



Antonio Ferrara

---

# Statistical and Structural Approaches to Algorithmic Fairness

---

## DOCTORAL THESIS

to achieve the university degree of  
Doctor of Technical Sciences

submitted to

**Graz University of Technology**

### Supervisor

Univ.-Prof. Dr. Fariba Karimi  
Institute of Human-Centred Computing

Graz, 19<sup>th</sup> June 2026

## **AFFIDAVIT**

I declare that I have authored this thesis independently, that I have not used other than the declared sources/resources, and that I have explicitly indicated all material which has been quoted either literally or by content from the sources used. The text document uploaded to TUGRAZonline is identical to the present doctoral thesis.

---

Date, Signature

# Abstract

Modern machine learning systems have outgrown their origins as isolated predictive constructs, evolving into complex socio-technical architectures that actively mediate human opportunity. As algorithms increasingly determine access to economic and social opportunities, it has become widely recognized that these systems are deeply embedded with the structural inequalities and prejudices of their environments. The field of algorithmic fairness emerged in response to the growing recognition that models optimized for predictive accuracy can systematically disadvantage marginalized groups. Early mitigation strategies, however, rested on fragile simplifications that limited their effectiveness in complex socio-technical environments. This thesis identifies and addresses two fundamental limitations of contemporary fairness paradigms: the reliance on deterministic point estimates for auditing and the treatment of individuals as isolated entities devoid of structural context.

First, the diagnosis of algorithmic unfairness has traditionally depended on scalar metrics that fail to capture the nuances of real-world deployment. This deterministic approach ignores the high statistical variance inherent in small, intersectional groups, often leading to false alarms or missed detections of bias. Furthermore, standard auditing struggles with the opacity of black-box models, frequently conflating unjustifiable bias with the influence of legitimate features. Moreover, traditional metrics also overwhelmingly focus on disparate outcomes, neglecting the procedural logic of the model and failing to detect when groups are subjected to distinct, discriminatory decision-making processes. To resolve these diagnostic failures, this thesis proposes a transition toward statistical hypothesis testing, ensuring that fairness assessments are statistically robust, causally valid, and capable of inspecting the underlying explanations of model decisions.

Second, this thesis challenges the prevailing focus on isolated predictions by examining algorithmic fairness through a structural lens. In networked and hierarchical systems, fairness is an emergent property of the interactions, connectivity, and comparative processes that govern the domain. Network topologies are not neutral; when optimization objectives interact with these structures, they can actively concentrate visibility and marginalize already peripheral communities. Similarly, hierarchical structures and rankings frequently crystallize human prejudices and biases into systemic disadvantages. By shifting the focus to these structural dependencies, the thesis demonstrates that achieving fairness requires deliberately reshaping how opportunities flow through networks and how merit is inferred and aggregated.

Ultimately, this thesis advances comprehensive frameworks that marry statistical reliability with structural awareness. By replacing brittle auditing metrics with statistical hypothesis testing, introducing concepts that actively mitigate bias in structural systems including physical routing, social networks, and rankings, and complementing these with operational safeguards such as abstention under uncertainty and lifecycle-wide bias governance, this thesis provides a robust foundation for the deployment of trustworthy artificial intelligence.

# Acknowledgments

I am deeply grateful to Prof. Fariba Karimi for supervising me throughout my entire Ph.D., providing a great combination of academic freedom and kind guidance. Her insightful advice and wise feedback have been invaluable in shaping this work.

Furthermore, I extend my deepest gratitude to Prof. Claudia Wagner for her mentoring and support during the first years of my doctorate, and to Prof. Francesco Bonchi for his guidance and inspiration during the final years of my journey.

I also want to thank all my colleagues and friends from TU Graz, GESIS, NoBias, and CENTAI, for their wonderful friendship and intellectual stimulation.

A special thank you to my girlfriend, Veronica, for her endless patience while I wrote this thesis and for surviving stressful deadlines together, even a NeurIPS rebuttal during our vacation in the Maldives! Grazie mille amorino.

Finally, my deepest thanks go to my family, for their unconditional support, for believing in me, and for always giving me the freedom to follow the path I chose.

# Contents

<b>1</b>	<b>Introduction</b>	<b>1</b>
1.1	The Foundations and Challenges of Algorithmic Fairness . . . . .	1
1.2	Research Questions . . . . .	8
1.3	List of Publications . . . . .	10
1.4	Roadmap . . . . .	12
<b>2</b>	<b>Background and Related work</b>	<b>14</b>
2.1	Definitions of Algorithmic Fairness . . . . .	14
2.2	Detecting Unfairness . . . . .	17
2.3	Mitigating Unfairness . . . . .	18
<b>3</b>	<b>Summary of Contributions</b>	<b>24</b>
3.1	Contributions to Fairness Testing and Auditing . . . . .	24
3.2	Contributions to Fairness in Network Structures . . . . .	26
3.3	Contributions to Fairness in Ranking and Pairwise Comparisons	28
3.4	Contributions to Reliability and Safety . . . . .	30
<b>4</b>	<b>Testing and Auditing for Fairness</b>	<b>32</b>
4.1	Size-adaptive Hypothesis Testing for Fairness . . . . .	32
4.2	Auditing For Demographic Bias in Opaque Rankings . . . . .	64
4.3	Beyond Demographic Parity: Redefining Equal Treatment . . . . .	79
<b>5</b>	<b>Fairness in Network Structures</b>	<b>107</b>
5.1	Beyond Shortest paths: Node Fairness in Route Recommendation	108
5.2	Link Recommendations: Their Impact on Network Structure and Minorities . . . . .	122
5.3	Super-Resolution of Urban Socioeconomic Indicators via Graph- Based Recommender Systems . . . . .	134
<b>6</b>	<b>Fairness in Ranking and Pairwise Comparisons</b>	<b>146</b>
6.1	Bias-Aware Ranking from Pairwise Comparisons . . . . .	147
6.2	Fairness-Aware Ranking Recovery from Pairwise Comparisons . .	173
6.3	FairMC Fair-Markov Chain Rank Aggregation Methods . . . . .	184
<b>7</b>	<b>Safety and Policy for Fairness</b>	<b>192</b>
7.1	Bounded-Abstention Pairwise Learning to Rank . . . . .	193
7.2	Policy Advice and Best Practices on Bias and Fairness in AI . .	214
<b>8</b>	<b>Conclusions, Limitations and Future Work</b>	<b>241</b>

# 1 Introduction

*“Technology is neither good nor bad; nor is it neutral.”*

– Melvin Kranzberg [1]

## 1.1 The Foundations and Challenges of Algorithmic Fairness

The integration of Artificial Intelligence into the foundational infrastructure of modern society represents a technological shift of unprecedented magnitude. We live in an era where the most consequential decisions of our lives, how we find employment, how we access credit, how we consume information, and even how we navigate the physical world, are mediated by artificial intelligence. Every day, billions of human needs are translated into queries, and billions of algorithmic responses shape the trajectory of those desires.

For the first few decades of the digital age, the primary challenge for these systems was accuracy: minimizing error rates on independent, identically distributed data points. Success was defined by a single number, e.g., accuracy, precision, or AUC, calculated on an often static test set. The optimization landscape was viewed as a technical frontier, devoid of moral weight. The underlying assumption was one of neutrality: if an algorithm is trained on data to maximize a mathematical objective function, it acts as an objective arbiter of quality.

This thesis proceeds from the fundamental premise that the era of assumed neutrality has irrevocably ended. As algorithmic systems have transitioned from passive tools to active gatekeepers of social and economic opportunity, they have begun to function less like technical instruments and more like institutions. They do not merely describe the world; they shape it. Today, algorithms determine who accesses credit, who is interviewed for employment, which neighborhoods receive infrastructure investment, and how information propagates through the public sphere.

A critical realization in the field of socio-technical systems is that an algorithm can be highly accurate on average while systematically discriminating against specific subpopulations. A credit scoring model might maximize overall profit while denying loans to creditworthy minority applicants due to historical redlining encoded in the training data. An online marketplace might boost overall sales by highlighting popular brands while burying highly rated products

from small, minority-owned businesses. A route recommendation system might optimize for global traffic flow while economically strangling local businesses in specific neighborhoods by diverting all foot traffic away from them.

The field of Algorithmic Fairness emerged to address these disparities, initially by defining statistical constraints such as Statistical Parity [2] (requiring equal positive prediction rates across groups) or Equalized Odds [3] (requiring equal true positive and false positive error rates) to enforce equitable outcomes across groups defined by sensitive attributes like race, gender, or age. While foundational, this early era of fairness research relied on several critical simplifications that now limit the efficacy of auditing and intervention in complex, real-world scenarios. Specifically, this thesis aims to address two major limitations in the current literature: the overreliance on point estimates for fairness assessment, and the failure to account for the interdependence between individuals, particularly the structural relationships embedded within networks and hierarchies.

### From Point Estimates to Fairness Testing

One of the first fundamental challenges in algorithmic fairness is the *diagnosis* of the presence of inequalities. Before an algorithmic system can be corrected, its unfairness must be reliably measured. However, the operationalization of algorithmic fairness has traditionally relied on fragile simplifications, including the calculation of disparity as point estimates. In standard practice, a practitioner selects a metric, such as Statistical Parity [2] or Equal Opportunity [3], computes it as a scalar value over a test set, and compares the result to a fixed threshold (e.g., the “four-fifths rule” [4]).

This thesis argues that this deterministic, scalar approach is insufficient for the complexity of modern socio-technical systems. The reliance on simple point estimates fails to account for several critical dimensions of real-world deployment:

1. **Reliability on Small Groups:** It ignores the high variance of estimators in finite, intersectional samples, leading to false alarms in small groups and missed detections in large ones.
2. **Direct and Indirect Influences:** It cannot distinguish between unjustifiable bias and disparities explained by legitimate task-relevant features, especially in opaque “black-box” systems where the internal logic is inaccessible.
3. **Process Transparency:** It measures only the final outcome distributions,

failing to detect when a model arrives at equitable outcomes through discriminatory reasoning or proxy variables.

In this thesis, we address these limitations by introducing comprehensive auditing frameworks that transition from comparing point estimates to conducting statistical hypothesis tests.

**Reliability on Small Groups:** The first failure mode of standard auditing is the illusion of precision. As we disaggregate data to audit intersectional subgroups, defined by combinations of protected attributes such as race, gender, and age, sample sizes naturally shrink. As the granularity of the audit increases, the variance of fairness estimators explodes. In PAPER 1 (*Size-adaptive Hypothesis Testing for Fairness*), we demonstrate that standard metrics frequently flag violations in intersectional groups that are essentially noise, while simultaneously missing significant disparities in larger groups due to rigid thresholds. We resolve this by reframing fairness auditing as a hypothesis testing problem. We introduce a size-adaptive framework that employs Wald tests for large samples and Bayesian inference for small samples. This approach allows us to define the *resolution limit* of fairness: the minimal detectable disparity for a given subgroup size, effectively creating a “no-power zone” where data is insufficient to reject the null hypothesis of fairness.

**Disentangling Direct and Indirect Influence:** Even when sample sizes are sufficient, standard disparity metrics can be misleading because they often only measure marginal dependence rather than considering also conditional dependence. In many high-stakes ranking applications, such as hiring or credit scoring, the auditor typically has access to the input features, the protected attributes, and the output ranking, but not the internal scoring function of the model. A machine learning system might exhibit a correlation with a protected attribute (e.g., gender) simply because that attribute is correlated with a legitimate, task-relevant feature (e.g., education level). Standard metrics like Statistical Parity would flag this as unfair, potentially forcing a correction that reduces utility. Conversely, a model might be ostensibly fair on average but harbor “residual” bias where, for two individuals with identical task-relevant features, the protected group member is consistently ranked lower. In PAPER 2 (*Auditing for Demographic Bias in Opaque Rankings*), we propose a method to detect this residual dependence under strict black-box assumptions. We move beyond point estimates of representation to test the conditional independence hypothesis. We introduce a statistical framework called CONDOR that residualizes the ranking and protected attributes with respect to the observables using kernels in a Reproducing Kernel Hilbert Space [5] (RKHS), and then quantifies the remaining as-

sociation using distance correlation. This method allows auditors to distinguish between disparities rooted in direct or indirect influence of protected attributes.

**Process Transparency:** The final limitation of standard point estimates is their highly prevalent focus on *outcomes* (Disparate Impact) rather than on the underlying *process* (Disparate Treatment). Historically, doctrines such as “fairness through unawareness” attempted to ensure procedural fairness through strict blindness, i.e., by simply removing the protected attribute from the data. However, this naive approach fails to achieve true Equal Treatment (the formal absence of Disparate Treatment) because it ignores how sensitive attributes are indirectly encoded via proxies. Equal Treatment demands that a model’s internal logic does not depend on group membership, either directly or indirectly. Crucially, a model can satisfy outcome-based metrics like Statistical Parity while still violating Equal Treatment. For example, a model might positively discriminate in favor of a subgroup based on a certain feature, while negatively discriminating against them on another feature, causing the biases to cancel out in the final prediction distribution. While the aggregated outcome appears fair, the underlying process is not; individuals are still being subjected to distinct, biased decision logic based on their demographic group. In PAPER 11 (*Beyond Demographic Parity: Redefining Equal Treatment*), we introduce the metric of Explanation Disparity to diagnose this failure mode. Instead of comparing the distributions of predictions, we compare the distributions of *explanations*, specifically, the Shapley value contributions of the features. We propose an Equal Treatment Inspector, a meta-classifier trained to predict the protected attribute solely from the explanations of the model’s decisions. If this inspector can predict the protected attribute with accuracy better than random chance, it proves that the model is treating groups differently, even if the final outcome rates are identical.

Together, these three methodologies constitute a unified diagnostic layer for algorithmic fairness that far exceeds the capabilities of traditional point-estimate audits. By ensuring statistical validity against noise (PAPER 1), causal validity against confounding (PAPER 2), and procedural validity against proxy discrimination (PAPER 11), we establish a robust foundation for the auditing of fairness strategies discussed in the subsequent chapters of this thesis.

## From Isolated Individuals to Structured Systems

In the previous section, we explained problems and challenges of auditing for fairness. A further limitation of traditional fairness lies in its treatment of individuals as isolated data points. Indeed, many contemporary algorithmic systems do not operate on independent individuals. Instead, they function over struc-

tured domains, where entities are connected, compared, ordered, or embedded in networks of mutual influence. In such environments, fairness is not solely a property of isolated predictions, but of the entire system of interactions through which outcomes are produced.

In this thesis, we adopt a broad interpretation of the term **Structural**, referring to any setting in which relationships among entities play a central role in shaping outcomes. Such relationships may arise through graph connectivity, network diffusion processes, ranking positions, or pairwise comparisons. We argue that fairness cannot be fully understood by examining individuals and their characteristics in isolation; rather, it requires confronting the structural challenges, such as biased connectivity patterns, feedback loops, and distorted comparative processes, that govern these systems. Accordingly, this thesis extends the scope of algorithmic fairness beyond the analysis of independent predictions to encompass relational structures, identifying critical sources of failure in two fundamental forms of organization: **Network Structures**, which regulate how opportunities flow and become visible, and **Hierarchical Structures**, which determine how merit is inferred, ordered, and aggregated.

### Unfairness in Network Structures

In networked systems, algorithms do not merely predict individual outcomes, they actively shape the distribution of visibility, access, and opportunity across the underlying structure. Crucially, network topology is not neutral: it reflects historical constraints, spatial frictions, and social divisions that influence how advantages and disadvantages propagate. When optimization objectives focus narrowly on local efficiency or predictive accuracy, they interact with these structural properties to generate effects that progressively concentrate exposure and marginalize already peripheral nodes. As a result, inequality in networked systems is not simply the product of biased data or flawed predictions, but an emergent property of the interplay between topology and optimization, where visibility, connectivity, and opportunity become unevenly distributed. This structural perspective provides a unifying lens through which several seemingly distinct challenges can be understood.

In physical transportation networks, this dynamic appears as a tension between individual efficiency and systemic equity. Classical routing systems optimize for minimal distance or minimal travel time, yet this objective induces winner-take-all patterns in which traffic, and therefore economic visibility, is funneled through a narrow set of “optimal” corridors, leaving nearby alternatives

systematically deprived of exposure. The root cause is a structural bottleneck of optimality: in weighted graphs, the shortest path is frequently unique, and when an algorithm is constrained to always select it, fairness becomes structurally infeasible rather than merely overlooked. In PAPER 3 (*Beyond Shortest Paths: Node Fairness in Route Recommendation*) we overcome these limitations by relaxing strict optimality and expanding the feasible solution space through a novel definition of paths. Specifically, we generate routes that maintain a user’s progress toward their destination without strictly minimizing distance. In this way, the exposure of business locations (the network nodes) to the customers traversing these paths can be redistributed toward the worst-off nodes while sufficiently preserving the overall user experience. In this sense, routing algorithms shift from passive optimizers of efficiency to active mediators of opportunities.

A closely related process governs social and recommendation networks, where the challenge is rooted in the dynamic evolution of the network. Social graphs are shaped by homophily [6] and preferential attachment [7], structural forces that naturally produce clustering and inequality in connectivity. When link recommendation systems rely on existing topology, optimizing for structural proximity naturally reproduces these patterns. As we demonstrate in PAPER 5 (*Link Recommendations: Their Impact on Network Structure and Minorities*), this creates a severe feedback loop in which popular nodes become increasingly central while minority or peripheral groups remain isolated. Over time, the network itself becomes a barrier to opportunity, restricting access to information and social centrality. Crucially, we show that the objectives of purely topological similarity and structural fairness are often fundamentally misaligned: algorithms that prioritize within-cluster connections inadvertently intensify segregation. Addressing this requires more than re-ranking recommendations; it involves structural interventions that deliberately bridge disconnected regions of the graph, preventing persistent marginalization and counteracting network segregation effects.

These structural inequalities are further obscured by a granularity gap that limits our ability to observe them directly. In many geographical and social contexts, socioeconomic indicators are measured at coarse spatial or temporal resolution, masking fine-grained disparities that emerge from the actual flow of people, resources, and attention across networks. The challenge is therefore one of structural inference: how to extract localized inequality from weak or aggregated signals. Interaction graphs, such as user–business mobility networks, implicitly encode such information because movement patterns often exhibit homophily, linking individuals and places of similar socioeconomic status. In PAPER 10 (*Super-Resolution of Urban Socioeconomic Indicators via Graph-Based Recommender Systems*), we study how to use Graph Neural Networks to prop-

agate latent signals across the network, effectively refining coarse observations and revealing otherwise invisible pockets of disadvantage.

Taken together, these phenomena highlight a unifying principle: inequality in networked systems is not solely a consequence of biased data or imperfect predictions, but an emergent property of the interaction between topology and optimization. Achieving fairness therefore requires moving beyond local objective optimization toward algorithms that explicitly reason about, and when necessary reshape, the structure of connectivity and visibility that governs access to opportunity.

### Unfairness in Hierarchical Structures

Just as networks are structures of connection, rankings are structures of hierarchy. A major challenge in algorithmic fairness is that these hierarchies are rarely “given”; they are often derived from noisy, biased preference relationships. If the process of comparison itself is flawed, the resulting ranking will crystallize that bias into a systemic disadvantage.

The first point of failure lies in the input to these systems. Rankings are frequently aggregated from human judgments, which are rarely neutral. Evaluators often harbor implicit group biases, such as in-group favoritism or out-group prejudice, that distort their perception of an item’s quality. Standard ranking models often fail to account for this, effectively assuming evaluators are objective sensors of latent quality. This conflation of prejudice with merit propagates discriminatory inputs directly into the final ranking, making the algorithmic output a reflection of human bias rather than true utility. In PAPER 4 (*Bias-Aware Ranking from Pairwise Comparisons*), we tackle this problem by developing a parametric method to account for evaluators’ biases in rankings obtained from pairwise comparisons.

Even if evaluators were neutral, fairness is compromised by the process of candidate selection. In many systems, not all pairs are compared; sampling strategies determine *who* gets the opportunity to be evaluated. Biases in sampling, where privileged individuals are selected for comparison more often due to popularity or representation bias, create a distorted comparison graph. Standard ranking recovery algorithms can interpret this lack of comparisons as a lack of merit, systematically under-ranking minority groups simply because they were denied the “opportunity to compete”. We study this phenomenon in PAPER 8 (*Fairness-Aware Ranking Recovery from Pairwise Comparisons*).

Finally, the aggregation mechanism itself can become a vehicle for unfairness. When combining multiple preference lists into a consensus, algorithms often follow transition probabilities derived from the input data. If the original rankings contain position bias or consistently favor certain groups, the aggregation process will naturally converge to a consensus that marginalizes the other groups. The challenge is to intervene in these aggregation algorithms to ensure that the final consensus reflects a fair representation of all groups without faithfully reproducing the biases of the inputs. We develop such techniques in PAPER 9 (*FairMC Fair-Markov Chain Rank Aggregation Methods*).

By shifting the focus from isolated individuals to structural challenges, this thesis argues that fairness cannot be achieved merely by constraining final outcomes. It requires diagnosing and repairing the inputs (biased judgments), the processes (skewed sampling), and the mechanisms (aggregation and optimization) that constitute the system itself.

## 1.2 Research Questions

This thesis is grounded in the observation that algorithmic systems have transitioned from passive technical tools to active institutional gatekeepers that distribute social and economic opportunities, arguing that the traditional assumption of algorithmic neutrality has ended, as these systems now shape the world rather than merely describing it.

However, the current methods for ensuring fairness in these systems are failing due to several limitations. First, standard auditing relies on fragile “point estimates”, scalar metrics that ignore statistical uncertainty and fail to detect bias in complex, black-box models. Furthermore, current approaches often treat individuals as isolated data points, ignoring the “structural” reality where opportunities are shaped by networks, connectivity, and hierarchies. Consequently, this research proposes a shift toward statistical validity (via hypothesis testing) and structural awareness (via network and ranking analysis). In more detail, in this thesis we want to address the following research questions:

RQ1 – How can the diagnosis of algorithmic unfairness transition from point estimates to statistical hypothesis testing?

RQ2 – How do structural dependencies in networks create inequalities, and how can they be mitigated?

RQ3 – How is unfairness embedded in hierarchical structures, and how can it

be addressed?

RQ4 – How can systems be designed to ensure reliability and safety in the face of biased inputs and opaque logic?

The research questions outlined above are addressed through the papers presented in the following Section 1.3.

PAPERS 1, 2 and 11 of this thesis address the first research question by proposing a comprehensive shift from deterministic point estimates to robust statistical hypothesis testing frameworks. To handle the high statistical variance inherent in small intersectional subgroups, PAPER 1 introduces a unified hypothesis-testing approach utilizing Bayesian inference to provide reliable credible intervals when data is scarce. To tackle the influence of sensitive attributes, PAPER 2 presents a model-agnostic auditing method that tests for conditional independence by measuring residual demographic dependence, effectively distinguishing between task-relevant features and unjustifiable bias. Lastly, PAPER 11 moves beyond disparate outcomes to inspect procedural logic. By comparing the distributions of feature attributions and training a meta-classifier to detect disparate treatment, the framework ensures models do not apply distinct, discriminatory reasoning across demographic groups, even when final acceptance rates appear equitable.

To answer the second research question, the thesis demonstrates how inequalities naturally emerge when algorithms focus exclusively on narrow goals like efficiency or accuracy, often interacting with the underlying network to hide or marginalize vulnerable individuals or communities. In connected systems like navigation networks, PAPER 3 of this thesis shows how to spread out exposure more fairly by recommending diverse, near-optimal routes instead of rigidly forcing everyone down a single shortest path. PAPER 5 contributes to RQ2 by inspecting how link recommendation algorithms, applied over time, can reinforce inequalities and segregation of communities, for example, by reducing the visibility of already marginalized minority groups. Instead, in PAPER 10, we propose a GNN framework that learns business representations from a bipartite user-business interaction graph. The representations are then used to better infer socioeconomic indicators, and thereby reveal underlying socioeconomic inequalities.

To answer RQ3, this thesis explores how unfairness permeates the entire pipeline of hierarchical structures, rankings, and pairwise comparisons. First, to address the distortion of human prejudice in the input data, PAPER 4 proposes a probabilistic framework that explicitly estimates and mathematically corrects

individual evaluator biases, allowing for the recovery of an unbiased latent ranking. Furthermore, PAPER 8 investigates the ranking recovery phase, evaluating how skewed sampling strategies interact with standard and fairness-aware algorithms, demonstrating the need to prevent structural invisibility for underrepresented candidates. Finally, tackling the aggregation of multiple rankings into a consensus, PAPER 9 introduces an in-processing Markov Chain method that rescales edge weights to ensure balanced visibility across demographic groups directly within the aggregation mechanism.

PAPER 6 bridges RQ3 and RQ4 by introducing a model-agnostic safety mechanism that enables ranking systems to selectively abstain from predictions when the underlying uncertainty is high. This is operationalized by estimating conditional risk and rejecting uncertain pairwise orderings without requiring the underlying model to be retrained.

Beyond direct algorithmic interventions, PAPER 7 answers RQ4 by synthesizing technical findings into actionable governance, proposing a holistic bias management architecture. The proposed governance framework champions continuous monitoring for temporal distribution shifts, the integration of causal reasoning to explicitly model discriminatory mechanisms, and a cautious approach to explainable artificial intelligence to manage the vulnerabilities of opaque systems across the entire lifecycle.

## 1.3 List of Publications

### Publications in International Journals and Conferences (Published and Forthcoming)

#### As First Author

- PAPER 1 – *Size-adaptive Hypothesis Testing for Fairness* [8]  
**A. Ferrara**, F. Cozzi, A. Perotti, A. Panisson, and F. Bonchi  
Advances in Neural Information Processing Systems 38 (NeurIPS 2025)
- PAPER 2 – *Auditing for Demographic Bias in Opaque Rankings* [9]  
**A. Ferrara**, C. Abrate, F. Vitale, and F. Bonchi  
Proceedings of the VLDB Endowment 19 (VLDB 2026)
- PAPER 3 – *Beyond Shortest Paths: Node Fairness in Route Recommendation* [10]  
**A. Ferrara**, D. García-Soriano, and F. Bonchi

Proceedings of the VLDB Endowment 18(9) (VLDB 2025)

- PAPER 4 – *Bias-aware ranking from pairwise comparisons* [11]  
**A. Ferrara**, F. Bonchi, F. Fabbri, F. Karimi, and C. Wagner  
Data Mining and Knowledge Discovery, 38(4) (DAMI 2024)
- PAPER 5 – *Link recommendations: Their impact on network structure and minorities* [12]  
**A. Ferrara**, L. Espín-Noboa, F. Karimi, and C. Wagner  
Proceedings of the 14<sup>th</sup> ACM Web Science Conference (WEBSCI 2022)
- PAPER 6 – *Bounded-Abstention Pairwise Learning to Rank* [13]  
**A. Ferrara**<sup>\*</sup>, A. Pugnana<sup>\*</sup>, F. Bonchi, and S. Ruggieri  
Proceedings of the 32<sup>nd</sup> ACM SIGKDD Conference on Knowledge Discovery and Data Mining (KDD 2026)

#### **As Co-author**

- PAPER 7 – *Policy advice and best practices on bias and fairness in AI* [14]  
J. M. Alvarez, A. B. Colmenarejo, A. Elobaid, S. Fabbri, M. Fahimi, **A. Ferrara**, S. Ghodsi, C. Mougan, I. Papageorgiou, P. Reyer, M. Russo, K. M. Scott, L. State, X. Zhao, and S. Ruggieri  
Ethics and Information Technology 26(2) 2024
- PAPER 8 – *Fairness-Aware Ranking Recovery from Pairwise Comparisons* [15]  
G. Ahnert, **A. Ferrara**, and C. Wagner  
Proceedings of the 18<sup>th</sup> ACM Web Science Conference (WEBSCI 2026)
- PAPER 9 – *FairMC Fair-Markov chain rank aggregation methods* [16]  
C. Balestra, **A. Ferrara**, and E. Muller  
International Conference on Big Data Analytics and Knowledge Discovery (DaWaK 2024)

---

<sup>\*</sup>Equal contribution.

## Pre-Prints, Under Review and Workshop papers

### As Co-author

PAPER 10 – *Super-Resolution of Urban Socioeconomic Indicators via Graph-Based Recommender Systems* [17]

F. P. Nerini, C. Borile, **A. Ferrara**, and A. Panisson

Accepted at WebAndTheCity workshop at The WebConf 2026

PAPER 11 – *Beyond demographic parity: Redefining equal treatment* [18]

C. Mougan, L. State, **A. Ferrara**, S. Ruggieri, and S. Staab

### Additional Publications of the Author which are not part of the thesis

PAPER 12 – *A Multidisciplinary Lens of Bias in Hate Speech* [19]

P. Reyero Lobo, J. Kwarteng, M. Russo, M. Fahimi, K. Scott, **A. Ferrara**, I. Sen, and M. Fernandez

Proceedings of the International Conference on Advances in Social Networks Analysis and Mining (ASONAM 2023)

## 1.4 Roadmap

The thesis is structured as follows. In Chapter 1, we introduce the foundations and limits of algorithmic fairness, highlighting the necessary transition from simple point estimates to robust fairness testing, and from treating individuals as isolated entities to understanding them within structured systems. In Chapter 2 we introduce preliminary notations and the related work, while Chapter 3 contains a summary of the contributions of this thesis.

The core technical contributions are divided into four macro themes, from Chapter 4 to Chapter 7. In Chapter 4, we address testing and auditing for fairness. We introduce *Size-Adaptive Hypothesis Testing for Fairness* (PAPER 1), a unified framework that turns fairness assessment into an evidence-based statistical decision to handle the high variance of small intersectional groups. Following this, we present *Auditing for Demographic Bias in Opaque Rankings* (PAPER 2), which utilizes conditional distance correlation to measure the residual dependence of a ranking on protected attributes within black-box models. Finally, we move beyond disparate outcomes to inspect procedural logic in *Beyond demographic parity: Redefining equal treatment* (PAPER 11), introducing Explanation Disparity to detect when models use different reasoning for different demographic

groups.

In Chapter 5, the focus shifts to fairness in network structures, examining how graph topology shapes the distribution of opportunity. In *Beyond Shortest Paths: Node Fairness in Route Recommendation* (PAPER 3), we propose the MMFP algorithm to guarantee individual fairness for network nodes by utilizing forward paths. In *Link Recommendations: Their Impact on Network Structure and Minorities* (PAPER 5), we then analyze how link recommendation algorithms impact social networks and their structure, demonstrating their tendency to exacerbate popularity bias and reinforce homophily. To bridge the spatial granularity gap, we also introduce a framework for the *Super-Resolution of Urban Socioeconomic Indicators* (PAPER 10) using Graph Neural Networks on user-business interaction graphs.

Chapter 6 explores fairness in ranking and pairwise comparisons, dealing with the end-to-end pipeline of hierarchical structures. In *Bias-Aware Ranking from Pairwise Comparisons* (PAPER 4), we propose a probabilistic model that estimates individual evaluator biases to recover an unbiased latent ranking. We further address the recovery phase in *Fairness-Aware Ranking Recovery from Pairwise Comparisons* (PAPER 8), evaluating how sampling strategies interact with ranking algorithms to prevent structural invisibility. For rank aggregation, we introduce FairMC (PAPER 9), an in-processing Markov Chain method that rescales edge weights to ensure balanced visibility for protected groups.

In Chapter 7, we connect these contributions to the reliability and safety of AI deployment. We present BALToR (Bounded-Abstention Learning to Rank) (PAPER 6), a framework that allows ranking models to safely abstain from predictions when uncertainty is high without requiring retraining. The thesis concludes with *Policy advice and best practices on bias and fairness in AI* (PAPER 7), synthesizing our technical findings into actionable AI governance, including continuous monitoring and a holistic Bias Management architecture.

We conclude in Chapter 8 by presenting concluding remarks, limitations, and future work of this thesis.

## 2 Background and Related work

*“Life can only be understood backwards; but it must be lived forwards.”*

– Søren Kierkegaard [20]

### 2.1 Definitions of Algorithmic Fairness

The study of algorithmic fairness emerged at the intersection of machine learning, law, and political philosophy in response to the growing societal impact of automated decision-making systems. Foundational literature has focused on formalizing the ethical concept of “fairness” into mathematical definitions, establishing theoretical limitations of these definitions, and identifying the root causes of algorithmic bias.

A central organizing distinction in the algorithmic fairness literature is the difference between individual and group-level fairness metrics.

#### Individual Fairness

Individual fairness was introduced by Dwork et al. [2] in their seminal paper “Fairness Through Awareness” and it is based on the Aristotelian principle that “similar individuals should be treated similarly” [21]. Mathematically, this is often framed as a Lipschitz condition: for a distance metric  $d$  in the feature space and a distance metric  $D$  in the outcome space, a mapping  $M$  is individually fair if for any individual  $x, y$ :  $D(M(x), M(y)) \leq d(x, y)$ . However, while conceptually robust, applying individual fairness in practice is often hindered by the inherent difficulty of defining appropriate similarity metrics  $d$  and  $D$  that correctly capture domain-specific nuances and ethical intuitions.

**Maxmin Fairness** In this thesis, in particular in PAPER 3, we consider an alternative framework of Individual Fairness known as Maxmin Fairness, as defined by García-Soriano and Bonchi [22], [23]. This approach bypasses the need to explicitly define the distance metrics  $d$  and  $D$ , and instead prioritizes the most disadvantaged individuals. Inspired by John Rawls’s theory of distributive justice [24], which argues that social inequalities should be arranged to benefit the worst-off, this definition evaluates fairness through an ex-ante probabilistic lens. Informally, a probability distribution over the set of solutions of a problem is

maxmin-fair if it is impossible to improve the satisfaction probability of any individual without decreasing it for some other individual which is no better off [23] (where an individual’s satisfaction probability is the probability that they receive a favorable or desired outcome under the chosen randomized distribution over all feasible deterministic solutions).

### Group Fairness

In contrast to individual fairness, group fairness assesses whether aggregate statistical properties of a model’s outputs are equal across predefined demographic groups (often defined by “sensitive” or “protected” attributes like race, gender, or age).

The literature categorizes group fairness into several distinct mathematical criteria, mainly depending on the relationship between the sensitive attribute  $A$ , the predicted score or label  $\hat{Y}$ , and the true label  $Y$ . A comprehensive list of fairness definitions can be found in Verma et al. [25]. We recall, here, a few of the most relevant definitions.

**Independence (Demographic / Statistical Parity):** Requires the prediction to be statistically independent of the sensitive attribute

$$\hat{Y} \perp A.$$

It mandates that the rate of positive outcomes (e.g., being hired or receiving a loan) is identical across all demographic groups, regardless of underlying qualification distributions.

**Separation (Equalized Odds):** Formalized by Hardt et al. [3], Equalized Odds requires that the prediction is independent of the sensitive attribute conditional on the true label

$$\hat{Y} \perp A \mid Y.$$

Practically, this means the model must achieve equal True Positive Rates (TPR) and equal False Positive Rates (FPR) across all demographic groups.

**Sufficiency (Predictive Rate Parity / Calibration):** This requires that the true label is independent of the sensitive attribute conditional on the prediction

$$Y \perp A \mid \hat{Y}.$$

Perhaps one of the most crucial foundational result in algorithmic fairness is the mathematical incompatibility of certain group fairness metrics. Concurrent and independent work by Kleinberg et al. [26] and Chouldechova [27], spurred by the controversy surrounding the COMPAS recidivism risk algorithm, proved what is now known as the *Impossibility Theorem of Fairness*. They demonstrated that if the underlying base rates of the target variable differ between demographic groups, it is impossible to simultaneously satisfy Separation (Equalized Odds) and Sufficiency (Calibration), except in highly restrictive cases. Formally, when

$$P(Y = 1 | A = a) \neq P(Y = 1 | A = b),$$

no predictor  $\hat{Y}$  can satisfy both

$$\hat{Y} \perp A | Y \quad \text{and} \quad Y \perp A | \hat{Y}$$

simultaneously.

This inherent trade-off forced the research community to acknowledge that algorithmic fairness cannot be solved by simply finding a “perfect” metric; practitioners must explicitly choose which ethical trade-offs to make based on the specific context of the domain.

Furthermore, subsequent foundational work expanded the study of fairness into causal modeling.

**Causal Fairness.** Kusner et al. [28] introduced the concept of *Counterfactual Fairness*, grounded in Pearl’s causal inference framework [29]. A model is considered counterfactually fair if its prediction for an individual remains the same in a counterfactual world in which the individual’s sensitive attribute had taken a different value.

Formally, a predictor  $\hat{Y}$  is counterfactually fair if

$$\hat{Y}_{A \leftarrow a}(U) = \hat{Y}_{A \leftarrow a'}(U)$$

for all individuals with latent attributes  $U$ , where  $\hat{Y}_{A \leftarrow a}$  denotes the prediction under an intervention setting the sensitive attribute to  $a$ . Operationalizing this definition requires specifying a causal Directed Acyclic Graph (DAG) that represents the structural relationships between variables and allows the identification of the direct and indirect pathways through which a sensitive attribute influences an outcome.

## 2.2 Detecting Unfairness

The theoretical formalization of algorithmic fairness into mathematical definitions, such as Statistical Parity, Equalized Odds, and Counterfactual Fairness, establishes first constraints required for equitable machine learning. However, transitioning from theoretical definitions to the practical, operational detection of unfairness in deployed systems represents a profound epistemic and engineering challenge. Detecting unfairness is not merely the act of evaluating a static metric on a hold-out dataset; it requires determining whether observed statistical disparities are artifacts of random sampling variance, reflections of historical systemic prejudices embedded within training data, or the direct mechanical consequences of an algorithm’s internal architecture and decision boundaries.

The earliest and most rudimentary approaches to detecting unfairness relied on computing a single point estimate of a chosen fairness metric—such as the difference in selection rates between two demographic groups—and comparing it against a predefined, often arbitrary threshold (for example, the U.S. Equal Employment Opportunity Commission’s traditional “four-fifths rule” [4]). Typically, these metrics are reported pointwise, and the decision to deem an observed metric’s value as a potential issue is addressed by defining a threshold: if the value of the metric is above this threshold, it is considered as a fairness violation, otherwise, it isn’t ([8], [30], [31]).

To address the limitations of fixed thresholds the literature started to consider confidence intervals and hypothesis testing for detecting fairness violations. Confidence Intervals, obtained via Bootstrapping, for example, have been advocated by Besse et al. [32] and Cherian and Candès [31], and are supported by open library tools like FAIRLEARN [33]. Del Barrio et al. [34], Besse et al. [32], and Lo et al. [35] instead used the asymptotic normality of certain fairness metrics to produce hypothesis tests for fairness violations.

Differently from prior works, in this thesis and in particular in Section 4.1, we propose a general fairness testing methodology that easily applies to all group fairness metrics based on the confusion matrix and related conditional probabilities. Furthermore, we address statistical reliability in both small and large samples.

Besides uncertainty and reliability, another key aspect of unfairness detection is the disentanglement of direct and indirect influence on model outcomes. For example, Marx et al. [36] use SHAP values to distinguish between the two types of influences. Adler et al. [37] focuses on detecting indirect influence, in partic-

ular, how some features might indirectly influence outcomes via other, related features. In Section 4.2 we show how to combine a conditional and an unconditional independence test to audit for direct and indirect influence in ranking outcomes. Related to our work are hence conditional independence tests such as KCI [38] and pdCor [39], and the concept of conditional statistical parity [2]. Furthermore, strictly related are also the concepts of Structural Causal Models [29] and Interventional Fairness [40].

## 2.3 Mitigating Unfairness

Algorithmic unfairness mitigation techniques are traditionally categorized into three distinct approaches based on when they intervene in the machine learning lifecycle: pre-processing, in-processing, and post-processing.

**Pre-processing methods** tackle bias at the very beginning of the pipeline, before the machine learning model is trained. They work by directly modifying the initial training dataset to remove underlying historical biases, sanitize feature distributions, or eliminate spurious correlations between sensitive attributes and target outcomes. Common techniques include assigning different weights to specific demographic samples [41] or mathematically adjusting the features to remove disparate impact [42]. The main advantage of pre-processing is that it is highly model-agnostic. Once the dataset is debiased, practitioners can use it to train standard machine learning algorithms. However, the main disadvantage is that altering the underlying data can inadvertently destroy legitimate, highly predictive patterns. Consequently, these methods often lack strong theoretical guarantees regarding how much they will negatively impact the final model’s predictive accuracy.

**In-processing methods** mitigate bias during the model’s training phase. Instead of changing the input data, they modify the learning algorithm itself. This is typically achieved by adding strict fairness constraints or penalty terms directly into the model’s objective loss function, forcing the algorithm to learn fair representations. The main advantage of in-processing is that because the model simultaneously optimizes for both predictive accuracy and fairness during optimization, these methods typically achieve the most optimal mathematical trade-off between utility and fairness. Conversely, the main disadvantage is that they are strictly tied to specific model architectures.

**Post-processing methods** operate at the end of the pipeline, after the model has been trained. They do not modify the input data or the algorithm; in-

stead, they treat the trained model as a static opaque model and systematically adjust its final predictions, thresholds, or rankings to ensure the final outputs satisfy certain fairness metrics or fairness constraints. The main advantage of post-processing is that these methods are very versatile and completely avoid the need for expensive, time-consuming model retraining. This makes them the ideal choice for retrofitting fairness into proprietary or legacy systems that are already deployed in production. The main disadvantage is that modifying outputs artificially often disrupts the model’s quality and properties.

### **Unfairness Mitigation in Network Structures**

Traditional algorithmic fairness research has primarily focused on predictive models operating on independent data points. However, many real-world systems involve relational data, where entities interact through network structures. In such settings, outcomes are influenced not only by individual attributes but also by the topology of the network and the dynamics of interaction among nodes. As a result, fairness must be studied not only at the level of individual predictions but also at the level of structural relationships and connectivity patterns.

A central insight from network science is that network topology itself can encode structural inequalities. Individuals occupying peripheral or sparsely connected positions may experience reduced access to information, influence, or opportunities compared to highly connected nodes. Classic work in social network analysis has shown that structural position, captured by measures such as degree centrality [43], betweenness centrality [43], and PageRank [44], plays a crucial role in determining visibility and influence within networks. When algorithmic systems rely on such structural features, existing inequalities in connectivity can translate directly into disparities in algorithmic outcomes [45].

These concerns have motivated a growing body of research on algorithmic fairness in graph-based systems. Recent surveys highlight several core tasks where fairness issues arise, including node classification, link prediction, ranking, and influence maximization [46], [47]. In these tasks, structural dependencies violate the independence assumptions underlying many traditional fairness metrics, creating new forms of bias propagation through the network.

One important source of unfairness in networked systems is homophily [6], the tendency of individuals to connect with others who share similar attributes. Homophily has long been recognized as a fundamental mechanism shaping social

networks [6]. While homophily is a natural social phenomenon, it can lead to the formation of tightly connected clusters that isolate minority groups from the rest of the network [48]. When machine learning models exploit network connectivity, for instance through random walks, graph embeddings or message passing, these structural patterns can lead to biased representations and discriminatory predictions. Because models often aggregate information from neighboring nodes, they can inadvertently propagate demographic biases present in the network structure. Several studies have shown that node embeddings learned from biased graphs can encode sensitive attributes even when these attributes are not explicitly provided as input [49], [50]. As a result, downstream tasks built on top of these embeddings may inherit and amplify structural disparities. To address these issues, a number of fairness-aware graph learning methods have been proposed. One line of work focuses on modifying the random walk sampling process used in graph embeddings. For example, FairWalk [50] and Crosswalk [51] alter transition probabilities in random walks to balance visits across demographic groups, thereby reducing bias in learned node representations. Another line of research introduces fairness constraints directly into graph neural network training objectives. Methods such as FairGNN [52] incorporate adversarial learning mechanisms to prevent node embeddings from encoding sensitive attributes, while other approaches introduce regularization terms that enforce group fairness in node classification tasks [49], [53]. These in-processing techniques aim to jointly optimize predictive performance and fairness during model training. Beyond representation learning, fairness issues also arise in graph-based ranking algorithms. Ranking methods such as PageRank are widely used to measure node importance and allocate visibility in information networks. However, because these algorithms rely heavily on link structure, they may disproportionately favor nodes that already occupy central positions in the network. To mitigate such disparities, researchers have proposed fairness-aware variants of PageRank and other ranking algorithms that incorporate group-level constraints or adjust teleportation probabilities to ensure more balanced exposure [54], [55].

A further important challenge concerns the dynamic evolution of networks under algorithmic recommendations. In many online platforms, algorithms suggest new connections or interactions between users. These link recommendation systems are typically optimized for predictive accuracy, often reinforcing existing patterns of homophily and preferential attachment. As a result, recommendation algorithms can unintentionally amplify structural inequalities, further isolating minority groups and reinforcing network segregation [48], [56].

Finally, fairness concerns also arise in network processes such as routing and resource allocation, where algorithmic decisions determine how traffic, informa-

tion, or opportunities flow through the network. Optimization objectives that focus solely on efficiency may produce winner-take-all dynamics, concentrating traffic or visibility along a small set of highly optimized paths while leaving alternative nodes systematically underutilized. These dynamics illustrate how fairness challenges in networks often emerge from the interaction between topology and optimization objectives, rather than from biased predictions alone. Taken together, this body of work highlights that unfairness in networked systems is fundamentally structural. It arises from the interplay between connectivity patterns, learning algorithms, and optimization goals that govern how visibility and opportunities propagate through the network. Consequently, addressing fairness in these settings requires methods that explicitly account for relational dependencies and, in some cases, intervene directly on the network structure itself.

In this thesis, we explore several aspects of inequalities that may arise in network structures. In particular, we study how unfairness and inequalities can propagate and exacerbate in social networks due to link recommendation algorithms. Furthermore, we propose a method to guarantee individual fairness in route recommendation systems operating on network structures. Finally, we investigate how graph neural networks can be used to better understand socio-economic indicators associated with geographic locations, illustrating how graph-based learning models can provide insights into structural patterns of inequality.

### **Unfairness Mitigation in Hierarchical Structures**

In many algorithmic systems, individuals or items are not evaluated in isolation but are placed within ordered lists that determine access to opportunities such as jobs, loans, university admissions, or visibility in search results. These hierarchical structures translate comparisons into positions, and positions into opportunities. As a consequence, small biases in the comparative process can propagate and crystallize into large disparities in outcomes. Unlike classification systems, which produce independent predictions for each individual, ranking systems operate on relative judgments. An item’s position depends not only on its own attributes but also on how it compares with all other candidates. This structural dependence means that fairness cannot be evaluated solely at the level of individual predictions; instead, it must consider the entire comparative process through which merit is inferred, ordered, and aggregated.

A first source of unfairness arises in the input data used to construct rankings. In many real-world applications, rankings are derived from human judgments or pairwise comparisons, such as peer review processes, crowd-sourced evaluations,

hiring assessments, or product ratings. However, extensive research in social psychology and behavioral economics has shown that human evaluators are often influenced by implicit biases, including in-group favoritism and stereotypes affecting perceived competence or quality [57], [58]. When ranking algorithms treat these judgments as unbiased measurements of latent quality, they effectively conflate prejudice with merit. Preference learning models such as the Bradley–Terry model [59] or the Plackett–Luce model [60] typically assume that comparisons are generated by rational agents observing a latent utility signal. In practice, however, the observed comparisons may systematically favor certain demographic groups, causing the inferred ranking to reflect social biases rather than true ability. This issue is particularly pronounced in crowdsourced evaluation settings, where annotators differ in reliability, expertise, and bias. Recent work has therefore explored models that explicitly estimate evaluator bias and reliability in order to disentangle true item quality from systematic judgment distortions [61], [62], [63]. Such approaches aim to recover a more accurate latent ranking by modeling the evaluation process itself rather than assuming unbiased comparisons.

Beyond data collection, unfairness may also arise in the algorithmic mechanisms used to generate rankings. A growing body of research has therefore proposed fairness-aware ranking methods that explicitly incorporate equity constraints into ranking objectives. One influential line of work focuses on exposure fairness, which studies how visibility in ranked lists is distributed across demographic groups. Because higher-ranked items receive disproportionate attention from users, small positional differences can translate into large differences in exposure or opportunity. Methods such as FA\*IR [64] and subsequent fairness-aware ranking frameworks aim to guarantee that protected groups receive a minimum level of representation among the top-ranked results. Another research direction investigates fair ranking under relevance constraints, where algorithms attempt to balance fairness with ranking utility. Approaches such as the fairness-of-exposure framework [65] model ranking as a constrained optimization problem that redistributes exposure while preserving relevance as much as possible. Related work has also explored fairness in ranking-based recommender systems, where feedback loops between ranking algorithms and user behavior can amplify disparities over time [66]. These dynamics illustrate how algorithmic hierarchies can interact with user attention patterns to reinforce existing inequalities.

A further challenge arises when multiple rankings must be aggregated into a consensus hierarchy, as in meta-search engines, committee evaluations, or ensemble recommender systems. In such settings, the aggregation mechanism itself can become a source of unfairness. Many classical rank aggregation algorithms,

including the Borda count [67] and Markov chain–based approaches such as [68], combine rankings by repeatedly reinforcing majority preferences. If the input rankings systematically favor certain groups due to position bias or representation bias, the aggregation process can amplify these disparities, producing a consensus ranking that marginalizes protected groups. Recent research has therefore investigated fairness-aware aggregation mechanisms that adjust transition probabilities or reweight input rankings to prevent the convergence process from reproducing biased structures. These approaches aim to ensure that the final consensus ranking reflects a fair representation of competing candidates rather than merely mirroring the biases embedded in the inputs.

## 3 Summary of Contributions

*“The task is not so much to see what no one has yet seen; but to think what nobody has yet thought, about that which everybody sees.”*

– Arthur Schopenhauer [69]

### 3.1 Contributions to Fairness Testing and Auditing

The first stage of the thesis focuses on the **diagnostic** challenge: how to reliably detect discrimination when data is scarce, models are opaque, or the definition of fairness requires looking beyond simple outcomes.

**Contributions of PAPER 1: *Size-adaptive Hypothesis Testing for Fairness*.** The paper addresses the statistical brittleness of traditional fairness auditing, which often relies on point estimates and arbitrary thresholds that fail to account for sampling error, especially in small intersectional groups.

- **Methodological:** We introduce Size-Adaptive Fairness Testing (SAFT), a unified hypothesis-testing framework that turns fairness assessment into an evidence-based statistical decision.
- **Theoretical:** For sufficiently large subgroups, we derive Central-Limit results for general group fairness metrics. For smaller, granular intersectional groups, we construct a Bayesian Dirichlet-multinomial estimator to produce reliable Monte-Carlo credible intervals.
- **Empirical:** We provide empirical evidence showing that the Bayesian estimator converges to the theoretical asymptotic behavior. Additionally, we highlight the pitfalls of previously existing fairness measures, especially in the context of intersectional groups.

**Contributions of PAPER 2: *Auditing for Demographic Bias in Opaque Rankings*.** The paper introduces Condor (CONditional Distance cOrrelation for Rankings), a model-agnostic auditing framework to measure the residual dependence of a ranking on protected attributes after accounting for task-relevant features.

- **Methodological:** Condor residualizes the ranking and protected attributes within a reproducing kernel Hilbert space and then quantifies the remain-

ing association to provide a conditional independence hypothesis test.

- **Theoretical** We prove how to combine the conditional test of **Condor** with an unconditional independence test to achieve a comprehensive causal understanding of the system. The causal interpretation evaluates whether the ranking shows an overall dependence on protected attributes, and whether that dependence remains after adjusting for task-relevant features, allowing auditors to effectively pinpoint the exact nature of the bias.
- **Empirical:** We validate the framework on synthetic data and semi-synthetic rankings derived from real-world datasets using explicitly controlled parameters for direct and indirect bias. We demonstrate that **Condor** accurately detects residual demographic dependence regardless of the data’s underlying non-linearities.

**Contributions of PAPER 11: *Beyond demographic parity: Redefining equal treatment.*** The paper moves beyond outcome disparities to inspect the procedural logic of a model.

- **Conceptual:** Drawing on the principle of “Equal Treatment,” we introduce the metric of *Explanation Disparity*.
- **Methodological:** We exploit feature attribution methods (Shapley values) to compare the distributions of explanations across groups, training a meta-classifier to detect when a model relies on different reasoning for different demographic groups, even if the final acceptance rates appear fair.
- **Theoretical:** We demonstrated that while independent explanation distributions guarantee independent prediction distributions, the converse does not hold, meaning Statistical Parity can easily mask disparate treatment. Additionally, we establish the theoretical validity of the Equal Treatment Inspector by proving that under the null hypothesis of statistical independence between the explanations and the protected attribute, the Area Under the Curve of any Classifier Two-Sample Test is exactly 0.5.
- **Empirical:** We validate the Explanation Disparity metric and the Equal Treatment Inspector on synthetic data and real-world datasets. The experiments confirmed that the inspector accurately detects proxy discrimination and identifies the specific features driving unequal treatment, successfully flagging fairness violations in scenarios where standard metrics like Statistical Parity falsely indicated compliance.

## 3.2 Contributions to Fairness in Network Structures

We now shift the focus from individual predictions to **relational structures**, examining how graph topology and connectivity shape the distribution of opportunity.

**Contributions of PAPER 3: *Beyond Shortest Paths: Node Fairness in Route Recommendation.***

- **Conceptual:** We introduce the novel problem of guaranteeing individual fairness for network nodes in point-to-point route recommendation systems. The problem adopts a Rawlsian notion of maxmin distributional fairness, utilizing randomization to maximize the minimum probability of eligible nodes being included in a recommended route. To achieve this without extreme deviations in travel distance, the paper introduces the concept of *forward paths*, routes where every step strictly decreases the distance to the destination, providing a diverse and fair basis of near-shortest alternatives.
- **Methodological:** We design the DAG-FP algorithm to construct a Directed Acyclic Graph (DAG) that encapsulates all possible forward paths between a source and a destination, effectively avoiding the need to explicitly enumerate a potentially exponential number of routes. We then frame the search for a maxmin-fair probabilistic distribution as a network flow problem on this DAG. This is solved iteratively through the MMFP algorithm using a sequence of small linear programs (LPs).
- **Theoretical:** The research proves that the DAG of forward paths can be constructed in  $\Theta(|E| + |V| \log |V|)$  time, matching the asymptotic computational complexity of solving a single shortest-path query via Dijkstra’s algorithm. Furthermore, we show that the MMFP algorithm is optimal and we demonstrate that our compact LP formulation requires only polynomially many constraints and variables, ensuring that a maxmin-fair distribution of forward paths can be found in polynomial time.
- **Empirical:** The framework is tested on several real-world road networks, including massive datasets with millions of edges like the state of Florida and the Eastern part of the USA from OpenStreetMaps. The experiments confirm that the MMFP method achieves a highly equitable distribution of node visits, evidenced by significantly lower Gini coefficients, compared to diversity-based baselines, while keeping path lengths competitive. Addi-

tionally, the method proves highly scalable on commodity hardware and outperforms baselines in runtime when generating high volumes of path recommendations for the same query.

**Contributions of PAPER 5: *Link recommendations: Their impact on network structure and minorities*.** In the paper we investigate people recommender systems in social networks, analyzing how unsupervised link recommendation algorithms (like Personalized PageRank [70] and Who-To-Follow [71]) influence network evolution.

- **Methodological:** We systematically compared five link recommendation algorithms by iteratively applying them to several synthetic bi-populated directed networks to control for varying levels of homophily and minority group sizes. To simulate continuous feedback loops, we added new algorithmic link recommendations and sequentially removed random out-links to maintain constant edge density. Finally, we evaluated the resulting structural changes using the global clustering coefficient, the Gini coefficient of the in-degree distribution, and the visibility of the minority group among the most important nodes.
- **Empirical:** Our experiments demonstrated that all evaluated algorithms increased the clustering coefficient, making the networks more cohesive by closing triangles. However, we also show how these algorithms often exacerbate “rich-get-richer” dynamics and reinforce homophily, potentially trapping minority groups in visibility deficits. We highlight *node2vec* [72] as a more robust alternative that can mitigate polarization by learning structural roles.

**Contributions of PAPER 10: *Super-Resolution of Urban Socioeconomic Indicators via Graph-Based Recommender Systems*.** The paper addresses the spatial “granularity gap” where coarse data obscures localized structural variations. It introduces a framework that infers high-resolution demographic indicators by using GNNs to learn enriched business representations from user-business interaction graphs. By rendering hidden structural inequalities measurable, this methodology reveals how advantage and disadvantage are distributed across urban topologies.

- **Methodological:** We propose a GNN framework that models cities as bipartite user-business interaction graphs. The model explicitly enriches business representations with semantic categories and coarse spatial context (postal codes). We introduce a Socioeconomic Super-Resolution pipeline

to infer fine-grained attributes (Census Block Groups) using only coarse-grained training labels.

- **Empirical:** Yelp dataset experiments confirm user mobility traces contain strong, quantifiable signals of socioeconomic homophily. Injecting geographic context significantly improves representation quality over standard baselines. The framework successfully bridges the “granularity gap” by recovering local socioeconomic variations, and the learned embeddings naturally capture spatial neighborhood structures without explicit supervision.

### 3.3 Contributions to Fairness in Ranking and Pairwise Comparisons

Chapter 6 examines **hierarchical structures**, specifically the end-to-end pipeline of obtaining and aggregating pairwise comparisons and rankings.

**Contributions of PAPER 4: *Bias-Aware Ranking from Pairwise Comparisons*.** The paper introduces BARP, a probabilistic model extending the Bradley-Terry framework [59]. BARP explicitly models and estimates the specific group biases of individual human annotators, allowing for the recovery of a debiased latent ranking from prejudiced pairwise judgments.

- **Conceptual:** We frame the challenge of biased pairwise comparisons as an evaluator-specific distortion of latent item quality. We recognize that by correcting this distortion directly at the level of individual evaluators, without requiring any group to be pre-designated as protected, the method naturally prevents systemic disadvantages from propagating into the final ranking.
- **Methodological:** We develop BARP (Bias-Aware Ranking from Pairwise Comparisons), a novel probabilistic extension of the classic Bradley-Terry model. It introduces individual evaluator bias parameters that distort the perceived scores of items based on their group membership. The framework formulates an explicit log-likelihood function to jointly estimate unbiased item scores and individual evaluator biases via maximum likelihood optimization, while also accommodating multiple, non-binary, and intersectional attributes.
- **Empirical:** We validate the model on both synthetic data with ground-

truth labels and real-world datasets. Experiments demonstrate that BARP accurately quantifies hidden individual evaluator biases, achieving a highly accurate reconstruction of the true, unbiased ranking compared to standard and fairness-aware baselines. Furthermore, correcting these evaluation biases naturally resulted in more equalized group exposure in the final ranking.

**Contributions of PAPER 8: *Fairness-Aware Ranking Recovery from Pairwise Comparisons*.** The paper addresses the effects of sampling bias that determines who gets compared in rankings obtained from the pairwise comparisons.

- **Methodological:** We systematically model the end-to-end ranking pipeline, developing three distinct sampling strategies (Random, Oversampling, and Rank-Based) to simulate representation and popularity biases. We evaluate how these sampling strategies interact with standard (David’s Score, RankCentrality, GNNRank) and fairness-aware (Fairness-Aware PageRank) ranking recovery and post-processing algorithms (FA\*IR, EPIRA).
- **Empirical:** The findings emphasize that when comparisons are sparse or unevenly sampled, sophisticated graph-based recovery methods are required to prevent structural invisibility from translating into low rankings.

**Contributions of PAPER 9: *FairMC Fair-Markov Chain Rank Aggregation Methods*.** In the paper, we address the aggregation of multiple rankings into a single consensus ranking.

- **Methodological:** We develop FairMC, an in-processing rank aggregation algorithm that modifies the underlying directed graph of Markov Chain methods. It rescales edge weights so that the total transition probability to protected nodes equals that to non-protected nodes, ensuring balanced visibility directly within the aggregation mechanism.
- **Empirical:** FairMC outperforms both traditional and state-of-the-art fair aggregation methods in group exposure and top-k fairness. It successfully increased the visibility of protected groups while maintaining an acceptably low Kemeny distance, meaning the final output remained closely aligned with the original input rankings.

### 3.4 Contributions to Reliability and Safety

The final chapter connects these technical contributions to the broader requirements of deploying trustworthy AI in high-stakes environments.

**Contributions of PAPER 6: *Bounded-Abstention Pairwise Learning to Rank*.** The paper introduces BALToR, a framework that enhances safety by allowing ranking models to abstain from making a prediction when the underlying uncertainty is high.

- **Theoretical:** We provide a mathematical characterization of the optimal abstention strategy, proving that the optimal selection function relies on thresholding the conditional risk of the ranker based on a target coverage constraint.
- **Methodological:** We develop BALToR (Bounded-Abstention Learning To Rank), a model-agnostic, plug-in algorithm that equips any pre-trained ranking model with a safety deferral mechanism. It operationalizes the theoretical strategy by estimating conditional risk (via prediction confidence or margin) and selectively abstaining from uncertain pairwise comparisons without requiring model retraining.
- **Empirical:** We validate the framework across four benchmark learning-to-rank datasets and demonstrate that BALToR significantly improves ranking accuracy on the accepted pairs, strictly respects the predefined abstention budget (coverage constraint), and evenly distributes rejections across classes to ensure the abstention mechanism itself does not introduce new biases.

**Contributions of PAPER 7: *Policy advice and best practices on bias and fairness in AI*.** In the paper, we broadly synthesize the technical findings on bias and fairness in AI into best practices.

- **Methodological:** We propose a holistic Bias Management architecture that addresses vulnerabilities across the entire AI lifecycle rather than relying on isolated, post-hoc debiasing interventions. The framework integrates causal reasoning to explicitly model discriminatory mechanisms and champions knowledge-informed AI approaches, which leverage external semantic sources to compensate for the representational gaps and nuances missed by raw observational data.

- **Policy and Practical:** We detail the regulatory friction between EU data protection regimes (GDPR) and non-discrimination mandates, noting that privacy restrictions on sensitive data severely complicate demographic auditing and debiasing. We outline actionable governance practices, including formal AI auditing, documenting the human labor behind data production, implementing continuous monitoring for temporal distribution shifts and feedback loops, and treating Explainable AI with caution due to its susceptibility to instability and secondary biases.

## 4 Testing and Auditing for Fairness

*“Doubt is an uncomfortable condition, but certainty is a ridiculous one.”*

– Voltaire [73]

This chapter presents the research on methods for detecting algorithmic unfairness, focusing on the statistical and methodological challenges involved in auditing complex machine learning systems. The works presented in this chapter contribute to RQ1 by proposing rigorous frameworks for fairness auditing that move beyond deterministic thresholds toward statistically grounded testing procedures. These approaches aim to improve the reliability of fairness assessments, particularly in scenarios involving small demographic groups, opaque machine learning models, and decision-making pipelines.

In Section 4.1, we introduce Size-Adaptive Fairness Testing (SAFT), a statistical framework that replaces threshold-based fairness checks with hypothesis testing procedures that account for sampling variability and subgroup size. In Section 4.2, we address the challenge of auditing opaque ranking systems, proposing a model-agnostic approach that detects residual demographic dependence in rankings even when the internal logic of the model is inaccessible. Finally, in Section 4.3, we move beyond outcome disparities to examine the decision-making process of models, introducing methods that analyze explanation distributions in order to detect cases where models apply different reasoning across demographic groups.

Together, these contributions advance fairness auditing from simple descriptive metrics toward statistically driven diagnostic tools, enabling more reliable assessments of algorithmic systems.

### 4.1 Size-adaptive Hypothesis Testing for Fairness

In this section we introduce Size-Adaptive Fairness Testing (SAFT), a statistical framework designed to improve the reliability of fairness audits. In standard practice, fairness metrics such as statistical parity are computed as single point estimates and compared to predefined thresholds, such as the widely used “four-fifths rule.” However, this deterministic approach ignores the statistical uncertainty of these estimates and treats demographic groups of very different sizes equivalently. As a result, fairness audits may incorrectly flag discrimina-

tion in small subgroups due to random fluctuations, or fail to detect significant disparities in larger populations.

SAFT addresses this limitation by transforming fairness evaluation into a hypothesis testing problem. Instead of relying on arbitrary thresholds, the framework evaluates whether observed disparities are statistically distinguishable from zero, explicitly accounting for the variance of the estimator. The method combines two complementary strategies: an asymptotic test based on the theoretical distribution of fairness metrics, and a Bayesian inference approach that remains reliable when intersectional subgroups are very small and asymptotic assumptions do not hold.

By providing size-adaptive confidence intervals and hypothesis tests, SAFT enables fairness audits that remain robust across both large and small populations. The framework therefore improves the reliability of fairness diagnosis and contributes to reducing both false positives and false negatives in the detection of discriminatory outcomes.

#### Authors' Contributions

---


<b>Contribution</b>	<b>Authors</b>
<b>Conceptualization:</b>	A. Ferrara and all authors
<b>Writing:</b>	A. Ferrara and all authors
<b>Methodology:</b>	A. Ferrara
<b>Formal Analysis:</b>	A. Ferrara
<b>Code:</b>	A. Ferrara, F. Cozzi
<b>Experiments:</b>	F. Cozzi, A. Ferrara, A. Perotti, A. Panisson


---

---

## Size-adaptive Hypothesis Testing for Fairness


---

**Antonio Ferrara**   
 CENTAI, Turin, Italy  
 Graz University of Technology, Austria  
 antonio.ferrara@centai.eu

**Francesco Cozzi**   
 Sapienza University, Rome, Italy  
 CENTAI, Turin, Italy  
 f.cozzi@uniroma1.it

**Alan Perotti**   
 CENTAI, Turin, Italy  
 alan.perotti@centai.eu

**André Panisson**   
 CENTAI, Turin, Italy  
 panisson@centai.eu

**Francesco Bonchi**   
 CENTAI, Turin, Italy  
 EURECAT, Barcelona, Spain  
 bonchi@centai.eu

### Abstract

Determining whether an algorithmic decision-making system discriminates against a specific demographic typically involves comparing a single point estimate of a fairness metric against a predefined threshold. This practice is statistically brittle: it ignores sampling error and treats small demographic subgroups the same as large ones. The problem intensifies in intersectional analyses, where multiple sensitive attributes are considered jointly, giving rise to a larger number of smaller groups. As these groups become more granular, the data representing them becomes too sparse for reliable estimation, and fairness metrics yield excessively wide confidence intervals, precluding meaningful conclusions about potential unfair treatments.

In this paper, we introduce a unified, size-adaptive, hypothesis-testing framework that turns fairness assessment into an evidence-based statistical decision. Our contribution is twofold. (i) For sufficiently large subgroups, we prove a Central-Limit result for the statistical parity difference, leading to analytic confidence intervals and a Wald test whose type-I (false positive) error is guaranteed at level  $\alpha$ . (ii) For the long tail of small intersectional groups, we derive a fully Bayesian Dirichlet–multinomial estimator; Monte-Carlo credible intervals are calibrated for any sample size and naturally converge to Wald intervals as more data becomes available. We validate our approach empirically on benchmark datasets, demonstrating how our tests provide interpretable, statistically rigorous decisions under varying degrees of data availability and intersectionality.

### 1 Introduction

As machine learning (ML) systems play an increasingly central role in decision-making in consequential domains – ranging from education and hiring to healthcare and criminal justice – concerns over algorithmic fairness have gained prominence, prompting the development of various fairness metrics [19, 29, 12, 41] and intervention strategies [46, 24]. Early proposals framed the problem as ensuring *statistical parity* across protected demographic groups defined by a single sensitive attribute such as race or gender. Demographic Parity [19], Equalized Odds and Equal Opportunity [29], Predictive Parity [12], and related criteria remain cornerstones of the field and are implemented in popular toolkits (e.g., FAIRLEARN [44]). These metrics are ordinarily reported pointwise, and the decision to classify an observed metric’s value as a potential issue is addressed by defining a threshold: everything below this threshold is ignored, while everything above this threshold is treated as an issue [4]. Such a threshold-based approach ignores the statistical uncertainty inherent in estimating population parameters from finite samples, treating small and large populations equivalently [36].

39th Conference on Neural Information Processing Systems (NeurIPS 2025).

Minor disparities in large groups might unjustly be overlooked, while larger disparities in smaller groups may not provide sufficient statistical evidence for meaningful conclusions [23, 33].

The issue of uncertainty of fairness measures is further exacerbated by *intersectionality* – an essential concept indicating the unique disadvantages faced by individuals belonging to multiple protected groups [14]. In intersectional settings, numerous subgroups emerge as multiple sensitive attributes are considered jointly. As these groups become more granular, the data representing them becomes too sparse for reliable estimation, and fairness metrics yield excessively wide confidence intervals, precluding meaningful conclusions about potential unfairness [45, 23]. This phenomenon produces a sort of “*resolution limit*” of *intersectionality*: as we show in our empirical assessment (Section 4) using the standard datasets commonly employed in fairness research, even the intersection of just two sensitive attributes can create conditions where existing methodologies appear to detect unfair treatment, when the uncertainty on the adopted metric is actually so large to make any unfairness claim statistically not significant.

This observation prompts a critical research question: *At what granularity should fairness be rigorously guaranteed, and how can we decide this in a principled, data-driven manner?* Specifically, there is a need for principled methodologies that identify a meaningful balance between the comprehensiveness of intersectionality and the statistical robustness of fairness assessments [30, 34].

**Our contributions.** In this work, we provide a principled methodology to measure fairness while accounting for uncertainty and group size. Specifically, we propose a theoretically grounded fairness measure based on hypothesis testing, and we introduce two tests to detect fairness violations. The first test relies on the asymptotic theoretical behavior of statistical parity. In particular, we demonstrate the asymptotic normality of statistical parity, which allows the construction of confidence intervals and tests for fairness violations. Secondly, we propose a test based on Bayesian inference, which is particularly useful when intersectional groups are very small and asymptotic assumptions do not hold. We further provide empirical evidence showing that the Bayesian estimator converges to the theoretical asymptotic behavior. Additionally, we highlight the pitfalls of current fairness measures, especially in the context of intersectional groups. We show that existing metrics can incorrectly detect unfairness in cases where no unfairness exists, and conversely, fail to detect statistically significant discriminatory behavior when it is present.

**How our work advances beyond prior research.** Kearns et al. [33] account for the size of intersectional groups by scaling fairness metrics – such as statistical parity – by multiplying the metrics by the probability of belonging to a subgroup. However, to determine whether a group is treated unfairly, one still needs to rely on a predefined threshold. Kim et al. [34] use Bayesian models to augment labeled data with unlabeled data, producing more accurate and lower-variance estimates. Unlike our work, they focus on unlabeled data and do not provide asymptotic results or hypothesis tests. Foulds et al. [22, 23] employ a Dirichlet-Multinomial model distribution; however, unlike us, they still rely on thresholds to detect which group is treated unfairly and do not provide hypothesis tests for fairness violation. Besse et al. [6, 7] compute the asymptotic distributions of the ratios of certain fairness metrics. We generalize their results to a broader class of fairness metrics and, in contrast to their approach, we also address and connect our findings to the case of small intersectional groups where the large-sample assumption does not hold.

A more exhaustive coverage of related literature is presented in Appendix A.

## 2 Problem Definition

Our objective is to move beyond the arbitrary nature of hand-picked thresholds by introducing a rigorous, uncertainty-aware test for detecting group-level discrimination. To set the stage, we first formalize our notation, then assess existing threshold-based criteria, and finally, we present and motivate our alternative approach rooted in significance testing.

**Notation and preliminary definitions.** Let  $\mathcal{X}$  denote the input space and  $\mathcal{Y} = \{0, 1\}$  the binary label space. For each individual  $x \in \mathcal{X}$ , let  $y \in \mathcal{Y}$  represent the *ground truth label*, and let  $f(x) \in \mathcal{Y}$  denote the predicted label given by a deterministic classifier  $f : \mathcal{X} \rightarrow \mathcal{Y}$ . A prediction  $f(x) = 1$  corresponds to a favorable decision. Protected attributes are encoded by a space of  $p$  discrete values  $\mathbb{S} = \mathbb{S}_1 \times \dots \times \mathbb{S}_p$ . Each  $S \in \mathbb{S}$  represents the description of an *intersectional subgroup* and  $S(\mathcal{X})$  the population of the subgroup. We also denote  $\bar{S}$  for the complement of  $S$  in  $\mathbb{S}$ .

## 4.1 Size-adaptive Hypothesis Testing for Fairness

**Definition 1** (Statistical parity, or SP). For any subgroup  $S$  and classifier  $f$  we measure disparate positive-decision rates via

$$\text{SP}(S) := \mathbb{P}(f(x) = 1 \mid x \in S(\mathcal{X})) - \mathbb{P}(f(x) = 1 \mid x \in \bar{S}(\mathcal{X})) . \quad (1)$$

Perfect statistical parity corresponds to  $\text{SP}(S) = 0$ .

We note that we use  $\bar{S}$  as the reference group, following common practice. Alternatively, one could use the entire population as the reference group; however, the differences are typically minimal, especially when  $S$  represents a small intersectional group.

**Definition 2** ( $\delta$ -Statistical parity, or  $\delta\text{SP}$ ). A predictor  $f$  satisfies statistical parity at level  $\delta$  when

$$\forall S \in \mathcal{S} : |\text{SP}(S)| \leq \delta . \quad (2)$$

A threshold  $\theta$  is typically chosen (such as the Equal Employment Opportunity Commission “four-fifths rule” [28], where  $\theta = 0.2$ ), and unfairness is identified when  $|\text{SP}(S)| > \theta$ . However, this approach does not account for sample variability, treating a subgroup of size 10 the same as one with 10,000.

To partially compensate for heterogeneous support, Kearns et al. [33] propose

**Definition 3** ( $\gamma$ -Statistical parity, or  $\gamma\text{SP}$ ). A predictor  $f$  is  $\gamma$ -Statistical Parity subgroup fair if:

$$\forall S \in \mathcal{S} : |\text{SP}(S)| \cdot \mathbb{P}(x \in S(\mathcal{X})) \leq \gamma . \quad (3)$$

However, in practice, to identify unfairly treated groups we have to choose a threshold  $\theta$  and claim fairness violation when  $|\text{SP}(S)| \cdot \mathbb{P}(x \in S(\mathcal{X})) > \theta$ . Moreover, as Gohar and Cheng [27] observe: “The second term reweights the difference by the proportion of the size of each subgroup in relation to the population. Consequently, the unfairness of smaller-sized groups is down-weighted in the final  $\gamma$ -Statistical Parity estimation. Thus, it may not adequately protect small subgroups, even if they have high levels of unfairness.”

**From thresholds to significance.** Both (2) and (3) require the practitioner to fix a global threshold  $\theta$  without guidance on how to adapt it to subgroup size or estimation variance. Motivated by the shortcomings above and by recent calls for uncertainty-aware auditing [18, 42, 39], we recast fairness checking as a statistical hypothesis test and propose the following definition:

**Definition 4** (Statistical Parity violation (this work)). Given a significance level  $\alpha \in [0, 1]$  and a test statistic  $T$  with null hypothesis  $H_0 : \text{SP}(S) = 0$ , we say a classifier  $f$  violates statistical parity for subgroup  $S$  if the null hypothesis  $H_0$  is rejected at level  $\alpha$ .

Hence fairness is assessed by whether the observed disparity could plausibly arise from sampling noise. Crucially, the decision threshold is no longer arbitrary: it is determined by the chosen test and  $\alpha$ , automatically adjusting to the subgroup’s sample size.

### 3 A Statistical Testing Framework for Size-Adaptive Fairness Assessment

In this section we operationalise our guiding idea: *replacing ad-hoc thresholds with statistically principled tests for group-level discrimination that remain valid even when intersectional subgroups are small.*

We do so by proposing two tests to detect statistical parity violations: (i) a large-sample **Wald test** that leverages an analytic asymptotic variance, and (ii) a **Bayesian small-sample test** that yields finite-sample credible intervals via Monte-Carlo draws from a Dirichlet–multinomial posterior. Both deliver a  $p$ -value (or posterior tail-probability) that can be compared with a user-selected significance level  $\alpha$ , automatically adapting to subgroup size and sampling noise.

This unified framework yields *size-adaptive, uncertainty-aware* fairness conclusions, removing the need for arbitrary global thresholds while retaining statistical guarantees for both common and rare intersectional groups.

## 4.1 Size-adaptive Hypothesis Testing for Fairness

### 3.1 Large-sample test: asymptotic normality of $\text{SP}_n(S)$

For an intersectional group  $s$  let us define the following probabilities:

$$p_{0,S} = \mathbb{P}(f(x) = 0, x \in S(\mathcal{X})), \quad p_{1,S} = \mathbb{P}(f(x) = 1, x \in S(\mathcal{X})), \\ p_{0,\bar{S}} = \mathbb{P}(f(x) = 0, x \in \bar{S}(\mathcal{X})), \quad p_{1,\bar{S}} = \mathbb{P}(f(x) = 1, x \in \bar{S}(\mathcal{X})),$$

Furthermore, let us define the marginal  $p_S = \mathbb{P}(x \in S(\mathcal{X}))$  and  $p_{\bar{S}} = \mathbb{P}(x \in \bar{S}(\mathcal{X}))$ .

For an i.i.d. test sample  $(x_i)_{i=1}^n$  we consider the following *plug-in estimator* of statistical parity:

$$\text{SP}_n(S) := \frac{\sum_{i=1}^n \mathbb{1}_{f(x_i)=1, x_i \in S(\mathcal{X})}}{\sum_{i=1}^n \mathbb{1}_{x_i \in S(\mathcal{X})}} - \frac{\sum_{i=1}^n \mathbb{1}_{f(x_i)=1, x_i \in \bar{S}(\mathcal{X})}}{\sum_{i=1}^n \mathbb{1}_{x_i \in \bar{S}(\mathcal{X})}},$$

where  $\mathbb{1}$  denotes the indicator function. Furthermore, let  $V = \left( \frac{p_{0,S}}{(p_S)^2}, \frac{-p_{1,S}}{(p_S)^2}, \frac{-p_{0,\bar{S}}}{(p_{\bar{S}})^2}, \frac{p_{1,\bar{S}}}{(p_{\bar{S}})^2} \right)$  and

$$\Sigma_4 = \begin{pmatrix} p_{1,S}(1-p_{1,S}) & -p_{1,S}p_{0,S} & -p_{1,S}p_{1,\bar{S}} & -p_{1,S}p_{0,\bar{S}} \\ -p_{0,S}p_{1,S} & p_{0,S}(1-p_{0,S}) & -p_{0,S}p_{1,\bar{S}} & -p_{0,S}p_{0,\bar{S}} \\ -p_{1,\bar{S}}p_{1,S} & -p_{1,\bar{S}}p_{0,S} & p_{1,\bar{S}}(1-p_{1,\bar{S}}) & -p_{1,\bar{S}}p_{0,\bar{S}} \\ -p_{0,\bar{S}}p_{1,S} & -p_{0,\bar{S}}p_{0,S} & -p_{0,\bar{S}}p_{1,\bar{S}} & p_{0,\bar{S}}(1-p_{0,\bar{S}}) \end{pmatrix}. \quad (4)$$

The following result (proof in Appendix B) provides the asymptotic distribution of the statistical parity.

**Theorem 1** (Central Limit Theorem for Statistical Parity). *Let  $\sigma(S) = \sqrt{V^\top \Sigma_4 V}$ , where  $V$  and  $\Sigma_4$  are defined above. Then*

$$\frac{\sqrt{n}}{\sigma(S)} (\text{SP}_n(S) - \text{SP}(S)) \xrightarrow{d} N(0, 1), \quad \text{as } n \rightarrow \infty,$$

where  $\xrightarrow{d}$  denotes convergence in distribution and  $N(0, 1)$  indicates the standard normal distribution.

From Theorem 1 we obtain the  $(1 - \alpha)$  two-sided Wald confidence interval:

$$\left[ \text{SP}_n(S) \pm \frac{\sigma(S)}{\sqrt{n}} \Phi^{-1}\left(1 - \frac{\alpha}{2}\right) \right],$$

and the corresponding  $p$ -value  $p = 2(1 - \Phi(|\sqrt{n} \cdot \text{SP}_n(S) - \text{SP}(S)| / \sigma(S)))$ , where  $\Phi(\cdot)$  is the cumulative distribution function of the standard normal distribution and  $\Phi^{-1}(\cdot)$  the quantile. We reject the null “no disparity” whenever  $p < \alpha$ . Because  $\sigma(S)$  depends on *population* probabilities, we estimate it by plugging empirical counts into Equation (4).

### 3.2 Bayesian inference for small samples

Theorem 1 describes how confidence intervals for  $\text{SP}(S)$  can be computed with large samples. In the particular case of small intersectional groups this assumption is, in general, not met and the theoretical asymptotic estimations of  $\text{SP}(S)$  and  $\Sigma_4$  might not be reliable. We thus move our attention to deriving credible intervals via Bayesian inference.

**Prior, likelihood and posterior.** We consider the probability space over  $p_{0,S}, p_{1,S}, p_{0,\bar{S}}$ , and  $p_{1,\bar{S}}$ . Since the  $p_{i,j}$ ,  $i \in \{0, 1\}, j \in \{S, \bar{S}\}$  are mutually exclusive, we can assume that observations are drawn from a categorical distribution. Hence, given  $n$  trials, let  $n_{i,j}$ ,  $i \in \{0, 1\}, j \in \{S, \bar{S}\}$  denote the counts for each outcome, with  $\sum_{i,j} n_{i,j} = n$ .  $n_{i,j}$  follows a multinomial distribution:  $(n_{0,S}, n_{0,\bar{S}}, n_{1,S}, n_{1,\bar{S}}) \sim \text{Multinomial}(n, p_{0,S}, p_{0,\bar{S}}, p_{1,S}, p_{1,\bar{S}})$ . One can consider a Dirichlet prior over  $p_{i,j}$ :  $(p_{0,S}, p_{0,\bar{S}}, p_{1,S}, p_{1,\bar{S}}) \sim \text{Dirichlet}(n, \alpha_{0,S}, \alpha_{0,\bar{S}}, \alpha_{1,S}, \alpha_{1,\bar{S}})$ . By conjugacy, the posterior distribution remains Dirichlet with updated parameters:

$$(p_{0,S}, p_{0,\bar{S}}, p_{1,S}, p_{1,\bar{S}}) \mid \text{data} \sim \text{Dirichlet}(n, \alpha_{0,S} + n_{0,S}, \alpha_{0,\bar{S}} + n_{0,\bar{S}}, \alpha_{1,S} + n_{1,S}, \alpha_{1,\bar{S}} + n_{1,\bar{S}}) \quad (5)$$

## 4.1 Size-adaptive Hypothesis Testing for Fairness

**Posterior draws and credible interval.** We are now interested in the posterior estimate of  $\text{SP}(S)$ . Since there is not known closed-form expression for the posterior distribution of  $\text{SP}(S)$ , we can approximate it using Monte Carlo sampling.

The procedure is as follows. Sample  $K$  times from the posterior, let the  $k$ -th sample be:  $(p_{0,S}^{(k)}, p_{0,\bar{S}}^{(k)}, p_{1,S}^{(k)}, p_{1,\bar{S}}^{(k)})$ , for  $k = 1, \dots, K$ , and let the  $k$ -th estimate of  $\text{SP}(S)$  be:

$$\text{SP}^{(k)}(S) := \frac{p_{1,S}^{(k)}}{p_{0,S}^{(k)} + p_{1,S}^{(k)}} - \frac{p_{1,\bar{S}}^{(k)}}{p_{0,\bar{S}}^{(k)} + p_{1,\bar{S}}^{(k)}}.$$

Then:

- An unbiased estimate of the posterior mean of  $\text{SP}(S)$  is given by:

$$\mathbb{E}[\text{SP}(S) \mid \text{data}] = \frac{1}{K} \sum_{k=1}^K \text{SP}^{(k)}(S)$$

- The  $(1 - \alpha)$  credible interval is given by:

$$\text{CI}_{1-\alpha}(S) = \left[ \hat{Q}_{\frac{\alpha}{2}}(\{\text{SP}^{(k)}(S)\}_{k=1}^K), \hat{Q}_{1-\frac{\alpha}{2}}(\{\text{SP}^{(k)}(S)\}_{k=1}^K) \right],$$

where the empirical-quantile at level  $u$  is defined by:

$$\hat{Q}_u(\{\text{SP}^{(k)}(S)\}_{k=1}^K) = \inf \left\{ t : \frac{1}{K} \sum_{k=1}^K \mathbb{1}\{\text{SP}^{(k)}(S) \leq t\} \geq u \right\}.$$

The interval reflects posterior uncertainty over the statistical parity difference given the observed data and prior. We can, hence, perform a two-sided hypothesis test for the null  $H_0 : \text{SP}(S) = 0$  from the credible interval. Specifically, we reject the null hypothesis at level  $\alpha$  if the value 0 is not contained in the  $(1 - \alpha)$  credible interval.

**Choice of prior.** We adopt a weakly informative symmetric (flat) Dirichlet prior, i.e. with concentration parameters  $(1, 1, 1, 1)$ , by default; domain knowledge (e.g. historical results), when available, can be injected via the prior parameters. We explore the possibility of incorporating additional information into the prior in Appendix C.7.

**Statistical Fairness Testing Framework.** Algorithm 1 summarizes our rigorous statistical framework for fairness assessment, which is specifically designed to handle varying subgroup sizes in intersectional settings. It integrates large-sample hypothesis testing with Bayesian inference, ensuring that fairness evaluations remain reliable even when data availability differs across subgroups. It dynamically adjusts significance thresholds, thus accounting for statistical uncertainty and preventing misleading conclusions about bias.

### 3.3 Resolution limits for statistical parity fairness violation

Auditing rare intersectional subgroups naturally raises the question: how small is too small? Even with uncertainty-aware tests, a subgroup composed of only a few samples may fail to provide statistically conclusive evidence of bias, regardless of how pronounced the observed disparity might be. Our framework addresses this challenge by computing, for each overall negative prediction probability  $\mathbb{P}(f(x) = 0)$  and protected group size  $n_S = n_{0,S} + n_{1,S}$ , the minimum fraction of negative outcomes in  $S$  required to reject the null hypothesis  $H_0 : \text{SP}(S) = 0$  at a specified significance level  $\alpha$ .

Figure 1 visualizes this boundary when evaluating the hypothesis that a group is being *disadvantaged* (the dual figure showing the boundary for deciding if a group is being *advantaged*, is reported in Figure 5 of the Appendix). The plot has on the  $y$ -axis the fraction  $p_{0,S}$  of 0s predicted in the given group, while on the  $x$ -axis the size  $n_S$  of the group. The plot reports 9 different lines corresponding to the fraction of 0s predicted in the overall population. The figure uses  $\alpha = 0.05$ .

## 4.1 Size-adaptive Hypothesis Testing for Fairness

---

### Algorithm 1 Size-Adaptive Fairness Testing (SAFT)

---

- 1: **Input:** Subgroup  $S$ , significance level  $\alpha$ , minimum support  $\tilde{n}$  (we use  $\tilde{n}=30$ )
  - 2: **Output:** Fairness decision (Reject  $H_0$  or Fail to Reject  $H_0$ )
  - 3: Compute  $n_{i,j}$ ,  $i \in \{0, 1\}, j \in \{S, \bar{S}\}$
  - 4: **if**  $\min\{n_{0,S}, n_{1,S}, n_{0,\bar{S}}, n_{1,\bar{S}}\} \geq \tilde{n}$  **then**
  - 5:     apply the Wald test of §3.1 {large-sample regime}
  - 6: **else**
  - 7:     use the Bayesian test of §3.2 {small-sample regime}
  - 8: **end if**
  - 9: Compute statistical parity measure  $SP(S)$
  - 10: Report point estimate  $SP_n(S)$  or posterior mean
  - 11: Report  $(1 - \alpha)$  confidence/credible interval
  - 12: Report  $p$ -value or posterior tail probability
  - 13: **if**  $p < \alpha$  **then**
  - 14:     Reject  $H_0$  {Fairness violation detected}
  - 15: **else**
  - 16:     Fail to reject  $H_0$  {No statistically significant violation}
  - 17: **end if**
- 

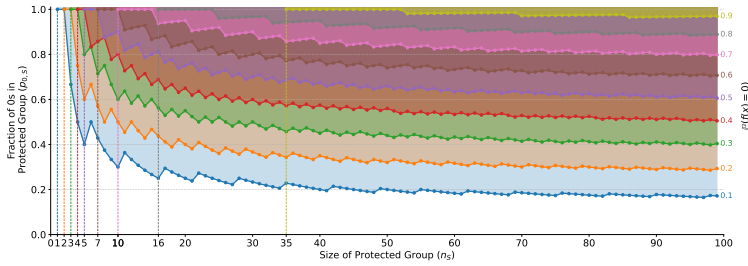


Figure 1: Resolution limits for Statistical Parity violations under varying global negative rates  $\mathbb{P}(f(x) = 0)$ , when detecting *disadvantaged* groups (the dual figure showing the boundary for deciding if a group is being *advantaged*, is reported in Figure 5 of the Appendix). Each curve traces the minimal fraction of negative outcomes needed to reject  $H_0$ :  $SP(S) = 0$  at  $\alpha = 0.05$  as a function of the group size  $n_s$ . To the left of each vertical bar is the “no-power” zone, where subgroups are too small to detect discrimination, regardless of the observed disparity. The shaded region above each curve is the “discrimination zone”, where the subgroup’s negative rate is enough to establish a statistically significant parity violation.

A pair  $(n_s, p_{0,S})$  needs to be *above the line* to indicate significant disparity. For instance, the point  $(10, 0.6)$  on the green line ( $\mathbb{P}(f(x) = 0) = 0.3$ ) indicates that, when in the overall population there are 30% of 0s predicted, a demographic subgroup of size 10 needs to have at least 6 individuals predicted 0, in order to have a negative discrimination case. When in the overall population there are 40% of 0s predicted (red line), a group of size 10 requires 8 negative cases to have unfairness. When instead the prediction in the overall population is balanced (purple line,  $\mathbb{P}(f(x) = 0) = 0.5$ ) a subgroup of size 10 requires at least 9 negative cases to have a legitimate discrimination complaint.

We can observe that, as the global negative rate  $\mathbb{P}(f(x) = 0)$  increases, the required subgroup size  $n_s$  grows steeply to evaluate *disadvantaged* groups. For example, when 90% of the population is predicted negative, a group needs to be composed of at least 35 individuals, all predicted negative, to have any statistically valid unfairness, highlighting the difficulty of auditing under severe class imbalance.

By charting these boundaries, our framework highlights the resolution limits of intersectionality, while providing practitioners a tool to determine exactly how much data each intersectional slice needs to be audit-worthy, preventing spurious signalling of fairness violations on small subgroups.

### 3.4 Generalisation to other fairness measures

Analogous results can be derived for other fairness metrics. Indeed, it holds the general form of the theorem (we defer the proof to Appendix B):

**Theorem 2.** Let  $\mathbf{p} = (p_1, \dots, p_q)$  a set of probabilities of  $q$  disjoint events, with  $\sum_i^q p_i = 1$ ; let  $C = (C_1, \dots, C_q) \sim \text{Categorical}(\mathbf{p})$  be the related categorical distribution, and let  $C^1, \dots, C^n$  be  $n$  i.i.d. realizations of  $C$ . Let  $\phi$  be a continuously differentiable (in a neighborhood of  $\mathbb{E}C$ ) function  $\phi: \mathbb{R}^q \rightarrow \mathbb{R}$ . Then

$$\frac{\sqrt{n}}{\sigma} \left( \phi\left(\frac{1}{n} \sum_{i=1}^n C^i\right) - \phi(\mathbb{E}C) \right) \xrightarrow{d} N(0, 1), \quad \text{as } n \rightarrow \infty,$$

where  $\sigma = \sqrt{V^\top \Sigma V}$ ,  $V = \nabla(\phi(\mathbb{E}C))$  is the gradient of  $\phi$ , and  $\Sigma = [\text{diag}(\mathbf{p}) - \mathbf{p}\mathbf{p}^\top]$  is the covariance matrix of  $C$ , where  $\text{diag}(\mathbf{p})$  indicates a diagonal matrix with entries  $p_i$ .

For example, considering **Equal Opportunity**:

$$\text{EO}(S) := \mathbb{P}(f(x) = 1 \mid y = 1, x \in S(\mathcal{X})) - \mathbb{P}(f(x) = 1 \mid y = 1, x \in \mathcal{X}),$$

Theorem 2 can be applied by choosing  $p_1 = \mathbb{P}(f(x) = 0, x \in S(\mathcal{X}) \mid y = 1)$ ,  $p_2 = \mathbb{P}(f(x) = 1, x \in S(\mathcal{X}) \mid y = 1)$ ,  $p_3 = \mathbb{P}(f(x) = 0, x \in \bar{S}(\mathcal{X}) \mid y = 1)$ ,  $p_4 = \mathbb{P}(f(x) = 1, x \in \bar{S}(\mathcal{X}) \mid y = 1)$ , and  $\phi(x_1, x_2, x_3, x_4) = \frac{x_2}{x_1+x_2} - \frac{x_4}{x_3+x_4}$ .

From Theorem 2, one can also obtain equivalent results to [6, 7] (but with a simpler computation of the covariance matrix). Indeed, for example, the asymptotic behaviour of the **Disparate Impact** assessment:

$$\text{DI}(S) := \frac{\mathbb{P}(f(x) = 1 \mid x \in S(\mathcal{X}))}{\mathbb{P}(f(x) = 1 \mid x \in \bar{S}(\mathcal{X}))},$$

can be obtained by choosing  $p_1 = \mathbb{P}(f(x) = 0, x \in S(\mathcal{X}))$ ,  $p_2 = \mathbb{P}(f(x) = 1, x \in S(\mathcal{X}))$ ,  $p_3 = \mathbb{P}(f(x) = 0, x \in \bar{S}(\mathcal{X}))$ ,  $p_4 = \mathbb{P}(f(x) = 1, x \in \bar{S}(\mathcal{X}))$ , and  $\phi(x_1, x_2, x_3, x_4) = \frac{x_2}{x_1+x_2} \cdot \frac{x_3+x_4}{x_4}$ .

The results for the Bayesian test can be extended under analogous conditions. Indeed, one can consider a general probability space over  $\mathbf{p} = (p_1, \dots, p_q)$  of  $q$  disjoint events. Consider  $n$  trials and indicate with  $(n_1, \dots, n_q)$  the counts for each outcome. The likelihood is again Multinomial( $n, \mathbf{p}$ ), and with a Dirichlet prior over  $\mathbf{p}$  with concentration parameters  $(\alpha_1, \dots, \alpha_q)$ , by conjugacy we obtain a posterior distribution distributed as a Dirichlet( $n, \alpha_1 + n_1, \dots, \alpha_q + n_q$ ). One can then consider a fairness metric  $\phi: \mathbb{R}^q \rightarrow \mathbb{R}$  and via Monte Carlo sampling can construct a  $(1 - \alpha)$  credible interval and hypothesis test for  $\phi$ , analogously to the procedure used for SP( $S$ ).

In general, our framework can model all those fairness metrics based on the confusion matrix and related conditional probabilities.

## 4 Experiments

In this section, we empirically validate our size-adaptive testing framework on two canonical fairness benchmarks under increasingly fine-grained intersectional slices.

### 4.1 Datasets and Models

We selected two standard datasets<sup>1</sup> used in fairness benchmarks: the Adult Income dataset [5] and the COMPAS recidivism dataset [2]. We include additional experiments on two other datasets in the Appendix. We apply standard data preprocessing and train an XGBoost classifier  $g: \mathcal{X} \rightarrow \mathcal{Y}$  (training details are in Appendix C.2). To examine intersectional effects, we first audit non-intersectional subgroups (*race*, *age* and *sex*) and then all two-way and three-way intersections of these protected attributes.

<sup>1</sup>COMPAS from propublica (compas-scores-two-years.csv); Adult from fairlearn.org, originally from UCI.

## 4.1 Size-adaptive Hypothesis Testing for Fairness

**COMPAS** The COMPAS dataset is widely used in the study of algorithmic fairness and risk assessment in the criminal justice system. It is often cited in fairness literature due to observed disparities in prediction outcomes across racial groups, most notably between Black and White defendants [2]. It includes information about criminal defendants, such as the number of prior convictions and charge degree. The protected variables are *race* ("African-American", "Asian", "Caucasian", "Hispanic", "Native American", "Other"), *age* ("Under 25", "25-45", "Over 45"), and *sex* ("Female", "Male"). The binary target variable indicates whether a defendant is predicted to reoffend within two years ( $y = 0$ ) or not ( $y = 1$ ).

**Adult** The Adult Income dataset is based on census data, which includes 14 categorical and numerical features (e.g. education, marital status, occupation, etc.). The protected variables are *race* ("Amer-Indian-Eskimo", "Asian-Pacific-Islander", "Black", "Other", "White"), *age* ("Under 18", "18-40", "40-65", "Over 65"), and *sex* ("Female", "Male"). The binary target is whether the individual annual income exceeds 50k per year ( $y = 1$ ) or not ( $y = 0$ ).

**Reproducibility** All experiments were run on a server equipped with an Intel Xeon Gold 6312U CPU and 256 GB of RAM. Our full codebase—including data preprocessing, model training, and auditing notebooks—can be found at <https://github.com/alanturin-g/SAFT>.

### 4.2 Comparison with point-wise estimations

We consider both COMPAS and Adult datasets over 20 random 2:1 train-test splits, followed by model training and fairness auditing each subgroup on every split. In each case, we compare our approach against the fixed-threshold  $\delta$ SP criterion ( $\theta = \pm 1$ , as, e.g., in [1]), to highlight how a threshold-based audit, while common, fails to account for sampling variability.

Figure 2 illustrates a selection of intersectional subgroups (one per panel) from the COMPAS dataset. In each panel, we specify the minimum ( $n_{min}$ ) and maximum ( $n_{max}$ ) size of the protected group across different train-test splits. The gray band marks the no-detection region under a fixed-threshold approach. For each train-test split we compute the point-wise SP estimation, the Bayesian (blue) and the asymptotic (red) credible/confidence intervals. In panel (a) we observe a scenario where  $\delta$ SP would detect a violation, since all point estimates are outside the gray band, and our approach agrees, since we can reject  $H_0$ . In panel (b), with a smaller intersectional group,  $\delta$ SP would detect fairness violations, but our approach shows that, due to the wide confidence interval, we cannot reject  $H_0$  and detect a violation. It is worth observing that in this scenario, due to the small size of the protected group, the asymptotic behaviour would not be reliable; our approach SAFT would indeed rely on the Bayesian inference instead. In panel (c), we show how, for small groups, the train-test split can have a strong impact:  $\delta$ SP would detect fairness violations in roughly half the cases, while our answer is consistent across all splits. A similar pattern, but with a fairness violation consistently detected on our side, is shown in panel (d) for a bigger group.

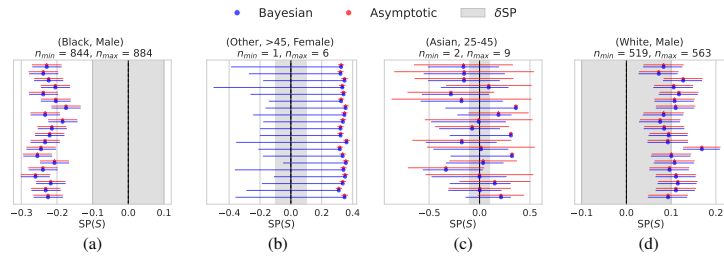


Figure 2: Point-wise estimation versus confidence intervals, COMPAS dataset.

Figure 3 shows analogous results for the Adult dataset. In panel (a) we show a cross-split, cross-approach agreement on a fairness violation detection. In panel (b) we have a disagreement, as  $\delta$ SP would detect fairness violations, but our approach cannot reject  $H_0$ . In panel (c) we have the opposite disagreement:  $\delta$ SP would not detect fairness violations, but we show that with such big group  $H_0$  can

## 4.1 Size-adaptive Hypothesis Testing for Fairness

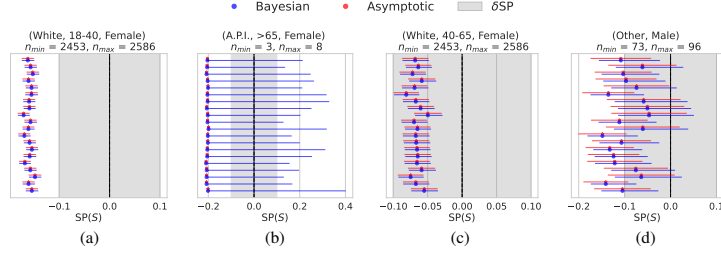


Figure 3: Point-wise estimation versus confidence intervals, Adult dataset.

be rejected, and a fairness violation warning raised. In panel (c) we show a scenario where the train-test split impacts both  $\delta$ SP and our approach. In general, these results show how a fixed-threshold approach cannot accommodate groups of different size even within the same dataset-model scenario, and can be sensitive to different train-test split. Conversely, our approach takes into account the group size and is generally more robust regarding train-test splits.

### 4.3 Comparison with $\gamma$ SP

We again consider all intersectional groups (across all 20 train-test splits) on COMPAS and Adult to compare the decision from our framework with those from a threshold-based  $\gamma$ SP approach. We plot the size of the protected group against its  $\gamma$ SP score computed according to Equation 3. We also compute the fairness violation with our statistical testing approach SAFT (Algorithm 1), and use the results as color-code in the scatterplots: red for fairness violation detection, blue for no violation. Figure 4 (COMPAS on the left, Adult on the right) shows that no single threshold (horizontal line) on  $\gamma$ SP can cleanly separate true violations from non-violations. These plots further support the need for a size-adaptive hypothesis-testing approach.

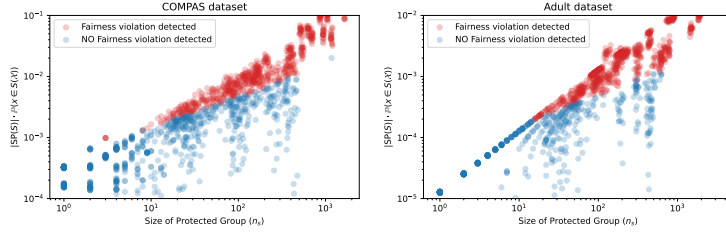


Figure 4: Protected groups size,  $\gamma$ SP scores, and interval-based fairness violations.

## 5 Conclusions

In this work, we have shown how fairness auditing can move beyond brittle point estimates and arbitrary thresholds. By providing an analytic Central-Limit result for the statistical parity difference and coupling it with a Bayesian Dirichlet-multinomial estimator, our framework conveys size-adaptive confidence and credible intervals that remain valid from the most common to the rarest intersectional subgroups.

**Limitations.** Our Bayesian framework inherently requires the specification of a prior distribution, which encodes assumptions about the parameters before observing the data. Even when employing weakly informative (flat) priors, one is still making a modelling choice. However, this is standard within the Bayesian framework and should be understood as a natural consequence of its formulation.

## 4.1 Size-adaptive Hypothesis Testing for Fairness

---

Moreover, while we discuss the generalization to other fairness measures, our focus is on statistical parity (and on equal opportunity in Appendix C.9) and leaves open empirical validation for additional group fairness definitions.

**Future work.** Looking ahead, we intend to extend our methodology to consider tests for individual fairness [17, 25, 21] and counterfactual fairness [35], which evaluate whether the model behaves fairly for individuals and under hypothetical changes to sensitive attributes, and represent an additional classes of fairness metrics, different from the group fairness metrics considered in this work.

**Broader Impact.** Our testing framework strengthens fairness audits by providing transparent, size-adaptive confidence intervals, which can reduce both false alarms and overlooked harms, especially for under-represented intersectional groups. At the same time, because fairness admits many metrics and any auditor can choose the one most favourable to their goals, there is a risk of using selective reporting to hide genuine bias. We therefore urge practitioners to apply our methods responsibly: report all tested metrics and provide transparent interpretations of confidence intervals rather than as standalone justifications for deployment.

### Acknowledgments and Disclosure of Funding

This work is conducted as part of the Horizon Europe project PRE-ACT (Prediction of Radiotherapy side effects using explainable AI for patient communication and treatment modification). It is supported by the European Commission through the Horizon Europe Program (Grant Agreement number 101057746), by the Swiss State Secretariat for Education, Research and Innovation (SERI) under contract number 22 00058, and by the UK government (Innovate UK) under application number 10061955.

Furthermore, the authors wish to thank Filippo Ascolani for the fruitful discussions regarding the statistical framework.

### References

- [1] Avinash Agarwal, Harsh Agarwal, and Nihaarika Agarwal. Fairness score and process standardization: framework for fairness certification in artificial intelligence systems. *AI and Ethics*, 3(1):267–279, 2023.
- [2] Julia Angwin, Jeff Larson, Surya Mattu, and Lauren Kirchner. Machine bias. In *Ethics of data and analytics*, pages 254–264. Auerbach Publications, 2022.
- [3] Ainhize Barrainkua, Paula Gordaliza, Jose A Lozano, and Novi Quadrianto. Uncertainty matters: stable conclusions under unstable assessment of fairness results. In *International Conference on Artificial Intelligence and Statistics*, pages 1198–1206. PMLR, 2024.
- [4] Joachim Baumann, Anikó Hannák, and Christoph Heitz. Enforcing group fairness in algorithmic decision making: Utility maximization under sufficiency. In *Proceedings of the 2022 ACM Conference on Fairness, Accountability, and Transparency*, pages 2315–2326, 2022.
- [5] Barry Becker and Ronny Kohavi. Adult. UCI Machine Learning Repository, 1996.
- [6] Philippe Besse, Eustasio del Barrio, Paula Gordaliza, and Jean-Michel Loubes. Confidence intervals for testing disparate impact in fair learning. *arXiv preprint arXiv:1807.06362*, 2018.
- [7] Philippe Besse, Eustasio del Barrio, Paula Gordaliza, Jean-Michel Loubes, and Laurent Rissler. A survey of bias in machine learning through the prism of statistical parity. *The American Statistician*, 76(2):188–198, 2022.
- [8] Umang Bhatt, Javier Antorán, Yunfeng Zhang, Q Vera Liao, Prasanna Sattigeri, Riccardo Fogliato, Gabrielle Melançon, Ranganath Krishnan, Jason Stanley, Omesh Tickoo, et al. Uncertainty as a form of transparency: Measuring, communicating, and using uncertainty. In *Proc. of the 2021 AAAI/ACM Conference on AI, Ethics, and Society*, pages 401–413, 2021.
- [9] Joy Buolamwini and Timnit Gebru. Gender shades: Intersectional accuracy disparities in commercial gender classification. In *Conference on fairness, accountability and transparency*, pages 77–91. PMLR, 2018.

## 4.1 Size-adaptive Hypothesis Testing for Fairness

---

- [10] Tianqi Chen and Carlos Guestrin. Xgboost: A scalable tree boosting system. In *Proceedings of the 22nd ACM SIGKDD International Conference on Knowledge Discovery and Data Mining*, pages 785–794, 2016.
- [11] John J Cherian and Emmanuel J Candès. Statistical inference for fairness auditing. *Journal of Machine Learning Research*, 25(149):1–49, 2024.
- [12] Alexandra Chouldechova. Fair prediction with disparate impact: A study of bias in recidivism prediction instruments. *Big Data*, 5(2):153–163, 2017.
- [13] Paulo Cortez and Alice Maria Gonçalves Silva. Using data mining to predict secondary school student performance. In *Proceedings of the 5th Annual Future Business Technology Conference (FUBUTEC 2008)*, pages 5–12, April 2008.
- [14] Kimberle Crenshaw. Mapping the margins: Intersectionality, identity politics, and violence against women of color. *Stanford Law Review*, 43(6):1241–1299, 1991.
- [15] Kimberlé Crenshaw. Demarginalizing the intersection of race and sex: A black feminist critique of antidiscrimination doctrine, feminist theory and antiracist politics. In *Feminist legal theories*, pages 23–51. Routledge, 2013.
- [16] Eustasio Del Barrio, Paula Gordaliza, and Jean-Michel Loubes. A central limit theorem for  $l_p$  transportation cost on the real line with application to fairness assessment in machine learning. *Information and Inference: A Journal of the IMA*, 8(4):817–849, 2019.
- [17] Cynthia Dwork, Moritz Hardt, Toniann Pitassi, Omer Reingold, and Richard Zemel. Fairness through awareness. In *Proceedings of the 3rd innovations in theoretical computer science conference*, pages 214–226, 2012.
- [18] Kawin Ethayarajh. Is your classifier actually biased? measuring fairness under uncertainty with bernstein bounds. In *Proceedings of the 58th Annual Meeting of the Association for Computational Linguistics*, pages 2914–2919. Association for Computational Linguistics, July 2020.
- [19] Michael Feldman, Sorelle A Friedler, John Moeller, Carlos Scheidegger, and Suresh Venkatasubramanian. Certifying and removing disparate impact. In *Proc. of the 21th ACM SIGKDD international conference on knowledge discovery and data mining*, pages 259–268, 2015.
- [20] Antonio Ferrara, Francesco Bonchi, Francesco Fabbri, Fariba Karimi, and Claudia Wagner. Bias-aware ranking from pairwise comparisons. *Data Mining and Knowledge Discovery*, 38(4):2062–2086, 2024.
- [21] Antonio Ferrara, David García-Soriano, and Francesco Bonchi. Beyond shortest paths: Node fairness in route recommendation. *Proc. of the VLDB Endowment*, 18(9):3230–3242, 2025.
- [22] James R Foulds, Rashidul Islam, Kamrun Naher Keya, and Shimei Pan. Bayesian modeling of intersectional fairness: The variance of bias. In *Proceedings of the 2020 SIAM International Conference on Data Mining*, pages 424–432. SIAM, 2020.
- [23] James R Foulds, Rashidul Islam, Kamrun Naher Keya, and Shimei Pan. An intersectional definition of fairness. In *2020 IEEE 36th international conference on data engineering (ICDE)*, pages 1918–1921. IEEE, 2020.
- [24] Sorelle A Friedler, Carlos Scheidegger, Suresh Venkatasubramanian, Sonam Choudhary, Evan P Hamilton, and Derek Roth. A comparative study of fairness-enhancing interventions in machine learning. In *Proceedings of the conference on fairness, accountability, and transparency*, pages 329–338, 2019.
- [25] David García-Soriano and Francesco Bonchi. Maxmin-fair ranking: individual fairness under group-fairness constraints. In *Proceedings of the 27th ACM SIGKDD Conference on Knowledge Discovery & Data Mining*, pages 436–446, 2021.
- [26] Avijit Ghosh, Lea Genuit, and Mary Reagan. Characterizing intersectional group fairness with worst-case comparisons. In *Artificial Intelligence Diversity, Belonging, Equity, and Inclusion*, pages 22–34. PMLR, 2021.

## 4.1 Size-adaptive Hypothesis Testing for Fairness

---

- [27] Usman Gohar and Lu Cheng. A survey on intersectional fairness in machine learning: Notions, mitigation, and challenges. In *International Joint Conference on Artificial Intelligence*, 2023.
- [28] Irwin Greenberg. An analysis of the eoccc “four-fifths” rule. *Management Science*, 25(8):762–769, 1979.
- [29] Moritz Hardt, Eric Price, and Nati Srebro. Equality of opportunity in supervised learning. *Advances in neural information processing systems*, 29, 2016.
- [30] Ursula Hébert-Johnson, Michael Kim, Omer Reingold, and Guy Rothblum. Multicalibration: Calibration for the (computationally-identifiable) masses. In *International Conference on Machine Learning*, pages 1939–1948. PMLR, 2018.
- [31] Johannes Himmelreich, Arbie Hsu, Ellen Veomett, and Kristian Lum. The intersectionality problem for algorithmic fairness. In *Proceedings of the Algorithmic Fairness Through the Lens of Metrics and Evaluation*, volume 279, pages 68–95. PMLR, 14 Dec 2025.
- [32] Hans Hofmann. Statlog (German Credit Data). UCI Machine Learning Repository, 1994.
- [33] Michael Kearns, Seth Neel, Aaron Roth, and Zhiwei Steven Wu. Preventing fairness gerrymandering: Auditing and learning for subgroup fairness. In *International conference on machine learning*, pages 2564–2572. PMLR, 2018.
- [34] Michael P Kim, Amirata Ghorbani, and James Zou. Multiaccuracy: Black-box post-processing for fairness in classification. In *Proceedings of the 2019 AAAI/ACM Conference on AI, Ethics, and Society*, pages 247–254, 2019.
- [35] Matt J Kusner, Joshua Loftus, Chris Russell, and Ricardo Silva. Counterfactual fairness. *Advances in neural information processing systems*, 30, 2017.
- [36] Selim Kuzucu, Jiaee Cheong, Hatice Gunes, and Sinan Kalkan. Uncertainty as a fairness measure. *Journal of Artificial Intelligence Research*, 81:307–335, 2024.
- [37] Erich L Lehmann and George Casella. *Theory of point estimation*. Springer Science & Business Media, 2006.
- [38] Edward Mascha and Thomas Vetter. Significance, errors, power, and sample size: The blocking and tackling of statistics. *Anesthesia and analgesia*, 126:691–698, 02 2018.
- [39] Mathieu Molina and Patrick Loiseau. Bounding and approximating intersectional fairness through marginal fairness. *Advances in Neural Information Processing Systems*, 35:16796–16807, 2022.
- [40] Giulio Morina, Viktoriia Oliinyk, Julian Waton, Ines Marusic, and Konstantinos Georgatzis. Auditing and achieving intersectional fairness in classification problems. *arXiv preprint arXiv:1911.01468*, 2019.
- [41] Cecilia Panigutti, Alan Perotti, André Panisson, Paolo Bajardi, and Dino Pedreschi. Fairlens: Auditing black-box clinical decision support systems. *Information Processing & Management*, 58(5):102657, 2021.
- [42] Manish Raghavan and Pauline T Kim. Limitations of the “four-fifths rule” and statistical parity tests for measuring fairness. *Geo. L. Tech. Rev.*, 8:93, 2024.
- [43] Eugen Slutsky. Über stochastische asymptoten und grenzwerte. *Metron*, 1925.
- [44] Hilde Weerts, Miroslav Dudík, Richard Edgar, Adrin Jalali, Roman Lutz, and Michael Madaio. Fairlearn: Assessing and improving fairness of ai systems. *Journal of Machine Learning Research*, 24(257):1–8, 2023.
- [45] Ke Yang, Joshua R. Loftus, and Julia Stoyanovich. Causal intersectionality and fair ranking. In *Symposium on Foundations of Responsible Computing*, 2021.
- [46] Muhammad Bilal Zafar, Isabel Valera, Manuel Gomez Rodriguez, and Krishna P Gummadi. Fairness beyond disparate treatment & disparate impact: Learning classification without disparate mistreatment. In *Proceedings of the 26th International World Wide Web Conference, WWW ’17*, pages 1171–1180, 2017.

## Appendices

<b>A Background and Related Work</b>	<b>13</b>
<b>B Proofs</b>	<b>14</b>
<b>C Additional experiments and discussions</b>	<b>16</b>
C.1 Additional datasets	16
C.2 Training Details	16
C.3 Additional results for Statistical Parity	16
C.4 Bayesian vs. Asymptotic Interval Convergence	24
C.5 Effects of small sample size on the asymptotic results	25
C.6 Choice of $\tilde{n}$	25
C.7 Influence of the prior	25
C.8 Comparison with Bootstrapping	26
C.9 Results for Equal Opportunity	26

### A Background and Related Work

Early research on algorithmic fairness framed the problem as ensuring Statistical Parity across sensitive groups defined by single attributes such as race or gender. Demographic Parity [19], Equalized Odds and Equal Opportunity [29], Predictive Parity [12], and related criteria remain cornerstones of the field and are implemented in popular toolkits (e.g., FAIRLEARN [44]). A large body of work subsequently proposed pre-, in-, and post-processing interventions to satisfy one or more of these metrics [46, 24].

While the above metrics are ordinarily reported as single numbers, they are in fact noisy estimates computed on finite samples. Angwin et al. [2] and the ensuing debate around COMPAS highlighted how small data perturbations can flip an “unfair” judgment. Kearns et al. [33] observed that even with large overall data sets, fairness estimates for minority sub-groups can have extremely high variance, a problem magnified under intersectionality. Recent surveys [7, 8] consolidate evidence that ignoring estimation error leads to both false alarms (flagging random fluctuation as bias) and missed harms (overlooking small but significant disparities in large groups).

Intersectionality [15, 27, 26, 20] demands analysis at the cross-sections of multiple protected attributes (e.g. “Black women over 50”). Empirical studies such as *Gender Shades* [9] revealed accuracy gaps that only appear at such intersections. Yet the number of subgroups grows exponentially with attribute count, leaving most groups sparsely represented. Foulds et al. [23] formalized this “resolution limit” and demonstrated that point estimates become statistically meaningless in the low-data regime. Subsequent work proposed auditing algorithms that search adaptively for large-effect subgroups without exhaustively enumerating all intersections [33, 40], but these methods still deliver binary verdicts on noisy estimates. Complementary to these estimation strategies, Molina and Loiseau [39] provide high-probability *bounds* that connect easily measured *marginal* fairness to otherwise intractable intersectional fairness. Their analysis shows when marginal guarantees suffice and offers computable certificates that scale to many attributes.

A direct frequentist remedy is to report confidence intervals (CIs) around each fairness metric. Bootstrap CIs for Demographic Parity, Equalized Odds, and related metrics are supported in FAIRLEARN and have been advocated by Besse et al. [6], Del Barrio et al. [16], and Cherian and Candès [11]. In NLP, Ethayarajh [18] introduces *Bernstein-bounded unfairness*, deriving analytic Bernstein bounds that convert a small, partially annotated sample into a tight confidence interval on bias. Wide inter-

vals immediately signal when data are insufficient to draw conclusions, a property exploited in the *FairlyUncertain* benchmark [3]. Nevertheless, Bootstrap CIs are not reliable when sample sizes are extremely small. Additionally, Himmelreich et al. [31] advocate for hypothesis testing for fairness in intersectional settings; however, differently from us they focus on the accuracy computed per group and solely rely on central limit results, without considering alternatives for small sample sizes.

Beyond estimating metrics more precisely, several authors treat disparities in predictive uncertainty themselves as indicators of unfairness. Bhatt et al. [8] decompose aleatoric and epistemic uncertainty across groups; higher epistemic uncertainty for a subgroup suggests under-representation in the training data. Kuzucu et al. [36] leverage uncertainty estimates from deep ensembles and Bayesian neural networks to design uncertainty-aware mitigation strategies.

Existing solutions thus improve fairness assessment along isolated axes—frequentist intervals or Bayesian models—but none provides a unified, scalable framework that (i) quantifies estimation uncertainty, (ii) adapts gracefully to the extreme sparsity of intersectional subgroups, and (iii) remains agnostic to the choice of fairness metric. We address this gap by introducing a statistically principled method that merges Bayesian modeling with concentration-inequality guarantees, yielding valid uncertainty bounds at small subgroup granularity without prohibitive computation.

## B Proofs

We first prove Theorem 2 which is the general version. Then, we show how Theorem 1 follows consequently.

**Theorem 2.** Let  $\mathbf{p} = (p_1, \dots, p_q)$  a set of probabilities of  $q$  disjoint events, with  $\sum_i p_i = 1$ ; let  $C = (C_1, \dots, C_q) \sim \text{Categorical}(\mathbf{p})$  be the related categorical distribution, and let  $C^1, \dots, C^n$  be  $n$  i.i.d. realizations of  $C$ . Let  $\phi$  be a continuously differentiable (in an neighbourhood of  $\mathbb{E}C$ ) function  $\phi : \mathbb{R}^q \rightarrow \mathbb{R}$ . Then

$$\frac{\sqrt{n}}{\sigma} \left( \phi \left( \frac{1}{n} \sum_{i=1}^n C^i \right) - \phi(\mathbb{E}C) \right) \xrightarrow{d} N(0, 1), \quad \text{as } n \rightarrow \infty,$$

where  $\sigma = \sqrt{V^\top \Sigma V}$ ,  $V = \nabla \phi(\mathbb{E}C)$  is the gradient of  $\phi$ , and  $\Sigma = [\text{diag}(\mathbf{p}) - \mathbf{p}\mathbf{p}^\top]$  is the covariance matrix of  $C$ , where  $\text{diag}(\mathbf{p})$  indicates a diagonal matrix with entries  $p_i$ .

*Proof of Theorem 2.* Let  $C^1, \dots, C^n$  be i.i.d. samples from the categorical distribution  $C \sim \text{Categorical}(\mathbf{p})$ , where each  $C^i$  is a one-hot vector in  $\mathbb{R}^q$  (i.e.,  $C^i \in \{e_1, \dots, e_q\}$  and  $\mathbb{E}C^i = \mathbb{E}C = \mathbf{p}$ ).

Define the sample mean:

$$\bar{C}_n := \frac{1}{n} \sum_{i=1}^n C^i.$$

Then, by the multivariate Central Limit Theorem [37], we have:

$$\sqrt{n}(\bar{C}_n - \mathbf{p}) \xrightarrow{d} \mathcal{N}(0, \Sigma),$$

where  $\Sigma = \text{diag}(\mathbf{p}) - \mathbf{p}\mathbf{p}^\top$  is the covariance matrix of the categorical variable  $C$ .

Now, let  $\phi : \mathbb{R}^q \rightarrow \mathbb{R}$  be a function continuously differentiable in an neighbourhood of  $\mathbf{p} = \mathbb{E}C$ . Then, by the multivariate Delta Method [37], we have:

$$\sqrt{n}(\phi(\bar{C}_n) - \phi(\mathbf{p})) \xrightarrow{d} \mathcal{N}(0, \sigma^2),$$

where  $\sigma^2 = V^\top \Sigma V$ , with  $V = \nabla \phi(\mathbb{E}C) = \nabla \phi(\mathbf{p})$ , and, hence:

$$\frac{\sqrt{n}}{\sigma} (\phi(\bar{C}_n) - \phi(\mathbf{p})) \xrightarrow{d} \mathcal{N}(0, 1).$$

□

## 4.1 Size-adaptive Hypothesis Testing for Fairness

Furthermore, we point out that by Slutsky's Theorem [43] one can use the covariance  $\hat{\sigma}$  estimated from the data, instead of the population one.

We now show that the asymptotic normality of the Statistical Parity estimator  $\text{SP}_n(S)$  (Theorem 1) follows from Theorem 2 by expressing it as a smooth function of the empirical mean of a categorical random variable.

**Theorem 1** (Central Limit Theorem for Statistical Parity). *Let  $\sigma(S) = \sqrt{V^\top \Sigma_4 V}$ , where  $V = \left( \frac{p_{0,S}}{(p_S)^2}, \frac{-p_{1,S}}{(p_S)^2}, \frac{-p_{0,\bar{S}}}{(p_{\bar{S}})^2}, \frac{p_{1,\bar{S}}}{(p_{\bar{S}})^2} \right)$ , and  $\Sigma_4$  is defined in Equation 4 of the paper. Then*

$$\frac{\sqrt{n}}{\sigma(S)} (\text{SP}_n(S) - \text{SP}(S)) \xrightarrow{d} N(0, 1), \quad \text{as } n \rightarrow \infty,$$

where  $\xrightarrow{d}$  denotes convergence in distribution and  $N(0, 1)$  indicates the standard normal distribution.

*Proof of Theorem 1.* Define the following four mutually exclusive and exhaustive events:

$$\begin{aligned} e_1 &\equiv (f(x) = 1, x \in S(\mathcal{X})), & e_2 &\equiv (f(x) = 0, x \in S(\mathcal{X})), \\ e_3 &\equiv (f(x) = 1, x \in \bar{S}(\mathcal{X})), & e_4 &\equiv (f(x) = 0, x \in \bar{S}(\mathcal{X})). \end{aligned}$$

Let  $C \in \mathbb{R}^4$  be a categorical random variable representing a one-hot encoding over these events, with probability vector  $\mathbf{p} = (p_{1,S}, p_{0,S}, p_{1,\bar{S}}, p_{0,\bar{S}})$ .

Let  $C^1, \dots, C^n$  be i.i.d. realizations of  $C$ , and define the empirical mean:

$$\hat{p} = \frac{1}{n} \sum_{i=1}^n C^i.$$

Then  $\hat{p}$  is a consistent estimator of the population vector  $\mathbb{E}C = \mathbf{p}$ .

Now define the function  $\phi: \mathbb{R}^4 \rightarrow \mathbb{R}$  by

$$\phi(p_1, p_2, p_3, p_4) = \frac{p_1}{p_1 + p_2} - \frac{p_3}{p_3 + p_4},$$

which corresponds to the population Statistical Parity:

$$\text{SP}(S) = \phi(\mathbf{p}), \quad \text{SP}_n(S) = \phi(\hat{p}).$$

Note that  $\phi$  is continuously differentiable in a neighborhood of  $\mathbf{p}$ , provided the denominators  $p_1 + p_2$  and  $p_3 + p_4$  are nonzero, which holds under standard assumptions.

By Theorem 2, we have the convergence:

$$\frac{\sqrt{n}}{\sigma(S)} (\phi(\hat{p}) - \phi(\mathbf{p})) \xrightarrow{d} \mathcal{N}(0, 1),$$

where  $\sigma(S) = \sqrt{V^\top \Sigma V}$ ,  $V = \nabla \phi(\mathbf{p})$ , and  $\Sigma = \text{diag}(\mathbf{p}) - \mathbf{p}\mathbf{p}^\top$  is the covariance matrix of the categorical variable  $C$ .

Direct computation of the gradient yields:

$$V = \left( \frac{p_{0,S}}{(p_S)^2}, \frac{-p_{1,S}}{(p_S)^2}, \frac{-p_{0,\bar{S}}}{(p_{\bar{S}})^2}, \frac{p_{1,\bar{S}}}{(p_{\bar{S}})^2} \right),$$

with  $p_S = p_{1,S} + p_{0,S}$  and  $p_{\bar{S}} = p_{1,\bar{S}} + p_{0,\bar{S}}$ .

The covariance matrix  $\Sigma$  for this 4-category categorical variable coincides with the matrix  $\Sigma_4$  defined in Equation (4) of the main paper. Hence, the asymptotic variance is exactly

$$(\sigma(S))^2 = V^\top \Sigma_4 V.$$

Thus,

$$\frac{\sqrt{n}}{\sigma(S)} (\text{SP}_n(S) - \text{SP}(S)) \xrightarrow{d} \mathcal{N}(0, 1),$$

which proves Theorem 1 as a special case of Theorem 2.  $\square$

The results for Equal Opportunity and Disparate Impact are obtained analogously, as special cases of Theorem 2.

## C Additional experiments and discussions

Due to space constraints, the main paper focused on a selected set of datasets and results. Here, we present broader discussions and analysis.

### C.1 Additional datasets

The additional experiments include the German Credit [32] and the Student Performance [13] datasets.

**German** The German Credit dataset, sourced from a German bank, comprises 1000 loan applicants characterized by twenty attributes (three of which are considered protected), including financial and personal details. Its primary use is in binary classification tasks to predict creditworthiness, with binary target "bad" ( $y = 0$ ) and "good" ( $y = 1$ ). The three protected variables considered are: *Sex* ("Male", "Female"), *Foreign worker* ("Foreign", "Not foreign"), and *Age* ("Under 30", "30-40", "40-50", "Over 50").

**Student** The Student Performance dataset focuses on student achievement in secondary education at two Portuguese schools. It includes attributes related to student grades, demographics, social factors, and school-related characteristics. The data was gathered for 649 students through school reports and questionnaires. The binary target variable indicates whether a student's final grade falls within the range of 0 to 10 ( $y = 0$ ) or exceeds 10 ( $y = 1$ ). The protected variables considered are: *age* ("Adult" ( $\geq 18$ ), "Minor" ( $< 18$ )), *Sex* ("F", "M") for Female and Male students, *Pstatus* ("T", "A"), which indicates the parent's cohabitation status, living Together or Apart, and *Address* ("U", "R"), which indicates student's home address type, Urban or Rural areas.

### C.2 Training Details

In all experiments, we train an XGBoost classifier [10] on each dataset without hyperparameter tuning, since our focus is on fairness auditing rather than maximizing predictive performance. We perform 20 independent 2:1 stratified train-test splits to account for sampling variability. The following default XGBoost parameters were used for all runs:

- `n_estimators = 100`
- `max_depth = 6`
- `learning_rate = 0.3`
- `subsample = 1.0`
- `colsample_bytree = 1.0`
- `objective = "binary:logistic"`
- `eval_metric = "logloss"`

After training on each split, we evaluate accuracy on the held-out test set. Table 1 reports the mean and standard deviation of test accuracy over the 20 splits for each dataset.

Table 1: Mean accuracy and standard deviation of the XGBoost model over 20 random 2:1 splits.

Dataset	Mean Accuracy	Std. Deviation
Adult	0.8702	0.0021
COMPAS	0.7141	0.0094
German	0.7633	0.0229
Student	0.7681	0.0177

### C.3 Additional results for Statistical Parity

Figure 5 shows the resolution limits for Statistical Parity violations when detecting when a group is *advantaged*.

## 4.1 Size-adaptive Hypothesis Testing for Fairness

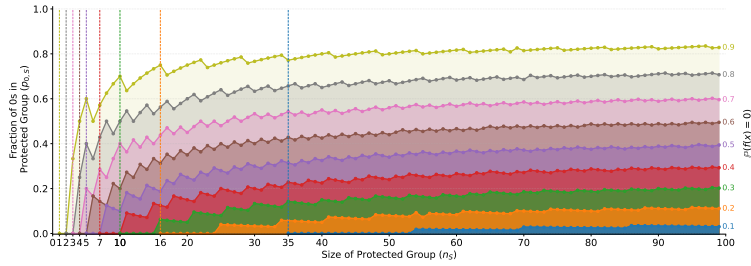


Figure 5: Resolution limits for Statistical Parity violations under varying global negative rates  $\mathbb{P}(f(x) = 0)$ , when detecting *advantaged* groups (the dual figure showing the boundary for deciding if a group is being *disadvantaged* is reported in Figure 1 in the main paper). Each curve traces the maximal fraction of negative outcomes needed to reject  $H_0: SP(S) = 0$  at  $\alpha = 0.05$  as a function of the group size  $n_s$ . To the left of each vertical bar is the “no-power” zone, where subgroups are too small to detect discrimination, regardless of the observed disparity. The shaded region below each curve is the “discrimination zone”, where the subgroup’s negative rate is enough to establish a statistically significant parity violation.

In Figures 2 and 3 of the main paper, we showed the results for Statistical Parity for a selection of intersectional subgroups (one per panel) from the COMPAS and Adult datasets. In each panel, we specified the minimum ( $n_{min}$ ) and maximum ( $n_{max}$ ) size of the protected group across different train-test splits. In Figures 6, 7, 8, 9, 10, 11 we show the complete set of intersectional subgroups for the four datasets *Adult*, *COMPAS*, *German* and *Student*. We have omitted panels for empty intersectional groups (‘Asian’, ‘Less than 25’, ‘Female’) and (‘N.A.’, ‘Less than 25’, ‘Female’) in COMPAS, (‘A.P.I.’, ‘Under 18’, ‘Male’) in Adult). For every split, we plot the Bayesian credible interval (blue), and the asymptotic normal confidence interval (red). In certain panels, such as the final one in Figure 10, some lines are absent. This occurs because, in some train-test splits, the intersectional group had no instances in the test fold.

As for the results in the main paper, these findings highlight the limitations of a fixed-threshold approach, which struggles to account for variations in group size within the same dataset-model setup and remains sensitive to different train-test splits. In contrast, our method considers group size, demonstrating greater robustness across train-test variations.

## 4.1 Size-adaptive Hypothesis Testing for Fairness

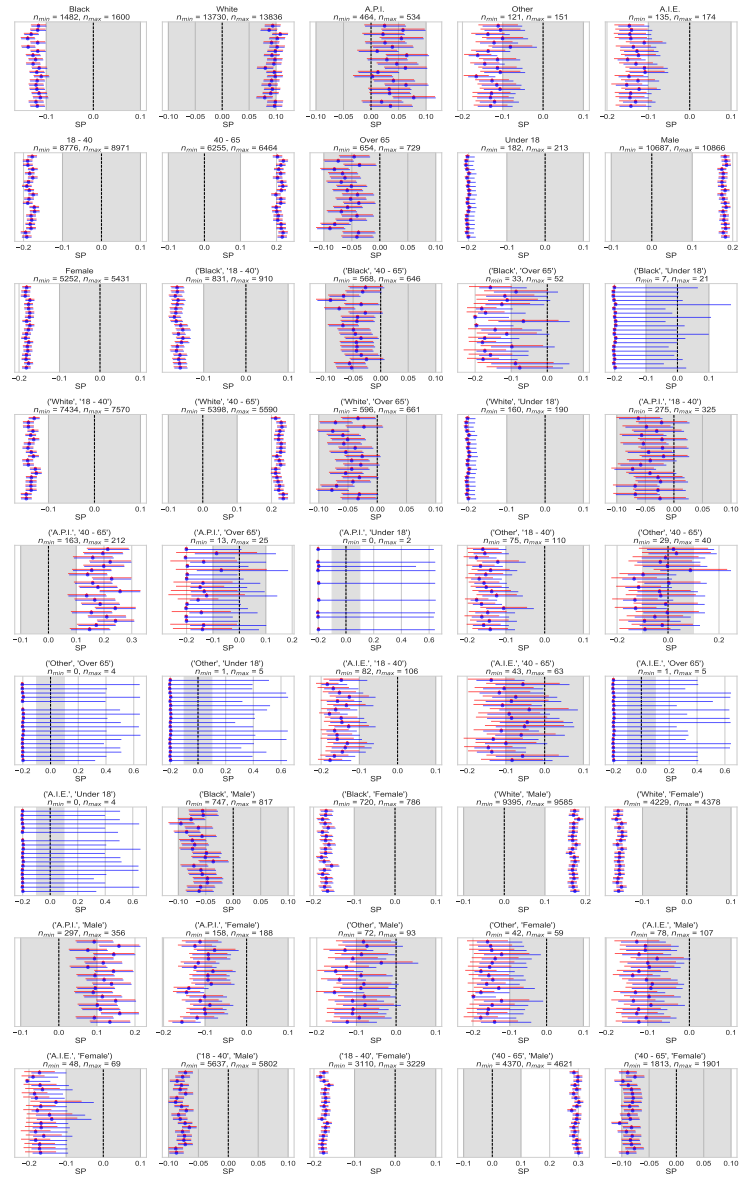


Figure 6: Point-wise estimation versus confidence intervals, Adult dataset.

## 4.1 Size-adaptive Hypothesis Testing for Fairness

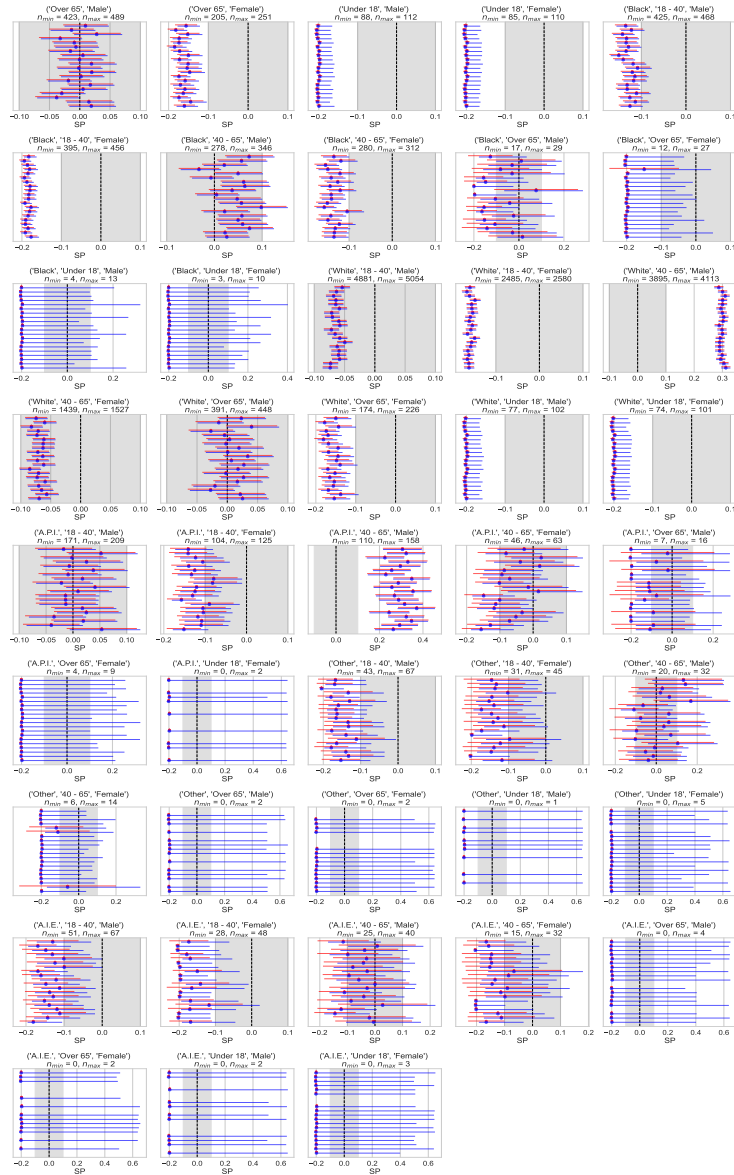


Figure 7: Point-wise estimation versus confidence intervals, Adult dataset (continued).

## 4.1 Size-adaptive Hypothesis Testing for Fairness

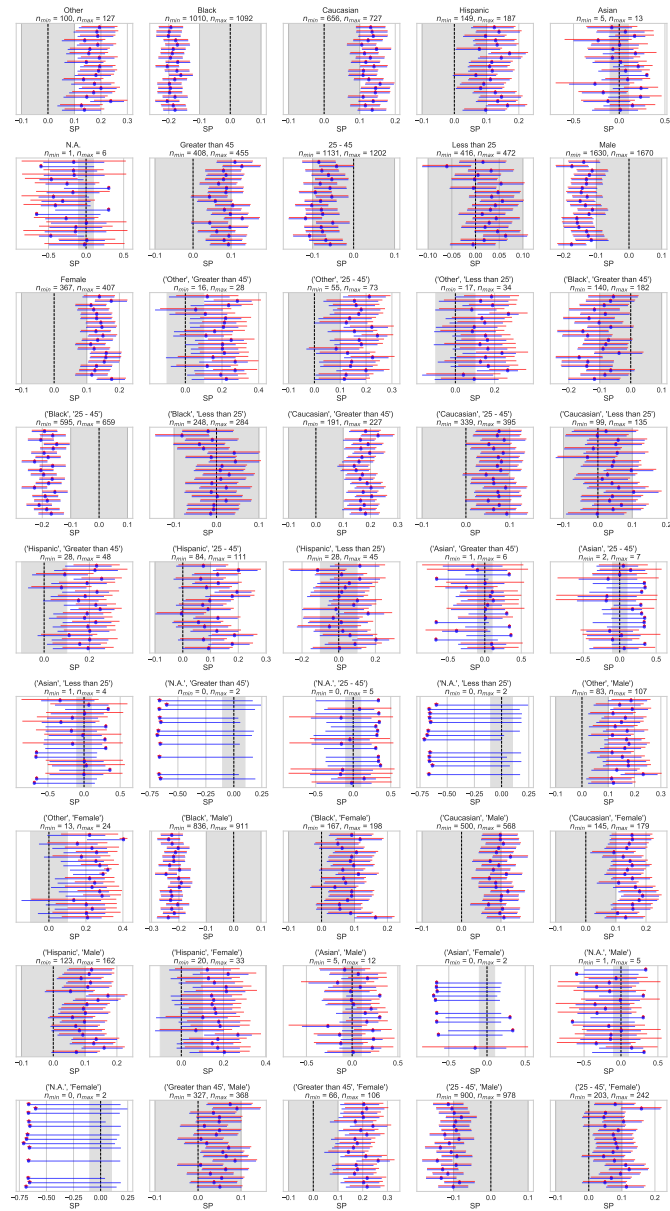


Figure 8: Point-wise estimation versus confidence intervals, COMPAS dataset.

## 4.1 Size-adaptive Hypothesis Testing for Fairness

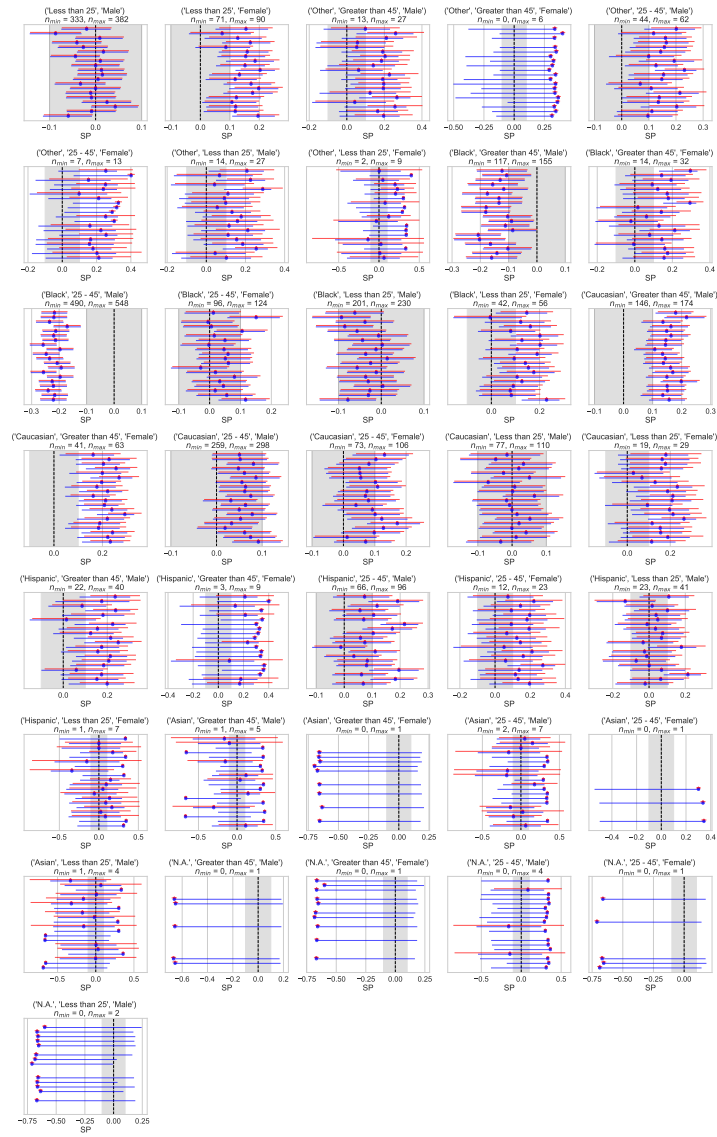


Figure 9: Point-wise estimation versus confidence intervals, COMPAS dataset (continued).

## 4.1 Size-adaptive Hypothesis Testing for Fairness

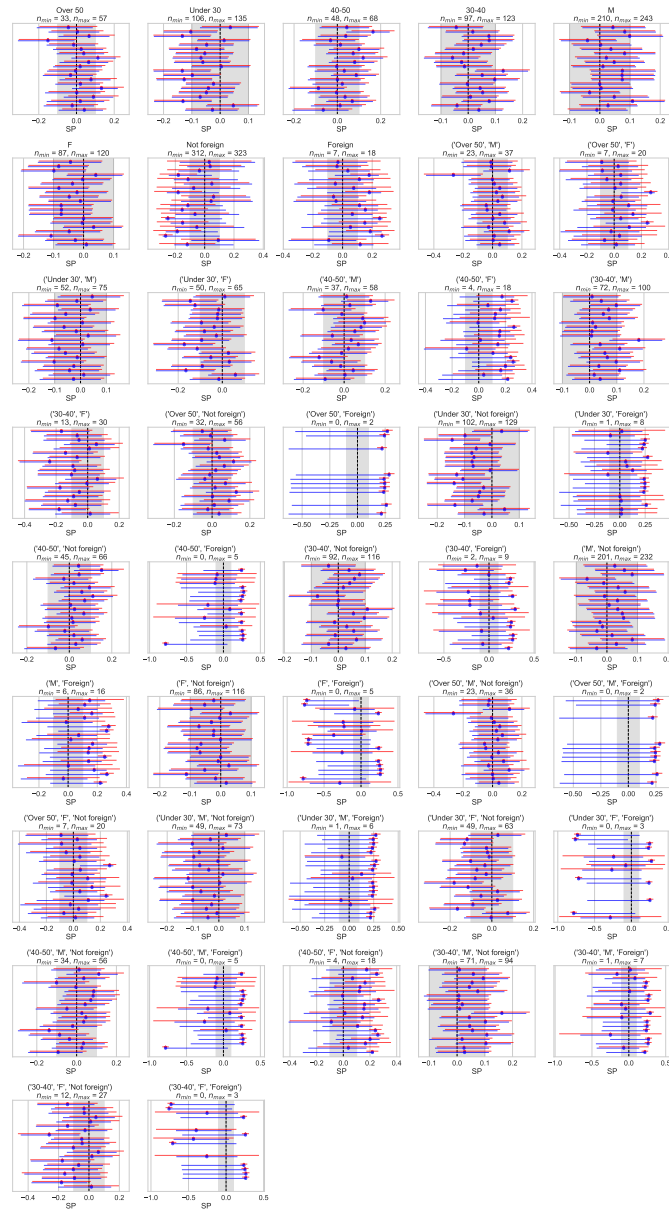


Figure 10: Point-wise estimation versus confidence intervals, German dataset

## 4.1 Size-adaptive Hypothesis Testing for Fairness

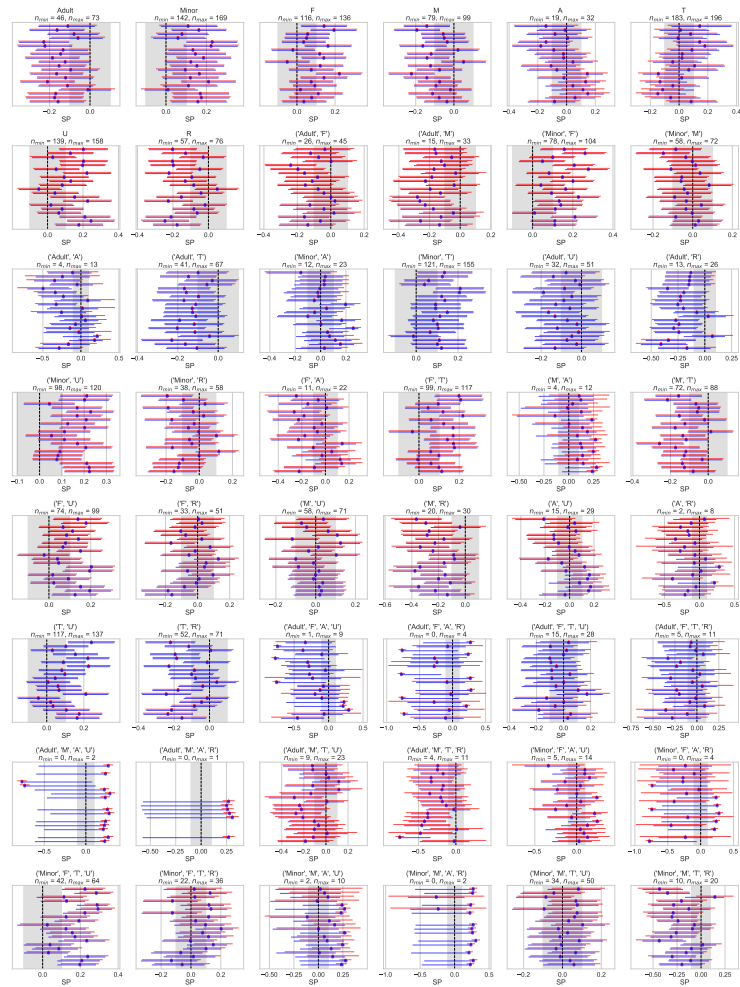


Figure 11: Point-wise estimation versus confidence intervals, Student dataset

## 4.1 Size-adaptive Hypothesis Testing for Fairness

Furthermore, in Figure 4, we considered all intersectional groups (across all 20 train-test splits) on COMPAS and Adult to compare the decision from our framework with those from a threshold-based  $\gamma$ SP approach. In Figure 12, we extend the same approach for the two other datasets, German and Student. The results show that a fixed threshold on  $\gamma$ SP fails to consistently distinguish fairness violations, highlighting the necessity of a size-adaptive hypothesis-testing approach like SAFT.

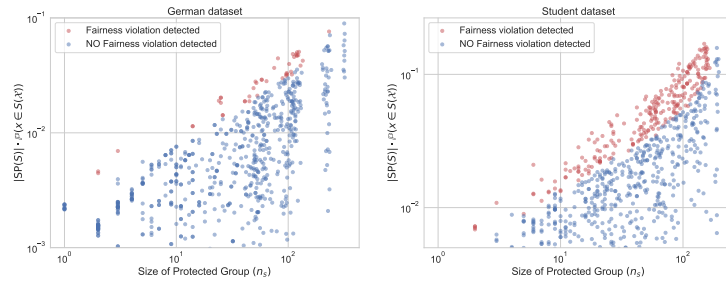


Figure 12: Protected groups size,  $\gamma$ SP scores, and interval-based fairness violations.

### C.4 Bayesian vs. Asymptotic Interval Convergence

To illustrate how our Bayesian credible intervals smoothly interpolate between robust small-sample uncertainty and asymptotic normality, Figure 13 shows four synthetic subgroups with sizes  $n \in \{1, 10, 100, 1025\}$ . In each panel we plot (i) the posterior density of the statistical-parity gap under a uniform Dirichlet prior (blue curve), (ii) the corresponding 95% credible interval (blue shaded region), and (iii) the asymptotic 95% confidence interval from Theorem 1 (red curve region) centered at the same point estimate. As  $n$  grows, the two intervals converge and the posterior density sharpens, while for very small  $n$  the Bayesian interval remains appropriately wide, reflecting high epistemic uncertainty.

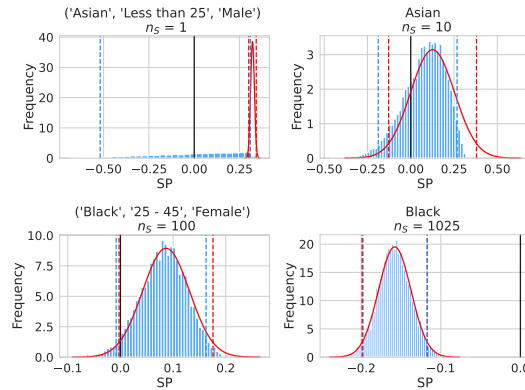


Figure 13: Comparison of Bayesian credible intervals (blue) and asymptotic normal confidence intervals (red) for subgroups of size  $n_S$ . As  $n_S$  increases, the posterior density concentrates and the two intervals converge; for small  $n_S$ , the Bayesian interval remains larger, correctly encoding high uncertainty.

## 4.1 Size-adaptive Hypothesis Testing for Fairness

### C.5 Effects of small sample size on the asymptotic results

The Wald variance for subgroup  $S$  can be rewritten as:

$$\sigma^2 = \frac{\frac{p_{1,S}}{p_{1,S}+p_{0,S}} \left(1 - \frac{p_{1,S}}{p_{1,S}+p_{0,S}}\right)}{n_S} + \frac{\frac{p_{1,\bar{S}}}{p_{1,\bar{S}}+p_{0,\bar{S}}} \left(1 - \frac{p_{1,\bar{S}}}{p_{1,\bar{S}}+p_{0,\bar{S}}}\right)}{n_{\bar{S}}}$$

Since  $n_S \approx n \cdot P(S)$  (and analogously for  $n_{\bar{S}}$ ) the variance decreases at rate  $1/n$ , even for rare groups. Both asymptotically and for small samples, small subgroups do not lead to inflated variance.

That said, the more subtle issue is that in finite samples, the plug-in variance  $\sigma^2$  may actually underestimate uncertainty when  $n_S$  is small. In particular, when the estimate of  $\frac{p_{1,S}}{p_{1,S}+p_{0,S}}$  is very close to 0 or 1, the estimation of the term  $\frac{p_{1,S}}{p_{1,S}+p_{0,S}} \left(1 - \frac{p_{1,S}}{p_{1,S}+p_{0,S}}\right)$  in the variance formula becomes near zero. This drives the Wald variance estimate to be artificially small, even though the underlying sampling uncertainty is high for such extreme proportions with small  $n_S$ .

This can make the Wald test *anti-conservative*, falsely rejecting the null due to high variance in small groups not captured by the asymptotic approximation. This effect can be seen, for example, in the top-left plot of Figure 13.

This is why we introduce the Bayesian Dirichlet–multinomial test to provides calibrated inference in the small-sample regime. Hence, the problem is not variance inflation, but undercoverage due to inappropriate reliance on asymptotics when subgroup counts are small.

### C.6 Choice of $\tilde{n}$

In Algorithm 1 we suggested choosing  $\tilde{n} = 30$ , since thirty observations is a widely used rule-of-thumb to trust CLT-based Wald tests [38] because coverage and power stabilize around that cell size in typical multinomial settings. In Table 2 we analyze the effect of the choice of  $\tilde{n}$  for SAFT applied to the Adult dataset. One can observe how from around twenty observations the total number (over all train-test splits and over all possible sub-groups) of fairness violations detected stabilizes. Hence, also our empirical results confirm thirty observations as a safe choice to switch from the bayesian to the asymptotic test. With a smaller  $\tilde{n}$ , e.g.,  $\tilde{n} = 5$ , the amount of samples appears to be too small to rely on asymptotic results, indeed the CLT might induce to over-reject the null, as explained in Appendix C.5.

Table 2: Total number of fairness violations detected by SAFT in Adult for all train-test splits and for all sub-groups for different values of  $\tilde{n}$

$\tilde{n}$	1	2	5	10	20	30	40	50	100	200	500	1000
# of violations	1159	1144	1118	1098	1097	1097	1097	1096	1098	1097	1097	1097

Clearly, users may raise or lower  $\tilde{n}$  if their data warrant it.

### C.7 Influence of the prior

We now explore the impact of the prior choice and the incorporation of prior information, derived from the training set. We consider:

- Uniform (flat) Dirichlet prior, which imposes no substantive prior information;
- Empirical Bayes priors derived from training-set frequencies.

For each subgroup we set

$$\alpha = \frac{\lambda}{\max(1, \min(c_{0,s}, c_{0,\bar{s}}, c_{1,s}, c_{1,\bar{s}}))} [c_{0,s} + 1, c_{0,\bar{s}} + 1, c_{1,s} + 1, c_{1,\bar{s}} + 1], \quad \lambda \in \{0.5, 1, 2, 5\}$$

where  $c_{i,j}$  is the number of training samples with label  $i \in \{0, 1\}$  in group  $j \in \{s, \bar{s}\}$ .

## 4.1 Size-adaptive Hypothesis Testing for Fairness

This construction scales the prior strength by  $\lambda$  while preserving the empirical class proportions, and caps the influence when any cell count is extremely small. Table 3 shows the results with the confidence/credible intervals (CIs) for some selected subgroups from the Adult dataset.

The results show prior influence for extremely small subgroups, while all CIs rapidly converge to the asymptotic regime as  $n_S$  grows. For the smaller  $n_S$  case, the Wald intervals are spuriously narrow, clearly under-representing the true sampling uncertainty. In contrast, the uniform-prior Bayesian credible intervals are much larger, appropriately reflecting the scarcity of data. As we introduce empirical-Bayes priors, these intervals shrink toward the Wald width but remain more conservative than asymptotic bounds, demonstrating that modest data-informed priors can stabilize inference without overconfidence. With hundreds or thousands of samples, all methods produce nearly identical intervals, illustrating that prior effects vanish once more data is available.

Table 3: Influence of the prior

$n_S$	Other, Under 18,	A.P.L., Over 65,	White, Over 65,	Black
	Female	Male	Female	
	2	12	210	1522
Asymptotic normal CI	[-0.204, -0.192]	[-0.271, 0.041]	[-0.182, -0.123]	[-0.130, -0.097]
Bayesian CI with uniform prior	[-0.190, 0.488]	[-0.176, 0.176]	[-0.174, -0.115]	[-0.127, -0.097]
Bayesian CI with empirical prior, $\lambda = 0.5$	[-0.240, 0.014]	[-0.196, 0.048]	[-0.179, -0.121]	[-0.138, -0.114]
Bayesian CI with empirical prior, $\lambda = 1$	[-0.236, 0.037]	[-0.196, 0.052]	[-0.179, -0.123]	[-0.138, -0.113]
Bayesian CI with empirical prior, $\lambda = 2$	[-0.228, 0.035]	[-0.177, 0.037]	[-0.177, -0.125]	[-0.138, -0.114]
Bayesian CI with empirical prior, $\lambda = 5$	[-0.195, 0.000]	[-0.156, 0.011]	[-0.176, -0.128]	[-0.139, -0.113]
Bootstrapping CI	[-0.204, -0.192]	[-0.203, 0.073]	[-0.178, -0.118]	[-0.130, -0.098]

### C.8 Comparison with Bootstrapping

In moderate to large subgroups, nonparametric bootstrap intervals (e.g., [44]) coincide, both theoretically and empirically, with the Wald limits obtained from our CLT analysis, so bootstrapping adds computation without accuracy gains at that scale. In small intersectional subgroups where Wald approximations fail, the bootstrap typically inherits the same pathologies: with pronounced class imbalance, resamples frequently yield zero counts in one or more contingency cells (e.g., no predicted positives for group  $S$ ), producing degenerate or undefined disparity estimates and a highly discrete, skewed resampling distribution that yields off-center, overly narrow intervals. In the last row of Table 3, the bootstrap intervals closely track the asymptotic confidence interval even at small  $n_S$ , indicating that resampling does not remedy the underlying approximation error in this setting. Accordingly, we use analytic CLT intervals when regularity conditions are met, and Dirichlet-multinomial credible intervals when any cell counts are in the single digits, where they remain well-calibrated and avoid degeneracy.

### C.9 Results for Equal Opportunity

In Figures 14 and 15 (Adult dataset) and Figures 16 and 17 (COMPAS dataset), we present the results for Equal Opportunity. In each panel,  $n_{min}$  and  $n_{max}$  denote the minimum and maximum number of instances belonging to the protected group with  $y = 1$  across different train-test splits. Compared to the plots for Statistical Parity Figures 6 to 9, those for Equal Opportunity show wider CIs, consistently reflecting lower  $n_{i,j}$  counts given the additional conditioning on  $y = 1$  for Equal Opportunity.

## 4.1 Size-adaptive Hypothesis Testing for Fairness

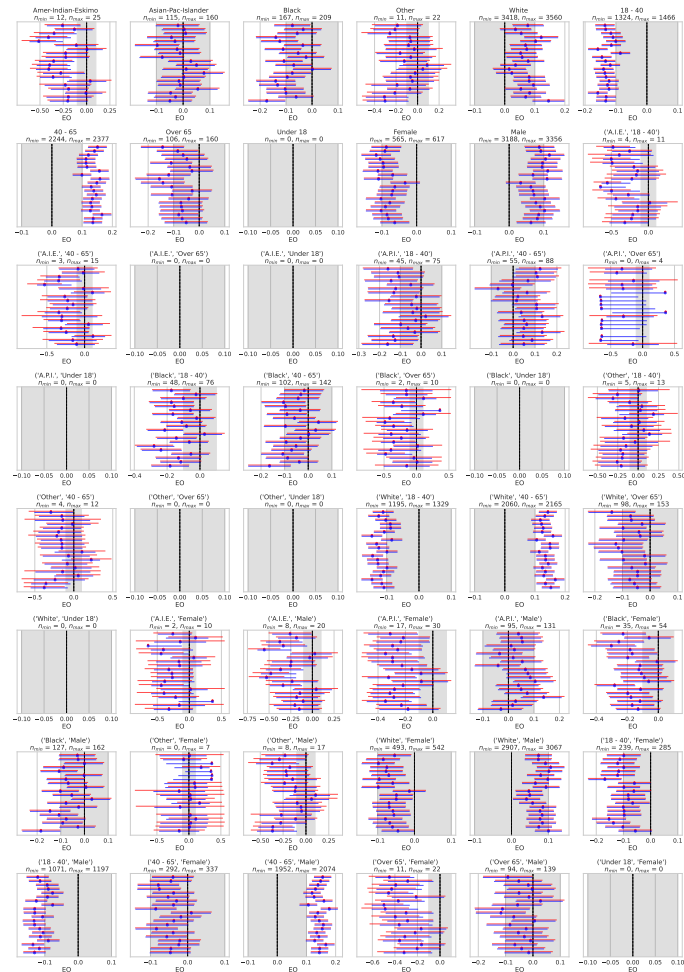


Figure 14: Point-wise estimation versus confidence intervals for Equal Opportunity, Adult dataset.

## 4.1 Size-adaptive Hypothesis Testing for Fairness

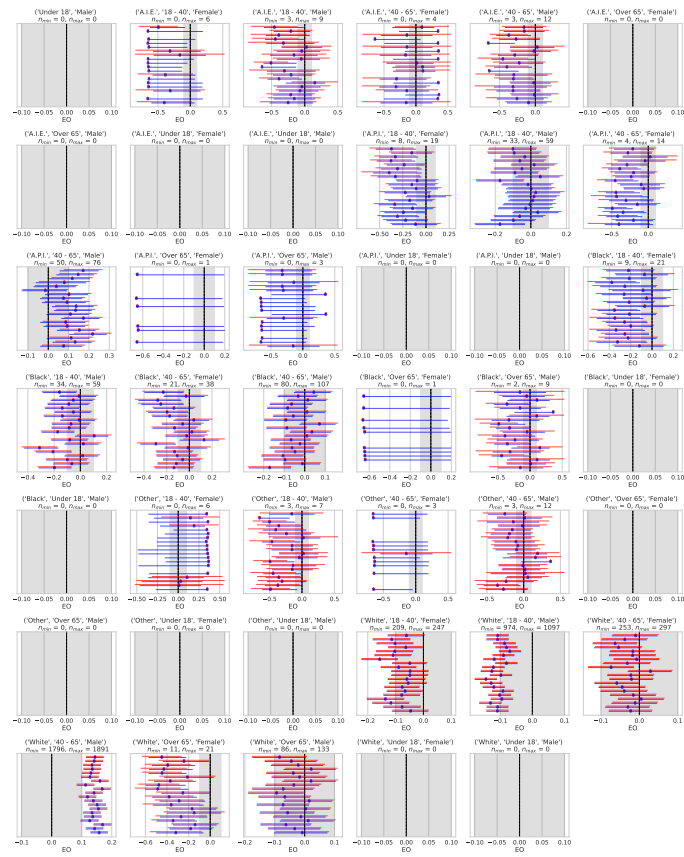


Figure 15: Point-wise estimation versus confidence intervals for Equal Opportunity, Adult dataset (continued).

## 4.1 Size-adaptive Hypothesis Testing for Fairness

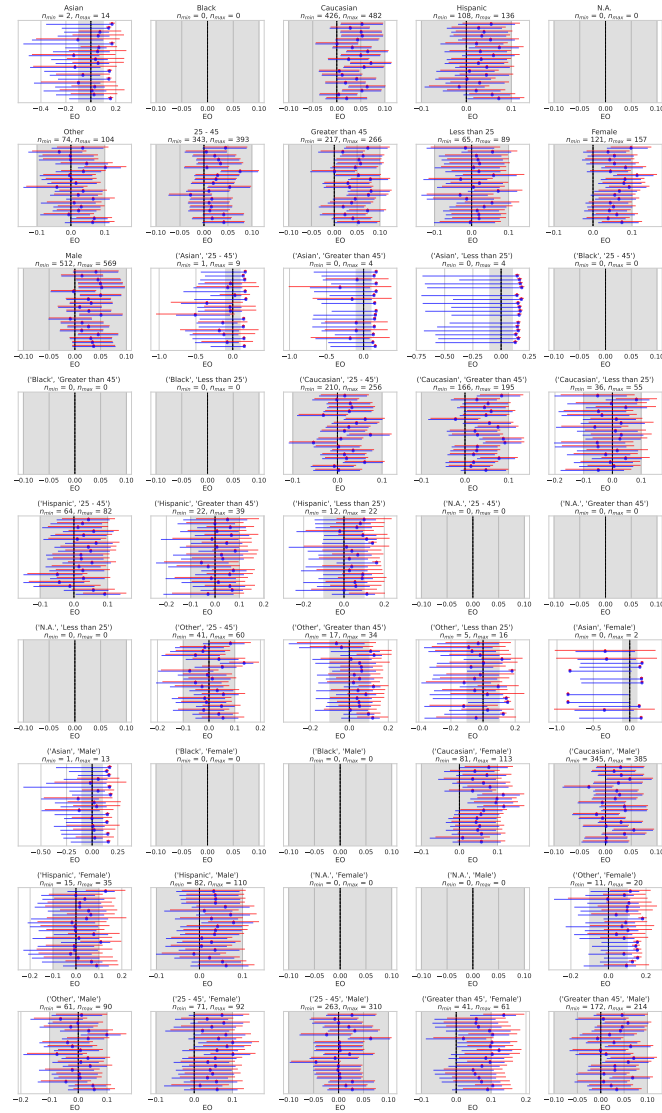


Figure 16: Point-wise estimation versus confidence intervals for Equal Opportunity, COMPAS dataset

## 4.1 Size-adaptive Hypothesis Testing for Fairness

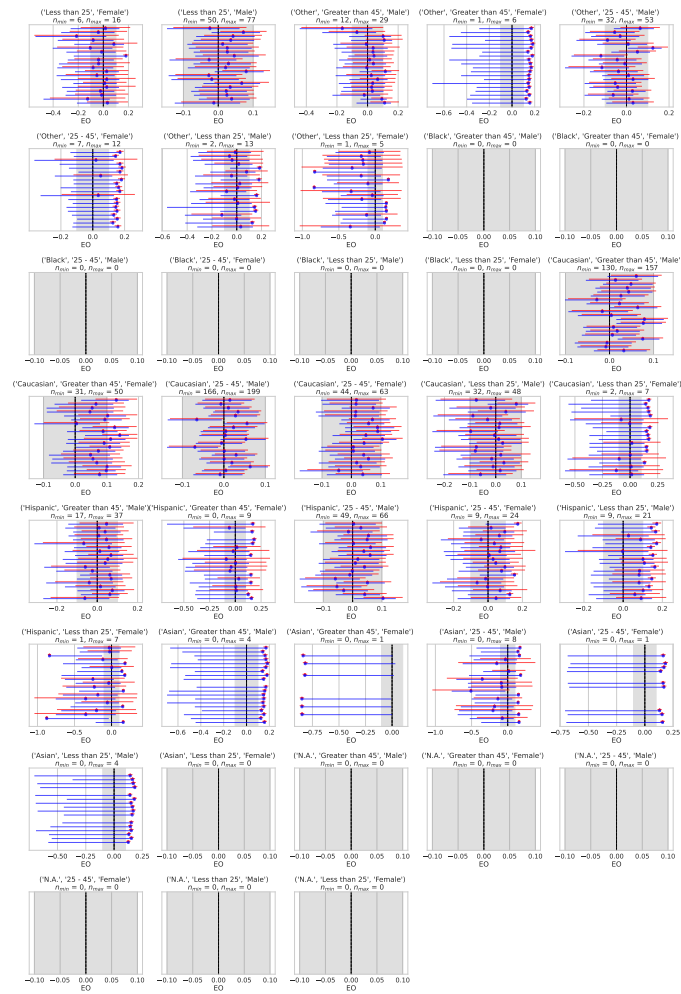


Figure 17: Point-wise estimation versus confidence intervals for Equal Opportunity, COMPAS dataset (continued)

## 4.2 Auditing For Demographic Bias in Opaque Rankings

While fairness metrics can be computed directly for classification models, auditing ranking systems presents additional challenges, particularly when the underlying model is opaque or proprietary. In many real-world applications, such as search engines, recommender systems, and hiring platforms, the internal logic of the ranking algorithm may not be accessible to auditors. In such cases, detecting unfairness requires analyzing the observable outputs of the system without relying on knowledge of its internal structure.

This section addresses this challenge by proposing a model-agnostic auditing framework for detecting demographic bias in opaque ranking systems. The central idea is to evaluate whether the ranking produced by the system exhibits residual dependence on protected attributes, after accounting for legitimate task-relevant features. If the ranking remains statistically dependent on demographic attributes even after conditioning on relevant variables, this dependence may indicate the presence of unjustifiable bias.

To operationalize this idea, the proposed framework measures conditional dependence between rankings and protected attributes using statistical tools capable of capturing complex, non-linear relationships. By doing so, the method enables fairness audits that remain applicable even in black-box scenarios where the internal decision-making process of the model cannot be inspected directly.

### Authors' Contributions

---

<b>Contribution</b>	<b>Authors</b>
<b>Conceptualization:</b>	A. Ferrara and all authors
<b>Writing:</b>	A. Ferrara and all authors
<b>Methodology:</b>	F. Vitale, A. Ferrara
<b>Formal Analysis:</b>	Theorem 1: A. Ferrara; Theorems 2 and 3: F. Vitale
<b>Code:</b>	A. Ferrara, C. Abrate
<b>Experiments:</b>	C. Abrate, A. Ferrara

---

## Auditing for Demographic Bias in Opaque Rankings

Antonio Ferrara  
Intesa Sanpaolo AI Research, Turin, Italy  
antonio.ferrara@intesaspaolo.com

Fabio Vitale  
Intesa Sanpaolo Innovation Center, Turin, Italy  
fabio.vitale@intesaspaolo.com

Carlo Abrate  
Intesa Sanpaolo AI Research, Turin, Italy  
carlo.abrate@intesaspaolo.com

Francesco Bonchi  
Intesa Sanpaolo AI Research, Turin, Italy  
francesco.bonchi@intesaspaolo.com

### ABSTRACT

Auditing algorithmic fairness is a critical challenge in high-stakes domains like hiring and credit scoring, especially given the intrinsic opacity of algorithmic decision-making systems. In this paper, we tackle the following problem: given a ranking of individuals, how can we assess whether the order is driven by protected attributes (e.g., gender or race) rather than task-relevant features, under a strict black-box assumption where the ranking mechanism cannot be queried?

Building on kernel conditional independence and partial distance correlation, we introduce CONDOR, a model-agnostic audit framework. CONDOR first residualizes the ranking and protected attributes with respect to observables in a reproducing kernel Hilbert space. It then quantifies the remaining association via distance correlation on the residualized embeddings, returning a normalized effect-size score. This procedure captures general nonlinear dependencies without assuming access to latent scores, requires no hyperparameter fine-tuning, and naturally accommodates mixed continuous and categorical data. From CONDOR’s effect-size score, we derive a hypothesis test for conditional independence. By combining this test with an unconditional independence test, auditors can achieve a comprehensive causal understanding of the protected attributes’ influence.

We validate our proposal on real and semi-synthetic datasets with controlled influence of the protected attributes on the ranking: our method reliably detects the influence of protected attributes, outperforming established statistical auditing baselines.

### PVLDB Reference Format:

Antonio Ferrara, Carlo Abrate, Fabio Vitale, and Francesco Bonchi. Auditing for Demographic Bias in Opaque Rankings. PVLDB, 14(1): XXX-XXX, 2020.  
doi:XX.XX/XXX.XX

### PVLDB Artifact Availability:

The source code, data, and/or other artifacts have been made available at [https://github.com/Ambress92/Audit\\_ranking](https://github.com/Ambress92/Audit_ranking).

This work is licensed under the Creative Commons BY-NC-ND 4.0 International License. Visit <https://creativecommons.org/licenses/by-nc-nd/4.0/> to view a copy of this license. For any use beyond those covered by this license, obtain permission by emailing [info@vldb.org](mailto:info@vldb.org). Copyright is held by the owner/author(s). Publication rights licensed to the VLDB Endowment.  
Proceedings of the VLDB Endowment, Vol. 14, No. 1 ISSN 2150-8097.  
doi:XX.XX/XXX.XX

### 1 INTRODUCTION

Algorithmic rankings govern high-stakes decisions in hiring, credit scoring, and college admissions. Ensuring these rankings are not unduly influenced by protected demographic attributes (e.g., gender or race) is a critical requirement often mandated by fairness regulations [30, 43, 64]. However, auditing these systems is complicated by their opacity: auditors typically observe only the input features and the output ranking, without access to the internal scoring logic or training data. Several authors have explored this *black-box auditing* challenge in various forms. Adler et al. [1] have introduced a framework for detecting indirect influence in black-box models using controlled perturbations and influence functions. More recently, Cherian and Candès [9] have proposed a general statistical testing framework for model-agnostic fairness auditing, leveraging disparity metrics and bootstrapping techniques. In parallel, methods based on counterfactual reasoning – such as [52] – aim to explain individual predictions and identify fairness violations through feature perturbation, even without access to internal model parameters. Despite these advances, existing approaches tend to focus either on binary classification tasks or on testing specific hypotheses (e.g., the presence or absence of group disparity), rather than assessing whether a ranking depends on protected attributes.

In this paper, we tackle the problem of detecting whether an observed ranking  $R$  depends on protected attributes  $Z$  after accounting for legitimate, task-relevant attributes  $X$  (see Figure 1). Formally, this requires testing the conditional independence hypothesis:

$$H_0 : Z \perp\!\!\!\perp R \mid X$$

To solve this problem, we introduce CONDOR (*CONDitional Distance-cOrrelation for Rankings*), a model-agnostic audit framework that quantifies the residual dependence of a ranking on protected attributes (see Figure 1). Our primary contributions are:

(1) **The CONDOR method:** We combine kernel-based residualization with distance correlation. By projecting the ranking and protected attributes into a Reproducing Kernel Hilbert Space (RKHS; see, e.g., [48]), we “regress out” the influence of task-relevant features  $X$ . Measuring the association between the remaining residuals using distance correlation yields the Protected Attribution Score (PAS), a normalized effect size in  $[0, 1]$  capable of capturing complex non-linear dependencies without hyperparameter tuning. We theoretically characterize the PAS showing that it ensures exact null alignment under conditional independence and exhibits predictable local sensitivity to emerging biases.

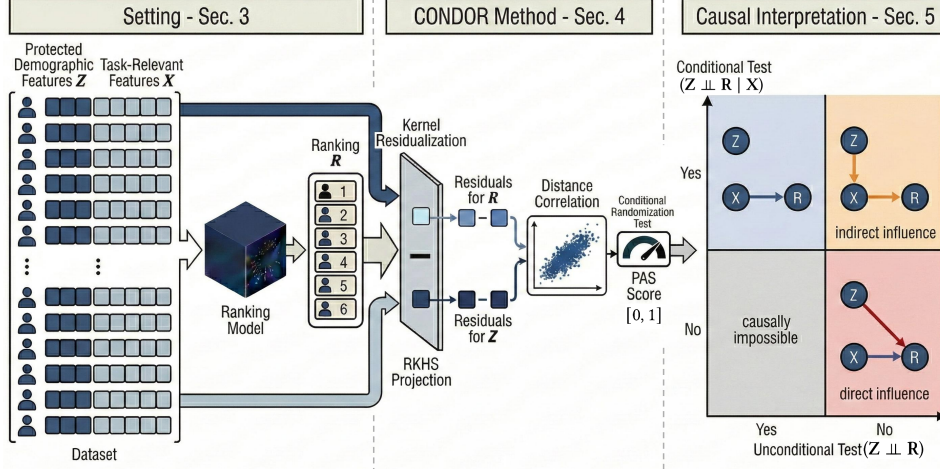


**Figure 1: CONDOR Pipeline and Causal Diagnostic Framework.** (Left) We observe a dataset of  $n$  individuals with protected attributes  $Z$  and task-relevant features  $X$ , alongside an opaque ranking  $R$  (§3). (Center) CONDOR audits this black box by projecting  $R$  and  $Z$  into a Reproducing Kernel Hilbert Space (RKHS) to residualize (“regress out”) the legitimate influence of  $X$ . Distance correlation on these residuals yields the Protected Attribution Score (PAS), which is then calibrated via a Conditional Randomization Test to produce a robust p-value for the null hypothesis  $Z \perp R | X$  (§4). (Right) Pairing this conditional test with an unconditional baseline ( $Z \perp R$ ) creates a  $2 \times 2$  causal matrix, allowing auditors to distinguish between a passed audit (no influence), indirect (mediated by task features) influence, and direct discrimination (§5).

As raw effect sizes depend heavily on dataset scale and variance, PAS values across different datasets are not directly comparable. To provide a definitive binary verdict, CONDOR calibrates the PAS against a “no residual effect” null hypothesis via a Conditional Randomization Test (CRT), converting the score into an interpretable one-sided p-value [12, 17, 35].

(2) **Causal interpretation:** By combining our conditional test ( $Z \perp R | X$ ) with an unconditional test ( $Z \perp R$ ), we provide a causal diagnostic framework. This allows auditors to distinguish between cases where the audit is passed (no influence), and cases where the protected attributes exert either a direct influence (violating conditional independence) or an indirect influence (mediated by task features) on the ranking.

(3) **Empirical assessment:** We validate CONDOR in 3 settings: (i) Both input data and ranking are synthetic, so that we can control the extent to which the protected information influences the ranking; (ii) Real-world datasets and grey-box ranking obtained by mixing a merit term with a tunable protected term, so the same protected-signal strength parameter governs *by design* the share of protected influence while preserving real-world feature distributions; (iii) Real-world dataset with black-box ranking.

We compare our method against three established baselines: a kernel-based conditional test (KCI [65]), a distance correlation

based technique (pdCOR [53]), and an information-theoretic conditional mutual information estimator (CMI – KSG  $k$ -NN [32]). Our experiments confirm the suitability of CONDOR as a conditional independence test and its superiority over the baselines.

## 2 RELATED WORK

Besides the topic of black-box auditing, which we already covered in Section 1, this work is related – on the technical level – to non-parametric measures of conditional dependence, while – at higher level – it collocates within the literature about fairness in ranking.

**Measures of conditional independence.** Kernel-based tests of conditional independence (e.g., KCI [65]) first residualize  $Z$  and  $R$  with respect to  $X$  in an RKHS via a regularized projection, and then quantify the remaining association using the Hilbert–Schmidt Independence Criterion [25], a kernel-based dependence measure that equals zero under independence [26]. CONDOR draws inspiration from this kernel-based framework but translates the kernel-residualization idea of KCI into a distance–correlation setting, thus producing a normalized effect size.

A complementary line relies on distance correlation dCOR[54], which characterizes independence for multivariate vectors; its partial variant pdCOR [53] provides a closed-form, distance-based effect size for residual association between  $R$  and  $Z$  after accounting for  $X$ . Building on this line, CONDOR augments pdCOR with an RKHS

residualization step and kernel-induced distances. This hybrid design preserves the geometric invariances and closed-form interpretability of pdCOR, while adding the conditioning strength of kernel methods to capture complex (nonlinear, interaction) effects of the observables. Other conditional independence approaches, such as conditional distance correlation (CDCor) [57] and conditional-mutual-information (CMI) estimators [33], yield measures that are zero *if and only if* conditional independence holds, but they require estimating conditional densities/expectations and introduce multiple tuning knobs (kernels, bandwidths, neighborhood sizes), which can be brittle in black-box audits.

Relative to these conditional independence tools, CONDOR sidesteps the estimation of conditional objects altogether and limits tuning to robust defaults (kernel family and a small ridge). In practice, this yields a normalized effect size (PAS) that is more sensitive to residual dependence than plain pdCOR when the influence of the observables is nonlinear, and it accommodates mixed continuous/categorical data through product kernels with stable defaults.

**Fair ranking.** Fairness in algorithmic ranking has attracted a growing attention [30, 36, 41, 43, 64]. Much of such literature frames the problem as one of equitable resource allocation. With a few exceptions that focus on individual fairness [5, 15, 46], or that tackle individual and group fairness jointly [22, 63], the bulk of the literature on fairness in ranking [4, 8, 24, 50, 60–62] and learning-to-rank [16, 37, 51] deals with *group fairness* along the lines of *demographic parity* [15] or *equal opportunity* [28]. This typically requires defining *a priori* demographic groups that have to be protected from discrimination, as enforced by legal norms [18, 19]. This is typically casted as the problem of maximizing utility under a *group-fairness constraint*, that requires a minimum fraction of individuals from the protected group to be included in the top- $k$  positions [8, 50, 62]. Such methods are inherently prescriptive: they aim to devise algorithms that produce fair rankings by balancing utility and fairness, often relying on explicit models of attention, such as the position-based discount functions used in Discounted Cumulative Gain (DCG) [31]. They face key challenges in defining the individual merit, the strength of group-fairness constraints, or even which groups should be protected in the first place [40].

Our work adopts a fundamentally different, *descriptive* posture: we do not prescribe how to rank fairly but instead provide a post-hoc, forensic tool to audit an *existing*, opaque ranking. The objective is not to manage exposure allocation but to quantify the *residual influence* of protected attributes on the observed ranking.

### 3 PRELIMINARIES

We are given  $n$  individuals each described by an attribute vector  $\mathbf{v}_i = (\mathbf{x}_i, \mathbf{z}_i)$  for  $i \in \{1, \dots, n\}$ , where  $\mathbf{x}_i$  are *observable task-relevant* attributes and  $\mathbf{z}_i$  are *protected demographic* attributes. We are also given a deterministic ranking of the  $n$  individuals: i.e., a bijective function  $r : [n] \rightarrow [n]$ , such that  $r(i)$  is the position of the individual  $i$  in the observed ranking, with  $r(i) = 1$  being the top (best) position. The positions in the ranking are hereafter viewed as stacked into the vector  $\mathbf{r} := (r(1), \dots, r(n))^T$ . We represent task-relevant and protected attributes by the matrices  $\mathbf{X} \in \mathbb{R}^{n \times d_o}$  and  $\mathbf{Z} \in \mathbb{R}^{n \times d_p}$ , whose  $i$ -th rows are  $\mathbf{x}_i^T$  and  $\mathbf{z}_i^T$ , respectively. As

our target is a property of the underlying data-generating mechanism, not of a single dataset, we adopt a *population-level* viewpoint, i.e., we use random variables  $X, Z, R$  for task-relevant attributes, protected attributes, and the ranking respectively, and study the conditional-independence hypothesis  $H_0 : Z \perp\!\!\!\perp R \mid X$ .

For sake of completeness and clarity of treatment, we next recall the fundamental definition of a kernel function and its associated spaces, which will be used in the next section, pointing the reader to standard texts for comprehensive treatments [34, 48, 49].

**DEFINITION 1 (KERNEL FUNCTION).** Let  $X$  be a non-empty set. A function  $k : X \times X \rightarrow \mathbb{R}$  is a **kernel** if there exists a Hilbert space  $\mathcal{H}$  (a feature space) and a feature map  $\phi : X \rightarrow \mathcal{H}$  such that for all  $\mathbf{u}, \mathbf{u}' \in X$ , the kernel computes the inner product in  $\mathcal{H}$ :

$$k(\mathbf{u}, \mathbf{u}') = \langle \phi(\mathbf{u}), \phi(\mathbf{u}') \rangle_{\mathcal{H}}. \quad (1)$$

In our setting,  $X$  can be, e.g., the space of task attributes  $\mathbb{R}^{d_o}$  or protected attributes  $\mathbb{R}^{d_p}$ . To rigorously ground this feature space, we define a Reproducing Kernel Hilbert Space, which ensures that point evaluations are well-behaved.

**DEFINITION 2 (REPRODUCING KERNEL HILBERT SPACE (RKHS)).** Let  $\mathcal{H}$  be a Hilbert space of functions  $f : X \rightarrow \mathbb{R}$ .  $\mathcal{H}$  is a **Reproducing Kernel Hilbert Space** if, for all  $\mathbf{x} \in X$ , the linear evaluation functional  $L_{\mathbf{x}} : \mathcal{H} \rightarrow \mathbb{R}$  defined by  $L_{\mathbf{x}}(f) = f(\mathbf{x})$  is bounded. By the Riesz representation theorem [34], this implies that for every  $\mathbf{x} \in X$ , there exists a unique function  $k_{\mathbf{x}} \in \mathcal{H}$  (the representer of evaluation) such that the reproducing property holds:

$$f(\mathbf{x}) = \langle f, k_{\mathbf{x}} \rangle_{\mathcal{H}}, \quad \forall f \in \mathcal{H}. \quad (2)$$

By the Moore-Aronszajn theorem [48], every positive-definite kernel  $k$  is associated with a unique RKHS where  $k(\mathbf{u}, \mathbf{u}') = \langle k_{\mathbf{u}}, k_{\mathbf{u}'} \rangle_{\mathcal{H}}$ . A standard choice for continuous variables or rankings is the radial basis function (RBF) kernel:

$$k(\mathbf{u}, \mathbf{u}') = \exp\left(-\frac{\|\mathbf{u} - \mathbf{u}'\|^2}{2\sigma^2}\right), \quad (3)$$

where  $\sigma > 0$  is the bandwidth parameter. For categorical variables, a common choice is the exponentiated Hamming kernel:

$$k(\mathbf{u}, \mathbf{u}') = \exp(-\gamma \cdot d_H(\mathbf{u}, \mathbf{u}')), \quad (4)$$

where  $d_H(\mathbf{u}, \mathbf{u}')$  is the Hamming distance and  $\gamma > 0$  is an inverse width scaling parameter.

**DEFINITION 3 (GRAM MATRIX).** Given a kernel function  $k$  and a dataset of  $n$  individuals with attributes  $\{\mathbf{u}_1, \dots, \mathbf{u}_n\} \subseteq X$ , the **Gram matrix** (or **kernel matrix**)  $\mathbf{K} \in \mathbb{R}^{n \times n}$  is the symmetric, positive semi-definite matrix defined by the pairwise kernel evaluations [49]:

$$\mathbf{K}_{ij} = k(\mathbf{u}_i, \mathbf{u}_j) = \langle \phi(\mathbf{u}_i), \phi(\mathbf{u}_j) \rangle_{\mathcal{H}}, \quad \forall i, j \in \{1, \dots, n\}. \quad (5)$$

Next, given a Gram matrix  $\mathbf{K}$ , we define the **Ridge residualizer matrix**  $\mathbf{R} \in \mathbb{R}^{n \times n}$  as:

$$\mathbf{R} = \mathbf{I}_n - \mathbf{K}(\mathbf{K} + n\varepsilon\mathbf{I}_n)^{-1}, \quad (6)$$

where  $\varepsilon > 0$  is a regularization parameter and  $\mathbf{I}_n$  is the  $n \times n$  identity matrix. Furthermore, we define the **centering matrix**  $\mathbf{H} \in \mathbb{R}^{n \times n}$  as:

$$\mathbf{H} = \mathbf{I}_n - \frac{1}{n}\mathbf{1}\mathbf{1}^T, \quad (7)$$

where  $\mathbf{1} \in \mathbb{R}^n$  is the column vector of all ones.

Table 1 summarizes the main notations of the paper.

## 4.2 Auditing For Demographic Bias in Opaque Rankings

### 4 CONDOR

We next present in detail the CONDOR method (Algorithm 1), which builds upon both Partial Distance Correlation (pDCOR) [53] and the residualization machinery of kernel-based conditional independence tests, such as KCI [65].

**Intuition.** CONDOR begins by constructing Gram matrices (kernel similarity matrices) that capture the pairwise similarities between individuals regarding their task-relevant attributes ( $X$ ), protected attributes ( $Z$ ), and the observed ranking ( $r$ ). It then residualizes the ranking and protected attributes using a projection operator, effectively “subtracting” the variation that is already explained by the task-relevant attributes ( $X$ ). Next, it computes the distance correlation between these residualized embeddings to produce a Protected Attribution Score (PAS)  $\in [0, 1]$ , where higher values indicate a residual dependence on protected attributes. Finally, it performs a Conditional Randomization Test (CRT) to calibrate the PAS, generating a  $p$ -value to determine if the result is statistically significant against the null hypothesis  $H_0 : Z \perp\!\!\!\perp R | X$ .

**Formalization.** First, given positive semi-definite kernel functions  $k_X, k_Z, k_R$ , CONDOR computes the Gram matrices  $\mathbf{K}_X, \mathbf{K}_Z, \mathbf{K}_R$  as:

$$(\mathbf{K}_X)_{ij} = k_X(\mathbf{x}_i, \mathbf{x}_j); (\mathbf{K}_Z)_{ij} = k_Z(z_i, z_j); (\mathbf{K}_R)_{ij} = k_R(r(i), r(j)).$$

Then, it uses  $\mathbf{R}_X$ , the Ridge residualizer matrix derived from  $\mathbf{K}_X$ , to remove the variation from  $\mathbf{K}_Z$  and  $\mathbf{K}_R$  that is already explained by the task-relevant attributes  $X$ . This is achieved by left- and right-multiplying  $\mathbf{K}_Z$  and  $\mathbf{K}_R$  by  $\mathbf{R}_X$ . Hence, the resulting matrices  $\tilde{\mathbf{K}}_R = \mathbf{R}_X \mathbf{K}_R \mathbf{R}_X$  and  $\tilde{\mathbf{K}}_Z = \mathbf{R}_X \mathbf{K}_Z \mathbf{R}_X$  represent the remaining pairwise similarities once the effect of  $X$  has been removed. These similarities are transformed into pairwise distances, obtaining:

$$\tilde{\mathbf{D}}_{ij}^{(r)} = \tilde{\mathbf{K}}_{R,ii} + \tilde{\mathbf{K}}_{R,jj} - 2\tilde{\mathbf{K}}_{R,ij}, \quad \tilde{\mathbf{D}}_{ij}^{(z)} = \tilde{\mathbf{K}}_{Z,ii} + \tilde{\mathbf{K}}_{Z,jj} - 2\tilde{\mathbf{K}}_{Z,ij}.$$

Next, to ensure that comparisons depend only on relative distances, CONDOR applies double-centering by left- and right-multiplying by the centering matrix  $\mathbf{H}$ :

$$\tilde{\mathbf{D}}^{(z)} = \mathbf{H} \tilde{\mathbf{D}}^{(z)} \mathbf{H}, \quad \tilde{\mathbf{D}}^{(r)} = \mathbf{H} \tilde{\mathbf{D}}^{(r)} \mathbf{H}.$$

From these centered residual distances, we compute the distance-correlation Protected Attribute Score (PAS):

$$\text{PAS} := \text{dCOR}(\tilde{\mathbf{D}}^{(r)}, \tilde{\mathbf{D}}^{(z)}) \in [0, 1],$$

where dCOR is calculated as a normalized measure of association between the two double-centered distance matrices  $\tilde{\mathbf{D}}^{(r)}$  and  $\tilde{\mathbf{D}}^{(z)}$  [54]. Formally, letting  $(\mathbf{A}, \mathbf{B})_F = \sum_{i,j} A_{ij} B_{ij}$  denote the Frobenius inner product, the sample distance covariance is computed via the centered matrices as:

$$\text{dCov}(\mathbf{D}^{(r)}, \mathbf{D}^{(z)}) = \frac{1}{n^2} \langle \tilde{\mathbf{D}}^{(r)}, \tilde{\mathbf{D}}^{(z)} \rangle_F,$$

and the corresponding distance variances are  $\text{dVar}(\mathbf{D}^{(r)}) = \text{dCov}(\mathbf{D}^{(r)}, \mathbf{D}^{(r)})$  and  $\text{dVar}(\mathbf{D}^{(z)}) = \text{dCov}(\mathbf{D}^{(z)}, \mathbf{D}^{(z)})$ . The distance correlation is then obtained as:

$$\text{dCOR}(\tilde{\mathbf{D}}^{(r)}, \tilde{\mathbf{D}}^{(z)}) = \frac{\text{dCov}(\mathbf{D}^{(r)}, \mathbf{D}^{(z)})}{\sqrt{\text{dVar}(\mathbf{D}^{(r)}) \text{dVar}(\mathbf{D}^{(z)})}}. \quad (8)$$

which takes values in  $[0, 1]$ . CONDOR’s pseudocode is reported in Algorithm 1.

Table 1: Notation

Notation	Description
$\mathbf{x}_i, \mathbf{z}_i$	Feature vectors for individual $i$
$\mathbf{X}, \mathbf{Z}$	Matrices of task-relevant and protected attributes
$\mathbf{r}$	Observed ranking vector
$X, Z, R$	Population random variables
$k_X, k_Z, k_R$	Positive-semidefinite kernel functions
$\mathbf{K}_X, \mathbf{K}_Z, \mathbf{K}_R$	Gram (similarity) matrices from $k_X, k_Z, k_R$
$\mathbf{R}_X$	Ridge residualizer matrix
$\tilde{\mathbf{K}}_R, \tilde{\mathbf{K}}_Z$	Residualized kernel matrices (removing $X$ influences)
$\tilde{\mathbf{D}}^{(r)}, \tilde{\mathbf{D}}^{(z)}$	Kernel-induced distance matrices from $\tilde{\mathbf{K}}_R$ and $\tilde{\mathbf{K}}_Z$
$\mathbf{H}$	Centering matrix, $\mathbf{H} = \mathbf{I}_n - \frac{1}{n} \mathbf{1}\mathbf{1}^\top$
$\tilde{\mathbf{D}}^{(r)}, \tilde{\mathbf{D}}^{(z)}$	Double-centered residual distance matrices
dCov, dVar	Distance covariance and distance variance
dCOR	Distance correlation metric

#### Algorithm 1 CONDOR

**Input:** Observed data  $\mathbf{X} \in \mathbb{R}^{n \times d_X}$  (task attributes),  $\mathbf{Z} \in \mathbb{R}^{n \times d_Z}$  (protected attributes), ranking map  $r : [n] \rightarrow [n]$

**Output:** PAS  $\in [0, 1]$  – residual dependence of  $\mathbf{r}$  on  $\mathbf{Z}$  given  $\mathbf{X}$

1: **Step 1: Build kernel matrices.** Select positive-semidefinite kernels  $k_X, k_Z, k_R$ . Compute Gram matrices:

$$(\mathbf{K}_X)_{ij} = k_X(\mathbf{x}_i, \mathbf{x}_j), (\mathbf{K}_Z)_{ij} = k_Z(z_i, z_j), (\mathbf{K}_R)_{ij} = k_R(r(i), r(j)).$$

2: **Step 2: Remove predictable variation (residualization).**

Build the ridge residualizer in the RKHS of  $X$ :

$$\mathbf{R}_X = \mathbf{I}_n - \mathbf{K}_X (\mathbf{K}_X + n\epsilon \mathbf{I}_n)^{-1},$$

with a small regularization parameter  $\epsilon > 0$  (default  $10^{-3}$ ) to ensure numerical stability. Apply it to  $\mathbf{K}_Z$  and  $\mathbf{K}_R$ :

$$\tilde{\mathbf{K}}_Z = \mathbf{R}_X \mathbf{K}_Z \mathbf{R}_X, \quad \tilde{\mathbf{K}}_R = \mathbf{R}_X \mathbf{K}_R \mathbf{R}_X.$$

These residual kernels retain only the variation in  $\mathbf{Z}$  and  $\mathbf{r}$  that cannot be explained by  $X$ .

3: **Step 3: Convert residual kernels into distances.**

For all pairs  $i, j$ , convert similarities to kernel-induced distances:

$$\tilde{\mathbf{D}}_{ij}^{(z)} = \tilde{\mathbf{K}}_{Z,ii} + \tilde{\mathbf{K}}_{Z,jj} - 2\tilde{\mathbf{K}}_{Z,ij}, \quad \tilde{\mathbf{D}}_{ij}^{(r)} = \tilde{\mathbf{K}}_{R,ii} + \tilde{\mathbf{K}}_{R,jj} - 2\tilde{\mathbf{K}}_{R,ij}.$$

This expresses distance once the influence of  $X$  is removed.

4: **Step 4: Double-center the distance matrices.**

Let  $\mathbf{H} = \mathbf{I}_n - \frac{1}{n} \mathbf{1}\mathbf{1}^\top$ . Apply centering on both sides:

$$\tilde{\mathbf{D}}^{(z)} = \mathbf{H} \tilde{\mathbf{D}}^{(z)} \mathbf{H}, \quad \tilde{\mathbf{D}}^{(r)} = \mathbf{H} \tilde{\mathbf{D}}^{(r)} \mathbf{H}.$$

This operation removes global offsets (location effects) so that dependence is measured only through relative distances.

5: **Step 5: Compute distance-correlation dependence.** Define:

$$\text{dCov} = \frac{1}{n^2} \langle \tilde{\mathbf{D}}^{(r)}, \tilde{\mathbf{D}}^{(z)} \rangle_F, \quad \text{dVar}_r = \frac{1}{n^2} \langle \tilde{\mathbf{D}}^{(r)}, \tilde{\mathbf{D}}^{(r)} \rangle_F,$$

$$\text{dVar}_z = \frac{1}{n^2} \langle \tilde{\mathbf{D}}^{(z)}, \tilde{\mathbf{D}}^{(z)} \rangle_F.$$

Then set:

$$\text{PAS} = \text{dCOR}(\tilde{\mathbf{D}}^{(r)}, \tilde{\mathbf{D}}^{(z)}) = \frac{\text{dCov}}{\sqrt{\text{dVar}_r \text{dVar}_z}} \in [0, 1].$$

6: **return** PAS.

#### 4.1 PAS Characterization

We next provide the intuition of two key properties establishing the correctness of the PAS. For readability sake, the corresponding theorems are provided in the Appendix.

**Null Alignment:** If the ranking does not use  $Z$  beyond what  $X$  already explains (i.e., under the null hypothesis  $Z \perp R \mid X$ ), the population PAS score is exactly zero, and the sample estimate converges to zero as  $n$  grows (Theorem 2 in the Appendix). This ensures the score conceptually aligns with the conditional-independence null tested by the CRT (see Section 4.2).

**Local Sensitivity:** When the ranking  $R$  begins to leverage  $Z$  slightly beyond what  $X$  already explains, the population PAS departs from 0 linearly in relation to the small signal (Theorem 3 in the Appendix).

Taken together, these calibrated behaviors—at the null and under weak effects—justify reading PAS as a simple, model-agnostic effect size for the residual dependence of the ranking on  $Z$  beyond  $X$ .

#### 4.2 Statistical Calibration

To translate the PAS into a binary decision with finite-sample error control, we use conditional randomization [12, 17, 35] to test the null hypothesis  $H_0 : Z \perp R \mid X$ . This is how the Conditional Randomization Calibration (CRT) works in practice. We first fix the observed task attributes  $X$  and the ranking  $r$ , we regenerate protected attributes under a model that enforces  $H_0$ , and we ask how often the resulting score exceeds the observed one. Concretely, given an audit mapping  $\text{PAS}(X, Z, r) \in [0, 1]$ , compute  $s_{\text{obs}} = \text{PAS}(X, Z, r)$ ; fit a conditional model  $\hat{P}(Z \mid X)$  (e.g., logistic/multinomial models, tree-based conditionals, or CTGAN [59]); draw  $B$  independent resamples  $Z^{(b)} \sim \hat{P}(Z \mid X)$  and form  $s^{(b)} = \text{PAS}(X, Z^{(b)}, r)$  for  $b = 1, \dots, B$ . The one-sided Monte Carlo  $p$ -value is

$$p = \frac{|\{b : s^{(b)} \geq s_{\text{obs}}\}|}{B}. \quad (9)$$

For a pre-set level  $\alpha$  (e.g.,  $\alpha = 0.05$ ), reject when  $p \leq \alpha$ ; otherwise report “no evidence of residual use”. When benchmarking multiple audits on the same dataset, reuse the same  $\{Z^{(b)}\}_{b=1}^B$  to reduce Monte Carlo variability and ensure fair comparison. Larger  $B$  increases  $p$ -value resolution at linear computational cost; we used  $B = 1000$  in the experiments. CRT is finite-sample exact if  $P(Z \mid X)$  is known; with an estimate  $\hat{P}$ , sample-splitting or cross-fitting improves robustness [7]. The pseudocode of the CRT calibration is provided in Algorithm 2.

---

#### Algorithm 2 Conditional-Randomization Test

---

**Input:** Observed  $(X, Z, r)$ , function  $\text{PAS}(\cdot)$ , number of resamples  $B$

**Output:** One-sided  $p$ -value testing  $H_0 : R \perp Z \mid X$

- 1: **Step 1: Compute observed score.**  $s_{\text{obs}} \leftarrow \text{PAS}(X, Z, r)$ .
  - 2: **Step 2: Generate null resamples.** For  $b = 1, \dots, B$ : sample  $Z^{(b)} \sim \hat{P}(Z \mid X)$  (fitted from data), then compute  $s^{(b)} = \text{PAS}(X, Z^{(b)}, r)$ .
  - 3: **Step 3: Compute empirical tail probability**  $p$  as in Equation 4.2
  - 4: **return**  $(s_{\text{obs}}, p)$ .
- 

#### 4.3 Computational Complexity

We analyze the time complexity of CONDOR w.r.t. the sample size  $n$ , the dimension of task-relevant ( $d_o$ ) and protected attributes ( $d_p$ ), and the number of bootstrap resamples  $B$  used for calibration.

**Algorithm 1 - Step 1: Kernel Matrix Construction.** Constructing the Gram matrices requires computing pairwise similarities for all  $n$  individuals.

- For the task-relevant attributes  $K_X$  (using inputs  $X \in \mathbb{R}^{n \times d_o}$ ), the complexity is  $O(n^2 d_o)$ . Similarly, for the protected attributes  $K_Z$ , the complexity is  $O(n^2 d_p)$ .
- For the ranking  $K_R$ , the complexity is  $O(n^2)$ .

**Algorithm 1 - Step 2: Ridge Residualization.** This step involves two computationally intensive operations: Computing the ridge residualizer  $R_X = I_n - K_X(K_X + n\epsilon I_n)^{-1}$  requires inverting a dense  $n \times n$  matrix, which scales as  $O(n^3)$ ; applying the residualizer to obtain  $\tilde{K}_Z = R_X K_Z R_X$  and  $\tilde{K}_R = R_X K_R R_X$  requires dense matrix-matrix multiplication, scaling as  $O(n^3)$  for each kernel.

**Algorithm 1 - Steps 3–5: Distance Conversion and Correlation.** Converting kernel matrices to distances ( $\tilde{D}^{(z)}, \tilde{D}^{(r)}$ ), performing double-centering via  $H$ , and computing the final distance correlation involve element-wise operations on  $n \times n$  matrices. The total complexity for these steps is  $O(n^2)$ .

**Statistical Calibration (Algorithm 2).** CRT repeats the score calculation for  $B$  resamples to generate a  $p$ -value. Since  $X$  and the ranking  $r$  remain fixed throughout the permutation test, the residualizer  $R_X$  and the residualized ranking kernel  $\tilde{K}_R$  can be pre-computed only once at the cost of  $O(n^3 + n^2 d_o)$ . Then, for each  $b \in \{1, \dots, B\}$  (bootstrap loop):

- **Resampling (Step 1):** Generating new protected attributes  $Z^{(b)}$  and building the corresponding kernel  $K_{Z^{(b)}}$  takes  $O(n^2 d_p)$ .
- **Projection (Step 2):** The new protected kernel must be projected into the residual space:  $\tilde{K}_{Z^{(b)}} = R_X K_{Z^{(b)}} R_X$ . This matrix multiplication is the bottleneck of the loop, scaling as  $O(n^3)$ .
- **Scoring (Steps 3–5):** Re-evaluating the PAS takes  $O(n^2)$ .

**Total Complexity.** Aggregating the costs from Algorithm 1 and Algorithm 2, the total time complexity is:  $O(n^2 d_o + B \cdot (n^3 + n^2 d_p))$ .

While the algorithm scales linearly with the feature dimension  $d_p$ ,  $d_o$  and the number of resamples  $B$ , it is cubic with respect to the sample size  $n$  due to matrix multiplications required during the residualization of  $Z$ .

**Scalable Approximations.** This  $O(n^3)$  bottleneck can be effectively circumvented using standard scalable kernel techniques. Replacing direct matrix factorizations with Krylov iterative solvers (e.g., Conjugate Gradient or MINRES) [29, 38, 45] reduces the inversion cost to a sequence of  $T$  matrix-vector multiplications. By further combining this with low-rank approximations, such as the Nyström method or Random Fourier Features using  $m \ll n$  components [13, 27, 58], the memory footprint drops from  $O(n^2)$  to  $O(nm)$ . Correspondingly, the bottleneck time complexity reduces to  $O(Tnm)$  or  $O(nm^2)$  (where  $T$  is the number of solver iterations), allowing CONDOR to scale efficiently to large datasets without computing the exact dense matrices.

5

## 5 CAUSAL INTERPRETATION

CONDOR captures the residual dependence of the ranking on protected attributes, once task-relevant observables are accounted for. As anticipated in Section 1, to have an effective audit we need to adopt the formal language of causality [6, 20]. By combining the the conditional-independence test  $Z \perp\!\!\!\perp R \mid X$  of CONDOR with an unconditional test  $Z \perp\!\!\!\perp R$ , while properly keeping in account the causal assumptions at the basis of our setting, we obtain the  $2 \times 2$  matrix in the right-most panel of Figure 1. We next prove that the causal structures provided in the  $2 \times 2$  matrix are correct.

First, let us observe that by the characteristics of our setting, we have the following causal assumptions:

- (1)  $X$  is a cause of  $R$ , ( $X \rightarrow R$ ): whatever algorithm has been used to produce  $R$ , it surely has seen as (part of the) input the task-relevant attributes  $X$ , as there is no other type of information available (besides the “forbidden”  $Z$ ).
- (2)  $R$  cannot be a cause of  $X$  ( $R \not\rightarrow X$ ): whatever is the decision-making process, the output ( $R$ ) cannot be a cause of the input ( $X$ ), as the input *existed before* the output.
- (3)  $Z$  does not have any ancestors ( $\nexists U : U \rightarrow Z$ ): as often is the case, we assume that the demographic attributes such as gender or race are not determined by any cause.

Next, we recall that in a Structural Causal Model, which uses a DAG (directed acyclic graph) to represent the causal relations, the key notion of **directional separation** (see e.g., [23, 42]) determines that two variables are conditionally independent if all informational paths between them are “blocked”. Conversely, they are dependent if there exists at least an “open path” between them.

**DEFINITION 4 (d-SEPARATION).** Let  $C \subseteq V$  be a set of variables we condition on. Two nodes  $A, B \in V$  are said to be *d-separated* by  $C$  if every path (considered on the undirected version of the DAG) between them is “blocked” by the conditioning set  $C$ . A path  $P$  is blocked by  $C$  if it satisfies any of the following conditions:

- **Chain:**  $P$  contains a chain  $A \cdots \leftarrow M \leftarrow \cdots B$  or  $A \cdots \rightarrow M \rightarrow \cdots B$ , and the middle node  $M$  is conditioned on (i.e.,  $M \in C$ ).
- **Fork:**  $P$  contains a fork  $A \cdots \leftarrow M \rightarrow \cdots B$ , and the middle node  $M$  is conditioned on (i.e.,  $M \in C$ ).
- **Collider:**  $P$  contains a collider  $A \cdots \rightarrow M \leftarrow \cdots B$ , such that the collision node  $M$  is not conditioned on ( $M \notin C$ ) and no descendant of  $M$  is conditioned on (i.e.,  $\text{Desc}(M) \cap C = \emptyset$ ).

We consider the following two statements:

**S1:**  $Z$  is unconditionally independent of  $R$  ( $Z \perp\!\!\!\perp R$ );

**S2:**  $Z$  is conditionally independent of  $R$ , given  $X$  ( $Z \perp\!\!\!\perp R \mid X$ ).

Our analysis of the four scenarios hinges on which paths are open or blocked by default (S1) and which become open or blocked after conditioning on  $X$  (S2).

**THEOREM 1.** Under the causal assumptions (1)-(3) above, based on the truthfulness of S1 and S2 the following four cases hold:

- (I)  $S1 \wedge S2 \implies Z$  is unrelated to  $X \rightarrow R$
- (II)  $S1 \wedge \neg S2 \implies$  causally impossible
- (III)  $\neg S1 \wedge S2 \implies Z \rightarrow X \rightarrow R$
- (IV)  $\neg S1 \wedge \neg S2 \implies Z \rightarrow R$

**PROOF.** We prove the four mutually exclusive cases.

(I) Satisfying S1 ( $Z \perp\!\!\!\perp R$ ): For  $Z$  and  $R$  to be unconditionally independent, there must be no open paths between them. Given the constraints (1)-(3), the absence of open paths requires: that  $Z$  does not cause  $R$  directly ( $Z \not\rightarrow R$ ), and that  $Z$  does not cause  $X$  ( $Z \not\rightarrow X$ ), otherwise the path  $Z \rightarrow X \rightarrow R$  would be open. Furthermore, no fork due to a confounder  $U$  ( $Z \leftarrow U \rightarrow R$  or  $Z \leftarrow U \rightarrow X$ ) is possible due to constraint (3) ( $U$  cannot be ancestor of  $Z$ ).

Satisfying S2 ( $Z \perp\!\!\!\perp R \mid X$ ): If no path exists between  $Z$  and  $R$ , then conditioning on any set of variables, including  $X$ , cannot create or open a path. Thus, independence holds trivially. Therefore, the only viable causal structure is when  $Z$  is isolated from  $X \rightarrow R$ .

(II) There is no open path between  $Z$  and  $R$  (S1), but conditioning on  $X$  creates an open path (S2). This requires  $X$  to be a collider on a path  $P$  between  $Z$  and  $R$ , or a descendant of such a collider.

- Case 1:  $X$  is the collider. The path is  $Z \rightarrow X \leftarrow R$ . This graph violates constraint (2) which states  $R \not\rightarrow X$ .
- Case 2:  $X$  is a descendant of the collider ( $C \rightarrow X$ ). The path is  $Z \rightarrow C \leftarrow R$  with  $C \rightarrow X$ . Adding constraint (1),  $X \rightarrow R$ , produces the structure  $R \rightarrow C \rightarrow X \rightarrow R$ , which is a causal cycle, violating the acyclicity assumption of causal structures.

Therefore, the case  $S1 \wedge \neg S2$ , is causally impossible.

(III) We seek a DAG where an open path exists between  $Z$  and  $R$  ( $\neg S1$ ), such that it is blocked by conditioning on  $X$  (S2). This requires  $X$  to be a non-collider (chain or fork center) on every path. Only two structures are possible:

- Chain:  $Z \rightarrow X \rightarrow R$ , which satisfies all requirements;
- Fork center:  $Z \leftarrow U \rightarrow X \rightarrow R$ , which is not admissible due to constraint (3) ( $U$  cannot be ancestor of  $Z$ ).

(IV) We seek a DAG where at least one path is open ( $\neg S1$ ), and at least one path remains open after conditioning on  $X$  ( $\neg S2$ ). This implies the existence of an unblocked path between  $Z$  and  $R$  bypassing  $X$ . Only three structures are, in principle, possible:

- Direct link bypass:  $Z \rightarrow R$ .
- Direct link bypass + chain: besides  $Z \rightarrow R$  a second path  $Z \rightarrow X \rightarrow R$  might exist. However, from an auditing standpoint, the second path is less relevant than the fact that  $Z \rightarrow R$ .
- Confounding bypass:  $Z \rightarrow X \rightarrow R$  and  $Z \leftarrow U \rightarrow R$  which is not viable due to constraint (3).

In both of the first two structures holds  $Z \rightarrow R$ , which proves case (IV), concluding our proof.  $\square$

**Connection to Interventional Fairness.** Our causal diagnostic framework is deeply connected to the concept of *interventional fairness* [47]. A system is considered interventional fair if changing an individual’s protected attribute does not affect their outcome, assuming all legitimate, task-relevant features are held constant. While formally proving this requires knowing the system’s exact internal causal rules, CONDOR provides a practical, observational proxy. Under our causal assumptions, passing the CONDOR audit provides strong empirical evidence that an opaque ranking mechanism is interventional fair, as it rules out direct discrimination.

6

## 6 EXPERIMENTAL SETTINGS

In this section, we describe the datasets (synthetic and real-world) and the baselines. Finally, we introduce the specific unconditional dependence test that we couple with CONDOR to provide the final causal interpretation.

### 6.1 Synthetic Data and Ranking Generation

We next present the process to generate synthetic data where we can control the influence of  $Z$  over  $X$ , and the influence of  $Z$  and  $X$  over  $r$ . We create cohorts of size  $n$ , with task-relevant features  $\mathbf{X} \in \mathbb{R}^{n \times d_o}$ , protected features  $\mathbf{Z} \in \mathbb{R}^{n \times d_p}$ , and a ranking  $r$ . The generation process proceeds as follows:

(1) **Draw protected features  $Z$ :**  $Z$  is drawn from a *Gaussian Cluster Generation* process:  $k_q$  cluster centers are picked in  $d_p$ -dimensional space, and  $n$  samples are drawn from Gaussian distributions centered at a randomly assigned cluster mean.

(2) **Draw latent features  $T$ :** Latent task factors  $T \in \mathbb{R}^{n \times d_o}$  are generated using the same Gaussian Cluster process described in step (1).

(3) **Generate task-relevant features  $X$ :** We generate  $X$  combining latent factors and protected attributes, controlled by an entanglement parameter  $\gamma \in [0, 1]$ :

$$\mathbf{X} = \gamma \mathbf{T} + (1 - \gamma) \mathbf{Z}' + \boldsymbol{\varepsilon}_X,$$

where  $\mathbf{Z}'$  is a projection of  $\mathbf{Z}$  onto  $\mathbb{R}^{n \times d_o}$ , and where the  $i$ -th row of  $\boldsymbol{\varepsilon}_X$  is  $\varepsilon_{X,i} \stackrel{\text{i.i.d.}}{\sim} \mathcal{N}(0, \Sigma_X)$ . Here,  $\gamma = 1$  implies  $\mathbf{X} \perp \mathbf{Z}$  (independence), while  $\gamma = 0$  implies  $X$  is fully determined by  $Z$ .

(4) **Generate underlying scores  $s$ :** We generate scores as a convex combination of task and protected components, controlled by an entanglement parameter  $\beta \in [0, 1]$ :

$$s = (1 - \beta) s_X + \beta s_Z + \boldsymbol{\varepsilon}_s, \quad \text{with } \boldsymbol{\varepsilon}_s \sim \mathcal{N}(0, \sigma_s^2 \mathbf{I}_n).$$

We use linear projections  $s_X = \mathbf{X} \mathbf{w}_X$  and  $s_Z = \mathbf{Z} \mathbf{w}_Z$  (with uniform weights  $\mathbf{w}_X \in \mathbb{R}^{d_o}$  and  $\mathbf{w}_Z \in \mathbb{R}^{d_p}$ ).  $\beta$  governs direct bias:  $\beta = 0$  yields scores dependent only on  $X$ , while  $\beta = 1$  yields scores dependent only on  $Z$ .

(5) **Generate final ranking  $r$ :** Individuals are sorted by  $s$ , and ranks are normalized:  $r_i := (\text{pos}_i - 0.5)/n$ .

In our experiments,  $\gamma$  and  $\beta$  vary across  $[0, 1]$ . Further specific parametrizations are detailed in Section 7.

### 6.2 Real Data

We use five publicly-available real-world datasets:

- **ADULT:** Individuals with demographic and work information [14] (individuals  $n = 48842$ , number of task-relevant features  $d_o = 12$ , number of protected features  $d_p = 2$ ). Task: ranking for high income potential.
- **COMPAS:** Data on criminal defendants used to generate recidivism risk scores [3] ( $n = 6172$ ,  $d_o = 9$ ,  $d_p = 2$ ). Task: ranking based on likelihood of recidivism.
- **LAW SCHOOL:** Individuals with law school admission records including LSAT and GPA [44] ( $n = 20798$ ,  $d_o = 2$ ,  $d_p = 2$ ). Task: ranking for law school success.

- **STUDENT PERFORMANCE:** Students with demographic, social, and school-related information from two Portuguese schools [10] (individuals  $n = 1044$ ,  $d_o = 30$ ,  $d_p = 2$ ). Task: ranking for academic performance.
- **STRESS LEVEL:** Individuals with smartphone usage behavior, sleep patterns, and productivity analytics [2] ( $n = 50000$ ,  $d_o = 9$ ,  $d_p = 2$ ). Task: ranking for stress levels.

Real-world data allows us to test CONDOR in realistic scenarios where complex relationships between  $X$  and  $Z$  exist naturally in the data (beyond our control). We exploit this in two different ways.

**Grey-Box Ranker.** In Section 7.2, we assess performance with real-world feature distributions and correlations while still maintaining control over the influence of  $Z$  and  $X$  over  $r$ . We first estimate one-sided scoring functions from the observed data,

$$s_X := f_X(\mathbf{X}), \quad s_Z := f_Z(\mathbf{Z}).$$

When  $Y$  is binary, we take  $s_X = \widehat{\mathbb{P}}(Y = 1 | \mathbf{X})$  and  $s_Z = \widehat{\mathbb{P}}(Y = 1 | \mathbf{Z})$  from off-the-shelf probabilistic classifiers (e.g., logistic regression or XGBoost) trained with 5-fold cross-validation. We then mix the two components through a direct-influence knob  $\beta \in [0, 1]$  and add noise,

$$\mathbf{s} = (1 - \beta) \mathbf{s}_X + \beta \mathbf{s}_Z + \boldsymbol{\varepsilon}_s, \quad \boldsymbol{\varepsilon}_s \sim \mathcal{N}(0, \sigma_s^2 \mathbf{I}_n),$$

and obtain the final ranking  $r$  by sorting  $s$  and normalizing the ranks via

$$r_i := (\text{pos}_i - 0.5)/n.$$

This construction injects a controlled amount of  $Z$ -driven signal (through  $\beta$ ) while preserving the empirical correlation structure within  $X$  and between  $X$  and  $Z$ .

**Black-Box Ranker.** In Section 7.4, we use real-world features and employ as ranker directly the ‘‘target’’ feature provided in the dataset. This allows us to test CONDOR in a truly black-box setting where we ignore the inner logic that produced the ranking.

### 6.3 Baselines

We consider three baseline methods to test for conditional independence between  $R$  and  $Z$  given  $X$ .

**KCI [65].** Kernel Conditional Independence estimates residual dependence between  $Z$  and  $r$  after regressing out  $X$  in the RKHS induced by a positive-definite kernel  $k_X$ . Defining

$$\mathbf{R}_X = \mathbf{I}_n - \mathbf{K}_X (\mathbf{K}_X + n\boldsymbol{\varepsilon} \mathbf{I}_n)^{-1},$$

the residualized kernel matrices are  $\widetilde{\mathbf{K}}_R = \mathbf{R}_X \mathbf{K}_R \mathbf{R}_X$  and  $\widetilde{\mathbf{K}}_Z = \mathbf{R}_X \mathbf{K}_Z \mathbf{R}_X$ . The empirical dependence is then measured by the Hilbert-Schmidt covariance:

$$\text{KCI}_n(r, z | \mathbf{x}) = \frac{1}{(n-1)^2} \text{tr}(\widetilde{\mathbf{K}}_R \mathbf{H} \widetilde{\mathbf{K}}_Z \mathbf{H}),$$

which is then normalized by the kernel self-variances. The p-value is then obtained generating the approximate null distribution with Monte Carlo simulation by computing a weighted sum of chi-squared samples [65]. We used the publicly available implementation from the Python library Causal-learn [66].

**PDCOR [53].** Partial distance correlation instead operates on pairwise distances, projecting out the contribution of  $X$  at the level of distance matrices. For centered distance matrices

7

$\bar{D}^{(r)}, \bar{D}^{(z)}, \bar{D}^{(x)}$ —obtained by left- and right-multiplying each pairwise distance matrix by  $H = I_n - \frac{1}{n}\mathbf{1}\mathbf{1}^\top$ —one computes

$$\text{pDCOR}(r, z | x) = \frac{\text{dCOR}_{r,z} - \text{dCOR}_{r,x} \text{dCOR}_{z,x}}{\sqrt{(1 - \text{dCOR}_{r,x}^2)(1 - \text{dCOR}_{z,x}^2)}}, \quad (10)$$

where  $\text{dCOR}$  is defined as in Equation 8,  $\text{dCOR}_{r,z} = \text{dCOR}(\bar{D}^{(r)}, \bar{D}^{(z)})$ ,  $\text{dCOR}_{r,x} = \text{dCOR}(\bar{D}^{(r)}, \bar{D}^{(x)})$ , and  $\text{dCOR}_{z,x} = \text{dCOR}(\bar{D}^{(z)}, \bar{D}^{(x)})$ . This closed form yields a normalized measure in  $[-1, 1]$ , interpretable as the correlation between residualized distance-embeddings of  $r$  and  $z$ . The  $p$ -value is then computed via a non-parametric permutation test, as provided in the Python library Hyppo [39].

**CMI (Conditional Mutual Information)** [11, 21, 32, 55]. Conditional Mutual Information (CMI) is an information-theoretic quantity that measures how much additional information the protected attributes  $Z$  provide about the ranking  $r$  once the observable attributes  $X$  are known. Formally, it is defined as

$$I(R; Z | X) = \mathbb{E} \left[ \log \frac{p(r, z | x)}{p(r | x) p(z | x)} \right] \geq 0,$$

and equals zero if and only if  $R$  and  $Z$  are conditionally independent given  $X$  [11]. This makes CMI a natural population-level analogue of our auditing null  $H_0 : R \perp\!\!\!\perp Z | X$ . We used the publicly available Python library npeet [56] and we calibrate CMI via the Conditional-Randomization Test, as done with CONDOR, to obtain a  $p$ -value assessing evidence against  $H_0$ .

#### 6.4 Unconditional Test

We adopt HSIC [26] as our test for **unconditional independence**,  $R \perp\!\!\!\perp Z$ . HSIC correspond to an unconditional version of KCI. In more details, let  $k_r, k_z$  be positive-definite kernels on the domains of  $r, z$ , again define the  $n \times n$  Gram matrices  $(K_r)_{ij} = k_r(r_i, r_j)$ ,  $(K_z)_{ij} = k_z(z_i, z_j)$ , then HSIC is defined as:

$$\text{HSIC}(r, z) = \frac{\text{tr}(K_r H K_z H)}{\sqrt{\text{tr}(K_r H K_r H) \text{tr}(K_z H K_z H)}} \in [0, 1].$$

The  $p$ -value is then computed as in [65], using the open source Python library Hyppo [39].

## 7 EXPERIMENT RESULTS

The goal of our empirical assessment is to answer the following research questions:

- RQ1:** How accurately can CONDOR detect the influence of protected attributes  $Z$  on ranking  $r$  in a fully controlled setting, with varying levels of influence of  $Z$  over  $X$ , and of  $Z$  and  $X$  over  $r$ ?
- RQ2:** How does CONDOR performs when applied to real-world feature distributions with naturally occurring correlations? Furthermore, does it reliably avoid false positives when tested against spurious correlations (e.g., random noise as a protected attribute)?
- RQ3:** When paired with an unconditional independence test, can CONDOR effectively distinguish between the ideal scenario of no influence of  $Z$  on  $r$ , indirect influence mediated by  $X$ , and direct influence?

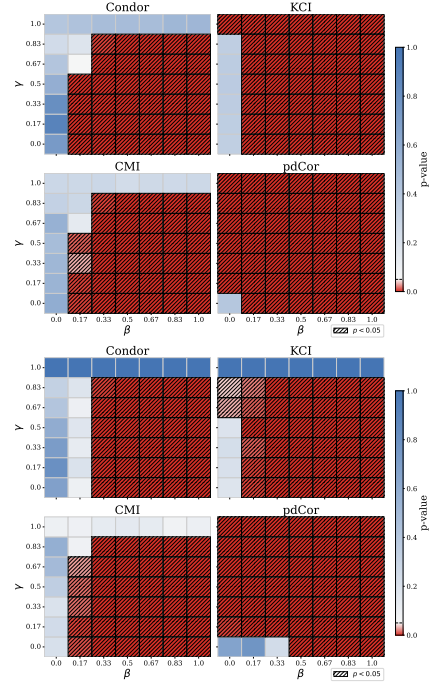


**Figure 2: Heatmap of  $p$ -values on synthetic data ( $n=1000$ ,  $k_x=k_t=5$ ). Top four heatmaps:  $d_0=5$ ,  $d_p=2$ . Bottom four heatmaps:  $d_0=10$ ,  $d_p=5$ . Each panel corresponds to one scoring rule; axes report the influence of  $X$  on  $Z$  ( $\gamma$ ) and of  $Z$  on the ranking ( $\beta$ ), and the red/white/blue scale marks respectively strong evidence against, the  $\alpha = 0.05$  boundary, and little evidence against  $H_0 : R \perp\!\!\!\perp Z | X$ .**

**RQ4:** How does CONDOR work as an audit in a purely black-box setting?

**RQ5:** How does CONDOR compare to the baselines in terms of run-time?

### 7.1 Synthetic Data (RQ1)

We evaluate the performance of CONDOR and the baseline methods in detecting conditional dependence  $H_0 : R \perp\!\!\!\perp Z | X$ . We present the results as heatmaps of  $p$ -values, where red indicates strong evidence against  $H_0$  ( $p \leq 0.05$ ), blue indicates little evidence against  $H_0$ , and white corresponds to boundary values. Figure 2 show the  $p$ -value heatmaps for two synthetic data settings, with different numbers of protected and task features. The  $x$ -axis ( $\beta$ ) controls the direct influence of the protected attribute  $Z$  on the ranking score  $S$ , while the  $y$ -axis ( $\gamma$ ) controls the dependence between  $Z$  and the task-relevant features  $X$ .

## 4.2 Auditing For Demographic Bias in Opaque Rankings

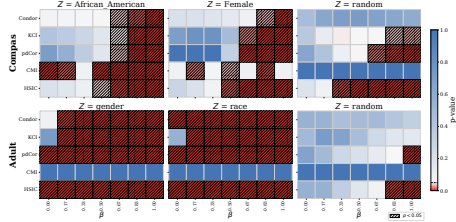


**Figure 3: COMPAS and ADULT datasets.** Heatmap of  $p$ -values on COMPAS and ADULT rankings. Each row corresponds to one dataset and each heatmap to a specific composition of the protected features  $Z$ . For each heatmap, the scoring rule is reported on the row and on the columns the influence of  $Z$  on the ranking ( $\beta$ ), and the red/white/blue scale marks respectively strong evidence against, the  $\alpha = 0.05$  boundary, and little evidence against  $H_0: R \perp\!\!\!\perp Z \mid X$ .

The ideal audit tool should reject  $H_0$  (show red) for  $\beta > 0$ , as this is when  $Z$  has a direct influence on the ranking  $R$  that is not mediated by  $X$ . The result should be insensitive to  $\gamma < 1$ , which only models the correlation between  $X$  and  $Z$  (a potential source of indirect discrimination, but not a violation of  $H_0$ ). Furthermore, in the special case of  $\gamma = 1$ , which indicates that  $X$  contains fully  $Z$  (or all its information), a method should indicate the independence between  $R$  and  $Z$  given  $X$  (blue), since conditioning on  $X$  is removing all the information on  $Z$ .

As shown in the figure, CONDOR achieves this ideal behavior. It reliably shows high  $p$ -values (blue) in the first column where  $\beta = 0$ , correctly finding no evidence of residual dependence. For all columns where  $\beta > 0$ , it shows low  $p$ -values (red or white if close to the boundary), successfully detecting the injected direct bias, regardless of the value of  $\gamma$ .

KCI, instead, fails in the case of  $\gamma = 1$  in the top heatmap of Figure 2 and also over-rejects the null when  $\beta = 0$ , in two cases in the bottom heatmap. CMI performs similarly to CONDOR on this synthetic-data setting, however, as we will see in the rest of this section, it does not perform as expected when dealing with the complex relationships of real data. Finally, pdCOR over-reject the null hypothesis in all cases, except when  $\beta = \gamma = 0$ .

### 7.2 Real Data with Grey-Box Ranker (RQ2)

Figure 3 presents the results from the COMPAS and ADULT datasets with generated rankings. Here, we only vary  $\beta$ , as the complex real-world relationship between  $X$  and  $Z$  is given by the datasets themselves. We test using different protected attributes  $Z$  for each dataset, and we also include a  $Z = \text{random}$  case as a sanity check, where the protected attribute  $Z$  is replaced with random noise and no dependence should be found.

For the protected attributes, CONDOR, KCI, and pdCOR show similar results, in particular, it is reasonable and correct that with the increase of  $\beta$  the methods reject more and more the null hypothesis, indicating the conditional dependence between the protected attributes and the ranking. CMI, on the other hand, does not exhibit this desired behaviour. In the  $Z = \text{random}$  control case, CONDOR

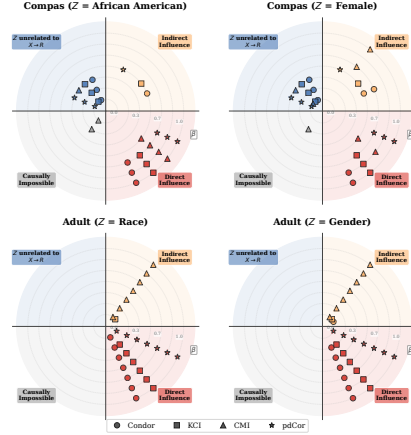


**Figure 4: The four panels map the audit outcomes for the COMPAS and ADULT datasets onto the  $2 \times 2$  causal matrix introduced in Figure 1.** Each marker represents an audited ranking, with concentric dotted lines indicating the strength of the injected direct bias ( $\beta$ ). As the true bias  $\beta$  increases (moving outward from the center), CONDOR correctly tracks the transition from no influence ( $\beta \approx 0$ ) to either “Direct Influence” or “Indirect Influence” ( $\beta > 0$ ), successfully diagnosing the causal structure of the opaque ranker.

correctly reports high  $p$ -values (blue) for all  $\beta$ , confirming it does not find spurious correlations. KCI and pdCOR, instead, fail and reject the null in this scenario.

### 7.3 Causal Interpretation (RQ3)

We now show how CONDOR can be combined with an unconditional test to understand the possible causal relationships between the protected attributes, the ranking, and the task features. As mentioned, we use HSIC as an unconditional test; however, in principle, any other unconditional test can be used.

The empirical analysis is reported in Figure 4. In each figure, the four quadrants correspond to the four quadrants of the  $2 \times 2$  matrix on Figure 1. Concentric circular lines represent different values of the parameter  $\beta$ , which controls the influence of  $Z$  on  $R$ : recall that  $\beta = 0$  indicates that the ranking only depends on the task-relevant features  $X$ , while  $\beta = 1$  indicates that the ranking depends only on the protected attributes  $Z$ . It is worth recalling that, for both datasets, this analysis is not directly on the datasets themselves, but it represents an audit of the ranking produced according to the procedure described in Section 4.2.

First, we can observe that the *causally impossible* remains rightfully unpopulated in all the experiments, with the exception of CMI which, however, already showed discordant behaviours in Section 7.2. In the COMPAS dataset, we observe that, for both settings of  $Z$ , when the impact of  $Z$  on the ranking is small ( $\beta < 0.5$ ) all the methods correctly report the first quadrant ( $Z$  (unrelated to

## 4.2 Auditing For Demographic Bias in Opaque Rankings

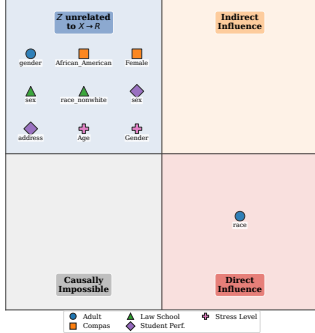


Figure 5: Causal interpretation of CONDOR’s audit on fully black-box models.

$X \rightarrow R$ ). As  $\beta$  increases, all the methods start signaling  $Z \rightarrow R$ . When  $\beta$  is neither too strong nor too weak, we can observe some influence of  $Z$  on  $X$ , i.e., the quadrant  $Z \rightarrow X \rightarrow R$ . In the ADULT dataset, the influence of  $Z$  on the original binary label of the dataset is very strong, and thus it remains strong in the ranking we generated according to the procedure described in Section 4.2. That explains why all the methods are concordant in producing  $Z \rightarrow R$ , with again the exception of CMI.

### 7.4 Complete Black-Box Setting (RQ4)

We now apply CONDOR as an auditor on fully black box and fully empirical data, to reproduce a real life application example.

Figure 5 maps various protected attributes ( $Z$ ) from five real-world datasets (ADULT, COMPAS, LAW SCHOOL, STUDENT PERFORMANCE, and STRESS LEVEL) onto the four quadrants of the causal interpretation matrix. Most protected attributes fall into the top-left quadrant, indicating no influence. Conversely, the *race* attribute in the ADULT dataset falls into the bottom-right quadrant, revealing a direct influence on the ranking.

### 7.5 Run-time Analysis (RQ5)

In Figure 6, we report the runtime of CONDOR and the baselines. The linear growth of CONDOR in the log-log plot confirms the polynomial runtime, w.r.t. the input size  $n$ , proven in Section 4.3. As expected, KCI which has the same complexity of CONDOR, shows the same asymptotic runtime. Also as expected, CMI is faster, while pdCOR is significantly slower.

## 8 CONCLUSIONS

In this work, we introduced CONDOR, a model-agnostic framework designed to audit opaque ranking systems for demographic bias. By bridging reproducing kernel Hilbert space (RKHS) residualization with distance correlation, CONDOR rigorously isolates and quantifies the residual influence of protected attributes beyond legitimate, task-relevant features. Beyond its practical utility, our framework is backed by solid theoretical guarantees: we prove that the Protected Attribution Score ensures exact null alignment under conditional

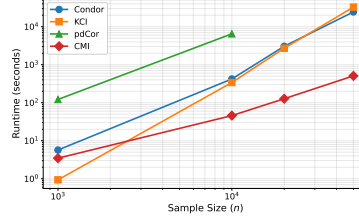


Figure 6: Runtime (in seconds) of each method as a function of the sample size  $n$  on synthetic data with  $d_o = d_p = 5$ ,  $\gamma = \beta = 0.5$ ,  $K = 5$  folds and  $B = 200$  permutations per fold. Both axes use a logarithmic scale. Experiments are run on a CPU Intel Xeon Gold 6248R, with 172 GB of RAM, running Ubuntu 24.04 LTS with Python 3.12.3.

independence and exhibits predictable local sensitivity to emerging biases. Furthermore, by pairing this conditional test with an unconditional independence baseline, we provide a comprehensive causal diagnostic tool capable of distinguishing between direct discrimination and indirect, feature-mediated influence.

Our empirical evaluation confirms that CONDOR is robust, natively accommodates mixed data types, and reliably outperforms established statistical baselines across both synthetic and real-world scenarios. Ultimately, CONDOR equips auditors with a practical, statistically sound forensic tool to hold black-box systems accountable. Moving forward, we plan to extend this framework toward prescriptive auditing, translating statistical bias signals into concrete, accountable rank interventions that restore conditional independence under explicit utility budgets, and to broaden its scope to encompass intersectional fairness guarantees.

## A APPENDIX

**THEOREM 2 (NULL ALIGNMENT AND SAMPLE CONVERGENCE).** Assume i.i.d. sampling of  $(R, Z, X)$ . Let  $\phi_R : R \rightarrow \mathcal{H}_R$  and  $\phi_Z : Z \rightarrow \mathcal{H}_Z$  be feature maps into separable Hilbert spaces, and assume

$$\mathbb{E} \|\phi_R(R)\|_{\mathcal{H}_R}^4 < \infty, \quad \mathbb{E} \|\phi_Z(Z)\|_{\mathcal{H}_Z}^4 < \infty.$$

Define the population residual features

$$\tilde{\phi}_R := \phi_R(R) - \mathbb{E}[\phi_R(R) | X], \quad \tilde{\phi}_Z := \phi_Z(Z) - \mathbb{E}[\phi_Z(Z) | X],$$

and adopt the normalization under which, for any Hilbert-valued random elements  $U, V$  with finite second moments,

$$d\text{Cov}_*^2(U, V) = \|\text{Cov}(U, V)\|_{\text{HS}}^2.$$

If  $Z \perp\!\!\!\perp R | X$ , then  $\text{PAS}_* := d\text{COR}(\tilde{\phi}_R, \tilde{\phi}_Z) = 0$ .

Moreover, for each sample size  $n$  suppose there exist measurable maps  $f_{R,n}, f_{Z,n} : R \times Z \times X \rightarrow \mathcal{H}_R, \mathcal{H}_Z$  such that, for i.i.d. copies  $\{(R_i, Z_i, X_i)\}_{i=1}^n$  of  $(R, Z, X)$ ,

$$\tilde{\phi}_R^{(i)} = f_{R,n}(R_i, Z_i, X_i), \quad \tilde{\phi}_Z^{(i)} = f_{Z,n}(R_i, Z_i, X_i), \quad i = 1, \dots, n,$$

and  $f_{R,n}(R, Z, X) \rightarrow \tilde{\phi}_R$ ,  $f_{Z,n}(R, Z, X) \rightarrow \tilde{\phi}_Z$  in  $L_2$ .

Assume in addition that the fourth moments are uniformly bounded:

$$\sup_n \mathbb{E} \|f_{R,n}(R, Z, X)\|_{\mathcal{H}_R}^4 < \infty, \quad \sup_n \mathbb{E} \|f_{Z,n}(R, Z, X)\|_{\mathcal{H}_Z}^4 < \infty.$$

## 4.2 Auditing For Demographic Bias in Opaque Rankings

Let  $\widehat{\text{PAS}}$  be the usual sample distance correlation (U- or V-statistic) computed from  $\{(\widehat{\phi}_R^{(i)}, \widehat{\phi}_Z^{(i)})\}_{i=1}^n$ . Then, under  $Z \perp\!\!\!\perp R \mid X$ ,

$$\widehat{\text{PAS}} \xrightarrow{\mathbb{P}} 0 \quad \text{as } n \rightarrow \infty.$$

**PROOF.** Population. Set  $U := \phi_R(R) \in \mathcal{H}_R$ ,  $V := \phi_Z(Z) \in \mathcal{H}_Z$ . By the fourth-moment assumption we have  $\mathbb{E}\|U\|_{\mathcal{H}_R}^2 < \infty$  and  $\mathbb{E}\|V\|_{\mathcal{H}_Z}^2 < \infty$ , so the Bochner conditional expectations  $\mathbb{E}[U \mid X]$  and  $\mathbb{E}[V \mid X]$  and the tensor product  $U \otimes V \in \mathcal{H}_R \otimes \mathcal{H}_Z$  are well defined. Define  $\widetilde{\phi}_R := U - \mathbb{E}[U \mid X]$ ,  $\widetilde{\phi}_Z := V - \mathbb{E}[V \mid X]$ , so that  $\mathbb{E}[\widetilde{\phi}_R \mid X] = \mathbb{E}[\widetilde{\phi}_Z \mid X] = 0$  a.s. The residual cross-covariance operator is

$$C_{RZ}^{\text{res}} := \mathbb{E}[(U - \mathbb{E}[U \mid X]) \otimes (V - \mathbb{E}[V \mid X])] \in \mathcal{H}_R \otimes \mathcal{H}_Z.$$

Expanding and using the tower property plus  $X$ -measurability of the conditional expectations,

$$\begin{aligned} C_{RZ}^{\text{res}} &= \mathbb{E}[U \otimes V] - \mathbb{E}[\mathbb{E}[U \mid X] \otimes V] - \mathbb{E}[U \otimes \mathbb{E}[V \mid X]] \\ &\quad + \mathbb{E}[\mathbb{E}[U \mid X] \otimes \mathbb{E}[V \mid X]] \\ &= \mathbb{E}[U \otimes V] - \mathbb{E}[\mathbb{E}[U \mid X] \otimes \mathbb{E}[V \mid X]]. \end{aligned}$$

Under  $Z \perp\!\!\!\perp R \mid X$  we have, a.s.,

$$\mathbb{E}[U \otimes V \mid X] = \mathbb{E}[U \mid X] \otimes \mathbb{E}[V \mid X].$$

Taking expectations yields

$$\mathbb{E}[U \otimes V] = \mathbb{E}[\mathbb{E}[U \mid X] \otimes \mathbb{E}[V \mid X]],$$

and therefore  $C_{RZ}^{\text{res}} = 0$ . By the adopted normalization for distance covariance on Hilbert-valued arguments,

$$\text{dCov}_\star^2(\widetilde{\phi}_R, \widetilde{\phi}_Z) = \|\text{Cov}(\widetilde{\phi}_R, \widetilde{\phi}_Z)\|_{\text{HS}}^2 = \|C_{RZ}^{\text{res}}\|_{\text{HS}}^2 = 0.$$

Thus  $\text{PAS}_\star = \text{dCOR}(\widetilde{\phi}_R, \widetilde{\phi}_Z) = 0$ , with the convention that  $\text{dCOR} = 0$  if a distance variance vanishes.

*Sample.* Let  $\{(R_i, Z_i, X_i)\}_{i=1}^n$  be i.i.d. copies of  $(R, Z, X)$  and define

$$U_n := f_{R,n}(R, Z, X), \quad V_n := f_{Z,n}(R, Z, X).$$

By assumption,  $U_n \rightarrow \widetilde{\phi}_R$ ,  $V_n \rightarrow \widetilde{\phi}_Z$  in  $L_2$ , so in particular  $U_n \rightarrow \widetilde{\phi}_R$  and  $V_n \rightarrow \widetilde{\phi}_Z$  in  $L_1$ , and

$$\sup_n \mathbb{E}\|U_n\|_{\mathcal{H}_R}^2 < \infty, \quad \sup_n \mathbb{E}\|V_n\|_{\mathcal{H}_Z}^2 < \infty.$$

The same uniform fourth moment assumption implies

$$\sup_n \mathbb{E}\|U_n\|_{\mathcal{H}_R}^4 < \infty, \quad \sup_n \mathbb{E}\|V_n\|_{\mathcal{H}_Z}^4 < \infty.$$

As in the population case, the covariance of Hilbert-valued variables is continuous with respect to  $L_2$ ; from  $U_n, V_n \rightarrow \widetilde{\phi}_R, \widetilde{\phi}_Z$  in  $L_2$ , it follows that  $\text{Cov}(U_n, V_n) \rightarrow \text{Cov}(\widetilde{\phi}_R, \widetilde{\phi}_Z)$  in Hilbert-Schmidt norm. By continuity of the norm,

$$\text{dCov}_\star^2(U_n, V_n) = \|\text{Cov}(U_n, V_n)\|_{\text{HS}}^2 \rightarrow$$

$$\|\text{Cov}(\widetilde{\phi}_R, \widetilde{\phi}_Z)\|_{\text{HS}}^2 = \text{dCov}_\star^2(\widetilde{\phi}_R, \widetilde{\phi}_Z) = 0.$$

An analogous argument with  $U_n = V_n$  yields the convergence of the distance variances associated with  $U_n$  and  $V_n$  towards those of  $\widetilde{\phi}_R$  and  $\widetilde{\phi}_Z$ .

For each  $n$ , the pairs

$$\left(\widehat{\phi}_R^{(i)}, \widehat{\phi}_Z^{(i)}\right) = \left(f_{R,n}(R_i, Z_i, X_i), f_{Z,n}(R_i, Z_i, X_i)\right), \quad i = 1, \dots, n,$$

are i.i.d. with the same distribution as  $(U_n, V_n)$ . The sample distance covariance and the sample distance variances are finite-order U- or V-statistics constructed from these pairs via a kernel  $h$  which is a polynomial in the distances  $\|U_n^{(i)} - U_n^{(j)}\|, \|V_n^{(i)} - V_n^{(j)}\|$ . From the uniform fourth moment assumptions on  $U_n$  and  $V_n$ , it follows

$$\sup_n \mathbb{E}[h^2] < \infty,$$

i.e., the kernel has a second moment uniformly bounded in  $n$ . The usual variance bounds for U- and V-statistics then give

$$\text{VAR}\left(\widehat{\text{dCov}}_\star^2(\widehat{\phi}_R, \widehat{\phi}_Z)\right) \leq \frac{C}{n}, \quad \text{VAR}\left(\widehat{\text{dVar}}_\star(\widehat{\phi}_\bullet)\right) \leq \frac{C'}{n},$$

for some constants  $C, C'$  independent of  $n$  and for  $\bullet \in \{R, Z\}$ . In particular,

$$\widehat{\text{dCov}}_\star^2(\widehat{\phi}_R, \widehat{\phi}_Z) - \text{dCov}_\star^2(U_n, V_n) \xrightarrow{\mathbb{P}} 0,$$

$$\widehat{\text{dVar}}_\star(\widehat{\phi}_\bullet) - \text{dVar}_\star(U_n) \xrightarrow{\mathbb{P}} 0,$$

and similarly for  $V_n$ .

Combining these convergences with those of the population functionals (two applications of Slutsky's theorem), we obtain

$$\widehat{\text{dCov}}_\star^2(\widehat{\phi}_R, \widehat{\phi}_Z) \xrightarrow{\mathbb{P}} \text{dCov}_\star^2(\widetilde{\phi}_R, \widetilde{\phi}_Z) = 0,$$

$$\widehat{\text{dVar}}_\star(\widehat{\phi}_\bullet) \xrightarrow{\mathbb{P}} \text{dVar}_\star(\widetilde{\phi}_\bullet),$$

for  $\bullet \in \{R, Z\}$ . If  $\text{dVar}_\star(\widetilde{\phi}_R) \text{dVar}_\star(\widetilde{\phi}_Z) > 0$ , the continuity of  $(a, b, c) \mapsto a/\sqrt{bc}$  and the continuous mapping theorem imply

$$\widehat{\text{PAS}} = \widehat{\text{dCOR}}(\widehat{\phi}_R, \widehat{\phi}_Z) \xrightarrow{\mathbb{P}} \text{dCOR}(\widetilde{\phi}_R, \widetilde{\phi}_Z) = 0.$$

If one of the limit distance variances is 0, we adopt the same convention at the sample level (setting  $\text{dCOR} = 0$  when an estimated distance variance is zero), and the convergence to 0 remains valid. In all cases  $\widehat{\text{PAS}} \xrightarrow{\mathbb{P}} 0$  as  $n \rightarrow \infty$ .  $\square$

**THEOREM 3 (QUADRATIC SENSITIVITY OF SQUARED PAS UNDER VANISHING SIGNALS).** Assume bounded kernels  $k_X, k_R, k_Z$  with finite second moments;  $k_R, k_Z$  are characteristic and distance-induced. Assume the local submodel  $R_\delta = \varphi(g(X) + \delta h(Z) + \eta)$  is DQM at  $\delta = 0$  with score  $S$ , and  $\varphi \in C^1$  has strictly positive bounded derivative on the support. Assume realizability for the RKHS  $L_2$  residualization:  $m_R(x) := \mathbb{E}[\phi_R(R) \mid X = x] \in \overline{\mathcal{G}}_R$  and  $m_Z(x) := \mathbb{E}[\phi_Z(Z) \mid X = x] \in \overline{\mathcal{G}}_Z$ . Assume moreover  $\eta \perp\!\!\!\perp Z \mid X$ ,  $\mathbb{E}[\eta \mid X, Z] = 0$ ,  $\text{VAR}(\eta \mid X, Z) > 0$  a.s.,  $Z$  is nondegenerate, and  $h(Z)$  is nonconstant given  $X$  on a set of positive  $\mathbb{P}_X$ -measure.

**Explicit non-degeneracy condition.** Let  $\mathbb{P}_0$  be the null distribution (i.e., at  $\delta = 0$ ), and define the residualized features under  $\mathbb{P}_0$ :

$$\widetilde{\phi}_R^0 := \phi_R(R_0) - \mathbb{E}_0[\phi_R(R_0) \mid X], \quad \widetilde{\phi}_Z^0 := \phi_Z(Z) - \mathbb{E}_0[\phi_Z(Z) \mid X].$$

Equivalently,  $\mathbb{E}_0[\cdot \mid X]$  is the  $L_2(\mathbb{P}_0)$  orthogonal projection onto the closed subspace of  $\sigma(X)$ -measurable Hilbert-valued functions. Set

$$A := \mathbb{E}_0[(S \widetilde{\phi}_R^0) \otimes \widetilde{\phi}_Z^0] + \mathbb{E}_0[\widetilde{\phi}_R^0 \otimes (S \widetilde{\phi}_Z^0)] \in \mathcal{H}_R \otimes \mathcal{H}_Z,$$

and assume

$$\|A\|_{\text{HS}} > 0 \quad \left(\text{equivalently } \mathbb{E}_0[h_0(W_1, W_2) (S_1 + S_2)^2] > 0\right),$$

where  $W = (R, Z, X)$ ,  $S_i := S(W_i)$ , and

$$h_0(W_1, W_2) := \langle \widetilde{\phi}_R^0(W_1), \widetilde{\phi}_R^0(W_2) \rangle_{\mathcal{H}_R} \langle \widetilde{\phi}_Z^0(W_1), \widetilde{\phi}_Z^0(W_2) \rangle_{\mathcal{H}_Z}.$$

## 4.2 Auditing For Demographic Bias in Opaque Rankings

Then, after residualization w.r.t.  $X$ ,

$$\text{PAS}_\star^2(\delta) = c \delta^2 + o(\delta^2), \quad c > 0.$$

**PROOF.** We work at the population level. In the local submodel, only  $R$  depends on  $\delta$ ;  $(Z, X)$  do not depend on  $\delta$ .

For arbitrary  $\delta$ , define the residualized features

$$\tilde{\phi}_R(\delta) := \phi_R(R_\delta) - \mathbb{E}_\delta[\phi_R(R_\delta) | X], \quad \tilde{\phi}_Z := \phi_Z(Z) - \mathbb{E}_0[\phi_Z(Z) | X].$$

We also fix population-centering at the null: let  $k_R^c, k_Z^c$  be the kernels centered under  $\mathbb{P}_0$ , so that  $\mathbb{E}_0[\tilde{\phi}_R(0)] = 0$  and  $\mathbb{E}_0[\tilde{\phi}_Z] = 0$ .

Let the residual cross-covariance operator be

$$C_{RZ}^{\text{res}}(\mathbb{P}_\delta) := \mathbb{E}_\delta[\tilde{\phi}_R(\delta) \otimes \tilde{\phi}_Z].$$

With distance-induced kernels, fix the normalization so that  $c_d = 1$  in the dCov-RKHS equivalence:

$$\Psi(\mathbb{P}_\delta) := \text{dCov}_\star^2(\tilde{\phi}_R(\delta), \tilde{\phi}_Z) = \|C_{RZ}^{\text{res}}(\mathbb{P}_\delta)\|_{\text{HS}}^2.$$

By realizability and null alignment, under  $H_0 : Z \perp\!\!\!\perp R | X$  (i.e.,  $\delta = 0$ ) we have  $C_{RZ}^{\text{res}}(\mathbb{P}_0) = 0$ ; hence the sample counterpart is a symmetric order-2 U-statistic with first Hoeffding projection equal to zero (order-1 degeneracy). Define, for each  $\delta$ , the order-2 kernel induced by the residualized features:

$$h_\delta(W_1, W_2) := \langle \tilde{\phi}_R(\delta; W_1), \tilde{\phi}_R(\delta; W_2) \rangle_{\mathcal{H}_R} \langle \tilde{\phi}_Z(W_1), \tilde{\phi}_Z(W_2) \rangle_{\mathcal{H}_Z},$$

so that  $\Psi(\mathbb{P}_\delta) = \mathbb{E}_\delta[h_\delta(W_1, W_2)]$ . By  $L_2$ -continuity of  $\delta \mapsto \tilde{\phi}_R(\delta)$  at 0 and boundedness of the kernels,

$$\mathbb{E}_\delta[h_\delta(W_1, W_2)] - \mathbb{E}_0[h_0(W_1, W_2)] = o(\delta^2).$$

Therefore,  $\Psi(\mathbb{P}_\delta) = \mathbb{E}_\delta[h_0(W_1, W_2)] + o(\delta^2)$ .

Consider the local parametric submodel  $\{\mathbb{P}_\delta : \delta \in (-\delta_0, \delta_0)\}$  that is DQM at  $\delta = 0$  with score  $S(W)$ . Applying the second-order Le Cam expansion to the linear functional  $\delta \mapsto \mathbb{E}_\delta[h_0(W_1, W_2)]$  (with respect to the product measure  $\mathbb{P}_\delta^{\otimes 2}$ ), order-1 degeneracy removes the first-order term and yields

$$\mathbb{E}_\delta[h_0(W_1, W_2)] = \frac{\delta^2}{2} \mathbb{E}_0[h_0(W_1, W_2) (S(W_1) + S(W_2))^2] + o(\delta^2).$$

Hence  $\Psi(\mathbb{P}_\delta) = \frac{\delta^2}{2} \mathbb{E}_0[h_0(W_1, W_2) (S(W_1) + S(W_2))^2] + o(\delta^2)$ . By Lemma 1,  $\mathbb{E}_0[h_0(W_1, W_2) (S_1 + S_2)^2] = \frac{1}{2} \|A\|_{\text{HS}}^2$ . Therefore,  $\Psi(\mathbb{P}_\delta) = \frac{1}{4} \delta^2 \|A\|_{\text{HS}}^2 + o(\delta^2)$ . By the explicit non-degeneracy condition,  $\|A\|_{\text{HS}} > 0$ . Set  $c_0 := \frac{1}{4} \|A\|_{\text{HS}}^2 > 0$ , so

$$\Psi(\mathbb{P}_\delta) = c_0 \delta^2 + o(\delta^2).$$

Since  $\varphi \in C^1$  with strictly positive bounded derivative and moments are finite,  $\delta \mapsto \phi_R(R_\delta)$  is  $L_2$ -continuous; consequently the residual distance variances

$$v_R(\delta) := \text{dCov}_\star(\tilde{\phi}_R(\delta), \tilde{\phi}_R(\delta)), \quad v_Z(\delta) := \text{dCov}_\star(\tilde{\phi}_Z, \tilde{\phi}_Z)$$

are continuous at 0. Moreover,  $v_Z(0) > 0$  because  $Z$  is nondegenerate, and  $v_R(0) > 0$  under  $\text{VAR}(\eta | X, Z) > 0$ . By definition of PAS,

$$\text{PAS}_\star^2(\delta) = \frac{\Psi(\mathbb{P}_\delta)}{v_R(\delta) v_Z(\delta)} = \frac{c_0}{v_R(0) v_Z(0)} \delta^2 + o(\delta^2).$$

Finally, set  $c := c_0 / \{v_R(0) v_Z(0)\} > 0$ ,

which completes the proof.  $\square$

**LEMMA 1 (POLARIZATION IDENTITY FOR RESIDUAL RKHS FEATURES).** Let  $W = (R, Z, X) \sim \mathbb{P}_0$ , and let  $(\mathcal{H}_R, \langle \cdot, \cdot \rangle_{\mathcal{H}_R})$  and  $(\mathcal{H}_Z, \langle \cdot, \cdot \rangle_{\mathcal{H}_Z})$  be separable Hilbert spaces. Consider measurable feature maps  $\phi_R : R \rightarrow \mathcal{H}_R$  and  $\phi_Z : Z \rightarrow \mathcal{H}_Z$  with  $\mathbb{E}_0 \|\phi_R(R)\|_{\mathcal{H}_R}^2 < \infty$  and  $\mathbb{E}_0 \|\phi_Z(Z)\|_{\mathcal{H}_Z}^2 < \infty$ . Define

$$\tilde{\phi}_R^0 := \phi_R(R) - \mathbb{E}_0[\phi_R(R) | X], \quad \tilde{\phi}_Z^0 := \phi_Z(Z) - \mathbb{E}_0[\phi_Z(Z) | X].$$

Assume (null alignment)  $\mathbb{E}_0[\tilde{\phi}_R^0 \otimes \tilde{\phi}_Z^0] = 0$  in  $\mathcal{H}_R \otimes \mathcal{H}_Z$ . Let  $S \in L_2(\mathbb{P}_0)$  be real-valued and assume the integrability condition

$$\mathbb{E}_0[(1 + S(W)^2) \|\tilde{\phi}_R^0(W)\|_{\mathcal{H}_R} \|\tilde{\phi}_Z^0(W)\|_{\mathcal{H}_Z}] < \infty.$$

For i.i.d. copies  $W_1, W_2$  of  $W$ , define

$$h_0(W_1, W_2) := \langle \tilde{\phi}_R^0(W_1), \tilde{\phi}_R^0(W_2) \rangle_{\mathcal{H}_R} \langle \tilde{\phi}_Z^0(W_1), \tilde{\phi}_Z^0(W_2) \rangle_{\mathcal{H}_Z}.$$

Write  $S_i := S(W_i)$  and  $\tilde{\phi}_\star^{0,i} := \tilde{\phi}_\star^0(W_i)$ . Then

$$\mathbb{E}_0[h_0(W_1, W_2) (S_1 + S_2)^2] = \frac{1}{2} \|A\|_{\text{HS}}^2,$$

where we use the canonical isometric identification  $\mathcal{H}_R \otimes \mathcal{H}_Z \cong \text{HS}(\mathcal{H}_Z, \mathcal{H}_R)$ , and  $A := \mathbb{E}_0[(S \tilde{\phi}_R^0 \otimes \tilde{\phi}_Z^0) \otimes (S \tilde{\phi}_Z^0)]$ .

**PROOF.** All expectations are under  $\mathbb{P}_0$ .

**Integrability.** By independence of  $(W_1, W_2)$  and Cauchy-Schwarz,

$$\begin{aligned} \mathbb{E}_0[h_0(W_1, W_2)] &\leq \mathbb{E}_0[\|\tilde{\phi}_R^{0,1}\|_{\mathcal{H}_R} \|\tilde{\phi}_Z^{0,1}\|_{\mathcal{H}_Z} \|\tilde{\phi}_R^{0,2}\|_{\mathcal{H}_R} \|\tilde{\phi}_Z^{0,2}\|_{\mathcal{H}_Z}] \\ &= \left( \mathbb{E}_0[\|\tilde{\phi}_R^0\|_{\mathcal{H}_R} \|\tilde{\phi}_Z^0\|_{\mathcal{H}_Z}] \right)^2 \leq (\mathbb{E}_0[\|\tilde{\phi}_R^0\|_{\mathcal{H}_R}^2] \mathbb{E}_0[\|\tilde{\phi}_Z^0\|_{\mathcal{H}_Z}^2]) < \infty, \end{aligned}$$

so  $h_0 \in L_1$ . Moreover, independence gives

$$\mathbb{E}_0[h_0(S_1^2)] \leq \mathbb{E}_0[S^2 \|\tilde{\phi}_R^0\|_{\mathcal{H}_R} \|\tilde{\phi}_Z^0\|_{\mathcal{H}_Z}] \mathbb{E}_0[\|\tilde{\phi}_R^0\|_{\mathcal{H}_R} \|\tilde{\phi}_Z^0\|_{\mathcal{H}_Z}] < \infty,$$

and similarly for  $S_2^2$ . Hence the tower property and Fubini-Tonelli (Bochner) apply. In particular,

$$T := \mathbb{E}_0[S \tilde{\phi}_R^0 \otimes \tilde{\phi}_Z^0] \in \mathcal{H}_R \otimes \mathcal{H}_Z$$

is well defined.

**Preparation.** With the canonical identification,

$$h_0(W_1, W_2) = \langle \tilde{\phi}_R^{0,1} \otimes \tilde{\phi}_Z^{0,1}, \tilde{\phi}_R^{0,2} \otimes \tilde{\phi}_Z^{0,2} \rangle_{\text{HS}}.$$

**(i) First-order degeneracy.** Using the previous identity and  $\mathbb{E}_0[\tilde{\phi}_R^0 \otimes \tilde{\phi}_Z^0] = 0$ ,

$$\mathbb{E}_0[h_0(W_1, W_2) | W_1] = \langle \tilde{\phi}_R^{0,1} \otimes \tilde{\phi}_Z^{0,1}, \mathbb{E}_0[\tilde{\phi}_R^0 \otimes \tilde{\phi}_Z^0] \rangle_{\text{HS}} = 0,$$

and symmetrically for  $| W_2$ . Therefore

$$\mathbb{E}_0[h_0(S_1^2)] = \mathbb{E}_0[\mathbb{E}_0[h_0 | W_1] S_1^2] = 0, \quad \mathbb{E}_0[h_0(S_2^2)] = 0.$$

**(ii) Cross term.** By independence of  $(W_1, W_2)$  and Fubini-Tonelli (Bochner),

$$\mathbb{E}_0[h_0(S_1 S_2)] = \langle \mathbb{E}_0[S \tilde{\phi}_R^0 \otimes \tilde{\phi}_Z^0], \mathbb{E}_0[S \tilde{\phi}_R^0 \otimes \tilde{\phi}_Z^0] \rangle_{\text{HS}} = \|T\|_{\text{HS}}^2.$$

**(iii) Conclusion.** Hence

$$\mathbb{E}_0[h_0(W_1, W_2) (S_1 + S_2)^2] = 2 \mathbb{E}_0[h_0(S_1 S_2)] = 2 \|T\|_{\text{HS}}^2.$$

Since  $S$  is scalar,  $A = 2 \mathbb{E}_0[S \tilde{\phi}_R^0 \otimes \tilde{\phi}_Z^0] = 2T$ , so  $\|A\|_{\text{HS}}^2 = 4 \|T\|_{\text{HS}}^2$  and therefore

$$\mathbb{E}_0[h_0(W_1, W_2) (S_1 + S_2)^2] = 2 \|T\|_{\text{HS}}^2 = \frac{1}{2} \|A\|_{\text{HS}}^2,$$

which completes the proof.  $\square$

12

## 4.2 Auditing For Demographic Bias in Opaque Rankings

### REFERENCES

- [1] Philip W Adler, Casey Falk, Sorelle A Friedler, Gabriel Rybeck, Carlos Scheidegger, Brandon Smith, and Suresh Venkatasubramanian. 2016. Auditing black-box models for indirect influence. In *2016 IEEE 16th International Conference on Data Mining (ICDM)*. IEEE, 1–10.
- [2] amar5693. 2024. Screen Time, Sleep and Stress Analysis Dataset. <https://www.kaggle.com/datasets/amar5693/screen-time-sleep-and-stress-analysis-dataset>. Accessed: 2026-02-27.
- [3] Julia Angwin, Jeff Larson, Surya Mattu, and Lauren Kirchner. 2016. Machine Bias: There’s Software Used Across the Country to Predict Future Criminals. And It’s Biased Against Blacks. *ProPublica* (May 2016). <https://www.propublica.org/article/machine-bias-risk-assessments-in-criminal-sentencing>
- [4] Abolfazl Asudeh, H. V. Jagadish, Julia Stoyanovich, and Gautam Das. 2019. Designing Fair Ranking Schemes. In *SIGMOD*. 1259–1276.
- [5] Asia J Biega, Krishna P Gummadi, and Gerhard Weikum. 2018. Equity of attention: Amortizing individual fairness in rankings. In *The 41st international acm sigir conference on research & development in information retrieval*. 405–414.
- [6] Francesco Bonchi, Sara Hajian, Bud Mishra, and Daniele Ramazzotti. 2017. Exposing the probabilistic causal structure of discrimination. *Int. J. Data Sci. Anal.* 3, 1 (2017), 1–21.
- [7] Emmanuel J. Candès, Yingying Fan, Lucas Janson, and Jinchi Lv. 2018. Panning for gold: Model-X knockoffs for high-dimensional controlled variable selection. *Journal of the Royal Statistical Society: Series B (Statistical Methodology)* 80, 3 (2018), 551–577.
- [8] L. Eliss Celis, Damian Straszak, and Nisheeth K. Vishnoi. 2018. Ranking with Fairness Constraints. In *ICALP*.
- [9] John J. Chertan and Emmanuel J. Candès. 2024. Statistical Inference for Fairness Auditing. *Journal of Machine Learning Research* 25, 149 (2024), 1–49. <https://www.jmlr.org/papers/v25/23-0739.html> Earlier version: arXiv:2305.03712.
- [10] P. Cortez and Alice Maria Gonçalves Silva. 2008. Using data mining to predict secondary school student performance. <https://api.semanticscholar.org/CorpusID:16621299>
- [11] Thomas M. Cover and Joy A. Thomas. 2006. *Elements of Information Theory* (2nd ed.). Wiley, Hoboken, NJ.
- [12] A. C. Davison and D. V. Hinkley. 1997. *Bootstrap Methods and Their Application*. Cambridge University Press, Cambridge.
- [13] Petros Drineas and Michael W. Mahoney. 2005. On the Nyström Method for Approximating a Gram Matrix for Improved Kernel-Based Learning. *Journal of Machine Learning Research* 6 (2005), 2153–2175.
- [14] Dheeru Dua and Casey Graff. 2019. Adult (Census Income) Data Set. UCI Machine Learning Repository. <https://archive.ics.uci.edu/ml/datasets/Adult> University of California, Irvine. Donors: Barry Becker and Ron Kohavi.
- [15] Cynthia Dwork, Moritz Hardt, Toniann Pitassi, Omer Reingold, and Richard Zemel. 2012. Fairness through Awareness. In *Proceedings of the 3rd Innovations in Theoretical Computer Science Conference (ITCS ’12)*. 214–226.
- [16] Cynthia Dwork, Michael P. Kim, Omer Reingold, Guy N. Rothblum, and Gal Yona. 2019. Learning from Outcomes: Evidence-Based Rankings. In *FOCS*. 106–125.
- [17] Bradley Efron and Robert J. Tibshirani. 1993. *An Introduction to the Bootstrap*. Chapman & Hall/CRC, New York.
- [18] U.S. Equal Employment Opportunity Commission. [n.d.]. <https://www.eeoc.gov/laws/index.cfm>.
- [19] European Commission Diversity Charters. [n.d.]. [https://ec.europa.eu/info/policies/justice-and-fundamental-rights/combating-discrimination/tackling-discrimination/diversity-management/diversity-charters-eu-country\\_en](https://ec.europa.eu/info/policies/justice-and-fundamental-rights/combating-discrimination/tackling-discrimination/diversity-management/diversity-charters-eu-country_en).
- [20] Sheila R Foster. 2004. Causation in antidiscrimination law: Beyond intent versus impact. *Hous. L. Rev.* 41 (2004), 1469.
- [21] Sebastian Frenzel and Bernd Pompe. 2007. Partial Mutual Information for Coupling Analysis of Multivariate Time Series. *Physical Review Letters* 99, 20 (2007), 204101.
- [22] David García-Soriano and Francesco Bonchi. 2021. Maxmin-Fair Ranking: Individual Fairness under Group-Fairness Constraints. In *Proceedings of the 27th ACM SIGKDD Conference on Knowledge Discovery and Data Mining (KDD ’21)*. 436–446.
- [23] Dan Geiger, Thomas Verma, and Judea Pearl. 1990. *d*-separation: From theorems to algorithms. In *Machine intelligence and pattern recognition*. Vol. 10. Elsevier, 139–148.
- [24] Sahin Cem Geyik, Stuart Ambler, and Krishnaram Kenthapadi. 2019. Fairness-Aware Ranking in Search & Recommendation Systems with Application to LinkedIn Talent Search. In *KDD*. 2221–2231.
- [25] Arthur Gretton, Olivier Bousquet, Alex Smola, and Bernhard Schölkopf. 2005. Measuring statistical dependence with Hilbert-Schmidt norms. In *International conference on algorithmic learning theory*. Springer, 63–77.
- [26] Arthur Gretton, Kenji Fukumizu, Choon Teo, Le Song, Bernhard Schölkopf, and Alex Smola. 2007. A kernel statistical test of independence. *Advances in neural information processing systems* 20 (2007).
- [27] Nathan Halko, Per-Gunnar Martinsson, and Joel A. Tropp. 2011. Finding Structure with Randomness: Probabilistic Algorithms for Constructing Approximate Matrix Decompositions. *SIAM Rev.* 53, 2 (2011), 217–288.
- [28] Moritz Hardt, Eric Price, and Nati Srebro. 2016. Equality of Opportunity in Supervised Learning. In *NeurIPS*. 3315–3323.
- [29] Magnus R. Hestenes and Eduard Stiefel. 1952. Methods of Conjugate Gradients for Solving Linear Systems. *J. Res. Nat. Bur. Standards* 49, 6 (1952), 409–436.
- [30] H. V. Jagadish, Francesco Bonchi, Tina Eliassi-Rad, Lise Getoor, Krishna Gummadi, and Julia Stoyanovich. 2019. The Responsibility Challenge for Data. In *Proceedings of the 2019 International Conference on Management of Data (Amsterdam, Netherlands) (SIGMOD ’19)*. 412–414.
- [31] Kaleruo Järvelin and Jaana Kekäläinen. 2002. Cumulated gain-based evaluation of IR techniques. *ACM Transactions on Information Systems* 20, 4 (2002), 422–446. <https://doi.org/10.1145/582415.582418>
- [32] Alexander Kraskov, Harald Stögbauer, and Peter Grassberger. 2004. Estimating mutual information. *Physical Review E* 69, 6 (2004), 066138. <https://doi.org/10.1103/PhysRevE.69.066138>
- [33] Alexander Kraskov, Harald Stögbauer, and Peter Grassberger. 2004. Estimating mutual information. *Physical Review E* 69, 6 (2004), 066138.
- [34] Erwin Kreyszig. 1989. *Introductory Functional Analysis with Applications*. John Wiley & Sons.
- [35] Erich L. Lehmann and Joseph P. Romano. 2005. *Testing Statistical Hypotheses* (3rd ed.). Springer.
- [36] Shira Mitchell, Eric Potash, Solon Barocas, Alexander D’Amour, and Kristian Lum. 2021. Algorithmic Fairness: Choices, Assumptions, and Definitions. *Annual Review of Statistics and Its Application* 8, 1 (2021), 141–163.
- [37] Hari Krishna Narasimhan, Andrew Cotter, Maya R. Gupta, and Serena Wang. 2020. Pairwise Fairness for Ranking and Regression. In *AAAI*.
- [38] Christopher C. Paige and Michael A. Saunders. 1975. Solution of Sparse Indefinite Systems of Linear Equations. *SIAM J. Numer. Anal.* 12, 4 (1975), 617–629.
- [39] Sambit Panda, Satish Palaniappan, Junhao Xiong, Eric W Bridgeford, Ronak Mehta, Cen Cheng Shen, and Joshua T Vogelstein. 2019. *hyppo*: A multivariate hypothesis testing Python package. *arXiv preprint arXiv:1907.02088* (2019).
- [40] Eliana Pastor and Francesco Bonchi. 2024. Intersectional fair ranking via subgroup divergence. *Data Min. Knowl. Discov.* 38, 4 (2024), 2186–2222.
- [41] Gourab K. Patro, Lorenzo Porcaro, Laura Mitchell, Quyuze Zhang, Meike Zehlike, and Nikhil Garg. 2022. Fair Ranking: A Critical Review, Challenges, and Future Directions. In *2022 ACM Conference on Fairness, Accountability, and Transparency (FACT ’22)*. 1929–1942.
- [42] Judea Pearl. 1995. Causal diagrams for empirical research. *Biometrika* 82, 4 (1995), 669–688.
- [43] Evangelia Pitoura, Kostas Stefanidis, and Georgia Koutrika. 2022. Fairness in rankings and recommendations: an overview. *The VLDB Journal* 31, 3 (2022), 431–458.
- [44] Salvatore Ruggieri and Jose Manuel Alvarez. 2023. Counterfactual Situation Testing: Uncovering Discrimination under Fairness given the Difference. In *Equity and Access in Algorithms, Mechanisms, and Optimization (EAAMO ’23)*. ACM, 1–11. <https://doi.org/10.1145/3617694.3623222>
- [45] Yousef Saad. 2003. *Iterative Methods for Sparse Linear Systems* (2 ed.). Society for Industrial and Applied Mathematics, Philadelphia, PA, USA.
- [46] Yuta Saito and Thorsten Joachims. 2022. Fair ranking as fair division: Impact-based individual fairness in ranking. In *Proceedings of the 28th ACM SIGKDD Conference on Knowledge Discovery and Data Mining*. 1514–1524.
- [47] Babak Salimi, Luke Rodriguez, Bill Howe, and Dan Suciu. 2019. Interventional Fairness: Causal Database Repair for Algorithmic Fairness. In *Proceedings of the 2019 International Conference on Management of Data, SIGMOD Conference 2019, Amsterdam, The Netherlands, June 30 - July 5, 2019*. ACM, 793–810.
- [48] Bernhard Schölkopf and Alexander J. Smola. 2002. *Learning with Kernels: Support Vector Machines, Regularization, Optimization, and Beyond*. MIT Press.
- [49] John Shawe-Taylor and Nello Cristianini. 2004. *Kernel Methods for Pattern Analysis*. Cambridge University Press, Cambridge, UK.
- [50] Ashudeep Singh and Thorsten Joachims. 2018. Fairness of Exposure in Rankings. In *KDD*. 2219–2228.
- [51] Ashudeep Singh and Thorsten Joachims. 2019. Policy Learning for Fairness in Ranking. In *NeurIPS*. 5427–5437.
- [52] Igor Stepin, Jose M Oramas, and Alejandro Coca-Catalina. 2021. Certifi: Counterfactual explanations for black-box models. In *Proceedings of the IEEE/CVF International Conference on Computer Vision (ICCV)*. 1518–1527.
- [53] Gábor J Székely and Maria L Rizzo. 2014. Partial distance correlation with methods for dissimilarities. *The Annals of Statistics* 42, 6 (2014), 2382–2412.
- [54] Gábor J Székely, Maria L Rizzo, and Nail K Bakirov. 2007. Measuring and testing dependence by correlation of distances. *Annals of Statistics* 35, 6 (2007), 2769–2794.
- [55] Martin Vejmelka and Milan Paluš. 2008. Inferring the Directionality of Coupling with Conditional Mutual Information. *Physical Review E* 77, 2 (2008), 026214.
- [56] Greg Ver Steeg. 2000. Non-parametric entropy estimation toolbox (npeet). *Non-parametric entropy estimation toolbox (NPEET)* (2000).

## 4.2 Auditing For Demographic Bias in Opaque Rankings

---

- [57] Xueqin Wang, Wenliang Pan, Wenhao Hu, Yuan Tian, and Heping Zhang. 2015. Conditional distance correlation. *J. Amer. Statist. Assoc.* 110, 512 (2015), 1726–1734.
- [58] Christopher K. I. Williams and Matthias Seeger. 2001. Using the Nyström Method to Speed Up Kernel Machines. In *Advances in Neural Information Processing Systems*, Vol. 13. 682–688.
- [59] Lei Xu, Maria Skoularidou, Alfredo Cuesta-Infante, and Kalyan Veeramachani. 2019. Modeling Tabular Data Using Conditional GAN. *arXiv preprint arXiv:1907.00503* (2019).
- [60] Ke Yang, Vasilis Gkatzelis, and Julia Stoyanovich. 2019. Balanced Ranking with Diversity Constraints. In *IJCAI*. 6035–6042.
- [61] Ke Yang and Julia Stoyanovich. 2017. Measuring Fairness in Ranked Outputs. In *SSDBM*. 22:1–22:6.
- [62] Meike Zehlike, Francesco Bonchi, Carlos Castillo, Sara Hajian, Mohamed Megahed, and Ricardo Baeza-Yates. 2017. FA\*IR: A Fair Top-k Ranking Algorithm. In *CIKM*. 1569–1578.
- [63] Meike Zehlike, Philipp Hacker, and Emil Wiedemann. 2020. Matching code and law: achieving algorithmic fairness with optimal transport. *Data Mining and Knowledge Discovery* 34, 1 (2020), 163–200.
- [64] Meike Zehlike, Ke Yang, and Julia Stoyanovich. 2022. Fairness in ranking, part i: Score-based ranking. *Comput. Surveys* 55, 6 (2022), 1–36.
- [65] Kun Zhang, Jonas Peters, Dominik Janzing, and Bernhard Schölkopf. 2011. Kernel-based Conditional Independence Test and Application in Causal Discovery. In *Proceedings of the 27th Conference on Uncertainty in Artificial Intelligence (UAI)*. AUAI Press, Barcelona, Spain, 804–813.
- [66] Yujia Zheng, Biwei Huang, Wei Chen, Joseph Ramsey, Mingming Gong, Ruichu Cai, Shohei Shimizu, Peter Spirtes, and Kun Zhang. 2024. Causal-learn: Causal discovery in python. *Journal of Machine Learning Research* 25, 60 (2024), 1–8.

### 4.3 Beyond Demographic Parity: Redefining Equal Treatment

Traditional fairness auditing focuses primarily on disparate outcomes, evaluating whether different demographic groups receive favorable decisions at similar rates. However, equal outcomes do not necessarily imply fair treatment. A model may achieve parity in outcomes while still relying on different reasoning or decision-making logic for different groups, for example by using different proxy variables or feature interactions.

The work presented in this section addresses this limitation by introducing a framework for auditing procedural fairness, focusing on how decisions are made rather than only on their final outcomes. The key idea is to analyze the distributions of model explanations or feature attributions across demographic groups. If the explanations that justify decisions differ systematically across groups, this may indicate that the model relies on distinct reasoning processes when evaluating individuals from different demographics.

To detect such disparities, the proposed approach compares explanation distributions and trains a meta-classifier capable of distinguishing whether a given explanation corresponds to one demographic group or another. If the meta-classifier can successfully distinguish between groups, it suggests that the model's decision-making process differs across groups, revealing a form of disparate treatment that would remain undetected by traditional outcome-based fairness metrics.

By extending fairness auditing to the analysis of explanation distributions, this work highlights the importance of examining the procedural logic of algorithmic systems, complementing traditional metrics focused solely on outcome disparities.

**Authors' Contributions**

---

<b>Contribution</b>	<b>Authors</b>
<b>Conceptualization:</b>	C. Mougan, A. Ferrara, and all authors
<b>Writing:</b>	C. Mougan and all authors
<b>Methodology:</b>	C. Mougan, A. Ferrara, and all authors
<b>Formal Analysis:</b>	C. Mougan, A. Ferrara, S. Ruggieri
<b>Code:</b>	C. Mougan
<b>Experiments:</b>	C. Mougan

---

---

# Beyond Demographic Parity: Redefining Equal Treatment

---

**Carlos Mougan**  
University of Southampton  
United Kingdom

**Laura State**  
Scuola Normale Superiore  
University of Pisa, Italy

**Antonio Ferrara**  
TU Graz, Austria  
AI Research Intesa Sanpaolo

**Salvatore Ruggieri**  
University of Pisa  
Italy

**Steffen Staab**  
University of Southampton  
University of Stuttgart, Germany

### Abstract

Liberalism-oriented political philosophy reasons that all individuals should be treated equally independently of their protected characteristics. Related work in machine learning has translated the concept of *equal treatment* into terms of *equal outcome* and measured it as *demographic parity* (also called *statistical parity*). Our analysis reveals that the two concepts of equal outcome and equal treatment diverge; therefore, demographic parity does not faithfully represent the notion of *equal treatment*. We propose a new formalization for equal treatment by (i) considering the influence of feature values on predictions, such as computed by Shapley values decomposing predictions across its features, (ii) defining distributions of explanations, and (iii) comparing explanation distributions between populations with different protected characteristics. We show the theoretical properties of our notion of equal treatment and devise a classifier two-sample test based on the AUC of an equal treatment inspector. We study our formalization of equal treatment on synthetic and natural data. We release `explanationspace`, an open-source Python package with methods and tutorials.

## 1 Introduction

In philosophy, long-held discussions about what constitutes a fair or an unfair political system have led to established frameworks of distributive justice (Lamont & Favor, 2017; Kymlicka, 2002). From the *egalitarian* school of thought, the *equal opportunity* concept was argued by Rawls (1958). The concept has been translated into computable metrics with the same name (Hardt et al., 2016). From a machine learning perspective, the technical drawback is that metrics for equal opportunity require label annotations, which are not always available after the deployment of a model.

The *liberalism* school of thought<sup>1</sup>, put forward by scholars such as Friedman et al. (1990) and Nozick (1974), requires *equal treatment* of individuals regardless of their protected characteristics. This concept has been translated by the machine learning literature (Simons et al., 2021; Heidari et al., 2019; Wachter et al., 2020) into the requirement that machine learning predictions should achieve *equal outcomes* for groups with different protected characteristics. The corresponding measure, *demographic parity* (also called *statistical parity*), compares the different distributions of predicted outcomes of a model  $f$  for different social groups. We will show, however, that the metric of demographic parity may indicate fairness, although groups are indeed treated differently.

<sup>1</sup>We use the term *liberalism* to refer to the perspective exemplified by Friedman et al. (1990). This perspective can also be referred to as *neoliberalism* or *libertarianism* (Lamont & Favor, 2017; Friedman, 2022).

Preprint. Under review.

We leave the normative discussion of which philosophical paradigm should be pursued by policy to the discourse in the social sciences and the broad public. However, our analysis contributes to a foundational understanding of fairness in machine learning. Moreover, we remedy the divergence between the liberalism-oriented philosophical requirement of equal treatment and actual measures used in fair machine learning approaches by proposing a novel method for measuring equal treatment.

Comparing different social groups, we measure how non-protected features of individuals interact with the trained model  $f$  as explained by Shapley value attributions (Lundberg & Lee, 2017). If two social groups are treated the same, the distributions of interaction behavior, which we call *explanation distributions*, will not be distinguishable. We introduce a tool, the “Equal Treatment Inspector”, that implements this idea. When detecting unequal treatment, it explains the features involved in such an inequality, supporting understanding of the causes of unfairness in the machine learning model. In summary, our contributions are:

1. The definition of a novel method for recognizing and explaining unequal treatment.
2. The study of the formal relationship between equal outcome and equal treatment.
3. An open-source Python package `explanationspace` implementing the “Equal Treatment Inspector” that is `scikit-learn` compatible together with documentation and tutorials.

## 2 Foundations and Related work

### 2.1 Basic Notations and Formal Definitions of Fairness in Related Work

In supervised learning, a function  $f_\theta : X \rightarrow Y$ , also called a model, is induced from a set of observations, called the training set,  $\mathcal{D} = \{(x_1, y_1), \dots, (x_n, y_n)\} \sim X \times Y$ , where  $X = \{X_1, \dots, X_p\}$  represents predictive features and  $Y$  is the target feature. The domain of the target feature is  $\text{dom}(Y) = \{0, 1\}$  (binary classification) or  $\text{dom}(Y) = \mathbb{R}$  (regression). For binary classification, we assume a probabilistic classifier, and we denote by  $f_\theta(x)$  the estimate of the probability  $P(Y = 1|X = x)$  over the (unknown) distribution of  $X \times Y$ . For regression,  $f_\theta(x)$  estimates  $E[Y|X = x]$ . We call the projection of  $\mathcal{D}$  on  $X$ , written  $\mathcal{D}_X = \{x_1, \dots, x_n\} \sim X$ , the *empirical input distribution*. The dataset  $f_\theta(\mathcal{D}_X) = \{f_\theta(x) \mid x \in \mathcal{D}_X\}$  is called the *empirical prediction distribution*.

We assume a feature modeling protected social groups denoted by  $Z$ , called *protected feature*, and assume it to be binary valued in the theoretical analysis.  $Z$  can either be included in the predictive features  $X$  used by a model or not. If not, we assume that it is still available for a test dataset. Even without the protected feature in training data, a model can discriminate against the protected groups by using correlated features as a proxy of the protected one (Pedreschi et al., 2008).

We write  $A \perp B$  to denote statistical independence between the two sets of random variables  $A$  and  $B$ , or equivalently, between two multivariate probability distributions. We define two common fairness notions and corresponding fairness metrics that quantify a model’s degree of discrimination or unfairness (Mehrabi et al., 2022).

**Definition 2.1.** (*Demographic Parity (DP)*). A model  $f_\theta$  achieves demographic parity if  $f_\theta(X) \perp Z$ .

Thus, demographic parity holds if  $\forall z. P(f_\theta(X)|Z = z) = P(f_\theta(X))$ . For binary  $Z$ ’s, we can derive a metric as  $d(P(f_\theta(X)|Z = 1), P(f_\theta(X)))$ , where  $d(\cdot)$  is probability distributions distance.

**Definition 2.2.** (*Equal Opportunity (EO)*) A model  $f_\theta$  achieves equal opportunity if  $\forall z. P(f_\theta(X)|Y = 1, Z = z) = P(f_\theta(X) = 1|Y = 1)$ .

As before, we can measure unfairness for binary  $Z$ ’s as  $d(P(f_\theta(X)|Y = 1, Z = 1), P(f_\theta(X) = 1|Y = 1))$ . Equal opportunity comes with the problem that labels for correct outcomes are required, but difficult or even impossible to collect Ruggieri et al. (2023).

### 2.2 Philosophical Foundations and Computable Fairness Metrics

Political and moral philosophers from the *egalitarian* school of thought often consider *equal opportunity* to be the key promoter of fairness and social justice, providing qualified individuals with equal chances to succeed regardless of their background or circumstances Rawls (1958, 1991), Dworkin (1981a,b), Arneson (1989), Cohen (1989). In fair ML, Hardt et al. (2016) proposed translating equal opportunity into the inter-group difference of the true positive rates. (Heidari et al., 2019) provided a moral framework to ground such a metric of equal opportunity.

## 4.3 Beyond Demographic Parity: Redefining Equal Treatment

---

The **liberalism** school of thought argues that individuals should be treated equally independently of outcomes [Friedman et al. \(1990\)](#); [Nozick \(1974\)](#). Equal treatment has also been defined as “equal treatment-as-blindness” or neutrality [Sunstein \(1992\)](#); [Miller & Howell \(1959\)](#). From a technical perspective, the notion of *equal treatment* has often been understood as *equal outcomes* and translated to metrics such as demographic parity or statistical parity (used synonymously). As we will analyze in Section 4.2, equal outcomes imply that two demographic groups experience the same distribution of outcomes, even if the first of the two groups have much better prospects for achieving the predicted outcome. Thus, a model  $f$  that achieves equal outcome may have to prefer individuals from one group over those from another group, violating the requirement for equal treatment of all individuals. Our metric for equal treatment remedy this drawback.

### 2.3 Fairness Notions: Paper Blind Reviews Use Case

To illustrate the difference between equal opportunity, equal outcomes, and equal treatment, based on the previously discussed framework, we consider the example of conference papers’ blind reviews and focus on the protected attribute of the country of origin of the paper’s author, comparing Germany and the United Kingdom.

For *equal opportunity*, we quantify fairness by the true positive rate (cf. Definition 2.2). In words, it is the acceptance ratio given that the quality of the paper is high. Achieving equal opportunity will imply that these ratios are similar between the two countries. In blind reviews, the purpose is to evaluate the paper’s quality and the research’s merit without being influenced by factors such as the author’s identity, affiliations, background or country. If we were to enforce equal opportunity in this use case, we would aim for similar true positive rates for submissions from different countries. However, this approach could lead to unintended consequences, such as unintentionally favouring, reverse discrimination, overcorrection or quotas of affirmative action towards certain countries.

For *equal outcomes*, we require that the distribution of acceptance rates is similar, independently of the quality of the paper (cf. Definition 2.1). Note that the outcomes can have similar rates due to random chance, even if there is a country bias in the acceptance procedure.

For *equal treatment*, we require that the contributions of the features used to make a decision on paper’s acceptance has similar distributions (cf. Definition 3.2). Equality of treatment through blindness is more desirable than equal opportunity or equal outcomes because it ensures that all submissions are evaluated solely on the basis of their quality, without any bias or discrimination towards any particular country. By achieving equality of treatment through blindness, we can promote fairness and objectivity in the review process and ensure that all papers have an equal chance to be evaluated on their merits.

In comparing our introduced measure of *equal treatment* with *equal outcomes* (or demographic or statistical parity, used as synonymous), we note that the latter looks at the distributions of predictions and measures their similarity. Equal treatment goes a step further by evaluating whether the contribution of features to the decision, is similar. Our definition of *equal treatment* implies the notion of *equal outcome*, but the converse is not necessarily true, as we showed in Section 4.3.1.

### 2.4 Related Work

**Measuring Demographic Parity.** Previous work has relied on the notion of equal outcomes and measured DP on the model predictions using statistics such as Mann–Whitney, Kolmogorov–Smirnov or Wasserstein distance ([Raji et al., 2020](#); [Kearns et al., 2018](#); [Cho et al., 2020](#)). Other research lines have aimed to measure DP when the protected attribute is a continuous variable ([Jiang et al., 2022](#)). We measure DP by using a classifier two-sample test (see later on) of statistical independence.

**Classifier two-sample test (C2ST).** We introduce a new classifier two-sample test (C2ST) to measure the independence of sets of random variables. While such a kind of approach has been previously explored by [Lopez-Paz & Oquab \(2017\)](#), our proposal relies on AUC rather than accuracy.

**Explainability for fair supervised learning.** [Lundberg \(2020\)](#) apply Shapley values to statistical parity. While there is a slight overlap with our work, their extended abstract is not comparable to our paper wrt. objectives, breadth, and depth.

### 3 A Model for Monitoring Equal Treatment

#### 3.1 Formalizing Equal Treatment

To establish a criterion for equal treatment, we rely on the notion of explanation distributions.

**Definition 3.1.** (*Explanation Distribution*) An explanation function  $S : \mathcal{F} \times X \rightarrow \mathbb{R}^p$  maps a model  $f_\theta \in \mathcal{F}$  and an input instance  $x \in X$  into a vector of reals  $S(f_\theta, x) \in \mathbb{R}^p$ . We extend it by mapping an input distribution  $\mathcal{D}_X$  into an (empirical) *explanation distribution* as follows:  $S(f_\theta, \mathcal{D}_X) = \{S(f_\theta, x) \mid x \in \mathcal{D}_X\} \subseteq \mathbb{R}^p$ .

We use Shapley values as an explanation function. Let us introduce next the new fairness notion of Equal Treatment, which considers the independence of the explanations with the social group.

**Definition 3.2.** (*Equal Treatment (ET)*) A model  $f_\theta$  achieves ET if  $S(f_\theta, X) \perp Z$ .

Such a definition characterizes the philosophical notion of Equal Treatment by encoding the “treatment” performed by the model through the attribution of the importance of its input features. As we will see later in Section 4, Equal Treatment is a stronger notion than Demographic Parity since it not only requires that the distributions of the predictions are similar but that the processes of how predictions are made (i.e., the explanations) are also similar.

#### 3.2 Equal Treatment Inspector

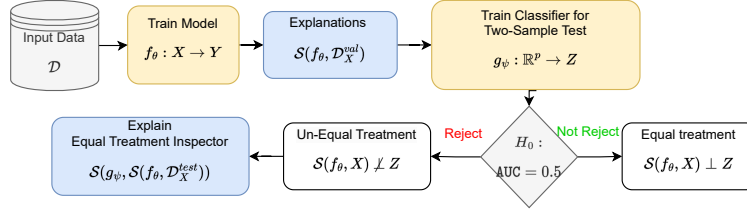


Figure 1: Equal Treatment Inspector workflow. The model  $f_\theta$  is learned based on training data,  $\mathcal{D}^{tr} = \{(x_i, y_i)\}$ , and outputs the explanations  $S(f_\theta, \mathcal{D}_X^{val})$ . The C2ST receives the explanations to predict the protected attribute,  $Z$  on validation data  $\mathcal{D}^{val}$ . The AUC of the C2ST classifier  $g_\psi$  on test data  $\mathcal{D}^{te}$  decides for or against *equal treatment*. We can interpret the driver for unequal treatment on  $g_\psi$  with explainable AI techniques.

Our approach is based on the properties of the Shapley values and on a novel classifier two-sample test. We split the available data into three parts  $\mathcal{D}^{tr}, \mathcal{D}^{val}, \mathcal{D}^{te} \subseteq X \times Y$ . Here  $\mathcal{D}^{tr}$  is the training set of  $f_\theta \in \mathcal{F}$  (not required if  $f_\theta$  is already trained). Following the intuition above,  $\mathcal{D}^{val}$  is used to train another model  $g_\psi$ , called the “Equal Treatment Inspector”. Here, the predictive features are the explanation distribution  $S(f_\theta, \mathcal{D}_{X \setminus Z}^{val})$  (excluding  $Z$ ) and the target feature is the protected feature  $Z$ . The model  $g_\psi$  belongs to a family  $\mathcal{G}$ , possibly different from  $\mathcal{F}$ . The parameter  $\psi$  optimizes a loss function  $\ell$ :

$$\psi = \arg \min_{\tilde{\psi}} \sum_{(x, z) \in \mathcal{D}^{val}} \ell(g_{\tilde{\psi}}(S(f_\theta, x)), z) \quad (1)$$

To evaluate whether there is an equal treatment violation, we perform a statistical test of independence based on the AUC of  $g_\psi$  on a test set  $\mathcal{D}^{te}$ . We also use  $\mathcal{D}^{te}$  for testing the approach w.r.t. baselines. Besides detecting fairness violations, a common desideratum is to understand what are the specific features driving such violations. The “Equal Treatment Inspector”  $g_\psi$  can provide information on *which features are the cause of the un-equal treatment*. See Figure 1 for a visualization of the whole workflow.

#### 4 Theoretical Analysis

Throughout this section, we assume an exact calculation of the Shapley values  $\mathcal{S}(f_\theta, x)$  for an instance  $x$ , possibly for the observational and interventional variants (Aas et al., 2021). In the experimental section, we will use non-IID data and non-linear models.

##### 4.1 Equal Treatment Given Shapley Values of Protected Attribute

Can we measure ET by looking only at the Shapley value of the protected feature? The following result considers a linear model (with unknown coefficients) over *independent* features. In such a very simple case, resorting to Shapley values leads to an exact test of both DP and ET, which turn out to coincide. In the following, we write  $\text{distinct}(\mathcal{D}_X, i)$  for the number of distinct values in the  $i$ -th feature of dataset  $\mathcal{D}_X$ , and  $\mathcal{S}(f_\beta, \mathcal{D}_X)_i \equiv 0$  if the Shapley values of the  $i$ -th feature are all 0's.

**Lemma 4.1.** *Consider a linear model  $f_\beta(x) = \beta_0 + \sum_j \beta_j \cdot x_j$ . Let  $Z$  be the  $i$ -th feature, i.e.  $Z = X_i$ , and let  $\mathcal{D}_X$  be such that  $\text{distinct}(\mathcal{D}_X, i) > 1$ . If the features in  $X$  are independent, then  $\mathcal{S}(f_\beta, \mathcal{D}_X)_i \equiv 0 \Leftrightarrow f_\beta(X) \perp Z \Leftrightarrow \mathcal{S}(f_\beta, X) \perp Z$ .*

*Proof.* It turns out  $\mathcal{S}(f_\beta, x)_i = \beta_i \cdot (x_i - E[X_i])$ . This holds in general for the interventional variant, and assuming independent features, also for the observational variant (Aas et al., 2021). Since  $\text{distinct}(\mathcal{D}_X, i) > 1$ , we have that  $\mathcal{S}(f_\beta, \mathcal{D}_X)_i \equiv 0$  iff  $\beta_i = 0$ . By independence of  $X$ , this is equivalent to  $f_\beta(X) \perp X_i$ , i.e.,  $f_\beta(X) \perp Z$ . Moreover, by the propagation of independence, this is also equivalent to  $\mathcal{S}(f_\beta, X) \perp Z$ .  $\square$

However, the result does not extend to the case of dependent features.

**Example 4.1.** Consider  $Z = X_2 = X_1^2$ , and the linear model  $f_\beta(x_1, x_2) = \beta_0 + \beta_1 \cdot x_1$  with  $\beta_1 \neq 0$  and  $\beta_2 = 0$ , i.e., the protected feature is not used by the model. In the interventional variant, the unformativeness property implies that  $\mathcal{S}(f_\beta, x)_2 = 0$ . However, this does not mean that  $Z = X_2$  is independent of the output because  $f_\beta(X_1, X_2) = \beta_0 + \beta_1 \cdot X_1 \not\perp X_2$ . In the observational variant, Aas et al. (2021) show that:

$$\text{val}(T) = \sum_{i \in N \setminus T} \beta_i \cdot E[X_i | X_T = x_T^*] + \sum_{i \in T} \beta_i \cdot x_i^*$$

from which, we calculate:  $\mathcal{S}(f_\beta, x^*)_2 = \frac{\beta_1}{2} E[X_1 | X_2 = x_2^*]$ . We have  $\mathcal{S}(f_\beta, \mathcal{D}_X)_2 \equiv 0$  iff  $E[X_1 | x_2 = x_2^*] = 0$  for all  $x_2^*$  in  $\mathcal{D}_X$ . For the marginal distribution  $P(X_1 = v) = 1/4$  for  $v = 1, -1, 2, -2$ , and considering that  $X_2 = X_1^2$ , it holds that  $E[X_1 | x_2 = v] = 0$  for all  $v$ . Thus  $\mathcal{S}(f, \mathcal{D}_X)_2 \equiv 0$ . However, again  $f_\beta(X_1, X_2) = \beta_0 + \beta_1 \cdot X_1 \not\perp X_2$ .

The counterexample shows that focusing only on the Shapley values of the protected feature is not a viable way to prove DP of a model – and, neither to prove ET of the model, as we show in Lemma 4.2.

##### 4.2 Equal Treatment vs Equal Outcomes vs Fairness of the Input

We start by observing that *equal treatment* (independence of the explanation distribution from the protected attribute) is a sufficient condition for *equal outcomes* measured as demographic parity (independence of the prediction distribution from the protected attribute).

**Lemma 4.2.** *If  $\mathcal{S}(f_\theta, X) \perp Z$  then  $f_\theta(X) \perp Z$ .*

*Proof.* By the propagation of independence in probability distributions, the premise implies  $(\sum_i \mathcal{S}_i(f_\theta, X) + c) \perp Z$  where  $c$  is any constant. By setting  $c = E[f(X)]$  and by the efficiency property, we have the conclusion.  $\square$

Therefore, a DP violation (on the prediction distribution) is also an ET violation (in the explanation distribution). ET accounts for a stricter notion of fairness. The other direction does not hold. We can have dependence of  $Z$  from the explanation features, but the sum of such features cancels out resulting in perfect DP on the prediction distribution.

### 4.3 Beyond Demographic Parity: Redefining Equal Treatment

**Example 4.2.** Consider the model  $f(x_1, x_2) = x_1 + x_2$ . Let  $Z \sim \text{Ber}(0.5)$ ,  $A \sim U(-3, -1)$ , and  $B \sim N(2, 1)$  be independent, and let us define:

$$X_1 = A \cdot Z + B \cdot (1 - Z) \quad X_2 = B \cdot Z + A \cdot (1 - Z)$$

We have  $f(X_1, X_2) = A + B \perp Z$  since  $A, B, Z$  are independent. Let us calculate  $\mathcal{S}(f, X)$  in the two cases  $Z = 0$  and  $Z = 1$ . If  $Z = 0$ , we have  $f(X_1, X_2) = B + A$ , and then  $\mathcal{S}(f, X)_1 = B - E[B] = B - 2 \sim N(0, 1)$  and  $\mathcal{S}(f, X)_2 = A - E[A] = A + 2 \sim U(-1, 1)$ . Similarly, for  $Z = 1$ , we have  $f(X_1, X_2) = A + B$ , and then  $\mathcal{S}(f, X)_1 = A - E[A] = A + 2 \sim U(-1, 1)$  and  $\mathcal{S}(f, X)_2 = B - E[B] = B - 2 \sim N(0, 1)$ . This shows:

$$P(\mathcal{S}(f, X)|Z = 0) \neq P(\mathcal{S}(f, X)|Z = 1)$$

and then  $\mathcal{S}(f, X) \not\perp Z$ . Notice this example holds both for the interventional and the observational cases, as we exploited Shapley values of a linear model over independent features, namely  $A, B, Z$ .

Statistical independence between the input  $X$  and the protected attribute  $Z$ , i.e.,  $X \perp Z$ , is another fairness notion. It targets fairness of the (input) datasets, disregarding the model  $f_\theta$ . For fairness-aware training algorithms, which are able not to (directly or indirectly) rely on  $Z$ , violation of such a notion of fairness does not imply ET violation nor DP violation.

**Example 4.3.** Let  $X = X_1, X_2, X_3$  be independent features such that  $E[X_1] = E[X_2] = E[X_3] = 0$ , and  $X_1, X_2 \perp Z$ , and  $X_3 \not\perp Z$ . The target feature is defined as  $Y = X_1 + X_2$ , hence it is also independent from  $Z$ . Assume a linear regression model  $f_\beta(x_1, x_2, x_3) = \beta_1 \cdot x_1 + \beta_2 \cdot x_2 + \beta_3 \cdot x_3$  trained from a sample data from  $(X, Y)$  with  $\beta_1, \beta_2 \approx 1$  and  $\beta_3 \approx 0$ . Intuitively, this occurs when a number of features are collected to train a classifier without a clear understanding of which of them contributes to the prediction. It turns out that  $X \not\perp Z$  but, for  $\beta_3 = 0$  (which can be obtained by some fairness regularization method (Kamishima et al., 2011)), we have  $f_\beta(X_1, X_2, X_3) = \beta_1 \cdot X_1 + \beta_2 \cdot X_2 \perp Z$ . By reasoning as in the proof of Lemma 4.1, we have  $\mathcal{S}(f_\beta, X) = (\beta_1 \cdot X_1, \beta_2 \cdot X_2, 0)$  and then  $\mathcal{S}(f_\beta, X) \perp Z$ . This holds both in the interventional and in the observational variants.

The above represents an example where the input data depends on the protected feature, but the model and the explanations are independent.

#### 4.3 Equal Treatment Inspection via Explanation Distributions

##### 4.3.1 Statistical Independence Test via Classifier AUC Test

In this subsection, we introduce a statistical test of independence based on the AUC of a binary classifier. The test of  $W \perp Z$  is stated in general form for multivariate random variables  $W$  and a binary random variable  $Z$  with  $\text{dom}(Z) = \{0, 1\}$ . In the next subsection, we will instantiate it to the case  $W = \mathcal{S}(f_\theta, X)$ .

Let  $\mathcal{D} = \{(w_i, z_i)\}_{i=1}^n$  be a dataset of realizations of the random sample  $(W, Z)^n \sim \mathcal{F}^n$  where  $\mathcal{F}$  is unknown. The independence  $W \perp Z$  can be tested via a two-sample test. In fact, we have  $W \perp Z$  iff  $P(W|Z) = P(W)$  iff  $P(W|Z = 1) = P(W|Z = 0)$ . We test whether the positives and negatives instances in  $\mathcal{D}$  are drawn from the same distribution by a novel two-sample test, which does not require permutation of data nor equal proportion of positive and negatives as in (Lopez-Paz & Oquab, 2017, Sections 2 and 3). We rely on a probabilistic classifier  $f : W \rightarrow [0, 1]$ , for which  $f(w)$  estimates  $P(Z = 1|W = w)$ , and on its AUC:

$$AUC(f) = E_{(W, Z), (W', Z') \sim \mathcal{F}}[I((Z - Z')(f(W) - f(W')) > 0) + 1/2 \cdot I(f(W) = f(W'))|Z \neq Z'] \quad (2)$$

Under the null hypothesis  $H_0 : W \perp Z$ , we have  $AUC(f) = 1/2$ .

**Lemma 4.3.** *If  $W \perp Z$  then  $AUC(f) = 1/2$  for any classifier  $f$ .*

*Proof.* Let us recall the definition of the Bayes Optimal classifier  $f_{opt}(w) = P(Z = 1|W = w)$ . For any classifier  $f$ , we have:

$$AUC(f_{opt}) \geq AUC(f) \geq 1 - AUC(f_{opt}) \quad (3)$$

The first bound  $AUC(f_{opt}) \geq AUC(f)$  follows because the Bayes Optimal classifier minimizes the Bayes risk (Gao & Zhou, 2015). Assume the second bound does not hold, i.e., for some  $f$  we

have  $AUC(f_{opt}) < 1 - AUC(f)$ . Consider the classifier  $\bar{f}(w) = 1 - f(w)$ . We have  $AUC(\bar{f}) \geq 1 - AUC(f)$ , and then  $\bar{f}$  would contradict the first bound because  $AUC(f_{opt}) < AUC(\bar{f})$ .

If  $W \perp Z$ , then  $P(Z = 1|W = w) = P(Z = 1)$ , and then  $f_{opt}(w)$  is constant. By (2), this implies  $AUC(f_{opt}) = 1/2$ . By (3), this implies  $AUC(f) = 1/2$  for any classifier.  $\square$

As a consequence, any statistics to test  $AUC(f) = 1/2$  can be used for testing  $W \perp Z$ . A classical choice is to resort to the Wilcoxon–Mann–Whitney test, which, however, assumes that the distributions of scores for positives and negatives have the same shape. Better alternatives include the Brunner–Munzel test (Neubert & Brunner, 2007) and the Fligner–Pollicello test (Fligner & Pollicello, 1981). The former is preferable, as the latter assumes that the distributions are symmetric.

## 5 Experimental Evaluation

We perform measures of equal treatment by systematically varying the model  $f$ , its parameters  $\theta$ , and the input data distributions  $\mathcal{D}_X$ . We adopt `xgboost` (Chen & Guestrin, 2016) for the model  $f_\theta$ , and logistic regression for the inspectors. We compare the AUC performances of several inspectors:  $g_\psi$  (see Eq. 1) for ET (see Def. 3.2),  $g_v$  for DP (see Def. 2.1),  $g_\Upsilon$  for fairness of the input (i.e.,  $X \perp Z$  as discussed in Section 4.2), and a combination  $g_\phi$  of the last two inspectors to test  $f_\theta(X)$ ,  $X \perp Z$ . These are the formal definitions:

$$\begin{aligned} \Upsilon &= \arg \min_{\Upsilon} \sum_{(x,z) \in \mathcal{D}^{val}} \ell(g_\Upsilon(x), z) & v &= \arg \min_v \sum_{(x,z) \in \mathcal{D}^{val}} \ell(g_v(f_\theta(x)), z) \\ \phi &= \arg \min_{\phi} \sum_{(x,z) \in \mathcal{D}^{val}} \ell(g_\phi(f_\theta(x), x), z) \end{aligned}$$

### 5.1 Experiments with Synthetic Data

We generate synthetic datasets by first drawing 10,000 samples from normally distributed features  $X_1 \sim N(0, 1)$ ,  $X_2 \sim N(0, 1)$ ,  $(X_3, X_4) \sim N\left(\begin{bmatrix} 0 \\ 0 \end{bmatrix}, \begin{bmatrix} 1 & \gamma \\ \gamma & 1 \end{bmatrix}\right)$ . Then, we define a binary protected feature  $Z$  with values  $Z = 1$  if  $X_4 > 0$  and  $Z = 0$  otherwise. We compare the methods and baselines while varying the correlation  $\gamma = r(X_3, Z)$  from 0 to 1. We define two experimental scenarios below. In both of them, the model  $f_\beta$  is a function over the domain of the features  $X_1, X_2, X_3$  only.

**Indirect Case: Unfairness in the data and in the model.** We consider all of the three features in the dataset  $X_1, X_2, X_3$ . This gives raise to unfairness of the input parameterized by  $\gamma = r(X_3, Z)$ . To generate DP violation in the model, we create the target  $Y = \sigma(X_1 + X_2 + X_3)$ , where  $\sigma$  is the logistic function.

**Uninformative Case: Unfairness in the data and fairness in the model.** The unfairness in the input data remains the same as in the previous case, while we now remove unfairness in the model. The target feature is now defined as  $Y = \sigma(X_1 + X_2)$ . The  $\gamma$  parameter controls unfairness in the dataset, which should not be captured by the model, since  $X_1, X_2 \perp Z$  implies  $Y \perp Z$  by propagation of independence.

In Figure 2, we compare the AUC performances of the different inspectors on synthetic data split into  $1/3$  for training the model,  $1/3$  for training the inspectors and  $1/3$  for testing them. Overall, the ET inspector  $g_\psi$  is able to detect unfairness in both scenarios. The DP inspector  $g_v$  works fine in the indirect case, but it is not sensitive to unfairness both in the data and in the model in the indirect case. Finally, the inspectors  $g_\Upsilon$  and  $g_\phi$  detect unfairness in the input but not in the model.

### 5.2 Use Case: ACS US Income Data

We experiment here with the ACS Income dataset<sup>2</sup> (Ding et al., 2021). The fairness notions are tested against all pairs of groups from the protected attribute ‘‘Race’’. Figure 3 (left) shows the AUC performances of the ET inspector  $g_\psi$  and the DT inspector  $g_v$ . Standard deviation of the AUC is calculated over 30 bootstrap runs, each one splitting the data into  $1/3$  for training the model,  $1/3$  for training the inspectors and  $1/3$  for testing them. The AUCs for the EP inspectors are greater than for the DP inspectors, as expected due to Lemma 4.2.

<sup>2</sup>ACS PUMS documentation: <https://www.census.gov/programs-surveys/acs/microdata/documentation.html>

### 4.3 Beyond Demographic Parity: Redefining Equal Treatment

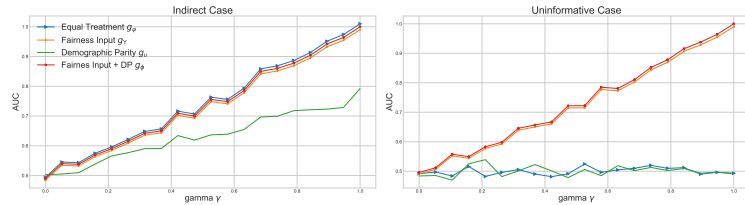


Figure 2: In the “Indirect case” (left): good unfairness detection methods should follow an increasing steady slope to capture the fairness violation; the DT inspector appears less sensitive due to the low dimensionality of its input. In the “Uninformative case” (right): good unfairness detection methods should remain constant with an  $AUC \approx 0.5$ ; the inspectors based on input data ( $g_T$  and  $g_D$ ) flag a false positive case of unfairness.

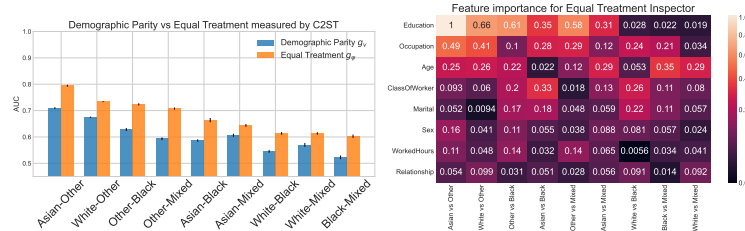


Figure 3: In the left figure, a comparison of ET and DP measures on the US Income data. The AUC range for ET is notably wider, and aligning with the theoretical section, there are indeed instances where DP fails to identify discrimination that ET successfully detects. Right figure provides insight into the influential features contributing to unequal treatment. Higher feature values correspond to a greater likelihood of these features being the underlying causes of unequal treatment.

Figure 3 (right) shows the Wasserstein distance between the coefficients of the linear regressor  $g_\psi$  compared to a baseline where groups are assigned at random in the input dataset. This feature importance post-hoc explanation method provides insights into the impact of different features as sources of unfairness. We observe “Education” as a highly discriminatory proxy while the role of the feature “Worked Hours Per Week” is less relevant. This allows us to identify areas where adjustments or interventions may be needed to move closer to the ideal of equal treatment.

## 6 Conclusions

We introduced a novel approach for fairness in machine learning by measuring *equal treatment*. While related work reasoned over model predictions to measure *equal outcomes*, our notion of equal treatment is more fine-grained, accounting for the usage of attributes by the model via explanation distributions. Consequently, equal treatment implies equal outcomes, but the converse is not necessarily true, which we confirmed both theoretically and experimentally.

This paper also seeks to improve the understanding of how theoretical concepts of fairness from liberalism-oriented political philosophy align with technical measurements. Rather than merely comparing one social group to another based on disparities within decision distributions, our concept of equal treatment takes into account differences through the explanation distribution of all non-protected attributes, which can act as proxies for protected characteristics. Implications warrant further techno-philosophical discussions.

**Limitations:** Political philosophical notions of distributive justice are more complex than we can account for in this paper. Our research has focused on tabular data using Shapley values, which allow for theoretical guarantees but may differ from their computational approximations. It is possible that alternative AI explanation techniques, such as feature attribution methods, logical reasoning,

argumentation, or counterfactual explanations, could be useful and offer their unique advantages to definitions of equal treatment. It is important to note that employing fair AI techniques does not necessarily ensure fairness in socio-technical systems based on AI, as stated in [Kulynych et al. \(2020\)](#).

#### Reproducibility Statement

To ensure the reproducibility of our results, we make publicly the open-source Python package `explanationspace` <https://github.com/cmougan/explanationspace>. We use default `scikit-learn` parameters ([Pedregosa et al., 2011](#)), unless stated otherwise. Our experiments were run on a 4 vCPU server with 32 GB RAM.

#### References

- Kjersti Aas, Martin Jullum, and Anders Løland. Explaining individual predictions when features are dependent: More accurate approximations to shapley values. *Artif. Intell.*, 298:103502, 2021.
- Julius Adebayo, Justin Gilmer, Michael Muelly, Ian J. Goodfellow, Moritz Hardt, and Been Kim. Sanity checks for saliency maps. In *NeurIPS*, pp. 9525–9536, 2018.
- Osman Aka, Ken Burke, Alex Bäuerle, Christina Greer, and Margaret Mitchell. Measuring model biases in the absence of ground truth. In *AIES*, pp. 327–335. ACM, 2021.
- David Alvarez-Melis and Tommi S. Jaakkola. Towards robust interpretability with self-explaining neural networks. In *NeurIPS*, pp. 7786–7795, 2018.
- Richard J Arneson. Equality and equal opportunity for welfare. *Philosophical Studies: An international journal for philosophy in the analytic tradition*, 56(1):77–93, 1989.
- Alejandro Barredo Arrieta, Natalia Díaz Rodríguez, Javier Del Ser, Adrien Bannetot, Siham Tabik, Alberto Barbado, Salvador García, Sergio Gil-Lopez, Daniel Molina, Richard Benjamins, Raja Chatila, and Francisco Herrera. Explainable artificial intelligence (XAI): concepts, taxonomies, opportunities and challenges toward responsible AI. *Inf. Fusion*, 58:82–115, 2020.
- Robert J Aumann and Jacques H Dreze. Cooperative games with coalition structures. *Int. J. of Game Theory*, 3:217–237, 1974.
- Vadim Borisov, Tobias Leemann, Kathrin Seßler, Johannes Haug, Martin Pawelczyk, and Gjergji Kasneci. Deep neural networks and tabular data: A survey, 2021.
- Hugh Chen, Joseph D. Janizek, Scott M. Lundberg, and Su-In Lee. True to the model or true to the data? *CoRR*, abs/2006.16234, 2020.
- Jianbo Chen, Le Song, Martin J. Wainwright, and Michael I. Jordan. L-shapley and c-shapley: Efficient model interpretation for structured data. In *ICLR (Poster)*. OpenReview.net, 2019.
- Tianqi Chen and Carlos Guestrin. Xgboost: A scalable tree boosting system. In *KDD*, pp. 785–794. ACM, 2016.
- Jaewoong Cho, Gyeongjo Hwang, and Changho Suh. A fair classifier using kernel density estimation. In *NeurIPS*, 2020.
- Alexandra Chouldechova. Fair prediction with disparate impact: A study of bias in recidivism prediction instruments. *Big Data*, 5(2):153–163, 2017.
- Gerald A Cohen. On the currency of egalitarian justice. *Ethics*, 99(4):906–944, 1989.
- Sam Corbett-Davies, Emma Pierson, Avi Feller, Sharad Goel, and Aziz Huq. Algorithmic decision making and the cost of fairness. In *KDD*, pp. 797–806. ACM, 2017.
- Anupam Datta, Shayak Sen, and Yair Zick. Algorithmic transparency via quantitative input influence: Theory and experiments with learning systems. In *IEEE Symposium on Security and Privacy*, pp. 598–617. IEEE Computer Society, 2016.

### 4.3 Beyond Demographic Parity: Redefining Equal Treatment

---

- Frances Ding, Moritz Hardt, John Miller, and Ludwig Schmidt. Retiring adult: New datasets for fair machine learning. In *NeurIPS*, pp. 6478–6490, 2021.
- Cynthia Dwork, Moritz Hardt, Toniann Pitassi, Omer Reingold, and Richard S. Zemel. Fairness through awareness. In *ITCS*, pp. 214–226. ACM, 2012.
- Ronald Dworkin. What is equality? Part 1: Equality of welfare. *Philosophy & public affairs*, pp. 185–246, 1981a.
- Ronald Dworkin. What is equality? Part 2: Equality of resources. *Philosophy & public affairs*, pp. 283–345, 1981b.
- Harrison Edwards and Amos J. Storkey. Censoring representations with an adversary. In *ICLR (Poster)*, 2016.
- Carl McBride Ellis. Kaggle: What is adversarial validation? <https://www.kaggle.com/code/carlmcbrideellis/what-is-adversarial-validation>, 2023. Accessed 03/04/23.
- Shereen Elsayed, Daniela Thyssens, Ahmed Rashed, Lars Schmidt-Thieme, and Hadi Samer Jomaa. Do we really need deep learning models for time series forecasting? *CoRR*, abs/2101.02118, 2021.
- Simone Fabbrizzi, Symeon Papadopoulos, Eirini Ntoutsi, and Ioannis Kompatsiaris. A survey on bias in visual datasets. *Comput. Vis. Image Underst.*, 223:103552, 2022.
- Michael A Fligner and George E Policello. Robust rank procedures for the behrens-fisher problem. *Journal of the American Statistical Association*, (373):162–168, 1981.
- Milton Friedman. Wikipedia, the free encyclopedia, 2022. URL [https://en.wikipedia.org/wiki/Milton\\_Friedman#cite\\_note-Reason1995June-1](https://en.wikipedia.org/wiki/Milton_Friedman#cite_note-Reason1995June-1). [Online; accessed 12-May-2023].
- Milton Friedman, Rose D Friedman, and Rose D Friedman. *Free to choose*. Free to Choose Enterprise, 1990.
- Christopher Frye, Colin Rowat, and Ilya Feige. Asymmetric shapley values: incorporating causal knowledge into model-agnostic explainability. In *NeurIPS*, 2020.
- Wei Gao and Zhi-Hua Zhou. On the consistency of AUC pairwise optimization. In *IJCAI*, pp. 939–945. AAAI Press, 2015.
- Saurabh Garg, Sivaraman Balakrishnan, J. Zico Kolter, and Zachary C. Lipton. RATT: leveraging unlabeled data to guarantee generalization. In *ICML*, volume 139 of *Proceedings of Machine Learning Research*, pp. 3598–3609. PMLR, 2021.
- Saurabh Garg, Sivaraman Balakrishnan, Zachary Chase Lipton, Behnam Neyshabur, and Hanie Sedghi. Leveraging unlabeled data to predict out-of-distribution performance. In *ICLR*. OpenReview.net, 2022.
- Amirata Ghorbani and James Y. Zou. Data shapley: Equitable valuation of data for machine learning. In *ICML*, volume 97 of *Proceedings of Machine Learning Research*, pp. 2242–2251. PMLR, 2019.
- Przemysław A. Grabowicz, Nicholas Perello, and Aarshee Mishra. Marrying fairness and explainability in supervised learning. In *FACt*, pp. 1905–1916. ACM, 2022.
- Léo Grinsztajn, Edouard Oyallon, and Gaël Varoquaux. Why do tree-based models still outperform deep learning on typical tabular data? In *NeurIPS*, 2022.
- Riccardo Guidotti, Anna Monreale, Salvatore Ruggieri, Franco Turini, Fosca Giannotti, and Dino Pedreschi. A survey of methods for explaining black box models. *ACM Comput. Surv.*, 51(5): 93:1–93:42, 2019.
- Alexander Guschin, Dmitry Ulyanov, Mikhail Trofimov, Dmitry Altukhov, and Mario Michaidilis. How to win a data science competition: Learn from top kagglers - national research university higher school of economics. <https://www.coursera.org/lecture/competitive-data-science/categorical-and-ordinal-features-qu1TF>, 2018. Accessed 02/11/20.

### 4.3 Beyond Demographic Parity: Redefining Equal Treatment

---

- Moritz Hardt, Eric Price, and Nati Srebro. Equality of opportunity in supervised learning. In *NIPS*, pp. 3315–3323, 2016.
- Hoda Heidari, Michele Loi, Krishna P. Gummadi, and Andreas Krause. A moral framework for understanding fair ML through economic models of equality of opportunity. In *FAT*, pp. 181–190. ACM, 2019.
- Zhimeng Jiang, Xiaotian Han, Chao Fan, Fan Yang, Ali Mostafavi, and Xia Hu. Generalized demographic parity for group fairness. In *ICLR*. OpenReview.net, 2022.
- Toshihiro Kamishima, Shotaro Akaho, and Jun Sakuma. Fairness-aware learning through regularization approach. In *ICDM Workshops*, pp. 643–650. IEEE Computer Society, 2011.
- Michael J. Kearns, Seth Neel, Aaron Roth, and Zhiwei Steven Wu. Preventing fairness gerrymandering: Auditing and learning for subgroup fairness. In *ICML*, volume 80 of *Proceedings of Machine Learning Research*, pp. 2569–2577. PMLR, 2018.
- Jon M. Kleinberg, Sendhil Mullainathan, and Manish Raghavan. Inherent trade-offs in the fair determination of risk scores. In *ITCS*, volume 67 of *LIPICs*, pp. 43:1–43:23. Schloss Dagstuhl - Leibniz-Zentrum für Informatik, 2017.
- Bogdan Kulynych, Rebekah Overdorf, Carmela Troncoso, and Seda F. Gürses. Pots: protective optimization technologies. In *FAT\**, pp. 177–188. ACM, 2020.
- Matt J. Kusner, Joshua R. Loftus, Chris Russell, and Ricardo Silva. Counterfactual fairness. In *NIPS*, pp. 4066–4076, 2017.
- Yongchan Kwon, Manuel A. Rivas, and James Zou. Efficient computation and analysis of distributional shapley values. In *AISTATS*, volume 130 of *Proceedings of Machine Learning Research*, pp. 793–801. PMLR, 2021.
- Will Kymlicka. *Contemporary political philosophy: An introduction*. oxford: oxford University Press, 2002.
- Julian Lamont and Christi Favor. Distributive justice. In Edward N. Zalta (ed.), *The Stanford Encyclopedia of Philosophy (Winter 2017 Edition)*. Stanford, 2017. <https://plato.stanford.edu/archives/win2017/entries/justice-distributive/>.
- Feng Liu, Wenkai Xu, Jie Lu, Guangquan Zhang, Arthur Gretton, and Danica J. Sutherland. Learning deep kernels for non-parametric two-sample tests. In *ICML*, volume 119 of *Proceedings of Machine Learning Research*, pp. 6316–6326. PMLR, 2020.
- David Lopez-Paz and Maxime Oquab. Revisiting classifier two-sample tests. In *ICLR (Poster)*. OpenReview.net, 2017.
- Scott M Lundberg. Explaining quantitative measures of fairness. In *Fair & Responsible AI Workshop@CHI2020*, 2020.
- Scott M. Lundberg and Su-In Lee. A unified approach to interpreting model predictions. In *NIPS*, pp. 4765–4774, 2017.
- Scott M Lundberg, Bala Nair, Monica S Vavilala, Mayumi Horibe, Michael J Eisses, Trevor Adams, David E Liston, Daniel King-Wai Low, Shu-Fang Newman, Jerry Kim, et al. Explainable machine-learning predictions for the prevention of hypoxaemia during surgery. *Nature Biomedical Eng.*, 2(10):749–760, 2018.
- Scott M. Lundberg, Gabriel G. Erion, Hugh Chen, Alex J. DeGrave, Jordan M. Prutkin, Bala Nair, Ronit Katz, Jonathan Himmelfarb, Nisha Bansal, and Su-In Lee. From local explanations to global understanding with explainable AI for trees. *Nat. Mach. Intell.*, 2(1):56–67, 2020.
- Marta Marchiori Manerba and Riccardo Guidotti. Fairshades: Fairness auditing via explainability in abusive language detection systems. In *CogMI*, pp. 34–43. IEEE, 2021.
- Masayoshi Mase, Art B. Owen, and Benjamin Seiler. Explaining black box decisions by shapley cohort refinement. *CoRR*, abs/1911.00467, 2019.

### 4.3 Beyond Demographic Parity: Redefining Equal Treatment

---

- Ninareh Mehrabi, Fred Morstatter, Nripsuta Saxena, Kristina Lerman, and Aram Galstyan. A survey on bias and fairness in machine learning. *ACM Comput. Surv.*, 54(6):115:1–115:35, 2022.
- Arthur S Miller and Ronald F Howell. The myth of neutrality in constitutional adjudication. *University of Chicago Law Review*, 27:661, 1959.
- Brent D. Mittelstadt, Chris Russell, and Sandra Wachter. Explaining explanations in AI. In *FAT*, pp. 279–288. ACM, 2019.
- Christoph Molnar. *Interpretable Machine Learning*. , 2019. <https://christophm.github.io/interpretable-ml-book/>.
- Carlos Mougán and Dan Saattrup Nielsen. Monitoring model deterioration with explainable uncertainty estimation via non-parametric bootstrap. In *AAAI*, pp. 15037–15045. AAAI Press, 2023.
- Carlos Mougán, Klaus Broelemann, Gjergji Kasneci, Thanassis Tiropanis, and Steffen Staab. Explanation shift: Detecting distribution shifts on tabular data via the explanation space. *CoRR*, abs/2210.12369, 2022.
- Ece Çigdem Mutlu, Niloofar Yousefi, and Özlem Özmen Garibay. Contrastive counterfactual fairness in algorithmic decision-making. In *AIES*, pp. 499–507. ACM, 2022.
- Karin Neubert and Edgar Brunner. A studentized permutation test for the non-parametric behrens-fisher problem. *Comput. Stat. Data Anal.*, 51(10):5192–5204, 2007.
- Robert Nozick. *Anarchy, state, and utopia*, volume 5038. New York: Basic Books, 1974.
- Fabian Pedregosa, Gaël Varoquaux, Alexandre Gramfort, Vincent Michel, Bertrand Thirion, Olivier Grisel, Mathieu Blondel, Peter Prettenhofer, Ron Weiss, Vincent Dubourg, Jake VanderPlas, Alexandre Passos, David Cournapeau, Matthieu Brucher, Matthieu Perrot, and Edouard Duchesnay. Scikit-learn: Machine learning in python. *J. Mach. Learn. Res.*, 12:2825–2830, 2011.
- Dino Pedreschi, Salvatore Ruggieri, and Franco Turini. Discrimination-aware data mining. In *KDD*, pp. 560–568. ACM, 2008.
- Inioluwa Deborah Raji, Andrew Smart, Rebecca N. White, Margaret Mitchell, Timnit Gebru, Ben Hutchinson, Jamila Smith-Loud, Daniel Theron, and Parker Barnes. Closing the AI accountability gap: defining an end-to-end framework for internal algorithmic auditing. In *FAT\**, pp. 33–44. ACM, 2020.
- John Rawls. Justice as fairness. *The philosophical review*, 67(2):164–194, 1958.
- John Rawls. Justice as fairness: Political not metaphysical. In *Equality and Liberty*, pp. 145–173. Springer, 1991.
- Marco Tulio Ribeiro, Sameer Singh, and Carlos Guestrin. Model-agnostic interpretability of machine learning, 2016a.
- Marco Túlio Ribeiro, Sameer Singh, and Carlos Guestrin. "why should I trust you?": Explaining the predictions of any classifier. In *KDD*, pp. 1135–1144. ACM, 2016b.
- Benedek Rozemberczki, Lauren Watson, Péter Bayer, Hao-Tsung Yang, Oliver Kiss, Sebastian Nilsson, and Rik Sarkar. The shapley value in machine learning. In *IJCAI*, pp. 5572–5579. ijcai.org, 2022.
- Boris Ruf and Marcin Detyniecki. Towards the right kind of fairness in AI. *CoRR*, abs/2102.08453, 2021.
- Salvatore Ruggieri, José M. Álvarez, Andrea Pugnana, Laura State, and Franco Turini. Can we trust fair-AI? In *AAAI*, pp. 15421–15430. AAAI Press, 2023.
- Andrew D Selbst and Solon Barocas. The intuitive appeal of explainable machines. *Fordham L. Rev.*, 87:1085, 2018.

### 4.3 Beyond Demographic Parity: Redefining Equal Treatment

---

- Lloyd S Shapley. A value for n-person games. *Classics in game theory*, 69, 1997.
- Joshua Simons, Sophia Adams Bhatti, and Adrian Weller. Machine learning and the meaning of equal treatment. In *AIES*, pp. 956–966. ACM, 2021.
- Dylan Slack, Sophie Hilgard, Emily Jia, Sameer Singh, and Himabindu Lakkaraju. Fooling LIME and SHAP: adversarial attacks on post hoc explanation methods. In *AIES*, pp. 180–186. ACM, 2020.
- Alexander Stevens, Peter Deruyck, Ziboud Van Veldhoven, and Jan Vanthienen. Explainability and fairness in machine learning: Improve fair end-to-end lending for kiva. In *SSCI*, pp. 1241–1248. IEEE, 2020.
- Erik Strumbelj and Igor Kononenko. Explaining prediction models and individual predictions with feature contributions. *Knowl. Inf. Syst.*, 41(3):647–665, 2014.
- Mukund Sundararajan and Amir Najmi. The many shapley values for model explanation. In *ICML*, volume 119 of *Proceedings of Machine Learning Research*, pp. 9269–9278. PMLR, 2020.
- Cass R Sunstein. Neutrality in constitutional law (with special reference to pornography, abortion, and surrogacy). *Columbia Law Review*, 92:1, 1992.
- Pauli Virtanen, Ralf Gommers, Travis E. Oliphant, Matt Haberland, Tyler Reddy, David Cournapeau, Evgeni Burovski, Pearu Peterson, Warren Weckesser, Jonathan Bright, Stéfan J. van der Walt, Matthew Brett, Joshua Wilson, K. Jarrod Millman, Nikolay Mayorov, Andrew R. J. Nelson, Eric Jones, Robert Kern, Eric Larson, C J Carey, İlhan Polat, Yu Feng, Eric W. Moore, Jake VanderPlas, Denis Laxalde, Josef Perktold, Robert Cimrman, Ian Henriksen, E. A. Quintero, Charles R. Harris, Anne M. Archibald, Antônio H. Ribeiro, Fabian Pedregosa, Paul van Mulbregt, and SciPy 1.0 Contributors. SciPy 1.0: Fundamental Algorithms for Scientific Computing in Python. *Nature Methods*, 17:261–272, 2020. doi: 10.1038/s41592-019-0686-2.
- Sandra Wachter, Brent Mittelstadt, and Chris Russell. Bias preservation in machine learning: the legality of fairness metrics under european union non-discrimination law. *West Virginia Law Review*, 123:735, 2020.
- Eyal Winter. The Shapley value. In *Handbook of Game Theory with Economic Applications*, volume 3, pp. 2025–2054. Elsevier, 2002.
- Kaiyu Yang, Klint Qinami, Li Fei-Fei, Jia Deng, and Olga Russakovsky. Towards fairer datasets: filtering and balancing the distribution of the people subtree in the imagenet hierarchy. In *FAT\**, pp. 547–558. ACM, 2020.
- Artjom Zern, Klaus Broelemann, and Gjergji Kasneci. Interventional SHAP values and interaction values for piecewise linear regression trees. In *AAAI*, pp. 11164–11173. AAAI Press, 2023.
- Jieyu Zhao, Tianlu Wang, Mark Yatskar, Vicente Ordonez, and Kai-Wei Chang. Men also like shopping: Reducing gender bias amplification using corpus-level constraints. In *EMNLP*, pp. 2979–2989. Association for Computational Linguistics, 2017.

**Contents**

<b>1 Introduction</b>	<b>1</b>
<b>2 Foundations and Related work</b>	<b>2</b>
2.1 Basic Notations and Formal Definitions of Fairness in Related Work . . . . .	2
2.2 Philosophical Foundations and Computable Fairness Metrics . . . . .	2
2.3 Fairness Notions: Paper Blind Reviews Use Case . . . . .	3
2.4 Related Work . . . . .	3
<b>3 A Model for Monitoring Equal Treatment</b>	<b>4</b>
3.1 Formalizing Equal Treatment . . . . .	4
3.2 Equal Treatment Inspector . . . . .	4
<b>4 Theoretical Analysis</b>	<b>5</b>
4.1 Equal Treatment Given Shapley Values of Protected Attribute . . . . .	5
4.2 Equal Treatment vs Equal Outcomes vs Fairness of the Input . . . . .	5
4.3 Equal Treatment Inspection via Explanation Distributions . . . . .	6
4.3.1 Statistical Independence Test via Classifier AUC Test . . . . .	6
<b>5 Experimental Evaluation</b>	<b>7</b>
5.1 Experiments with Synthetic Data . . . . .	7
5.2 Use Case: ACS US Income Data . . . . .	7
<b>6 Conclusions</b>	<b>8</b>
<b>A Definition and Properties of Shapley values</b>	<b>15</b>
<b>B Detailed Related Work</b>	<b>16</b>
B.1 Fairness Notions: Paper Blind Reviews Use Case . . . . .	16
B.2 Measuring Fairness . . . . .	16
B.3 Explainability and fair supervised learning . . . . .	17
B.4 Classifier Two-Sample Test (C2ST) . . . . .	17
<b>C True to the Model or True to the Data?</b>	<b>18</b>
<b>D Experiments on datasets derived from the US Census</b>	<b>19</b>
D.1 ACS Employment . . . . .	19
D.2 ACS Travel Time . . . . .	19
D.3 ACS Mobility . . . . .	20
<b>E Additional Experiments</b>	<b>20</b>
E.1 Statistical Independence Test via Classifier AUC Test . . . . .	20
E.2 Hyperparameters Evaluation . . . . .	21

E.3 Varying Estimator and Inspector . . . . . 22  
 E.4 Explaining ET Unfairness . . . . . 22  
 E.5 Statistical Comparison of Demographic Parity versus Equal Treatment . . . . . 23  
**F LIME as an Alternative to Shapley Values . . . . . 25**  
 F.1 Runtime . . . . . 25

**A Definition and Properties of Shapley values**

Explainability has become an important concept in legal and ethical guidelines for data processing and machine learning applications (Selbst & Barocas, 2018). A wide variety of methods have been developed, aiming to account for the decision of algorithmic systems (Guidotti et al., 2019; Mittelstadt et al., 2019; Arrieta et al., 2020). One of the most popular approaches to explainability in machine learning is Shapley values.

Shapley values are used to attribute relevance to features according to how the model relies on them (Lundberg et al., 2020; Lundberg & Lee, 2017; Rozemberczki et al., 2022). Shapley values are a coalition game theory concept that aims to allocate the surplus generated by the grand coalition in a game to each of its players (Shapley, 1997).

For set of players  $N = \{1, \dots, p\}$ , and a value function  $\text{val} : 2^N \rightarrow \mathbb{R}$ , the Shapley value  $\mathcal{S}_j$  of the  $j$ 'th player is defined as the average marginal contribution of player  $j$  in all possible coalitions of players:

$$\mathcal{S}_j = \sum_{T \subseteq N \setminus \{j\}} \frac{|T|!(p - |T| - 1)!}{p!} (\text{val}(T \cup \{j\}) - \text{val}(T))$$

In the context of machine learning models, players correspond to features  $X_1, \dots, X_p$ , and the contribution of the feature  $X_j$  is with reference to the prediction of a model  $f$  for an instance  $x^*$  to be explained. Thus, we write  $\mathcal{S}(f, x^*)_j$  for the Shapley value of feature  $X_j$  in the prediction  $f(x^*)$ . We denote by  $\mathcal{S}(f, x^*)$  the vector of Shapely values  $(\mathcal{S}(f, x^*)_1, \dots, \mathcal{S}(f, x^*)_p)$ .

There are two variants for the term  $\text{val}(T)$  (Aas et al., 2021; Chen et al., 2020; Zern et al., 2023): the *observational* and the *interventional*. When using the observational conditional expectation, we consider the expected value of  $f$  over the joint distribution of all features conditioned to fix features in  $T$  to the values they have in  $x^*$ :

$$\text{val}(T) = E[f(x_T^*, X_{N \setminus T}) | X_T = x_T^*] \tag{4}$$

where  $f(x_T^*, X_{N \setminus T})$  denotes that features in  $T$  are fixed to their values in  $x^*$ , and features not in  $T$  are random variables over the joint distribution of features. Opposed, the interventional conditional expectation considers the expected value of  $f$  over the marginal distribution of features not in  $T$ :

$$\text{val}(T) = E[f(x_T^*, X_{N \setminus T})] \tag{5}$$

In the interventional variant, the marginal distribution is unaffected by the knowledge that  $X_T = x_T^*$ . In general, the estimation of (4) is difficult, and some implementations (e.g., SHAP) actually consider (5) as the default one. In the case of decision tree models, TreeSHAP offers both possibilities.

The Shapley value framework is the only feature attribution method that satisfies the properties of efficiency, symmetry, uninformative and additivity (Molnar, 2019; Shapley, 1997; Winter, 2002; Aumann & Dreze, 1974). We recall next the key properties of efficiency and uninformative:

**Efficiency.** Feature contributions add up to the difference of prediction for  $x^*$  and the expected value of  $f$ :

$$\sum_{j \in N} \mathcal{S}(f, x^*)_j = f(x^*) - E[f(X)] \tag{6}$$

The following property only holds for the interventional variant (e.g., for SHAP values), but not for the observational variant.

**Uninformativeness.** A feature  $X_j$  that does not change the predicted value (i.e., for all  $x, x'_j$ :  $f(x_{N \setminus \{j\}}, x_j) = f(x_{N \setminus \{j\}}, x'_j)$ ) has a Shapley value of zero, i.e.,  $S(f, x^*)_j = 0$ .

In the case of a linear model  $f_\beta(x) = \beta_0 + \sum_j \beta_j \cdot x_j$ , the SHAP values turns out to be  $S(f, x^*)_i = \beta_i(x_i^* - \mu_i)$  where  $\mu_i = E[X_i]$ . For the observational case, this holds only if the features are independent (Aas et al., 2021).

## B Detailed Related Work

This section provides an in-depth review of the related theoretical work that informs our research. We contextualize our contribution within the broader field of explainable AI and fairness auditing. We discuss the use of fairness measures such as demographic parity, as well as explainability techniques like Shapley values and counterfactual explanations.

### B.1 Fairness Notions: Paper Blind Reviews Use Case

To illustrate the difference between equal opportunity, equal outcomes, and equal treatment, based on the previously discussed framework, we consider the example of conference papers' blind reviews and focus on the protected attribute of the country of origin of the paper's author, comparing Germany and the United Kingdom.

For *equal opportunity*, we quantify fairness by the true positive rate (cf. Definition 2.2). In words, it is the acceptance ratio given that the quality of the paper is high. Achieving equal opportunity will imply that these ratios are similar between the two countries. In blind reviews, the purpose is to evaluate the paper's quality and the research's merit without being influenced by factors such as the author's identity, affiliations, background or country. If we were to enforce equal opportunity in this use case, we would aim for similar true positive rates for submissions from different countries. However, this approach could lead to unintended consequences, such as unintentionally favouring, reverse discrimination, overcorrection or quotas of affirmative action towards certain countries.

For *equal outcomes*, we require that the distribution of acceptance rates is similar, independently of the quality of the paper (cf. Definition 2.1). Note that the outcomes can have similar rates due to random chance, even if there is a country bias in the acceptance procedure.

For *equal treatment*, we require that the contributions of the features used to make a decision on paper's acceptance has similar distributions (cf. Definition 3.2). Equality of treatment through blindness is more desirable than equal opportunity or equal outcomes because it ensures that all submissions are evaluated solely on the basis of their quality, without any bias or discrimination towards any particular country. By achieving equality of treatment through blindness, we can promote fairness and objectivity in the review process and ensure that all papers have an equal chance to be evaluated on their merits.

In comparing our introduced measure of *equal treatment* with *equal outcomes* (or demographic or statistical parity, used as synonymous), we note that the latter looks at the distributions of predictions and measures their similarity. Equal treatment goes a step further by evaluating whether the contribution of features to the decision, is similar. Our definition of *equal treatment* implies the notion of *equal outcome*, but the converse is not necessarily true, as we showed in Section 4.3.1.

### B.2 Measuring Fairness

Selecting a measure to compare fairness between two sensitive groups has been a highly discussed topic, where results such as (Chouldechova, 2017; Hardt et al., 2016; Kleinberg et al., 2017), have highlighted the impossibility to satisfy simultaneously three type of fairness measures: demographic parity (Dwork et al., 2012), equalized odds (Hardt et al., 2016), and predictive parity (Corbett-Davies et al., 2017; Ruf & Detyniecki, 2021; Wachter et al., 2020).

Previous work has relied on measuring and calculating demographic parity on the model predictions (Raji et al., 2020; Kearns et al., 2018), or on the input data (Fabrizzi et al., 2022; Yang et al., 2020; Zhao et al., 2017). In this work, we perform equal treatment measures on the explanation distribution, which measures that each feature contributes equally to the prediction, which differs from the previous notions.

In this work, we focus on Equal Treatment (ET), as this fairness metric does not require a ground truth target variable, allowing for our method to work in its absence (Aka et al., 2021), and under distribution shift conditions (Mougan et al., 2022) where model performance metrics are not feasible to calculate (Garg et al., 2021, 2022; Mougan & Nielsen, 2023). Demographic Parity requires independence of the model’s output from the protected features, written  $f_\theta(X) \perp Z$ , while Equal Treatment requires independence across the feature attributions of the model  $\mathcal{S}(f_\theta(X), X) \perp Z$ .

#### B.3 Explainability and fair supervised learning

The intersection of fairness and explainable AI has been an active topic in recent years. The work most close to our approach is Lundberg (2020) where Shapley values are aimed at testing for demographic parity. This concise workshop paper emphasizes the importance of “decomposing a fairness metric among each of a model’s inputs to reveal which input features may be driving any observed fairness disparities”. In terms of statistical independence, the approach can be rephrased as decomposing  $f_\theta(X) \perp Z$  by examining  $\mathcal{S}(f_\theta, X)_i \perp Z$  for  $i \in [1, p]$ . Actually, the paper limits to consider difference in means, namely testing for  $E[\mathcal{S}(f_\theta, X)_i | Z = 1] \neq E[\mathcal{S}(f_\theta, X)_i | Z = 0]$ . Our approach goes beyond this, as we consider different distributions, and introduce the ET fairness notion for that. On the contrary, Lundberg (2020) claims a decomposition method specific of DP. However, the decomposition method proposed is not sufficient nor necessary to prove DP, as showed next.

**Lemma B.1.**  $f_\theta(X) \perp Z$  is neither implied by nor it implies  $(\mathcal{S}(f_\theta, X))_i \perp Z$  for  $i \in [1, p]$ .

*Proof.* Consider  $f_\theta(X_1, X_2) = X_1 - X_2$  with  $X_1, X_2 \sim \text{Ber}(0.5)$  and  $Z = 1$  if  $X_1 = X_2$ , and  $Z = 0$  otherwise. Hence  $Z \sim \text{Ber}(0.5)$ . We have  $\mathcal{S}(f_\theta, X_1) = X_1 \perp Z$  and  $\mathcal{S}(f_\theta, X_2) = -X_2 \perp Z$ . However,  $f_\theta(X_1, X_2) = X_1 - X_2$  does not satisfy  $f_\theta(X_1, X_2) \perp Z$ , e.g.,  $P(Z = 0 | f_\theta(X_1, X_2) = 0) = P(Z = 0 | X_1 - X_2 = 0) = 1$ . Example 4.2 illustrates a case where  $f_\theta(X) \perp Z$  yet  $\mathcal{S}(f_\theta, X)_1$  and  $\mathcal{S}(f_\theta, X)_2$  are not independent of  $Z$ .  $\square$

Our approach to ET considers the independence of the *multivariate* distribution of  $\mathcal{S}(f, X)$  with respect to  $Z$ , rather than the independence of each marginal distribution  $\mathcal{S}(f_\theta, X)_i \perp Z$ . With such a definition, we obtain a sufficient condition for DP, as shown in Lemma 4.2.

Stevens et al. (2020) presents an approach based on adapting the Shapley value function to explain model unfairness. They also introduce a new meta-algorithm that considers the problem of learning an additive perturbation to an existing model in order to impose fairness. In our work, we do not adopt the Shapley value function. Instead, we use the theoretical Shapley properties to provide fairness auditing guarantees. Our “Equal Treatment Inspector” is not perturbation-based but uses Shapley values to project the model to the explanation distribution, and then measures *un-equal treatment*. It also allows us to pinpoint what are the specific features driving this violation.

Grabowicz et al. (2022) present a post-processing method based on Shapley values aiming to detect and nullify the influence of a protected attribute on the output of the system. For this, they assume there are direct causal links from the data to the protected attribute and that there are no measured confounders. Our work does not use causal graphs but exploits the theoretical properties of the Shapley values to obtain fairness model auditing guarantees.

A few works have researched fairness using other explainability techniques such as counterfactual explanations (Kusner et al., 2017; Manerba & Guidotti, 2021; Mutlu et al., 2022). We don’t focus on counterfactual explanations but on feature attribution methods that allow us to measure unequal feature contribution to the prediction. Further work can be envisioned by applying explainable AI techniques to the “Equal Treatment Inspector” or constructing the explanation distribution out of other techniques.

#### B.4 Classifier Two-Sample Test (C2ST)

The use of classifiers as a statistical tests of independence  $W \perp Z$  for a binary  $Z$  has been previously explored in the literature (Lopez-Paz & Oquab, 2017). The approach relies on testing accuracy of a classifier trained to distinguish  $Z = 1$  (positives) from  $Z = 0$  (negatives) given  $W = w$ . In the null hypothesis that the distributions of positives and negatives are the same, no classifier is better than a random answer with accuracy  $1/2$ . This assumes equal proportion of instances of the two distributions in the training and test set. Our approach builds on this idea, but it considers testing the AUC instead

of the accuracy. Thus, we remove the assumption of equal proportions<sup>3</sup>. We also show in Section E.1 that using AUC may achieve a better power than using accuracy.

Liu et al. (2020) propose a kernel-based approach to two-sample tests classification. Alike work has also been used in Kaggle competitions under the name of “Adversarial Validation” (Ellis, 2023; Guschin et al., 2018), a technique which aims to detect which features are distinct between train and leaderboard datasets to avoid possible leaderboard shakes.

Edwards & Storkey (2016) focuses on removing statistical parity from images by using an adversary that tries to predict the relevant sensitive variable from the model representation and censoring the learning of the representation of the model and data on images and neural networks. While methods for images or text data are often developed specifically for neural networks and cannot be directly applied to traditional machine learning techniques, we focus on tabular data where techniques such as gradient boosting decision trees achieve state-of-the-art model performance (Grinsztajn et al., 2022; Elsayed et al., 2021; Borisov et al., 2021). Furthermore, our model and data projection into the explanation distributions leverages Shapley value theory to provide fairness auditing guarantees. In this sense, our work can be viewed as an extension of their work, both in theoretical and practical applications.

#### C True to the Model or True to the Data?

Many works discuss the application of Shapley values for feature attribution in ML models (Strumbelj & Kononenko, 2014; Lundberg et al., 2020; Lundberg & Lee, 2017; Lundberg et al., 2018). However, the correct way to connect a model to a coalitional game, which is the central concept of Shapley values, is a source of controversy, with two main approaches: an interventional (Aas et al., 2021; Frye et al., 2020; Zern et al., 2023), and an observational formulation of the conditional expectation, see (4,5) (Sundararajan & Najmi, 2020; Datta et al., 2016; Mase et al., 2019).

In the following experiment, we compare the impact of the two approaches on our “Equal Treatment Inspector”. We benchmark this experiment on the four prediction tasks based on the US census data (Ding et al., 2021) and use linear models for both the  $f_\theta(X)$  and  $g_\psi(\mathcal{S}(f_\theta, X))$ . We calculate the two variants of Shapley values using the SHAP linear explainer.<sup>4</sup> The comparison will be parametric to a feature perturbation hyperparameter. The interventional SHAP values break the dependence structure between features in the model to uncover how the model would behave if the inputs are changed (as it was an intervention). This option is said to stay “true to the model” meaning it will only give allocation credit to the features that are actually used by the model. On the other hand, the full conditional approximation of the SHAP values respects the correlations of the input features. If the model depends on one input that is correlated with another input, then both get some credit for the model’s behaviour. This option is said to say “true to the data”, meaning that it only considers how the model would behave when respecting the correlations in the input data (Chen et al., 2020). We will measure the difference between the two approaches by looking at the AUC and at the linear coefficients of the inspector  $g_\psi$ , for this case only for the pair White-Other. In Table 1 and Table 2, we can see that differences in AUC and coefficients are negligible.

Table 1: AUC comparison of the “Equal Treatment Inspector” between estimating the Shapley values between the interventional and the observational approaches for the four prediction tasks based on the US census dataset. The % column is the relative difference.

	Interventional	Correlation	%
Income	0.736438	0.736439	1.1e-06
Employment	0.747923	0.747923	4.44e-07
Mobility	0.690734	0.690735	8.2e-07
Travel Time	0.790512	0.790512	3.0e-07

<sup>3</sup>For unequal proportions, one can consider the accuracy of the majority class, but this still make the requirement to know the true proportion of positives and negatives.

<sup>4</sup><https://shap.readthedocs.io/en/latest/generated/shap.explainers.Linear.html>

### 4.3 Beyond Demographic Parity: Redefining Equal Treatment

Table 2: Linear regression coefficients comparison of the “Equal Treatment Inspector” between estimating the Shapley values between the interventional and the observational approaches for the ACS Income prediction task. The % column is the relative difference.

	Interventional	Correlation	%
Marital	0.348170	0.348190	2.0e-05
Worked Hours	0.103258	-0.103254	3.5e-06
Class of worker	0.579126	0.579119	6.6e-06
Sex	0.003494	0.003497	3.4e-06
Occupation	0.195736	0.195744	8.2e-06
Age	-0.018958	-0.018954	4.2e-06
Education	-0.006840	-0.006840	5.9e-07
Relationship	0.034209	0.034212	2.5e-06

## D Experiments on datasets derived from the US Census

In the main body of the paper, we considered the ACS Income dataset. Here, we experiment with additional datasets derived from the US census database (Ding et al., 2021): ACS Travel Time, ACS Employment and ACS Mobility. We compare fairness of the prediction tasks for pairs of protected attribute groups over the California 2014 district data.

We follow the same methodology as in the experimental Section 5.2. The choice of  $xgboost$  (Chen & Guestrin, 2016) for the model  $f_\beta$  is motivated as it achieves state-of-the-art performance Grinsztajn et al. (2022); Elsayed et al. (2021); Borisov et al. (2021). The choice of logistic regression for the inspector  $g_\psi$  is motivated by its direct interpretability.

### D.1 ACS Employment

The goal of this task is to predict whether an individual, is employed. Figure 4 shows a low DP violation, compared to the other prediction tasks based on the US census dataset. The AUC of the “Equal Treatment Inspector” is ranging from 0.55 to 0.70. For Asian vs Black un-equal treatment we see that there significant variation of the AUC, indicating that the method achieves different values on the bootstrapping folds. Looking at the features driving the ET violation, we see particularly high values when comparing “Asian” and “Black” populations, and for features “Citizenship” and “Employment”. On average, the most important features across all group comparisons are also “Education” and “Area”. Interestingly, features such as “difficulties on the hearing or seeing”, do not play a role.

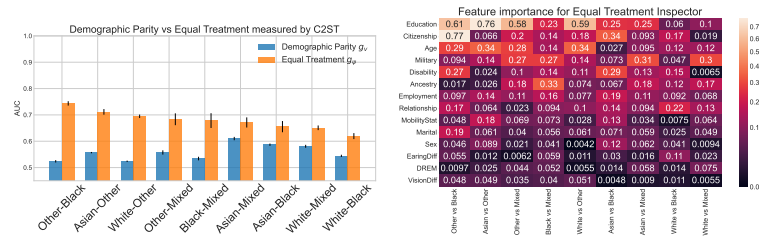


Figure 4: Left: AUC of the inspector for ET and DP, over the district of California 2014 for the ACS Employment dataset. Right: contribution of features to the ET inspector performance.

### D.2 ACS Travel Time

The goal of this task is to predict whether an individual has a commute to work that is longer than 20 minutes. The threshold of 20 minutes was chosen as it is the US-wide median travel time to work based on 2018 data. Figure 5 shows an AUC for the ET inspector in the range of 0.50 to 0.60. By

### 4.3 Beyond Demographic Parity: Redefining Equal Treatment

looking at the features, they highlight different ET drivers depending on the pair-wise comparison made. In general, the feature “Education”, “Citizenship” and “Area” are the those with the highest difference. Even though for Asian-Black pairwise comparison “Employment” is also one of the most relevant features.

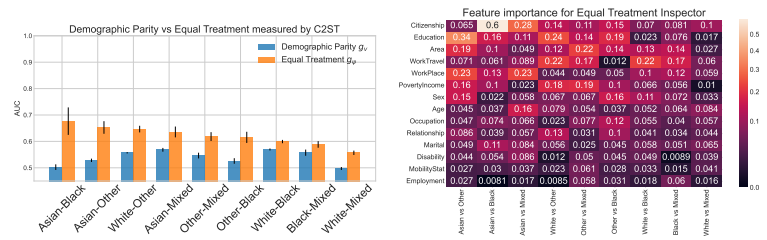


Figure 5: Left: AUC of the inspector for ET and DP, over the district of California 2014 for the ACS Travel Time dataset. Right: contribution of features to the ET inspector performance.

### D.3 ACS Mobility

The goal of this task is to predict whether an individual had the same residential address one year ago, only including individuals between the ages of 18 and 35. This filtering increases the difficulty of the prediction task, as the base rate of staying at the same address is above 90% for the general population (Ding et al., 2021). Figure 6 show an AUC of the ET inspector in the range of 0.55 to 0.80. By looking at the features, they highlight different source of the ET violation depending on the group pair-wise comparison. In general the feature “Ancestry”, i.e. “ancestors’ lives with details like where they lived, who they lived with, and what they did for a living”, plays a high relevance when predicting ET violation.

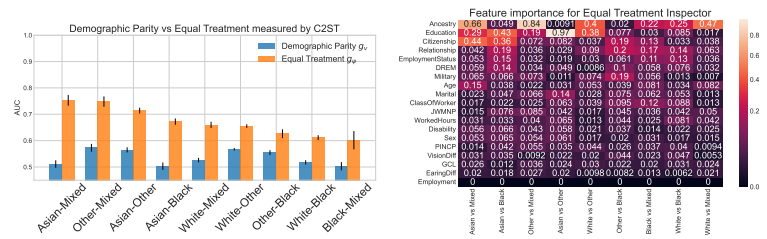


Figure 6: Left: AUC of the inspector for ET and DP, over the district of California 2014 for the ACS Mobility dataset. Right: contribution of features to the ET inspector performance.

## E Additional Experiments

In this section, we run additional experiments regarding C2ST, hyperparameters, and models for estimators  $f_\theta$  and inspectors  $g_\psi$ .

### E.1 Statistical Independence Test via Classifier AUC Test

We complement the experiments of Section 5.2 by reporting in Table 3 the results of the C2ST for group pair-wise comparisons. As discussed in Section 4.3.1, we perform the statistical test  $H_0 : AUC = 1/2$  of the “Equal Treatment Inspector” using a Brunner-Munzel one tailed test against  $H_1 : AUC > 1/2$  as implemented in Virtanen et al. (2020). Table 3 reports the empirical AUC on test

### 4.3 Beyond Demographic Parity: Redefining Equal Treatment

set, the confidence intervals at 95% confidence level (columns “Low” and “High”), and the p-value of the test. The “Random” row regards a randomly assigned group and represents a baseline for comparison. The statistical tests clearly show that the AUC is significantly different from  $1/2$ , also when correcting for multiple comparison tests.

Table 3: Results of the C2ST on the “Equal Treatment Inspector”.

Pair	AUC	Low	High	pvalue	Test Statistic
Random	0.501	0.494	0.507	0.813	0.236
White-Other	0.735	0.731	0.739	$< 2.2e-16$	97.342
White-Black	0.62	0.612	0.627	$< 2.2e-16$	27.581
White-Mixed	0.615	0.607	0.624	$< 2.2e-16$	23.978
Asian-Other	0.795	0.79	0.8	$< 2.2e-16$	107.784
Asian-Black	0.667	0.659	0.676	$< 2.2e-16$	38.848
Asian-Mixed	0.644	0.634	0.653	$< 2.2e-16$	28.235
Other-Black	0.717	0.708	0.725	$< 2.2e-16$	48.967
Other-Mixed	0.697	0.688	0.707	$< 2.2e-16$	39.925
Black-Mixed	0.598	0.586	0.61	$< 2.2e-16$	15.451

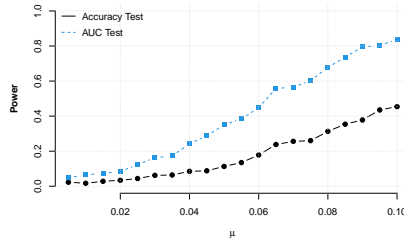


Figure 7: Comparing the power of C2ST based on Accuracy vs AUC.

We also compare the power of the C2ST based on the AUC against the two-sample test of Lopez-Paz & Oquab (2017), which is based on accuracy. We generate synthetic datasets where  $Y \sim \text{Ber}(0.5)$  and  $X = (X_1, X_2)$  with positives distributed as  $N((\mu, \mu), \Sigma)$  and negatives distributed as  $N((- \mu, - \mu), \Sigma)$ , where  $\Sigma = \begin{bmatrix} 1 & 0.5 \\ 0.5 & 1 \end{bmatrix}$ . Thus, the larger the  $\mu$ , the easier it is to distinguish the two distributions. Figure 7 reports the power of the AUC-based test vs the accuracy-based test using a logistic regression classifier, estimated by 1000 runs for each of the  $\mu$ 's ranging from 0.005 to 0.1. The figure highlights that, under such a setting, testing the AUC rather than the accuracy leads to a better power (probability of rejecting  $H_0$  when it does not hold).

#### E.2 Hyperparameters Evaluation

This section presents an extension to our experimental setup, where we increase the model complexity by varying the model hyperparameters. We use the US Income dataset for the population of the CA14 district. We consider three models for  $f_\theta$ : Decision Trees, Gradient Boosting, and Random Forest. For the Decision Tree models, we vary the depth of the tree, while for the Gradient Boosting and Random Forest models, we vary the number of estimators. Shapley values are calculated by means of the TreeExplainer algorithm (Lundberg et al., 2020). For the ET inspector  $g_\psi$ , we consider logistic regression, and XGB.

Figure 8 shows that less complex models, such as Decision Trees with maximum depth 1 or 2, are also less unfair. However, as we increase the model complexity, the unequal treatment of the model becomes more pronounced, achieving a plateau when the model has enough complexity. Furthermore, when we compare the results for different ET inspectors, we observe minimal differences (note that the y-axis takes different ranges).

### 4.3 Beyond Demographic Parity: Redefining Equal Treatment

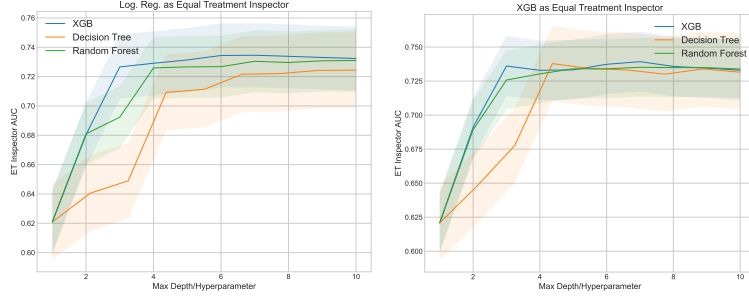


Figure 8: AUC of the inspector for ET, over the district of CA14 for the US Income dataset.

#### E.3 Varying Estimator and Inspector

We vary here the model  $f_\theta$  and the inspector  $g_\psi$  over a wide range of well-known classification algorithms. Table 4 shows that the choice of model and inspector impacts on the measure of Equal Treatment, namely the AUC of the inspector. By Theorem ??, the larger the AUC of any inspector the smaller is the  $p$ -value of the null hypothesis  $\mathcal{S}(f_\theta, X) \perp Z$ . Therefore, inspectors able to achieve the best AUC should be considered. Weak inspectors have lower probability of rejecting the null hypothesis when it does not hold.

Inspector $g_\psi$	Model $f_\theta$				
	DecisionTree	SVC	Logistic Reg.	RF	XGB
DecisionTree	0.631	0.644	0.644	0.664	0.634
KNN	0.737	0.754	0.75	0.744	0.751
Logistic Reg.	0.767	0.812	0.812	0.812	0.821
MLP	0.786	0.795	0.795	0.813	0.804
RF	0.776	0.782	0.781	0.758	0.795
SVC	0.743	0.807	0.807	0.790	0.810
XGB	0.775	0.780	0.780	0.789	0.790

Table 4: AUC of the ET inspector for different combinations of models and inspectors.

#### E.4 Explaining ET Unfairness

We complement the results of the experimental Section 5.1 with a further experiment relating the correlation hyperparameter  $\gamma$  to the coefficients of an explainable ET inspector. We consider a synthetic dataset with one more feature, by drawing 10,000 samples from a  $X_1 \sim N(0, 1)$ ,  $X_2 \sim N(0, 1)$ , and  $(X_3, X_5)$  and  $(X_4, X_5)$  following bivariate normal distributions  $N([0, 0], [1 \ \gamma \ \gamma \ 1])$  and  $N([0, 0], [1 \ \gamma \ 0.5 \ \gamma \ 0.5 \ 1])$ , respectively. We define the binary protected feature  $Z$  with values  $Z = 1$  if  $X_5 > 0$  and  $Z = 0$  otherwise. As in Section 5.1, we consider two experimental scenarios. In the first scenario, the indirect case, we have unfairness in the data and in the model. The target feature is  $Y = \sigma(X_1 + X_2 + X_3 + X_4)$ , where  $\sigma$  is the logistic function. In the second scenario, the uninformative case, we have unfairness in the data and fairness in the model. The target feature is  $Y = \sigma(X_1 + X_2)$ .

Figure 9 shows how the coefficients of the inspector  $g_\psi$  vary with correlation  $\gamma$  in both scenario. In the indirect case, coefficients for  $\mathcal{S}(f_\theta, X_1)_1$  and  $\mathcal{S}(f_\theta, X_1)_2$  correctly attributes zero importance to such variables, while coefficients for  $\mathcal{S}(f_\theta, X_1)_3$  and  $\mathcal{S}(f_\theta, X_1)_4$  grow linearly with  $\gamma$ , and with the one for  $\mathcal{S}(f_\theta, X_1)_3$  with higher slope as expected. In the uninformative case, coefficients are correctly zero for all variables.

### 4.3 Beyond Demographic Parity: Redefining Equal Treatment



Figure 9: Coefficient of  $g_\psi$  over  $\gamma$  for synthetic datasets in two experimental scenarios.

#### E.5 Statistical Comparison of Demographic Parity versus Equal Treatment

So far, we measured ET and DP fairness using the AUC of an inspector,  $g_\psi$  and  $g_\nu$  respectively (see Section 5). For DP, however, other probability density distance metrics can be considered, including the p-value of the Kolmogorov–Smirnov (KS) test and the Wasserstein distance. Table 5 reports all such distances in the format “mean  $\pm$  stdev” calculated over 100 random sampled datasets. The pairs of group comparisons are sorted by descending AUC values. We highlight in red values below the threshold of 0.05 for the KS test, of 0.55 for the AUC of the C2ST, and of 0.05 for the Wasserstein distance. They represent cases where ET violation occurs, but no DP violation is measured (with different metrics).

### 4.3 Beyond Demographic Parity: Redefining Equal Treatment

Table 5: Comparison of ET and DP measured in different ways. Case of ET violation but no DP violation are highlighted in red.

Pair	Data	Equal treatment	Demographic Parity		
		C2ST(AUC)	C2ST(AUC)	KS(pvalue)	Wasserstein
Asian-Other	Income	0.794 ± 0.004	0.709 ± 0.004	0.338 ± 0.007	0.256 ± 0.004
White-Other	Income	0.734 ± 0.002	0.675 ± 0.003	0.282 ± 0.003	0.209 ± 0.002
Other-Black	Income	0.724 ± 0.004	0.628 ± 0.006	0.216 ± 0.007	0.143 ± 0.004
Other-Mixed	Income	0.707 ± 0.005	0.593 ± 0.005	0.169 ± 0.006	0.117 ± 0.004
Asian-Black	Income	0.664 ± 0.008	0.587 ± 0.004	0.142 ± 0.005	0.111 ± 0.004
Asian-Mixed	Income	0.644 ± 0.005	0.607 ± 0.006	0.159 ± 0.008	0.128 ± 0.006
White-Mixed	Income	0.613 ± 0.005	0.546 ± 0.005	0.082 ± 0.004	<b>0.058 ± 0.002</b>
White-Black	Income	0.613 ± 0.005	0.57 ± 0.007	0.113 ± 0.008	0.08 ± 0.006
Black-Mixed	Income	0.603 ± 0.006	<b>0.523 ± 0.007</b>	<b>0.055 ± 0.007</b>	<b>0.023 ± 0.004</b>
Asian-Black	TravelTime	0.677 ± 0.052	<b>0.502 ± 0.011</b>	<b>0.021 ± 0.009</b>	<b>0.01 ± 0.003</b>
Asian-Other	TravelTime	0.653 ± 0.024	<b>0.528 ± 0.006</b>	<b>0.053 ± 0.011</b>	<b>0.027 ± 0.004</b>
Asian-Mixed	TravelTime	0.647 ± 0.013	0.557 ± 0.003	0.096 ± 0.004	<b>0.045 ± 0.002</b>
White-Other	TravelTime	0.636 ± 0.02	0.568 ± 0.007	0.107 ± 0.01	0.06 ± 0.005
Other-Mixed	TravelTime	0.618 ± 0.017	<b>0.546 ± 0.011</b>	0.079 ± 0.012	<b>0.043 ± 0.006</b>
Other-Black	TravelTime	0.615 ± 0.021	<b>0.526 ± 0.011</b>	<b>0.049 ± 0.014</b>	<b>0.026 ± 0.006</b>
White-Black	TravelTime	0.599 ± 0.006	0.569 ± 0.004	0.12 ± 0.006	<b>0.057 ± 0.003</b>
Black-Mixed	TravelTime	0.588 ± 0.012	0.557 ± 0.012	0.098 ± 0.015	<b>0.0557 ± 0.001</b>
White-Mixed	TravelTime	0.557 ± 0.008	<b>0.497 ± 0.006</b>	<b>0.016 ± 0.004</b>	<b>0.006 ± 0.002</b>
Other-Black	Employment	0.744 ± 0.008	<b>0.524 ± 0.005</b>	<b>0.036 ± 0.005</b>	<b>0.036 ± 0.004</b>
Asian-Other	Employment	0.711 ± 0.011	0.557 ± 0.003	0.066 ± 0.004	0.066 ± 0.003
White-Other	Employment	0.695 ± 0.007	<b>0.524 ± 0.003</b>	0.019 ± 0.005	0.019 ± 0.002
Other-Mixed	Employment	0.683 ± 0.022	0.557 ± 0.008	0.083 ± 0.005	0.083 ± 0.003
Black-Mixed	Employment	0.678 ± 0.028	<b>0.534 ± 0.007</b>	<b>0.049 ± 0.007</b>	<b>0.048 ± 0.004</b>
Asian-Mixed	Employment	0.671 ± 0.019	0.61 ± 0.006	0.0144 ± 0.006	0.145 ± 0.004
Asian-Black	Employment	0.655 ± 0.021	0.587 ± 0.004	0.106 ± 0.006	0.106 ± 0.004
White-Mixed	Employment	0.651 ± 0.009	0.581 ± 0.006	0.095 ± 0.004	0.095 ± 0.003
White-Black	Employment	0.619 ± 0.011	<b>0.544 ± 0.004</b>	<b>0.049 ± 0.003</b>	<b>0.049 ± 0.002</b>
Asian-Mixed	Mobility	0.753 ± 0.02	<b>0.511 ± 0.014</b>	<b>0.04 ± 0.012</b>	<b>0.014 ± 0.006</b>
Other-Mixed	Mobility	0.748 ± 0.02	0.573 ± 0.015	0.113 ± 0.017	<b>0.062 ± 0.009</b>
Asian-Other	Mobility	0.714 ± 0.011	0.565 ± 0.01	0.114 ± 0.011	<b>0.054 ± 0.005</b>
Asian-Black	Mobility	0.672 ± 0.012	<b>0.503 ± 0.014</b>	<b>0.032 ± 0.011</b>	<b>0.012 ± 0.004</b>
Other-Black	Mobility	0.66 ± 0.012	<b>0.526 ± 0.009</b>	<b>0.044 ± 0.009</b>	<b>0.02 ± 0.004</b>
White-Mixed	Mobility	0.655 ± 0.007	0.568 ± 0.005	0.105 ± 0.007	<b>0.044 ± 0.003</b>
White-Other	Mobility	0.626 ± 0.017	0.555 ± 0.009	0.091 ± 0.01	<b>0.046 ± 0.005</b>
White-Black	Mobility	0.611 ± 0.009	<b>0.518 ± 0.008</b>	<b>0.043 ± 0.008</b>	<b>0.017 ± 0.004</b>
Black-Mixed	Mobility	0.602 ± 0.035	<b>0.503 ± 0.016</b>	<b>0.031 ± 0.013</b>	<b>0.012 ± 0.006</b>

## F LIME as an Alternative to Shapley Values

The definition of ET (Def. 3.2) is parametric in the explanation function. We used Shapley values for their theoretical advantages (see Appendix A). Another widely used feature attribution technique is LIME (Local Interpretable Model-Agnostic Explanations). The intuition behind LIME is to create a local linear model that approximates the behavior of the original model in a small neighbourhood of the instance to explain (Ribeiro et al., 2016b,a), whose mathematical intuition is very similar to the Taylor/Maclaurin series. This section discusses the differences in our approach when adopting LIME instead of the SHAP implementation of Shapley values. First of all, LIME has certain drawbacks:

- **Computationally Expensive:** Its current implementation is more computationally expensive than current SHAP implementations such as TreeSHAP (Lundberg et al., 2020), Data SHAP (Kwon et al., 2021; Ghorbani & Zou, 2019), or Local and Connected SHAP (Chen et al., 2019). This problem is exacerbated when producing explanations for multiple instances (as in our case). In fact, LIME requires sampling data and fitting a linear model, which is a computationally more expensive approach than the aforementioned model-specific approaches to SHAP. A comparison of the execution time is reported in the next sub-section.
- **Local Neighborhood:** The randomness in the calculation of local neighbourhoods can lead to instability of the LIME explanations. Works including Slack et al. (2020); Alvarez-Melis & Jaakkola (2018); Adebayo et al. (2018) highlight that several types of feature attributions explanations, including LIME, can vary greatly.
- **Dimensionality:** LIME requires, as a hyperparameter, the number of features to use for the local linear model. For our method, all the features in the explanation distribution should be used. However, linear models suffer from the curse of dimensionality. In our experiments, this is not apparent, since our synthetic and real datasets are low-dimensional.

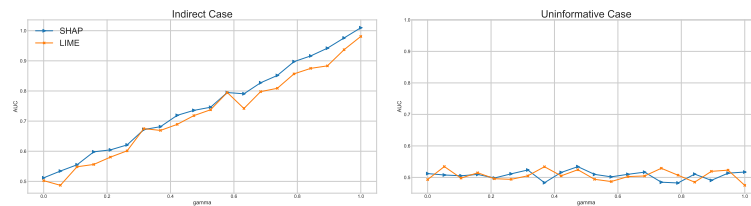


Figure 10: AUC of the ET inspect using SHAP vs using LIME.

Figure 10 compares the AUC of the ET inspector using SHAP and LIME as explanation functions over the synthetic dataset of Section 5.1. In both scenarios (indirect case and uninformative case), the two approaches have similar results. In both cases, however, the stability of using SHAP is better than using LIME.

### F.1 Runtime

We conduct an analysis of the runtimes of generating the explanation distributions using TreeShap vs LIME. We adopt shap version 0.41.0 and lime version 0.2.0.1 as software packages. In order to define the local neighborhood for both methods in this example, we used all the data provided as background data. The model  $f_\theta$  is set to xgboost. As data we produce a random generated data matrix, of varying dimensions. When varying the number of samples, we use 5 features, and when varying the number of features, we use 1000 samples. Figure 11 shows the elapsed time for generating explanation distributions with varying numbers of samples and columns.

The runtime required to generate explanation distributions using LIME is considerably greater than using SHAP. The difference becomes more pronounced as the number of samples and features increases.

### 4.3 Beyond Demographic Parity: Redefining Equal Treatment

---

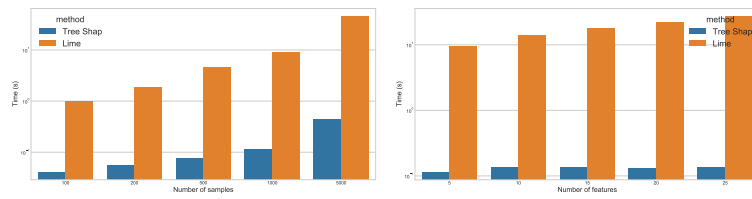


Figure 11: Elapsed time for generating explanation distributions using SHAP and LIME with different numbers of samples (left) and features (right) on synthetically generated datasets. Note that the y-scale is logarithmic.

## 5 Fairness in Network Structures

*“When we try to pick out anything by itself, we find it hitched to everything else in the Universe.”*

– John Muir [74]

This chapter presents the research on algorithmic fairness in networked systems, focusing on how structural properties of networks can influence the distribution of opportunities, visibility, and resources among individuals or entities. Many real-world algorithmic systems operate on relational data, where outcomes are determined not only by individual attributes but also by the topology of interactions and the dynamics of information flow. In such contexts, algorithmic decisions can reinforce or exacerbate structural inequalities embedded in the network.

The publications presented in this chapter contribute to RQ2 by investigating different mechanisms through which unfairness may arise in network structures and by proposing methods to better understand and mitigate such effects. Specifically, the works examine fairness in three distinct but related contexts: route recommendation systems, link recommendation algorithms, and graph-based models for socioeconomic analysis.

In Section 5.1, we study fairness in route recommendation systems, showing how traditional shortest-path approaches can lead to uneven exposure of nodes within transportation or navigation networks and proposing a fairness-aware alternative. In Section 5.2, we investigate link recommendation algorithms in social networks, analyzing how these systems can influence the evolution of network structure and potentially reinforce inequalities affecting minority groups. Finally, in Section 5.3, we explore the use of graph-based recommender systems to infer fine-grained socioeconomic indicators in urban environments, illustrating how graph learning techniques can reveal structural patterns in geographic data.

Together, these studies illustrate how fairness concerns arise across different types of network-based algorithms and highlight the importance of incorporating structural considerations into the design and analysis of such systems.

## 5.1 Beyond Shortest paths: Node Fairness in Route Recommendation

Route recommendation systems are widely used in navigation applications and logistics platforms to suggest optimal paths between locations. Most existing systems rely on shortest-path algorithms, which optimize efficiency criteria such as travel time or distance. While effective in improving individual navigation efficiency, these approaches may produce unintended structural consequences when deployed at scale.

In particular, repeatedly recommending the same optimal routes may concentrate traffic or attention on a limited subset of nodes or edges in the network. As a result, certain locations may systematically receive more exposure or benefits, while others remain largely ignored. This raises concerns about fairness at the node level, especially in contexts where exposure to traffic or visitors may have economic or social implications.

The work presented in this section contributes to RQ2 by investigating how fairness considerations can be incorporated into route recommendation systems. Specifically, we introduce a framework for node fairness in route recommendations, which aims to balance traditional efficiency objectives with a more equitable distribution of exposure across nodes in the network.

### Authors' Contributions

---

Contribution	Authors
<b>Conceptualization:</b>	A. Ferrara and all authors
<b>Writing:</b>	A. Ferrara and all authors
<b>Methodology:</b>	A. Ferrara and D. Garcia-Soriano (equally)
<b>Formal Analysis:</b>	Prop. 1, 2, 3 and 4: A. Ferrara and D. Garcia-Soriano Lemma 4.1 and Theorem 4.2: D. Garcia-Soriano and A. Ferrara
<b>Code:</b>	A. Ferrara
<b>Experiments:</b>	A. Ferrara

---

## Beyond Shortest Paths: Node Fairness in Route Recommendation

Antonio Ferrara  
antonio.ferrara@centai.eu  
CENTAI, Turin, Italy  
TU Graz, Austria

David García-Soriano  
david.garcia.soriano@upc.edu  
Universitat Politècnica de Catalunya  
Serra Hünter Fellow, Barcelona, Spain

Francesco Bonchi  
bonchi@centai.eu  
CENTAI, Turin, Italy  
Eurecat, Barcelona, Spain

### ABSTRACT

Traditionally, route recommendation systems focused on minimizing distance (or time) to travel between two points. However, recent attention has shifted to other factors beyond mere length. This paper addresses the challenge of ensuring a fair distribution of visits among network nodes when handling a high volume of point-to-point path queries. In doing so, we adopt a *Rawlsian* notion of individual-level fairness exploiting the power of randomization. Specifically, we aim to create a probabilistic distribution over paths that maximizes the minimum probability of any eligible node being included in the recommended path.

A key idea of our work is the notion of *forward paths*, i.e., paths where travelling along any edge decreases the distance to the destination. In unweighted graphs forward paths and shortest paths coincide, but in weighted graphs forward paths provide a richer set of alternative routes, involving many more nodes while remaining close in length to the shortest path. Thus, they offer diversity and a wider basis for fairness, while maintaining near-optimal path lengths. We devise an algorithm that extracts a directed acyclic graph (DAG) containing all the forward paths in the input graph, with the same computational runtime as solving a single shortest-path query. This avoids enumerating all possible forward paths, which can be exponential in the number of nodes. We then design a flow problem on this DAG to derive the probabilistic distribution over forward paths with the desired fairness property, solvable in polynomial time through a sequence of small linear programs.

Our experiments on real-world datasets validate our theoretical results, demonstrating that our technique provides individual node satisfaction while maintaining near-optimal path lengths. Moreover, our experiments show that our method can handle networks with millions of nodes and edges on a commodity laptop, and scales better than the baselines when there is a large volume of path queries for the same source and destination pair.

### PVLDB Reference Format:

Antonio Ferrara, David García-Soriano, and Francesco Bonchi. Beyond Shortest Paths: Node Fairness in Route Recommendation. PVLDB, 18(9): 3230 - 3242, 2025.  
doi:10.14778/3746405.3746440

### PVLDB Artifact Availability:

The source code, data, and/or other artifacts have been made available at <https://github.com/Ambres92/MaxMinFairForwardPaths>.

This work is licensed under the Creative Commons BY-NC-ND 4.0 International License. Visit <https://creativecommons.org/licenses/by-nc-nd/4.0/> to view a copy of this license. For any use beyond those covered by this license, obtain permission by emailing [info@vldb.org](mailto:info@vldb.org). Copyright is held by the owner/author(s). Publication rights licensed to the VLDB Endowment.  
Proceedings of the VLDB Endowment, Vol. 18, No. 9 ISSN 2150-8097.  
doi:10.14778/3746405.3746440

### 1 INTRODUCTION

Route recommendation systems have become essential tools in everyday life for navigation, deliveries, and trip planning [7, 8, 28, 35, 37, 45]. In every smartphone or personal device, apps such as Google Maps help users find the most effective route from a source to a destination by driving, public transportation, or walking. Such point-to-point queries can be solved by classic shortest-path algorithms [2, 14, 31, 40, 44] by converting the physical space into a graph structure, where nodes represent locations, edges represent road segments, and the edge weights can be used to represent travel costs in terms of time, distance, or other criteria.

Modern route recommendation systems are able to take into consideration other factors beyond the physical space (e.g., traffic status, delays in public transportation, varying user preferences, weather, etc.), thus recommending routes beyond the mere utilitarian value of shortest paths. Researchers have also studied methods to recommend routes that maximize human factors such as enjoyment, perceived safety, and overall positive experience of users, while minimizing the risk of crime, accidents, or pollution [33, 39]. While most of this research focuses on the system's benefit for the users, scant attention has been paid to ensuring fair exposure of the items forming the recommendation, i.e., nodes or points-of-interest (POIs), which may or may not be part of the recommended route. In this paper we tackle a novel problem thus far overlooked in the literature: *how to guarantee a fair distribution of visits among the nodes of the network, when providing route recommendations*.

Consider the following motivating example:

**EXAMPLE 1 (NODE INDIVIDUAL FAIRNESS.).** *The tourism office of the municipality of Florence develops an app to help tourists navigate the city center and move between the key attractions and historic landmarks. Shortly after the release of the app, an ice-cream parlor, located in a strategic position for tourists flowing between the Central Train Station and the Uffizi Gallery, suffers a sudden drop in sales. Upon investigation, they realize that all tourists moving between the two landmarks were being routed through the same shortest path, greatly reducing the visibility of the ice-cream parlor, which was located along a slightly different path. At the same time, a newly opened ice-cream parlor located on the recommended shortest path experiences a surge in sales.*

The notion of *item fairness*, which concerns whether the recommendation allocates exposure to items fairly, is well established in the literature on fairness in recommender systems [5, 12, 42]. However, it has received very little attention in the context of route recommendations. Some previous work considered a *group-level* notion of fairness in point-to-point shortest path queries on *vertex-colored graphs*, requiring that paths pass through a balanced number of nodes of different colors [3, 4]. The problem we introduce in this paper, however, departs significantly from previous formulations,

## 5.1 Beyond Shortest paths: Node Fairness in Route Recommendation

as we focus on *individual fairness* for the nodes, requiring that they are *equitably covered* by the recommendations. To the best of our knowledge, we are the first to address this requirement.

Related to our proposal is the notion of *diversity* of the recommendation. In fact, it is well known that improvements in the items' individual fairness are likely to increase diversity [42], due to the larger number of different items covered by some recommendations [27]. However, the converse need not hold: increasing diversity does not necessarily improve item fairness [42]. Although providing a set of diverse paths also enlarges the set of nodes covered by the recommended routes, as our experiments in Section 5 prove, this does not guarantee that the nodes in the graph are *equitably covered*. **Forward paths.** When addressing diversity along with fairness, it is often necessary to relax the requirement that the route be the shortest, as in weighted networks – like real-world road networks – the point-to-point shortest path is typically unique. This relaxation is usually achieved by introducing a parameter to control the desired path-length deviation from the shortest path [23, 25]. However, in this paper, we take a different approach.

Our first contribution is the concept of *forward paths*. Intuitively, each step along a forward path brings you closer to your destination. This aligns well with user preferences in real-world applications, as travelers generally favor routes that consistently progress toward their destination without backtracking or moving in circles. In unweighted graphs, forward paths coincide with shortest paths, while, in weighted graphs, forward paths visit a wider variety of nodes, making them a suitable foundation for fairness. Figure 1(a) provides a toy example depicting the shortest path, a forward path that is not a shortest path, and another path that is neither.

Although instances can be constructed where the ratio between forward path length and shortest path length may be arbitrarily large, we show empirically that in many real-world weighted graphs, *forward paths are very close in length to the shortest path*.<sup>1</sup> For example, in the network of drivable streets of Piedmont (California, USA) shown in Figure 1(b), for randomly sampled source-destination pairs of nodes, there are on average 634 different forward paths while the shortest path is almost always unique. Forward paths visit 81% more nodes on average than the shortest paths, and the longest forward path is only 11% longer than the shortest path.

Based on these observations, we adopt forward paths as our notion of near-shortest paths, removing the need for the parameter to control path-length deviation from the shortest path.

**Maxmin distributional fairness.** The second ingredient of our solution is the fairness criterion we employ. In particular, given our focus on fairness from the individual perspective of the nodes of the network, we adopt the notion of *maxmin distributional fairness* [17, 18, 26, 32, 36]. Such a paradigm exploits the power of randomization to provide *individual ex-ante fairness* and is inspired by Rawls's theory of justice [34], which advocates arranging social and financial inequalities to the benefit of the worst-off.

In the context of route recommendation, this translates into the goal of producing a probabilistic distribution over valid routes, such that it is impossible to improve the probability of any suitable location being visited, without decreasing it for some other location which already has a lower probability. In our context, the routes

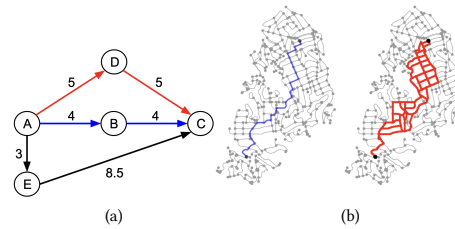


**Figure 1:** (a) Toy example: in red, a forward path that is not the shortest path (blue). Moving from the source (A) to (D) reduces the distance to the destination (C) from 8 to 5, satisfying the definition of forward path. In black, a path that is not forward: moving from (A) to (E) increases the distance to (C) from 8 to 8.5. (b) Drivable street network of Piedmont (California). For a random pair of source-destination nodes, the shortest path is shown in blue, while the union of the forward paths is highlighted in red. In this dataset, the shortest path between random pairs is almost always unique. By contrast, on average there are 634 different forward paths, visiting 81% more nodes than the shortest path, with the longest forward path being only 11% longer than the shortest path.

that we consider valid are forward paths, and the nodes that are subject to the fairness requirement are precisely the nodes that belong to at least one forward path.

Wrapping up, the technical problem we address in this paper (formally defined as Problem 1 in Section 4) is the following: *given a network, a source node  $s$ , a destination node  $t$ , produce a probabilistic distribution over forward paths from  $s$  to  $t$  that is maxmin-fair for all the eligible nodes (i.e., those that belong to at least one forward path).*

**EXAMPLE 2 (MAXMIN-FAIR DISTRIBUTION OVER FORWARD PATHS.)** In Figure 2 we use the setting of Example 1 to showcase the input and output of the problem we address. In Figure 2(a) we show a portion of the real road network of the city center of Florence. Our input is a source-destination pair of nodes, marked in yellow: node 1 (Central Train Station) and node 46 (Uffizi Gallery). The union of all forward paths is depicted in red. A maxmin-fair distribution assigns probabilities to the possible paths. In Figure 2(b) we report the output, a maxmin-fair distribution over forward paths: a list of paths from the source to the destination, each associated to its probability of being recommended, satisfying the desired fairness property.

**Practical implications and deployment.** Our proposal embraces randomization to produce a probability distribution over forward paths that guarantees the maximum possible visibility to all eligible nodes. This distributional fairness approach is very well suited to contexts in which the same query can be served many times for different users of a platform. Consider again Example 1, where tens of thousands of path requests may be received every day for top landmarks, such as Florence Central Station and the Uffizi Gallery. Having precomputed a maxmin-fair distribution, such as the one in Figure 2(b), it becomes easy to serve all the requests simply by sampling a route recommendation for any request independently,

<sup>1</sup>See Table 1 in Section 3 for empirical results on real-world road networks.

## 5.1 Beyond Shortest paths: Node Fairness in Route Recommendation

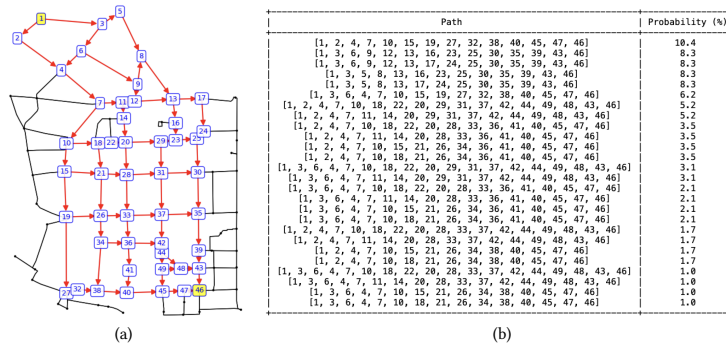


Figure 2: (a) A portion of the Florence city-center road network. The input to our problem, along with the map, is a source-destination pair: here the user needs to go from the Central Train Station (node 1) to the Uffizi Gallery (node 46). The first step of our solution is constructing the DAG of forward paths (Algorithm 1 in Section 3), shown in red. The DAG is fed into Algorithm 2 (Section 4.1), which produces a probability distribution over forward paths (b) with the required fairness property (Problem 1, Section 4). Finally, the system samples one path according to the computed probabilities and suggests it to the user.

with the guarantee of fairness in the spirit of *amortized fairness over multiple trials* [5, 18, 38].

In contrast, the baseline methods from the literature on diverse path recommendations face significant challenges when computing high volumes of different alternative paths. We will show in Section 5 that, as the number of paths requested for a point-to-point query increases, our method becomes significantly faster than the baseline approaches. Additionally, it is worth noting that each source-destination pair defines its own problem instance, independent of other instances. Consequently, our proposal is highly parallelizable, since computations for different pairs can proceed concurrently. Moreover, the maxmin-fair distribution for a source-target pair needs only be computed once; after storing it, the only computation needed at query time is sampling from the distribution.

**Technical challenges and roadmap.** A first technical difficulty towards developing our solution is the need to enumerate the set of all possible forward paths, which, in the worst case, is exponential in the number of nodes. We show that it is possible to compute, with the same asymptotic computational runtime as solving a single shortest-path query, the Directed Acyclic Graph (DAG) representing all the forward paths from a given source to a given target, avoiding the need to explicitly enumerate the set of all possible forward paths.

The main technical challenge is to ensure a maxmin-fair distribution of forward paths. While the work of [18] proposes a general framework for a wide class of combinatorial problems based on solving numerous linear programs (LPs), applying it to our problem presents significant obstacles to overcome.

Firstly, such a method requires the existence of a *separation oracle* [21], which is a method to detect quickly a violated constraint in an exponentially large set of constraints. While this oracle can be shown to exist for exact shortest paths, it is unlikely to exist for near-shortest paths (see Section 4 for details).

Secondly, the general approach in [18] is purely theoretical, relying on solving an exponentially large LP via the ellipsoid algorithm [21], which is the only known algorithm to solve LPs in polynomial time using separation oracles. There is no practical implementation of the ellipsoid algorithm: all real-world LP solvers need all constraints provided upfront or added lazily (with no guarantee of polynomial-time efficiency in the latter case). We propose a compact LP formulation of maxmin-fair forward path distributions with polynomially many constraints and variables. This allows us to use any LP solver, yielding a practically efficient algorithm.

In summary, the contributions of this paper are as follows:

- We introduce the novel problem of individual fairness for the nodes of the network in point-to-point path queries, following the paradigm of maxmin distributional fairness.
- We introduce the concept of forward paths and show that, in weighted graphs, they provide a much wider set of alternative paths than shortest paths, without being much longer. We thus adopt them as our notion of near-shortest paths.
- We provide an algorithm to compute a Directed Acyclic Graph (DAG) representing all forward paths in  $\Theta(|E| + |V| \log |V|)$  time, avoiding explicit enumeration of the set of all possible forward paths (of which there can be exponentially many).
- We design a flow problem which allows us to derive the desired maxmin-fair probabilistic distribution over forward paths. It can be solved in polynomial time by solving a sequence of small linear programs.
- We test our method on several real-world road networks. The experiments confirm our theoretical results showing that our method provides a more equitable distribution of visits among nodes than the baselines. We also demonstrate that our method can handle graphs with millions of edges on a commodity laptop.

The rest of the paper is organized as follows. Section 2 presents a brief survey of the related literature. Section 3 introduces the concept of forward paths and the algorithm to compute the DAG containing all forward paths. Section 4 provides the formal problem statement and our method for obtaining a maxmin-fair distribution on forward paths. Section 5 describes the experiments on real-world datasets. Finally, Section 6 discusses limitations and future work.

## 2 RELATED WORK

As clarified in the previous section, our work is the first to address the problem of guaranteeing an equitable distribution of visits among the nodes of the network when handling a high volume of route recommendations. On the one hand, our contribution can be placed within the wide literature on route recommendation systems (see, e.g., [45] for a recent survey). On the other hand, it naturally belongs in the literature about fairness in recommender systems, especially the part focusing on *item fairness*, i.e., the equitable allocation of exposure to the items being recommended (see, e.g., [12, 42] for recent surveys). However, neither of these two bodies of research offers closely related methods to be used as baselines in our evaluation. We already mentioned the work of Bentert et al. [3, 4] which, however, deals with a completely different notion of group fairness that is not relevant in our context. Hence, in order to identify suitable methods for comparison, we turn our attention to the literature about *diversity* in point-to-point path queries.

**Diversity in point-to-point path queries.** Chondrogiannis et al. [9] aim to find a set of  $k$  paths that are sufficiently dissimilar and as short as possible. Similarly, Luo et al. [30] study the top- $k$  shortest paths under a maximum similarity threshold, using an edge deletion/concatenation method to avoid expensive graph searches.

Häcker et al. [23] limit the maximum path length to identify the  $k$  most diverse paths within the length constraint. Abraham et al. [1] explore alternative routes through single-via paths, formed by concatenating shortest paths through an intermediate vertex.

Hanaka et al. [25] focus on maximizing the sum of pairwise Hamming distances among the  $k$  shortest paths, but this is unsuitable for real-world weighted graphs due to the uniqueness of the shortest path. To address the challenge of finding diverse solutions, Hanaka et al. [24] present a framework for approximation algorithms in combinatorial problems.

Routing scenarios with precomputed roadmaps that restrict routes to avoid newly introduced obstacles are studied by Voss et al. [41]. Fahmin et al. [15] use precomputed hub labels to calculate shortest paths and prune already-visited hubs for alternative paths. Xie et al. [43] focus on the space complexity of storing alternative paths excluding specific vertices or edges.

While this literature does not address fairness, the diverse set of paths produced ensures that various nodes are visited. In our experiments (Section 5), we use the methods by Chondrogiannis et al. [9] and the DKSP algorithm from Luo et al. [30] as baselines. Additionally, we compare against Yen’s algorithm [44], which computes the  $k$  shortest paths without diversity constraints.

**Maxmin distributional fairness.** The notion of fairness considered in this work is the maxmin distributional fairness originally defined by García-Soriano and Bonchi [17] in the context of bipartite matching, and later extended to different contexts: individual

fairness in ranking under group-fairness constraints by García-Soriano and Bonchi [18], individual fairness in bipartite matching under group-fairness constraints by Panda et al. [32], max-cut and other combinatorial optimization problems by Salem et al. [36] and other graph-theoretic optimization problems Hojny et al. [26].

## 3 FORWARD PATHS

We are given a simple, directed, weighted graph  $G = (V, E, \ell)$ , where  $V$  is a finite set of nodes,  $E$  is a set of directed edges (ordered pairs of nodes,  $(u, v) : u, v \in V$ ), and  $\ell : E \rightarrow \mathbb{R}^{>0}$  is a positive weight function associating each edge  $e = (u, v) \in E$  with its length  $\ell(e)$ . A path in a simple directed graph is a finite sequence of distinct nodes  $P = (v_1, \dots, v_k)$  such that  $\forall i \in [k - 1], (v_i, v_{i+1}) \in E$ . The length of  $P$  is given by

$$\ell(P) = \sum_{i=1}^{k-1} \ell(v_i, v_{i+1}).$$

Given a pair of distinct nodes  $s, t \in V$ , an  $s$ - $t$ -path is a path  $P = (v_1, \dots, v_k)$  such that  $v_1 = s$  and  $v_k = t$ . We denote the set of  $s$ - $t$ -paths by  $\mathcal{P}_{s,t}$ . Assuming  $\mathcal{P}_{s,t} \neq \emptyset$ , a shortest  $s$ - $t$ -path is any  $s$ - $t$ -path  $S$  such that

$$S \in \arg \min_{P \in \mathcal{P}_{s,t}} \ell(P).$$

The *shortest-path distance* between any two distinct nodes  $s, t \in V$ ,  $s \neq t$  is  $d(s, t) = \min_{P \in \mathcal{P}_{s,t}} \ell(P)$  if the minimum exists and  $+\infty$  otherwise (i.e., if  $\mathcal{P}_{s,t} = \emptyset$ ). When  $s = t$ , we define  $d(s, t) = 0$ .

In the remainder of the paper, we might omit the  $s$ - $t$ -prefix when the start and end point of the path are clear from the context.

In a directed weighted graph, it is quite common for many  $s$ - $t$  pairs to have a unique shortest path, which does not provide a good basis for fairness. Next, to address the uniqueness issue of the shortest path in weighted graphs, we define a novel type of path called *forward path* that provides a much larger set of alternatives, at the price of a slight increase in path length.

**DEFINITION 1 (S-T-FORWARD PATH).** An  $s$ - $t$ -path  $P = (v_1 = s, \dots, v_k = t)$  in a graph  $G$  is called *forward* if for  $i = 1, \dots, k - 1$ ,

$$d(v_{i+1}, t) < d(v_i, t),$$

where  $d$  represents the shortest path distance function in  $G$ . We will write  $\mathcal{FP}_{s,t}$  for set of forward paths from  $s$  to  $t$ .

Intuitively, the distance to the target decreases along each step in a forward path. Clearly, any shortest path is a forward path:

**PROPOSITION 1.** Let  $G = (V, E, \ell)$  be a directed weighted graph. Any shortest  $s$ - $t$ -path in  $G$  is a forward path.

**PROOF.** Let  $S = (v_1 = s, \dots, v_k = t)$  be an  $s$ - $t$ -shortest path and take any edge  $(v_i, v_{i+1})$  in  $S$ . Then  $d(v_i, t) = d(v_{i+1}, t) + \ell(v_i, v_{i+1})$ , because  $(v_i, v_{i+1})$  belongs to a shortest path. Then, since  $\ell(v_i, v_{i+1}) > 0$ ,  $d(v_{i+1}, t) < d(v_i, t)$ . This holds for any  $i = 1, \dots, k - 1$ , hence  $S$  satisfies the forward path condition.  $\square$

In unweighted graphs, i.e., graphs in which the weights are all one (i.e.,  $\ell \equiv 1$ ), it is more common to have various alternative shortest paths. In this case, shortest paths and forward paths coincide:

## 5.1 Beyond Shortest paths: Node Fairness in Route Recommendation

**Table 1:** The table contains data from the road networks of five cities extracted from OpenStreetMap and two datasets from the 9th DIMACS Implementation Challenge – Shortest Paths, namely the Florida and the Eastern USA datasets. Nodes represent locations and points of interest with a geographic position, stored as latitude-longitude pairs. Edges represent connections between these locations. The table reports, for 100 source-target pairs sampled uniformly at random, the average shortest path (SP), the average length of the longest forward path (LFP), and the ratio of the LFP length to the SP length. The ratio is computed per pair and averaged across all pairs. The remaining three columns show the average number of nodes visited by SP, FP (i.e., the node count of the DAG), and the mean and standard deviation of their ratio. Overall, we observe that with a minimal increase in the worst-case forward path length, the number of locations visited increases significantly.

Dataset	# nodes	# edges	SP length	LFP length	LFP/SP length	SP nodes	FP nodes	FP/SP nodes
Piedmont, California	352	937	1 860.07	2 061.58	1.11 ± 0.11	19.91	39.48	1.81 ± 0.66
Essaouira, Morocco	1 277	3 429	3 650.36	3 967.11	1.13 ± 0.14	37.20	107.03	2.52 ± 1.33
Florence, Italy	6 096	11 737	6 909.52	7 287.29	1.05 ± 0.05	75.10	121.27	1.58 ± 0.65
Buenos Aires, Argentina	17 890	37 474	9 065.83	9 642.57	1.06 ± 0.04	89.10	387.50	4.00 ± 2.12
Kyoto, Japan	44 828	118 087	8 501.42	9 243.75	1.09 ± 0.06	117.90	536.77	4.16 ± 2.21
Florida, USA	1 070 376	2 687 902	4.12 · 10 <sup>6</sup>	4.22 · 10 <sup>6</sup>	1.02 ± 0.02	1 194.27	2 720.63	2.33 ± 0.95
Eastern USA	3 598 623	8 708 058	4.39 · 10 <sup>6</sup>	4.57 · 10 <sup>6</sup>	1.04 ± 0.02	1 924.43	7 046.97	3.28 ± 1.45

**PROPOSITION 2.** Let  $G = (V, E, \ell)$  be a directed unweighted (i.e.,  $\ell \equiv 1$ ) graph. An  $s$ - $t$ -path  $P = (v_1, \dots, v_k)$  is a shortest path if and only if it is a forward path.

**PROOF.** The “only if” part is a special case of Proposition 1. Conversely, let  $F = (v_1 = s, \dots, v_k = t)$  be a forward path. Its length is  $\ell(F) = k - 1$ . From the forward path condition, we have  $d(v_{i+1}, t) < d(v_i, t)$ , and by the triangle inequality and the existence of the edge  $(v_i, v_{i+1})$ , we conclude that  $d(v_i, t) \leq d(v_{i+1}, t) + 1$ . Hence  $d(v_i, t) > d(v_{i+1}, t) \geq d(v_i, t) - 1$ . Since  $d$  can assume only integer values, we must in fact have  $d(v_{i+1}, t) = d(v_i, t) - 1$ . It follows that  $d(s, t) = d(v_2, t) + 1 = \dots = d(v_{k-1}, t) + k - 2 = k - 1 = \ell(F)$ , so  $F$  is a shortest path.  $\square$

Forward paths not only have the desirable property of getting closer to the target after traversing any edge, but also offer the flexibility of allowing for various alternatives and visiting a wider set of nodes, while remaining competitive in terms of length compared to the shortest path. Table 1 reports statistics on seven real-world road networks, confirming that forward paths, with a minimal increase in length, allow us to visit a significantly larger number of locations. We thus adopt them as our notion of near-shortest paths.

**Constructing the DAG of all forward paths.** In Section 4, we will discuss how to create a maxmin-fair distribution over forward paths. A preliminary step in our solution is to compute the Directed Acyclic Graph (DAG) representing all the forward paths from a given source to a given target, avoiding the need to explicitly enumerate the set of all possible forward paths, which, in the worst case, is exponential in the number of nodes of the DAG.<sup>2</sup> This is done by Algorithm 1, presented next.

DAG-FP takes as input a directed graph, a source, and a target node. It outputs a DAG in which any path from  $s$  to  $t$  is an  $s, t$ -forward path. The algorithm proceeds by computing a list containing the distance from the source to all the nodes, and the distance from any node to the target. These distances can be computed by Dijkstra’s algorithm [14], once on the input graph and once more

<sup>2</sup>In fact, the longest forward path lengths reported in Table 1 have been computed by dynamic programming on this DAG.

**Algorithm 1** DAG-FP: Creates a DAG containing the Forward Paths from  $s$  to  $t$

---

**Input:** Graph  $G = (V, E, \ell)$ , source node  $s$ , target node  $t$   
**Output:** DAG with Forward Paths

```

1:  $dist\_from\_s \leftarrow \text{distance}(G, s, V)$ 
2:  $dist\_to\_t \leftarrow \text{distance}(G, V, t)$ 
3:  $reachable\_from\_s \leftarrow \{i \mid dist\_from\_s[i] < \infty\}$ 
4:  $reachable\_to\_t \leftarrow \{i \mid dist\_to\_t[i] < \infty\}$ 
5:  $reachable \leftarrow reachable\_from\_s \cap reachable\_to\_t$ 
6:  $G' \leftarrow G.\text{induced\_subgraph}(reachable)$ 
7: for all  $(u, v)$  in  $G'.edges$  do
8:   if  $dist\_to\_t[u] \leq dist\_to\_t[v]$  then
9:     remove  $(u, v)$  from  $G'$ 
10:  end if
11: end for
12: return  $G'$ 

```

---

on the reversed graph. Then, it removes any node  $v$  for which there does not exist an  $s$ - $t$ -path that also visits  $v$ . The induced subgraph containing all the remaining nodes and the edges among them is then considered, and all the edges for which the forward path property is not respected are removed. The resulting graph is returned.

**PROPOSITION 3.** Algorithm 1 produces a DAG whose edge set is exactly the edges in  $G$  in some forward path from  $s$  to  $t$ .

**PROOF.** The DAG returned contains exactly those edges  $(u, v)$  where (a)  $d(s, u) < \infty$ , (b)  $d(v, t) < \infty$ , and (c)  $d(u, t) > d(v, t)$ . Indeed, edges where (a) or (b) fail are removed in line 6, and edges where (c) fails are removed in line 9; all other edges are kept. We need to show that an edge  $(u, v)$  belongs to some forward path if and only if these three conditions hold. The “only if” part follows directly from the definition of forward path. For the “if” part, assume that the three conditions hold. Then there is a path in  $G$  from  $s$  to  $u$  and another one from  $t$  to  $v$ ; in particular,  $G$  has a shortest (hence forward) path from  $s$  to  $u$  and another shortest (hence forward) path from  $t$  to  $v$ . By pasting these two paths together with the edge  $(u, v)$  we obtain a forward path from  $s$  to  $t$  traversing  $(u, v)$ , because  $d(u, t) > d(v, t)$ .

## 5.1 Beyond Shortest paths: Node Fairness in Route Recommendation

Finally, observe that the resulting graph is acyclic since the distance to  $t$  is finite and strictly decreasing along any path.  $\square$

Furthermore, the algorithm has the same asymptotic complexity as computing the distance from a source to all the nodes, which can be done with Dijkstra's algorithm. The following holds:

**PROPOSITION 4.** *Algorithm 1 has computational complexity  $\Theta(|E| + |V| \log |V|)$ .*

**PROOF.** Line 1 is computed with Dijkstra's algorithm, and also line 2, after reversing the direction of all the edges in the graph, can be computed with Dijkstra's algorithm starting from the target. Lines 3 to 11 have time complexity  $\Theta(|E|)$ . Dijkstra's algorithm with a Fibonacci heap priority queue has a worst-case running time of  $\Theta(|E| + |V| \log |V|)$  [16], and hence also does Algorithm 1.  $\square$

Given the ability to efficiently compute the DAG that contains all the forward paths, one might be tempted to randomly sample paths from it. However, such random selection would lack fairness guarantees: one could end up visiting certain nodes too often, while ignoring others for no good reason, causing inequalities in terms of nodes' exposure. To avoid such inequalities, our goal is to produce a distribution on the forward paths that is individually fair to the nodes. We formalize this notion in the next section.

### 4 MAXMIN-FAIR FORWARD PATHS

Consider a general instance  $\mathcal{T}$  of our path search problem, defined by a directed weighted graph  $G = (V, E, \ell)$  and a pair of terminal nodes  $s, t \in V$ , which in turn implicitly defines the set of feasible solutions  $\text{FP}_{s,t}$  (i.e., the set of forward paths from  $s$  to  $t$ ), which is finite and assumed to be non-empty. Let us associate with each path  $P \in \text{FP}_{s,t}$  and each node  $v \in V$  a binary satisfaction  $A(P, v) \in \{0, 1\}$  such that  $A(P, v) = 1$  if  $v \in P$  and 0 otherwise. Consider a randomized algorithm  $\mathcal{A}$  that, for any given search problem  $\mathcal{T}$ , always halts and selects a solution path  $\mathcal{A}(\mathcal{T}) \in \text{FP}_{s,t}$ . Then  $\mathcal{A}$  induces a probability distribution  $\mathbb{D}$  over  $\text{FP}_{s,t}$  by  $\mathbb{P}_{\mathbb{D}}[P] = \mathbb{P}[\mathcal{A}(\mathcal{T}) = P]$ ,  $\forall P \in \text{FP}_{s,t}$ . Let us denote the *expected satisfaction* of each node  $u \in V$  under  $\mathbb{D}$  by  $\mathbb{D}[u] := \mathbb{E}_{P \sim \mathbb{D}}[A(P, u)]$ .

**EXAMPLE 3 (EXPECTED SATISFACTION).** *Consider again the maxmin-fair distribution of Figure 2(b). The expected satisfaction of all nodes (except the source and destination, which are trivially always satisfied) are reported in Table 2. This is simply the probability of being part of a forward path sampled from the distribution.*

It is worth highlighting that a distribution being fair does not require providing equal satisfaction probability to all eligible nodes. In fact, there are nodes that are better positioned to be part of a forward path from the given source to the given destination. Their "strategic" position should be naturally rewarded by a fair distribution, rather than penalized. Intuitively, a maxmin-fair distribution provides, on any given input instance, the strongest guarantee possible for all nodes, in terms of expected satisfaction [17]. In other words, a distribution  $\mathbb{F}$  over  $\text{FP}_{s,t}$  is maxmin-fair for a set of nodes  $U \subseteq V$  if it is impossible to improve the expected satisfaction of any node in  $U$  without decreasing it for some other node which is no better off. This is formalized in the following definition.

**Table 2: Expected satisfaction of the nodes in Figure 2(a) under the probability distribution in Figure 2(b). Source and destination nodes are omitted, as they are always satisfied.**

$u$	$\mathbb{D}[u]$ (%)	$u$	$\mathbb{D}[u]$ (%)	$u$	$\mathbb{D}[u]$ (%)	$u$	$\mathbb{D}[u]$ (%)
4	66.7	25	33.3	48	22.2	22	16.7
7	66.7	30	33.3	49	22.2	23	16.7
3	58.3	35	33.3	5	16.7	24	16.7
43	55.6	39	33.3	8	16.7	26	16.7
10	50.0	15	25.0	9	16.7	27	16.7
40	44.4	18	25.0	11	16.7	28	16.7
45	44.4	36	22.2	12	16.7	29	16.7
47	44.4	37	22.2	14	16.7	31	16.7
2	41.7	38	22.2	16	16.7	32	16.7
6	41.7	41	22.2	17	16.7	33	16.7
13	33.3	42	22.2	19	16.7	34	16.7
20	33.3	44	22.2	21	16.7	–	–

**DEFINITION 2.** *A distribution  $\mathbb{F}$  over  $\text{FP}_{s,t}$  is **maxmin-fair** for  $U \subseteq V$  if for all distributions  $\mathbb{D}$  over  $\text{FP}_{s,t}$  and all  $u \in U$ ,*

$$\mathbb{D}[u] > \mathbb{F}[u] \Rightarrow \exists v \in U \mid \mathbb{D}[v] < \mathbb{F}[v] \leq \mathbb{F}[u].$$

With these concepts in place, we can now formally state our problem as follows:

**PROBLEM 1.** *Given a graph  $G = (V, E, \ell)$  and  $s, t \in V$ , our problem consists of finding a maxmin-fair distribution  $\mathbb{F}$  over  $\text{FP}_{s,t}$  for the set  $U = \{u \in V \mid \exists P \in \text{FP}_{s,t} \text{ such that } u \in P\}$ .*

There is some flexibility in choosing the graph  $G$ . Practical applications may require including only a subset of "valuable" nodes (such as points of interest, major intersections, or important landmarks) for fairness consideration. In these cases, a weighted graph based on the shortest distances between the valuable nodes can be constructed, which can serve as the input to our problem.

In the remainder of this section, we present a solution to Problem 1 by a carefully crafted linear programming algorithm, which avoids the need to compute the set of all possible forward paths (which can be exponential in the number of nodes in the DAG).

### 4.1 Algorithm

In [18], the authors introduce a general framework to solve maxmin-fair distributional problems. The problem defined above specializes their framework to forward paths, and is thus amenable to their techniques provided that one shows the existence of a certain separation oracle [21]. Specifically, given an assignment of non-negative weights to users, the separation oracle needs to find a feasible solution of maximum weight. The method of [18] applies whenever such a separation oracle admits an efficient implementation. When the set of feasible solutions is large (as in our setting), avoiding explicit enumeration is paramount.

We remark that the choice of forward paths in Problem 1 has the additional benefit of making the separation oracle tractable. Indeed, if we were to define the feasible set  $S$  as the set of simple paths from  $s$  to  $t$ , the separation oracle would ask for a simple path from  $s$  to  $t$  of maximum node weight. As the Hamiltonian path problem can be reduced to this question, it follows that the separation oracle problem for simple  $s, t$ -paths is NP-hard. However, when the graph is a DAG, there is a linear-time algorithm to find a simple path of maximum node weight: it suffices to process the

**Table 3: The LP (1) encapsulating our problem and its dual (2).**

$$\begin{aligned}
 & \text{maximize } \lambda \in \mathbb{R} \quad \text{subject to} \\
 & \sum_{u|(u,t) \in E} f_{u,t} = 1 \\
 & \sum_{u|(s,u) \in E} -f_{s,u} = -1 \\
 & \sum_{u|(u,v) \in E} f_{u,v} - \sum_{w|(v,w) \in E} f_{v,w} = 0 \quad \forall v \neq s, t \\
 & \lambda - \sum_{u|(u,v) \in E} f_{u,v} \leq 0 \quad \forall v \notin K \\
 & - \sum_{u|(u,v) \in E} f_{u,v} \leq -\alpha_v \quad \forall v \in K \\
 & f_{u,v} \geq 0 \quad \forall (u,v) \in E
 \end{aligned} \tag{1}$$

$$\begin{aligned}
 & \text{minimize } d_t - d_s - \sum_{v \in K} \alpha_v w_v \quad \text{subject to} \\
 & d_v - d_u - w_v \geq 0 \quad \forall (u,v) \in E \\
 & \sum_{v \in K} w_v = 1 \\
 & w_v \geq 0 \quad \forall v \in V \\
 & d_v \in \mathbb{R} \quad \forall v \in V
 \end{aligned} \tag{2}$$

vertices in topological order and apply dynamic programming (DP) (Section 24.2 of [11]). As we have shown in Section 3 that the set of all forward paths forms a DAG, it follows that the separation oracle for forward paths is polynomial-time solvable.

Using the DP-based separation oracle for the forward path DAG, one could theoretically apply the techniques from [18] to solve Problem 1. Unfortunately, the general algorithm proposed therein, while efficient in theory, requires the use of the impractical ellipsoid algorithm to solve exponential-sized linear programs in polynomial time. The ellipsoid method is the only known theoretically efficient method to solve large LPs via separation oracles, but it suffers from numerical stability issues and its performance is far from being competitive with the simplex or interior point methods used in established solvers. In fact, [18] poses as an open problem the development of faster algorithms for concrete problems.

We address this challenge by taking a different approach. By interpreting the probabilities of traversing the edges in a maxmin-fair solution as flows in a network, in the following we provide a compact Linear Programming (LP) formulation for maxmin-fair forward paths with only polynomially many constraints, thus bypassing the need of separation oracles and the ellipsoid algorithm.

Throughout our discussion, we use  $E$  to represent the set of edges in the forward path DAG for a certain fixed pair  $s, t$  of source-target vertices. To exclude trivial cases, we assume that the set  $U = \{s, t\}$  is non-empty. Let us introduce a flow variable  $f_{u,v}$  for each directed edge  $(u, v) \in E$  denoting the (unconditional) probability that the edge  $u \rightarrow v$  will be traversed in a path drawn from the solution. We interpret the search for a maxmin-fair distribution as a flow

problem in  $G$ , where the probabilities “flow” from one vertex to its successors in the DAG. As every path starts at the source and ends at the target (and does not stall at any intermediate vertex), we need to ensure that (a) the incoming flow for the target and the outgoing flow from the source is 1; (b) flow conservation holds, i.e., the incoming flow equals the outgoing flow for every vertex other than  $s$  and  $t$ ; and (c) the minimum incoming flow of a vertex is maximized (as required by the maxmin-fairness condition). All of these are expressible as linear constraints in the flow variables.

However, this does not quite suffice, since maxmin-fairness yields the lexicographically largest vector of sorted satisfaction probabilities [17]. To achieve this ordering, we need to solve several optimization problems. In order to do so, let  $\alpha_v$  denote the satisfaction probability of  $v$  in the maxmin-fair distribution. We will obtain these values step by step, assuming that the values of  $\alpha_v$  are known for an (initially empty) subset  $K \subseteq V$  and augmenting  $K$  in each iteration. Thus, we wish to ensure that all members of  $K$  are visited with probabilities indicated by  $\alpha$ , while we maximize the minimum visiting probability among the rest. Our problem is thus encapsulated by LP (1) in Table 3 or, equivalently, its dual (2).

**LEMMA 4.1.** *Let  $K \subseteq V$  and  $\alpha \in \mathbb{R}^K$ . Any distribution of forward paths from  $s$  to  $t$  satisfying the two conditions below gives rise to a solution  $(\lambda, \{f_{u,v}\}_{(u,v) \in E})$  to LP (1):*

- (a) *The probability of visiting each vertex  $v \in K$  is at least  $\alpha_v$ ;*
- (b) *The probability of visiting each vertex  $v \notin K$  is at least  $\lambda$ .*

*Conversely, from any solution  $(\lambda, \{f_{u,v}\}_{(u,v) \in E})$  to LP (1), one may construct a distribution of forward paths from  $s$  to  $t$  such that (a) and (b) above hold.*

**PROOF.** Consider a distribution  $\mathbb{D}$  of forward paths from  $s$  to  $t$  satisfying (a) and (b). Define  $f_{u,v} = \Pr_{p \in \mathbb{D}}[\text{edge } (u, v) \text{ is traversed in } p] \geq 0$ . Notice that when drawing a path from  $\mathbb{D}$ , the probability of entering vertex  $v \neq s$  is  $\sum_{u|(u,v) \in E} f_{u,v}$ , and the probability of exiting vertex  $v \neq t$  is  $\sum_{w|(v,w) \in E} f_{v,w}$ . Hence these two must be equal for every  $v \neq s, t$ . Also, since the source and the target are visited with probability 1, the constraints  $\sum_{u|(u,t) \in E} f_{u,t} = 1$  and  $\sum_{u|(s,u) \in E} f_{s,u} = 1$  hold. Finally, we also have  $\sum_{u|(u,v) \in E} f_{u,v} \geq \lambda$  when  $v \notin K$  by condition (b) and  $\sum_{u|(u,v) \in E} f_{u,v} \geq \alpha_v$  by (a). Hence all constraints are satisfied.

Conversely, take any solution  $(\lambda, \{f_{u,v}\}_{(u,v) \in E})$  to LP (1). For each  $(u, v) \in E$ , let

$$p_{u,v} = \begin{cases} f_{u,v} & \text{if } u = s \\ \frac{f_{u,v}}{\sum_{w|(w,u) \in E} f_{w,u}} \geq 0 & \text{if } u \neq s \end{cases} \tag{3}$$

(We leave  $p_{u,v}$  undefined when the denominator is zero.) Note that  $\sum_{v|(u,v) \in E} p_{u,v} = 1$  for all  $u \neq t$  because of the constraint  $\sum_{u|(u,v) \in E} f_{u,v} = \sum_{w|(v,w) \in E} f_{v,w}$ . So consider a random walk starting at  $s$  and stopping at  $t$  with transition probabilities  $\{p_{u,v}\}_{(u,v) \in E}$ , and define  $e(v) = \sum_{u|(u,v) \in E} f_{u,v}$  if  $v \neq s$  and 1 otherwise.

We show that  $\Pr[v \text{ is visited}] = e(v)$ . The proof proceeds by induction on the maximum length  $q(v)$  of a path from  $s$  to  $v$  in the DAG  $G$ . The base case is when  $q(v) = 0$  (i.e.,  $v = s$ ), and the property holds in this case because the path starts at  $s$  and  $e(v) = 1$ . For the inductive step, consider a vertex  $v$  and suppose that the

## 5.1 Beyond Shortest paths: Node Fairness in Route Recommendation

---

### Algorithm 2 MMFP - MaxMin Fair Forward Paths

---

**Input:** DAG  $G$ , source node  $s$ , target node  $t$   
**Output:** Encoding of a maxmin-fair distribution for  $s, t$ -forward paths

- 1:  $K \leftarrow \emptyset$
- 2: **while**  $K \neq V$  **do**
- 3:   Solve LP (1) and its dual LP (2);
- 4:   let  $\lambda^*, \{f_{u,v}^*\}, \{w_v^*\}$  be the optimum values
- 5:    $K' \leftarrow \{v \notin K \mid w_v^* > 0\}$
- 6:    $K \leftarrow K \cup K'$
- 7:   **for all**  $v \in K'$  **do**
- 8:      $\alpha_v \leftarrow \lambda^*$
- 9:   **end for**
- 10: **end while**
- 11: Return the flow values  $f_{u,v}^*$

---

claim holds for all  $u$  with  $q(u) < q(v)$ . Observing that  $(u, v) \in E$  implies  $q(u) < q(v)$ , we have

$$\Pr[v \text{ is visited}] = \sum_{u|(u,v) \in E} p_{u,v} \cdot \Pr[u \text{ is visited}] = \sum_{u|(u,v) \in E} \frac{f_{u,v}}{e(u)} \cdot e(u) = \sum_{u|(u,v) \in E} f_{u,v} = e(v).$$

This establishes our claim.

Now observe that the walk must end (because the graph is finite and acyclic), but cannot end anywhere else than  $t$  (as for any vertex  $u \neq t$  visited with non-zero probability  $e(u) > 0$ , the probability that the walk exits  $u$  is  $\sum_{v|(u,v) \in E} p_{u,v} = 1$ ). In particular  $t$  is visited with probability one<sup>3</sup>. Moreover, properties (a) and (b) follow from the constraints  $\sum_{u|(u,v) \in E} f_{u,v} \geq \lambda$  when  $v \notin K$  by condition (b) and  $\sum_{u|(u,v) \in E} f_{u,v} \geq \alpha_v$  when  $v \in K$  by condition (a).  $\square$

Algorithm 2 outlines the complete procedure. It takes as input the DAG, constructed with Algorithm 1, as well as the source and target nodes, and outputs the flow values. The algorithm goes through the following steps. We maintain a set  $K$  containing the bottom nodes for which we already ensured a maxmin-fair probabilistic satisfaction; it is initialized with the empty set. Then, the algorithm iteratively performs the following steps until  $K$  contains all the nodes. First, LP (1) and its dual LP (2) are solved. Then  $K'$ , a set containing all the nodes with dual weights greater than zero and not yet in  $K$ , is computed, and  $K$  gets updated with the nodes of  $K'$ . The nodes in  $K'$  then have their maxmin probabilistic satisfaction value  $\alpha_v$  assigned to the optimum LP value  $\lambda^*$ ; these values are then used as input for the updated LP (1). Finally, when the loop terminates, the flow values in the solution of the last LP 1 are returned.

**THEOREM 4.2.** *Algorithm 2 finds a maxmin-fair distribution of forward paths in polynomial time.*

**PROOF.** Given  $K \subseteq V$  and  $\{\alpha_v\}_{v \in K}$ , call a distribution  $\mathbb{D}$  of  $s$ - $t$ -forward paths *compatible with  $(K, \alpha)$*  if  $\mathbb{D}[v] = \alpha_v$  for all  $v \in K$  and  $\mathbb{D}[v] \geq \alpha_w$  for all  $v \notin K, w \in K$ . We show that at the start of each

<sup>3</sup>In fact, this shows that the constraint  $\sum_{u|(u,t) \in E} f_{u,t} = 1$  in LP (1) is actually redundant, and the variable  $d_t$  in the dual can be taken to be zero.

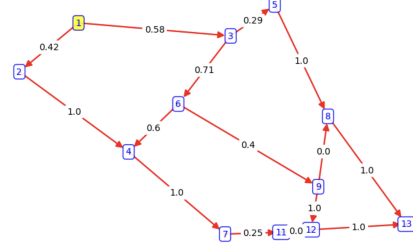


**Figure 3:** A portion of the DAG from Figure 2(a). The weights on the edges computed by Algorithm 2 encode the maxmin-fair distribution in Figure 2(b). Performing a random walk from the source to the target with the computed transition probabilities yields the maxmin-fair distribution.

iteration of the while loop, the maxmin-fair distribution  $\mathbb{F}$  is compatible with  $(K, \alpha)$ . Furthermore, the size of  $K$  is strictly increasing on each iteration. This implies that the algorithm terminates with  $\alpha_v = \mathbb{F}[v]$  for all  $v \in V$ .

The case  $K = \emptyset$  is vacuous. We establish the general claim by induction. Assuming  $\mathbb{F}$  was compatible with  $(K, \alpha)$  at line 3, we need to argue that  $\mathbb{F}$  is compatible with the next pair  $(K \cup K', \alpha')$  after line 9 in the same iteration, where  $\alpha'$  denotes the modified values of  $\alpha$ . To this end, we employ the lexicographic characterization of maxmin-fairness [17]: a distribution is maxmin-fair iff its vector of satisfaction probabilities, sorted from low to high, is lexicographically largest. Since we know that  $\mathbb{F}$  is compatible with  $(K, \alpha)$ , it follows from the aforementioned characterization and Lemma 4.1 that LP (1) is feasible and its optimum value  $\lambda^*$  equals  $\min_{v \notin K} \mathbb{F}[v]$ . Observe that  $K' \neq \emptyset$  because of the constraint  $\sum_{v \notin K} w_v = 1$  in the dual. Moreover, by complementary slackness, the constraints in any optimal solution to the primal that are complementary to the non-zero dual variables are tight. Hence  $\sum_{u|(u,v) \in E} f_{u,v}^* = \lambda^*$  for all  $v \in K'$ . In other words, any distribution  $\mathbb{D}$  compatible with  $(K, \alpha)$  and maximizing  $\min_{v \notin K} \mathbb{D}[v]$  needs to satisfy  $\mathbb{D}[v] = \lambda^*$  for all  $v \in K'$ . In particular this holds for  $\mathbb{F}$ , which implies that  $\mathbb{F}$  is compatible with the next pair  $(K \cup K', \alpha')$ .

After the last iteration, we can recover a distribution of forward paths  $\mathbb{D}$  determined by the last set of flow variables  $f_{u,v}^*$  by performing the random walk described in the proof of the “conversely” part of Lemma 4.1. This distribution is maxmin-fair, since the satisfaction probabilities of  $\mathbb{D}$  and  $\mathbb{F}$  agree everywhere on  $V$ .

Regarding the running time, the number of iterations of the while loop is bounded by  $n$ , since  $|K|$  is strictly increasing. Therefore at most  $n$  calls to the LP solver are made. The rest of the algorithm, including computing the forward path DAG, takes linear time. Since LP is solvable in polynomial time, so is the Maxmin Fair Forward Paths problem. Sampling each path from this distribution after the  $f_{u,v}^*$  values have been found takes linear time as well.  $\square$

It is worth noting that our method does not explicitly materialize the maxmin-fair distribution shown in Figure 2(b) due to its redundancy and space demands; indeed, many of the different

routes share a common prefix. Instead, it encodes the distribution compactly by labeling the DAG edges with the correct transition probabilities (line 11 of Algorithm 2). We showed in Lemma 4.1 that a DAG always exists such that performing a random walk from the source to the target with its transition probabilities is equivalent to sampling directly a path from the maxmin-fair distribution.

**EXAMPLE 4 (ENCODING THE MAXMIN-FAIR DISTRIBUTION.).** *Figure 3 illustrates how we encode the maxmin-fair distribution in Figure 2(b) by labeling the edges of the DAG in Figure 2(b) with the correct transition probabilities as computed by Algorithm 2. For space reasons, the figure only shows a portion of the DAG.*

**Complexity and scalability.** Recall that the DAG can be constructed in the same asymptotic time it takes to perform a single-source shortest path computation (Algorithm 1). Moreover, the time taken to sample each path given the flow values is linear in the path length. Hence, the bulk of the overall computational effort is spent on solving the sequence of LPs in Algorithm 2. The fastest algorithm to date for linear programming by [10] takes roughly  $p^{2.37}D$ , where  $p$  is the number of variables and  $D$  is the largest absolute value of the determinant of any submatrix of the matrix of coefficients. Since LP is not known to be solved in strongly polynomial time, such dependence on a parameter like  $D$  is unavoidable. In the worst case, our algorithm may need to solve up to  $n$  linear programs. However, as demonstrated in Section 5, these bounds are overly pessimistic. One reason is that, because we update  $K$  based on the value of the dual variables in line 6 of Algorithm 2 rather than one element at a time, the number of intermediate LP problems needed is much smaller than  $n$  in practice. Furthermore, our LPs are sparse if the original graph is, since the constraints follow the edge structure of the DAG of the graph. Finally, the actual practical performance LP solvers is much faster than the bounds suggest, and state-of-the-art commercial solvers like Gurobi [22] can handle LPs with hundreds of thousands of non-zeros.

## 5 EXPERIMENTAL EVALUATION

In this section, we compare our proposal against several baselines. Our empirical analysis focuses on assessing (i) fairness of node exposure, (ii) path lengths, and (iii) runtime and scalability.

**Datasets.** We consider five real-world road networks extracted from OpenStreetMap (publicly available) with the OSMnx Python library [6]. Furthermore, we consider the graph of the state of Florida from the 9th DIMACS Implementation Challenge - Shortest Paths [13] and the Eastern region of the USA from the same collection. Statistics of the seven datasets used are reported in Table 1.

**Queries.** For the first six networks in Table 1, we sample uniformly at random 100 source to target pairs. For the Eastern USA network, we sample 100 pairs uniformly at random from the set of pairs within the distance range  $\left[\frac{d_{\max}}{16}, \frac{d_{\max}}{8}\right]$ , where  $d_{\max}$  represents the estimated diameter of the graph. Following Luo et al. [30], we indicate these constrained pairs with Q1.

**Measures.** The main goal of our method is to guarantee individual fairness in terms of nodes' satisfaction. For our purposes, we compute the generalized Lorenz curve [29] between the bottom fraction of the nodes and the cumulative sum of the nodes' satisfaction,

when the satisfactions are sorted in increasing order. Furthermore, we compute the Gini inequality coefficient [19], as  $1 - 2 \cdot B$ , where  $B$  is the area under the Lorenz curve. The Gini coefficient ranges in  $[0, 1]$ ; higher values are undesirable and indicate higher inequality levels between methods with similar total cumulative satisfactions.

As an (unattainably optimistic) reference line, we compute, for every  $k$  between 1 and the number  $n$  of nodes, the maximum cumulative satisfaction probability by a distribution of forward paths. We refer to the curve thus obtained as the *pointwise best*. It has been calculated for the four smallest networks using the sequence of majorized LPs devised in Section 3.1 of [20]. By definition, the generalized Lorenz curve of any method cannot be above it at any point. Although every point  $(k, y)$  in this curve can be attained by *some* distribution of paths, the entire curve cannot, in general, be attained by any fixed distribution. Indeed, the only case in which the pointwise best is attainable is when it coincides with the maxmin-fair distribution. However, it provides a useful reference as to how suboptimal each method is for different values of  $k$  simultaneously.

We also consider the length of the paths, as well as the running time of the methods, measured as wall-time. Due to the runtime of some baselines on the larger datasets, along with the need to run 100 different source-target pairs, we allow a maximum computational time of 1000 seconds per point-to-point query.

Experiments were run on a MacBook Pro with Apple M1 chip, 8 cores, and 16 GB RAM. To solve the LP problems, we have used the Gurobi optimizer [22].

**Baselines.** To the best of our knowledge, we are the first to investigate node fairness in path recommendations. As no direct comparison with previous work is possible, we use baselines from the literature on diversity in short paths. Specifically:

- **Yen's  $k$ -shortest path algorithm** [44] computes a shortest path and then proceeds to find  $k - 1$  deviations of the shortest path.
- **Two heuristic algorithms from Chondrogiannis et al. [9]: OnePass+ (OP+) and ESX-C.** The goal of these methods is to find a set of  $k$  paths as short as possible and for which their pairwise similarity (defined as a weighted fraction of edges shared by two paths) is below a certain pre-specified threshold  $\theta \in [0, 1]$ . Given a source node  $s$  and a target node  $t$ , OnePass+ traverses the road network expanding every path from the source to any node  $v \in V$  satisfying certain shortness and diversity properties, until  $k$  paths are found. ESX-C, instead, executes shortest-path searches while progressively excluding edges from the road network. We use the default parameter value of  $\theta = 0.8$  and consider  $k = 10$  paths, unless stated otherwise in the tables and figures. In a preliminary analysis, smaller  $\theta$  and higher  $k$  did not improve the results on node fairness, instead significantly increasing the runtime and path length.
- **Moreover, we compare against DKSP**, Luo et al. [30], an edge deviation and concatenation method, based on shortest path trees, which aims to diversify the top- $k$  paths between a source-destination pair such that their pairwise similarities are under a threshold while their total length is minimal. To run DKSP, we set the similarity upper bound between each pair of paths to 0.9.
- **Lastly, we consider random paths drawn uniformly at random from the set of all forward paths (Random FP).** This is equivalent

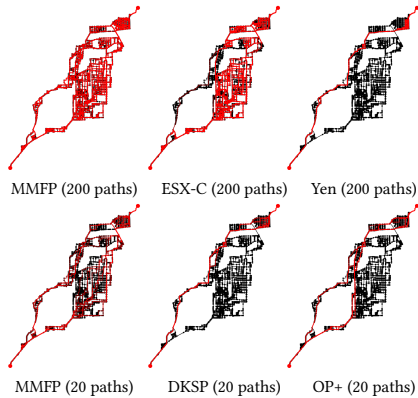


**Figure 4:** Visualization of the paths (in red) produced by different methods, applied to the DAG obtained for a source-target pair of the Kyoto dataset (nodes and edges in black). Our method, MMFP (top-left), visits nearly all the nodes. ESX-C (top-center) also performs well, leaving only a small portion of nodes unvisited. Yen (top-right) finds only minimal deviations from the shortest path. Due to the runtime limits of DKSP and OP+, the second row reports a comparison generating only 20 different paths. Even in this setting, MMFP with the same number of paths covers significantly more nodes.

to drawing random walks from  $s$  to  $t$  in the DAG, where the transition probability is uniform on the outgoing edges of a vertex. We sample 100 paths for each source-destination pair. Essentially, this results in the use of random forward paths only, without the maxmin-fairness optimization.

### 5.1 Comparison against the baselines

We start with the anecdotal evidence reported in Figure 4, where the union of the paths recommended by various methods is colored red. In the first row, we compare methods for which we could compute 200 paths, while in the bottom row we compare our method against baselines for which a maximum of 20 different paths could be computed. For our method MMFP, we sample from a maxmin-fair distribution the exact number of paths, while for the other methods the number of paths is a parameter to the algorithm. To facilitate visual comparison, all methods are applied directly to the DAG constructed for a random source-destination pair from the Kyoto dataset. The figure highlights how MMFP is able to recommend paths covering a broader set of nodes than the baselines. In particular, Yen and DKSP appear to produce only limited deviations from the shortest path. OP+ satisfies a few additional nodes, while ESX-C visits several more nodes but still leaves some groups of nodes uncovered.

**Fairness.** The first column of Tables 4-10 reports the mean and standard deviation of the Gini coefficient. MMFP obtains the lowest level

of inequality with respect to the visibility of the nodes, consistently across all different datasets. This is further illustrated in Figure 5 (Left), where the generalized Lorenz curve for different methods is depicted (results for different source-target pairs and other datasets are analogous and not reported for space reasons). The horizontal axis represents the fraction of nodes receiving the least visibility, while the vertical axis contains the cumulative visibility received by that bottom fraction. Observe that the curve for our method lies consistently above the others, especially in its initial segment, corresponding to the least visible nodes. This highlights how our approach aligns with Rawls’s theory of justice, which advocates maximizing benefits for the least advantaged. Note also how closely our method is to the ideal (yet unattainable) *pointwise best* curve.

So far, we have focused on the fact that MMFP guarantees ex-ante individual fairness. In Figure 5 (Center), we investigate the convergence of ex-post fairness in terms of the allocation of visibility as provided by forward paths sampled from the maxmin-fair distribution. As expected, increasing the number of sampled paths leads to an allocation that closely approximates the theoretical optimum. Specifically, with around 100 paths, the empirical generalized Lorenz curve is already very close to the ideal, while for 1000 sampled paths it becomes essentially identical. This shows the convergence of our technique to maxmin-fairness when serving a large volume of path queries.

**Length of the paths.** The second column of Tables 4-10 reports the average path length. Our method is competitive in this respect, aligning with our earlier observation in Table 1 that the longest forward paths closely approximate shortest paths. MMFP paths are slightly longer than randomly sampled forward paths, reflecting a trade-off between fairness and path length. Yen’s algorithm, focused on finding the  $k$   $s$ - $t$ -paths as short as possible, naturally yields the shortest average lengths. OP+ and DKSP still produce quite short paths. By contrast, those returned by ESX-C are longer; the length of its paths increases as the similarity threshold  $\theta$  decreases and the number  $k$  of requested paths increases.

**Runtime analysis.** The third column of Tables 4-10 reports the runtime in seconds. Our method is quite competitive and scales well with larger networks. It is worth highlighting that, on the commodity laptop we use for our experiments, computing the maxmin-fair distribution takes on average 150 seconds in a network with 3.6M nodes and 8.7M edges.

Unsurprisingly, random forward paths are faster to compute than MMFP. As for the other methods, their runtime is highly dependent on the number of paths  $k$  requested which, unlike our method, needs to be specified in advance. Requesting around  $k = 10$  paths is reasonably fast for all the baselines, except for very large road networks (Table 7 and 10). However, asking for a larger  $k$  was computationally expensive for a single source-destination pair, even for small networks. This was particularly noticeable for OnePass+ and, to a lesser degree, for Yen and DKSP. Although ESX-C is able to produce a higher number of different paths  $k$ , it becomes prohibitively slow on large networks.

In Figure 5 (Right), we investigate further the relationship between the number of requested paths and the runtime for the Florence dataset (for larger datasets, we couldn’t run several baselines

## 5.1 Beyond Shortest paths: Node Fairness in Route Recommendation

**Table 4: Essaouira, Morocco.** We report the Gini coefficient, path lengths, and runtime averaged over 100 random source-destination pairs. The maximum computational time allowed per pair is 1000 seconds. For DAG and MMFP (Algorithms 1 and 2), Gini and the expected length are computed exactly from the distribution; for the rest, they refer to the empirical average over the  $k$  paths produced.

Method	Gini	Length	Runtime (s)
DAG & MMFP	0.27 ± 0.13	3936 ± 3664	0.48 ± 0.81
Random FP	0.36 ± 0.19	3822 ± 3582	0.05 ± 0.01
Yen	0.48 ± 0.22	3692 ± 3485	0.27 ± 0.29
OP+	0.43 ± 0.16	4040 ± 3831	0.07 ± 0.38
DKSP	0.46 ± 0.20	3704 ± 3562	3.70 ± 25.47
ESX-C $\theta=0.5$ $k=10$	0.47 ± 0.13	5537 ± 4500	0.03 ± 0.02
ESX-C $\theta=0.8$ $k=10$	0.50 ± 0.12	6055 ± 5863	0.04 ± 0.03
ESX-C $\theta=0.5$ $k=100$	0.46 ± 0.17	6089 ± 3618	0.18 ± 0.17
ESX-C $\theta=0.8$ $k=100$	0.50 ± 0.16	9871 ± 4882	1.03 ± 1.08

**Table 5: Florence, Italy.** Same as in Table 4.

Method	Gini	Length	Runtime (s)
DAG & MMFP	0.18 ± 0.10	7233 ± 3859	0.59 ± 0.42
Random FP	0.20 ± 0.12	7155 ± 3791	0.28 ± 0.04
Yen	0.29 ± 0.17	6953 ± 3598	0.97 ± 0.95
OP+	0.32 ± 0.09	7301 ± 3572	0.82 ± 4.02
DKSP	0.29 ± 0.12	6996 ± 3171	0.43 ± 1.17
ESX-C $\theta=0.5$ $k=10$	0.46 ± 0.07	13985 ± 4830	0.17 ± 0.18
ESX-C $\theta=0.8$ $k=10$	0.46 ± 0.06	9517 ± 3671	0.03 ± 0.01
ESX-C $\theta=0.5$ $k=100$	0.55 ± 0.15	29075 ± 10320	2.75 ± 2.03
ESX-C $\theta=0.8$ $k=100$	0.62 ± 0.10	37191 ± 8903	30.6 ± 15.3

**Table 6: Kyoto, Japan.** Same as in Table 4.

Method	Gini	Length	Runtime (s)
DAG & MMFP	0.40 ± 0.12	9214 ± 4973	12.66 ± 15.19
Random FP	0.56 ± 0.19	8931 ± 4806	2.18 ± 0.15
Yen	0.66 ± 0.20	8510 ± 4589	35.88 ± 45.45
OP+	0.61 ± 0.18	8600 ± 4599	1.12 ± 3.10
DKSP	0.64 ± 0.20	8533 ± 4672	1.53 ± 5.96
ESX-C $\theta=0.5$ $k=10$	0.57 ± 0.10	9883 ± 4892	0.31 ± 0.39
ESX-C $\theta=0.8$ $k=10$	0.61 ± 0.13	9066 ± 4681	0.10 ± 0.02
ESX-C $\theta=0.5$ $k=100$	0.63 ± 0.12	25868 ± 12884	198.4 ± 179.6
ESX-C $\theta=0.8$ $k=100$	0.66 ± 0.09	17015 ± 6365	15.08 ± 44.80

**Table 7: Eastern USA (Q1).** Same as in Table 4.

Method	Gini	Length	Runtime (s)
DAG & MMFP	0.37 ± 0.11	(1.60 ± 0.24) · 10 <sup>6</sup>	149.8 ± 83.0
Random FP	0.45 ± 0.14	(1.58 ± 0.24) · 10 <sup>6</sup>	67.5 ± 6.0
Yen $k=5$	0.51 ± 0.17	(1.51 ± 0.25) · 10 <sup>6</sup>	641.9 ± 476.8
OP+ $k=5$	0.53 ± 0.14	(1.54 ± 0.24) · 10 <sup>6</sup>	229.9 ± 622.3
DKSP $k=5$	-	-	> 10 <sup>3</sup>
ESX-C $\theta=0.5$ $k=10$	0.57 ± 0.08	(1.68 ± 0.26) · 10 <sup>6</sup>	9.5 ± 9.1
ESX-C $\theta=0.8$ $k=10$	0.59 ± 0.10	(1.60 ± 0.26) · 10 <sup>6</sup>	4.5 ± 1.3
ESX-C $\theta=0.5$ $k=100$	-	-	> 10 <sup>3</sup>
ESX-C $\theta=0.8$ $k=100$	-	-	> 10 <sup>3</sup>

**Table 8: Piedmont, California, USA.** Same as in Table 4.

Method	Gini	Length	Runtime (s)
DAG & MMFP	0.20 ± 0.11	2038 ± 1004	0.29 ± 0.24
Random FP	0.26 ± 0.14	2034 ± 1001	0.02 ± 0.03
Yen	0.34 ± 0.17	1958 ± 855	0.04 ± 0.03
OP+	0.34 ± 0.13	2125 ± 835	0.02 ± 0.00
DKSP	0.34 ± 0.16	2004 ± 856	0.02 ± 0.00
ESX-C $\theta=0.5$ $k=10$	0.38 ± 0.09	4395 ± 1739	0.02 ± 0.00
ESX-C $\theta=0.8$ $k=10$	0.41 ± 0.09	3447 ± 1195	0.02 ± 0.00
ESX-C $\theta=0.5$ $k=100$	0.30 ± 0.11	3315 ± 1354	0.05 ± 0.02
ESX-C $\theta=0.8$ $k=100$	0.30 ± 0.10	4264 ± 1843	0.08 ± 0.04

**Table 9: Buenos Aires, Argentina.** Same as in Table 4.

Method	Gini	Length	Runtime (s)
DAG & MMFP	0.39 ± 0.13	8824 ± 3996	4.14 ± 5.81
Random FP	0.53 ± 0.18	8668 ± 3915	0.57 ± 0.15
Yen	0.62 ± 0.21	8364 ± 3747	5.44 ± 6.20
OP+	0.57 ± 0.15	8476 ± 3734	0.72 ± 3.76
DKSP	0.61 ± 0.19	8392 ± 3748	0.05 ± 0.04
ESX-C $\theta=0.5$ $k=10$	0.54 ± 0.10	9643 ± 3776	0.07 ± 0.05
ESX-C $\theta=0.8$ $k=10$	0.58 ± 0.11	9098 ± 3814	0.06 ± 0.01
ESX-C $\theta=0.5$ $k=100$	0.64 ± 0.07	21793 ± 6057	26.64 ± 28.35
ESX-C $\theta=0.8$ $k=100$	0.67 ± 0.05	22593 ± 5751	3.45 ± 2.97

**Table 10: Florida, USA.** Same as in Table 4.

Method	Gini	Length	Runtime (s)
DAG & MMFP	0.43 ± 0.12	(4.22 ± 2.01) · 10 <sup>6</sup>	232.1 ± 213.6
Random FP	0.50 ± 0.17	(4.19 ± 2.00) · 10 <sup>6</sup>	14.2 ± 2.0
Yen $k=5$	-	-	> 10 <sup>3</sup>
OP+ $k=5$	-	-	> 10 <sup>3</sup>
DKSP $k=5$	-	-	> 10 <sup>3</sup>
ESX-C $\theta=0.5$ $k=10$	0.64 ± 0.08	(4.49 ± 2.01) · 10 <sup>6</sup>	61.3 ± 64.9
ESX-C $\theta=0.8$ $k=10$	0.66 ± 0.08	(4.28 ± 2.00) · 10 <sup>6</sup>	3.2 ± 1.6
ESX-C $\theta=0.5$ $k=100$	-	-	> 10 <sup>3</sup>
ESX-C $\theta=0.8$ $k=100$	-	-	> 10 <sup>3</sup>

for  $k$  larger than 5). Increasing the number of paths per point-to-point query, the baseline methods become slower when several paths are requested, while MMFP is hardly affected. These observations highlight another advantage of our method: by constructing a distribution over multiple distinct paths, we eliminate the need to pre-specify the number of paths required. This approach enables us to efficiently generate a larger set of paths without the computational overhead associated with increasing  $k$  in other methods.

## 5.2 Ablation study and scalability

We analyze the scalability of our method by breaking it into three components: DAG construction (Algorithm 1), maxmin-fair distribution computation (Algorithm 2), and path sampling.

Figure 6 (Left) shows the average runtime of each of the three components across the seven datasets. As expected, MMFP is the most computationally intensive. However, the linear trend in the log-log plot suggests polynomial growth, consistent with Sections 3 and 4. Figure 6 (Center) plots runtime against DAG size for random source-target pairs from the Kyoto dataset. For each pair, we build the DAG and report its number of nodes on the horizontal axis. MMFP shows sublinear growth in the semi-log plot, aligning with theoretical expectations. DAG construction time depends mainly on the input graph size, not the (smaller) output DAG size, as Algorithm 1 relies on distance computations from sources to all nodes and from all nodes to the target. Path sampling time increases only slightly with DAG size.

Finally, Figure 6 (Right) reports peak memory usage. We can observe that MMFP’s LP optimization uses minimal memory. DAG construction memory usage is comparable to that of storing the original graph, as Dijkstra’s algorithm operates on it directly.

## 6 CONCLUSIONS

To the best of our knowledge, our work is the first to address the problem of individual fairness towards the nodes of a network in route recommendation. We introduce the concept of forward paths

## 5.1 Beyond Shortest paths: Node Fairness in Route Recommendation

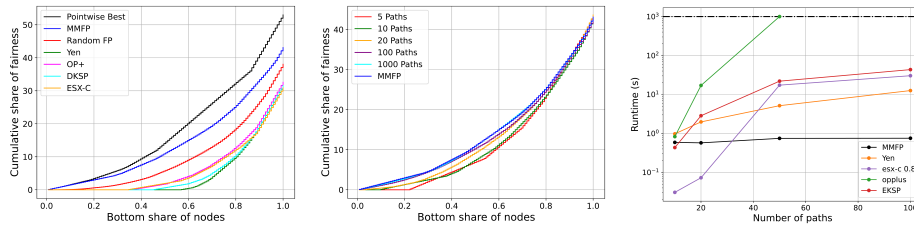


Figure 5: (Left) and (Center) Generalized Lorenz curve for a source-destination random pair of the Essaouira dataset. The horizontal axis reports the cumulative fraction of nodes that are receiving the least amount of satisfaction, while the vertical axis contains the cumulative amount of satisfaction received by the corresponding bottom share of nodes. On the left, the curve is depicted for different methods and Pointwise Best (black) represents an idealistic, in general unattainable, curve that maximizes the cumulative share of fairness, for each fixed the bottom share of nodes. In the center, as more paths are sampled from the maxmin-fair distribution, the observed fairness allocation increasingly converges to the one of the maxmin-fair distribution. (Right) Average runtime w.r.t. number of requested paths per point-to-point query, (Florence dataset). Baseline methods becomes slower when several paths are requested. The time complexity of MMFP is due to the optimization of the maxmin-fair distribution; sampling several paths does not increase its runtime significantly.

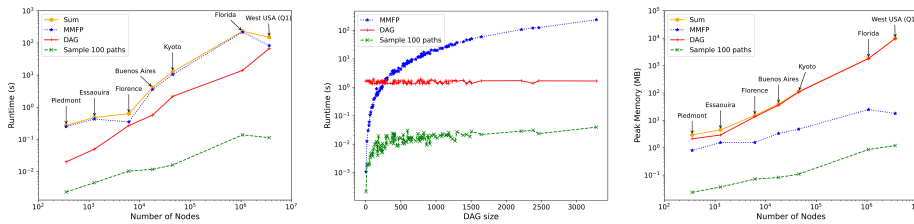


Figure 6: (Left) Average runtime over 100 random source-target pairs for each component of our method, as well as their total sum, across datasets of varying sizes. (Center) Runtime for each component of our method for the Kyoto dataset. Each point corresponds to a source-target pair, with the number of nodes in the corresponding DAG reported on the horizontal axis. The sub-linear growth in the semi-log plot of MMFP corresponds to the theoretical polynomial runtime. The constant runtime of the DAG creation is in accordance with the fact that the cost to construct the DAG is asymptotically the same as Dijkstra’s algorithm, which mainly depends on the size of the original graph. (Right) The Peak Memory allocated, averaged across multiple source-target pairs. The memory allocated by MMFP is very low, as the LPs iteratively solved are small.

and show their viability as an alternative to shortest paths. We show how to compute a DAG that contains all the forward paths and how a probability distribution on the forward paths, such that the individual nodes receive a maxmin-fair individual satisfaction, can be obtained by solving a flow problem by linear programming. Our experimental results confirm the benefits and practical relevance of our proposal.

One limitation of our work is that even though forward paths tend to be short in practice, this property is not guaranteed. The degree to which forward paths approximate shortest paths is data-dependent, whereas for some applications a strict pre-specified upper bound on the deviation from the optimal path length may be desirable. In this regard, we note that it is straightforward to modify LP (1) to include a constraint on the *expected* length of the forward paths found, which is given by  $\sum f_{u,v} \cdot \ell(u, v)$ ; and by using

rejection sampling, we can constrain the *maximum* path length to be at most  $1 + \alpha$  times its expectation by sampling  $O(1/\alpha)$  paths (in expectation) and rejecting those that are too long. However, such a modification would not conform to the strict definition of maxmin-fairness. Reconciling maxmin-fairness with hard bounds on path lengths remains an open problem for future research.

We have focused on fairness from a locational perspective, assuming users aim to reach their destination in a reasonable time. However, users may have diverse preferences: for example, a tourist might prefer routes with museums, while another might favor architecturally significant sites. Incorporating such personalized preferences into our fairness framework is a compelling challenge for future work. Additionally, our method assumes static graphs; extending it to dynamic networks or incorporating evolving edge weights would be valuable directions for future research.

## REFERENCES

- [1] Ittai Abraham, Daniel Delling, Andrew V Goldberg, and Renato F Werneck. 2013. Alternative routes in road networks. *Journal of Experimental Algorithms (JEA)* 18 (2013), 1–1.
- [2] Richard Bellman. 1958. On a routing problem. *Quarterly of applied mathematics* 16, 1 (1958), 87–90.
- [3] Matthias Bentert, Leon Kellerhals, and Rolf Niedermeier. 2022. The structural complexity landscape of finding balance-fair shortest paths. *Theoretical Computer Science* 933 (2022), 149–162.
- [4] Matthias Bentert, Leon Kellerhals, and Rolf Niedermeier. 2023. Fair short paths in vertex-colored graphs. In *Proceedings of the AAAI Conference on Artificial Intelligence*, Vol. 37. 12346–12354.
- [5] Asia J. Biega, Krishna P. Gummadi, and Gerhard Weikum. 2018. Equity of Attention: Amortizing Individual Fairness in Rankings. In *The 41st International ACM SIGIR Conference on Research & Development in Information Retrieval, SIGIR 2018*. 405–414.
- [6] Geoff Boeing. 2025. Modeling and analyzing urban networks and amenities with OSMnx. *Geographical Analysis* (2025).
- [7] Igo Brilhante, Jose Antonio Macedo, Franco Maria Nardini, Raffaele Perego, and Chiara Renso. 2013. Where shall we go today? Planning touristic tours with TripBuilder. In *Proceedings of the 22nd ACM international conference on Information & Knowledge Management*. 757–762.
- [8] Xin Cao, Lisi Chen, Gao Cong, and Xiaokui Xiao. 2012. Keyword-aware Optimal Route Search. *Proc. VLDB Endow* 5, 11 (2012), 1136–1147.
- [9] Theodoros Chondrogiannis, Panagiotis Bouras, Johann Gamper, Ulf Leser, and David B Blumenthal. 2020. Finding k-shortest paths with limited overlap. *The VLDB Journal* 29, 5 (2020), 1023–1047.
- [10] Michael B Cohen, Yin Tat Lee, and Zhao Song. 2021. Solving linear programs in the current matrix multiplication time. *Journal of the ACM (JACM)* 68, 1 (2021), 1–39.
- [11] Thomas H Cormen, Charles E Leiserson, Ronald L Rivest, and Clifford Stein. 2022. *Introduction to algorithms*. MIT press.
- [12] Yashar Deldjoo, Dietmar Jannach, Alejandro Bellogin, Alessandro Difonzo, and Dario Zanzonelli. 2024. Fairness in recommender systems: research landscape and future directions. *User Modeling and User-Adapted Interaction* 34, 1 (2024), 59–108.
- [13] Camil Demetrescu, Andrew V Goldberg, and David S Johnson. 2009. *The shortest path problem: Ninth DIMACS implementation challenge*. Vol. 74. American Mathematical Soc.
- [14] Edsger W. Dijkstra. 1959. A Note on Two Problems in Connexion with Graphs. *Numer. Math.* 50 (1959), 269–271.
- [15] Ahmed Fahmin, Bojie Shen, Muhammad Aamir Cheema, Adel N. Toosi, and Mohammed Eunus Ali. 2024. Efficient alternative route planning in road networks. *IEEE Transactions on Intelligent Transportation Systems* 25, 10 (Oct. 2024), 14220–14232.
- [16] Michael I. Fredman and Robert Endre Tarjan. 1987. Fibonacci heaps and their uses in improved network optimization algorithms. *Journal of the ACM (JACM)* 34, 3 (1987), 596–615.
- [17] David Garcia-Soriano and Francesco Bonchi. 2020. Fair-by-design matching. *Data Mining and Knowledge Discovery* 34 (2020), 1291–1335.
- [18] David Garcia-Soriano and Francesco Bonchi. 2021. Maxmin-fair ranking: individual fairness under group-fairness constraints. In *Proceedings of the 27th ACM SIGKDD Conference on Knowledge Discovery & Data Mining*. 436–446.
- [19] Corrado Gini. 1936. On the measure of concentration with special reference to income and statistics. Colorado College Publication. *General series* 208, 1 (1936), 301–323.
- [20] Ashish Goel and Adam Meyerson. 2006. Simultaneous optimization via approximate majorization for concave profits or convex costs. *Algorithmica* 44 (2006), 301–323.
- [21] Martin Grötschel, László Lovász, and Alexander Schrijver. 1988. *Geometric Algorithms and Combinatorial Optimization*. Algorithms and Combinatorics, Vol. 2. Springer.
- [22] Gurobi Optimization, LLC. 2024. Gurobi Optimizer Reference Manual. <https://www.gurobi.com>
- [23] Christian Häcker, Panagiotis Bouras, Theodoros Chondrogiannis, and Ernst Althaus. 2021. Most diverse near-shortest paths. In *Proceedings of the 29th International Conference on Advances in Geographic Information Systems*. 229–239.
- [24] Teshu Hanaka, Masashi Kiyomi, Yasuaki Kobayashi, Yusuke Kobayashi, Kazuhiro Kurita, and Yota Otachi. 2023. A framework to design approximation algorithms for finding diverse solutions in combinatorial problems. In *Proceedings of the AAAI Conference on Artificial Intelligence*, Vol. 37. 3968–3976.
- [25] Teshu Hanaka, Yasuaki Kobayashi, Kazuhiro Kurita, See Woo Lee, and Yota Otachi. 2022. Computing diverse shortest paths efficiently: A theoretical and experimental study. In *Proceedings of the AAAI Conference on Artificial Intelligence*, Vol. 36. 3758–3766.
- [26] Christopher Hojny, Frits Spieksma, and Sten Wessel. 2025. Fairness in graph-theoretical optimization problems. *Discrete Applied Mathematics* 375 (2025), 178–192.
- [27] Chen Karako and Putra Manggala. 2018. Using image fairness representations in diversity-based re-ranking for recommendations. In *Proceedings of the 26th Conference on User Modeling, Adaptation and Personalization*. 23–28.
- [28] Shan Liu, Hai Jiang, Shuiping Chen, Jing Ye, Renqing He, and Zhizhao Sun. 2020. Integrating Dijkstra’s algorithm into deep inverse reinforcement learning for food delivery route planning. *Transportation Research Part E: Logistics and Transportation Review* 142, Article 102070 (Oct. 2020), 102070 pages.
- [29] Max O Lorenz. 1905. Methods of measuring the concentration of wealth. *Publications of the American statistical association* 9, 70 (1905), 209–219.
- [30] Zihan Luo, Lei Li, Mengxuan Zhang, Wen Hua, Yehong Xu, and Xiaofang Zhou. 2022. Diversified Top-k Route Planning in Road Network. *Proc. VLDB Endow* 15, 11 (2022), 3199–3212.
- [31] Amgad Madkour, Walid G Aref, Faizan Ur Rehman, Mohamed Abdur Rahman, and Saleh Basalamah. 2017. A survey of shortest-path algorithms. *arXiv preprint arXiv:1705.02044* (2017).
- [32] Atasi Panda, Anand Louis, and Prajakta Nimbhorkar. 2024. Individual Fairness under Group Fairness Constraints in Bipartite Matching - One Framework to Approximate Them All. In *Proceedings of the Thirty-Third International Joint Conference on Artificial Intelligence, IJCAI 2024*. 175–183.
- [33] Daniele Quercia, Rossano Schifanella, and Luca Maria Aiello. 2014. The shortest path to happiness: Recommending beautiful, quiet, and happy routes in the city. In *Proceedings of the 25th ACM conference on Hypertext and social media*. 116–125.
- [34] John Rawls. 1971. *A theory of justice*. MA: Harvard University Press.
- [35] Senjuti Basu Roy, Gautam Das, Sihem Amer-Yahia, and Cong Yu. 2011. Interactive itinerary planning. In *2011 IEEE 27th International Conference on Data Engineering*. IEEE, 15–26.
- [36] Jad Salem, Reuben Tate, and Stephan Eidenbenz. 2024. Expected Maximin Fairness in Max-Cut and other Combinatorial Optimization Problems. *arXiv preprint arXiv:2410.02589* (2024).
- [37] Joy Lal Sarkar, Abhishek Majumder, Chhabi Rani Panigrahi, Sudipta Roy, and Bibudhendu Pati. 2023. Tourism recommendation system: A survey and future research directions. *Multimedia tools and applications* 82, 6 (2023), 8983–9027.
- [38] Ashudeep Singh and Thorsten Joachims. 2018. Fairness of Exposure in Rankings. In *Proceedings of the 24th ACM SIGKDD International Conference on Knowledge Discovery & Data Mining, KDD 2018, London, UK, August 19–23, 2018*, Yike Guo and Faisal Farooq (Eds.), 2219–2228.
- [39] Panote Siriaraya, Yuanyuan Wang, Yihong Zhang, Shoko Wakamiya, Péter Jeszenszky, Yukiko Kawai, and Adam Jatowt. 2020. Beyond the Shortest Route: A Survey on Quality-Aware Route Navigation for Pedestrians. *IEEE Access* 8 (2020), 135569–135590.
- [40] Christian Sommer. 2014. Shortest-path queries in static networks. *ACM Computing Surveys (CSUR)* 46, 4 (2014), 1–31.
- [41] Caleb Voss, Mark Moll, and Lydia E Kavrakı. 2015. A heuristic approach to finding diverse short paths. In *2015 IEEE International Conference on Robotics and Automation (ICRA)*. IEEE, 4173–4179.
- [42] Yifan Wang, Weizhi Ma, Min Zhang, Yiqun Liu, and Shaoping Ma. 2023. A Survey on the Fairness of Recommender Systems. *ACM Trans. Inf. Syst.* 41, 3 (2023).
- [43] Kexin Xie, Ke Deng, Shuo Shang, Xiaofang Zhou, and Kai Zheng. 2012. Finding alternative shortest paths in spatial networks. *ACM Transactions on Database Systems (TODS)* 37, 4 (2012), 1–31.
- [44] Jin Y Yen. 1970. An algorithm for finding shortest routes from all source nodes to a given destination in general networks. *Quarterly of applied mathematics* 27, 4 (1970), 526–530.
- [45] Shiming Zhang, Zhipeng Luo, Li Yang, Fei Teng, and Tianrui Li. 2024. A survey of route recommendations: Methods, applications, and opportunities. *Inf. Fusion* 108 (2024), 102413.

## 5.2 Link Recommendations: Their Impact on Network Structure and Minorities

Link recommendation algorithms play a central role in many online platforms, where they are used to suggest new connections between users. These systems are typically designed to maximize predictive accuracy or user engagement, relying on structural features of the network such as common neighbors, similarity measures, or learned node embeddings.

However, by shaping which connections are formed, link recommendation algorithms can also influence the long-term evolution of the network structure. In particular, they may reinforce existing patterns of homophily or preferential attachment, potentially amplifying structural inequalities affecting minority groups.

The work presented in this section contributes to RQ2 by examining the impact of link recommendation algorithms on the structural properties of social networks. Specifically, we analyze how commonly used recommendation strategies influence network evolution and investigate whether these mechanisms may exacerbate segregation or disadvantage minority groups over time. Through simulation analysis, this study provides insights into the systemic effects of recommendation algorithms, highlighting how seemingly neutral optimization objectives can have unintended consequences for fairness in evolving network structures.

### Authors' Contributions

---

<b>Contribution</b>	<b>Authors</b>
<b>Conceptualization:</b>	A. Ferrara and all authors
<b>Writing:</b>	A. Ferrara and all authors
<b>Methodology:</b>	A. Ferrara and all authors
<b>Code:</b>	A. Ferrara
<b>Experiments:</b>	A. Ferrara

---

## Link recommendations: Their impact on network structure and minorities

Antonio Ferrara  
GESIS - Leibniz Institute for the Social Sciences  
Cologne, Germany  
RWTH Aachen University  
Aachen, Germany  
antonio.ferrara@gesis.org

Fariba Karimi  
Complexity Science Hub  
Vienna, Austria  
karimi@csh.ac.at

Lisette Espín-Noboa  
Complexity Science Hub  
Vienna, Austria  
Central European University  
Vienna, Austria  
espin@csh.ac.at

Claudia Wagner  
GESIS - Leibniz Institute for the Social Sciences  
Cologne, Germany  
RWTH Aachen University  
Aachen, Germany  
Complexity Science Hub  
Vienna, Austria  
claudia.wagner@gesis.org

### ABSTRACT

Network-based people recommendation algorithms are widely employed on the Web to suggest new connections in social media or professional platforms. While such recommendations bring people together, the feedback loop between the algorithms and the changes in network structure may exacerbate social biases. These biases include rich-get-richer effects, filter bubbles, and polarization. However, social networks are diverse complex systems and recommendations may affect them differently, depending on their structural properties. In this work, we explore five people recommendation algorithms by systematically applying them over time to different synthetic networks. In particular, we measure to what extent these recommendations change the structure of bi-populated networks and show how these changes affect the minority group.

Our systematic experimentation helps to better understand when link recommendation algorithms are beneficial or harmful to minority groups in social networks. In particular, our findings suggest that, while all algorithms tend to close triangles and increase cohesion, all algorithms except Node2Vec are prone to favor and suggest nodes with high in-degree. Furthermore, we found that, especially when both classes are heterophilic, recommendation algorithms can reduce the visibility of minorities.

### CCS CONCEPTS

• **Information systems** → **Social networks; Recommender systems.**

Permission to make digital or hard copies of part or all of this work for personal or classroom use is granted without fee provided that copies are not made or distributed for profit or commercial advantage and that copies bear this notice and the full citation on the first page. Copyrights for third-party components of this work must be honored. For all other uses, contact the owner/author(s).  
WebSci '22, June 26–29, 2022, Barcelona, Spain  
© 2022 Copyright held by the owner/author(s).  
ACM ISBN 978-1-4503-9191-7/22/06.  
<https://doi.org/10.1145/3501247.3531583>

### KEYWORDS

Recommendation algorithms, friendship recommendations, network science, social networks, homophily, preferential attachment.

### ACM Reference Format:

Antonio Ferrara, Lisette Espín-Noboa, Fariba Karimi, and Claudia Wagner. 2022. Link recommendations: Their impact on network structure and minorities. In *14th ACM Web Science Conference 2022 (WebSci '22)*, June 26–29, 2022, Barcelona, Spain. ACM, New York, NY, USA, 11 pages. <https://doi.org/10.1145/3501247.3531583>

### 1 INTRODUCTION

Social networks are the infrastructure of our social and professional life. They impact, among others, our cooperation [18], our health [8], and our social perceptions [24]. The structure of modern online social networks is however not only shaped by well-studied social mechanisms (such as homophily or preferential attachment), but it is also affected by people recommender systems, complex algorithms that suggest new connections among social network users. How do these algorithms affect the structure of social networks over time? What are the consequences for different groups? In this paper, we aim to shed light on these questions.

**Problem:** Previous work has shown that recommendation algorithms are prone to reinforcing popularity bias [1]. A further subtle problem is that by matching users' preferences, these algorithms often lead to the formation of filter bubbles [7], echo chambers [5], and polarization [11]. In recent years, much attention has been paid to understanding when, and to what extent, such biases are being amplified. As an example, [15] and [14] have studied the correlation between network structure and the output of ranking algorithms in social networks. While these studies highlight that *homophily*—the tendency to connect to similar others—and *preferential attachment*—the tendency to connect to those that are already well-connected—are important structural factors that impact the visibility of nodes in algorithmic rankings, they do not compare effects over time. Feedback loops, instead, have been studied in [34]

## 5.2 Link Recommendations: Their Impact on Network Structure and Minorities

WebSci '22, June 26–29, 2022, Barcelona, Spain

Ferrara et al.

and [33], where they respectively analyze “rich-get-richer” and “glass ceiling” effects. Recently, also [16] and [9] have focused on feedback loops and long term effects of people recommender systems. The former analyzes inequalities in the exposure of minorities and the latter focuses on polarization and echo chambers. Our study integrates this body of research by providing a systematic analysis of how homophily and minority size relate to structural properties of the network and visibility of groups.

**Approach:** We systematically compare five recommendation algorithms and apply their recommendations to several synthetic networks. We focus on scale-free directed networks with adjustable homophily and minority group size [14] and quantify the global changes in network structure, as well as the changes in connectivity for the minority group over time. In particular, we assess whether certain types of links are created more often than others and whether the network becomes more cohesive or segregated. Similarly, we verify when, and at what rates, these algorithms put minorities at disadvantage by measuring the changes in their *visibility*, here defined as the fraction of minorities among the top most important nodes, based on their algorithmic ranking. To this end, we formulate the following research questions that will guide our analysis throughout this paper.

- RQ1: How do recommendation algorithms affect the structure of the network and the visibility of minorities?
- RQ2: To what extent is the change in visibility due to homophily?
- RQ3: Is the change in visibility inversely proportional to the size of the minority or proportional to the in-group links within the minority?

**Contributions:** Our contributions are the following: (1) We demonstrate that networks become more cohesive over time throughout multiple recommendations. However, the rate at which this cohesiveness gets stronger depends on the algorithm. (2) Not all algorithms suffer from the popularity bias problem, which means that certain algorithms may diversify their recommendations. (3) The visibility of the minority group gets affected differently depending on three main components: the algorithm, the initial conditions of homophily in the network, and the size of the minority group.

Moreover, our study sheds light on the weaknesses of algorithms under the initial conditions of network structure and can be used as key factors to improve recommendations, where necessary.

### 2 RELATED WORK

The related work is organized in two parts. First, we introduce the relevant literature on the mechanisms that drive the existence of biases in network structure. Then, we focus on the creation of new ties from link recommendations. In particular, we highlight the effects of recommendation algorithms on the network structure and the visibility of minorities.

**Biases in network structure and related consequences:** The rich-get-richer or Matthew effect [28] is one of the first mechanisms of edge formation discovered by sociologists to explain cumulative advantages in real-world networks. From the network perspective, the Matthew effect operates through the preferential attachment mechanism, that is the tendency of nodes to attach preferentially

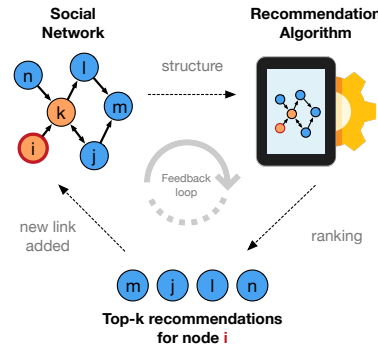


**Figure 1: The recommendation cycle:** A network-based recommendation algorithm uses the local or global structure of the network to recommend for each node  $i$  the top- $k$  best matches with whom node  $i$  may want to connect. If node  $i$  accepts the recommendations, the structure of the network changes. This creates a feedback loop since the new structure is pre-processed by the algorithm to infer new recommendations.

to those that are already well-connected [4]. This mechanism of edge formation and other structural characteristics may impact the visibility and importance of nodes, and thus, create and enlarge inequalities. For example, [3] and [23] propose mathematical models that integrate preferential attachment and homophily (the tendency to connect to similar others [27]) to explain the emergence of the “glass ceiling” effect in social networks. Glass ceiling, as defined by the US Federal Commission, is “the unseen, yet unbreakable barrier that keeps minorities and women from rising to the upper rungs of the corporate ladder, regardless of their qualifications or achievements”. Studies on glass ceiling are expanded in [30], where the authors consider the effect of the perceived gender on the visibility of users on Twitter. In particular, they reveal how users perceived as women are hampered from attaining equal visibility. Furthermore, [23] shed light on how homophily can put minority groups at disadvantage by restricting their ability to establish links with the majority group and by limiting their access to information. Recently, [35] observed that PageRank [31] might unfairly allocate importance scores to different classes, and proposed alternative fair versions of the algorithm.

Our work is built upon this body of literature and integrates social biases in feedback loops of people recommendations. In particular, we analyze the tendencies of groups to connect to each other, how these tendencies or mechanisms of edge formation affect the recommendations, and ultimately how these recommendations affect the structure of networks and the visibility of minorities.

**Effects of recommender systems on networks:** [34] analyzes the “rich-get-richer” phenomenon through social recommendations. In particular, they study how the “Who-to-Follow” algorithm affects

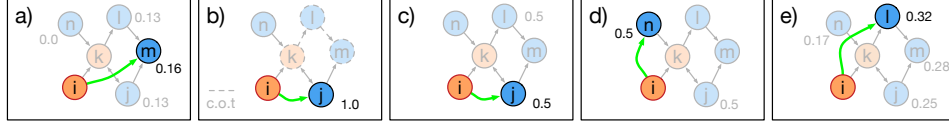


**Figure 2: Recommendation algorithms:** Given the network in Figure 1, here we explain the recommendation suggested to node  $i$  by each of our algorithms of interest. a) Personalized PageRank recommends the most visited nodes by performing random walks that restart from node  $i$ :  $i \rightarrow m$ . b) Who-to-follow builds the so called “circle of trust” (c.o.t.: nodes  $k$ ,  $l$ , and  $m$ ) for  $i$  and recommends nodes that are followed by the nodes in the c.o.t.:  $i \rightarrow j$ . c) Two-hops recommends nodes at a distance 2:  $i \rightarrow j$ . d) Common-followed suggests nodes with a similar set of out-links:  $i \rightarrow n$ . e) Node2Vec projects nodes into an euclidean space and recommends those with similar embeddings:  $i \rightarrow l$ . The values next to each node are the scores returned by each algorithm. The larger the value, the more important the node for  $i$ .

the structure of the follower network on Twitter. They found that most popular users profited substantially more than average from the user suggestions. They attributed this “rich-get-richer” effect to various factors, including the mismatch between users (being recommended proportional to their degree), and the baseline growth rate of users (whose asymptotic behavior is instead sub-linear in the degree). Users’ centrality and clustering coefficient may also vary depending on the recommendation algorithm in “Social-Blue”, an internal social networking site at IBM [10]. Similar effects have been found in Tumblr and Flickr, two social media platforms, where recommendations favor popular and well-connected nodes, and at the same time limit the growth of the diameter of the network [2].

In addition to these topological effects, social recommendations may also exacerbate the under-representation of certain demographic groups in the network. For instance, [14, 15, 33] show how the visibility of minorities can be amplified or mitigated by different levels of homophily within groups when using recommendation algorithms on scale-free networks. These inequalities have been also studied over time but only recently. [16] suggests that while the homophily level of the minority affects the speed of the growth of their disparate exposure, the relative size of the minority affects the magnitude of this effect.

One of the main differences between this body of research and our work is that we vary homophily systematically. This allows us to better understand the relationship between the initial homophily of the network and the long-term effects of the recommendations. In particular, to what extent they change network structure and the visibility of minorities over time. Moreover, we study Node2Vec [20], a more recent algorithm used to generate link recommendations through node embeddings.

### 3 METHODS

#### 3.1 Directed networks

We consider attributed directed networks of the following form: let  $G = (V, E, C)$  be a node-attributed graph where  $V = \{v_1, \dots, v_n\}$  is a set of  $n$  nodes,  $E \subseteq V \times V$  is a set of  $e$  unweighted directed edges, and  $C : V \rightarrow \{0, 1\}$  is a function that maps each node  $v_i$  into its group (or class) membership  $c_i$ . For the sake of simplicity we focus on binary group membership (e.g., black/white or male/non-male). The function  $C$ , hence, divides the nodes into two groups, a

minority, called  $m$ , and a majority, called  $M$ . We refer to the fraction of the minority group in the network as  $f_m$ .

Further definitions, peculiar to the synthetic network generation model employed, are provided in Section 3.3.

#### 3.2 Recommendation algorithms

In this section, we define the five recommendation algorithms of interest. All algorithms are class agnostic which means that their recommendations are solely based on topology. Note as well that for each node  $v_i \in V$ , the recommendation algorithm suggests a ranked list of  $k$  nodes that  $v_i$  is not yet connected with. The ranked list is sorted in descending order in terms of relevance scores according to each algorithm. In the case of ties, where multiple nodes are equally relevant, nodes are chosen randomly. We refer the reader to Section 3.3 for the details on the configuration of hyper-parameters for each algorithm.

**Personalized PageRank (PPR):** It is an extension of PageRank to rank nodes in a network from the perspective of a seed node [31]. In principle, random walks are performed and restarted at the origin (or seed node) multiple times to update the importance score of all nodes, see Figure 2(a). We compute the PPR vector  $\pi_i$  with respect to each node  $v_i \in V$  as follows:

$$\pi_i^T = (1 - \alpha)e_i^T + \alpha\pi_i^T W \quad (1)$$

where  $\alpha$  is the probability of following links,  $e_i$  denotes the personalized one-hot vector<sup>1</sup>,  $W$  is the transition matrix inferred from  $G$  and  $T$  represents the transpose operator. The ranking score given to node  $v_j$  is then the  $j^{\text{th}}$  component of  $\pi_i$ .

**Who-to-follow (WTF):** This algorithm, proposed by Twitter [21], suggests users who are followed by people that are similar to the one getting the recommendation, see Figure 2(b). For each user  $v_i$ , the algorithm looks for its *circle of trust*, which is the result of an egocentric random walk (similar to personalized PageRank [22]). Then, based on this circle-of-trust  $COT_i$ , WTF ranks (using the SALSA algorithm [25]) users that are not yet friends with  $v_i$  but are connected through the circle of trust  $\pi_{COT_i}^{\text{out}}$ .

$$WTF_i = \text{SALSA}(COT_i, \pi_{COT_i}^{\text{out}}) \quad (2)$$

<sup>1</sup> $(e_i)_i = 1$  and  $(e_i)_j = 0, \forall j \neq i$

**Two-hops (2H):** This algorithm follows the intuition behind *friends-of-friends*. In directed networks, the 2H algorithm recommends nodes  $v_j$  that are at a distance 2 from node  $v_i$ , see Figure 2(c). The more such paths, the more likely the recommendation. Calling  $\Gamma_a^{out}$  the set of nodes that  $v_a$  points towards (i.e., out-links), and  $\Gamma_a^{in}$  the set of nodes pointing to  $v_a$  (i.e., in-links), we define the 2H score function as the number of possible paths of length 2 from  $v_i$  to  $v_j$ :

$$2H(v_i, v_j) := |\Gamma_i^{out} \cap \Gamma_j^{in}| \quad (3)$$

**Common-followed (CF):** We extend the common neighbors approach [26], which is based on the idea that two nodes  $v_i$  and  $v_j$  are more likely to connect to each other if they have multiple friends in common. In the context of directed networks, the *common-followed* algorithm will recommend node  $v_j$  to node  $v_i$  if they follow partially or fully the same set of nodes, see Figure 2(d). Then, the algorithm ranks all nodes  $v_j$  based on the number of common-followed nodes with  $v_i$ . Let  $\Gamma_a^{out}$  be the set of nodes that  $v_a$  follows. We define the set of common-followed nodes between  $v_i$  and  $v_j$  as:

$$CF(v_i, v_j) := |\Gamma_i^{out} \cap \Gamma_j^{out}| \quad (4)$$

**Node2Vec (N2V):** A popular embedding algorithm that maps nodes to a low-dimensional space of features, by maximizing the likelihood of preserving nodes' neighborhoods [20]. It has been used for link prediction by evaluating the cosine similarity between nodes in the embedding space, see Figure 2(e). Here we use N2V to recommend to each node  $v_i$  the most similar node in the embedding space, according to cosine similarity of the embedded vectors. Calling respectively  $v_i^p$  and  $v_j^p$  the embedded vector projections for  $v_i$  and  $v_j$ , the cosine similarity between these projections is defined as:

$$\text{CosineSim}(v_i^p, v_j^p) := \frac{v_i^p \cdot v_j^p}{\|v_i^p\| \|v_j^p\|} \quad (5)$$

### 3.3 Experiments setup

Here we describe the networks employed in our experiments and explain how the recommendation algorithms are iteratively used to recommend new connections among nodes.

**Synthetic networks:** In order to systematically create networks as defined in Section 3.1, we employed the DPAH model [14]. This model allows to generate scale-free bi-populated directed networks with adjustable homophily (for each group), minority size, node activity, and edge density. DPAH is a growth model that generates networks as follows. First,  $n$  nodes are created and randomly assigned to one of two groups based on the fraction of minorities  $f_m$ . Then, the following steps are repeated until the desired edge density  $d$  is fulfilled. A source node  $v_i$  is drawn from a power-law distribution, modeled through the activity parameters  $\gamma_M$  and  $\gamma_m$  for the majority and the minority group, respectively. A target node  $v_j$  is drawn with a probability that is proportional to the product of its in-degree and the pair-wise homophily between the source and the target node. Lastly, a directed edge from  $v_i$  to  $v_j$  is created. Thus, the probability of creating a link from  $v_i$  to  $v_j$  is defined as:

$$\mathbb{P}(v_i \rightarrow v_j) = \frac{h_{ij} k_j^{in}}{\sum_{l=1}^n h_{il} k_l^{in}} \quad (6)$$

where  $k_j^{in}$  is the in-degree of  $v_j$ , and  $h_{ij}$  is the homophily between  $v_i$  and  $v_j$  and it is determined by their class membership.

In this work, we systematically modify the homophily within groups and the size of the minority, leaving the variation of node activity and edge density for a further study. In particular, in order to measure the influence of algorithms (RQ1) and homophily (RQ2) in the recommendations, we generate 4 networks for each combination of homophily parameters  $h_{mm}, h_{MM} \in \{0.0, 0.1, \dots, 1.0\}$  ( $h_{mM}$  and  $h_{Mm}$  are defined as  $1 - h_{mm}$  and  $1 - h_{MM}$ , respectively) and fix the number of nodes  $n = 1000$ , the size of the minority  $f_m = 0.3$ , the node activity  $\gamma_M = \gamma_m = 2.5$  and the edge density  $d = 0.03$ . We further adjust the size of the minority  $f_m \in \{0.1, 0.2, 0.3, 0.4\}$  to measure its influence in the visibility of minorities (RQ3).

**Recommendation:** Given an initial network  $G$ , we apply a recommendation algorithm  $R$  to suggest to each node  $v_i$  a node  $v_j$  to connect with. Then, we create a direct link  $v_i \rightarrow v_j$  for each top-1 of these recommendations. By doing so, in what we call "one step", we create a new out-link for each node  $v_i$ . This decision is motivated by the fact that the employed acceptance policy plays only a marginal role in shaping the network [9, 16]. Then, for every addition, we remove a random out-link. This is a procedure previously employed in the literature, for example in [9]. One of the main reasons for this choice is to prevent a significant increase in the edge density of the network. The evaluation metrics considered in Section 3.4 are sensible to edge density. By removing a link every time a new one is created we ensure to keep the density constant on every step and make sure that the changes are due to the recommendations and not to an increase in the total amount of connections. The link removal procedure is also grounded on the social theory for which people exhibit a finite communication capacity and, thus, they have a limit on the number of ties that they can maintain active in time [12, 29].

We repeat the above procedure 30 times to simulate an equal amount of recommendations per node.

**Hyper-parameters:** For PPR, we set the probability of following links to  $\alpha = 0.85$ , as suggested by Brin and Page [6] and widely used in many applications. In N2V, we use the default values for the dimensions of the embedding space  $dimensions = 64$ , the number of visited nodes in each random walk  $walk\_length = 10$ , and the number of random walks to be generated from each node in the graph  $num\_walks = 200$ . For WTF, we constrain the circle of trust to include only the top-10 nodes.

**Additional assumption:** We assume that the recommendations of different algorithms are similarly relevant, as our goal is not to evaluate which algorithm performs better in terms of utility metrics, but rather to study their effects on the structure and their impact on the visibility of the minorities (see Section 3.4).

### 3.4 Evaluation metrics

We use the global *clustering coefficient* [17] of the network and the *Gini coefficient* [19] of the in-degree distribution as proxies of network structure, and the fraction of minorities among the most important nodes as *visibility*. We measure these metrics before and after each round of recommendations to verify whether certain types of networks change these metrics faster or slower and by how much.

## 5.2 Link Recommendations: Their Impact on Network Structure and Minorities

Link recommendations: Their impact on network structure and minorities

WebSci '22, June 26–29, 2022, Barcelona, Spain

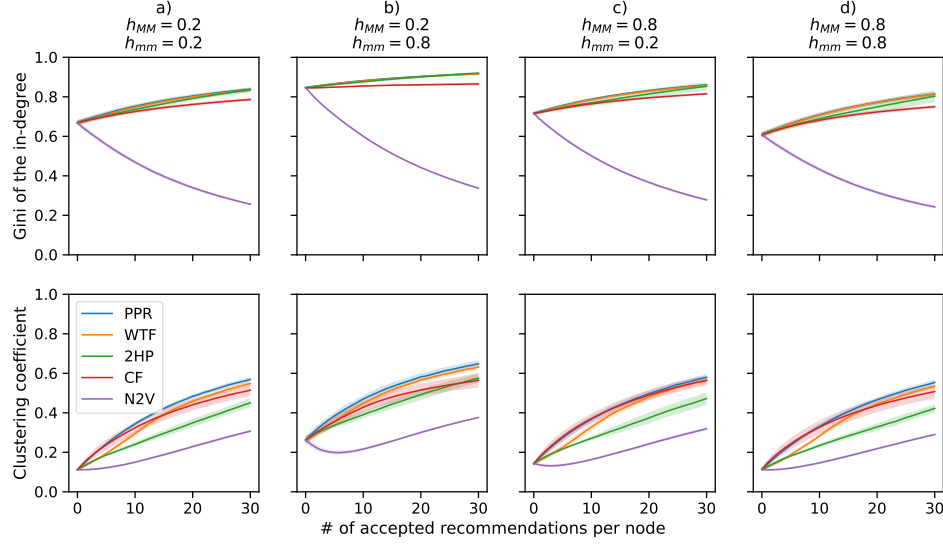


**Figure 3: The evolution of network structure for different recommendation algorithms and different values of homophily in the initial network. One can see that, regardless of the type of network (columns), all algorithms except N2V have similar effects on the Gini coefficient of the in-degree distribution (top row) and the clustering coefficient (bottom row). Surprisingly, N2V reduces the Gini coefficient of the in-degree distribution over time (x-axis) and increases the global clustering coefficient at lower rates compared to the other algorithms.**

**Clustering coefficient:** This metric allows to verify whether the recommendations are making the network more cohesive by closing more triangles. The clustering coefficient of node  $v_i$  is defined as:

$$c_{v_i} = \frac{2}{\text{deg}^{\text{tot}}(v_i) (\text{deg}^{\text{tot}}(v_i) - 1) - 2 \text{deg}^{\text{rec}}(v_i)} T(v_i) \quad (7)$$

where  $T(v_i)$  is the number of directed triangles through node  $v_i$ ,  $\text{deg}^{\text{tot}}(v_i)$  is the sum of in-degree and out-degree of  $v_i$ , and  $\text{deg}^{\text{rec}}(v_i)$  is the reciprocal degree of  $v_i$ . The global clustering coefficient of the network is then obtained by taking the mean across all nodes:  $c = 1/n \sum_{i=1}^n c_{v_i}$ .

**Gini coefficient of the in-degree distribution:** Popularity bias is a well-known issue reinforced by certain recommendation algorithms [1]. The Gini coefficient [19] allows us to demonstrate whether this bias is exacerbated by the algorithms regardless of the initial conditions of the network structure, or whether certain types of networks are exempt from this bias. The Gini coefficient of the in-degree distribution  $\pi^{\text{in}}$ , sorted in ascending order, is defined as follows:

$$\text{Gini}(\pi^{\text{in}}) = \frac{\sum_{i=1}^n (2i - n - 1) \pi_i^{\text{in}}}{n \sum_{i=1}^n \pi_i^{\text{in}}} \quad (8)$$

The higher the Gini coefficient, the more skewed or unequal the in-degree distribution across all nodes.

**Visibility of the minority group:** First, we measure the importance of nodes by computing their PageRank [31]. Then, out of the top-10% highest-scored nodes, we measure the fraction of nodes that belong to the minority group and refer to this fraction as the visibility of the minority group  $\hat{f}_m$ . We use the relative visibility  $\hat{f}_m^* = \hat{f}_m - f_m$  to verify how far the visibility of the minority is from statistical parity [13] before the recommendations. Finally, we measure the change in visibility by computing  $\hat{f}_m$  after and before the recommendations to verify whether the minority group is gaining or losing visibility:

$$\delta \hat{f}_m = \hat{f}_m(\text{after}) - \hat{f}_m(\text{before}) \quad (9)$$

**In-group links:** We also look at the fraction of links within groups to see what type of edges are being recommended more often by the algorithms. The in-group link ratio for group  $a$  is defined as:

$$I_a = \frac{e_{aa}}{e_{aa} + e_{ab}} \quad (10)$$

where  $a, b \in \{m, M\}$  and  $a \neq b$ .

WebSci '22, June 26–29, 2022, Barcelona, Spain

Ferrara et al.

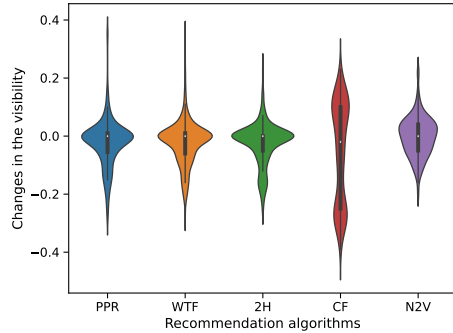


**Figure 4: Changes in the visibility of minorities for different recommendation algorithms.** After 30 recommendations for each node (in networks with different values of homophily and fixed minority size  $f_m = 0.3$ ), we see that all algorithms may increase (positive change), decrease (negative change) or keep constant (zero change) the visibility of the minority group. In particular, PPR, WTF and 2H mostly keep the visibility of minorities unchanged. However, their tails are asymmetric and denser in the negative direction, in correspondence with a decrease in visibility. CF maintains the initial visibility of minorities in a few cases, and otherwise it may drastically change the visibility in both directions. N2V generates less extreme changes in both directions.

#### 4 RESULTS

Here we address our three research questions and present the results obtained after applying the recommendation algorithms iteratively to the simulated directed networks described in Sections 3.2 and 3.3, respectively. First, we show the consequences of these recommendations on the structure of the network and on the visibility of the minority group (RQ1). Second, we explain the changes in structure and visibility as a function of homophily (RQ2). Third, we further investigate the role of the size of the minority group and in-group links in the effects of the recommendations (RQ3).

##### 4.1 RQ1: How do recommendation algorithms affect the structure of the network and the visibility of minorities?

**Changes in network structure:** To address this question, we first assess the changes in network structure in terms of global clustering coefficient and Gini coefficient of the in-degree distribution. The idea is to verify whether the algorithms (while connecting people together) make the network more cohesive and whether popularity bias increases at the same rate for all algorithms. Figure 3 shows the results for both metrics (top/bottom) on different types of networks (columns) across multiple rounds of recommendations (x-axis). Note that the x-axis reflects the iteration or step of recommendation, e.g., at step=20, each algorithm has independently recommended 20

connections to each node in the network. First, we see that overall, the evolution of these metrics is consistent across types of networks (columns) and recommendation algorithms (colors). Second, all recommendation algorithms increase the clustering coefficient of the network which means that the networks are becoming more cohesive as more triangles are getting closed. However, the rate at which this clustering increases, differs across algorithms, especially for N2V which, surprisingly, is the slowest. Third, we corroborate that PPR, WTF, 2H and CF reinforce the popularity bias issue since the Gini increases over time. This means that these algorithms make popular people (in terms of high in-degree) more popular. The exception is N2V, which after several recommendations makes the in-degree distribution less skewed (i.e., the recommendations are more diverse). One possible explanation is that similarity in the embedding space is only partially sensible to popularity bias.

**Changes in the visibility:** Now, we explore to what extent each recommendation algorithm changes the visibility of the minority group after several recommendations. We show the results in Figure 4. Each violin refers to one algorithm and the distribution of the violin represents the variation across a multiplicity of networks with different initial homophily values, fixed number of nodes and minority size (see Section 3.3 for details). PPR, WTF and 2H show similar patterns: they have median close to zero but denser tails in the negative direction. This indicates that these algorithms mostly keep the visibility of the minority unchanged, but, in certain cases, they decrease this visibility. CF shows the opposite behavior. First, it keeps the visibility unchanged for a few cases, but most of the time it drastically changes this visibility in either direction. Among all, N2V reveals more symmetric and smaller effects. Summarizing, Figure 4 suggests that four out of five algorithms are more prone to keep the visibility of the minority unchanged. Nevertheless, in certain regimes (explored next in RQ2) this visibility can be increased or reduced depending on the levels of homophily.

##### 4.2 RQ2: To what extent is the change in visibility due to homophily?

To understand how the initial levels of homophily in the network affect the recommendations, we compare the visibility of the minority before and after the recommendations for each algorithm, see Figure 5. We control for the number of nodes and the fraction of minorities by keeping them fixed, and vary homophily values (see Section 3.3 for more details). As defined in Section 3.4, visibility measures the fraction of nodes that belong to a particular group and make it to the top-10% of the rank. This rank reflects the importance of nodes in the network and it is assessed through their PageRank [31].

**Visibility before the recommendations:** Figure 5(a) shows the relative visibility of the minority before the recommendations. White regions (neutral visibility) represent statistical parity [13], in which the fraction of the minority in the top-10% is equal to the fraction of minority populating the whole network. Orange regions (positive visibility) represent higher amount of minority nodes at the top of the rank compared to the statistical parity condition. Blue regions (negative visibility), instead, represent under-representation of minorities in top ranks. We see that the minority is over-represented mostly when the majority is heterophilic

## 5.2 Link Recommendations: Their Impact on Network Structure and Minorities

Link recommendations: Their impact on network structure and minorities

WebSci '22, June 26–29, 2022, Barcelona, Spain

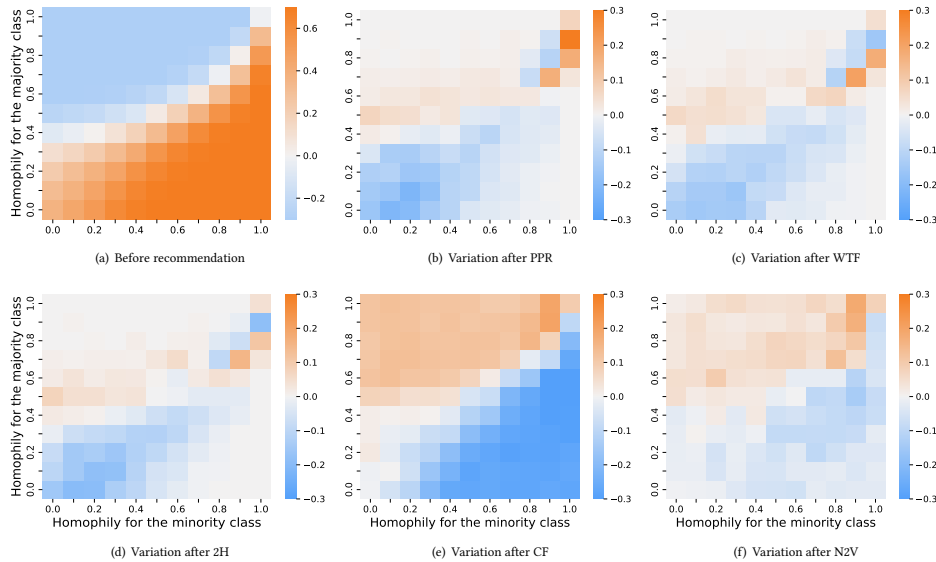


**Figure 5: Visibility of the minority group as a function of homophily.** Heatmaps show the visibility of the minority group before and after the recommendations for different algorithms and different combinations of homophily within the majority (y-axis) and the minority (x-axis) groups. The visibility of the minority group is measured by the fraction of minorities in the top-10% of nodes ranked by their PageRank. In (a), colors show the relative visibility of the minority group w.r.t., the fraction of minorities in the network  $f_m = 0.3$  before the recommendations. Positive visibility means that the minority is over-represented (orange), and negative visibility means that the minority is under-represented or the majority is over-represented (blue). Zero visibility refers to those cases where the top rank does not include any node from the minority group. In (b-f), colors represent the variation in the visibility due to different recommendation algorithms. For PPR, WTF and 2H one can see that the minority loses more visibility than the majority (especially in the heterophilic regime), while CF and N2V show more symmetric effects on the visibility of the minority and majority. Notice that the homophily values shown in the x- and y-axis of all plots represent the initial levels of homophily in the network before the recommendations.

$h_{MM} < 0.5$  or when the minorities are more homophilic than the majorities  $h_{mm} > h_{MM}$ .

**Changes in the visibility after the recommendations:** Figures 5(b) to 5(f) show the change in visibility after 30 recommendations per node. A positive change (orange) indicates that the visibility of the minority increased after the recommendations (relative to the initial visibility they had before the recommendations). Actual values in each cell denote the magnitude of this change. Conversely, a negative change (blue) indicates that the majority increased its visibility at the cost of reducing the visibility of the minority. No changes (white) indicate that the visibility did not vary across time. At first glance, we see that the visibility gets affected differently depending on the algorithm and the initial values of homophily. We further notice that there are slightly more blue than orange

regions in almost all plots (i.e., the majority increases its visibility more often than the minority across all regimes).

Among all the algorithms CF produces the strongest changes, while N2V is the most balanced. PPR, WTF and 2H, on the other hand, show a similar behavior. They penalize minorities especially in the heterophilic regimes for both classes, i.e.,  $h_{**} < 0.5$ , bottom-left corners of Figures 5(b) to 5(d).

Furthermore, when only one group is homophilic, PPR, WTF and 2H do not change the initial over-representation of the homophilic group, see top-left and bottom-right corners in Figures 5(b) to 5(d).

## 5.2 Link Recommendations: Their Impact on Network Structure and Minorities

WebSci '22, June 26–29, 2022, Barcelona, Spain

Ferrara et al.

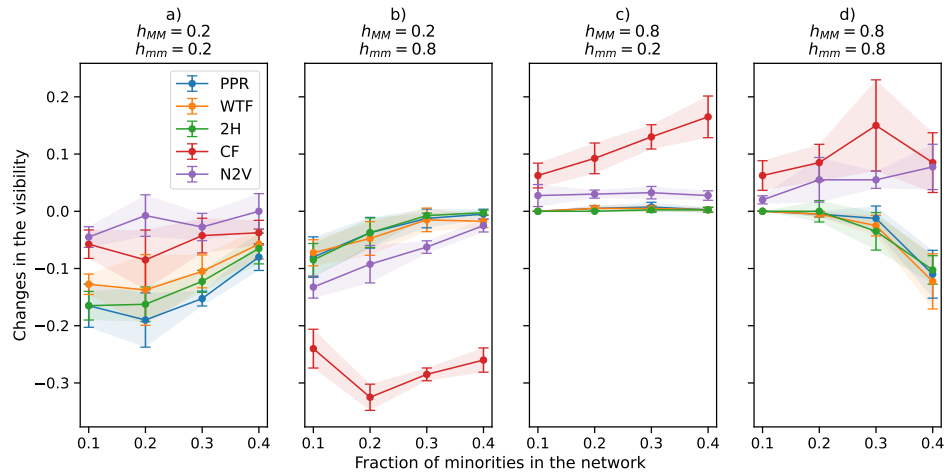


Figure 6: Changes in the visibility of minorities as a function of the minority size. The y-axis shows the change in visibility for the minority group after the recommendations. A positive (negative) change indicates that minorities appeared more (less) often in the top-10% compared to their initial representation before the recommendations. If this change is around zero, the visibility of minorities remained constant or invariant. The x-axis shows the size of the minority group as a fraction of all nodes in the network. In general, we see that larger minorities get penalized less than smaller ones when the majority is heterophilic (a,b). When the majority is homophilic, however, the changes in visibility not only depend on the fraction of the minority but also on its homophily level. For instance, when the minority is heterophilic (c), its visibility remains mostly constant for all algorithms except CF, and when the minority is homophilic (d), its visibility drops for larger-size minorities, unless N2V and CF are used.

### 4.3 RQ3: Is the change in visibility inversely proportional to the size of the minority or proportional to the in-group links within the minority?

**Size of the minority:** To answer RQ1 and RQ2, we kept the size of the minority fixed ( $f_m = 0.3$ ) to study the effects of homophily on the visibility of minorities after the recommendations. However, it is unclear whether the changes in visibility are inversely proportional to the size of the minority (e.g., larger changes for smaller minorities), or whether these are steady-state changes that appear regardless of the size of the minority. In Figure 6, we show how the change in visibility (y-axis) is affected by multiple factors including the size of the minority. First, we see a concordance among algorithms when the majority is heterophilic, Figures 6(a) and 6(b). In these cases, the larger the minority, the smaller the change in the visibility of the minority, except for CF which drastically reduces this visibility when the minority is more homophilic than the majority, Figure 6(b). When only the majority is homophilic, Figure 6(c), i.e., most out-links point to nodes in the majority group, the size of minorities has almost no effect on their final visibility

in algorithmic rankings unless CF is used as recommendation algorithm. When both groups are homophilic, Figure 6(d), however, only CF and N2V increase the visibility of larger minorities more than the visibility of smaller minorities.

**In-group links:** As we have seen previously, the visibility of the minority can be affected by different factors, including the initial homophily of the network. Since homophily depends on the mixing of types of edges (see [14] for a detailed derivation of homophily in DPAH networks), we further investigate the evolution of in-group links over time, see Figure 7. Here, we found two main patterns. First, results from PPR, WTF and 2H are consistent in each type of network (columns). These algorithms mostly increase the number of in-group minority links, see Figures 7(a), 7(b) and 7(e). Surprisingly, this advantage does not guarantee an increase in visibility for the minority group. On the contrary, they lose visibility, see Figures 6(a) and 6(b) for  $f_m = 0.3$ . Second, results from CF and N2V are also consistent in each type of network. We see in Figures 7(a) and 7(b) that these two algorithms increase the in-group majority links when the majority is initially heterophilic, and reduce them when the majority is initially homophilic, see Figures 7(c), 7(d) and 7(e).

Now, we analyze in details different possible homophily configurations.

## 5.2 Link Recommendations: Their Impact on Network Structure and Minorities

Link recommendations: Their impact on network structure and minorities

WebSci '22, June 26–29, 2022, Barcelona, Spain

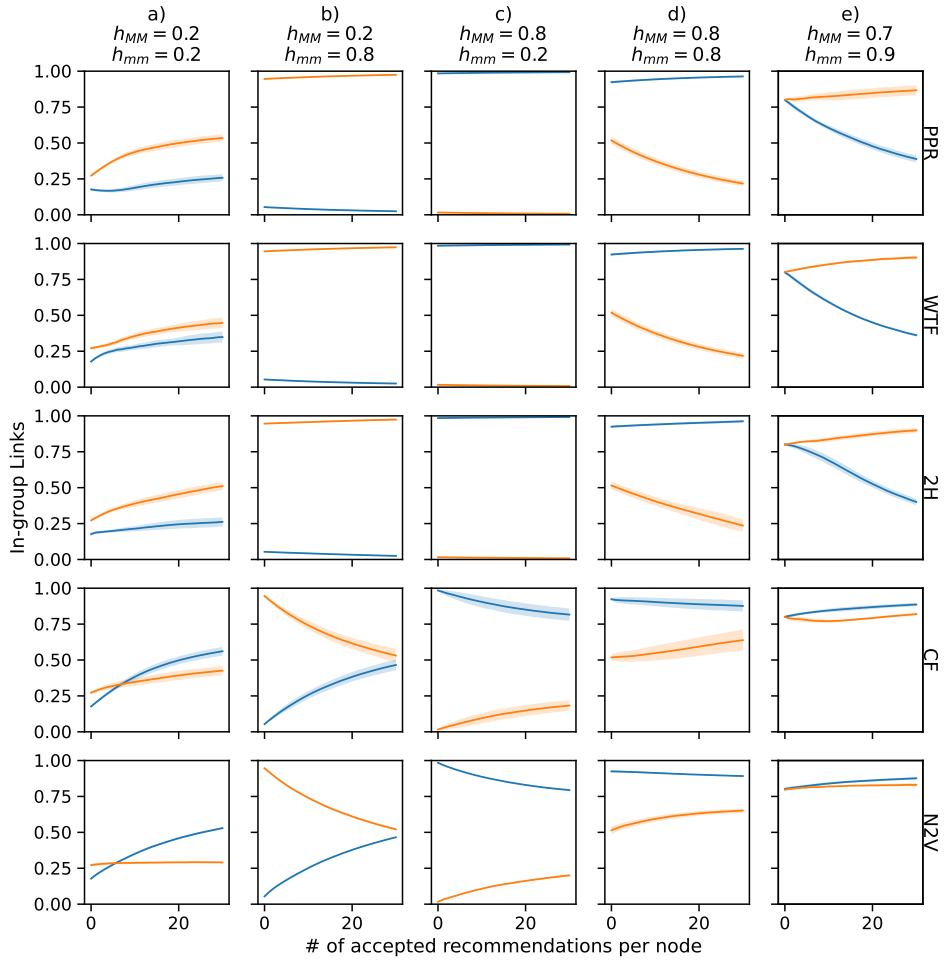


**Figure 7: The evolution of the in-group links within majority nodes (blue) and within minority nodes (orange) for different recommendation algorithms (rows) and different values of homophily (columns) in the initial network. These networks possess a fixed number of nodes and fraction of minorities  $f_m = 0.3$ .**

When one class is homophilic and the other class is heterophilic, the links coming from both classes are mostly directed to nodes in the homophilic class. Let us consider PPR, WTF and 2H where the values of homophily are  $h_{MM} = 0.2$  for the majority and  $h_{mm} = 0.8$

for the minority and vice-versa, see Figures 7(b) and 7(c), respectively. In these situations, these recommendation algorithms will keep increasing the in-group proportions of the homophilic group since the recommended links mostly point to nodes in this group.

These correspond to situations in the white regions at the top-left and bottom-right of Figures 5(b) to 5(d). Hence, this shows that the absence of variation in the fraction of minority is due to the fact that PPR, WTF and 2H do not modify connections between classes in these cases. This does not hold for CF and N2V. In fact, under the same homophily conditions, these methods make the in-group links for both classes more similar, decreasing structural differences between classes, see Figures 7(b) and 7(c).

Now, we will consider regimes where both classes are heterophilic,  $h_{mm} = h_{MM} = 0.2$ , see Figure 7(a). Here, CF and N2V are the only algorithms in which the initial conditions of in-group links are flipped. Note that the proportion of links within the majority group gets larger than the proportion of links within the minority after multiple rounds of recommendations. Consequently, the majority increases its visibility even further by pushing minorities to lower ranks, see Figures 5(e) and 5(f). Interestingly, the visibility of minorities decreases even if the flip does not occur in these heterophilic settings for PPR, WTF and 2H, see bottom-left of Figures 5(b) to 5(d).

On the other extreme of homophily, when both groups are homophilic,  $h_{mm} = h_{MM} = 0.8$ , we found two main patterns, see Figure 7(d). First, PPR, WTF and 2H tend to strengthen the connections towards the majority group by either recommending majority-to-majority or minority-to-majority links. This in turn penalizes the minorities at the top of the rank, see  $h_{mm} = h_{MM} = 0.8$  in Figures 5(b) to 5(d). In contrast, CF and N2V slowly increase the number of connections within the minority group. For N2V, one possible explanation is that the homophily levels are high enough so that the two classes (especially the minority class), are represented in the embeddings as, at least partially, separated clusters.

Lastly, the possibility to systematically vary the initial levels of homophily for both classes allows us to identify tipping points. For instance, in a homophilic regime, where both groups have the same level of initial homophily,  $h_{MM} = h_{mm} = 0.8$ , we found that PPR, WTF and 2H increase the number of links within the majority group after multiple recommendations, see Figure 7(d). However, the same algorithms may also increase the number of links within the minorities, and thus their visibility, if the minority group is initially more homophilic than the majority,  $h_{MM} = 0.7$  and  $h_{mm} = 0.9$ , see Figure 7(e). CF and N2V, on the other hand, do not show this tipping effect when both groups of nodes are initially homophilic. In either case, these two algorithms keep increasing the proportion of in-group links which induces segregation.

## 5 LIMITATIONS AND FUTURE WORK

We have limited our study to five recommendation algorithms, and in future work we aim to include more algorithms into this investigation, especially recent versions of popular algorithms that have been developed with the goal to increase fairness.

Furthermore, we focused on scale-free directed networks with homophily which represent a plausible configuration of online social networks. As next steps, we would like to include in our analysis different network simulation models that include other factors in the network generation process, such as multiple node-attributes, heterogeneous group mixing, the presence of communities, and triadic closure. We also acknowledge the fact that our analysis is

theoretical and has not been validated with real data. We plan to extend our study by considering empirical networks.

Importantly, link recommendation algorithms and datasets are generally proprietary. This is why simulation-based approaches are often necessary for this kind of investigations. In addition, the simulation approach enables us to examine different scenarios which might not occur in one instance of the data [32].

## 6 CONCLUSIONS

In this work, we systematically studied five link recommendation algorithms and quantified their feedback loop effects on bi-populated scale-free directed networks with homophily. In particular, we assessed two types of changes in these networks due to multiple link recommendations. First, we measured the changes in network structure in terms of clustering and in-degree distribution. Second, we measured the changes in the visibility of minorities at the top-10% of the rank with respect to their PageRank (importance) scores, highlighting the effects of homophily, minority size, and in-group links.

Our results show that four out of the five algorithms reduced on average the visibility of minorities more often than to the majority counterpart. In particular, PPR, WTF and 2H when both groups are initially heterophilic, and CF when the minority is initially more homophilic than the majority.

We also found that while all algorithms tend to close triangles and increase the clustering coefficient, all algorithms except N2V are prone to favor and suggest nodes with high in-degree. This is known as popularity bias, rich-get-richer effect or cumulative advantage, a well-known mechanism that contributes to inequality.

Link recommendations based on N2V rely on the proximity of nodes in the embedding space, which does not necessarily imply closeness to nodes with high in-degree. Consequently, N2V is a promising alternative to other link recommendation algorithms since it mitigates cumulative advantage.

## ACKNOWLEDGMENTS

This work has received funding by the European Union's Horizon 2020 research and innovation programme under the Marie Skłodowska-Curie Actions (grant agreement number 860630) for the project : "NoBIAS - Artificial Intelligence without Bias". Furthermore, this work reflects only the authors' view and the European Research Executive Agency (REA) is not responsible for any use that may be made of the information it contains. Moreover, Fariba Karimi was supported by the Austrian research agency (FFG) (project number 873927).

## REFERENCES

- [1] Himan Abdollahpour. 2019. Popularity bias in ranking and recommendation. In *Proceedings of the 2019 AAAI/ACM Conference on AI, Ethics, and Society*. 529–530.
- [2] Luca Maria Aiello and Nicola Barbieri. 2017. Evolution of ego-networks in social media with link recommendations. In *Proceedings of the Tenth ACM International Conference on Web Search and Data Mining*. 111–120.
- [3] Chen Avin, Barbara Keller, Zvi Lotker, Claire Mathieu, David Peleg, and Yvonne-Anne Pignolet. 2015. Homophily and the glass ceiling effect in social networks. In *Proceedings of the 2015 conference on innovations in theoretical computer science*. 41–50.
- [4] Albert-László Barabási and Réka Albert. 1999. Emergence of scaling in random networks. *science* 286, 5439 (1999), 509–512.

## 5.2 Link Recommendations: Their Impact on Network Structure and Minorities

- [5] Fabian Baumann, Philipp Lorenz-Spreen, Igor M Sokolov, and Michele Starnini. 2020. Modeling echo chambers and polarization dynamics in social networks. *Physical Review Letters* 124, 4 (2020), 048301.
- [6] Sergey Brin and Lawrence Page. 1998. The anatomy of a large-scale hypertextual web search engine. *Computer networks and ISDN systems* 30, 1-7 (1998), 107–117.
- [7] Uthav Chitra and Christopher Musco. 2020. Analyzing the impact of filter bubbles on social network polarization. In *Proceedings of the 13th International Conference on Web Search and Data Mining*, 115–123.
- [8] Nicholas A. Christakis and James H. Fowler. 2013. Social contagion theory: examining dynamic social networks and human behavior. *Statistics in Medicine* 32, 4 (2013), 556–577. <https://doi.org/10.1002/sim.5408> arXiv:<https://onlinelibrary.wiley.com/doi/pdf/10.1002/sim.5408>
- [9] Federico Cimis, Marco Minici, Corrado Monti, and Francesco Bonchi. 2021. The Effect of People Recommenders on Echo Chambers and Polarization. *arXiv preprint arXiv:2112.00626* (2021).
- [10] Elizabeth M Daly, Werner Geyer, and David R Millen. 2010. The network effects of recommending social connections. In *Proceedings of the fourth ACM conference on Recommender systems*, 301–304.
- [11] Pranav Dandekar, Ashish Goel, and David T Lee. 2013. Biased assimilation, homophily, and the dynamics of polarization. *Proceedings of the National Academy of Sciences* 110, 15 (2013), 5791–5796.
- [12] Robin IM Dunbar. 1992. Neocortex size as a constraint on group size in primates. *Journal of human evolution* 22, 6 (1992), 469–493.
- [13] Cynthia Dwork, Moritz Hardt, Toniann Pitassi, Omer Reingold, and Richard Zemel. 2012. Fairness through awareness. In *Proceedings of the 3rd innovations in theoretical computer science conference*, 214–226.
- [14] Lisette Espin-Noboa, Claudia Wagner, Markus Strohmaier, and Fariba Karimi. 2022. Inequality and inequity in network-based ranking and recommendation algorithms. *Scientific Reports* 12, 1 (2022).
- [15] Francesco Fabbri, Francesco Bonchi, Ludovico Boratto, and Carlos Castillo. 2020. The effect of homophily on disparate visibility of minorities in people recommender systems. In *Proceedings of the International AAAI Conference on Web and Social Media*, Vol. 14, 165–175.
- [16] Francesco Fabbri, Maria Luisa Croci, Francesco Bonchi, and Carlos Castillo. 2021. Exposure Inequality in People Recommender Systems: The Long-Term Effects. *arXiv preprint arXiv:2112.08257* (2021).
- [17] Giorgio Fagiolo. 2007. Clustering in complex directed networks. *Physical Review E* 76, 2 (2007), 026107.
- [18] James H. Fowler and Nicholas A. Christakis. 2010. Cooperative behavior cascades in human social networks. *Proceedings of the National Academy of Sciences* 107, 12 (2010), 5334–5338. <https://doi.org/10.1073/pnas.0913149107> arXiv:<https://www.pnas.org/content/107/12/5334.full.pdf>
- [19] Corrado Gini. 1912. Variabilità e mutabilità. *Reprinted in Memorie di metodologica statistica (Ed. Pizetti E (1912))*.
- [20] Aditya Grover and Jure Leskovec. 2016. node2vec: Scalable Feature Learning for Networks. *CoRR* abs/1607.00653 (2016). arXiv:1607.00653 <http://arxiv.org/abs/1607.00653>
- [21] Pankaj Gupta, Ashish Goel, Jimmy Lin, Aneesh Sharma, Dong Wang, and Reza Zadeh. 2013. Wf: The who to follow service at twitter. In *Proceedings of the 22nd international conference on World Wide Web*, 505–514.
- [22] Glen Jeh and Jennifer Widom. 2003. Scaling personalized web search. In *Proceedings of the 12th international conference on World Wide Web*, 271–279.
- [23] Fariba Karimi, Mathieu Génio, Claudia Wagner, Philipp Singer, and Markus Strohmaier. 2018. Homophily influences ranking of minorities in social networks. *Scientific reports* 8, 1 (2018), 1–12.
- [24] Eun Lee, Fariba Karimi, Claudia Wagner, Hang-Hyun Jo, Markus Strohmaier, and Mirta Galesic. 2019. Homophily and minority-group size explain perception biases in social networks. *Nature human behaviour* 3, 10 (2019), 1078–1087.
- [25] Ronny Lempel and Shlomo Moran. 2001. SALSA: the stochastic approach for link-structure analysis. *ACM Transactions on Information Systems (TOIS)* 19, 2 (2001), 131–160.
- [26] David Liben-Nowell and Jon Kleinberg. 2007. The link-prediction problem for social networks. *Journal of the American society for information science and technology* 58, 7 (2007), 1019–1031.
- [27] Miller McPherson, Lynn Smith-Lovin, and James M Cook. 2001. Birds of a feather: Homophily in social networks. *Annual review of sociology* 27, 1 (2001), 415–444.
- [28] Robert K Merton. 1988. The Matthew effect in science. II: Cumulative advantage and the symbolism of intellectual property. *isis* 79, 4 (1988), 606–623.
- [29] Giovanna Miritello, Rubén Lara, Manuel Cebrian, and Esteban Moro. 2013. Limited communication capacity unveils strategies for human interaction. *Scientific reports* 3, 1 (2013), 1–7.
- [30] Shirin Nilizadeh, Anne Groggel, Peter Lista, Srijita Das, Yong-Yeol Ahn, Apu Kapadia, and Fabio Rojas. 2016. Twitter’s glass ceiling: The effect of perceived gender on online visibility. In *Proceedings of the International AAAI Conference on Web and Social Media*, Vol. 10.
- [31] Lawrence Page, Sergey Brin, Rajeev Motwani, and Terry Winograd. 1999. *The PageRank citation ranking: Bringing order to the web*. Technical Report. Stanford InfoLab.
- [32] Mitja Steinbacher, Matthias Raddant, Fariba Karimi, Eva Camacho Cuenca, Simone Alfarano, Giulia Iori, and Thomas Lux. 2021. Advances in the agent-based modeling of economic and social behavior. *SN Business & Economics* 1, 7 (2021), 1–24.
- [33] Ana-Andreea Stoica, Christopher Riederer, and Augustin Chaintreau. 2018. Algorithmic Glass Ceiling in Social Networks: The effects of social recommendations on network diversity. In *Proceedings of the 2018 World Wide Web Conference*, 923–932.
- [34] Jessica Su, Aneesh Sharma, and Sharad Goel. 2016. The effect of recommendations on network structure. In *Proceedings of the 25th international conference on World Wide Web*, 1157–1167.
- [35] Sotiris Tsioutsoulis, Evaggelia Pitoura, Panayiotis Tsaparas, Ilias Klefakakis, and Nikos Mamoulis. 2021. Fairness-Aware PageRank. In *Proceedings of the Web Conference 2021*, 3815–3826.

## 5.3 Super-Resolution of Urban Socioeconomic Indicators via Graph-Based Recommender Systems

Graph-based machine learning methods are increasingly used to analyze complex relational datasets, including those describing urban environments. In cities, many socioeconomic phenomena, such as income distribution, access to services, or mobility patterns, are shaped by spatial and relational dependencies between geographic areas.

However, socioeconomic data are often available only at coarse spatial resolutions, limiting the ability of policymakers and researchers to analyze inequalities at finer geographic scales. Graph-based models provide an opportunity to address this limitation by exploiting structural relationships between locations to infer missing or higher-resolution information.

The work presented in this section contributes to RQ2 by exploring how graph-based recommender systems can be used to infer fine-grained socioeconomic indicators for urban areas. By modeling geographic regions as nodes in a graph and leveraging similarities between them, the proposed approach performs super-resolution of socioeconomic indicators, enabling the estimation of more detailed spatial distributions from limited data. Beyond its methodological contribution, this work illustrates how graph learning techniques can help uncover structural patterns of inequality in urban systems, providing tools for more informed analysis of socioeconomic disparities.

### Authors' Contributions

---

Contribution	Authors
<b>Conceptualization:</b>	F.P. Nerini, A. Ferrara, and all authors
<b>Writing:</b>	F.P. Nerini, A. Ferrara, and all authors
<b>Methodology:</b>	F.P. Nerini, A. Ferrara, and all authors
<b>Code:</b>	F.P. Nerini
<b>Experiments:</b>	F.P. Nerini

---

## Super-Resolution of Urban Socioeconomic Indicators via Graph-Based Recommender Systems

Francesco Paolo Nerini  
Sapienza University of Rome  
Rome, Italy  
nerini@diag.uniroma1.it

Antonio Ferrara  
Intesa Sanpaolo AI Research, Turin, Italy  
TU Graz, Austria  
antonio.ferrara@intesasanpaolo.com

Claudio Borile  
Independent  
Turin, Italy  
borileclaudio@gmail.com

André Panisson  
Intesa Sanpaolo AI Research  
Turin, Italy  
andre.panisson@intesasanpaolo.com

### Abstract

Detailed socioeconomic insights are essential for effective urban policy, yet traditional census data remains static, costly, and restricted to coarse spatial resolutions due to privacy constraints. To bridge this "granularity gap", we introduce a Socioeconomic Super-Resolution framework that infers fine-grained indicators from user-generated digital traces. We propose a Spatial-GNN framework that learns business representations from user-business interaction graphs, explicitly enriching them with semantic categories and coarse geographical context. We show that these embeddings, trained solely on coarse aggregate labels (Postal Codes), capture sufficient latent signal to recover fine-grained attributes at the Census Block Group level. Experiments on the Yelp dataset confirm that our approach effectively disaggregates urban data, with the learned embeddings naturally capturing spatial and socioeconomic homophily. This work bridges Recommender Systems and Urban Computing, offering a scalable methodology for high-resolution demographic inference.

### CCS Concepts

• **Information systems** → *Geographic information systems*; • **Computing methodologies** → **Supervised learning**; *Learning latent representations*.

### Keywords

Graph Learning, Socioeconomics, Recommender Systems

### ACM Reference Format:

Francesco Paolo Nerini, Claudio Borile, Antonio Ferrara, and André Panisson. 2026. Super-Resolution of Urban Socioeconomic Indicators via Graph-Based Recommender Systems. In *Companion Proceedings of the ACM Web Conference 2026 (WWW Companion '26)*, April 13–17, 2026, Dubai, United Arab Emirates. ACM, New York, NY, USA, 11 pages. <https://doi.org/10.1145/3774905.3795856>



This work is licensed under a Creative Commons Attribution 4.0 International License. [WWW Companion '26, Dubai, United Arab Emirates](https://creativecommons.org/licenses/by/4.0/)  
© 2026 Copyright held by the owner/author(s).  
ACM ISBN 979-8-4007-2308-7/2026/04  
<https://doi.org/10.1145/3774905.3795856>

### 1 Introduction

Detailed socioeconomic data is the cornerstone of modern urban planning. As cities grow in complexity, policymakers and businesses require fine-grained insights, such as neighborhood income levels or housing values, to target public health interventions, allocate resources, and address urban inequality [2, 5]. However, the "gold standard" for this information remains traditional census data, which suffers from critical issues: it is *infrequently updated* (often decennially), *resource-intensive* to collect, and, crucially, often released at a *coarse spatial resolution* (e.g., Postal Codes) to protect privacy [30]. This creates a "granularity gap": while decision-making happens at the street or block level, data is often only available at a much coarser granularity level.

Digital traces generated by users on online platforms offer a promising alternative to bridging this gap. Platforms like Yelp and Google Places generate millions of user-business interactions that implicitly encode the socioeconomic fabric of a city [15]. Sociological theories of *homophily* and *distinction* suggest that these interactions are not random; users tend to frequent businesses that align with their socioeconomic status, creating mobility corridors that connect geographically distant but socioeconomically similar neighborhoods [4]. However, leveraging these unstructured, noisy digital traces to infer rigorous socioeconomic indicators remains an open challenge. Existing approaches often rely on static data (e.g., satellite imagery [14]) or simple aggregations, failing to capture the dynamic, relational nature of urban life.

In parallel, recent advancements in Graph Neural Networks (GNNs) have shown exceptional promise in modelling complex, relational datasets across a variety of tasks, including recommendation systems, node classification, and spatial inference problems [6, 13, 31]. Particularly relevant to our context, GNNs have demonstrated an ability to effectively integrate spatial information into their learned representations, making them suitable tools for extracting insights from spatially-informed data [36]. However, their application to inferring fine-grained socioeconomic indicators from online review data remains largely unexplored, representing a novel intersection between recommender systems, spatial analytics, and urban socioeconomics.

In this paper, we propose a novel framework that leverages Graph Neural Networks (GNNs) to perform **Socioeconomic Super-Resolution**. We hypothesize that the user-business interaction

## 5.3 Super-Resolution of Urban Socioeconomic Indicators via Graph-Based Recommender Systems

WWW Companion '26, April 13–17, 2026, Dubai, United Arab Emirates

Francesco Paolo Nerini, Claudio Borile, Antonio Ferrara, & André Panisson

graph contains sufficient latent signal to "downscale" coarse aggregate statistics into fine-grained local estimates. By treating the city as a bipartite graph of users and businesses, we employ GNNs to learn business representations that capture not just geographic proximity, but *user homophily*. Unlike traditional spatial interpolation methods that smooth data over space, our graph-based approach allows information to "tunnel" through the network, enabling a business in a low-income ZIP code to be correctly identified as a high-end establishment if it shares clientele with high-income regions.

Our research is guided by three key questions:

- **RQ1 (Signal):** Do digital traces of user mobility contain quantifiable signals of socioeconomic homophily sufficient for predictive modeling?
- **RQ2 (Super-Resolution):** Can GNN-based business representations, trained solely on coarse regional labels, effectively recover fine-grained (Block Group level) socioeconomic variations?
- **RQ3 (Spatial Integration):** To what extent does the explicit injection of coarse geographical context and semantic features enhance the quality of the learned representations compared to pure interaction-based baselines?

Our specific contributions are as follows:

- **A Spatial-GNN Framework for Urban Inference:** We introduce a novel adaptation of graph-based recommender systems (specifically LightGCN and R-GCN) for the domain of urban analytics. We propose a composite embedding strategy that explicitly enriches business representations with semantic categories and coarse geographical context (postal codes), significantly improving representation quality over standard interaction-based baselines.
- **Socioeconomic Super-Resolution via Weak Supervision:** We demonstrate a method to bridge the "granularity gap" in urban data. By training our model solely on coarse-grained regional statistics (Postal Code averages), we successfully recover fine-grained socioeconomic indicators at the Census Block Group level. This confirms that the learned graph embeddings capture sufficient local variance to disaggregate coarse public data.

Through extensive evaluation, we validate the proposed methodology on the Yelp dataset, providing reproducible experimental results. Our study underscores the potential of combining graph-based recommendation models with spatial data as a powerful paradigm for socioeconomic analysis in urban environments.

Furthermore, in appendix A, we provide an analysis of the learned embedding space, showing that the model inherently captures meaningful spatial and semantic correlations. Even without explicit supervision, the business representations naturally cluster according to geographic neighborhoods and socioeconomic functions, validating the presence of strong homophily signals in user mobility traces.

The remainder of the paper is structured as follows. Section 2 reviews related literature. Section 3 details the Spatial-GNN framework and the super-resolution formulation. Section 4 discusses the experimental setup, presents the dataset, and performs a preliminary homophily analysis. Section 5 presents the experimental

results, and Section 6 concludes with implications for urban computing. We also release the code for reproducibility<sup>1</sup>.

## 2 Related Work

Our research sits at the intersection of urban computing, computational social science, and graph representation learning. In this Section, we review the relevant literature on inferring socioeconomic indicators and learning representations of urban environments.

### 2.1 Socioeconomic Inference and Disaggregation

The study of urban environments requires dealing with intricate interactions between various spatial, social, and functional elements [22]. With the increase in the availability of digital sources such as mobility networks, satellite images, points of interest (POIs), and social network data, a vast literature has emerged studying complex urban dynamics [1, 3, 9, 11, 32, 39].

Obtaining fine-grained socioeconomic data is a foundational challenge in urban analytics. Traditional methods rely on *dasymeric mapping*, which redistributes coarse census counts into finer spatial units using ancillary data like land cover or building footprints [21, 30]. While effective for population density, these heuristic methods often struggle to capture complex latent variables like income or social class.

**Remote Sensing Approaches.** With the advent of deep learning, significant attention has shifted to inferring socioeconomic indicators from high-resolution satellite imagery [10, 24, 26]. Recent foundation models like SatClip [14] and CSP [18] learn global location embeddings from visual data, serving as powerful proxies for static urban attributes. However, visual approaches face limitations in temporal resolution and fail to capture the *dynamic* social functions of a neighborhood (e.g., the difference between a high-end restaurant and a discount store in similar buildings).

**Digital Traces and LBSN.** To capture these social dynamics, researchers have turned to Location-Based Social Networks (LBSN). Mobility data has been successfully used to quantify urban segregation [4, 37], predict gentrification, and map local cultural fingerprints [25, 29]. Most relevant to our work, recent studies have employed knowledge graphs constructed from LBSN data to predict socioeconomic indicators [12, 38]. However, these works typically operate at a fixed spatial scale (predicting region-level attributes from region-level features). In contrast, our work tackles the harder *super-resolution* problem: training on coarse aggregates to predict fine-grained local variations.

### 2.2 Urban Region Representation Learning

Parallel to socioeconomic inference, there is a growing body of work on learning vector representations for urban regions. Early methods like *Region2Vec* and *Place2Vec* adapted Word2Vec to learn embeddings from spatial adjacency or mobility flow sequences.

**Multi-View and Contrastive Learning.** State-of-the-art approaches now utilize Multi-View representation learning. For instance, ReCP [17] leverages contrastive learning to align mobility flows with Point-of-Interest (POI) data, while other works integrate

<sup>1</sup>[https://github.com/Frappan/super\\_resolution\\_gnn](https://github.com/Frappan/super_resolution_gnn)

### 5.3 Super-Resolution of Urban Socioeconomic Indicators via Graph-Based Recommender Systems

street-view imagery with mobility networks [11, 39]. These methods focus on generating general-purpose region embeddings for tasks like land-use classification.

**GNNs in Recommendation vs. Urban Space.** Graph Neural Networks (GNNs) have become the standard for modeling interactions in recommender systems, with architectures like LightGCN [7], R-GCN [28], and STGCN [35] effectively capturing high-order collaborative signals. While some recent works have applied GNNs to spatial networks [16, 23], they often treat the city as a static grid or a physical road network.

Our framework differs by adapting GNN-based *recommendation* architectures to the urban domain. We treat the city not as a physical graph, but as a bipartite *interaction* graph. This allows us to exploit the "homophily of patronage"—the tendency of users to visit businesses of similar socioeconomic status—to propagate labels from coarse regions to specific businesses, enabling granular inference.

#### 3 Methodology

This section outlines our proposed framework for inferring fine-grained socioeconomic indicators from user-business interactions. The framework operates in two distinct stages: (1) *Spatial-Aware Representation Learning*, where a GNN encodes businesses into latent embeddings enriched with geographical and semantic context, and (2) *Socioeconomic Super-Resolution*, where these representations are used to bridge the granular gap between coarse-grained supervision and fine-grained estimation.

##### 3.1 Problem Formulation

**Input Data Structure.** We consider a set of users  $\mathcal{U}$  and a set of businesses  $\mathcal{V}$  interacting on a bipartite graph  $G = (\mathcal{U}, \mathcal{V}, \mathcal{E})$ , where an edge  $(u, v) \in \mathcal{E}$  indicates an interaction (e.g., a review) between user  $u$  and business  $v$ . Each business  $v$  is associated with a specific geographical location and a set of categorical features  $c_v \subseteq C$  (e.g.,  $\{\text{Restaurant, Retail}\}$ ), describing its function.

**Spatial Granularity Definitions.** To formalize the super-resolution task, we define two layers of spatial granularity:

- Coarse-grained layer ( $S_{coarse}$ ): A set of large spatial regions (e.g., ZIP Codes) denoted as  $\{Z_1, \dots, Z_m\}$ .
- Fine-grained layer ( $S_{fine}$ ): A set of small spatial units (e.g., Census Block Groups) denoted as  $\{B_1, \dots, B_n\}$ , such that each fine unit  $B_j$  is spatially contained within a coarse region  $Z_i$ .

**The Super-Resolution Task.** Let  $y_B$  be the true socioeconomic indicator (e.g., median income) of a fine-grained unit  $B$ , and  $y_Z$  the indicator for the encompassing coarse region  $Z$ . We assume  $y_Z$  is an aggregation of the underlying fine-grained values:

$$y_Z = \frac{1}{|Z|} \sum_{B \in Z} y_B \quad (1)$$

In practice, this aggregation is dataset-dependent, as  $y_Z$  and  $y_B$  may be collected via different census processes.

**Problem Definition (Spatial Super-Resolution)**

Given a dataset where socioeconomic labels are only observed at the coarse level  $\mathcal{Y}_{train} = \{y_Z \mid Z \in S_{coarse}\}$ , the goal is to learn a function  $f(\cdot)$  that utilizes the business interaction graph  $G$  to

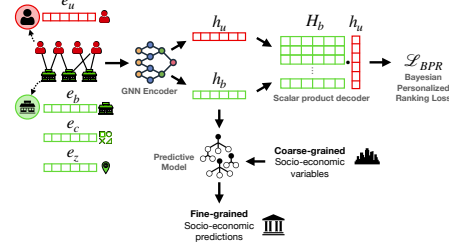


**Figure 1: Schematic overview of the Spatial-GNN framework. (Top) Spatial-Aware Representation Learning: The system initializes business representations by aggregating ID ( $e_b$ ), categorical ( $e_c$ ), and coarse spatial ( $e_z$ ) embeddings. A GNN encoder processes the bipartite user-business graph to produce refined embeddings  $h_u$  and  $h_b$ , optimized via Bayesian Personalized Ranking (BPR) loss. (Bottom) Socioeconomic Super-Resolution: The learned business embeddings  $h_b$  serve as input to a predictive model  $\mathcal{M}$ . In this stage, the model is trained using coarse-grained labels ( $y_Z$ , e.g., Postal Code averages) but is deployed to infer latent socioeconomic indicators at a fine-grained level ( $y_B$ , e.g., Census Block Groups), enabling spatial disaggregation.**

estimate the unobserved fine-grained labels  $\hat{y}_B$  for all  $B \in S_{fine}$ . The objective is to minimize the error against the hidden ground truth:

$$\min_{\theta} \sum_{B \in S_{fine}} \mathcal{L}(\hat{y}_B, y_B) \quad (2)$$

subject to the constraint that the model is trained solely using the coarse set  $\mathcal{Y}_{train}$ .

##### 3.2 Spatial-aware Representation Learning

To solve this problem, our framework operates as a two-stage pipeline, visually summarized in Figure 1. The first stage (Figure 1, Top) focuses on extracting robust vector representations of businesses via a GNN. We employ a GNN-based recommender system architecture trained on a link prediction task.

**Feature Initialization & Spatial Injection.** Standard recommender systems often rely solely on ID-based embeddings. However, to capture the spatial homophily required for socioeconomic inference, we explicitly inject geographical and semantic information into the input features. The input representation for a business node  $v$ , denoted as  $x_v$ , is constructed as the combination of three components:

$$x_v = e_v + e_c + e_z \quad (3)$$

where:

- $e_v \in \mathbb{R}^d$  is the unique latent identity embedding of the business.
- $e_c \in \mathbb{R}^d$  is a learnable embedding corresponding to the coarse geographical region  $Z_v$  (e.g., ZIP Code) where the business is located.

### 5.3 Super-Resolution of Urban Socioeconomic Indicators via Graph-Based Recommender Systems

WWW Companion '26, April 13–17, 2026, Dubai, United Arab Emirates

Francesco Paolo Nerini, Claudio Borile, Antonio Ferrara, & André Panisson

- $\mathbf{e}_c \in \mathbb{R}^d$  represents the semantic category. Since a business may be associated with a set of categories  $c_v$  (e.g., both "Bar" and "Jazz Club"), we calculate  $\mathbf{e}_c$  as the sum of the embeddings of its constituent categories:

$$\mathbf{e}_c = \sum_{k \in c_v} \mathbf{e}_k \quad (4)$$

This combination ensures that the initial node features encode not just *who* the business is, but *where* it is and *what* it does.

**Graph Encoding and Optimization.** We use a GNN encoder to propagate information across the bipartite graph. The encoder aggregate messages from a node's neighbors to update its representation. Formally, for a business node  $v$ , the final representation  $\mathbf{h}_v$  is obtained by aggregating information from interacting users  $\mathcal{N}_v$ :

$$\mathbf{h}_v = \text{Encoder}(\mathbf{x}_v, G) \quad (5)$$

The encoder is optimized using a Bayesian Personalized Ranking (BPR) loss, which encourages the model to rank observed user-business interactions higher than unobserved ones. This ensures that the learned embeddings  $\mathbf{h}_v$  preserve the structural properties of the interaction network, effectively capturing the socioeconomic profile of the business's visiting users.

#### 3.3 Socioeconomic Super-Resolution Framework

The core novelty of our approach lies in using the learned interaction-based embeddings  $\mathbf{h}_v$  to disaggregate coarse socioeconomic data.

**Coarse-to-Fine Inference.** We define the super-resolution task as a supervised learning problem where a predictive model  $\mathcal{M}$  maps business embeddings to socioeconomic indicators. The process consists of three steps:

- **Training (Coarse Supervision):** the model is trained using the coarse labels  $y_Z$ . Specifically, every business  $v$  located in a coarse region  $Z$  is assigned the aggregate label of that region as its training target:

$$y_v^{\text{train}} = y_Z, \quad \forall v \in Z \quad (6)$$

- **Inference (Fine Prediction):** Once trained, the model predicts the socioeconomic variable  $\hat{y}_v$  for each individual business using its embedding:

$$\hat{y}_v = \mathcal{M}(\mathbf{h}_v) \quad (7)$$

- **Spatial Aggregation:** Finally, to obtain estimates for the fine-grained spatial units  $B$ , we aggregate the predictions of all businesses located within that unit:

$$\hat{y}_B = \text{Agg}(\{\hat{y}_v \mid v \in B\}) \quad (8)$$

This framework relies on the hypothesis that the embeddings  $\mathbf{h}_v$ , refined by the GNN, capture latent signal variations that deviate from the spatially smoothed coarse mean  $y_Z$ . This hypothesis is grounded in the existence of *socioeconomic homophily*, as verified in our preliminary analysis (Section 4.3). While coarse labels  $y_Z$  impose a uniform value across all businesses in a region, the GNN aggregates interactions from users who, as shown empirically, traverse specific socioeconomic corridors. Consequently, the resulting embeddings  $\mathbf{h}_v$  inherently encode the distinct clientele profile of each business. This structural signal allows the predictive model to

break the uniformity of the coarse region  $Z$ , effectively recovering the local heterogeneity required for fine-grained inference.

## 4 Implementation and Experimental Setup

While the methodology described in Section 3 outlines the general theoretical framework, this section details the datasets used, the specific model instantiations, and validation protocols used in our experiments.

### 4.1 Business Reviews Dataset

We use the Yelp Open dataset<sup>2</sup>, comprising millions of user-generated reviews for various businesses in different metropolitan areas across the U.S.A. and Canada., and widely used for recommendation systems [7, 19, 34]. This data can be represented naturally as a bipartite graph of users and businesses, where edges correspond to reviews. Each business has information regarding its location, category, average ratings, etc., while users have information regarding their review activity and followers. Although users' review activity and followers are available, we limit our attention primarily to interactions reflected through reviews.

We select reviews from 2005 to 2019, expanding beyond the frequently-used 2018 subset, to ensure a comprehensive representation of user-business interactions. Businesses lacking postal code information and users with fewer than 10 reviews were filtered out to maintain robustness. The final dataset comprises 2,714,253 reviews, linking 96,825 users to 135,149 unique businesses.

### 4.2 Socio-demographic Data

We collected detailed demographic data at the postal-code level from the DataCommons API<sup>3</sup>. We focus on three widely used socio-demographic variables: Median Home Value, Mean Commute Time, and Median Income. We retrieved data at three different division granularities, covering the metropolitan areas within the Yelp dataset. In particular, we followed the geographical units made by the United States Census Bureau. At the finest level, we have Census Block Groups (BGs). At the coarsest geographical level, instead, we then have ZIP Code Tabulation Areas (ZCTA), which roughly correspond to the standard Postal Codes, although they are distinct. In general, ZCTAs are not an exact aggregation of BGs: a single BG can potentially contain areas belonging to different ZCTAs. However, we exclude such block groups from the experiments, using only block groups that are entirely contained in a ZCTA. We focus on the five largest urban areas in the Yelp dataset: Philadelphia (PA), Tampa (FL), Nashville (TN), Indianapolis (IN), and Saint Louis (MO). Table 1 summarizes the number of businesses in each urban area for which socio-demographic attributes are available.

To evaluate the super-resolution scenario, we utilize the hierarchical nature of the census data. We use the coarse-grained **ZCTA-level** statistics as our training data ( $\mathcal{M}_{\text{train}}$ ), mimicking the widely available public data. For evaluation, we use the fine-grained **Census Block Group-level** statistics as the ground truth ( $\mathcal{M}_{\text{test}}$ ), which we aim to recover. This setup realistically simulates the "granularity gap" where only aggregate data is available for training.

<sup>2</sup><https://business.yelp.com/data/resources/open-dataset>

<sup>3</sup><https://datacommons.org>

### 5.3 Super-Resolution of Urban Socioeconomic Indicators via Graph-Based Recommender Systems

**Table 1: Number of businesses used for each urban area and demographic variable combination (a business has a variable if its ZCTA and Block Group has it).**

Urban area	Businesses w/ median income	Businesses w/ median home value	Businesses w/ Median Age
Philadelphia (PA)	14,992	14,844	15,530
Tampa (FL)	8,411	8,064	8,603
Indianapolis (IN)	2,493	2,429	2,509
Saint Louis (MO)	2,397	2,352	2,462
Nashville (TN)	2,505	2,338	2,521

#### 4.3 Socioeconomic Homophily Analysis

A fundamental premise of our spatial-aware GNN framework is that user-business interactions encode latent socioeconomic signals. Specifically, we hypothesize that users exhibit *socioeconomic homophily*, the tendency to visit businesses located in neighborhoods with similar socioeconomic characteristics.

To validate this hypothesis prior to training, we analyze the *socioeconomic assortativity* of the user-business graph. We construct a 2-hop business-to-business network where an edge exists between two businesses if they have been reviewed by the same user. For each connected pair of businesses  $(v_i, v_j)$ , we calculate the absolute difference in the socioeconomic indicators of their respective Block Groups:  $\Delta_{ij} = |y_{v_i} - y_{v_j}|$ .

We compare the distribution of  $\Delta_{ij}$  in the actual interaction graph against a *Null Model*, where user interactions are randomly shuffled while preserving node degrees.

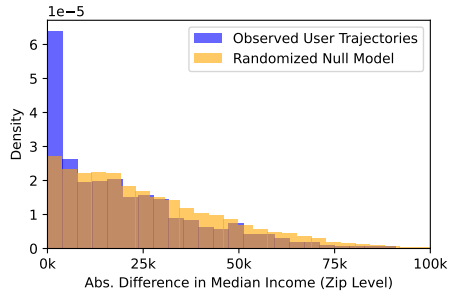


**Figure 2: Socioeconomic consistency in user trajectories. The distribution of absolute differences in Median Income between businesses visited by the same user. The observed data (Blue) shows a significantly higher concentration of low-difference pairs compared to the randomized null model (Orange), confirming strong socioeconomic homophily.**

As illustrated in Figure 2, the observed interactions show a significantly lower mean difference in socioeconomic attributes compared to the null model (Kolmogorov-Smirnov test,  $p < 0.001$ ). This confirms that users tend to move within “socioeconomic distinct”

corridors, providing the necessary signal for our GNN to propagate labels from coarse regions to fine-grained specific businesses.

**Theoretical Basis.** Our analysis draws upon the sociological concept of *homophily* [20], specifically the observation that social stratification constrains urban mobility [33]. According to Bourdieu’s theory of distinction, consumer choices act as markers of class, implying that a user’s set of visited businesses likely share latent socioeconomic attributes. In network science terms, this manifests as *attribute assortativity* within the bipartite graph. If the graph exhibits high assortativity, the user interactions effectively form “bridges” between geographically distant but socioeconomically similar locations, allowing the GNN to overcome the smoothing limitations of coarse spatial labels.

#### 4.4 GNN Architectures with Business and Spatial Context

To implement the spatial-aware representation learning, we explore three recommender system architectures to extract latent embeddings of businesses:

**Embeddings-only Model (Emb):** This baseline model directly learns embeddings for users ( $e_u$ ) and businesses ( $e_b$ ) without additional contextual information, focusing solely on the user-business interactions. Predictions are generated through a simple inner-product decoder between user and business embeddings, akin to a Generalized Matrix Factorization model [8].

**Relational Graph Convolutional Network (RGCN):** We adopt the RGCN [28] architecture with GraphSAGE convolutional layers [6] built on top of the learnable embeddings. This model allows for handling multi-relational data, and in this case it captures the complex relational information within the user-business interactions.

**LightGCN:** We employ the LightGCN model [7], a state-of-the-art simplification of general GNN architectures obtained by removing non-linearities, often resulting in better generalization for recommender systems. Unlike RGCN, LightGCN does not rely on additional neural transformations beyond embedding propagation, reducing computational complexity while maintaining strong predictive capabilities.

As detailed in Section 5.1, for RGCN and LightGCN, we consider three distinct configurations to assess the incremental impact of adding business and geographic information:

**Basic (RGCN, LightGCN):** Only the graph structure is used, and both users and businesses are represented by their embeddings  $e_u$  and  $e_b$ .

**Feat (Feat-RGCN, Feat-LightGCN):** Business embeddings are enriched with categorical business features ( $e_c$ ) (e.g., categories such as food, beauty, etc.).

**Feat&PC (Feat&PC-RGCN, Feat&PC-LightGCN):** Business embeddings are further enriched with spatial information encoded via learnable postal code embeddings ( $e_z$ ), explicitly embedding geographical context into the learned representations.

For the socioeconomic predictions, we also consider embeddings which were not pre-trained on the recommendation tasks (but are learned during the socioeconomic task). We call this embeddings “NoPreTrain” and use it as a further baseline for our framework.

### 5.3 Super-Resolution of Urban Socioeconomic Indicators via Graph-Based Recommender Systems

WWW Companion '26, April 13–17, 2026, Dubai, United Arab Emirates

Francesco Paolo Nerini, Claudio Borile, Antonio Ferrara, & André Panisson

#### 4.5 Socioeconomic Tasks Setup

We use the business representations ( $h_b$ ) obtained from the trained GNN recommender systems (Section 4.4) and a spatial, k-nearest neighbors graph with the businesses as input for an additional GNN performing supervised classification tasks over the business. The aim of these models is to distinguish between areas where the value of the sociodemographic is high (e.g., high median income), and areas where the value is low. Say that a business  $b$  belongs to area  $A \in \mathcal{A}_{train}$ , where  $\mathcal{A}_{train}$  is the set of geographical areas used for training. We binarize the label on a given area based on whether the value of the target variable,  $y_A$ , is above or below the median value  $\tilde{y} = \text{Median}(y_A, A \in \mathcal{A})$ , i.e.:

$$y'_A = \begin{cases} 1 & \text{if } y_A \geq \tilde{y} \\ 0 & \text{otherwise.} \end{cases}$$

As mentioned previously, each business in an area is assigned the same label of its region:

$$y_v = y'_A, \forall v \in A.$$

We then train a model using a binary cross-entropy loss as:

$$\min_{\theta} \sum_{A \in \mathcal{A}_{train}} \sum_{v \in A} (-\hat{y}_v \log y_v + (1 - \hat{y}_v) \log (1 - y_v)), \quad (9)$$

where  $\hat{y}_v$  is the probability, predicted by the GNN, that business  $v$  belongs to an area with target variable above the median. Since we are interested to perform a prediction for the geographical area  $A \in \mathcal{A}_{test}$ , we aggregate the business-level predictions by computing the mean between the businesses  $v \in A$  and output a geographical area prediction:

$$\hat{y}_A = \text{Mean}(\hat{y}_v, v \in A), A \in \mathcal{A}_{test}. \quad (10)$$

Finally, by defining the vectors  $y_{pred} = \{\hat{y}_A | A \in \mathcal{A}_{test}\}$  and  $y_{true} = \{y'_A | A \in \mathcal{A}_{test}\}$ , we use the area under the Receiver Operating Characteristic curve  $\text{AUC}(y_{true}, y_{pred})$  as evaluation metric.

In the super-resolution experiments (Section 5.3), we consider coarser geographical subdivision as training labels, and a finer subdivision as test labels. In our experiments, we use the ZCTAs to provide the training labels and the Census Block Groups as test labels (i.e.,  $\mathcal{A}_{train} = Z$  and  $\mathcal{A}_{test} = B$ ).

In the classification experiments of Section 5.2, instead, we consider a more standard scenario, where we split the Census Block Groups of each urban area into train and test sets ( $\mathcal{A}_{train} = B_{train}$ ,  $\mathcal{A}_{test} = B_{test}$ ).

#### 4.6 Validation Protocol

To validate the effectiveness of the super-resolution framework, we adopt a strict evaluation protocol based on the spatial hierarchy defined in Problem 1.

- **Input Features:** The GNN model receives the business embeddings  $h_b$  and the corresponding k-nearest neighbour graph as input.
- **Baselines:** We compare our model's fine-grained predictions against a *Coarse Baseline*. This baseline assumes perfect homogeneity within a coarse region, assigning the observed coarse value (e.g., ZIP Code value) to all constituent fine-grained units (e.g., Census Block Groups).

- **Success Metric:** The framework is considered successful if the error of the aggregated business predictions at the fine-grained level is consistently lower than the error of the Coarse Baseline. This explicitly demonstrates that the business embeddings contain latent signals capable of recovering local variance lost during spatial aggregation.

#### 4.7 GNN Training setup

To evaluate our recommendation models, we split each user's interactions into training (80%), validation (10%), and testing (10%) sets, as usually done in the literature [7, 34]. The link prediction (recommendation) task is optimized with the Bayesian Personalized Ranking (BPR) loss [27]. Test performance is averaged across 10 different splits. Each GNN model is trained for up to 5000 epochs, with early stopping based on the validation performance (Recall@20) to avoid overfitting. We use Adam optimization with a learning rate of 0.01, embedding dimensionality and hidden layers size of 64, 2 layers of message passing and early-stopping monitoring every epoch. The measured performance metric is Recall@20, measuring the fraction of relevant businesses successfully recommended within the top 20 predictions per user.

For the socioeconomic tasks, we follow a similar setup, with the same maximum epochs, learning rate, embedding dimensionality and early stopping. We test our models using the ROC-AUC. We also a validation set of areas for early stopping (using the cross-entropy loss as validation metric), not used for the train loss computation. We repeat each experiment, with a different split, 10 times for robustness.

### 5 Experimental Results

#### 5.1 Recommendation Results

Figure 3 compares the performances of the evaluated models. The results clearly show the benefit of incorporating categorical and spatial information into the recommendation task. In particular, adding postal code embeddings consistently improves the model's performance, confirming that geographical information effectively complements traditional user-business interaction signals. These results highlight that geographic context significantly enhances the quality and relevance of the learned business representations.

Additionally, the superior performance of LightGCN models compared to RGCN models in the same feature settings is consistent with previous findings in the recommendation literature [7], suggesting that a simpler and more efficient propagation mechanism can often achieve better or comparable performance.

Given the higher performance of LightGCN in the task, in the following we present results only on embeddings obtained from training these models. We report results also with RGCN architectures in the Appendix.

#### 5.2 Classification Results

As a benefit of our representation learning approach, the embeddings learned from the recommendation task can be used across a variety of different applications. We then first apply the embedding to a standard classification task. For each urban area, we split the Census Block Groups into a train set  $B_{train}$  (80% of the areas) and a test set  $B_{test}$  (20%), and use the business in the train set as described

### 5.3 Super-Resolution of Urban Socioeconomic Indicators via Graph-Based Recommender Systems

Super-Resolution of Urban Socioeconomic Indicators via Graph-Based Recommender Systems

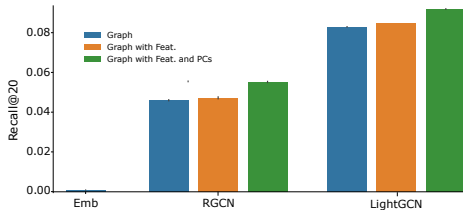


**Figure 3: Model Performance as Recall@20 over the dataset using the models defined in Section 4.4; Emb model obtains low Recall@20, around  $10^{-4}$ .**

in Section 4.5. The main difference with the super-resolution case is then that we do not employ the coarse grained labels for training. We report the results in Figure 4.

We observe that we always manage to obtain a classification ROC-AUC above 0.5, corresponding to random guessing, implying that the model are learning from the spatial distribution of the business how to identify characteristics of their neighbourhood. Additionally, it is interesting to observe that, especially for urban areas where we have the most businesses (Philadelphia and Tampa), the best performing recommendation systems tend to produce business embeddings with higher ROC-AUC. This suggests a link between latent representations useful for recommendations and those useful for sociodemographic variables predictions, although Feat-LightGCN often outperforms Feat&PC-LightGCN.

This latter hypothesis is further sustained by comparing the performance with the "NoPreTrain" model. In this case, each business is assigned an embedding, and the GNN model is only learning from the classification task. These models, ignoring latent information learned from the recommendation task, is the worst performing model for all areas and variables.

#### 5.3 Super-resolution Results

Our experiments illustrate that business embeddings learned through graph representation learning significantly improve the predictive capability of demographic inference, achieving meaningful super-resolution results. The results are presented in Table 2.

In particular, we show consistent improvements over the "NoPreTrain" model, highlighting the increased ability of embeddings' trained on a recommendation task to discriminate between neighborhoods with differing socioeconomic characteristics. We also observe that urban areas with higher number of business tend to achieve higher super-resolution results with respect to the coarse training labels.

Embeddings from the Feat-LightGCN model are on average the best performing across all target variables. In this case, using embeddings with explicit geographical information (the postal codes) does not improve the performance in the super-resolution tasks, but decreases it. This effect, observed partially also in Section 5.2, is possibly due to the scale of the postal codes areas used in the business embeddings, which limits the predictions of the model at finer levels.

WWW Companion '26, April 13–17, 2026, Dubai, United Arab Emirates

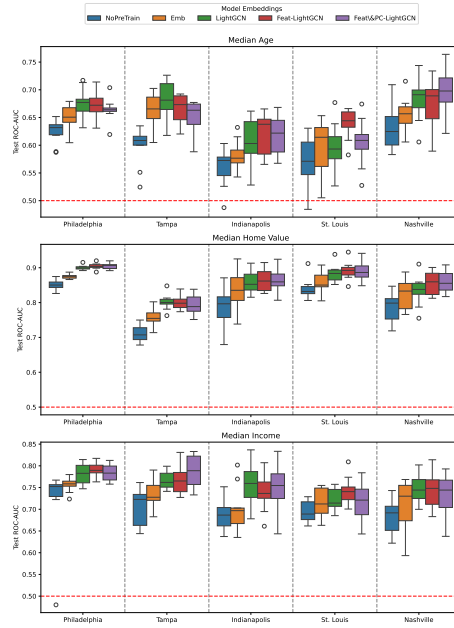


**Figure 4: Test ROC-AUC on classification (high vs low) sociodemographic variables on Census Block Groups, across different model embeddings and urban areas. The horizontal, dashed line correspond to random guessing.**

Figure 5 illustrates this for the Philadelphia area, demonstrating how the model that uses LightGCN embeddings to predict the Median Income variable significantly recovers detailed neighborhood-level variations in median income beyond what coarse-grained ZCTA averages alone can provide.

#### 6 Discussion and Limitations

The results show empirically that a representation learning approach allows to learn rich business representation, implicitly containing information regarding socio-economics information on the business' neighborhood and clientele. We obtain large improvements over our baselines on inferring fine-grained even when using coarser labels for training, showing the advantages of such framework for demographics inference.

However, our experiments still have various limitations. The main limit lies in the inherent sparsity of user-business interactions in smaller urban areas, which can affect the robustness of the learned embeddings. We are able to apply our method to large metropolitan cities, but on smaller settlements we would likely not have enough data to differentiate between different users distribution and preferences.

### 5.3 Super-Resolution of Urban Socioeconomic Indicators via Graph-Based Recommender Systems

WWW Companion '26, April 13–17, 2026, Dubai, United Arab Emirates

Francesco Paolo Nerini, Claudio Borile, Antonio Ferrara, & André Panisson

**Table 2: ROC-AUCs in super-resolution setup; Values in parenthesis correspond to difference to the Coarse Baseline, i.e., the ROC-AUCs obtained from assigning the train labels (ZIP Code-level) to all their constituent fine-grained units (Census Block Group-level)**

Target Variable	Model \ State	PA	FL	IN	MO	TN	Average
Median Age	NoPreTrain	66.8±0.2 (-0.1)	73.9±0.2 (+1.0)	64.2±0.6 (+0.4)	69.3±0.5 (-0.8)	73.2±0.7 (+1.4)	+0.4
	Emb	67.8±0.4 (+0.9)	75.9±0.2 (+3.0)	66.6±0.3 (+2.9)	70.6±0.2 (+0.5)	70.6±0.1 (-1.2)	+1.2
	LightGCN	68.8±0.1 (+1.9)	75.6±0.1 (+2.7)	68.2±0.2 (+4.4)	72.2±0.2 (+2.1)	72.7±0.2 (+1.0)	+2.4
	Feat-LightGCN	69.5±0.1 (+2.5)	75.4±0.1 (+2.5)	68.6±0.2 (+4.8)	72.4±0.2 (+2.3)	72.2±0.2 (+0.4)	+2.5
	Feat&PC-LightGCN	68.3±0.1 (+1.4)	75.1±0.1 (+2.2)	65.7±0.2 (+1.9)	69.7±0.1 (-0.4)	73.4±0.3 (+1.6)	+1.3
Median Home Value	NoPreTrain	85.4±0.2 (+0.6)	79.7±0.3 (+0.5)	82.2±0.5 (+2.3)	82.9±0.3 (-1.3)	74.7±1.3 (+1.3)	+0.7
	Emb	85.1±0.2 (+0.2)	82.7±0.2 (+3.5)	82.9±0.2 (+2.9)	85.6±0.2 (+1.4)	73.3±0.2 (-0.1)	+1.6
	LightGCN	86.8±0.1 (+1.9)	83.3±0.4 (+4.0)	82.2±0.1 (+2.3)	83.9±1.9 (-0.3)	74.7±0.1 (+1.3)	+1.8
	Feat-LightGCN	87.6±0.1 (+2.8)	83.3±0.1 (+4.1)	82.5±0.1 (+2.6)	87.5±0.1 (+3.2)	75.3±0.1 (+1.9)	+2.9
	Feat&PC-LightGCN	86.1±0.0 (+1.3)	82.4±0.2 (+3.2)	83.6±0.3 (+3.7)	85.7±0.2 (+1.5)	73.4±0.2 (0.0)	+1.9
Median Income	NoPreTrain	77.3±0.3 (+0.8)	77.7±0.3 (+0.8)	76.8±0.3 (+1.9)	75.8±0.4 (-1.0)	68.1±0.8 (+1.5)	+0.8
	Emb	76.8±0.3 (+0.2)	78.6±0.5 (+1.6)	77.5±0.2 (+2.6)	74.7±0.1 (-2.2)	66.1±0.2 (-0.5)	+0.4
	LightGCN	78.9±0.1 (+2.3)	80.1±0.2 (+3.2)	76.2±0.2 (+1.3)	77.1±0.5 (+0.3)	67.6±0.4 (+1.0)	+1.6
	Feat-LightGCN	80.1±0.1 (+3.5)	80.1±0.1 (+3.2)	77.9±0.2 (+3.0)	76.0±0.1 (-0.9)	70.7±0.3 (+4.1)	+2.6
	Feat&PC-LightGCN	79.3±0.1 (+2.8)	78.9±0.2 (+2.0)	77.6±0.2 (+2.7)	79.2±0.2 (+2.4)	69.2±0.3 (+2.6)	+2.5

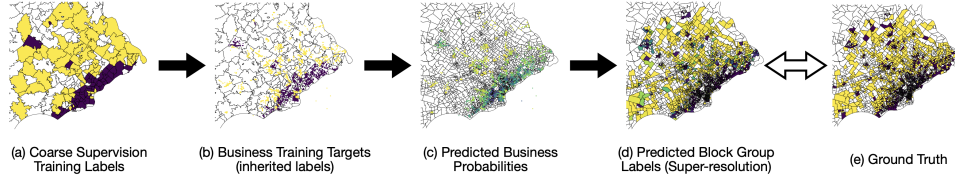


**Figure 5: Example maps of the super-resolution regression on the "Median Income", Philadelphia metropolitan area. Darker blue colors denote low income and bright yellow denotes high income areas. Block Groups without the values of the target variable are left in white. The business predictions depicted here are derived from the Feat-LightGCN model.**

Additionally, user-generated datasets, such as the Yelp dataset used here, can have several problems. Business density and user interactions intrinsically limits and bias our inference: we are not able to make predictions on any uncovered area, and demographic imbalances among users introduce bias which could affect the validity and fairness of our socio-demographic inferences. User data may also give rise to privacy concerns. For example, reviews can be leveraged to infer approximate residential and workplace locations, requiring additional privatization techniques for large scale application.

Finally, due to the data distribution in the Yelp dataset, we were severely limited in our experiments to only consider urban areas in the U.S.A., without being able to generalize to, e.g., Asian, or European urban areas.

## 7 Conclusion

In this paper, we presented a novel representation learning framework designed to perform super-resolution inference of socio-demographic variables using previously underused data from location-based social networks. By training GNNs on a recommendation task, we obtained business representations from Yelp user-business interactions, enriched with spatial information encoded through

postal code embeddings. These learned representations enabled the inference of fine-grained socio-demographic statistics from coarse-grained demographic data.

Our extensive experimental evaluation shows that explicitly incorporating geographical context into the GNN-based recommender systems consistently enhances recommendation performance. Moreover, we found that the learned embeddings can capture meaningful spatial structures, even when not encoding explicit geographic information, thus validating their potential as proxies for local socio-demographic characteristics.

However, as previously discussed, our method currently shows several limitations, with concerns due to the nature and distribution of the underlying user-generated datasets. Experimentally it should be tested on different regions, as the current dataset is limited to U.S.A. and Canada. Therefore, any results solely based on such data must be interpreted with caution. Future research should address these limitations with the use of larger and more comprehensive datasets, ideally including explicit temporal information, while developing techniques to deal with the privacy and bias concerns. Incorporating temporal dynamics could further enhance the framework's capability to analyze urban socio-demographic changes over time, providing valuable insights for urban policy and planning.

## 5.3 Super-Resolution of Urban Socioeconomic Indicators via Graph-Based Recommender Systems

### References

- [1] Mohit Agarwal, Mimi Sun, Chaitanya Kamath, Arbaaz Muslim, Prithul Sarker, Joydeep Paul, Hector Yee, Marcin Sieniek, Kim Jablonski, Yael Mayer, et al. 2024. *General Geospatial Inference with a Population Dynamics Foundation Model*. arXiv:2411.07207 doi:10.48550/arXiv.2411.07207
- [2] Michael Batty. 2013. *The new science of cities*. MIT press, Cambridge, MA 02142.
- [3] Ylenia Casali, Nazlı Yonca Aydin, and Tina Comes. 2022. Machine learning for spatial analyses in urban areas: a scoping review. *Sustainable Cities and Society* 85 (Oct. 2022), 104050.
- [4] Donald R Davis, Jonathan I Dingel, Joan Monras, and Eduardo Morales. 2019. How segregated is urban consumption? *Journal of Political Economy* 127, 4 (2019), 1684–1738.
- [5] Antonio Ferrara, David Garcia-Soriano, and Francesco Bonchi. 2025. Beyond Shortest Paths: Node Fairness in Route Recommendation. *Proc. VLDB Endow.* 18, 9 (2025), 3230–3242. doi:10.14778/3746405.3746440
- [6] Will Hamilton, Zhitao Ying, and Jure Leskovec. 2017. Inductive Representation Learning on Large Graphs. In *Advances in Neural Information Processing Systems*, I. Guyon, U. Von Luxburg, S. Bengio, H. Wallach, R. Fergus, S. Vishwanathan, and R. Garnett (Eds.), Vol. 30. Curran Associates, Inc. [https://proceedings.neurips.cc/paper\\_files/paper/2017/file/5dd94b5e033da9c6fb5ba83c7a7e99-Paper.pdf](https://proceedings.neurips.cc/paper_files/paper/2017/file/5dd94b5e033da9c6fb5ba83c7a7e99-Paper.pdf)
- [7] Xiangnan He, Kuan Deng, Xiang Wang, Yan Li, YongDong Zhang, and Meng Wang. 2020. LightGCN: Simplifying and Powering Graph Convolution Network for Recommendation. In *Proceedings of the 43rd International ACM SIGIR Conference on Research and Development in Information Retrieval*. ACM, Virtual Event China, 639–648.
- [8] Xiangnan He, Lizi Liao, Hanwang Zhang, Lijiang Nie, Xia Hu, and Tat-Seng Chua. 2017. Neural Collaborative Filtering. In *Proceedings of the 26th International Conference on World Wide Web (Perth, Australia) (WWW '17)*. International World Wide Web Conferences Steering Committee, Republic and Canton of Geneva, CHE, 173–182. doi:10.1145/3038912.3052569
- [9] Joanne Hinds and Adam N. Joinson. 2018. What demographic attributes do our digital footprints reveal? A systematic review. *PLoS ONE* 13, 11 (Nov. 2018), e0207112.
- [10] Neal Jean, Marshall Burke, Michael Xie, W. Matthew Alampay Davis, David B Lobell, and Stefano Ermon. 2016. Combining satellite imagery and machine learning to predict poverty. *Science* 353, 6301 (2016), 790–794.
- [11] Guangyin Jin, Yuxuan Liang, Yuchen Fang, Zexhi Shao, Jincai Huang, Junbo Zhang, and Yu Zheng. 2023. Spatio-temporal graph neural networks for predictive learning in urban computing: A survey. *IEEE Trans. Knowl. Data Eng.* 36, 10 (2023), 5388–5408.
- [12] Devashish Khulbe, Alexander Belyi, and Stanislav Sobolevsky. 2025. Commute Networks as a Signature of Urban Socioeconomic Performance: Evaluating Mobility Structures with Deep Learning Models. *Smart Cities* 8, 4 (2025), 125.
- [13] Thomas N. Kipf and Max Welling. 2017. Semi-Supervised Classification with Graph Convolutional Networks. In *International Conference on Learning Representations*. <https://openreview.net/forum?id=SJU4ayYgl>
- [14] Konstantin Klemmer, Esther Rolf, Caleb Robinson, Lester Mackey, and Marc Rufwurm. 2025. SatCLIP: Global, General-Purpose Location Embeddings with Satellite Imagery. *Proceedings of the AAAI Conference on Artificial Intelligence* 39, 4 (Apr. 2025), 4347–4355. doi:10.1609/aaai.v39i4.32457
- [15] David Lazer, Alex Pentland, Lada Adamic, Sinan Aral, Albert-László Barabási, Devon Brewer, Nicholas Christakis, Noshir Contractor, James Fowler, Myron Gutmann, et al. 2009. Computational social science. *Science* 323, 5915 (2009), 721–723.
- [16] Mengzhang Li and Zhanxing Zhu. 2021. Spatial-Temporal Fusion Graph Neural Networks for Traffic Flow Forecasting. *Proceedings of the AAAI Conference on Artificial Intelligence* 35, 5 (May 2021), 4189–4196. doi:10.1609/aaai.v35i5.16542
- [17] Zechen Li, Weiming Huang, Kai Zhao, Min Yang, Yongshun Gong, and Meng Chen. 2024. Urban Region Embedding via Multi-View Contrastive Prediction. *Proceedings of the AAAI Conference on Artificial Intelligence* 38, 8 (Mar. 2024), 8724–8732. doi:10.1609/aaai.v38i8.28718
- [18] Genchen Mai, Ni Lao, Yutong He, Jiaming Song, and Stefano Ermon. 2023. CSP: Self-Supervised Contrastive Spatial Pre-Training for Geospatial-Visual Representations. In *Proceedings of the 40th International Conference on Machine Learning (Proceedings of Machine Learning Research, Vol. 202)*. Andreas Krause, Emma Brunskill, Kyunghyun Cho, Barbara Engelhardt, Sivan Sabato, and Jonathan Scarlett (Eds.), PMLR, 23498–23515. <https://proceedings.mlr.press/v202/mai23a.html>
- [19] Kelong Mao, Jieming Zhu, Xi Xiao, Biao Lu, Zhaowei Wang, and Xiuqiang He. 2021. UltraGCN: Ultra Simplification of Graph Convolutional Networks for Recommendation. In *Proceedings of the 30th ACM International Conference on Information & Knowledge Management*. ACM, Virtual Event Queensland Australia, 1253–1262.
- [20] Miller McPherson, Lynn Smith-Lovin, and James M Cook. 2001. Birds of a feather: Homophily in social networks. *Annual review of sociology* 27, 1 (2001), 415–444.
- [21] Nando Metzger, John E Vargas-Muñoz, Rodrigo C Daudt, Benjamin Kellenberger, Thao Ton-That Whelan, Ferda Ofli, Muhammad Imran, Konrad Schindler, and Devis Tuia. 2022. Fine-grained population mapping from coarse census counts and open geodata. *Scientific Reports* 12, 1 (2022), 20085.
- [22] Anastasios Noulas, Salvatore Scellato, Renaud Lambiotte, Massimiliano Pontil, and Cecilia Mascolo. 2012. A tale of many cities: universal patterns in human urban mobility. *PLoS one* 7, 5 (2012), e37027.
- [23] Maximiliano Ojeda and Juan Reutter. 2025. Using publicly available data for predicting socioeconomic values in urban context. *Computational Urban Science* 5, 1 (2025), 32.
- [24] Simone Piaggese, Serena Giurgola, Márton Karsai, Yelena Mejova, André Panisson, and Michele Tizzoni. 2022. Mapping urban socioeconomic inequalities in developing countries through Facebook advertising data. *Frontiers in big Data* 5 (2022), 1006352.
- [25] Sohrab Rahimi, Sam Mottahedi, and Xi Liu. 2018. The Geography of Taste: Using Yelp to Study Urban Culture. *ISPRS International Journal of Geo-Information* 7, 9 (Sept. 2018), 376. Number: 9 Publisher: Multidisciplinary Digital Publishing Institute.
- [26] Nathan Ratledge, Gabriel Cadamuro, Brandon De la Cuesta, Matthieu Stigler, and Marshall Burke. 2021. *Using satellite imagery and machine learning to estimate the livelihood impact of electricity access*. Technical Report. National Bureau of Economic Research.
- [27] Steffen Rendle, Christoph Freudenthaler, Zeno Gantner, and Lars Schmidt-Thieme. 2009. BPR: Bayesian personalized ranking from implicit feedback. In *Proceedings of the Twenty-Fifth Conference on Uncertainty in Artificial Intelligence (Montreal, Quebec, Canada) (UAI '09)*. AUAI Press, Arlington, Virginia, USA, 452–461.
- [28] Michael Schlichtkrull, Thomas N. Kipf, Peter Bloem, Rianne van den Berg, Ivan Titov, and Max Welling. 2018. Modeling Relational Data with Graph Convolutional Networks. In *The Semantic Web, Aldo Gangemi, Roberto Navigli, Maria-Esther Vidal, Pascal Hitzler, Raphaël Troncy, Laura Hollink, Anna Tordai, and Mehwish Alam (Eds.)*. Springer International Publishing, Cham, 593–607.
- [29] Thiago H Silva and Daniel Silver. 2025. Using graph neural networks to predict local culture. *Environment and Planning B: Urban Analytics and City Science* 52, 2 (2025), 355–376. arXiv:https://doi.org/10.1177/23998083241262053 doi:10.1177/23998083241262053
- [30] Forrest R Stevens, Andrea E Gaughan, Catherine Linaard, and Andrew J Tatem. 2015. Disaggregating census data for population mapping using random forests with remotely-sensed and ancillary data. *PLoS one* 10, 2 (2015), e0170742.
- [31] Petar Veličković, Guillem Cucurull, Arantxa Casanova, Adriana Romero, Pietro Liò, and Yoshua Bengio. 2018. Graph Attention Networks. In *International Conference on Learning Representations*. <https://openreview.net/forum?id=rJXMpikCZ>
- [32] Pengyang Wang, Yanjie Fu, Jiawei Zhang, Xiaolin Li, and Dan Lin. 2018. Learning urban community structures: A collective embedding perspective with periodic spatial-temporal mobility graphs. *ACM Transactions on Intelligent Systems and Technology (TIST)* 9, 6 (2018), 1–28.
- [33] Qi Wang, Nolan Edward Phillips, Mario L Small, and Robert J Sampson. 2018. Urban mobility and neighborhood isolation in America's 50 largest cities. *Proceedings of the National Academy of Sciences* 115, 30 (2018), 7735–7740.
- [34] Xiang Wang, Xiangnan He, Meng Wang, Full Feng, and Tat-Seng Chua. 2019. Neural Graph Collaborative Filtering (SIGIR 19). Association for Computing Machinery, New York, NY, USA, 165–174. doi:10.1145/3331184.3331267
- [35] Zhaobo Wang, Yanmin Zhu, Qiaomei Zhang, Haobing Liu, Chunyang Wang, and Tong Liu. 2022. Graph-Enhanced Spatial-Temporal Network for Next POI Recommendation. *ACM Transactions on Knowledge Discovery from Data* 16, 6 (July 2022), 104:1–104:21.
- [36] Zonghan Wu, Shirui Pan, Fengwen Chen, Guodong Long, Chengqi Zhang, and S Yu Philip. 2020. A comprehensive survey on graph neural networks. *IEEE transactions on neural networks and learning systems* 32, 1 (2020), 4–24.
- [37] Fengli Xu, Qi Wang, Esteban Moro, Lin Chen, Arianna Salazar Miranda, Marta C. González, Michele Tizzoni, Chaoming Song, Carlo Ratti, Luis Bettencourt, Yong Li, and James Evans. 2025. Using human mobility data to quantify experienced urban inequalities. *Nature Human Behaviour* 9, 4 (01 Apr 2025), 654–664. doi:10.1038/s41562-024-02079-0
- [38] Zhilun Zhou, Yu Liu, Jingtao Ding, Depeng Jin, and Yong Li. 2023. Hierarchical Knowledge Graph Learning Enabled Socioeconomic Indicator Prediction in Location-Based Social Network. In *Proceedings of the ACM Web Conference 2023*. ACM, Austin TX USA, 122–132.
- [39] Xingchen Zou, Yibo Yan, Xixuan Hao, Yuehong Hu, Haomin Wen, Erdong Liu, Junbo Zhang, Yong Li, Tianrui Li, Yu Zheng, et al. 2025. Deep learning for cross-domain data fusion in urban computing: Taxonomy, advances, and outlook. *Information Fusion* 113 (2025), 102606.

### 5.3 Super-Resolution of Urban Socioeconomic Indicators via Graph-Based Recommender Systems

WWW Companion '26, April 13–17, 2026, Dubai, United Arab Emirates

Francesco Paolo Nerini, Claudio Borile, Antonio Ferrara, & André Panisson

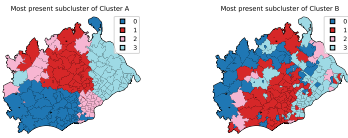


**Figure 7: Second K-Means clustering on the two business clusters in Philadelphia for the LightGCN model; we show the prevalent sub-cluster for each postal code depending on the macro-cluster.**

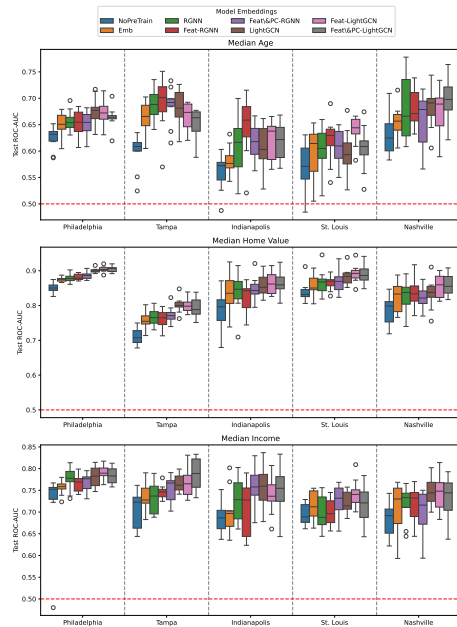


**Figure 8: Test ROC-AUC on classification (high vs low) sociodemographic variables on Census Block Groups, across different model embeddings and urban areas. The horizontal, dashed line correspond to random guessing.**

#### A Understanding Geographical and Semantic Information in Business Embeddings

To better understand what types of information are encoded in the learned business representations, we perform an exploratory analysis of their geographical and semantic structure. Specifically, we examine whether embeddings obtained from our GNN-based recommender systems naturally cluster according to business type

and geographic proximity, even without explicit spatial supervision. We focus on the urban area of Philadelphia, analyzing business embeddings produced by the standard LightGCN model. Importantly, this model variant uses only user–business interaction data and does not explicitly incorporate spatial embeddings, allowing us to test whether the embeddings inherently capture geographical or semantic correlations.

First, we reduce the dimensionality of the 64 dimensional business embeddings obtained to a lower-dimensional space (4 dimensions) using PCA. Then, we perform a K-means clustering in two steps. First, we partition business embeddings into two broad clusters to distinguish between the two dominant groups of businesses. Next, each of these two clusters is subdivided again into four sub-clusters, enabling us to observe more granular spatial patterns. To facilitate the interpretation, we categorize businesses into two intuitive macro-categories: *Food-related* and *Non-Food-related* businesses.

In Figure 6, we observe that cluster B, which is made up mainly of Food-related businesses, is geographically aligned with well-known urban districts, such as the dense central neighborhoods in southern Philadelphia. Similarly, Non-Food-related businesses are prevalent within Cluster A and exhibit a spatially coherent distribution, further strengthening the implicit encoding of spatial and categorical information in the embedding.

To further explore this spatial-semantic interplay, the second-level clustering provides additional insight into how geographical patterns emerge within the initial clusters. After subdividing the two primary clusters into finer sub-clusters, we observe a distinct geographical stratification. Specifically, Figure 7 reveals that within both groups, businesses naturally cluster according to their geographical proximity, clearly delineating neighborhoods and city districts.

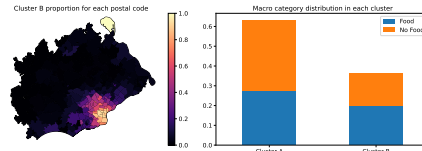


**Figure 6: (Left) Prevalence of cluster B across the business of each postal code on the business in Philadelphia for the LightGCN model; (Right) proportion of businesses for each macro-category in the two clusters obtained through K-Means clustering.**

#### B Additional results

We provide additional results to the experiments of Section 5.2 and Section 5.3. In particular, we show the results also with the RGNN architectures. In Figure 8 we show the results for the Block group classification experiments comparing also the additional architectures; while in Table 3 we show the complete results for the super resolution task.

### 5.3 Super-Resolution of Urban Socioeconomic Indicators via Graph-Based Recommender Systems

**Table 3: ROC-AUCs in super-resolution setup; Values in parenthesis correspond to difference to the Coarse Baseline, i.e., the ROC-AUCs obtained from assigning the train labels (ZIP Code-level) to all their constituent fine-grained units (Census Block Group-level)**

Target Variable	Model \ State	PA	FL	IN	MO	TN	Average
Median Age	NoPreTrain	66.8±0.2 (-0.1)	73.9±0.2 (+1.0)	64.2±0.6 (+0.4)	69.3±0.5 (-0.8)	73.2±0.7 (+1.4)	+0.4
	Emb	67.8±0.4 (+0.9)	75.9±0.2 (+3.0)	66.6±0.3 (+2.9)	70.6±0.2 (+0.5)	70.6±0.1 (-1.2)	+1.2
	RGNN	68.0±0.4 (+1.0)	75.0±0.2 (+2.1)	68.2±0.4 (+4.4)	65.9±3.9 (-4.2)	73.4±0.2 (+1.6)	+1.0
	Feat-RGNN	68.9±0.5 (+1.9)	74.6±0.2 (+1.7)	67.2±0.4 (+3.4)	72.0±0.8 (+1.9)	73.2±0.2 (+1.4)	+2.1
	Feat&PC-RGNN	68.0±0.3 (+1.0)	74.6±0.2 (+1.7)	63.3±2.8 (-0.4)	70.1±0.2 (0.0)	72.9±0.3 (+1.1)	+0.7
	LightGCN	68.8±0.1 (+1.9)	75.6±0.1 (+2.7)	68.2±0.2 (+4.4)	72.2±0.2 (+2.1)	72.7±0.2 (+1.0)	+2.4
	Feat-LightGCN	69.5±0.1 (+2.5)	75.4±0.1 (+2.5)	68.6±0.2 (+4.8)	72.4±0.2 (+2.3)	72.2±0.2 (+0.4)	+2.5
	Feat&PC-LightGCN	68.3±0.1 (+1.4)	75.1±0.1 (+2.2)	65.7±0.2 (+1.9)	69.7±0.1 (-0.4)	73.4±0.3 (+1.6)	+1.3
Median Home Value	NoPreTrain	85.4±0.2 (+0.6)	79.7±0.3 (+0.5)	82.2±0.5 (+2.3)	82.9±0.3 (-1.3)	74.7±1.3 (+1.3)	+0.7
	Emb	85.1±0.2 (+0.2)	82.7±0.2 (+3.5)	82.9±0.2 (+2.9)	85.6±0.2 (+1.4)	73.3±0.2 (-0.1)	+1.6
	RGNN	83.6±2.8 (-1.2)	77.7±3.5 (-1.6)	79.9±1.6 (-0.0)	86.9±0.6 (+2.6)	75.0±0.3 (+1.6)	+0.3
	Feat-RGNN	86.6±0.3 (+1.8)	79.9±1.5 (+0.7)	84.7±0.1 (+4.8)	85.8±0.4 (+1.6)	77.4±0.5 (+4.0)	+2.6
	Feat&PC-RGNN	86.3±0.3 (+1.5)	83.0±0.2 (+3.8)	81.0±0.2 (+1.1)	83.3±0.2 (-1.0)	74.6±0.1 (+1.2)	+1.3
	LightGCN	86.8±0.1 (+1.9)	83.2±0.4 (+4.0)	82.2±0.1 (+2.3)	83.9±1.9 (-0.3)	74.7±0.1 (+1.3)	+1.8
	Feat-LightGCN	87.6±0.1 (+2.8)	83.3±0.1 (+4.1)	82.5±0.1 (+2.6)	87.5±0.1 (+3.2)	75.3±0.1 (+1.9)	+2.9
	Feat&PC-LightGCN	86.1±0.0 (+1.3)	82.4±0.2 (+3.2)	83.6±0.3 (+3.7)	85.7±0.2 (+1.5)	73.4±0.2 (0.0)	+1.9
Median Income	NoPreTrain	77.3±0.3 (+0.8)	77.7±0.3 (+0.8)	76.8±0.3 (+1.9)	75.8±0.4 (-1.0)	68.1±0.8 (+1.5)	+0.8
	Emb	76.8±0.3 (+0.2)	78.6±0.5 (+1.6)	77.5±0.2 (+2.6)	74.7±0.1 (-2.2)	66.1±0.2 (-0.5)	+0.4
	RGNN	78.7±0.3 (+2.1)	77.5±0.8 (+0.6)	78.3±0.3 (+3.4)	77.5±0.3 (+0.7)	68.7±0.3 (+2.0)	+1.8
	Feat-RGNN	78.4±1.3 (-1.8)	79.3±0.3 (+2.3)	79.6±0.2 (+4.7)	77.7±0.4 (+0.9)	68.1±0.6 (+1.5)	+2.2
	Feat&PC-RGNN	79.5±0.2 (+2.9)	80.5±0.3 (+3.5)	74.7±0.2 (-0.2)	76.3±0.2 (-0.5)	70.8±1.1 (+4.2)	+2.0
	LightGCN	78.9±0.1 (+2.3)	80.1±0.2 (+3.2)	76.2±0.2 (+1.3)	77.1±0.5 (+0.3)	67.6±0.4 (+1.0)	+1.6
	Feat-LightGCN	80.1±0.1 (+3.5)	80.1±0.1 (+3.2)	77.9±0.2 (+3.0)	76.0±0.1 (-0.9)	70.7±0.3 (+4.1)	+2.6
	Feat&PC-LightGCN	79.3±0.1 (+2.8)	78.9±0.2 (+2.0)	77.6±0.2 (+2.7)	79.2±0.2 (+2.4)	69.2±0.3 (+2.6)	+2.5

The results are in large part coherent with those in the main text: although RGNN architectures can perform better than the

baselines, they usually underperform with respect to the LightGCN architectures, as it happens for the recommendation tasks.

## 6 Fairness in Ranking and Pairwise Comparisons

*“In all chaos there is a cosmos, in all disorder a secret order.”*

– Carl Jung [75]

This chapter investigates fairness in hierarchical systems, focusing on ranking algorithms and pairwise comparison frameworks. While the previous chapter examined fairness in network structures, where outcomes depend on patterns of connectivity, many algorithmic systems instead operate by ordering individuals or items into hierarchical structures. Rankings determine access to opportunities such as employment, funding, visibility in search results, or admission to selective programs. In such contexts, even small distortions in the ranking process can translate into large disparities in exposure and opportunity.

Unlike classification systems that produce independent predictions for each individual, ranking algorithms operate on relative judgments: the position of an item depends not only on its own attributes but also on how it compares to all other candidates. Consequently, fairness cannot be evaluated solely at the level of individual predictions. Instead, it requires examining the entire pipeline through which merit is inferred, compared, and aggregated into an ordered hierarchy.

The works presented in this chapter contribute to RQ3 by investigating different sources of unfairness that may arise throughout the ranking pipeline. In particular, the chapter considers three stages of this process: the generation of pairwise comparisons, the recovery of rankings from sampled comparisons, and the aggregation of rankings into a final ordered list. In Section 6.1, we introduce a probabilistic framework that models evaluator bias in pairwise comparisons in order to recover a more accurate latent ranking. In Section 6.2, we study how the sampling of pairwise comparisons interacts with ranking algorithms, showing how certain sampling strategies may lead to structural invisibility for some items. Finally, in Section 6.3, we examine the aggregation stage of ranking systems and present a fairness-aware Markov Chain method designed to ensure balanced visibility across demographic groups. Together, these studies analyze fairness across the entire ranking pipeline, highlighting how biases in human evaluations, data sampling, and aggregation algorithms can propagate through hierarchical systems and ultimately shape the distribution of opportunities.

## 6.1 Bias-Aware Ranking from Pairwise Comparisons

Many ranking systems rely on pairwise comparisons as a fundamental source of information. Instead of assigning absolute scores to items, evaluators are asked to compare pairs and indicate which item is preferred. This paradigm appears in a wide range of applications, including peer review, crowdsourced evaluations, hiring processes, and product ratings. Pairwise comparisons are often considered easier and more reliable for human annotators than direct scoring tasks.

However, human judgments are not always unbiased. Extensive research in psychology and behavioral economics has shown that evaluators may be influenced by implicit biases, stereotypes, or favoritism. When ranking algorithms treat these judgments as unbiased measurements of quality, the resulting rankings may inadvertently reflect these biases rather than the true merit of the evaluated items.

The work presented in this section addresses this challenge by introducing Bias-Aware Ranking from Pairwise Comparisons (BARP), a probabilistic model that explicitly estimates individual evaluator biases. By modeling the evaluation process itself, the method aims to disentangle systematic judgment distortions from the latent quality signal underlying the comparisons. The resulting framework enables the recovery of rankings that better reflect true item quality while accounting for heterogeneity and bias among evaluators.

### Authors' Contributions

---

<b>Contribution</b>	<b>Authors</b>
<b>Conceptualization:</b>	A. Ferrara and all authors
<b>Writing:</b>	A. Ferrara and all authors
<b>Methodology:</b>	A. Ferrara and all authors
<b>Formal Analysis:</b>	A. Ferrara
<b>Code:</b>	A. Ferrara
<b>Experiments:</b>	A. Ferrara

---

Data Mining and Knowledge Discovery (2024) 38:2062–2086  
<https://doi.org/10.1007/s10618-024-01024-z>



## Bias-aware ranking from pairwise comparisons

Antonio Ferrara<sup>1,2,3</sup> · Francesco Bonchi<sup>1,4</sup> · Francesco Fabbri<sup>5</sup> · Fariba Karimi<sup>3,6</sup> · Claudia Wagner<sup>2,7</sup>

Received: 5 December 2023 / Accepted: 14 April 2024 / Published online: 31 May 2024  
© The Author(s) 2024

### Abstract

Human feedback is often used, either directly or indirectly, as input to algorithmic decision making. However, humans are biased: if the algorithm that takes as input the human feedback does not control for potential biases, this might result in biased algorithmic decision making, which can have a tangible impact on people's lives. In this paper, we study how to detect and correct for evaluators' bias in the task of *ranking people (or items) from pairwise comparisons*. Specifically, we assume we are given pairwise comparisons of the items to be ranked produced by a set of evaluators. While the pairwise assessments of the evaluators should reflect to a certain extent the latent (unobservable) true quality scores of the items, they might be affected by each evaluator's own bias against, or in favor, of some groups of items. By detecting and amending evaluators' biases, we aim to produce a ranking of the items that is, as much as possible, in accordance with the ranking one would produce by having access to the latent quality scores. Our proposal is a novel method that extends the classic Bradley-Terry model by having a bias parameter for each evaluator which distorts the true quality score of each item, depending on the group the item belongs to. Thanks to the simplicity of the model, we are able to write explicitly its log-likelihood w.r.t. the parameters (i.e., items' latent scores and evaluators' bias) and optimize by means of the alternating approach. Our experiments on synthetic and real-world data confirm that our method is able to reconstruct the bias of each single evaluator extremely well and thus to outperform several non-trivial competitors in the task of producing a ranking which is as much as possible close to the unbiased ranking.

**Keywords** Pairwise comparisons · Evaluators' bias · Rankings · Bradley-Terry · Fairness

---

Responsible editor: Rita P. Ribeiro.

Extended author information available on the last page of the article

Springer

## 1 Introduction

Human decision bias is well-studied in the field of human computation (Chen et al. 2013; Kamar et al. 2015; Hube et al. 2019; Almaatouq et al. 2020; Liu et al. 2022): human characteristics, opinions, cognitive and social biases, as well as the way the human computation task is formulated, can result in biased human feedback. In turn, if the algorithm that takes as input the human feedback does not take into account and control for such potential biases, this might result in biased algorithmic decision making. In this paper, we focus on the task of ranking humans (or items) starting from pairwise comparisons, i.e., a collection of triples  $\langle i, j, e \rangle$  indicating that, according to the evaluator  $e$ , the item  $i$  is superior to  $j$ . Pairwise comparisons are widely used to collect relevance feedback from humans since comparative assessments of two items are easy and fast to obtain: this type of human feedback is typically collected by means of crowdsourcing experiments in which crowdworkers are presented with a pair of items/people from which they should select the more relevant one for a given task (e.g., searching for information about a certain topic, or selecting people for a given position). Alternatively, indirect relevance feedback can be inferred from human behavior (e.g., their click behavior, or the time they spend exploring certain options). Pairwise comparisons have been used in various contexts including hiring at scale (Kotturi et al. 2020; Sarma et al. 2016; Kuttal et al. 2021), investigating aspects of the labor activity (Koshkaldal et al. 2020), assessing political biases (Kuo et al. 2020), and comparing political texts (Carlson and Montgomery 2017). Furthermore, various methods have been proposed in the literature to rank from pairwise comparisons (Bradley and Terry 1952; Negahban et al. 2012; Chen et al. 2013). However, pairwise comparisons, based on human judgements, can be affected by the quality of the evaluators (Chen et al. 2013; Bugakova et al. 2019) and by various types of biases, including ordering effects and presentation biases (Bugakova et al. 2019; Beaver and Gokhale 1975; Davidson and Beaver 1977).

Of special interest for this paper, *in-group favoritism* and *out-group prejudice* are two prominent bias mechanisms that spring into action when humans judge people or items that belong to certain identity groups such as nationality, gender, or even political parties. These bias mechanisms produce systematic deviations from rational decision making that puts one group in an unfavorable position by systematically skewing the decisions against items/people of this group even if they objectively should be preferred. Our goal is to develop a method to accurately measure and account for group biases in pairwise comparisons.

More formally, we assume to have a collection of items (or people) to be ranked, and we assume that we are given pairwise comparisons of the items produced by a set of evaluators. While the pairwise assessments of the evaluators should reflect to a certain extent the latent (unobservable) true quality scores of the items, they might be affected by each evaluator's own bias against, or in favor, of some groups of items. By detecting and amending evaluators' biases, we aim to produce a ranking of the items that is, as much as possible, in accordance with the unbiased ranking, i.e., the one we would produce by having access to the latent quality scores.

Our proposed method, dubbed BARP (Bias-Aware Ranker from Pairwise comparisons), is based on a novel model that enhances the Bradley-Terry (BT) model (Bradley

and Terry 1952) by having a bias parameter for each evaluator which distorts the true quality score of each item, depending on the group the item belongs to. Thanks to the simplicity of the model, we are able to write explicitly its log-likelihood w.r.t. the parameters (i.e., items' latent scores and evaluators' bias). Then, the disentanglement of the true latent scores from the evaluators' bias can be achieved by maximum likelihood estimation.

The main principles and concepts of our problem and our proposed method are depicted in Fig. 1.

Interestingly and contrarily to most of the fair ranking literature, our method does not require to indicate any group as protected, instead, all groups are treated equivalently and the method is able to detect and fix bias in favor or against any group and without any prior information of the evaluators preferences.

We assess empirically, on both synthetic and real-world datasets, the performance of BARP in detecting evaluators' bias, thus producing a ranking that is, as much as possible, close to the unbiased ranking. We compare BARP with several non-trivial baselines, including the BT model (Bradley and Terry 1952) (which does not take into account the possibility of bias), some recent variants of the BT model, which take into consideration some forms of evaluators' quality and bias (Chen et al. 2013; Bugakova et al. 2019), spectral methods for ranking from pairwise comparison (Negahban et al. 2012), and methods for fair ranking (Zehlike et al. 2017) used as post-processing in combination with the BT model.

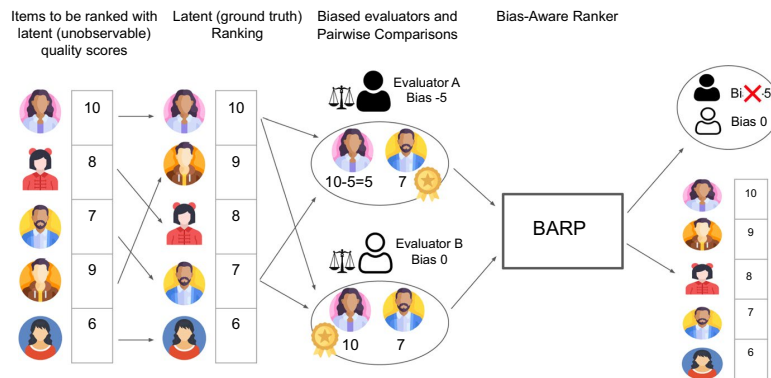


**Fig. 1** Depiction of the main principles and concepts of the problem and the proposed method, BARP. We are given a set of items to be ranked, in this case people, that belong to two groups: in this example, we consider binary gender as the attribute defining the two groups. Each items has a latent (unobservable) score which implicitly defines a ground truth (correct) ranking that we would like to produce, but we can not directly because we can not observe the latent scores. Instead, what we are given as input is a set of pairwise comparisons performed by some evaluators. The pairwise comparisons may be affected by the evaluators' own biases in favour or against a specific group. For instance, in the figure, Evaluator A has a bias against female candidates, while Evaluator B has no bias. As an effect of the implicit bias of Evaluator A, their pairwise comparisons are likely not to correctly reflect the true value of the candidates. BARP, by analyzing many input pairwise comparisons by many different evaluators, is able to detect and estimate evaluators' bias and to take this into account while producing a final ranking that is as close as possible to the ground-truth one

Our experiments on synthetic data (with ground-truth evaluators' bias) confirm that BARP is able to reconstruct the bias of each single evaluator extremely well ( $MSE < 0.3$ , w.r.t. evaluators' bias uniformly distributed in  $[-5, 5]$ ). Thanks to this, the ranking produced by BARP is much closer to the unbiased ranking than those produced by all the baselines: the stronger is the evaluators' bias, the larger the performance gap between our method and the baselines.

Our experiments on real-world data demonstrate the utility of BARP in identifying otherwise unknown biased evaluators. Utilizing the IMDB-WIKI-SbS dataset, which comprises pairwise comparisons of face snapshots, BARP effectively identify evaluators who frequently misperceive the ages of males compared to females, and vice versa. Furthermore, we showcase the applicability of our method in the context of admissions at law schools. We illustrate how BARP can mitigate differences in the rankings of individuals from different groups.

The rest of the paper is organized as follows. The next section presents a survey of the related literature. Section 3 introduces the formal problem statement, while Sect. 4 describes the BARP model, the learning method and its derivation. Section 5 contains the experiments on synthetic data. Results on real-word datasets are presented in Sect. 6. Finally, in Sect. 7, we conclude with a discussion on the limitations of our work and future research pathways.

## 2 Related work

Ranking from pairwise comparisons dates back to Kendall and Smith (1940) and, in the course of time, different methods have been proposed. Early works include counting and heuristic methods, such as David's score (David 1987). Seminal works, grounded in statistical and probability methods, like Bradley-Terry (1952) and Thurstone (1927) models, make distributional assumptions on the relationship between the comparisons and the ranking. The item's scores and ranking can, then, be recovered with maximum likelihood optimizations. Other methods exploit the interpretation of pairwise comparison as a directed graph, where nodes represent items and directed edges represent pairwise comparisons, leading to the use of random walk and spectral-based methods for ranking items. Examples in this category are RankCentrality (Negahban et al. 2012), SerialRank (Fogel et al. 2014), and GNNRank (He et al. 2022). Furthermore, Ranking from pairwise comparisons is substantially different from learning to rank, even when a pairwise learning to rank approach is employed. The goal of learning to rank is to construct a ranking model to rank new, unseen items by exploiting the information about features learned in the training data. Ranking from pairwise comparisons, instead, aims at constructing a rank of the available items, having at disposal only limited information about pairwise comparisons among them.

Several biases can affect pairwise comparisons. One of these is the order of presentation of the items in the pair. For example, in an experiment investigating a subject's sensitivity to small electrical shocks, the response to the second shock could be strongly modified by the first shock (Beaver and Gokhale 1975). In the literature, variations of the Bradley-Terry model have been proposed to model and account for such ordering effects (Beaver and Gokhale 1975; Davidson and Beaver 1977). An

additional series of effects relevant to our study are related to the evaluators and their behaviors. Evaluators's biases have received a lot of interest in other fields, for example in Natural Language Processing. How evaluators' demographics and beliefs can bias toxic language detection is pointed out in Sap et al. (2021), Liu et al. (2022), while Sap et al. (2019) highlights how insensitivity of evaluators to differences in dialect can lead to racial bias in automatic hate speech detection models. Finally, Geva et al. (2019) shows how the use of evaluator identifiers as features and the use of models that are able to recognize the most productive evaluators improves performances of Natural Language Processing models in various language understanding tasks.

Instead, the role of evaluators' biases in crowdsourced pairwise comparisons didn't receive an adequate attention. The main method that considers evaluators' quality is CrowdBT (Chen et al. 2013), where a parameter models evaluators' quality by quantifying the probability that an evaluator answers sincerely or not to the comparison tasks. Furthermore, evaluators' bias is considered in FactorBT (Bugakova et al. 2019). Similarly to FactorBT, our methods deal with evaluators' group biases, but with various significant differences. FactorBT models the probability that an evaluator, instead of basing their choices on the scores of the items of a pair, chose an item because of certain characteristics of the item, for example, being placed at the top of a screen. In FactorBT, how the perception of the scores is affected by evaluators' bias and how the perception of the scores relates to the probability that an item is selected are not considered. Instead, we model evaluators' behaviour with a parameter that directly relates to the perceived scores of the items and we establish a connection between the variation of the perceived score due to group biases and the probability of an item being selected. Furthermore, FactorBT analyzes the problem mainly from an accuracy perspective, while we investigate how our method affects the exposure and ranking of the different groups and we show how our method can be used to estimate the group bias of each individual evaluator.

Lastly, we want to point out the connection between the literature on fair ranking and our work. In a ranking, the desired good for an individual is to be ranked as higher as possible, and, in broad terms, fair ranking tries to avoid members of certain groups being systematically ranked lower than those of privileged groups (Zehlike et al. 2017). In the last years, various methods have been developed to achieve fair ranking, such as Singh and Joachims (2018), Zehlike and Castillo (2020), Celis et al. (2017), García-Soriano and Bonchi (2021). However, many of these methods are focused on learning to rank and are not well tailored to the task of ranking from pairwise comparisons considered in this paper.

### 3 Problem statement

We consider a collection of  $n$  items  $I = \{1, \dots, n\}$  where each item  $i \in I$  belongs to one group  $g_i \in G$  (where  $G$  is a discrete set), and has a latent (*unobservable*) quality score  $s_i \in \mathbb{R}$ . We denote  $\mathbf{g}$  and  $\mathbf{s}$  the vectors of groups membership and quality scores for all items.

We are given a set of pairwise comparisons among the items in  $I$ , produced by a set  $E$  of  $m$  evaluators. Each evaluator receives pairs of items to evaluate: we denote

the set of labeled pairs by the  $k$ -th evaluator as  $Q_k = \{(i, j) \in I \times I : i \succ_k j\}$ , where  $\succ_k$  is a relation, with  $i \succ_k j$  meaning that the  $k$ -th evaluator preferred the object  $i$  to the object  $j$ . Let  $Q$  be the multi-set of all the pairwise comparisons. In this paper, we assume that the multi-set  $Q$  is noisy and potentially inconsistent. Although the pairwise comparisons should reflect to a certain extent the latent quality scores of the items, the input comparisons might be affected by each evaluator's own bias against, or in favor, some groups in  $G$ . Moreover, inconsistent information might exist in  $Q$ , such as, for instance,  $i \succ_{k_1} j$  and  $j \succ_{k_2} i$  for two different evaluators  $k_1, k_2 \in E$ . Another example of inconsistent information is  $i \succ_k j$ ,  $j \succ_k l$ , and  $l \succ_k i$ .

The problem we tackle in this paper is to produce a ranking  $r^*$  of the items in  $I$ , that corrects for the evaluators bias, i.e., it is as close as possible to the ranking induced by the latent quality scores, denoted  $r(\mathbf{s})$ . We will hence evaluate the quality of the ranking  $r^*$  in terms of Kendall's Tau correlation (Kendall 1938, 1945) with  $r(\mathbf{s})$ .

#### 4 Method

In order to solve our problem we need to relate the scores  $\mathbf{s}$  and the pairwise comparisons  $Q$ . In devising our method, we build on top of the classic Bradley-Terry (BT) model (Bradley and Terry 1952). The BT model assumes that the probability that item  $i$  is preferred over  $j$  is defined as:

$$P(i \succ j) = \frac{e^{s_i}}{e^{s_i} + e^{s_j}}, \quad (1)$$

where  $e^x$  is the exponential function.

This probability has the following meaning: when evaluators are facing the decision of preferring one item over another, given the fact that they observe the item but they don't know the true score of the item, they prefer the correct item (i.e., the item with unknown higher score) with a certain probability that depends on the unknown scores. For example, when two items are similar (i.e. have similar unknown scores), it is hard for an evaluator to chose the correct one, while when one items is significantly better than the other, the evaluator is able to chose the best one correctly with a high probability.

Given the observed pairwise comparisons and the BT relational assumption, it is possible to estimate the underlying unknown scores according to the maximum likelihood principle. Indeed, the log-likelihood  $l$  of the scores can then be written as:

$$l(\mathbf{s}) = \sum_{(i,j) \in Q} \log \left( \frac{e^{s_i}}{e^{s_i} + e^{s_j}} \right), \quad (2)$$

and  $\hat{\mathbf{s}} = \arg \max_{\mathbf{s}} l(\mathbf{s})$  represents the vector of scores that better approximates the latent, unobserved vector of scores  $\mathbf{s}$ . The maximum of the log-likelihood can be found with standard numerical methods.

We observe that in the Bradley-Terry model, all evaluators are treated equally, and the model does not account for any differences in the quality of their contributions.

Hence, with some further assumptions, different behaviors of the evaluators can be modeled. For instance, in CrowdBT (Chen et al. 2013) it is assumed that evaluators might respond sincerely, randomly, or that they could be malicious or poorly informed. In particular, in CrowdBT, there is an additional parameter that models the probability that each evaluator agrees with the true pairwise preference, and allows for an interpolation between the possible behaviors above.

In our work, we focus on evaluators' behavior but from a different perspective. We assume that the perception of each evaluator is affected by the group membership of an item. For example, if evaluators, in a hiring scenario, exhibit a *gender bias* they might consider more frequently men as more fit for the position than women, when confronted with mixed-gender pairs. Essentially, we assume that evaluators can have an implicit preference for items belonging to a group which may lead to biased relevance feedback.

#### 4.1 Single binary attribute

For sake of simplicity of exposition, we start presenting the case of one single binary attribute (for example a binary version of the attribute gender), which induces two groups (males and females). Later we will extend our model to deal with multiple attributes and with non-binary attributes. It is worth stressing that *our method does not require to indicate any group as protected*: all groups are treated equivalently and the method is able to detect and fix bias in favor or against any group and without any prior information of the evaluators preferences.

In the binary setting, we model the bias of each evaluator  $k \in E$  with a bias parameter  $\theta_k \in \mathbb{R}$ . Taken one of the two groups as reference (it is not relevant which one), the interpretation is that an evaluator perceives the scores of the item  $i$  as  $s_i + \theta_k$ , if the item  $i$  belongs to the reference group, or equivalently,  $s_i - \theta_k$  if the item belongs to the other group. In the gender example, suppose we take the group females as reference: the evaluator  $k \in E$  with a bias parameter  $\theta_k \in \mathbb{R}$ , in a direct comparison between a male and a female, will be biased in favor of the female if  $\theta_k > 0$ , or in favor of the male if  $\theta_k < 0$ .

Formally, let  $\gamma_k = e^{\theta_k}$ , the probability that item  $i$  is preferred over  $j$  by the  $k$ -th evaluator is as follows:

$$P(i >_k j) = \frac{\gamma_k^{\delta_{g_i g}} e^{s_i}}{\gamma_k^{\delta_{g_i g}} e^{s_i} + \gamma_k^{\delta_{g_j g}} e^{s_j}}, \quad (3)$$

where  $\delta$  is the Kronecker delta, that is  $\delta_{g_i g} = 1$ , if  $g_i = g$  and  $\delta_{g_i g} = 0$ , if  $g_i \neq g$ . Such a multiplicative factor on the probability (or equivalently an additive factor on the scores) is grounded in the statistical literature of pairwise comparisons, as Davidson and Beaver (1977) used an analog parameter to model the effect of the order of presentation within the pairs, sometimes also referred to as the home advantage effect. Here, we take a similar functional form and, instead of using it to account for order of presentation effects, we extend it to account for group bias in the evaluations.

Furthermore, one may notice that when  $g_i = g_j$  the factor  $\gamma_k$  cancels out, correctly reflecting the assumption that the evaluators show only a preferential behavior when faced with the evaluation of items belonging to two different classes, and not affecting within classes evaluations.

Equation 3, can also be written in terms of  $\theta_k$  as:

$$P(i \succ_k j) = \frac{e^{s_i + \theta_k \delta_{g_i g}}}{e^{s_i + \theta_k \delta_{g_i g}} + e^{s_j + \theta_k \delta_{g_j g}}}, \tag{4}$$

This corresponds to Eq. 1, where, instead of the original scores  $s_i$ , we have biased scores  $s_i + \theta_k \delta_{g_i g}$  resulting from biased evaluations. This probability has the following meaning: when evaluators are facing the decision of preferring one item over another, they prefer the correct item with a certain probability that depends, not directly on the unknown scores as in BT model, but rather on their biased perception of the unknown scores.

Disentangling the contribution of the scores and the group bias of the evaluators, we can obtain an unbiased estimation of the unknown scores. Indeed, given the observed pairwise comparisons  $Q_k$  for each evaluator  $k$ , one can compute  $\hat{s}$  (i.e. the estimate of the scores  $\mathbf{s}$ ) and the estimate of  $\theta_k$  (we will call them  $\hat{\theta}_k$ ) via a maximum likelihood estimation. In particular, the log-likelihood for the parameters  $\mathbf{s}$  and  $\theta = (\theta_1, \dots, \theta_m)$  can be written as:

$$l(\mathbf{s}, \theta) = - \sum_{k=1}^m \sum_{(i,j) \in Q_k} \log \left( 1 + e^{-\left(s_i + \theta_k \delta_{g_i g} - s_j - \theta_k \delta_{g_j g}\right)} \right). \tag{5}$$

One way to optimize the objective function  $l(\mathbf{s}, \theta)$  is to use the alternating variables approach, also referred to as the coordinate descend or coordinate search method, Wright (2015), Nocedal and Wright (1999), which involves the iterative repetition of the following two steps. Firstly, keep  $\theta$  constant and optimize over  $\mathbf{s}$ . Then, keep  $\mathbf{s}$  constant and optimize over  $\theta$ . In particular, we used the equation of the first iteration of BFGS (Nocedal and Wright 1999) to determine, at each step, the parameters updates for both  $\mathbf{s}$  and  $\theta$ , with the gradients explicitly expressed as:

$$\begin{aligned} \frac{dl}{ds_i}(\mathbf{s}, \theta) = & \sum_{k=1}^m \left( \sum_{i:(i,j) \in Q_k} \left( 1 + e^{\left(s_i + \theta_k \delta_{g_i g} - s_j - \theta_k \delta_{g_j g}\right)} \right)^{-1} \right. \\ & \left. - \sum_{i:(j,i) \in Q_k} \left( 1 + e^{\left(s_i + \theta_k \delta_{g_i g} - s_j - \theta_k \delta_{g_j g}\right)} \right)^{-1} \right), \end{aligned} \tag{6}$$

where the sum on all  $i : (i, j) \in Q_k$  means the sum on all  $i$  such that  $i \succ_k j$  (by the definition of  $Q_k$ ), and

$$\frac{dl}{d\theta_k}(\mathbf{s}, \theta) = \sum_{(i,j) \in Q_k} \frac{\delta_{g_i g} - \delta_{g_j g}}{\left( 1 + e^{\left(s_i + \theta_k \delta_{g_i g} - s_j - \theta_k \delta_{g_j g}\right)} \right)}. \tag{7}$$

The pseudocode of our heuristic method, dubbed BARP (Bias-Aware Ranker from Pairwise comparisons), is summarized in Algorithm 1. BARP takes as input, the collection of items  $I$ , together with the classes that they belong  $\mathbf{g}$ , the set of pairwise comparison  $Q$ , the number of evaluators  $m$ . As stopping criteria, it also takes thresholds for the gradients and a maximum number of iterations. It outputs the maximum likelihood estimation of the scores  $\hat{\mathbf{s}}$ , from which the ranking of the object  $r^*$  is inferred, and the maximum likelihood estimation of the bias parameters of the evaluators  $\hat{\boldsymbol{\theta}}$ .

The algorithm starts by initializing  $\mathbf{s}^{(0)}$  and  $\boldsymbol{\theta}^{(0)}$ , until the maximum number of iterations or the stopping criteria are met, the algorithm updates the estimate for  $\mathbf{s}$  and  $\boldsymbol{\theta}$  with the following procedure. The algorithm computes the gradient with respect to  $\mathbf{s}$  and uses it to compute a one step update for  $\mathbf{s}$ . Then, the gradient of the log-likelihood with respect to the bias parameter vector  $\boldsymbol{\theta}$  is computed and used to update  $\boldsymbol{\theta}$ , in a similar way of what done for  $\mathbf{s}$ . The algorithm is flexible on how to exactly compute the updates of the parameters.

In details, we initialize  $\mathbf{s}^{(0)}$  and  $\boldsymbol{\theta}^{(0)}$  to the 0 vectors, alternatively the vectors could take any random initialization, we set the maximum number of iterations to 1000, and, as further stopping criteria, we stop if the norms of the gradient vectors for  $\mathbf{s}$  and  $\boldsymbol{\theta}$  are both smaller than  $10^{-5}$ .

#### Algorithm 1 BARP

---

**Input** :  $I, \mathbf{g}, Q, m$ , stopping criteria, max\_iters  
**Output**:  $\hat{\mathbf{s}}, \hat{\boldsymbol{\theta}}$   
 $\mathbf{s}^{(0)}, \boldsymbol{\theta}^{(0)} \leftarrow$  initialization;  
**for**  $t \leftarrow 0$  **to**  $(\text{max\_iters} - 1)$  **do**  
  **for**  $i \leftarrow 0$  **to**  $(n - 1)$  **do**  
    | compute  $\frac{dl}{ds_i}(\mathbf{s}^{(t)}, \boldsymbol{\theta}^{(t)})$  from eq. 6;  
  **end**  
  compute  $\mathbf{s}^{(t+1)}$  using  $\mathbf{s}^{(t)}$  and the gradient  $\frac{dl}{ds}$  ;  
  **for**  $k \leftarrow 0$  **to**  $(m - 1)$  **do**  
    | compute  $\frac{dl}{d\theta_k}(\mathbf{s}^{(t+1)}, \boldsymbol{\theta}^{(t)})$  from eq. 7;  
  **end**  
  compute  $\boldsymbol{\theta}^{(t+1)}$  using  $\boldsymbol{\theta}^{(t)}$  and the gradient  $\frac{dl}{d\boldsymbol{\theta}}$  ;  
  **if** *stopping criteria are met* **then**  
    | **Break**  
  **end**  
**end**  
**return**  $\hat{\mathbf{s}} = \mathbf{s}^{(t+1)}$  and  $\hat{\boldsymbol{\theta}} = \boldsymbol{\theta}^{(t+1)}$

---

#### 4.2 Multiple and non-binary attributes

We next extend BARP to account for the presence of multiple binary attributes and non-binary attributes.

Consider  $q$  binary attributes and for each item  $i$ , let  $\vec{g}_i \in \{0, 1\}^q$  be the vector of length  $q$ , where the  $t$ -th component is 1 if  $i$  belongs to the reference group for the  $t$ -th attribute and 0 otherwise. Similar to the single binary case, we model the behavior of the  $k$ -th evaluator by a bias parameter vector of length  $q$ ,  $\vec{\theta}_k \in \mathbb{R}^q$ . Equation 4, can hence be rewritten to account for the multiple binary attributes as:

$$P(i \succ_k j) = \frac{e^{s_i + \vec{\theta}_k \cdot \vec{g}_i}}{e^{s_i + \vec{\theta}_k \cdot \vec{g}_i} + e^{s_j + \vec{\theta}_k \cdot \vec{g}_j}}, \tag{8}$$

where  $\vec{x} \cdot \vec{y}$  indicates the scalar product between the vectors  $\vec{x}$  and  $\vec{y}$ . The log-likelihood for the parameters  $\mathbf{s}$  and the parameter matrix  $\vec{\theta} = (\vec{\theta}_1, \dots, \vec{\theta}_m)$  can be written as:

$$l(\mathbf{s}, \vec{\theta}) = - \sum_{k=1}^m \sum_{(i,j) \in Q_k} \log \left( 1 + e^{-(s_i + \vec{\theta}_k \cdot \vec{g}_i - s_j - \vec{\theta}_k \cdot \vec{g}_j)} \right), \tag{9}$$

while the gradients become:

$$\begin{aligned} \frac{dl}{ds_i}(\mathbf{s}, \vec{\theta}) &= \sum_{k=1}^m \left( \sum_{i:(i,j) \in Q_k} \left( 1 + e^{(s_i + \vec{\theta}_k \cdot \vec{g}_i - s_j - \vec{\theta}_k \cdot \vec{g}_j)} \right)^{-1} \right. \\ &\quad \left. - \sum_{i:(j,i) \in Q_k} \left( 1 + e^{(s_i + \vec{\theta}_k \cdot \vec{g}_i - s_j - \vec{\theta}_k \cdot \vec{g}_j)} \right)^{-1} \right), \end{aligned} \tag{10}$$

and

$$\frac{dl}{d(\vec{\theta}_k)_t}(\mathbf{s}, \vec{\theta}) = \sum_{(i,j) \in Q_k} \frac{(\vec{g}_i)_t - (\vec{g}_j)_t}{\left( 1 + e^{(s_i + \vec{\theta}_k \cdot \vec{g}_i - s_j - \vec{\theta}_k \cdot \vec{g}_j)} \right)}, \tag{11}$$

where  $(\vec{x})_t$  indicates the  $t$ -th component of the vector  $\vec{x}$ . In this way, we are able to estimate the bias of the evaluators with respect to multiple binary attributes.

The case of a single attribute with more than two groups is dealt with in an analogous way. Assume that the attribute of interest induces  $q$  groups. Then, we will need a vector  $\vec{\theta}_k \in \mathbb{R}^{q-1}$  of  $q - 1$  parameters to model the bias of the evaluator  $k$ . We only need  $q - 1$  parameters as the effect on the  $q$ -th group is implicitly determined as  $-\sum_{t=1}^{q-1} (\theta_k)_t$ , where  $(\theta_k)_t$  indicates the  $t$ -th component of  $\theta_k$ . (This extends the particular case of a single binary attribute, where there are two groups and one parameter and  $\theta_k$  for, e.g., male is equal to  $-\theta_k$  for, e.g., female). Furthermore, for an item  $i$ , the vector  $\vec{g}_i \in \{0, 1\}^{q-1}$  will have all components as 0 if  $i$  belongs to the  $q$ -th group and all components as 0 except the  $t$ -th equal to 1 if  $i$  belongs to the  $t$ -th of the other  $q - 1$  groups. Note that any of the groups can equivalently be the  $q$ -th group.

It is further possible to combine multiple (non binary) attributes. Let's assume to have  $\vec{g}_i \in \{0, 1\}^q$  and  $\vec{g}'_i \in \{0, 1\}^{q'}$  (representing two different attributes with  $q + 1$  and  $q' + 1$  groups respectively) we can simply stack  $\vec{g}_i$  on the top of  $\vec{g}'_i$ , obtaining a new vector of  $q + q'$  components. Analogously, it will be necessary a parameter vector  $\theta_k \in \mathbb{R}^{q+q'}$  of length  $q + q'$  for each evaluator  $k$ .

### 4.3 Dealing with intersectionality

Based on Crenshaw's theory (Crenshaw 2013), "Intersectionality states that interaction along multiple dimensions of identity produces unique and differing levels of discrimination for various possible sub-groups" (Gohar and Cheng 2023). Intersectionality focuses on the fact that sub-groups, defined as the intersection of multiple attributes (e.g., black women), might be particularly penalised or favored. BARP is able to deal with intersectionality by adding the following components. For each intersectional group that needs to be modeled, a new component, with value 1 if item  $i$  belong to that intersectional group and 0 otherwise, needs to be added to each vector  $\vec{g}_i$ . Furthermore, for each intersectional group and for each evaluators' bias vector  $\vec{\theta}_k$ , a new bias parameter, that will be estimated by BARP, needs to be added. In general, we recommend incorporating an intersectional component when experts' knowledge indicates potential discrimination issues related to such intersectionality. Furthermore, one can firstly use BARP without intersectional parameters and then compare the distributions of the scores of the items of intersectional groups with the distribution of all items' scores. If there are significative differences for an intersectional group, it suggests that such group has been discriminated/favoured and that explicit evaluators' bias parameters for that intersectional group should be added.

## 5 Experiments on synthetic data

In this section, we assess the effectiveness of our method using synthetic data. The advantage of using synthetic data is to have the ground truth for the evaluators' biases and the items' latent quality scores. In this way, we can assess how well our method is able to estimate evaluators' bias and if it can effectively reconstruct an unbiased ranking. Furthermore, it allows us to explore how certain factors, such as the total number of comparisons, affect the performance of our method. More in details, our empirical analysis is aimed at answering the following research questions:

- To what extent does evaluators' bias affect ranking from pairwise comparisons methods?
- To what extent can BARP reconstruct the ground truth (unobservable) ranking, thus mending evaluators' bias?
- Can BARP estimate the bias of each evaluator correctly?
- Which conditions affect the performance of our method?

In Sect. 6, we also present an empirical analysis on real-world datasets.

### 5.1 Synthetic dataset generation

Our experimental setup consists of 100 items to be ranked, each assigned a latent quality score (denoted as  $s$ ), drawn from a normal distribution  $N(0, 5)$ . Among these items, 70 belong to group  $g_a \in G$ , while the remaining 30 belonged to group  $g_b \in G$ . Additionally, we consider 50 evaluators, each characterized by a group bias parameter sampled from a normal distribution. The bias parameter represented an additive value, either positive or negative, applied uniformly to all elements within one of the two groups. Subsequently, taking into account their respective biases, each evaluator assesses 100 randomly generated pairs. More specifically, consider two items  $i, j \in I$  with latent quality score  $s_i$  and  $s_j$  respectively, that are to be compared by an evaluator  $k \in E$  with bias parameter  $\theta_k$ : following the literature, e.g., Chen et al. (2013), Negahban et al. (2012), Chen and Suh (2015), the pairwise comparison is produced stochastically according the probability in Eq. 4. This process allows us to accumulate a total of 5000 labeled pairwise comparisons.

### 5.2 Baselines and measures

As baselines for comparison we consider the Bradley-Terry model (Bradley and Terry 1952) (BT), which consists in the maximization of the likelihood of Eq. 2, as a baseline for parametric statistical methods. We also considered CrowdBT (Chen et al. 2013), a variation of the Bradley-Terry, that includes evaluators and estimation of their reliability, and FactorBT (Bugakova et al. 2019) a variation of CrowdBT, that assumes that evaluators, with a certain probability, instead of basing their choices on the scores of the items, can chose an item because of its belonging to a certain group. Furthermore, we include RankCentrality (Negahban et al. 2012) as a representative of graph and spectral methods, that exploit the representation of the items as nodes in a graph and of the pairwise comparisons as edges. With this graph representation, the ranking of the items can be seen as the stationary distribution of a random walk. Finally, we consider the FA\*IR post-processing method (Zehlke et al. 2017), that consists in re-ranking an output ranking (in this case the output of BT) to ensure that each group have enough members at the top of the ranking so to satisfy certain statistical constraints.

The main measure we consider is the reconstruction accuracy of the true latent ranking, computed in terms of Kendall's Tau correlation coefficient, adjusted for ties, Tau-b (Kendall 1945), between the true latent scores  $s$  and the scores  $\hat{s}$  estimated by the different methods. The measure ranges between  $-1$  (complete inversion) and  $1$  (perfect agreement). Any pair of pairs  $(s_i, \hat{s}_i)$  and  $(s_j, \hat{s}_j)$ , where  $i < j$ , is said to be concordant if either both  $s_i > s_j$  and  $\hat{s}_i > \hat{s}_j$  holds or both  $s_i < s_j$  and  $\hat{s}_i < \hat{s}_j$ ; otherwise, they are said to be discordant. The pair  $\{(s_i, \hat{s}_i), (s_j, \hat{s}_j)\}$  is said to be tied if and only if  $s_i = s_j$  or  $\hat{s}_i = \hat{s}_j$ ; a tied pair is neither concordant nor discordant. Then, the Kendall's Tau-b coefficient is defined as follows:

$$\tau_b = \frac{n_c - n_d}{\sqrt{(n_c + n_d + t_s)(n_c + n_d + t_{\hat{s}})}}$$

where  $n_c, n_d$  are respectively the the number of concordant and discordant pairs,  $t_s$  is the number of tied values in  $s$  only and  $t_{\hat{s}}$  is the number of tied values in  $\hat{s}$  only.

Further, we measure group specific differences in exposure in a ranking following Singh and Joachims (2018). We define the exposure for a group  $g$  as:

$$\text{Exposure}(g) := \frac{1}{|g|} \sum_{i \in g} \frac{1}{\log_2(r_i^* + 1) + 1}.$$

Then, the difference in exposure received on average by the items in two groups  $g_a$  and  $g_b$  is simply computed as  $\text{Exposure}(g_a) - \text{Exposure}(g_b)$ . Values, positive or negative, far from 0 are undesirable.

5.3 Results

Figures 2 (Left) and (Right) show that our method is able to correctly reconstruct the unbiased rank, despite the existence of group biases in the evaluators' judgments. In the two plots, we progressively increase the average group bias of the evaluators and its standard deviation, reporting on the horizontal axis the mean (or std) of the normal distribution from which the group bias of each evaluator is sampled. Our results show that the baseline methods become increasingly inaccurate when rising the average evaluators' group bias and also suffer from increases in the standard deviation, while the accuracy of our method is hardly affected.

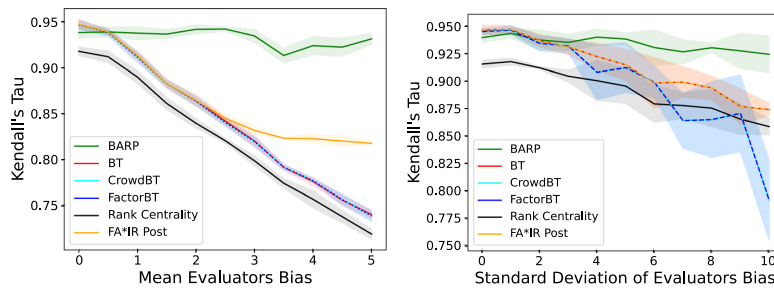


**Fig. 2** (Left) Comparison of different methods with increasing evaluators' group bias. As the group bias of the evaluators increases, the Kendall's Tau for all the methods, except BARP, decreases. This indicates that baseline methods, including FactorBT and FA\*IR that have access to the group information, are not able to correctly reconstruct the ranking of the items if the evaluators exhibit a systematic group bias. (Right) Comparison of different methods with increasing variance in evaluators' group bias. The mean of the evaluators is 0, hence, some evaluators favor one group and some others favor the other group, while on average the comparisons result equally biased in both directions. However, accounting for the group bias of the single evaluators ensures that the accuracy of our method is not decreasing

Increasing the mean of evaluators bias, BT and Rank Centrality are not able to deal with the fact that items of the penalized group are erroneously being relegated to lower positions in the ranking. CrowdBT and, interestingly, also FactorBT try to find evaluators that sometimes answer randomly, but, since the comparisons are driven by systematic bias, both fails to detect such evaluators' bias and they both behave as the simple BT model. Finally, the FA\*IR post-processing, when the group bias in the ranking become significative, by partially addressing this bias it is able to mitigate part of the accuracy reduction.

Instead, when the standard deviation is increased and some evaluators might show extreme group bias, CrowdBT and FactorBT, mistakenly, assume that some evaluators answer adversarially, that is always answers the opposite of what the true scores would suggest. We noticed this behaviour by looking at the estimated parameters of the evaluators, and this explains their worst performance. Furthermore, since on average evaluators are equally biased in both directions, FA\*IR does not detect significant violations and does not modify the ranking output of BT.

In the case in which the evaluators' mean bias is different from 0, the reduction in the accuracy of the methods, except BARP, is connected with the fact that the items of the group penalized are erroneously being relegated to lower positions in the ranking. In substance, methods that do not correctly model bias tend to penalize one group if the judgements of the evaluators are biased. We show this in Fig. 3 (Left) by computing the differences in the exposure received on average by the items in different groups. Our results indicate that with increasing average group bias of evaluators most methods show increasing differences in the exposure of different groups in a ranking. Unlike most methods, BARP based rankings are not affected by increasing evaluator bias and lead to relatively equal group exposure.

Besides being able to correctly rank items even in the presence of evaluators' group bias, our method further allows to identify the amount of group bias of each single evaluator. We investigate this in Fig. 3 (Right). In particular, we create

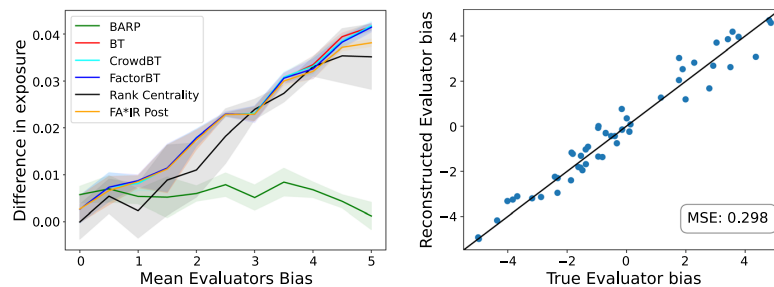


**Fig. 3** (Left) Difference in the exposure of the groups. Mending the bias of the evaluators BARP avoids that the items belonging to different groups receive different exposure in the ranking. (Right) Reconstruction of the individual bias of each evaluator. Each point represents an evaluator. The horizontal axis depicts the simulated ground-truth bias of each evaluator and the vertical axis represents the BARP based estimation of the individual biases. For each evaluator, we can individuate their bias quite accurately

comparisons where the single evaluators have different biases uniformly sampled in  $[-5, 5]$ . A negative bias means that the evaluator favors group  $g_a$  and a positive one means that the evaluator instead has a bias in favor of the items belonging to group  $g_b$ . Figure 3 (Right) reports a scatter-plot comparing the ground-truth evaluators' bias with the estimated one. Our results show that BARP allows to accurately reconstruct this bias starting from the pairwise comparisons of items only.

Next, we investigate multiple factors that might affect the performance of our method. Firstly, we are interested in how the total number of pairwise comparisons available, the amount of pairwise comparisons evaluated by each evaluator, and the number of evaluators affect the accuracy of our ranking recovery method. We analyze this in Fig. 4 (Left). We notice two main effects. The first is that when there are more total pairs, the method is able to better reconstruct the ground truth ranking (i.e. Kendall's Tau closer to 1). This is as expected, as having more pairwise comparisons implies having more information, allowing for better estimations. The second effect refers to the number of evaluators that produce a fixed total number of pairwise comparisons. Moving along the anti-diagonal in the heatmap, one can see that it is slightly better to have less evaluators evaluating more pairs rather than having more evaluators evaluating less pairs. This is because, with more information per evaluator, we are better able to estimate the group bias of each evaluator, and hence to better reconstruct the true ranking. However, this effect is less pronounced compared to the effect of the total amount of pairwise comparisons which is the most important factor that effects the accuracy of our method.

Another factor that might affect the results is the dispersion of the ground truth scores. If all items are similar to each other with respect to their ground truth scores, reconstructing the ranking is more difficult, even in the absence of bias. We study this factor in Fig. 4 (Right) by reporting the Kendall's Tau score achieved by our method while varying the relative distance between the scores. For example, when the scores are normally distributed with a small variance it is

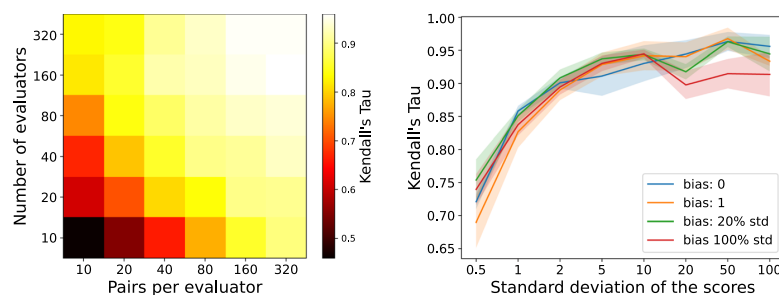


**Fig. 4** (Left) Number of pairwise comparisons. The heatmap contains the Kendall's Tau ranking reconstruction scores (1 is best), varying the number of evaluators and the number of pairs annotated by each evaluator. Increasing the total number of pairs, i.e. moving up or to the right in the heatmap, the ranking becomes more accurate. (Right) The effect of the values of the scores. The higher the distance between the scores, the easier it is to reconstruct the original ranking

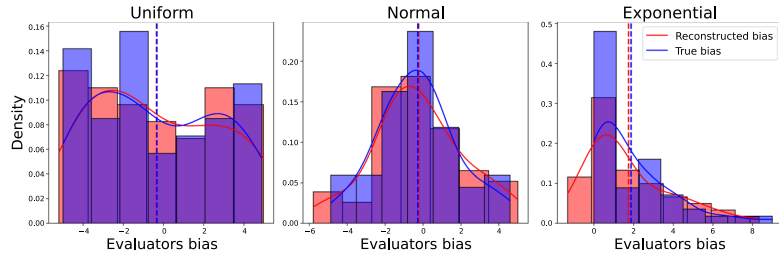


Fig. 5 Reconstruction of evaluators' bias under different distributions of the bias: uniform (Left), normal (Center), and exponential (Right)

harder to correctly recover the original ranking for the above-mentioned reasons (as the comparisons depend on the relative differences shifting the mean of the scores doesn't have any effect).

Furthermore, one could argue that the distribution of the group bias of the evaluators could depend on different situations and scenarios. Figure 5 illustrates the capability of BARP to reconstruct the bias under different distributions: uniform (Left), normal (Center), and exponential (Right). Our results show that independently of the shape of the group bias distribution that we use to sample the evaluator bias, BARP accurately estimates the bias of evaluators.

Finally, in Fig. 6, we examined evaluators with a bias against groups having attribute values of 1 for two binary attributes. This bias specifically penalizes items with both attribute values set to 1 (depicted as red items in the figure). On the left, we can see how the ranking obtained with Bradley-Terry (similarly happens for the other methods, except BARP), ranks systematically lower items of the disadvantaged groups. On the other hand, we illustrate how BARP can reconstruct the ranking of

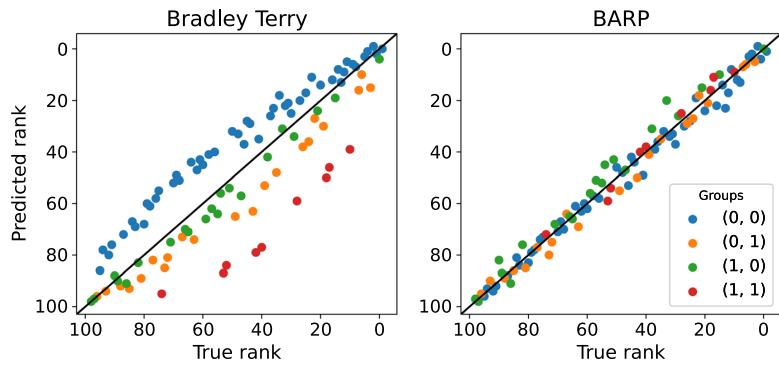


Fig. 6 Ranking with multiple groups. (Left) The ranking reconstruct by BT (as an example) penalizes certain groups over others due to its inability to account for evaluators group bias. (Right) BARP avoids inequalities between the groups and better reconstructs the true rank of the items

the items accurately and contrast the disadvantage of certain group of items, even in the presence of combined multiple groups effects.

## 6 Experiments on real-world data

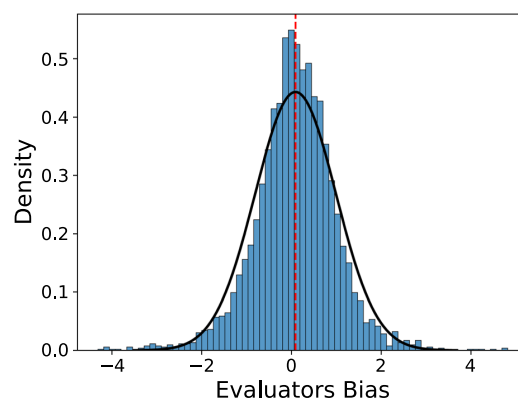
In this section we report applications of our method to two real-world datasets. In these cases, contrarily to the case of synthetic data discussed in the previous section, we do not have access to the evaluators' ground truth bias.

### 6.1 People's age evaluation dataset

For the empirical analysis, we consider the IMDB-WIKI-SbS (Pavlichenko and Ustalov 2021), a recently released large-scale dataset for evaluating pairwise comparisons. The dataset contains 9150 images appearing in 250,249 pairs annotated via crowdsourcing. The dataset uses a subset of images and information about age and gender from the IMBD-WIKI dataset (Rothe et al. 2018), with a balanced distributions of age and gender. In the pairwise comparison task crowdworker were asked to judge which of the two presented people is older. The pairs of face-shot images were presented to 4,091 workers, with each pair annotated by only one unique worker. In this way, on average, each worker annotated around 60 pairs (excluding additional control tasks).

In order to investigate the gender group bias of the evaluators, we apply BARP to the set of pairwise preferences. Figure 7 reports the distribution of the gender group bias of the annotators according to the estimation of our model. Choosing as convention the group  $g$  to be the male group, the interpretation of the bias of the evaluators is the following: an evaluator  $k$  with a bias of  $\theta_k > 0$ , perceives males as if they were  $\theta_k$  years older than what they are, when they are compared to females. Instead, a bias of  $\theta_k < 0$  implies that the males are perceived as  $\theta_k$  years younger than what

**Fig. 7** IMDB-WIKI-SbS dataset: Distribution of the group bias of the evaluators. Positive values indicate a tendency to perceive males as older, and negative values indicate a tendency to perceive females as older, when compared with the opposite gender



they are, when compared to the opposite gender. The distribution of the bias of the evaluators resembles the distribution of a Gaussian with a mean close to 0. This means that, averaging on all evaluators, we would not see a clear effect against a group, but single evaluators might still exhibit a gender bias in their age evaluations.

We further investigate, in Fig. 8, the estimated gender group bias of the individual evaluators by relating them to the amount and types of errors that evaluators are committing in the evaluation of gender-mixed and single-gender pairs. Note that the ground-truth scores for age are only used to calculate the errors while the BARP

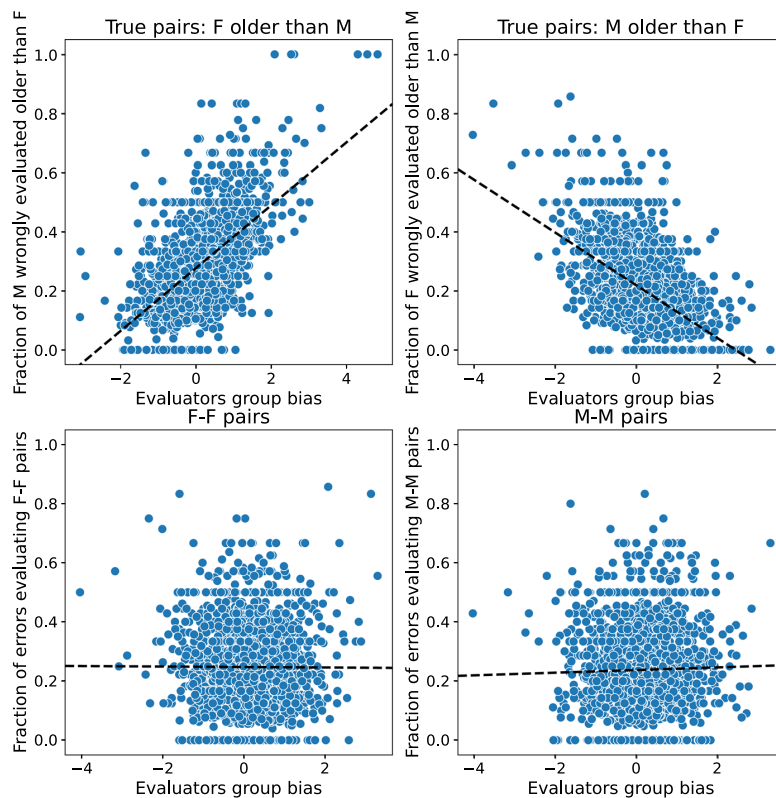


**Fig. 8** Relationship between evaluators' gender group bias and errors in the evaluation of pairwise comparisons. The plots in the first row depict pairs in which a male (M) face is compared with a female (F) face. The horizontal axis depicts the BARP estimate of the evaluator bias, while the vertical axis depicts the error rate. In the left plot only the pairs in which the woman is older than the man are depicted, and vice versa on the right. One can see that the BARP based estimate for the gender bias of the evaluator is correlated with the fraction of errors that evaluators conduct. The plots on the second row represent within group comparisons (i.e. male-male or female-female). While evaluators also commit errors here, the error seems to be unrelated from the group bias of evaluators

estimates do not use this information. In the plots of the first row, there are the pairs in which a male (M) is compared with a female (F). On the left plot, the pairs in which the female is older than the man, and vice versa on the right. The plots on the second row represent within groups comparisons (i.e. male-male or female-female). On the horizontal axis is displayed the bias of each evaluator as computed with our method, while on the vertical axis is represented the error rate that an evaluator has when evaluating pairs of specific groups. The results are as expected. In the first plot, a high positive bias (i.e. perceiving man as older) is associated with more often evaluating a man as older than a woman, when this is not true. The opposite happens in the second plot, evaluators with negative bias, tend to commit more often the error of wrongly evaluating a woman as older than a man. In the bottom row, instead, we can see how the evaluators' group bias doesn't affect error when evaluating pairs of the same gender.

## 6.2 Law schools scores

As an additional example of application of BARP, we consider the US data from the Law School Admission Council survey (Wightman 1998; Alvarez and Ruggieri 2023). The dataset contains information about students' law school admissions test scores (LSAT), undergraduate grade-point average (UGPA), and z-scores of the first-year average grades (ZFYA). It also contains demographic information about the students. Following Alvarez and Ruggieri (2023), we consider as attributes a student's binary gender (male/female) and a binary race variable (white/non-white). The dataset comes in the form of tabular data and, in order to apply ranking from pairwise comparison methods, we randomly select  $n = 1000$  students and simulate pairwise comparisons considering their scores and grades in the following way. For each of the three LSAT, UGPA, and ZFYA, we sample 10,000 pairs, creating a pairwise preference relationship based on which student has a higher score/grade.

While ranking students based on their scores and grades might be considered as an objective criterion, in reality, racial disparities in access to education may result in systematic variations in scores (Reeves and Halikias 2017). We aim to investigate whether our proposed method can detect this bias and control for it. First, we use BARP to estimate the bias of the different scores/grades, considering in one case the gender and in the other the race. The results are reported in table 1.

We can notice that, for gender, the bias of the columns used to evaluate are nearly symmetric and close to zero, while for race the biases are higher and of the same sign. When we are not expecting bias, i.e. the case of gender, algorithms non group-bias-aware reconstruct scores and rank similarly as BARP. This is shown in the first

**Table 1** Estimated group bias with the BARP model

	LSAT	UGPA	ZFYA
Gender	0.334	- 0.358	0.074
Race	- 1.532	- 0.728	- 1.786

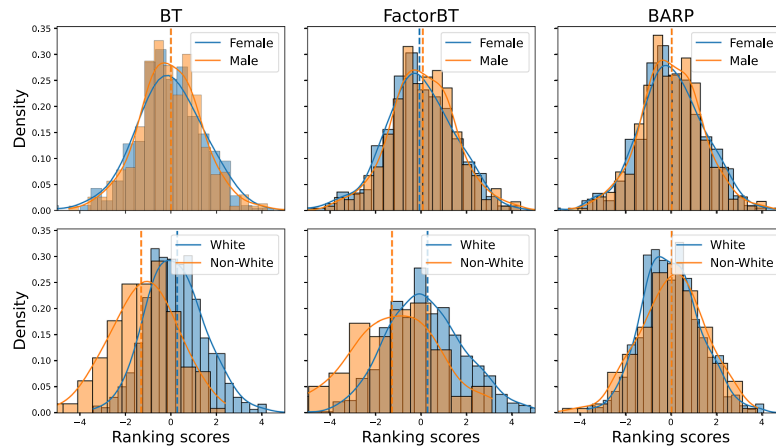


**Fig. 9** Distribution of the ranking scores. Even in the presence of group bias, the case of the attribute race, BARP tackles the differences in the distributions of the ranking scores across the different groups

row of Fig. 9. Instead, in the presence of group biases, i.e. the case of race, in the second row, we expect an algorithm that doesn't account for group bias to present inequalities in the distribution with respect to race. The second row on the left of Fig. 9 shows how Bradely-Terry, as an example of non group bias aware ranker, ranks a group, in this case white students, systematically higher than the other group, non-white students. Furthermore, also FactorBT is not able to correctly address the discrepancy in the scores in the presence of group biases. The reason can be traced in the fact that FactorBT does not models how the perception of the scores is affected by evaluators' bias. BARP, on the other hand, on the second row on the right of Fig. 9, by accounting for the group bias relative to the race, ranks the two groups more similarly.

## 7 Conclusions, limitations and future work

In this paper, we study the problem of correctly ranking items from pairwise comparisons in presence of evaluators' bias against some groups of items. We propose an algorithm that estimates the group bias of the individual evaluators and accounts for this bias while recovering the unknown ranking of the items. Our experiments confirm that our method is very effective at detecting and fixing the biases intrinsic in the pairwise comparisons, thus producing rankings which are closer to the latent one than methods that do not consider the possibility of biased evaluators. Furthermore, our experiments show how mending the bias of the evaluators avoids items from different groups receiving different exposure in the ranking.

We next discuss some limitations of this work which hint potential pathways for future research. First, it is often difficult to distinguish if the bias comes from

the evaluators or if it is the problem of different skill sets between different groups. Here, we assume that there should not be systematic differences in the true skills/scores for different groups. In reality, due to certain societal discrimination, the true scores may be related to the group identity. In such cases, our method can serve as a corrective method to reduce those systematic group-level biases. Second, we assume that the bias of each evaluator can be modeled with a constant parameter for each group, but there might be instances in which the bias might depend also on other factors, such as, for example, on the scores of the items themselves. We leave this as a future work. Furthermore, similar to all ranking methods from pairwise comparisons, BARP requires a minimum amount of pairwise comparison that scales with  $n \log n$ . Therefore the accuracy of the method decreases with the increasing the number of objects if this is not followed by an adequate increase in the number of comparisons.

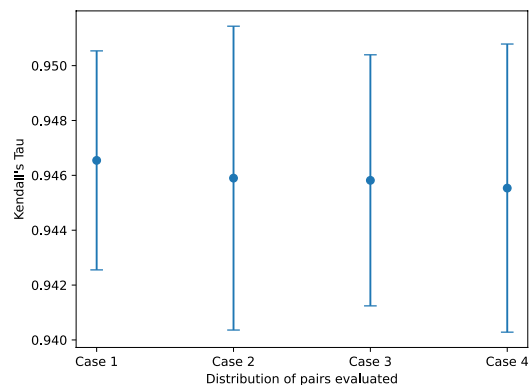
Despite these limitations, we believe that our model can be useful in detecting and addressing biases against groups of people in ranking from pairwise comparisons and we hope that our work can motivate further research in this topic.

## Appendix: Additional experiments

### Number of pairs evaluated by each evaluator

In the analysis with simulated data, we assumed that each evaluator assesses the same number of comparisons. However, in real-word scenarios, as for example happens in the IMDB-WIKI-SbS dataset, the number of pairs evaluated is different across evaluators. In Fig. 10, we show that this assumption does not significantly affect the recovery of the true ranking of the items. We consider four different distributions for the number of pairs evaluated by the evaluators. We keep fixed the number of evaluators at 50 and the total number of comparisons at 5000. As sake of

**Fig. 10** The distribution of pairs evaluated by the evaluators does not significantly affect the recovery of the true ranking of the items. On the horizontal axis are displayed four different distributions, while on the vertical axis, are reported the mean and standard deviation, across ten repetitions, of the Kendall's Tau correlation between the reconstructed ranking and the true ranking

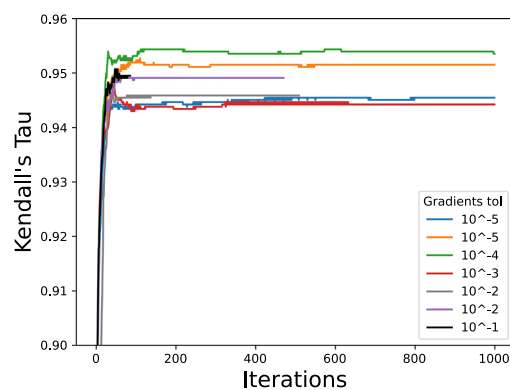


example, we consider four different alternatives. In the first case, all evaluators evaluate 100 comparisons each, in the second case we assume that the number of pairs evaluated by each evaluator is Poisson distributed with expected rate 100 (hence the total number of pairs evaluated is 5000 on average), in the third case, each of 10, 30, 50, 70, 90, 110, 130, 150, 170 and 190 pairs are evaluated by 5 evaluators, and lastly we consider an extreme case in which half evaluators evaluate only 5 pairs each while the other half evaluate 195 pairs each. In Fig. 10 we can see that despite considering different distributions for the pairs evaluated by the evaluators the Kendall's Tau between the reconstructed ranking and the true ranking does not differ significantly. One reason lies in the fact that even if the bias of a single evaluator could be less precise if they estimated only few pairs, it is also true that the impact on the reconstructed ranking of that evaluator is low since they only evaluated few pairs.

#### Approximation and stopping criteria

On the vertical axis of Fig. 11 we report the approximation obtained in terms of the Kendall's Tau, while on the horizontal axis we report the number of iterations of BARP. Each line correspond to a typical run with the tolerance for the gradient specified in the legend. Each run is performed on a different set of observed pairwise comparisons. Since multiple runs, even with different initial parameter initializations, on the same set of pairwise comparisons are almost equivalent, this allows us to compare how the approximation due to the choice of a stopping criteria compare with the overall noise in the observations. We can notice some facts. The first is that after the first around hundred of iterations, the Kendall's Tau is almost stable, meaning that at the ranking level the order of only very few pairs is swapped. The method does not rely very much on the choice of the values of stopping criteria on the gradient since even setting the values as big as  $10^{-1}$  leads to meaningful results. Lastly, the noise of stopping at a certain point (as long as we passed the initial

**Fig. 11** Approximation of BARP in reconstructing the original ranking in terms of the Kendall's Tau correlation with respect to the number of iterations and the stopping criteria on the gradients



around hundred iterations) is small compared to the overall noise that the actually observed comparisons induce.

**Acknowledgements** This work has received funding from the European Union’s Horizon 2020 research and innovation programme under Marie Skłodowska-Curie Actions (grant agreement number 860630) for the project “NoBIAS - Artificial Intelligence without Bias”. This work reflects only the authors’ views and the European Research Executive Agency (REA) is not responsible for any use that may be made of the information it contains.

**Funding** Open access funding provided by the project “NoBIAS - Artificial Intelligence without Bias”.

**Availability of data and materials** The code and datasets to reproduce our experiments can be found at: <https://github.com/Ambress92/Bias-Aware-Ranker-from-Pairwise-comparisons>.

### Declarations

**Ethics approval and consent to participate** This paper focuses on bias and fairness issues in ranking from pairwise comparisons. Although the goal is to mitigate such issues, there are several ethical aspects to be considered. First, in order to tackle bias issues we need access to the sensitive attributes (for example gender or race) for which we want to mitigate biases. Furthermore, ranking from pairwise comparison methods, and hence BARP as such, can be used in decision making contexts, such as hiring or university admissions, that can affect human lives. Moreover, we considered biases against groups of people, however discriminatory behaviours against single individuals might still exist and special attention is required in such cases.

**Open Access** This article is licensed under a Creative Commons Attribution 4.0 International License, which permits use, sharing, adaptation, distribution and reproduction in any medium or format, as long as you give appropriate credit to the original author(s) and the source, provide a link to the Creative Commons licence, and indicate if changes were made. The images or other third party material in this article are included in the article’s Creative Commons licence, unless indicated otherwise in a credit line to the material. If material is not included in the article’s Creative Commons licence and your intended use is not permitted by statutory regulation or exceeds the permitted use, you will need to obtain permission directly from the copyright holder. To view a copy of this licence, visit <http://creativecommons.org/licenses/by/4.0/>.

### References

- Almaatouq A, Krafft P, Dunham Y, Rand DG, Pentland A (2020) Turkers of the world unite: multilevel in-group bias among crowdworkers on amazon mechanical Turk. *Soc Psychol Personal Science* 11(2):151–159
- Alvarez JM, Ruggieri S (2023) Counterfactual situation testing: Uncovering discrimination under fairness given the difference. Preprint [arXiv:2302.11944](https://arxiv.org/abs/2302.11944)
- Beaver RJ, Gokhale D (1975) A model to incorporate within-pair order effects in paired comparisons. *Commun Stat Theory Methods* 4(10):923–939
- Bradley RA, Terry ME (1952) Rank analysis of incomplete block designs: I. the method of paired comparisons. *Biometrika* 39(3/4):324–345
- Bugakova N, Fedorova V, Gusev G, Drutsa A (2019) Aggregation of pairwise comparisons with reduction of biases. Preprint [arXiv:1906.03711](https://arxiv.org/abs/1906.03711)
- Carlson D, Montgomery JM (2017) A pairwise comparison framework for fast, flexible, and reliable human coding of political texts. *Am Polit Sci Rev* 111(4):835–843
- Celis LE, Straszak D, Vishnoi NK (2017) Ranking with fairness constraints. Preprint [arXiv:1704.06840](https://arxiv.org/abs/1704.06840)

- Chen X, Bennett PN, Collins-Thompson K, Horvitz E (2013) Pairwise ranking aggregation in a crowd-sourced setting. In: Proceedings of the sixth ACM international conference on web search and data mining, pp 193–202
- Chen Y, Suh C (2015) Spectral MLE: Top-K rank aggregation from pairwise comparisons. In: International conference on machine learning, pp 371–380
- Crenshaw K (2013) Demarginalizing the intersection of race and sex: a black feminist critique of antidiscrimination doctrine, feminist theory and antiracist politics. In: Feminist legal theories. Routledge, pp 23–51
- David HA (1987) Ranking from unbalanced paired-comparison data. *Biometrika* 74(2):432–436
- Davidson RR, Beaver RJ (1977) On extending the Bradley-Terry model to incorporate within-pair order effects. *Biometrics* 693–702
- Fogel F, d’Aspremont A, Vojnovic M (2014) Serialrank: spectral ranking using seriation. *Adv Neural Inf Process Syst* 27
- García-Soriano D, Bonchi F (2021) Maxmin-fair ranking: individual fairness under group-fairness constraints. In: KDD '21: The 27th ACM SIGKDD conference on knowledge discovery and data mining, pp 436–446
- Geva M, Goldberg Y, Berant J (2019) Are we modeling the task or the annotator? an investigation of annotator bias in natural language understanding datasets. In: Inui K, Jiang J, Ng V, Wan X (eds) Proceedings of the 2019 conference on empirical methods in natural language processing and the 9th international joint conference on natural language processing, EMNLP-IJCNLP, pp 1161–1166
- Gohar U, Cheng L (2023) A survey on intersectional fairness in machine learning: Notions, mitigation, and challenges. Preprint [arXiv:2305.06969](https://arxiv.org/abs/2305.06969)
- He Y, Gan Q, Wipf D, Reinert GD, Yan J, Cucuringu M (2022) GNNRank: learning global rankings from pairwise comparisons via directed graph neural networks. In: International conference on machine learning, pp 8581–8612
- Hube C, Fetahu B, Gadiraju U (2019) Understanding and mitigating worker biases in the crowdsourced collection of subjective judgments. In: Proceedings of the 2019 CHI conference on human factors in computing systems
- Kamar E, Kapoor A, Horvitz E (2015) Identifying and accounting for task-dependent bias in crowdsourcing. In: Proceedings of the AAAI conference on human computation and crowdsourcing, vol 3, no 1, pp 92–101
- Kendall MG (1938) A new measure of rank correlation. *Biometrika* 30(1/2):81–93
- Kendall MG (1945) The treatment of ties in ranking problems. *Biometrika* 33(3):239–251
- Kendall MG, Smith BB (1940) On the method of paired comparisons. *Biometrika* 31(3/4):324–345
- Koshkaldal I, Kniaz O, Rysanyanska A, Velieva V (2020) Motivation mechanism for stimulating the labor potential. *Res World Econ* 11(4):53–61
- Kotturi Y, Kahng A, Procaccia A, Kulkarni C (2020) Hirepeer: impartial peer-assessed hiring at scale in expert crowdsourcing markets. In: Proceedings of the AAAI conference on artificial intelligence, vol 34, pp 2577–2584
- Kuo T-S, Hankin M, Miranda L, Ying A, Wang C (2020) Assessing political bias using crowdsourced pairwise comparisons. In: Proceedings of the AAAI conference on human computation and crowdsourcing
- Kuttal SK, Chen X, Wang Z, Balali S, Sarma A (2021) Visual resume: exploring developers’s online contributions for hiring. *Inf Softw Technol* 138:106633
- Liu H, Thekinen J, Mollaoglu S, Tang D, Yang J, Cheng Y, Liu H, Tang J (2022) Toward annotator group bias in crowdsourcing. In: Proceedings of the 60th annual meeting of the association for computational linguistics
- Negahban S, Oh S, Shah D (2012) Iterative ranking from pair-wise comparisons. *Adv Neural Inf Process Syst* 25
- Nocedal J, Wright SJ (1999) Numerical optimization
- Pavlichenko N, Ustalov D (2021) IMDB-WIKI-SbS: an evaluation dataset for crowdsourced pairwise comparisons. Preprint [arXiv:2110.14990](https://arxiv.org/abs/2110.14990)
- Reeves RV, Halikias D (2017) Race gaps in sat scores highlight inequality and hinder upward mobility. Brookings Institute, Washington
- Rothe R, Timofte R, Gool LV (2018) Deep expectation of real and apparent age from a single image without facial landmarks. *Int J Comput Vis* 126(2–4):144–157

- Sap M, Card D, Gabriel S, Choi Y, Smith NA (2019) The risk of racial bias in hate speech detection. In: Proceedings of the 57th annual meeting of the association for computational linguistics, pp 1668–1678
- Sap M, Swayamdipta S, Vianna L, Zhou X, Choi Y, Smith NA (2021) Annotators with attitudes: how annotator beliefs and identities bias toxic language detection. Preprint [arXiv:2111.07997](https://arxiv.org/abs/2111.07997)
- Sarma A, Chen X, Kuttal S, Dabbish L, Wang Z (2016) Hiring in the global stage: profiles of online contributions. In: 2016 IEEE 11th international conference on global software engineering (ICGSE), pp 1–10
- Singh A, Joachims T (2018) Fairness of exposure in rankings. In: Proceedings of the 24th ACM SIGKDD international conference on knowledge discovery & data mining, pp 2219–2228
- Thurstone LL (1927) The method of paired comparisons for social values. *J Abnorm Soc Psychol* 21(4):384
- Wightman LF (1998) LSAC national longitudinal bar passage study. LSAC research report series
- Wright SJ (2015) Coordinate descent algorithms. *Math Program* 151(1):3–34
- Zehlike M, Bonchi F, Castillo C, Hajian S, Megahed M, Baeza-Yates R (2017) FA\*IR: a fair top-k ranking algorithm. In: Proceedings of the 2017 ACM on conference on information and knowledge management, pp 1569–1578
- Zehlike M, Castillo C (2020) Reducing disparate exposure in ranking: a learning to rank approach. In: Proceedings of the web conference, pp 2849–2855

**Publisher's Note** Springer Nature remains neutral with regard to jurisdictional claims in published maps and institutional affiliations.

### Authors and Affiliations

Antonio Ferrara<sup>1,2,3</sup> · Francesco Bonchi<sup>1,4</sup> · Francesco Fabbri<sup>5</sup> · Fariba Karimi<sup>3,6</sup> · Claudia Wagner<sup>2,7</sup>

✉ Antonio Ferrara  
antonio.ferrara@centai.eu

<sup>1</sup> CENTAI, Turin, Italy

<sup>2</sup> GESIS, Cologne, Germany

<sup>3</sup> TU Graz, Graz, Austria

<sup>4</sup> EURECAT, Barcelona, Spain

<sup>5</sup> Spotify, Barcelona, Spain

<sup>6</sup> Complexity Science Hub, Vienna, Austria

<sup>7</sup> RWTH Aachen University, Aachen, Germany

## 6.2 Fairness-Aware Ranking Recovery from Pairwise Comparisons

Even when pairwise comparisons are collected without systematic evaluator bias, the sampling process used to gather comparisons can still introduce structural distortions in the resulting ranking. In many real-world systems, it is infeasible to collect comparisons for every possible pair of items, and algorithms must instead recover rankings from a sparse set of sampled comparisons.

The way these comparisons are sampled can significantly influence the inferred ranking. Some items may receive many comparisons, while others may remain rarely evaluated. As a result, certain candidates may become structurally under-represented, limiting their chances of appearing in favorable ranking positions regardless of their true quality.

The work presented in this section studies the interaction between sampling strategies and ranking recovery algorithms. In particular, it investigates how different sampling mechanisms affect the visibility and representation of items in the resulting ranking.

### Authors' Contributions

---

Contribution	Authors
<b>Conceptualization:</b>	G. Ahnert, A. Ferrara, C. Wagner
<b>Writing:</b>	G. Ahnert, A. Ferrara, C. Wagner
<b>Methodology:</b>	G. Ahnert, A. Ferrara, C. Wagner
<b>Code:</b>	G. Ahnert, A. Ferrara
<b>Experiments:</b>	G. Ahnert

---

## Fairness-Aware Ranking Recovery from Pairwise Comparisons

Georg Ahnert  
georg.ahnert@uni-mannheim.de  
University of Mannheim  
Mannheim, Germany

Antonio Ferrara  
antonio.ferrara@intesasampaolo.com  
Intesa Sanpaolo AI Research  
Turin, Italy  
Graz University of Technology  
Graz, Austria

Claudia Wagner  
claudia.wagner@gesis.org  
GESIS–Leibniz Institute for the Social  
Sciences  
Cologne, Germany  
RWTH Aachen University  
Aachen, Germany

### Abstract

Pairwise comparisons based on human judgments are widely used to derive rankings, yet the biases embedded in these comparisons can propagate into downstream, algorithmically generated rankings. Such bias can reduce the visibility of underprivileged groups, with potentially profound consequences. In this work we analyze two points in the ranking pipeline where bias can emerge: (i) the selection of candidates that receive comparisons, and (ii) the comparison and ranking mechanisms themselves. To assess fairness in this context, we introduce a group-conditioned accuracy metric that captures how ranking quality varies across demographic groups.

Using both, synthetic and real-world datasets, we evaluate how state-of-the-art ranking recovery methods and sampling strategies influence accuracy and fairness. Our results show that Fairness-Aware PageRank and GNNRank with FA\*IR post-processing effectively mitigate existing biases in pairwise comparisons and improve the overall accuracy of recovered rankings. We discuss the trade-offs across approaches and release an open-source Python package to support reproducibility and further research on fair ranking recovery in Web-scale comparison systems.

### CCS Concepts

• **Information systems** → Content ranking; **Retrieval models and ranking**; • **Human-centered computing** → *Collaborative and social computing design and evaluation methods.*

### Keywords

Fairness, Ranking Recovery, Pairwise Comparisons

### ACM Reference Format:

Georg Ahnert, Antonio Ferrara, and Claudia Wagner. 2026. Fairness-Aware Ranking Recovery from Pairwise Comparisons. In *18th ACM Web Science Conference (WebSci '26)*, May 26–29, 2026, Braunschweig, Germany. ACM, New York, NY, USA, 10 pages. <https://doi.org/10.1145/3795766.3799744>

### 1 Introduction

Rankings of items or people are commonplace in, for instance, internet search [26], online hiring [16], academic admissions [42], or healthcare prioritization. Pairwise comparisons, which are judgements between pairs of items or individuals, are a commonly used

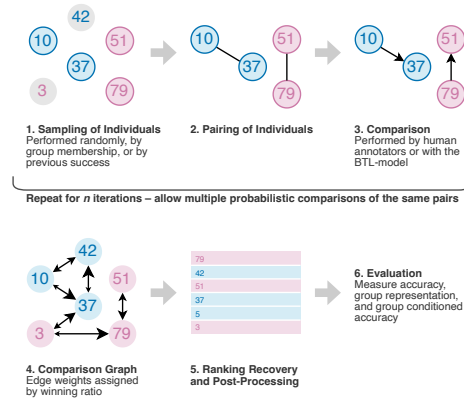


**Figure 1: Research Setup.** We investigate the effect of sampling individuals for pairwise comparison and of ranking recovery methods, on fairness and accuracy of a recovered ranking.

type of data from which to generate rankings. Rankings based on pairwise comparisons have been historically used in various contexts, including social science studies and psychometric measurements [21, 39, 40], the assessment of political preferences [24] and online hiring platforms [23, 25]. Recently, they have also been employed for human alignment of Large Language Models [38], to assess their outputs [27], and to extract data from them [28].

While pairwise comparisons are often considered to be less prone to inconsistencies and judgement errors than rating scale annotations [7, 22], they can still be subject to bias and systemic discrimination [29]. Research on algorithmic fairness has shown that with the increased relevance of machine learning, concerns regarding the introduction and perpetuation of discrimination must be taken seriously into consideration when algorithmic results are employed for decision making purposes [8]. While not without criticism [17], research on the quantification of fairness led to the development of fairness measures and the integration of fairness targets into machine learning algorithms [29]. In recent years, a sub-field on fairness in rankings has brought forth pre-, in-, and post-processing methods of ensuring fairness [47]. Still, existing



This work is licensed under a Creative Commons Attribution 4.0 International License. WebSci '26, Braunschweig, Germany © 2026 Copyright held by the owner/author(s). ACM ISBN 979-8-4007-2504-3/2026/05 <https://doi.org/10.1145/3795766.3799744>

ranking recovery from pairwise comparison methods have not been systematically evaluated regarding their impact on fairness, and the biases and the discrimination that may arise by skewed candidate selection in the pairwise assessments have not been adequately studied. Consider the following motivating example:

**EXAMPLE 1.** *A newly launched talent acquisition platform evaluates and ranks candidates by presenting pairs of CVs to human experts who work as external consultants to hiring companies. The experts assess which candidate from each pair has a stronger CV for a given position. Based on the evaluations of numerous candidate pairs, ranking recovery methods from pairwise comparison models are used to rank all candidates. Companies then use these rankings to hire suitable candidates. Although companies are generally satisfied with the rankings, it has been observed that certain demographic groups are consistently ranked lower. This discrepancy may be due to biases in the evaluations, the selection of candidate pairs, or the ranking recovery methods used.*

Our paper aims at bridging the gap in the knowledge about unfairness issues in ranking recovery from pairwise comparisons methods by (i) systematically analyzing how the biases in the selection of the pairs might perpetuate to the rankings, as shown in Figure 1, (ii) introducing a group-conditioned error measure tailored towards ranking recovery, and (iii) evaluating the performance of state-of-the-art ranking recovery methods and a fairness-aware algorithm developed for a different task and adapted to the ranking recovery problem, in terms of fairness and accuracy.

Our results on synthetic and empirical data show that under random sampling of individuals for comparison, resource-intense methods such as GNNRank [18] have little benefit over heuristics-based approaches such as David’s Score [10]. We find that Fairness-Aware PageRank [41], although not developed for ranking recovery from pairwise comparisons, is able to mitigate bias and to improve accuracy as measured against a latent ground-truth. Post-processing of recovered rankings using algorithms such as FA<sup>2</sup>IR [46] can further improve overall accuracy at the expense of group-conditioned accuracy. We provide an open-source Python package alongside our paper to facilitate replication and future work on fair ranking recovery<sup>1</sup>.

## 2 Related Work

Measuring perceived attributes through pairwise comparisons dates back to Thurstone [39], Zermelo [48], and Kendall and Smith [21]. Pairwise comparisons are generally incomplete and probabilistic, i.e., not all possible pairs are compared and a “stronger” individual might lose a comparison by chance. This probabilistic nature is also considered in models of rational choice theory [34], and can lead to the formation of *Condorcet cycles*, which are most prominently studied in the context of ballots [15, 45]. When only a limited number of comparisons between items or individuals can be drawn, pairing becomes crucial for accurate outcomes [36].

The context-agnostic problem of ranking recovery from pairwise comparisons has been addressed through approaches that can be roughly grouped into three categories: (i) heuristics-based methods such as David’s Score [10], (ii) eigenvector- or random-walk-based

such as RankCentrality [31], and (iii) similarity-based methods such as GNNRank [18]. Considering all three categories, we include a diverse set of state-of-the-art algorithms into our evaluation and describe them in more detail in Section 3.3.

Previous research evaluated the performance of ranking recovery methods regarding accuracy and efficiency. Zhang et al. [49] compare heuristics-based and learning-based ranking recovery methods. They conclude that “local inference heuristics” (e.g., David’s Score) are outperformed by “global inference heuristics” (i.e., random walk based methods). Further, they show that “global” heuristics have comparable performance to learning-based methods, as is also shown by Negahban et al. [31]. He et al. [18] include various baselines outperformed by GNNRank according to the authors’ original error measure. The results indicate that similarity based methods might have an accuracy advantage over eigenvector-based methods. Yet, none of these evaluations takes bias or fairness into account.

Initial work on fairness in machine learning primarily focused on classification tasks [8], with fairness in ranking recently attracting more attention [47]. Multiple methods have been proposed to achieve fair rankings in score-based ranking [5, 44] and (pairwise) learning-to-rank tasks [1, 16, 37, 46]. Both, however, substantially differ from ranking recovery from pairwise comparisons. In score-based ranking, a ranking is constructed given an utility score for each individual, and in (pairwise) learning-to-rank, a ranking is predicted from the individuals’ features. In contrast, pairwise comparisons between individuals is the only information available in ranking recovery from pairwise comparisons. Nevertheless, post-processing methods developed for score-based ranking and learning-to-rank tasks can also be applied to ranking recovery from pairwise comparisons. We include FA<sup>2</sup>IR [46] into our evaluation.

Furthermore, in the problem of rank aggregation, a list of rankings of all the candidates are aggregate to obtain a single ranking. The literature has started to study fairness in rank aggregation [6, 43]. In general, rank aggregation methods have rankings and not pairwise comparisons as input and they can not be applied to our problem. An exception is the post-processing method for rank aggregation, EPIRA [4], which we included in the analysis. The problem of ranking recovery from pairwise comparisons is also connected with ranked-choice voting system (election systems) methods [9, 11], since voters preferences often rely on pairwise ordering relationships. However, in our work, we focus on direct pairwise assessments, while voting is typically concerned with more than two alternatives in each comparison.

Lastly, it is worth to mention works that deal with annotators’ qualities and biases in ranking recovery from pairwise comparison methods [3, 7, 12]. In particular, Chen et al. [7] study how annotators might evaluate pairs randomly or intentionally wrong, and accounts for these behaviors. Instead, Bugakova et al. [3] analyses how confounding factors such as the position of online evaluated pairs in a screen might affect the rankings. Lastly, Ferrara et al. [12] investigate how group biases of each individual annotator might influence their assessments of pairs and consequently rank items of certain groups systematically higher or lower. However, all these works focus on the perspective of the annotators and strictly rely on having at disposal the identifier of which annotator evaluated which pairs. In many real world scenarios such annotators’ information is not available. For this reason, in our work, we take a

<sup>1</sup><https://github.com/wanLo/fairpair/>

different approach that it is not tied to annotators and their identifiers, instead, we focus on possible underlying scenarios that affect which candidate are selected for pairwise evaluation, and how these selection processes consequently affect the rankings of the items, possibly leading to unfair rankings.

### 3 Approach

The research setup is shown in Figure 1 and comprises six steps. We first establish pairwise comparisons through (step 1) sampling individuals from a population, (step 2) pairing them, and (step 3) comparing these pairs using human annotation or, when human annotation are not available, we simulate them with the Bradley-Terry-Luce (BTL) model [2]. Sampling, pairing and comparison is iteratively repeated to allow for multiple probabilistic comparisons of the same pair of individuals. We assume biases and discrimination to affect both the sampling and comparison steps, as we lay out in the following section, before describing derived sampling approaches.

From iterated pairwise comparisons, we obtain a comparison graph (step 4) in which edge weights indicate winning ratios. Ranking recovery methods take this comparison graph as input and output scores according to which the individuals in the graph are ranked (step 5). Post-processing might be applied to a recovered ranking to improve fairness. Finally, we evaluate the obtained ranking’s error and fairness against the latent skill score (step 6). For group fairness, we consider both measures of group representation and group-conditioned accuracy.

#### 3.1 Biases and Discrimination

We explore two stages in which bias and discrimination may enter and affect the final ranking: the selection of candidates for comparison and the comparison and ranking procedure.

Which individuals are included in pairwise comparisons can be subject to representation, popularity, or self-selection biases [29]. *Representation bias* occurs when the individuals sampled are not representative of the population, e.g., women might be under-represented in pairwise comparisons of job performance in male-dominated fields. *Popularity bias* describes popular items attracting more exposure, e.g., popular search results attract more pairwise comparisons as they appear at the top of the ranking. Finally, *self-selection bias* can happen if individuals select themselves, e.g., students whose parents did not attend college might see themselves as “not worthy” of applying and thus will not be included in the comparison of scholarship candidates. To study the potential impact of these biases, we include three distinct sampling approaches, which determines the likelihood for a candidate to be selected for comparisons, into our research setup (Figure 1, step 1): random, conditioned on the group membership, or conditioned on the previous success. These sampling approaches are laid out in more detail in the following section.

We consider systemic discrimination to be the origin of additional bias inherent to pairwise comparisons. *Systemic discrimination* describes policies or customs that perpetuate discrimination, even if they are performed with no ill intent [29]. For instance, an individual from a poor family might lose pairwise comparisons of candidates for a managerial position by lacking the expected

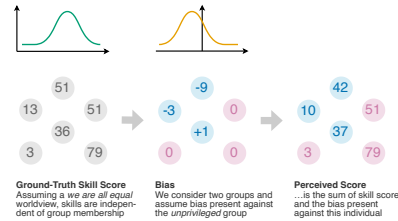


**Figure 2:** We consider the standard *We’re All Equal* worldview [14], where ground-truth unknown *skill score* and *bias* are considered separately. Ground-truth skill scores are independent of group membership, which means, e.g., that the underlying capability of individual are independent of their gender or race, but perceived scores are impacted by group membership, because of systemic discrimination, historical bias, or other types of biases.

habitus. In our setup, we focus on a single, binary sensitive attribute that separates a population into a “privileged” group  $G_{priv}$  and an “unprivileged” group  $G_{unpriv}$  (Fig. 2). We assume a *We’re All Equal* worldview [14] in which each individual has a latent ground-truth *skill score* on a given task, but pairwise comparisons are subject to *bias*.

#### 3.2 Candidate Pairs Selection

Resources for pairwise comparisons are generally limited, i.e., pairs must be selected for comparison. This can be seen as a two-step process, where individuals are (1) sampled from the population and then (2) paired, corresponding to steps 1 & 2 in Figure 1. We devise three distinct sampling approaches for step 1: Random Sampling, Oversampling, and Rank-Based Sampling. *Random Sampling* serves as a baseline sampling approach where in each iteration, we select 20% of individuals randomly from both groups. Since pairs are drawn without replacement, sampling already influences the possible pairings. For instance, if oversampling is applied, then there will always be different numbers of homogeneous pairs (both individuals from the same group) among the groups. Without oversampling, the number of same and different groups pairs is (almost) the same. We fix pairing to be random since biases from the literature [29] are more closely linked to sampling approaches rather than pairing.

*Oversampling.* One aspect according to which individuals could be sampled is group-membership. If designers of a pairwise competition are aware of *representation bias* (i.e., a group being under-represented in a sample), they might stratify their sample by oversampling this group. Further, designers of a pairwise competition might try to mitigate systemic discrimination or historical bias by allotting an unprivileged group disproportionate chances to compete (i.e., applying a form of affirmative action). For instance, this could be desirable for female job applicants in a male-dominated field. We therefore implement *Oversampling* as a group-dependent sampling approach, sampling more individuals from the unprivileged group. In this paper, we fix the oversampling rate at 75%,

i.e. we sample three times more individuals from the unprivileged group. We investigated different oversampling rates in a preliminary study and include the results in Appendix C. The effects of oversampling (especially for David’s Score and RankCentrality) increase with an increasing oversampling rate.

*Rank-Based Sampling.* Another possible aspect for sampling individuals is previous success. Our iterative setup of sampling, pairing, and comparing allows for the consideration of feedback loops between these components. Both *popularity* and *self-selection bias* can be the result of such a feedback loop, as they give more successful individuals a higher chance of being selected again for comparison. On one hand, popularity bias might be desirable if the accuracy of the top of the ranking matters most. On the other hand, the Matthew-Effect [30] can be a type of self-selection bias if more successful individuals are more eager to compete again. We thus implement *Rank-Based Sampling* using intermittently recovered ranks to condition the probabilities for sampling nodes in the next iteration. We normalize these probabilities to be independent of ranking length, to give exponentially higher chances to top-ranking individuals, and to keep a minimal probability for selection even at the bottom of the ranking.

### 3.3 Candidate Comparison & Ranking Recovery

*Problem Statement.* We are given a population  $N = \{1, \dots, n\}$  and two subgroups  $C_{\text{priv}}, C_{\text{unpriv}} \subseteq N$ . We assume that each individual  $i \in N$  has a ground truth unobservable latent skill score  $t_i$ . We indicate with  $\mathbf{t}$  the corresponding vector. The latent skill scores also induce a ground truth unobservable ranking  $r(\mathbf{t})$ . Furthermore, we assume that each item has a perceived score  $s_i$ , which is affected by the group membership of an item. We define bias for an item  $i$  the difference between its latent skill score and its perceived skill score. We assume that the bias depends only on the group membership of an item. While we cannot observe the perceived scores  $s$  either, they inform the human judgments and probabilistically determine the pairwise comparisons. From a multi-set  $P$  of pairwise assessments of the form  $(i \succ j)$ , indicating that the item  $i$  has been preferred over  $j$  in a certain assessment, the goal of ranking recovery methods is to produce a ranking  $r^*$  that best reconstructs the unbiased ranking  $r(\mathbf{t})$ . In this paper, we measure the alignment of  $r^*$  and  $r(\mathbf{t})$  using *Group-Conditioned Weighted Kemeny Distance*, which we introduce in the next Section. Ground truth skill scores  $\mathbf{t}$  serve as test data for this performance evaluation of ranking recovery methods. Ground truth skill scores are otherwise unobservable, and, in particular, inaccessible to the ranking recovery methods themselves.

From the human evaluated pairwise comparisons, it is possible to construct a pairwise comparisons graph, that is exploited by various ranking recovery methods, as follows. Let the individuals be the nodes of a directed, weighted comparison graph. For each pairwise comparison we observe between distinct individuals  $i$  and  $j$ , we then update the weight of the edge  $(i, j)$  to reflect the proportion of  $j$ ’s wins against  $i$  over the total number of comparisons between the pair. This results in an adjacency matrix  $A$ , with zeros on the diagonal (i.e., no self-loops), and in which  $A_{ij} = 1 - A_{ji}$  for each pair  $i, j$  that has been compared at least once. We assume the pairwise comparisons to be incomplete and potentially inconsistent. In other words, there are individuals  $i, j$  for

which  $A_{ij} = A_{ji} = 0$ , and the comparison graph contains Condorcet cycles such as  $A_{ij} = A_{jk} = A_{ki} = 1$ . If the comparisons were transitive and complete, ranking recovery could be trivially performed by any sorting method. Pairwise comparison graphs that contain Condorcet cycles, on the other hand, require algorithms that are specifically tailored towards ranking recovery.

*Ranking Recovery Algorithms.* Existing ranking recovery algorithms are based on heuristics, random walks, or similarity, and we include one state-of-the-art algorithm from each class into our evaluation. Implementation details are provided in Appendix Section B. As a baseline, we also include a *Random Rank Recovery* method that randomly assigns ranks to candidates.

*David’s Score.* David’s Score [10] is a heuristics-based approach to ranking recovery that estimates an individual  $i$ ’s rank from its direct wins and losses as follows:  $DS_i = w_i + \bar{w}_i - l_i - \bar{l}_i$ , where  $w_i = \sum_j A_{ji}$  is the sum of its winning ratios and  $l_i = \sum_j A_{ij}$  the sum of its losing ratios.  $\bar{w}_i = \sum_j A_{ji} w_j$  and  $\bar{l}_i = \sum_j A_{ij} l_j$  aggregate these sums from individuals  $j$  that  $i$  is compared to. While David’s Score does not require a connected comparison graph and can be computed very efficiently, it only considers an individual’s success (i.e., proportion of wins) over its neighbors and their successes. However, there might be a community of individuals that are weaker than everyone else globally, in which one individual would still have a high proportion of wins over the other individuals in this community locally.

*RankCentrality.* A possible “global heuristic” for ranking recovery is the stationary distribution of a random walk over the comparison graph. Using this idea, RankCentrality [31] obtains a ranking as follows: First, the adjacency matrix is normalized through dividing by the individuals’ out-degrees and adding self-loops. Then, the stationary distribution of a random walk is calculated as the top left eigenvector of this normalized adjacency matrix.

*GNNRank.* Another approach to ranking recovery assumes that individuals who win similarly often against the same other individuals should be ranked similarly. SerialRank [13] uses the Fiedler vector, i.e., the second smallest eigenvector of the Laplacian of the similarity matrix, to calculate this similarity. SerialRank does, however, require a considerable amount of consistent comparisons to recover an accurate ranking. GNNRank [18] tries to overcome this limitation by learning better suited similarity vectors using node embeddings obtained from the comparison graph through the use of graph neural networks.

*Fairness-Aware PageRank.* The PageRank algorithm [32] is designed to estimate the relevance of web pages based on the hyper-link network in which they are embedded. Using a random walk with restarts, it solves a problem related to, yet distinct from ranking recovery from pairwise comparisons. Fairness-Aware PageRank [41] introduces group-awareness into PageRank by equally distributing PageRank mass (i.e., relevance) to all subgroups. Fairness-Aware PageRank is similar to RankCentrality in that it belongs to the group of random walk based approaches to network centrality. While Fairness-Aware PageRank neglects edge weights, it allows for multi-edges in the comparison graph, i.e., individual comparisons can be expressed separately. In addition to a winning ratio,

## 6.2 Fairness-Aware Ranking Recovery from Pairwise Comparisons

Fairness-Aware Ranking Recovery from Pairwise Comparisons

multi-edges express the total number of comparisons between a pair. This is a potential benefit of Fairness-Aware PageRank over methods that allow for edge weights but not for multi-edges.

*Post-Processing.* In addition to the discussed ranking recovery methods, we also included two post-processing methods into our evaluation. FA\*IR [46] is a commonly used post-processing method that re-ranks individuals to ensure a specified representation in the top-k of a ranking, while maximizing utility. EPIRA [4] is a post-processing method tailored towards the exposure measure of group representation, which we also employ in our setup.

### 3.4 Measures

Given our research setup, a suitable error measure should (i) compare the recovered ranking against the ground truth skill scores  $\mathbf{t}$ , (ii) assign higher penalties to gross differences between order of skill scores and ranks, and (iii) consider subgroups in the ranking. Ground-truth skills scores  $\mathbf{t}$  serve as essential test data for the evaluation of ranking recovery error, but they are not available to the ranking recovery methods themselves. We modify the normalization term of [31]’s Weighted Kemeny Distance to also satisfy the third desired property.

Kemeny Distance [20] counts discordant pairs between the recovered ranking and the ground-truth skill scores, but requires normalization to make it comparable between rankings of different lengths. Weighted Kemeny Distance [31] introduces more sensitivity to discordant pairs that have a large weight difference and is normalized with regard to the number of nodes and the norm of the weight vector. This normalization cannot be applied to find a subgroup’s error, which we would expect to comprise both within-group and between-groups comparisons. We introduce Group-Conditioned Weighted Kemeny Distance by instead normalizing on all pairs involving a group, i.e., within- & between-group pairs. This normalization guarantees the error to be in the interval  $[0, 1] \subset \mathbb{R}$  and to be comparable between subgroups of different size.

*Group-Conditioned Weighted Kemeny Distance.* For a subgroup  $G$  of a population  $N$  ( $G \subseteq N$ ) with ground-truth skill scores  $\mathbf{t}$  and recovered ranks  $r$ , we define the Group-Conditioned Weighted Kemeny Distance as:

$$D_i^G(r) := \sqrt{\frac{\sum_{i < j} (t_i - t_j)^2 I_{(t_i - t_j)(r_i - r_j) > 0}}{\sum_{i < j} (t_i - t_j)^2}} \quad (1)$$

for all pairs of individuals  $(i, j)$  such that  $i \in N$  and  $j \in G$ , comparing the individuals of a group both in-group and out-of-group for evaluation. Further,  $I_{[\ ]}$  is the indicator function that has value of 1 for discordant pairs and 0 otherwise. Given a privileged group  $G_{\text{priv}}$  and an unprivileged group  $G_{\text{unpriv}}$ , we define the **error difference** as:

$$D_i^{\text{diff}}(r) = D_i^{G_{\text{unpriv}}}(r) - D_i^{G_{\text{priv}}}(r) \quad (2)$$

In this paper, we consider both the overall error of a recovered ranking and the error difference as a measure of fairness. Furthermore, we include *exposure* as a measure of group representation as introduced by [37]. In contrast to the (group-conditioned) error measure, exposure only takes to group membership of individuals into account, not their ground-truth skill scores. A logarithmic discount then ensures a focus on the top-k individual’s groups.

WebSci '26, May 26–29, 2026, Braunschweig, Germany

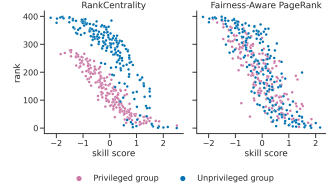


**Figure 3: Correlations of Skill Score (higher is better) and Rank (lower is better) by Recovery Method. 400 individuals in 2 equal size groups, compared in 1000 iterations using Oversampling and the BTL model. Left: Ranks recovered with RankCentrality [31]. Unprivileged individuals have a higher mean rank because of bias, but are sorted to the extremes of the ranking when Oversampling is applied with RankCentrality. Right: Ranks recovered with Fairness-Aware PageRank [41]. The correlations of both groups overlap, but within-group error is higher.**

*Exposure.* Group representation as exposure is measured for a group  $G$  in a ranking  $r$  as:

$$\text{Exp}^G(r) := \frac{1}{|G|} \sum_{d \in G} \frac{1}{\log_2(r_d + 2)} \quad (3)$$

Given a privileged group  $G_{\text{priv}}$  and an unprivileged group  $G_{\text{unpriv}}$ , we define the **exposure difference** as:

$$\text{Exp}^{\text{diff}}(r) = \text{Exp}^{G_{\text{unpriv}}}(r) - \text{Exp}^{G_{\text{priv}}}(r) \quad (4)$$

## 4 Synthetic Data

Given the introduced sampling strategies and ranking recovery methods, as well as the setup illustrated in Figure 1, we conduct experiments on both synthetic and empirical data. We create synthetic datasets by simulating 500 iterations of sampling, pairing, and comparing individuals using the Bradley-Terry-Luce (BTL) model [2], as illustrated in steps 1–3 in Figure 1. A detailed description of how we create synthetic data is provided in Appendix Section A and results after varying parameters are shown in Appendix Section C. We deploy the different sampling approaches described in Section 3.2 and obtain multisets of pairwise assessments on which we apply state-of-the-art ranking recovery algorithms. Two different outcomes of such a ranking recovery are illustrated in Figure 3. *Exposure difference*, *error difference*, and *error* (medians and ranges of 10 trials) are shown after 500 iterations in Figure 4.

### 4.1 Results from Simulated Comparisons

Regarding *exposure difference*, we find that David’s Score and Rank-Centrality in combination with Oversampling indeed lead to improved exposure of the unprivileged group. Upon closer inspection (Fig. 3), this is because RankCentrality sorts the oversampled group to both extremes of the ranking and can therefore not be relied upon to remedy existing bias. Whether this effect temporarily mitigates exposure differences as shown in Figure 4 depends on the amount of bias present in the data, so the oversampling rate might need to

## 6.2 Fairness-Aware Ranking Recovery from Pairwise Comparisons

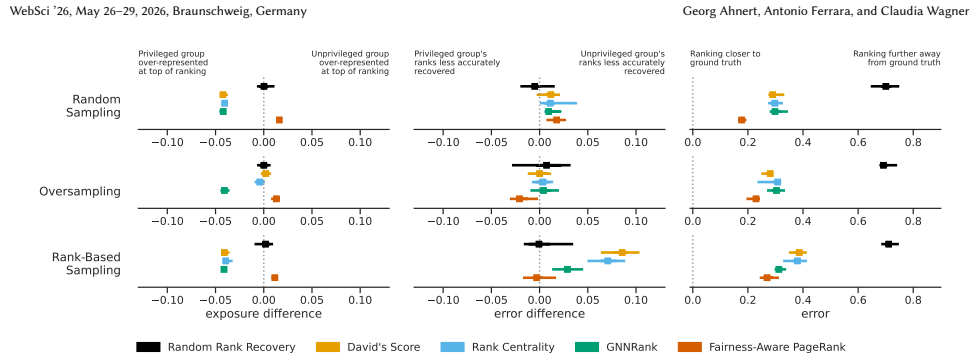


**Figure 4: Results of Simulated Pairwise Comparisons, by Sampling Approach (rows) and Ranking Recovery Method (colors). Medians and ranges of 10 trials. Exposure difference (left) and error difference (center) are group-conditioned measures of fairness, error (right) reflects the whole ranking—dashed lines indicate optimal values. David's Score and RankCentrality intermittently remove exposure difference when Oversampling is applied. Error difference is minimized by GNNRank and Fairness-Aware PageRank, even under Rank-Based Sampling. Fairness-Aware PageRank over-shoots on the unprivileged group's exposure but achieves best overall accuracy by partially mitigating bias.**

be adjusted accordingly. Still, we recommend against relying on this effect to mitigate bias, as it diminishes with an increasing number of comparisons being drawn. Fairness-Aware PageRank, by contrast, consistently improves the exposure of the unprivileged group across all sampling strategies and iterations. This ranking recovery method does, however, slightly overshoot and over-represents the unprivileged group at the top of the ranking.

Random Sampling and Oversampling have very little effect on *error difference*. Only Rank-Based Sampling creates higher error in the ranks recovered for the unprivileged group. This comes as no surprise, given that the privileged individuals are more likely to be found at the top of the ranking and will thus be compared more often. Among the ranking recovery methods that are not group-aware, GNNRank deals best with the Rank-Based Sampling scenario in terms of *error difference* and overall *error*.

In fact, if we do not simulate bias, GNNRank consistently performs similar to or outperforms David's Score and RankCentrality regarding *error*. This replicates the findings by He et al. [18] but using a different error measure. Notwithstanding GNNRank's performance in scenarios without bias, Fairness-Aware PageRank consistently outperforms the other ranking recovery methods if bias is assumed to be present. This is because it is the only group-aware recovery method investigated and it shares a *We're All Equal* worldview with our research setup. Further, Fairness-Aware PageRank is capable of minimizing error difference in Rank-Based Sampling scenarios as well.

### 4.2 Post-Processing Results

We apply the post-processing methods FA\*IR [46] and EPIRA [4], showing the results in Figure 5. The FA\*IR post-processing method has a larger impact on all individuals in the ranking. We find that it effectively reduces exposure difference while not overshooting and also greatly reduces error. Setting the proportion of protected

individuals  $p$  to a value even larger than 0.5 yields optimal results in our setup. In combination with GNNRank, FA\*IR is able to outperform Fairness-Aware PageRank regarding overall error, in particular under Rank-Based Sampling. This combination of ranking recovery and post-processing methods does, however, not mitigate the error difference observable under this sampling approach. Thus, Fairness-Aware PageRank might still be preferable.

The EPIRA method optimizes a ranking until a certain threshold on the exposure is satisfied. We find this method to effectively mitigate exposure difference. However, post-processing with EPIRA does not improve error or error difference. This is what we would expect from a post-processing method that optimizes this very measure (i.e., exposure) with minimal swaps in the ranking.

## 5 Empirical Data

Validating our findings on empirical data necessitates a dataset where both ground-truth values (i.e., *skill scores*) and pairwise comparisons are available and where *bias* is present in the data. Such datasets are scarce, but we identify one dataset that fulfills the criteria: IMDB-WIKI-SbS [33]. In contrast to the synthetic datasets discussed in the previous section, sampling and comparison was already performed when the dataset was gathered.

### 5.1 The IMDB-WIKI-SbS Dataset

The IMDB-WIKI-SbS dataset [33] is a large-scale dataset consisting of human-annotated pairwise comparisons of age between faces from IMDB.com and Wikipedia. The dataset consists of 9,150 images sampled from the IMDB-WIKI dataset [35] that are compared in 250,249 pairs by crowdworkers, tasked with selecting the older individual of each pair.

Pavlichenko and Ustalov [33] already acknowledge that many ground-truth labels for age and gender in the dataset are incorrect. To overcome these issues, we apply FairFace [19] to all pictures

## 6.2 Fairness-Aware Ranking Recovery from Pairwise Comparisons

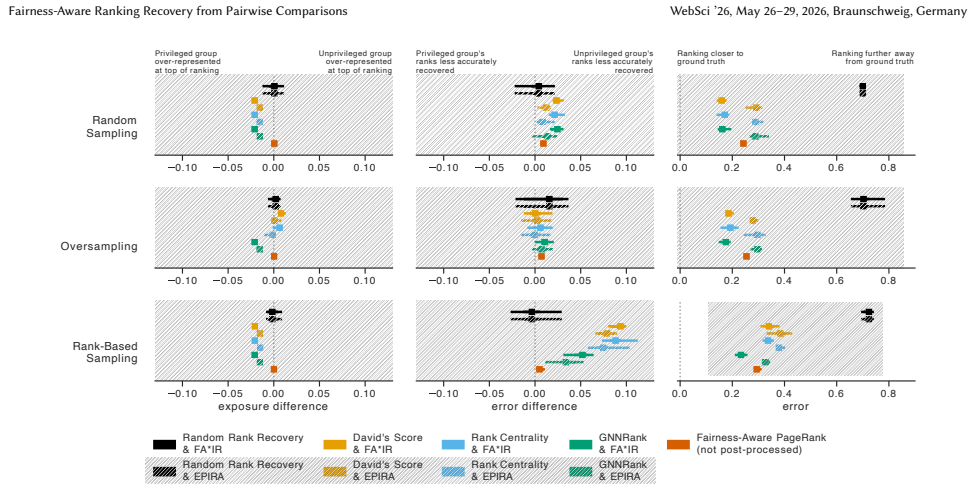


**Figure 5: Post-Processed Results the FA\*IR algorithm [46] and the EPIRA algorithm [4]. FA\*IR is able to effectively limit exposure difference while not over-shooting the way Fairness-Aware PageRank does. The post-processing technique also improves overall accuracy and is able to outperform Fairness-Aware PageRank, in particular if paired with GNNRank for ranking recovery. FA\*IR does, in contrast to Fairness-Aware PageRank, negatively impact error difference. While EPIRA effectively limits exposure difference between the groups, it does not improve error difference under Rank-Based Sampling. Overall error does not see any improvements when using EPIRA. Thus, in our simulations, Fairness-Aware PageRank outperforms post-processing with EPIRA.**

and classified age and gender. We then retrieve the image captions for all original images from IMDB.com and extract a list of linked actors for each image. Using the actor’s IMDB IDs, we extract their date of birth and gender from Wikidata and are able to reconstruct their approximate age given the year that the picture was taken. We then perform an exact match on gender and a closest match on age between each actor and the detected gender and age for a given face. We further remove all pictures in which no age match could be established within the age range identified by FairFace  $\pm 5$  years.

After re-labeling, we have 6,123 images on which women are on average younger than man (i.e., unequal *skill score* distributions). These differences in the ground-truth *skill scores* for men and women violate the *we-are-all-equal* worldview. Since this worldview is a necessary assumption for notions of group fairness [14], we shall not deploy any of the measures nor the Fairness-Aware PageRank ranking recovery method directly to this dataset. Instead, we first stratify it such that we keep the same number of men and women for each age. After stratification, we have 4,806 images of 2,403 women and 2,403 men, and the *we-are-all-equal* assumption is now satisfied. Because of the domains from which the pictures were gathered (movies and Wikipedia) our data is skewed towards young people, i.e., age does not follow a normal distribution. Our results, shown in Figure 6, also indicate the existence of *bias* in the form of gender ageism, i.e., women being systematically perceived younger than men of equal age.

### 5.2 Results for IMDB-WIKI-SbS

The results we obtain from David’s Score, RankCentrality, and GNNRank for the IMDB-WIKI-SbS dataset confirm our findings with synthetic data. All three fairness-unaware ranking recovery methods lead to an over-representation of the privileged group (i.e., men) at the top of the ranking, and to increased error for the unprivileged group (i.e., women). We also evaluate sub-sampling from the IMDB-WIKI-SbS dataset, following the same objectives (i.e., random, group-, or success-based), and then choose among existing edges between the sampled individuals. When sub-sampling the dataset in such a way that we oversample the unprivileged group, David’s Score and RankCentrality do not mitigate the under-representation of the unprivileged group. This is contrary to what we have observed with synthetic data and underlines that this effect cannot be relied upon.

We find that GNNRank generalized less well on the IMDB-WIKI-SbS comparison graph and thus re-trained the model after each iteration of sampling and comparison. In contrast to our experiments on synthetic data, GNNRank shows no advantage in error over the other ranking recovery methods, even under Rank-Based Sampling. We suspect this to be the case because of the absence of edge weights for the comparisons, i.e., each pair was only compared once. With less graph structure available, GNNRank cannot find better node embeddings, even if it is re-trained separately after each iteration.

## 6.2 Fairness-Aware Ranking Recovery from Pairwise Comparisons

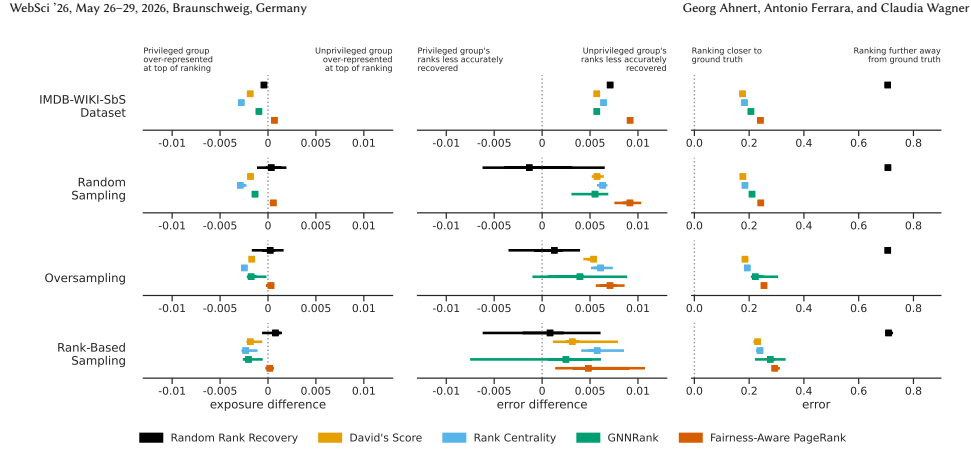


**Figure 6: Ranking Recovery Results from the IMDB-WIKI-SbS dataset [33] with Improved Labels, and Stratified by Gender. Rows show sampling approaches and colors indicate ranking recovery methods. Similar to the simulated comparisons data, Fairness-Aware PageRank overshoots on improving the unprivileged group's exposure. Further, Oversampling in combination with David's Score or RankCentrality leads to improved exposure for the unprivileged group as well. In contrast to our simulations, error is higher overall and for the unprivileged group when Fairness-Aware PageRank is applied in contrast to other ranking recovery methods. This can be explained by less bias and a less dense comparison graph observed for the IMDB-WIKI-SbS dataset.**

Same as we found with the synthetic dataset, Fairness-Aware PageRank slightly overshoots in correcting for the under-representation of the unprivileged group. This also affects error difference and overall error, where we find that Fairness-Aware PageRank performs worse than the other ranking recovery methods. We explain this with the fact that the observed bias against women is much smaller than in our simulations and it thus becomes more apparent that Fairness-Aware PageRank is designed to solve a different task than ranking recovery from pairwise comparisons. The FA<sup>IR</sup> post-processing algorithm cannot be applied to a ranking recovered from the IMDB-WIKI-SbS dataset, since only rankings with at most 400 individuals are supported and running the Python implementation<sup>2</sup> nonetheless results in a `RecursionError`. Similar to our experiments with synthetic data, we also found that applying EPIRA to the rankings recovered from IMDB-WIKI-SbS has little impact.

### 6 Discussion and Conclusion

This paper investigates fairness-aware ranking recovery in settings where only biased pairwise comparisons are observable, an increasingly common scenario in user-generated and platform-mediated evaluation systems. Since many platforms rely on implicit or explicit pairwise judgments (e.g., preference clicks, up-votes, A/B choices) to infer global rankings, understanding how bias in these comparisons propagates into downstream rankings is essential for ensuring equitable outcomes.

<sup>2</sup><https://github.com/fair-search/fairsearch-fair-python>

By focusing on a single binary sensitive attribute, we analyze group-level fairness under controlled conditions while studying how different forms of sampling bias shape the information available to ranking algorithms. Using both synthetic and empirical datasets, we systematically evaluate how state-of-the-art ranking-recovery methods perform with respect to accuracy and fairness under these varying conditions.

Our research provides three main insights: (i) When individuals are sampled uniformly at random for pairwise comparisons, computationally intensive algorithms such as GNNRank provide little advantage over simpler, group-unaware baselines such as David's Score. Given their vastly lower computational cost, heuristic methods may be preferable in settings where sampling is sufficiently diverse or random. (ii) Post-processing methods have the potential to improve both accuracy and fairness, but out of the methods we evaluated, only FA<sup>IR</sup> achieves this. This highlights the importance of carefully selecting post-processing techniques rather than assuming they will universally enhance fairness. (iii) Both Fairness-Aware PageRank and GNNRank followed by FA<sup>IR</sup> post-processing can partially mitigate pre-existing biases while improving overall ranking accuracy. GNNRank combined with FA<sup>IR</sup> achieves the lowest overall error, yet tends to amplify error disparities between demographic groups. In contrast, Fairness-Aware PageRank yields rankings that are fair with respect to exposure and error differences, but it may produce less accurate results when the underlying bias is weak. These trade-offs illustrate that no single approach dominates

## 6.2 Fairness-Aware Ranking Recovery from Pairwise Comparisons

across fairness and accuracy dimensions; method selection should therefore depend on the nature and severity of observed biases.

While our findings could be applied to more than two groups by considering each group separately against all others, future work should investigate multiple and multinary sensitive attributes, as well as different group sizes, other distributions for *skill score* and *bias*, and additional sampling approaches. Algorithms should also be evaluated against newly collected empirical data comprising both ground-truth scores and human annotated pairwise comparisons. Given the limitations of existing ranking recovery methods, we encourage the development of dedicated methods for fairness-aware ranking recovery. We provide a Python package under MIT license alongside our paper to facilitate replication and future work on fair ranking recovery<sup>3</sup>.

### References

- [1] Alex Beutel, Jilin Chen, Tulsee Doshi, Hai Qian, Li Wei, Yi Wu, Lukasz Heldt, Zhe Zhao, Lichan Hong, Ed H Chi, et al. 2019. Fairness in recommendation ranking through pairwise comparisons. In *Proceedings of the 25th ACM SIGKDD International Conference on Knowledge Discovery & Data Mining*, 2212–2220.
- [2] Ralph Allan Bradley and Milton E Terry. 1952. Rank analysis of incomplete block designs. I. The method of paired comparisons. *Biometrika* 39, 3/4 (1952), 324–345.
- [3] Nadezhda Bugakova, Valentina Fedorova, Gleb Gusev, and Alexey Drutsa. 2019. Aggregation of pairwise comparisons with reduction of biases. *arXiv preprint arXiv:1906.03711* (2019).
- [4] Kathleen Cachel and Elke Rundensteiner. 2023. Fairer Together: Mitigating Disparate Exposure in Kemeny Rank Aggregation. In *Proceedings of the 2023 ACM Conference on Fairness, Accountability, and Transparency*, 1347–1357.
- [5] L Elisa Celis, Damian Straszak, and Nisheeth K Vishnoi. 2018. Ranking with Fairness Constraints. In *45th International Colloquium on Automata, Languages, and Programming (ICALP 2018)*. Schloss Dagstuhl-Leibniz-Zentrum fuer Informatik.
- [6] Diparka Chakraborty, Syamantak Das, Arindam Khan, and Aditya Subramanian. 2022. Fair rank aggregation. *Advances in Neural Information Processing Systems* 35 (2022), 23965–23978.
- [7] Xi Chen, Paul N Bennett, Kevyn Collins-Thompson, and Eric Horvitz. 2013. Pairwise ranking aggregation in a crowdsourced setting. In *Proceedings of the sixth ACM international conference on Web search and data mining*, 193–202.
- [8] Alexandra Chouldechova and Aaron Roth. 2020. A snapshot of the frontiers of fairness in machine learning. *Commun. ACM* 63, 5 (2020), 82–89.
- [9] Arthur H Copeland. 1951. *A reasonable social welfare function*. Technical Report. mimeo, 1951. University of Michigan.
- [10] Herbert A David. 1987. Ranking from unbalanced paired-comparison data. *Biometrika* 74, 2 (1987), 432–436.
- [11] Peter Emerson. 2013. The original Borda count and partial voting. *Social Choice and Welfare* 40, 2 (2013), 353–358.
- [12] Antonio Ferrara, Francesco Bonchi, Francesco Fabbri, Fariba Karimi, and Claudia Wagner. 2024. Bias-aware ranking from pairwise comparisons. *Data Mining and Knowledge Discovery* (2024), 1–25.
- [13] Fajwel Fogel, Alexandre d’Aspremont, and Milan Vojnovic. 2014. Serialrank: Spectral ranking using seriation. *Advances in neural information processing systems* 27 (2014).
- [14] Sorelle A Friedler, Carlos Scheidegger, and Suresh Venkatasubramanian. 2021. The (im)possibility of fairness: Different value systems require different mechanisms for fair decision making. *Commun. ACM* 64, 4 (2021), 136–143.
- [15] William V Gehrlein and Dominique Lepelley. 2010. *Voting paradoxes and group coherence: the Condorcet efficiency of voting rules*. Springer Science & Business Media.
- [16] Sahin Cem Geyik, Stuart Ambler, and Krishnaram Kenthapadi. 2019. Fairness-aware ranking in search & recommendation systems with application to linkedin talent search. In *Proceedings of the 25th acm sigkdd international conference on knowledge discovery & data mining*, 2221–2231.
- [17] Thilo Hagendorff. 2022. Blind spots in AI ethics. *AI and Ethics* 2, 4 (2022), 851–867.
- [18] Yixuan He, Quan Gan, David Wipf, Gesine D Reinert, Junchi Yan, and Mihai Cucuringu. 2022. GNNRank: Learning global rankings from pairwise comparisons via directed graph neural networks. In *International Conference on Machine Learning*. PMLR, 8581–8612.
- [19] Kimmo Karkkainen and Jungsoek Joo. 2021. Fairface: Fair attribute dataset for balanced race, gender, and age for bias measurement and mitigation. In *Proceedings of the IEEE/CVF winter conference on applications of computer vision*, 1548–1558.
- [20] John G Kemeny. 1959. Mathematics without numbers. *Daedalus* 88, 4 (1959), 577–591.
- [21] Maurice G Kendall and B Babington Smith. 1940. On the method of paired comparisons. *Biometrika* 31, 3/4 (1940), 324–345.
- [22] Svetlana Kiritchenko and Saif M Mohammad. 2017. Best-worst scaling more reliable than rating scales: A case study on sentiment intensity annotation. *arXiv preprint arXiv:1712.01765* (2017).
- [23] Yasmine Kotturi, Anson Kahng, Ariel Procaccia, and Chinmay Kulkarni. 2020. Hirepeer: Impartial peer-assessed hiring at scale in expert crowdsourcing markets. In *Proceedings of the AAAI Conference on Artificial Intelligence*, Vol. 34, 2577–2584.
- [24] Tzu-Sheng Kuo, McArdle Hankin, Andrew Ying Miranda Li, and Cathy Wang. 2020. Assessing political bias using crowdsourced pairwise comparisons. In *Proceedings of the AAAI conference on human computation and crowdsourcing*.
- [25] Sandeep Kaur Kuttal, Xiaofan Chen, Zhendong Wang, Sogol Balali, and Anita Sarma. 2021. Visual Resume: Exploring developers’ online contributions for hiring. *Information and Software Technology* 138 (2021), 106633.
- [26] Kristina Lerman and Tad Hogg. 2014. Leveraging position bias to improve peer recommendation. *Plus one* 9, 6 (2014), e98914.
- [27] Ruosen Li, Teerth Patel, and Xinya Du. 2023. Prd: Peer rank and discussion improve large language model based evaluations. *arXiv preprint arXiv:2307.02762* (2023).
- [28] Hauke Licht, Rupak Sarkar, Patrick Y Wu, Pranav Goel, Niklas Stoehr, Elliott Ash, and Alexander Miserlis Hoyle. 2025. Measuring scalar constructs in social science with LLMs. In *Proceedings of the 2025 Conference on Empirical Methods in Natural Language Processing*, 32132–32159.
- [29] Ninareh Mehrabi, Fred Morstatter, Nripsuta Saxena, Kristina Lerman, and Aram Galstyan. 2021. A survey on bias and fairness in machine learning. *ACM computing surveys (CSUR)* 54, 6 (2021), 1–35.
- [30] Robert K Merton. 1988. The Matthew effect in science, II: Cumulative advantage and the symbolism of intellectual property. *isis* 79, 4 (1988), 606–623.
- [31] Sahand Negahban, Sewoong Oh, and Devavrat Shah. 2012. Iterative ranking from pair-wise comparisons. *Advances in neural information processing systems* 25 (2012).
- [32] Lawrence Page, Sergey Brin, Rajeev Motwani, and Terry Winograd. 1999. *The PageRank citation ranking: Bringing order to the web*. Technical Report. Stanford InfoLab.
- [33] Nikita Pavlichenko and Dmitry Ustalov. 2021. IMDB-WIKI-SbS: An evaluation dataset for crowdsourced pairwise comparisons. *arXiv preprint arXiv:2110.14990* (2021).
- [34] Michel Regenwetter, Jason Dana, and Clinton P Davis-Stober. 2011. Transitivity of preferences. *Psychological review* 118, 1 (2011), 42.
- [35] Rasmus Rothe, Radu Timofte, and Luc Van Gool. 2018. Deep expectation of real and apparent age from a single image without facial landmarks. *International Journal of Computer Vision* 126, 2-4 (2018), 144–157.
- [36] Dmitry Ryvkin. 2005. The predictive power of noisy elimination tournaments. *CERGE-EI Working Paper* 1, 252 (2005).
- [37] Ashudeep Singh and Thorsten Joachims. 2018. Fairness of exposure in rankings. In *Proceedings of the 24th ACM SIGKDD international conference on knowledge discovery & data mining*, 2219–2228.
- [38] Feifan Song, Bowen Yu, Minghao Li, Haiyang Yu, Fei Huang, Yongbin Li, and Houteng Wang. 2023. Preference ranking optimization for human alignment. *arXiv preprint arXiv:2306.17492* (2023).
- [39] Louis L Thurstone. 1927. A law of comparative judgment. *Psychological Review* 34 (1927), 273–286.
- [40] Louis L Thurstone. 1927. The method of paired comparisons for social values. *The Journal of Abnormal and Social Psychology* 21, 4 (1927), 384.
- [41] Sotiris Tsioutsoulis, Evaggelia Pitoura, Panayiotis Tsapras, Ilias Kleftakis, and Nikos Mamoulis. 2021. Fairness-aware pagerank. In *Proceedings of the Web Conference 2021*, 3815–3826.
- [42] Austin Waters and Risto Miikkilainen. 2014. Grade: Machine learning support for graduate admissions. *Ai Magazine* 35, 1 (2014), 64–64.
- [43] Dong Wei, Md Mouimul Islam, Baruch Schieber, and Senjuti Basu Roy. 2022. Rank aggregation with proportionate fairness. In *Proceedings of the 2022 international conference on management of data*, 262–275.
- [44] Ke Yang and Julia Stoyanovich. 2017. Measuring fairness in ranked outputs. In *Proceedings of the 29th international conference on scientific and statistical database management*, 1–6.
- [45] H Peyton Young and Arthur Levenglick. 1978. A consistent extension of Condorcet’s election principle. *SIAM Journal on applied Mathematics* 35, 2 (1978), 285–300.
- [46] Meike Zehlke, Francesco Bonchi, Carlos Castillo, Sara Hajian, Mohamed Megahed, and Ricardo Baeza-Yates. 2017. FAIR: A fair top-k ranking algorithm. In *Proceedings of the 2017 ACM on Conference on Information and Knowledge Management*, 1569–1578.
- [47] Meike Zehlke, Ke Yang, and Julia Stoyanovich. 2021. Fairness in ranking: A survey. *arXiv preprint arXiv:2103.14000* (2021).

<sup>3</sup><https://github.com/wanLo/fairpair/>

## 6.2 Fairness-Aware Ranking Recovery from Pairwise Comparisons

WebSci '26, May 26–29, 2026, Braunschweig, Germany

Georg Ahnert, Antonio Ferrara, and Claudia Wagner

- [48] Ernst Zermelo. 1929. Die Berechnung der Turnier-Ergebnisse als ein Maximumproblem der Wahrscheinlichkeitsrechnung. *Mathematische Zeitschrift* 29, 1 (1929), 436–460.
- [49] Xiaohang Zhang, Guoliang Li, and Jianhua Feng. 2016. Crowdsourced top-k algorithms: An experimental evaluation. *Proceedings of the VLDB Endowment* 9, 8 (2016), 612–623.

### A Synthetic Data

We consider a synthetic dataset of 400 individuals divided in two equal size groups. First, we draw *skill scores* from the same normal distribution  $\mathcal{N}_{\text{skill}}(\mu_{\text{skill}}, \sigma_{\text{skill}})$  for all individuals, then we add *bias* drawn from a different normal distribution  $\mathcal{N}_{\text{bias}}(\mu_{\text{bias}}, \sigma_{\text{bias}})$  to the scores of the unprivileged group. For results on datasets in which *skill scores* and *bias* are not normally distributed, see Section 5. For the privileged group, *skill scores* and *perceived scores* are identical, while for the unprivileged group, *perceived scores* comprise *bias*. This is without loss of generality since what is relevant in the pairwise comparisons is the relative difference in the (perceived) scores. We use the Bradley-Terry-Luce (BTL) model [2] to simulate human comparisons. The magnitude of scores matters for the BTL model, as it determines whether an individual is almost certain to win a comparison or only slightly more likely to win than to lose a comparison. To inform our choice of parameters for the *skill score* and *bias* distributions, we propose fixing the expected probabilities of (i) stronger individuals winning ( $p_{\text{stronger}}$ ), and (ii) privileged individuals winning ( $p_{\text{discr}}$ ) a pairwise comparison.

To simulate average amounts of comparison uncertainty and of bias against the unprivileged group, we set  $p_{\text{stronger}} = p_{\text{discr}} = 75\%$ , as well as  $\mu_{\text{skill}} = 0$  and  $\sigma_{\text{bias}} = \sigma_{\text{skill}}/2$ . In general, both the type of distribution and the parameters should be calibrated to a specific context. The IMDB-WIKI-SbS dataset discussed in Section 5.1, for instance, shows more conservative probabilities of  $p_{\text{stronger}} = 81.6\%$  and  $p_{\text{discr}} = 62.7\%$ .

We iteratively select 20% of all individuals according to the sampling approaches introduced in Section 3.2, pair them randomly, and probabilistically compare the pairs using the BTL model [2], also known as the *softmax* function.

*The Bradley-Terry-Luce (BTL) Model.* For two individuals  $i$  and  $j$  with *perceived scores*  $s_i$  and  $s_j$ , the probability of  $i$  winning a pairwise comparison against  $j$  is given by:

$$P(i \text{ wins over } j) = \frac{e^{s_i}}{e^{s_i} + e^{s_j}} = \frac{1}{1 + e^{s_j - s_i}} \quad (5)$$

Given the probability, we randomly identify the winner of a comparison. If we re-compare the same individuals  $i$  and  $j$  multiple times, we update the edge weight from  $j$  to  $i$  with the winning ratio of  $j$  over  $i$  and vice versa.

### B Recovery Algorithm Implementation

We used the implementations of David’s Score, RankCentrality, and other baseline ranking recovery methods provided in the official GNNRank code repository. We fixed an error in GNNRank’s implementation of RankCentrality that would prevent the algorithm from accurately recovering rankings. In addition to these algorithms, we implemented a baseline ranking recovery method that simply assigns random ranks to individuals. In order to facilitate fast experimentation, we trained GNNRank always only once every graph was strongly connected and then later employed the

same model without re-training even after more comparisons were conducted. The original paper highlights such generalization capabilities, and we were able to replicate these findings in preliminary experiments for our synthetically generated data. Only for a few trials did GNNRank not generalize in some iterations. The wrongly recovered rankings result in temporary spikes in the results over time and can easily be identified. Since the empirical dataset we evaluated [33] only has a single comparison for each pair of images, GNNRank does not generalize well on the subsampled comparison graph and needed to be re-trained for each evaluation. Fairness-Aware PageRank does not consider edge weights, i.e. comparisons are either won or lost. In contrast to all other ranking recovery algorithms, we thus did not supply it with the weighted edges of the comparison graph but with a directed multigraph of comparisons. We adopt the LFPR variant of Fairness-Aware PageRank, as the original authors report good performance on all tests for this variant.

### C Oversampling Parameter

In Figure 7, we show that for the RankCentrality recovery method, Oversampling can partially mitigate bias, leading to an exposure difference and an error difference close to zero. This effect, however, relies on the correct choice of over-sampling ratio and can thus not be relied upon. If the unprivileged group is smaller than 45% or larger than 55% of the whole population, only extreme (over-)sampling rates—selecting > 80% or < 20% unprivileged individuals—can mitigate bias in combination with RankCentrality.

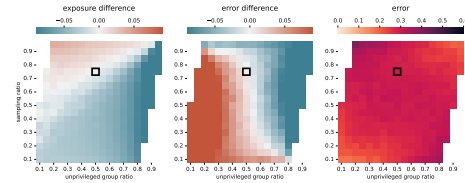


**Figure 7: Parameters for the Oversampling Method: Relative Size of the Unprivileged Group (x-axis) and Ratio of the Individuals Sampled from the Unprivileged Group in each Iteration (y-axis).** All experiments performed with the default parameters for skill and bias distributions, Oversampling—500 iterations, 20% of individuals selected in each iteration—and the RankCentrality ranking recovery method. The high-lighted rectangles represent the parameters used the main paper.

## 6.3 FairMC Fair-Markov Chain Rank Aggregation Methods

In many applications, rankings are not generated directly from raw data but instead emerge from the aggregation of multiple partial rankings or comparison signals. For example, search engines combine signals from various sources, recommender systems aggregate user feedback, and crowdsourcing platforms merge the judgments of multiple annotators.

Markov Chain-based methods are widely used for this purpose, as they model ranking as a stochastic process over pairwise preferences. However, when the input comparisons or rankings contain structural biases, standard aggregation methods may amplify these disparities, producing final rankings that systematically disadvantage certain groups.

The work presented in this section introduces **FairMC**, a fairness-aware rank aggregation method based on Markov Chains. The approach modifies the transition dynamics of the aggregation process by rescaling edge weights, enabling the algorithm to balance visibility across demographic groups while preserving the overall structure of the ranking signal. By incorporating fairness considerations directly into the aggregation procedure, the method provides a mechanism for mitigating disparities in the final ranking outcomes.

### Authors' Contributions

---

Contribution	Authors
<b>Conceptualization:</b>	A. Ferrara, C. Balestra
<b>Writing:</b>	C. Balestra, A. Ferrara
<b>Methodology:</b>	A. Ferrara, C. Balestra
<b>Code:</b>	C. Balestra, A. Ferrara
<b>Experiments:</b>	C. Balestra, A. Ferrara

---



## FairMC Fair–Markov Chain Rank Aggregation Methods

Chiara Balestra<sup>1</sup> (✉), Antonio Ferrara<sup>2,3</sup>, and Emmanuel Müller<sup>1</sup>

<sup>1</sup> TU Dortmund University, Dortmund, Germany  
chiara.balestra@cs.uni-dortmund.de

<sup>2</sup> Centai, Turin, Italy

<sup>3</sup> TU Graz, Graz, Austria

**Abstract.** Given a set of voters' preferences expressed as rankings, rank aggregation approaches combine them into a unique consensus ranking. Even if some methods guarantee fair representation of single voters, they still overlook unfair biases potentially affecting individuals from marginalized groups in the original rankings.

Rank aggregation is employed in many high-stakes decision-making processes, hence, due to the high societal influence, the development and study of fair rank aggregation approaches is essential. We introduce FairMC, a new fair rank aggregation approach based on Markov Chains to derive consensus rankings. By modifying the transition matrix and enforcing fairness in the transition probabilities across the groups, we obtain fairness in the representation of the items at the ranking level. The resulting ranking assures higher visibility for protected groups while being close to the original rankings.

**Keywords:** Rank aggregation · Fair rankings · Markov Chains

### 1 Introduction

Rankings are ubiquitous and arise as the output results of several automatized processes. The necessity of finding a unique consensus ranking has received interest due to its applicability in multiple domains [7, 8, 12]. Given a set of  $r$  preference rankings from multiple sources, rank aggregation methods find a consensus ranking out of a list of potentially numerous rankings. The problem of aggregating rankings is not trivial; the Kemeny optimal ranking problem, i.e., aggregating rankings under the minimal sum of Kendall's Tau distances constraint [10], is NP-hard [2, 7]. Various techniques have been proposed to find an approximation of the optimal solution: the well-known Borda counting method [8] but also several other combinatorial methods for Kemeny optimal ranking exist [1, 15]. Additional methods exploit the representation of the items and the ranking as nodes and edges of a graph [7].

Given a set of potentially many rankings, rank aggregation aims to obtain a unique consensus ranking. Far more complicated is when the “items” to be ranked are people with emerging fairness-related concerns; the rankers can be biased towards some categories, and rank aggregation methods can propagate or even expand such biases to the

© The Author(s), under exclusive license to Springer Nature Switzerland AG 2024  
R. Wrembel et al. (Eds.): DaWaK 2024, LNCS 14912, pp. 315–321, 2024.  
[https://doi.org/10.1007/978-3-031-68323-7\\_26](https://doi.org/10.1007/978-3-031-68323-7_26)

consensus rankings. The issue, often referred to as *position bias*, refers to the fact that the users need to explore the rankings fully, and elements not ranked in the top positions suffer from low visibility; this is particularly relevant when it affects differently the various groups of items. The challenge is that the fairness issue is present in both the original and the final rankings; the generated consensus ranking should represent the preferences of single voters and show no or slight bias against protected communities and marginalized groups. The goal is to satisfy some *group fairness* constraints, i.e., aiming at the same treatments in the various groups. We refer to [14] that defines constraints for fairness of exposure in ranking outputs, and [17] that deals with the fair top- $k$  ranking problem. The fairness-aware PageRank [13] comprehends various fair versions of the PageRank algorithm, ensuring a proportional allocation of scores to the different groups. Their Markov Chain considers unweighted graphs and doesn't allow for self-loops, two important ingredients that are instead needed to solve the rank aggregation problem and make fairness-aware PageRank not suited for our task. We finally cite some methods for fair rank aggregation: [5, 16] found theoretical bounds for picking the best fair version of the input rankings, [3, 4] use post-processing methods to re-rank the output of several other traditional non-fair rank aggregation methods with different fairness metrics, [11] represents an in-processing method.

We propose FairMC, an in-processing method, jointly aggregating rankings and achieving fairness; conversely to [11], FairMC does not assume that the number of input rankings is small. We focus on *group fairness*, i.e., aiming at the same treatments in the various groups, on a fixed number  $N$  of candidates and a fixed number of  $r$  voter input rankings; each ranker is supposed to provide a full rank of the candidates and each of the candidates belongs or not to a pre-specified, e.g., protected by law, *protected group*. We simplify the multi-class case, where several protected groups must be equally represented, to this binary distinction. Proposing FairMC as a fair rank aggregation method, we integrate group fairness into rank aggregation mechanisms. Particularly interesting is the fact that our contribution does not optimize for any group fairness evaluation metric; the approach builds on the well-known Markov Chains methods for ranking aggregation and modifies the underlying graphs to obtain a fair stationary probability distribution by enforcing group equality in the transition probabilities. Although not directly optimizing for any metric, we show in the experiments that FairMC performs reasonably well in most datasets.

## 2 Markov Chain Methods for Rank Aggregation

Markov Chain methods base the computation of a consensus ranking on the representation of the rankings as a graph, where the nodes represent the items to be ranked and the edges incorporate the ordering relationships of the input rankings.

**Graphs.** A directed graph is a pair  $G = (\mathcal{N}, \mathcal{E})$  where  $\mathcal{N}$  represents the set of the nodes while  $\mathcal{E}$  represents the set of the edges. We indicate with  $N = |\mathcal{N}|$  the total number of nodes. An edge in a directed graph  $e = (v, u)$  is an ordered pair of nodes  $v, u \in \mathcal{N}$ , and  $(v, u) \in \mathcal{E} \not\Rightarrow (u, v) \in \mathcal{E}$ . If the edges are weighted, we speak about weighted graphs; weights, designed by  $e_{u,v}$ , can be assigned to each edge, and they represent the strength of the link between  $u$  and  $v$ . Mathematically, we assign to

each edge a weight  $e_{u,v} > 0$ ; an edge is not part of the graph if and only if its weight is zero, i.e.,  $(u, v) \notin \mathcal{E} \Leftrightarrow e_{u,v} = 0$ . The adjacency matrix  $W \in \mathbb{R} \times \mathbb{R}$  whose entries are  $W_{u,v} = e_{u,v}$  entirely defines the graph  $(\mathcal{N}, \mathcal{E})$ . Given a node  $v \in \mathcal{N}$ ,  $\mathcal{N}_G(v)$  indicates the set of neighbors of  $v$ , i.e.,  $\mathcal{N}_G(v) = \{u \in \mathcal{N} \mid e_{u,v} > 0\}$ ; in the case  $G$  is a directed graph, we can distinguish between  $\mathcal{N}_G^+(v) = \{u \in \mathcal{N} \mid (v, u) \in \mathcal{E}\}$ , the *out-neighborhood* and  $\mathcal{N}_G^-(v) = \{u \in \mathcal{N} \mid (u, v) \in \mathcal{E}\}$ , the *in-neighborhood*.

**Markov Chains for Rank Aggregation.** We consider a finite set  $\Sigma = \{\sigma_1, \dots, \sigma_r\}$  of ranked lists of the  $\mathcal{N}$  elements where each  $\sigma_i$  represents the ranking provided by the ranker  $i$ . From the rankings in  $\Sigma$ , Markov Chain methods for rank aggregation construct a directed weighted graph  $G = (\mathcal{N}, \mathcal{E})$  whose nodes are the elements in  $\mathcal{N}$  and whose edges  $\mathcal{E}$  and respective weights represent their pairwise orderings in  $\Sigma$ . The pairwise relationships among elements of  $\mathcal{N}$  in the rankings  $\Sigma$  are used to determine the existence and the weight of the edges connecting them, i.e., given  $u, v \in \mathcal{N}$ , the weight  $e_{u,v}$  of the directed edge  $(u, v)$  is assigned so that it includes the frequency in which  $v$  is ranked higher than  $u$  by the input rankings. The Markov process is then defined by the obtained adjacency matrix  $W$ . Given a directed weighted graph, it is possible to normalize the edges such that  $\sum_{v \in \mathcal{N}_G^+(u)} e_{u,v} = 1$  for all  $u \in \mathcal{N}$  (in case, by adding self loops); thus, the adjacency matrix can be interpreted as a probability transition matrix, where  $W_{u,v}$  represents the probability for a random walker on the graph to transition from node  $u$  to node  $v$ . A probability matrix describes the underlying Markov Chain process, and it is called *ergodic* in the case that the probability of ending up in one node is bigger than 0 for each node  $u \in \mathcal{N}$ . The stationary probability distribution  $\pi$  is the vector satisfying  $\pi_u = \sum_{v \in \mathcal{N}_G^-(u)} W_{u,v} \pi_v$  where  $\pi_v$  represents the probability of being in the node  $v$ ;  $\pi$  can be efficiently computed when the Markov Chain is *ergodic*. From  $\pi$ , the consensus ranking is defined as the underlying ranking obtained using the probabilities of the stationary distribution as importance scores, i.e., the highest probability places the corresponding item in the first position of the consensus ranking. For the construction of the graphs given by the various rank aggregation approaches we refer to the literature [6, 7].

**Group Fairness.** Each ranker assigns an ordering to the elements in  $\mathcal{N}$ . Rank aggregation methods assume the existence of a *consensus ranking*, i.e., a ranking that equally and fairly considers the opinion of each ranker. The composition of  $\mathcal{N}$  is generally a priori unknown. We use the notation  $\mathcal{N} = \mathcal{P} \cup (\mathcal{N} \setminus \mathcal{P})$ , where  $\mathcal{P}$  is the protected category while  $\mathcal{N} \setminus \mathcal{P}$  is the set of non-protected items. For the moment, we reduce to study the case of  $\mathcal{P} = \mathcal{P}_1 \cup \dots \cup \mathcal{P}_k$  where  $\mathcal{P}_1, \dots, \mathcal{P}_k$  are  $k$  protected categories in  $\mathcal{N}$ ; thus, we have only a binary classification over the items. We indicate with  $p$  a protected item, i.e.,  $p \in \mathcal{P}$ ,  $u$  a non-protected item, i.e.,  $u \in \mathcal{N} \setminus \mathcal{P}$  and  $v \in \mathcal{N}$  for the general individual. Given a ranking  $\sigma_r$  generated by the  $r$ th ranker, we write  $\sigma_r(v)$  to indicate the ranking position of element  $v$  in the ranking  $\sigma_r$ . Each ranking  $\sigma_r$  is an element of  $S_N$ , the symmetric group or permutation group of  $N$  elements.

318 C. Balestra et al.

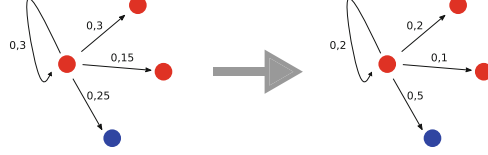


Fig. 1. Toy example for our proposed approach for the node  $v$  in the graph.

### 3 FairMC

Markov Chain methods allow interpreting the search of the consensus ranking in terms of transition probabilities among nodes of a graph and the graph-structured representation has advantages in terms of computational complexity and interpretability. However, as for the other rank aggregation methods, Markov Chain rank aggregation approaches do not consider whether the obtained consensus ranking satisfies fairness requirements. Markov Chain methods rely on the computation of the stationary probability distribution of the Markov process defined on the directed graph of items by an adjacency matrix; we state that it is sufficient to make the adjacency matrix fair in order to obtain a fair consensus ranking. Our claim derives from observing that the transition probability reflects the biases of the rankers, where the probability of transitioning to a protected node or to an unprotected node is not balanced.

Our approach is based on the same assumptions of the Markov Chain methods [6, 7]; the proposed modification is applicable to each of the three Markov Chain methods. We use the graph  $G = (\mathcal{N}, \mathcal{E})$  derived from Markov Chain and modify it obtaining a new graph  $\tilde{G} = (\tilde{\mathcal{N}}, \tilde{\mathcal{E}})$ , where  $\tilde{\mathcal{N}} = \mathcal{N}$ . The edges' weights are reweighted using the following definition

$$\tilde{e}_{u,v} = \begin{cases} e_{u,v} \cdot \frac{|\mathcal{P}|}{N \sum_{w \in \mathcal{P}} e_{u,w}} & \text{if } v \in \mathcal{P} \\ e_{u,v} \cdot \frac{|\mathcal{N} \setminus \mathcal{P}|}{N \sum_{w \in \mathcal{N} \setminus \mathcal{P}} e_{u,w}} & \text{if } v \in \mathcal{N} \setminus \mathcal{P} \end{cases} \quad (1)$$

Furthermore, for each node  $u$  for which  $\mathcal{N}_G^+(u) \cap \mathcal{P} \neq \emptyset$ , we create an edge from  $u$  to  $v$  with weight  $\tilde{e}_{u,v} = \frac{|\mathcal{P}|}{N}$  for each  $v \in \mathcal{P}$ ; instead, for each node  $u'$  for which  $\mathcal{N}_G^+(u') \cap (\mathcal{N} \setminus \mathcal{P}) \neq \emptyset$ , we create an edge from  $u'$  to  $v'$  with weight  $\tilde{e}_{u',v'} = \frac{|\mathcal{N} \setminus \mathcal{P}|}{N}$  for each  $v' \in \mathcal{N} \setminus \mathcal{P}$ .

Figure 1 illustrates a toy example of the rescaling mechanism. Recall that reweighting the edges' weights is equivalent to redefining the adjacency matrix and that the weights represent the probability of transitioning from one node to another one. The rescaled weights guarantee that

1. the relative importance of the original transition probabilities is respected,
2. the sum of the probabilities to transition to a protected node is equal to the sum of the probabilities to transition to a non-protected, i.e., it holds  $\sum_{v \in \mathcal{P}} \tilde{e}_{u,v} = \sum_{v \in \mathcal{N} \setminus \mathcal{P}} \tilde{e}_{u,v}$  for each  $u \in \mathcal{N}$ . Thus, the transition probabilities are *fair* with respect to the protected group.

In the experimental section, we show that our approach assures fairer consensus rankings without harshly disrupting the Kemeny distance.

## 4 Experiments

We use *group exposure* [9] and *fairness@k*, i.e., the difference in the percentage of items from the two groups in the top  $k$ , to evaluate the fairness of the consensus rankings. We group the methods in FairMC, Markov Chain methods (MC), non-fair aggregation approaches<sup>1</sup>, and the EPIRA methods<sup>2</sup>. We use the 30 Mallows datasets (with different dispersion parameters) described in [3]. The code is available on GitHub<sup>3</sup>.

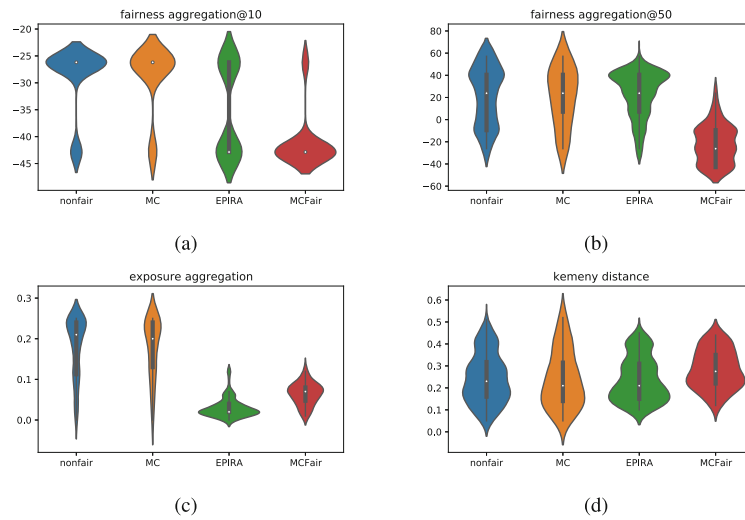


**Fig. 2.** Violin plots of summary statistics of performance.

### 4.1 Performance Evaluation

Figure 2a and 2b show the violin plots of *fairness@k* of the consensus rankings of the top 10% and 50% of the full ranking. At each level, the non-fair approaches, Markov Chain approaches, and the competing fair rank aggregation approaches tend to obtain

<sup>1</sup> best rank aggregated, Borda aggregation, exponential enhanced Borda, exponential weighting, highest rank, lowest rank, mc4, robust aggregation, round Robin, stability enhanced and stability selection.

<sup>2</sup> EPIK, EPIRA + {Kemeny, Copeland, Copeland noWiG, Schulze, Borda, Maximin Borda} [3].

<sup>3</sup> [github.com/chiarabales/fairMC](https://github.com/chiarabales/fairMC).

consensus rankings favoring the unprotected group; this is particularly visible at 50%, where a clear difference among fair and non-fair methods appears. On the contrary, the FairMC approaches tend to favor the protected group, both at 10 and 50%. In Fig. 2c, we do not expect to perform better than Cachel et al. [3] with respect to the exposure as their methods directly optimize for the exposure of the consensus rankings while we do not. Nevertheless, we can observe how the consensus rankings obtained through the FairMC approaches visibly outperform all non-fair methods in exposing the protected group.

The Kemeny distance in Fig. 2d evaluates the distance between the original rankings and the obtained consensus ranking, and it is not a fairness metric. Higher values of the Kemeny distance indicate that the consensus ranking is distant from the original rankings. We observe a slight tendency to increase the Kemeny distance when adding fairness constraints in the Markov Chain, as expected given the trade-off between optimizing for the Kemeny distance and for the fairness metrics.

## 5 Conclusions

We propose FairMC, introducing fairness at the level of the nodes in Markov Chain-based rank aggregation methods. Our method achieves extraordinarily good results with respect to the exposure of protected groups and the fairness@ $k$  with respect to common rank aggregation approaches without optimizing for any fairness metrics; furthermore, the Kemeny distance with respect to the original rankings remains acceptably low after the introduced modification. We believe in the potential of acting at the level of nodes to achieve fairer consensus rankings and that further development in this direction can achieve unbiased results.

## References

1. Ailon, N., Charikar, M., Newman, A.: Aggregating inconsistent information: ranking and clustering. *J. ACM (JACM)* **55**, 1–27 (2008)
2. Bartholdi, J., Tovey, C.A., Trick, M.A.: Voting schemes for which it can be difficult to tell who won the election. *Soc. Choice Welfare* **6**, 157–165 (1989)
3. Cachel, K., Rundensteiner, E.: Fairer together: Mitigating disparate exposure in Kemeny rank aggregation. In: *FACCT* (2023)
4. Cachel, K., Rundensteiner, E., Harrison, L.: Mani-rank: multiple attribute and intersectional group fairness for consensus ranking. In: *ICDE* (2022)
5. Chakraborty, D., Das, S., Khan, A., Subramanian, A.: Fair rank aggregation. In: *NeurIPS* (2022)
6. DeConde, R.P., Hawley, S., Falcon, S., Clegg, N., Knudsen, B., Etzioni, R.: Combining results of microarray experiments: a rank aggregation approach. *Stat. Appl. Genet. Mol. Biol.* **5** (2006)
7. Dwork, C., Kumar, R., Naor, M., Sivakumar, D.: Rank aggregation methods for the web. In: *WWW*, pp. 613–622 (2001)
8. Emerson, P.: The original Borda count and partial voting. *Soc. Choice Welfare* **40**, 353–358 (2013)
9. Ferrara, A., Bonchi, F., Fabbri, F., Karimi, F., Wagner, C.: Bias-aware ranking from pairwise comparisons. *Data Min. Knowl. Discov.* 1–25 (2024)

10. Kendall, M.G.: A new measure of rank correlation. *Biometrika* **30**, 81–93 (1938)
11. Kuhlman, C., Rundensteiner, E.: Rank aggregation algorithms for fair consensus. *VLDB* (2020)
12. List, C.: *Social choice theory* (2013)
13. Pitoura, E., Stefanidis, K., Koutrika, G.: Fairness in rankings and recommendations: an overview. *VLDB* (2022)
14. Singh, A., Joachims, T.: Fairness of exposure in rankings. In: *KDD* (2018)
15. van Zuylen, A., Williamson, D.P.: Deterministic algorithms for rank aggregation and other ranking and clustering problems. In: Kaklamanis, C., Skutella, M. (eds.) *WAOA 2007*. LNCS, vol. 4927, pp. 260–273. Springer, Heidelberg (2008). [https://doi.org/10.1007/978-3-540-77918-6\\_21](https://doi.org/10.1007/978-3-540-77918-6_21)
16. Wei, D., Islam, M.M., Schieber, B., Basu Roy, S.: Rank aggregation with proportionate fairness. In: *ICMD* (2022)
17. Zehlike, M., Bonchi, F., Castillo, C., Hajian, S., Megahed, M., Baeza-Yates, R.: FA\* IR: a fair top-k ranking algorithm. In: *CIKM* (2017)

## 7 Safety and Policy for Fairness

*“And now here is my secret, a very simple secret: It is only with the heart that one can see rightly; what is essential is invisible to the eye.”*

– Antoine de Saint-Exupéry [76]

This chapter focuses on the reliability, safety, and policy of algorithmic decision-making systems, addressing the challenges that arise when such systems are deployed in high-stakes, real-world environments. While the previous chapters examined how to detect unfairness and how structural inequalities emerge in networked and hierarchical systems, these analyses alone are not sufficient to ensure that AI systems behave safely in practice. In real-world deployments, models must operate under uncertainty, interact with incomplete or biased data, and remain robust to distributional shifts and opaque decision-making processes.

A key limitation of current approaches is that they often assume that models should always produce a prediction. However, in many high-stakes domains, such as healthcare, hiring, or public policy, forcing a decision under uncertainty can lead to harmful outcomes. As a result, ensuring safety requires mechanisms that allow models to recognize their own uncertainty and defer decisions when necessary, as well as broader governance frameworks that address risks across the entire lifecycle of AI systems.

The works presented in this chapter contribute to RQ4 by proposing both algorithmic and systemic approaches to reliability and safety. Rather than focusing solely on fairness metrics or structural properties, this chapter examines how to design systems that remain robust, trustworthy, and accountable under real-world conditions.

In Section 7.1, we introduce a method for incorporating abstention mechanisms into ranking systems, enabling models to defer uncertain decisions in a principled and controlled manner. In Section 7.2 we extend the perspective beyond individual algorithms, synthesizing the technical insights of this thesis into policy recommendations and best practices for managing bias and ensuring reliability across the AI lifecycle.

Together, these contributions connect fairness research with the broader goal of trustworthy AI, highlighting that achieving fairness in isolation is not sufficient without mechanisms that ensure safe and reliable deployment.

## 7.1 Bounded-Abstention Pairwise Learning to Rank

Ranking systems are increasingly used in high-stakes decision-making contexts, where outcomes depend directly on an individual’s position in an ordered list. In such settings, errors can have significant social and economic consequences. Despite this, most ranking models are designed to always produce a prediction, even when the underlying data is noisy or the model is uncertain.

This work addresses this limitation by introducing Bounded-Abstention Pairwise Learning to Rank (BALToR), a framework that equips ranking models with a safety mechanism based on abstention. Instead of forcing a potentially unreliable decision, the model is allowed to defer predictions when its confidence is low, enabling human intervention or the collection of additional information.

The approach is grounded in a theoretical characterization of the optimal abstention strategy, which is based on thresholding the conditional risk of the ranking model under a predefined coverage constraint. Building on this result, BALToR provides a model-agnostic, plug-in method that can be applied to existing ranking systems without requiring retraining.

By selectively abstaining on uncertain comparisons, the method improves the reliability of ranking outcomes while ensuring that the abstention mechanism itself does not introduce additional biases. This work highlights the importance of moving beyond models that always produce a prediction toward selective prediction frameworks, where models can explicitly manage uncertainty as part of their decision-making process.

### Authors’ Contributions

---


<b>Contribution</b>	<b>Authors</b>
<b>Conceptualization:</b>	A. Ferrara and all authors
<b>Writing:</b>	A. Ferrara and all authors
<b>Methodology:</b>	A. Ferrara, A. Pugnana
<b>Formal Analysis:</b>	A. Pugnana, A. Ferrara
<b>Code:</b>	A. Pugnana, A. Ferrara
<b>Experiments:</b>	A. Pugnana, A. Ferrara


---


---


## Bounded-Abstention Pairwise Learning to Rank

---

**Antonio Ferrara\***   
 CENTAI, Turin, Italy  
 Graz University of Technology, Graz, Austria  
 antonio.ferrara@centai.eu

**Andrea Pugnana\***   
 University of Trento, Trento, Italy  
 DISI  
 andrea.pugnana@unitn.it

**Francesco Bonchi**   
 CENTAI, Turin, Italy  
 EURECAT, Barcelona, Spain  
 francesco.bonchi@centai.eu

**Salvatore Ruggieri**   
 University of Pisa, Pisa, Italy  
 Department of Computer Science  
 salvatore.ruggieri@unipi.it

### Abstract

Ranking systems influence decision-making in high-stakes domains like health, education, and employment, where they can have substantial economic and social impacts. This makes the integration of safety mechanisms essential. One such mechanism is *abstention*, which enables algorithmic decision-making system to defer uncertain or low-confidence decisions to human experts. While abstention have been predominantly explored in the context of classification tasks, its application to other machine learning paradigms remains underexplored. In this paper, we introduce a novel method for abstention in pairwise learning-to-rank tasks. Our approach is based on thresholding the ranker’s conditional risk: the system abstains from making a decision when the estimated risk exceeds a predefined threshold. Our contributions are threefold: a theoretical characterization of the optimal abstention strategy, a model-agnostic, plug-in algorithm for constructing abstaining ranking models, and a comprehensive empirical evaluations across multiple datasets, demonstrating the effectiveness of our approach.

### 1 Introduction

Ranking systems have become deeply embedded in modern decision-making processes, affecting outcomes in high-stakes domains such as healthcare (e.g., prioritizing patients for clinical trials or organ transplants), education (e.g., university admission), and employment (e.g., job candidate screening). Because an individual’s outcome is often determined by their position in the ranking, these algorithmic decision-making systems can exert profound economic and social influence. As a result, it is essential to equip them with robust safety mechanisms. Among the emerging forms of “*AI guardrails*”, abstention mechanisms enable AI systems to refrain from issuing a low-confidence prediction. This allows for either direct human intervention—such as making a judgment on a specific case—or for the collection of additional, higher-quality data to be fed in input to the system.

So far, abstention—also referred to as “rejection”—has been primarily studied in the context of classification tasks (see §2.2 for the relevant literature), while receiving limited attention in other machine learning (ML) settings. In this paper, we address the problem of *bounded abstention in pairwise learning to rank with ties*. The objective of pairwise learning to rank is to train a model capable of predicting pairwise preferences between item pairs for a given query. For instance, in a hiring scenario, the query is a job opening, and the two items to be compared are two candidates. Notice that building a classifier can easily become computationally unfeasible when considering all

\*Equal contribution, listed by alphabetical order

## 7.1 Bounded-Abstention Pairwise Learning to Rank

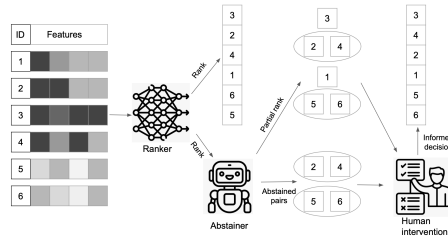


Figure 1: Illustration of the role of the abstainer in a ranking process. A standard ranker produces a complete ordering of items for a given query. However, it may exhibit low confidence in the relative ordering of certain item pairs. An abstainer identifies a number of these low-confidence pairs and defer them to an evaluator for further inspection. Such an evaluator - a human or even another model - leverages additional knowledge or higher-quality data to resolve the uncertainty on those pairs and, finally, producing a more reliable final ranking.

the pairs of instances. Hence, one needs to resort to learning-to-rank approaches, which derive a global ranking from a dataset of pairwise preferences (see §2.1). Therefore, given a trained ranker, i.e., a ML model trained for ranking, our goal is to build ad-hoc abstention strategies.

Regarding the abstention strategies, two main approaches are generally considered in the literature [Franc et al., 2023]: assigning a fixed cost to each abstention in the loss function (*cost-based model*) or balancing the fraction of allowed abstentions against the improvement in the ML model’s performance (*bounded-abstention model*). Mao et al. [2023] provide a theoretical analysis of the cost-based formulation in a pairwise ranking setting. However, in practice, establishing the cost of abstaining compared to making an error is very challenging. Therefore, we focus on the bounded-abstention formulation, where a fixed fraction of abstentions is specified in advance, and the goal is to optimize performance within such a constraint. This approach enables effective resource management, particularly in scenarios where human decision-making capacity is limited. For instance, in a recruitment setting, a company may allocate a specific budget for additional data collection or expert review to handle uncertain predictions made by the ML system. This budget naturally translates into a predefined threshold on the number of abstentions the system is allowed to make.

The setting addressed by our work is illustrated in Figure 1. Given a set of items (each represented by a feature vector) to be ranked for a specific query, a standard ranker would output a complete ordering of the items. In contrast, our approach introduces an *abstainer* that identifies item pairs for which the ranker’s confidence is low. These uncertain comparisons are then deferred to a human expert for further evaluation.

We propose BALToR (**B**ounded-**A**bstention **L**earning **T**o **R**ank), a novel method for abstention in pairwise learning-to-rank settings. To devise BALToR, we first characterize the optimal selection strategy that determines when the ranking model should abstain from providing a relative ordering between item pairs. This strategy is based on thresholding the model’s conditional risk: the system abstains when the estimated risk exceeds a predefined threshold. Given a bound on the allowable fraction of abstentions over pairwise comparisons, BALToR aims to maximize ranking performance on the remaining, non-abstained pairs.

Our contributions can be summarized as follows:

- (i) We formally introduce the problem of *bounded-abstention pairwise learning-to-rank* and provide a theoretical characterization of the optimal abstention strategy when *the ranker is given*, a common setting in the real world when retraining the ranker is computationally too expensive (e.g., for foundation models);
- (ii) We propose a *model-agnostic* plug-in algorithm for building an abstaining ranking model. Our approach relies on the optimal strategy of (i), and determines which pairs of instances the ranker should abstain on;

(iii) We conduct an empirical evaluation of our approach across multiple datasets and baseline methods, showing the effectiveness of the proposed methodology.

The paper is structured as follows. In §2, we introduce the frameworks of pairwise learning to rank and bounded abstention, highlighting the distinction of our work with the existing literature. In §3, we describe the proposed method for bounded-abstention pairwise learning to rank, present the theoretical characterization of the optimal abstention strategy, and provide the algorithmic details. In §4, we empirically evaluate the proposed method on various datasets. Finally, in §5, we conclude and outline limitations and future directions.

## 2 Background and Related Work

Let  $\mathcal{X}$  be an *input space*,  $\mathcal{Y}$  the *target space* and  $P$  a (unknown) joint probability distribution over  $\mathcal{X} \times \mathcal{Y}$ . Given a *hypothesis space*  $\mathcal{F}$  of functions that map  $\mathcal{X}$  to  $\mathcal{Y}$ , the goal of a ML algorithm (a *learner*) is to find a hypothesis  $f \in \mathcal{F}$ , called a *predictor*, that minimizes the *risk*:

$$R(f) = \mathbb{E}_{\mathbf{x}, Y \sim P}[l(f(\mathbf{X}), Y)]$$

where  $l : \mathcal{Y} \times \mathcal{Y} \rightarrow \mathbb{R}_{\geq 0}$  is a user-specified *loss function*.

### 2.1 Pairwise learning to rank with ties

We consider the standard pairwise learning to rank scenario where a set of queries  $Q = \{q_1, q_2, \dots, q_n\}$  and, for each query  $q$ , a set of item-query couples  $D^q = \{d_1^q, d_2^q, \dots, d_m^q\}$  are given. Typically, for each item-query couple, one has access to a set of features  $\mathbf{x}^q \in \mathcal{X}$ , representing characteristics of the item for that query. For instance, in a hiring scenario, a query is a job offer, and items are candidates. Features may regard attributes on a candidate (e.g., age) or also on the matching of the candidate to the job offer (e.g., share of job offer skills fulfilled by the candidate). Furthermore, given a pair of items for the same query, we call it a pair of instances  $\mathbf{x}^q, \mathbf{x}'^q \in \mathcal{X} \times \mathcal{X}$ , and we define pairwise preference as an ordering relationship ( $\succ_q, \prec_q, =_q$ ) where  $d_x^q \succ_q d_{x'}^q$  indicates that  $d_x^q$  is preferred over  $d_{x'}^q$ , for query  $q$ ,  $d_x^q \prec_q d_{x'}^q$ , that  $d_{x'}^q$  is preferred over  $d_x^q$ , and  $=_q$  indicates a tie. We consider a set of pairwise preferences given for each training query. Alternatively, a relevance score might be given for each document-query couple, from which pairwise preferences among two items for the same query are inferred. This preference ordering can be encoded by considering a target space  $\mathcal{Y} = \{-1, 0, 1\}$ , where  $-1$  means that the second instance is preferred (or ranked higher) than the first,  $1$  indicates that the first is preferred and  $0$  a tie. From now on, for easing the notations, we will omit the query indicators.

The objective of pairwise learning to rank is to learn a predictor  $f : \mathcal{X} \times \mathcal{X} \rightarrow \mathcal{Y}$ , called a *ranker*, which predicts the pairwise orders between all item pairs for each query. The canonical loss one aims to minimize in such a setting is the mis-ranking loss, which is defined as  $l_r(f(\mathbf{x}, \mathbf{x}'), y) = \mathbb{1}_{y \neq f}$ . In other words,  $f$  incurs a loss of one whenever the pair  $(\mathbf{x}, \mathbf{x}')$  is ranked by  $f$  differently from the ground truth order; if the ranking is correct, no loss is incurred. Let  $P$  be a probability distribution over  $\mathcal{X} \times \mathcal{X} \times \mathcal{Y}$ . We denote with  $R_l(f) = \mathbb{E}_{(\mathbf{x}, \mathbf{x}', Y) \sim P}[l(f(\mathbf{X}, \mathbf{X}'), Y)]$  the expected  $l$  loss of the ranker  $f$ . Typically, such a loss is not directly tractable. Hence, a few approaches propose to learn scores  $s : \mathcal{X} \rightarrow \mathbb{R}$  that provide a value for the relevance of the single item  $\mathbf{x}$ . Generally, these scores are learnt through (stochastic) gradient descent and boosting techniques, e.g., Ranknet, LambdaRank and LambdaMart [Burges, 2010]. Given  $s$ , one can estimate  $P(Y = 1 \mid \mathbf{X} = \mathbf{x}, \mathbf{X}' = \mathbf{x}')$ , i.e., the probability that  $\mathbf{x}$  is ranked higher than  $\mathbf{x}'$ ,  $P(Y = -1 \mid \mathbf{X} = \mathbf{x}, \mathbf{X}' = \mathbf{x}')$ , i.e., the probability that  $\mathbf{x}$  is ranked lower than  $\mathbf{x}'$ , and  $P(Y = 0 \mid \mathbf{X} = \mathbf{x}, \mathbf{X}' = \mathbf{x}')$ , i.e., the two instances are tied, through parametric probability models [Zhou et al., 2008]. The two most famous approaches are the *Bradley-Terry model* [Bradley and Terry, 1952] and the *Thurstone-Mosteller model* [Thurstone, 1994] (for tie-adjusted models, see, e.g., Zhou et al. [2008]). The former estimates probabilities as follows:

$$\begin{aligned} \hat{P}(Y = 1 \mid \mathbf{X} = \mathbf{x}, \mathbf{X}' = \mathbf{x}') &= \frac{e^{s(\mathbf{x})}}{e^{s(\mathbf{x})} + \theta e^{s(\mathbf{x}')}}, \\ \hat{P}(Y = -1 \mid \mathbf{X} = \mathbf{x}, \mathbf{X}' = \mathbf{x}') &= \frac{e^{s(\mathbf{x}')}}{e^{s(\mathbf{x}')} + \theta e^{s(\mathbf{x})}}, \\ \hat{P}(Y = 0 \mid \mathbf{X} = \mathbf{x}, \mathbf{X}' = \mathbf{x}') &= \frac{(\theta - 1)^2 e^{s(\mathbf{x})} e^{s(\mathbf{x}')}}{(\theta e^{s(\mathbf{x})} + e^{s(\mathbf{x}')})(e^{s(\mathbf{x})} + \theta e^{s(\mathbf{x}')})}, \end{aligned}$$

where  $\theta = e^\epsilon$ , with  $\epsilon$  a parameter regulating the probabilities for ties. The latter computes probabilities as follows:

$$\begin{aligned}\hat{P}(Y = 1 \mid \mathbf{X} = \mathbf{x}, \mathbf{X}' = \mathbf{x}') &= \Phi(s(\mathbf{x}) - s(\mathbf{x}') - \epsilon) , \\ \hat{P}(Y = -1 \mid \mathbf{X} = \mathbf{x}, \mathbf{X}' = \mathbf{x}') &= \Phi(s(\mathbf{x}') - s(\mathbf{x}) - \epsilon) , \\ \hat{P}(Y = 0 \mid \mathbf{X} = \mathbf{x}, \mathbf{X}' = \mathbf{x}') &= \Phi(s(\mathbf{x}) - s(\mathbf{x}') + \epsilon) - \Phi(s(\mathbf{x}) - s(\mathbf{x}') - \epsilon) ,\end{aligned}$$

where  $\Phi$  is the Gaussian cumulative distribution function.

Finally, the predictor is  $f$  is defined as a function of the estimated probabilities, e.g.,  $f(\mathbf{x}, \mathbf{x}') = \arg \max_{y \in \mathcal{Y}} \hat{P}(Y = y \mid \mathbf{X} = \mathbf{x}, \mathbf{X}' = \mathbf{x}')$ .

## 2.2 Abstaining Machine Learning

Abstention mechanisms have been predominantly explored in the context of classification [Geifman and El-Yaniv, 2017, 2019, Pugnana and Ruggieri, 2023, Feng et al., 2023], while limited attention has been devoted to other ML tasks.

The risk of a predictor can be controlled through a selection function  $g : \mathcal{X} \rightarrow \{0, 1\}$  that determines whether the predictor shall be invoked ( $g(\mathbf{x}) = 1$ ) or it should abstain from producing an output ( $g(\mathbf{x}) = 0$ ) [Cortes et al., 2024]. The former case is also denoted as accepting an instance, and the latter as rejecting the instance. Abstention mechanisms include *novelty rejection* [Cordella et al., 1995], which focuses on rejecting instances out of the training distribution, and *ambiguity rejection* [Hendrickx et al., 2024], which focuses on rejecting instances close to the decision boundary of the predictor. For approaches combining both strategies, see Prusa and Franc [2025]. This paper belongs to the ambiguity rejection research line, for which two main frameworks have been considered. Learning to Reject [Chow, 1970] considers a loss function parametric in the cost  $a$  of rejecting an instance [Herbei and Wegkamp, 2006, Tortorella, 2005, Condessa et al., 2013, Cortes et al., 2016]. However, determining the value of  $a$  is context-dependent and difficult to determine [Denis and Hebiri, 2020, Ruggieri and Pugnana, 2025]. Moreover, there is no *ex-ante* control on the fraction of abstentions, which is a critical requirement in practice. Selective Prediction methods solve those concerns by controlling the trade-off between performance and abstention through the *coverage*  $\phi(g) = \mathbb{E}[g(\mathbf{X})]$  [El-Yaniv and Wiener, 2010], namely the probability of acceptance. In the bounded-abstention formulation [Franc et al., 2023], this translates into the following objective:

$$\arg \min_{(f, g)} \frac{\mathbb{E}_{\mathbf{X}, Y \sim P}[l(f(\mathbf{X}), Y)g(\mathbf{X})]}{\phi(g)} \quad \text{s.t. } \phi(g) \geq c, \quad (1)$$

where  $c$  is the *target coverage*, i.e., the user-defined fraction of cases for which the selective predictor  $(f, g)$  must provide a prediction. Theoretical results can be found in Franc et al. [2023] for the classification task and in Zaoui et al. [2020] for the regression task.

To the best of our knowledge, in the setting of ranking, only the following approaches have been proposed: Cheng et al. [2010, 2012] study the problem of abstention, in particular for the label ranking setting, with the selective predictors returning partial orders (instead of total orders) on the labels; Mao et al. [2023] have considered pairwise ranking with abstention in the framework of Learning to Reject, introducing a cost for abstaining on a pair of instances. As for classification, such an approach hinders a practical implementation because specifying the correct cost for abstaining on a pair is not straightforward, making the cost-based model and the bounded-abstention approaches not directly comparable [Pugnana et al., 2024]. Our work complements theirs by: (i) formulating selective pairwise ranking as a bounded-abstention problem, with advantages in terms of practical usage; (ii) extending the setting to pairwise ranking with ties, providing optimal strategies also in that context.

## 3 Bounded Abstention Learning To Rank

We adopt a *selection function*  $g : \mathcal{X} \times \mathcal{X} \rightarrow \{0, 1\}$  to decide whether a ranker  $f$  should abstain (value 0) or should output (value 1) its prediction on the relative order of two input instances. A *selective ranker* is a pair  $(f, g)$ , that abstains if  $g(\mathbf{x}, \mathbf{x}') = 0$ , and returns  $f(\mathbf{x}, \mathbf{x}')$  if  $g(\mathbf{x}, \mathbf{x}') = 1$ . We extend the bounded-abstention paradigm of classification (see §2.2), by defining the (pairwise)

coverage  $\phi(g) = \mathbb{E}[g(\mathbf{X}, \mathbf{X}')] as the expected fraction of pairs of instances for which the ranker provides a prediction. We define the selective risk as follows:$

$$R_l(f, g) = \frac{\mathbb{E}_{\mathbf{x}, \mathbf{x}', Y \sim P} [l((f(\mathbf{X}, \mathbf{X}'), Y) g(\mathbf{X}, \mathbf{X}'))]}{\phi(g)}$$

where  $P$  is a (unknown) distribution over  $\mathcal{X} \times \mathcal{X} \times \mathcal{Y}$ . For a given ranker  $f$ , the bounded-abstention pairwise learning to rank problem is to find a selection function from a space of hypotheses  $\mathcal{G}$  that minimizes selective risk while achieving a (minimum) target coverage  $c$ :

$$\arg \min_{g \in \mathcal{G}} R_l(f, g) \quad \text{s.t.} \quad \phi(g) \geq c \quad (2)$$

Let us now characterize a solution to the problem (2). We write  $p(\mathbf{x}, \mathbf{x}', y)$  for the density of  $P$ . We denote the conditional expected risk on the pair  $(\mathbf{x}, \mathbf{x}')$  by:

$$r(\mathbf{x}, \mathbf{x}') = \sum_{y \in \mathcal{Y}} l(f(\mathbf{x}, \mathbf{x}'), y) p(y | \mathbf{x}, \mathbf{x}')$$

Moreover, we define the subspaces of  $\mathcal{X} \times \mathcal{X}$  where the conditional risk is lower, equal, or greater than  $a \in \mathbb{R}$  respectively as  $r(\mathcal{X} \times \mathcal{X})_{<a} = \{(\mathbf{x}, \mathbf{x}') \in \mathcal{X} \times \mathcal{X} : r(\mathbf{x}, \mathbf{x}') < a\}$ ;  $r(\mathcal{X}, \mathcal{X})_{=a} = \{(\mathbf{x}, \mathbf{x}') \in \mathcal{X} \times \mathcal{X} : r(\mathbf{x}, \mathbf{x}') = a\}$  and  $r(\mathcal{X}, \mathcal{X})_{>a} = \{(\mathbf{x}, \mathbf{x}') \in \mathcal{X} \times \mathcal{X} : r(\mathbf{x}, \mathbf{x}') > a\}$ . We assume that the loss is *symmetric*, namely  $l(f(\mathbf{x}, \mathbf{x}'), y) = l(f(\mathbf{x}', \mathbf{x}), -y)$ . This is a natural assumption in most contexts, since stating that  $\mathbf{x}$  is better than  $\mathbf{x}'$  ( $d_{\mathbf{x}}^q >_q d_{\mathbf{x}'}^q$ ) is equivalent to state that  $\mathbf{x}'$  is worse than  $\mathbf{x}$  ( $d_{\mathbf{x}'}^q <_q d_{\mathbf{x}}^q$ ), and, *a fortiori*, mistakes in predicting the relative rankings are symmetric. We can characterize now the solutions to problem (2).

**Theorem 3.1.** *Let us consider a symmetric loss. A selection function  $g^* : \mathcal{X} \times \mathcal{X} \rightarrow [0, 1]$  is an optimal solution to Eq. 2 if and only if the following conditions hold:*

$$\iint_{r(\mathcal{X} \times \mathcal{X})_{<\beta}} p(\mathbf{x}, \mathbf{x}') g^*(\mathbf{x}, \mathbf{x}') d\mathbf{x} d\mathbf{x}' = \iint_{r(\mathcal{X} \times \mathcal{X})_{<\beta}} p(\mathbf{x}, \mathbf{x}') d\mathbf{x} d\mathbf{x}'; \quad (\text{p1})$$

$$\iint_{r(\mathcal{X} \times \mathcal{X})_{=\beta}} p(\mathbf{x}, \mathbf{x}') g^*(\mathbf{x}, \mathbf{x}') d\mathbf{x} d\mathbf{x}' = c - \iint_{r(\mathcal{X} \times \mathcal{X})_{<\beta}} p(\mathbf{x}, \mathbf{x}') d\mathbf{x} d\mathbf{x}'; \quad (\text{p2})$$

$$\iint_{r(\mathcal{X} \times \mathcal{X})_{>\beta}} p(\mathbf{x}, \mathbf{x}') g^*(\mathbf{x}, \mathbf{x}') d\mathbf{x} d\mathbf{x}' = 0, \quad (\text{p3})$$

where  $\beta = \inf \left\{ a : \iint_{r(\mathcal{X} \times \mathcal{X})_{<a}} p(\mathbf{x}, \mathbf{x}') d\mathbf{x} d\mathbf{x}' \geq c \right\}$ .

Theorem 3.1 extends the result for probabilistic classifiers by Franc et al. [2023] to the pairwise-learning-to-rank-with-ties task. We provide the proof in Appendix A. Intuitively,  $\beta$  is the  $c$ -th conditional-risk quantile. The conditions of the theorem can be read as: we should abstain on those pairs where the conditional risk is above  $\beta$  (p3), and accept those where it is below  $\beta$  (p1). For pairs with conditional risk equal to  $\beta$ , the abstention is random with a probability that satisfies (p2). Moreover, notice that assuming a symmetric loss guarantees that we reject consistently both  $(\mathbf{x}, \mathbf{x}')$  and  $(\mathbf{x}', \mathbf{x})$  pairs for a given  $\beta$ . This intuition is further formalized in the following result, with the proof also provided in Appendix A.

**Theorem 3.2.** *Let us consider a symmetric loss. Consider the selection function:*

$$g^*(\mathbf{x}, \mathbf{x}') = \begin{cases} 1 & \text{if } r(\mathbf{x}, \mathbf{x}') < \beta \\ \xi & \text{if } r(\mathbf{x}, \mathbf{x}') = \beta \\ 0 & \text{if } r(\mathbf{x}, \mathbf{x}') > \beta, \end{cases} \quad (3)$$

where  $\xi = 0$  if

$$\iint_{r(\mathcal{X} \times \mathcal{X})_{=\beta}} p(\mathbf{x}, \mathbf{x}') d\mathbf{x} d\mathbf{x}' = 0$$

and  $\xi = \text{Bernoulli}(p_r)$  otherwise, where the probability  $p_r$  is defined as:

$$p_r = \frac{c - \iint_{r(\mathcal{X} \times \mathcal{X})_{<\beta}} p(\mathbf{x}, \mathbf{x}') d\mathbf{x} d\mathbf{x}'}{\iint_{r(\mathcal{X} \times \mathcal{X})_{=\beta}} p(\mathbf{x}, \mathbf{x}') d\mathbf{x} d\mathbf{x}'}$$

Then,  $g^*$  satisfies conditions (p1, p2, p3) of Theorem 3.1, and, thus, it is an optimal solution of Eq. 2.

---

**Algorithm 1: BALToR**


---

**Input** :  $\mathcal{D}_{cal}, f, c$  - held-out (un)labeled dataset  $\mathcal{D}_{cal}$ , trained ranker  $f$ , target coverage  $c$   
**Output**:  $g$  - selection function  
 1  $\hat{\mathbf{p}} \leftarrow \{f.pred.proba((\mathbf{x}, \mathbf{x}')_i)\}_{i \in \mathcal{D}_{cal}}$  // conditional probabilities on  $\mathcal{D}_{cal}$   
 2  $\hat{\mathbf{r}}_{cal} \leftarrow \{1 - \max_y \hat{\mathbf{p}}_i\}_{i \in \mathcal{D}_{cal}}$  // conditional risk on  $\mathcal{D}_{cal}$   
 3  $\hat{\beta}_c \leftarrow \text{quantile}(\hat{\mathbf{r}}_{cal}, c)$  //  $c$ -th quantile estimate  
 4  $g \leftarrow \text{lambda}(\mathbf{x}, \mathbf{x}') : \mathbb{1}_{(1 - \max_y f.pred.proba((\mathbf{x}, \mathbf{x}')_i) < \hat{\beta}_c)}$  // selection function  
 5 **return**  $g$

---

In the case of the 0-1 loss, we have the following closed form of conditional risk for the Bayes optimal ranker (proof in Appendix A).

**Proposition 3.3.** *Let us define the Bayes optimal ranker as:  $f^*(\mathbf{x}, \mathbf{x}') = \arg \max_{y \in \mathcal{Y}} p(y | \mathbf{x}, \mathbf{x}')$ . Its conditional risk w.r.t. the 0-1 loss is:*

$$r_{0-1}(\mathbf{x}, \mathbf{x}') = 1 - \max_{y \in \mathcal{Y}} p(y | \mathbf{x}, \mathbf{x}') \quad (4)$$

By applying a standard plug-in approach to the estimates above, we derive our BALToR proposal, shown in Algorithm 1.

We assume *as given*: a calibration set  $\mathcal{D}_{cal}$ , a ranker  $f$ , and a target coverage  $c$ . First, the algorithm estimates the conditional probabilities  $\hat{p}_y \approx p(y | \mathbf{x}, \mathbf{x}')$  for every  $y \in \mathcal{Y}$  and stack them in a vector  $\hat{\mathbf{p}} = \{\hat{p}_{y,i}\}_{y \in \mathcal{Y}, i \in \mathcal{D}_{cal}}$  (line 1). This can be done, e.g., by using the generalized Bradley-Terry approach or the Thurstone-Mollesler approach. Then, the algorithm estimates the conditional risk by computing  $r((\mathbf{x}, \mathbf{x}')_i) = 1 - \max_y \hat{\mathbf{p}}_i$  over each  $i \in \mathcal{D}_{cal}$  (line 2). Next, it computes the  $c$ -th quantile  $\hat{\beta}_c$  over the estimated conditional risks (line 3). The estimated quantile is used as a threshold in the returned selection function (line 4): if the estimated conditional risk of a pair of instances is below  $\hat{\beta}_c$ , the prediction is provided; otherwise, the selective ranker abstains.

## 4 Experiments

In this section, we empirically assess the effectiveness of BALToR using three popular and publicly available datasets for the learning-to-rank task. Our method aims to identify and abstain from pairs that are truly uncertain. By abstaining from a larger number of uncertain pairs, we expect improved performance on the remaining pairs. Additionally, we aim for the actual coverage to closely match the target coverage and for the rejections to maintain the overall distribution of classes in the pairwise comparisons.

More in details, we address the following questions:

- Q1:** Does the accuracy on the pairwise ordering relationship, i.e., the capability of predicting the relative order or a tie for pairs of items for a query, improve on the remaining ones when abstaining on a subset of pairs?
- Q2:** Is the coverage constraint satisfied at test time?
- Q3:** How is rejection distributed across classes, i.e., is BALToR (un)evenly rejecting pairs in which the first items is ranked higher than the second, or viceversa, or when there is a tie?

### 4.1 Experimental Settings

**Datasets** We consider three popular datasets from the related literature: Web-30k, OHSUMED and MQ2007.

Web-30k Qin and Liu [2013] contains more than 30,000 queries, with each query having 125 assessed items/documents on average. Each query-document pair is encoded with 136 features. Furthermore, relevance judgments are obtained from a retired labeling set of a commercial web search engine (Microsoft Bing), with values ranging from 0 (irrelevant) to 4 (perfectly relevant).

## 7.1 Bounded-Abstention Pairwise Learning to Rank

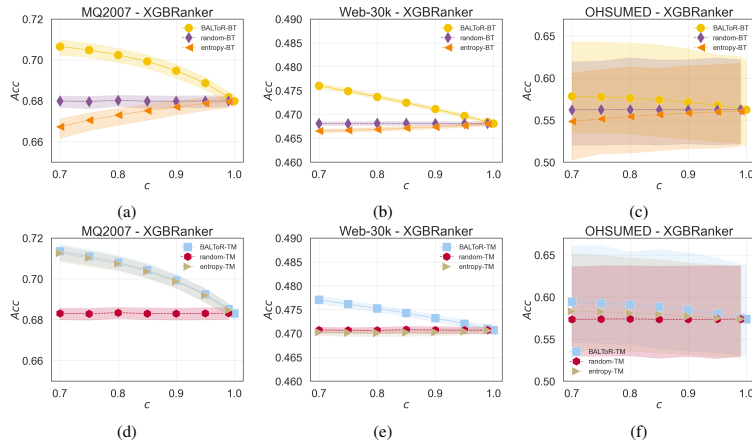


Figure 2: Accuracy  $Acc$  on the selected pairs ( $mean \pm std$  over five folds) for the BT model (top line) and the TM model (bottom line). For smaller target coverages  $c$  (i.e., more abstention), the accuracy increases for BALToR, remains stable for the random abstainer, has erratic performance for the entropy-based abstainer.

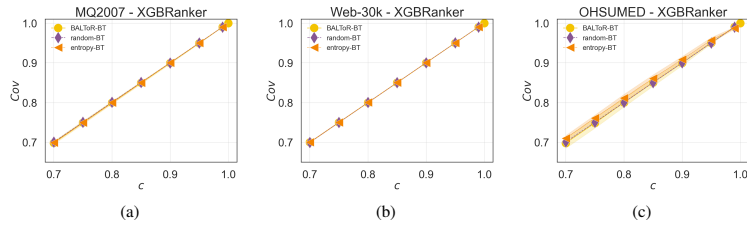


Figure 3: Actual (empirical) coverage  $Cov$  on the test set ( $mean \pm std$  over five folds) for the BT model. The actual coverage remains very close to the target coverage  $c$ .

OHSUMED [Hersh et al., 1994] is a MEDLINE database subset containing 106 queries with 16,140 query-documents pairs. Each query-document pair has a 25-dimensional feature vector that contains popular information-retrieval features, such as tf-idf and BM25 score. There are three levels of relevance judgments: not relevant, possibly relevant and definitely relevant.

MQ2007 Qin and Liu [2013] is a query set from the Million Query track of TREC 2007 and consist of 1,700 queries. The query-document pairs are represented with 46 features including scores such as BM25, PageRank, and HITS. The relevance labels are on a three-grade scale from 0 (irrelevant) to 2 (very relevant).

**Baselines** We consider the default implementation of LambdaMART [Burges, 2010] from the popular libraries XGBoost [Chen and Guestrin, 2016], CatBoost [Prokhorenkova et al., 2018] and LightGBM [Ke et al., 2017], as these are still state-of-the-art methods in learning to rank [Qin et al., 2021]. We report the results for XGBoost in the main body of the paper. Since the results for CatBoost and LightGBM are very similar and consistent with those of XGBoost, we report them in Appendix B. To obtain probabilities for Algorithm 1, we consider the Bradley-Terry (BT) approach and the Thurstone-Mosteller (TM) approach. As a baseline against BALToR, for each ranking model, we consider (i) a selection function that rejects pairs of instances thresholding the entropy of the

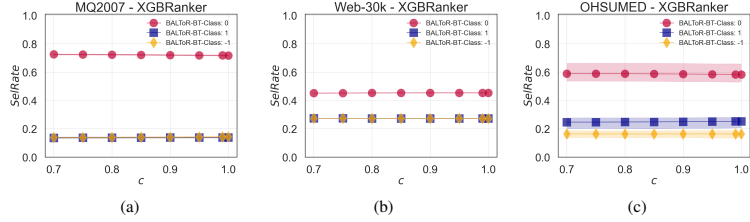


Figure 4: Distribution of classes  $SelRate$  on the selected pairs ( $mean \pm std$  over five folds) for the BT model. While the target coverage  $c$  varies, BALToR maintains stable the proportions of the classes in  $\mathcal{Y} = \{-1, 0, 1\}$ .

predicted probabilities rather than the conditional risk (the higher the entropy, the more uncertain the ranker); (ii) a random abstainer, namely a selection function that selects a fraction  $c$  of pairs of instances u.a.r. (uniformly at random).

**Metrics** Concerning **Q1**, we evaluate the effectiveness of our approach in correctly comparing pairs of instances, by computing the accuracy  $Acc$  (fraction of correctly ranked pairs) on the selected pairs at target coverage  $c$ . With respect to **Q2**, we evaluate the ability to meet the coverage constraint by calculating the actual coverage  $Cov = \frac{1}{|D_{test}|} \sum_{\mathbf{x}, \mathbf{x}' \in D_{test}} g(\mathbf{x}, \mathbf{x}')$  at target coverage  $c$ . Concerning **Q3**, we compute the fraction  $SelRate$  of each class ( $y \in \mathcal{Y} = \{-1, 0, 1\}$ ) in the selected pairs of instances at target coverage  $c$ .

**Setup** For each experimental dataset, we train rankers on the training set. Then, for each target coverage  $c \in \{.99, .95, .90, .85, .80, .75, .70\}$ , we calibrate  $\hat{\beta}_c$  on the calibration set. Then, we compute the metrics of interest on the test set. Each dataset provide five default folds, and in each fold the training, calibration (validation), and test splits are already predefined. Hence, we repeat the above procedure for each of the five default folds provided in each dataset.

Furthermore, we use default parameters for the learning to rank methods and we chose the tie probability parameter  $\theta = 2 \cdot n_{\text{pairs}} / n_{\text{no ties}} - 1$ , where  $n_{\text{no ties}}$  is the number of pairs without ties and  $n_{\text{pairs}}$  is the total number of pairs, as suggested in [Rao and Kupper, 1967].

**Reproducibility** All experiments were run on a 64-core machine with AMD EPYC 7313 16-Core Processor, RAM 1TB, OS Ubuntu 22.04.5 LTS. The code can be retrieved at <https://github.com/Ambress92/Bounded-Abstention-LTR>.

## 4.2 Experimental Results

**Q1: improving accuracy** Consider Figure 2 (and Figures 9 and 13 in Appendix B) on accuracy at target coverage  $c$ . The accuracy of the random abstainer remains flat across all datasets and probability models. The entropy-based approach might have an erratic behaviour. Such a behaviour occurs as the entropy density function might differ from the risk density function depending on how smoothed the predicted probabilities are, hence not always capturing when to abstain correctly (we show this in Appendix B). Conversely, BALToR shows an increasing accuracy when decreasing  $c$ 's, confirming the effectiveness of our approach in correctly detecting when to abstain.

For MQ2007, the  $Acc$  at full coverage is  $\approx .679 \pm .004$  for the BT and  $\approx .683 \pm .004$  for TM. When decreasing  $c$ , BALToR's accuracy keeps increasing reaching  $\approx .706 \pm .004$  for the BT model and  $\approx .713 \pm .004$  for the TM one at  $c = .70$ .

For Web-30k, the BT model with BALToR achieves an  $Acc$  of  $\approx .476 \pm .001$  at  $c = .70$ , starting from an  $Acc$  of  $\approx .471 \pm .002$  at full coverage. The TM model equipped with BALToR has a slightly better performance, with  $Acc \approx .477 \pm .001$  at  $c = .70$  and  $Acc \approx .470 \pm .003$  at full coverage.

For OHSUMED, we see a large variance between folds. On the one hand, when looking at the  $Acc$ , our approach reaches  $Acc \approx .578 \pm .07$  at  $c = .70$  and constantly drops to  $\approx .562 \pm .06$  at full coverage

for the BT model (Figure 2c). For BALToRwith TM, Figure 2f shows similar patterns, but with slightly increased performance:  $Acc$  is  $\approx .594 \pm .076$  at  $c = .70$ , and drops to  $\approx .573 \pm .07$  at full coverage.

**Q2: respecting coverage** Selection functions should respect the coverage constraint of our problem formulation Equation (2). Figure 3 (and Figures 10 and 14 in Appendix B) reports the actual (empirical) coverage  $Cov$  obtained at target coverage  $c$ . In all cases,  $Cov$  is very close to the target coverage  $c$ . For MQ2007 and Web-30k, the approach based on both the BT and the TM show an actual coverage distance from  $c$  less than  $\approx .001$ . The average distance is slightly larger for OHSUMED, with the largest difference of  $\approx .002$  at  $c = .75$  and  $c = .70$ . These results confirm the effectiveness of our approach in satisfying the coverage constraint at test time.

**Q3: evaluating the acceptance ratios** A critical aspect often underestimated in the literature, is the ability of abstaining systems to keep stable distribution of classes  $y \in \mathcal{Y} = \{-1, 0, 1\}$  in the selected (pairs of) instances. Abstention that concentrates on one class introduces forms of biases in the decision-making process [Pugnana et al., 2024]. Overall, all baselines show stable  $SelRate$  when varying  $c$ . Figure 4 (and Figures 11 and 15 in Appendix B) provide results for the three datasets, when considering BT paired with BALToR. For the sake of space, we provide the results for the entropy baseline and TM in Appendix B (the random baseline is stable by definition).

On MQ2007, when considering the BT model, the  $SelRate$  for the 0-class pairs ranges between  $\approx .718 \pm .005$  and  $\approx .725 \pm .005$ , the -1-class  $SelRate$  is between  $\approx .143 \pm .007$  and  $\approx .138 \pm .007$  and the 1-class  $SelRate$  is stable around  $\approx .139 \pm .007$  and  $\approx .136 \pm .007$ .

On Web-30k, for the Bradley-Terry model, the  $SelRate$  remain stable around  $\approx .272 \pm .002$  both for class -1 and 1, while the average  $SelRate$  for class 0 is  $\approx .456 \pm .004$ .

Also on OHSUMED, the  $SelRate$  remains almost flat : the former's  $SelRate$  is  $\approx .163 \pm .033$  for class -1,  $\approx .249 \pm .002$  for class 1, and  $\approx .586 \pm .082$  for class 0.

These results confirm that the rejections are evenly distributed across the classes and show no biases in rejecting pairs of instances belonging to specific classes.

## 5 Conclusions

Abstention methods have proven effective in mitigating the effects of uncertainty in ML models. In this paper, we introduced the bounded-abstention framework in the context of pairwise learning-to-rank. We provided a theoretical characterization of the optimal selection strategy and proposed a model-agnostic algorithm to implement it. Our experimental results demonstrated the effectiveness of the approach, showing improvements in accuracy and ranking performance, while satisfying coverage constraints and maintaining stable selection rates across different classes.

**Limitations** Our implementation relies on a given ranker provided by a learning-to-rank algorithm. In practice, obtaining a ranker with strong performances can be challenging. In turn, this could negatively affect the quality of the selection strategy, with limited improvements when abstention occurs, as known in the classification task [Franc et al., 2023, Pugnana et al., 2024]. While we considered the problem of optimizing the selection function  $g$ , with the ranker  $f$  given, an end-to-end approach is worth considering, where both  $f$  and  $g$  are optimized together.

**Future Works** We envision several future research directions. First, we aim at studying how to build optimal abstention strategy for other ranking tasks, such as listwise ranking. Second, our work focuses on ambiguity rejection. We intend to explore approaches targeting novelty rejection in the learning-to-rank setting by abstaining on pairs that are out-of-distribution. Finally, we implicitly assume that humans can correctly break ties when asked to. Such an assumption is challenged in the learning-to-defer framework [Madras et al., 2018], where humans can also make mistakes. Considering strategies for learning to defer in the context of ranking is an unexplored area.

**Broader Impact** This paper focuses on abstention mechanisms in learning to rank. The goal is to allow a ML system to avoid low-confidence decision and inform a human decision maker, who can then intervene directly or help the system to make a more informed decision. While in this paper we mainly focus on the abstention framework, eventual biases might especially arise from the interplay

between algorithms and humans decision making. We do not envision any direct ethical concern arising from our work, however a special attention might be necessary when abstention mechanisms are used in high-stakes domains.

### References

- Ralph Allan Bradley and Milton E Terry. Rank analysis of incomplete block designs: I. The method of paired comparisons. *Biometrika*, 39(3/4):324–345, 1952.
- Christopher JC Burges. From ranknet to lambdarank to lambdamart: An overview. *Learning*, 11(23-581):81, 2010.
- Tianqi Chen and Carlos Guestrin. Xgboost: A scalable tree boosting system. In *KDD*, pages 785–794. ACM, 2016.
- Weiwei Cheng, Michaël Rademaker, Bernard De Baets, and Eyke Hüllermeier. Predicting partial orders: ranking with abstention. In *Machine Learning and Knowledge Discovery in Databases: European Conference, ECML PKDD 2010, Barcelona, Spain, September 20-24, 2010, Proceedings, Part I 21*, pages 215–230. Springer, 2010.
- Weiwei Cheng, Eyke Hüllermeier, Willem Waegeman, and Volkmar Welker. Label ranking with partial abstention based on thresholded probabilistic models. In *NIPS*, pages 2510–2518, 2012.
- C. K. Chow. On optimum recognition error and reject tradeoff. *IEEE Trans. Inf. Theory*, 16(1):41–46, 1970.
- Filipe Condessa, José M. Bioucas-Dias, Carlos A. Castro, John A. Ozolek, and Jelena Kovacevic. Classification with reject option using contextual information. In *ISBI*, pages 1340–1343. IEEE, 2013.
- Luigi P. Cordella, Claudio De Stefano, Carlo Sansone, and Mario Vento. An adaptive reject option for LVQ classifiers. In *ICIAP*, volume 974 of *Lecture Notes in Computer Science*, pages 68–73. Springer, 1995.
- Corinna Cortes, Giulia DeSalvo, and Mehryar Mohri. Boosting with abstention. In *NIPS*, pages 1660–1668, 2016.
- Corinna Cortes, Giulia DeSalvo, and Mehryar Mohri. Theory and algorithms for learning with rejection in binary classification. *Ann. Math. Artif. Intell.*, 92(2):277–315, 2024.
- Christophe Denis and Mohamed Hebiri. Consistency of plug-in confidence sets for classification in semi-supervised learning. *J. of Nonpar. Statistics*, 32(1):42–72, 2020.
- Ran El-Yaniv and Yair Wiener. On the foundations of noise-free selective classification. *J. Mach. Learn. Res.*, 11:1605–1641, 2010.
- Leo Feng, Mohamed Osama Ahmed, Hossein Hajimirsadeghi, and Amir H. Abdi. Towards better selective classification. In *ICLR*. OpenReview.net, 2023.
- Vojtech Franc, Daniel Průša, and Václav Voráček. Optimal strategies for reject option classifiers. *J. Mach. Learn. Res.*, 24:11:1–11:49, 2023.
- Yonatan Geifman and Ran El-Yaniv. Selective classification for deep neural networks. In *NIPS*, pages 4878–4887, 2017.
- Yonatan Geifman and Ran El-Yaniv. Selectivenet: A deep neural network with an integrated reject option. In *ICML*, volume 97, pages 2151–2159. PMLR, 2019.
- Kilian Hendrickx, Lorenzo Perini, Dries Van der Plas, Wannes Meert, and Jesse Davis. Machine learning with a reject option: a survey. *Mach. Learn.*, 113(5):3073–3110, 2024.
- Radu Herbei and Maten H. Wegkamp. Classification with reject option. *Can. J. Stat.*, 34(4):709–721, 2006.

- William Hersh, Chris Buckley, TJ Leone, and David Hickam. Ohsumed: An interactive retrieval evaluation and new large test collection for research. In *SIGIR'94: Proceedings of the Seventeenth Annual International ACM-SIGIR Conference on Research and Development in Information Retrieval*, organised by Dublin City University, pages 192–201. Springer, 1994.
- Guolin Ke, Qi Meng, Thomas Finley, Taifeng Wang, Wei Chen, Weidong Ma, Qiwei Ye, and Tie-Yan Liu. Lightgbm: A highly efficient gradient boosting decision tree. *Advances in neural information processing systems*, 30, 2017.
- David Madras, Toniann Pitassi, and Richard S. Zemel. Predict responsibly: Improving fairness and accuracy by learning to defer. In *NeurIPS*, pages 6150–6160, 2018.
- Anqi Mao, Mehryar Mohri, and Yutao Zhong. Ranking with abstention. *CoRR*, abs/2307.02035, 2023.
- Liudmila Prokhorenkova, Gleb Gusev, Aleksandr Vorobev, Anna Veronika Dorogush, and Andrey Gulin. Catboost: unbiased boosting with categorical features. *Advances in neural information processing systems*, 31, 2018.
- Daniel Prusa and Vojtech Franc. Constrained binary decision making. In *NeurIPS*, 2025.
- Andrea Pugnana and Salvatore Ruggieri. Auc-based selective classification. In *AISTATS*, volume 206 of *Proceedings of Machine Learning Research*, pages 2494–2514. PMLR, 2023.
- Andrea Pugnana, Lorenzo Perini, Jesse Davis, and Salvatore Ruggieri. Deep neural network benchmarks for selective classification. *Journal of Data-centric Machine Learning Research (DMLR)*, 1(17):1–58, 2024.
- Tao Qin and Tie-Yan Liu. Introducing LETOR 4.0 datasets. *CoRR*, abs/1306.2597, 2013. URL <http://arxiv.org/abs/1306.2597>.
- Zhen Qin, Le Yan, Honglei Zhuang, Yi Tay, Rama Kumar Pasumarthi, Xuanhui Wang, Michael Bendersky, and Marc Najork. Are neural rankers still outperformed by gradient boosted decision trees? In *ICLR*. OpenReview.net, 2021.
- PV Rao and Lawrence L Kupper. Ties in paired-comparison experiments: A generalization of the bradley-terry model. *Journal of the American Statistical Association*, 62(317):194–204, 1967.
- Salvatore Ruggieri and Andrea Pugnana. Things machine learning models know that they don't know. In *AAAI*, pages 28684–28693. AAAI Press, 2025.
- Louis L Thurstone. A law of comparative judgment. *Psychological review*, 101(2):266, 1994.
- Francesco Tortorella. A ROC-based reject rule for dichotomizers. *Pattern Recognit. Lett.*, 26(2): 167–180, 2005.
- Ahmed Zaoui, Christophe Denis, and Mohamed Hebiri. Regression with reject option and application to knn. In *NeurIPS*, 2020.
- Ke Zhou, Gui-Rong Xue, Hongyuan Zha, and Yong Yu. Learning to rank with ties. In *Proceedings of the 31st annual international ACM SIGIR conference on Research and development in information retrieval*, pages 275–282, 2008.

## A Proofs

### Proof of Theorem 3.1

*Proof.* We adopt the same proof strategy as in Franc et al. [2023]. First, consider that: condition p1 implies that

$$g^*(\mathbf{x}, \mathbf{x}') = 1 \quad \forall (\mathbf{x}, \mathbf{x}') \in r(\mathcal{X} \times \mathcal{X})_{<\beta}$$

almost-surely. As  $p(\mathbf{x}, \mathbf{x}') \geq 0$  and since  $g(\mathbf{x}, \mathbf{x}') \in [0, 1]$  it must always be one on all the points with positive probability mass in  $r(\mathcal{X} \times \mathcal{X})_{<\beta}$  to make p1 hold.

Similarly, condition p3 implies that

$$g^*(\mathbf{x}, \mathbf{x}') = 0 \quad \forall (\mathbf{x}, \mathbf{x}') \in r(\mathcal{X} \times \mathcal{X}')_{>\beta}$$

almost-surely. As  $p(\mathbf{x}, \mathbf{x}') \geq 0$  and since  $g(\mathbf{x}, \mathbf{x}') \in [0, 1]$  it must always be zero on all the points with positive probability mass in  $r(\mathcal{X} \times \mathcal{X}')_{>\beta}$  to make p3 hold.

Now, let us consider  $R_l(f, g, y)$ . This can be decomposed as:

$$R_l(f, g, y) = \frac{\mathbb{E}_{(\mathbf{x}, \mathbf{x}', y)}[l(f(\mathbf{x}), f(\mathbf{x}'), y)g(\mathbf{x}, \mathbf{x}')]}{\mathbb{E}_{(\mathbf{x}, \mathbf{x}')}[g(\mathbf{x}, \mathbf{x}')]},$$

where the numerator is

$$\begin{aligned} & \mathbb{E}_{(\mathbf{x}, \mathbf{x}', y)}[l(f(\mathbf{x}), f(\mathbf{x}'), y)g(\mathbf{x}, \mathbf{x}')] = \\ & \iint_{\mathcal{X} \times \mathcal{X}} p(\mathbf{x}, \mathbf{x}')g(\mathbf{x}, \mathbf{x}') \left( \int_{\mathcal{Y}|\mathcal{X} \times \mathcal{X}} p(y | \mathbf{x}, \mathbf{x}')l(f(\mathbf{x}'), f(\mathbf{x}'), y) dy \right) dx dx' = \\ & \iint_{\mathcal{X} \times \mathcal{X}} p(\mathbf{x}, \mathbf{x}')g(\mathbf{x}, \mathbf{x}')r(\mathbf{x}, \mathbf{x}') dx dx', \end{aligned}$$

and the denominator is

$$\mathbb{E}_{(\mathbf{x}, \mathbf{x}')}[g(\mathbf{x}, \mathbf{x}')] = \iint_{\mathcal{X} \times \mathcal{X}} p(\mathbf{x}, \mathbf{x}')g(\mathbf{x}, \mathbf{x}') dx dx'$$

If conditions (p1), (p2) and (p3) are met, then for every  $f \in \mathcal{F}$ ,  $g^* : \mathcal{X} \times \mathcal{X} \rightarrow [0, 1]$  satisfies:

$$R(f, g^*, y) = \beta + \frac{1}{c} \iint_{r(\mathcal{X} \times \mathcal{X})_{<\beta}} p(\mathbf{x}, \mathbf{x}') dx dx' - \frac{\beta}{c} \iint_{r(\mathcal{X} \times \mathcal{X})_{<\beta}} p(\mathbf{x}, \mathbf{x}') dx dx', \quad (5)$$

as it holds that

$$\begin{aligned} & \iint_{\mathcal{X} \times \mathcal{X}} p(\mathbf{x}, \mathbf{x}')g^*(\mathbf{x}, \mathbf{x}')r(\mathbf{x}, \mathbf{x}') dx dx' = \\ & = \iint_{r(\mathcal{X} \times \mathcal{X})_{<\beta}} p(\mathbf{x}, \mathbf{x}')g^*(\mathbf{x}, \mathbf{x}')r(\mathbf{x}, \mathbf{x}') dx dx' + \iint_{r(\mathcal{X} \times \mathcal{X}')_{=\beta}} p(\mathbf{x}, \mathbf{x}')g^*(\mathbf{x}, \mathbf{x}')r(\mathbf{x}, \mathbf{x}') dx dx' + \\ & \quad + \iint_{r(\mathcal{X} \times \mathcal{X}')_{>\beta}} p(\mathbf{x}, \mathbf{x}')g^*(\mathbf{x}, \mathbf{x}')r(\mathbf{x}, \mathbf{x}') dx dx' = \\ & = \iint_{r(\mathcal{X} \times \mathcal{X})_{<\beta}} p(\mathbf{x}, \mathbf{x}')g^*(\mathbf{x}, \mathbf{x}')r(\mathbf{x}, \mathbf{x}') dx dx' + \beta \iint_{r(\mathcal{X} \times \mathcal{X}')_{=\beta}} p(\mathbf{x}, \mathbf{x}')g^*(\mathbf{x}, \mathbf{x}') dx dx' = \\ & = \iint_{r(\mathcal{X} \times \mathcal{X})_{<\beta}} p(\mathbf{x}, \mathbf{x}')g^*(\mathbf{x}, \mathbf{x}')r(\mathbf{x}, \mathbf{x}') dx dx' + \beta[c - \iint_{r(\mathcal{X} \times \mathcal{X})_{<\beta}} p(\mathbf{x}, \mathbf{x}') dx dx'] = \\ & = \beta c + \iint_{r(\mathcal{X} \times \mathcal{X})_{<\beta}} p(\mathbf{x}, \mathbf{x}') (g^*(\mathbf{x}, \mathbf{x}')r(\mathbf{x}, \mathbf{x}') - \beta) dx dx' = \\ & = \beta c + \iint_{r(\mathcal{X} \times \mathcal{X})_{<\beta}} p(\mathbf{x}, \mathbf{x}') (r(\mathbf{x}, \mathbf{x}') - \beta) dx dx', \end{aligned}$$

where the last equality comes from the fact that  $g^*(\mathbf{x}, \mathbf{x}')$  is one on all the points in  $r(\mathcal{X} \times \mathcal{X})_{<\beta}$ . Concerning the denominator, we can see that it is equal to:

$$\mathbb{E}_{(\mathbf{x}, \mathbf{x}')}[g^*(\mathbf{x}, \mathbf{x}')] = \iint_{\mathcal{X} \times \mathcal{X}_{r(\mathbf{x}, \mathbf{x}') < \beta}} p(\mathbf{x}, \mathbf{x}') d\mathbf{x} d\mathbf{x}' + c - \iint_{\mathcal{X} \times \mathcal{X}_{r(\mathbf{x}, \mathbf{x}') < \beta}} p(\mathbf{x}, \mathbf{x}') d\mathbf{x} d\mathbf{x}' = c$$

Hence,  $g^*$  is feasible. To prove the theorem, we show that for each  $g$  that is feasible (i.e.,  $g$  is such that  $\phi(g) \geq c$ ) and does not satisfy one of the conditions, we can always define another  $g'$  with a lower risk. We first show that if we consider  $g$  such that  $p1$  is violated, but  $p2$  and  $p3$  hold, then  $g$  is not optimal. Then, we show that if  $p1$  and  $p3$  holds but  $p2$  is violated,  $g$  is not optimal. Then, we show that if  $p3$  does not hold, we also have a violation of  $p1$ .

**Case 1: violation of  $p1$ .** Let us assume that  $p2$  and  $p3$  hold. If  $p1$  is violated, it means that :

$$\iint_{r(\mathcal{X} \times \mathcal{X})_{<\beta}} p(\mathbf{x}, \mathbf{x}') g(\mathbf{x}, \mathbf{x}') d\mathbf{x} d\mathbf{x}' < \iint_{r(\mathcal{X} \times \mathcal{X})_{<\beta}} p(\mathbf{x}, \mathbf{x}') d\mathbf{x} d\mathbf{x}' \quad (6)$$

This implies that  $\exists \tilde{\mathcal{X}} \subseteq \mathcal{X} \times \mathcal{X}$  s.t.

$$\forall (\mathbf{x}, \mathbf{x}') \in \tilde{\mathcal{X}} : r(\mathbf{x}, \mathbf{x}') \geq \beta \quad (7)$$

Alternatively, we can think of  $\tilde{\mathcal{X}}$  as the set of points for which it holds that:  $(\mathbf{x}, \mathbf{x}') \in \mathcal{X} \times \mathcal{X} : 0 < g(\mathbf{x}, \mathbf{x}') < 1$

and

$$\begin{aligned} & \iint_{\tilde{\mathcal{X}}} p(\mathbf{x}, \mathbf{x}') g(\mathbf{x}, \mathbf{x}') d\mathbf{x} d\mathbf{x}' = \\ &= \iint_{r(\mathcal{X} \times \mathcal{X})_{<\beta}} p(\mathbf{x}, \mathbf{x}') d\mathbf{x} d\mathbf{x}' - \iint_{r(\mathcal{X} \times \mathcal{X})_{<\beta}} p(\mathbf{x}, \mathbf{x}') g(\mathbf{x}, \mathbf{x}') d\mathbf{x} d\mathbf{x}' > 0 \end{aligned} \quad (8)$$

Now, let us consider the following  $g'$ :

$$g'(\mathbf{x}, \mathbf{x}') = \begin{cases} 1 & \text{if } r(\mathbf{x}, \mathbf{x}') < \beta \\ 0 & \text{if } (\mathbf{x}, \mathbf{x}') \in \tilde{\mathcal{X}} \\ g(\mathbf{x}, \mathbf{x}') & \text{otherwise} \end{cases} \quad (9)$$

Now notice that  $g'$  is feasible, as

$$\begin{aligned} \phi(g') &= \iint_{\mathcal{X} \times \mathcal{X}} p(\mathbf{x}, \mathbf{x}') g'(\mathbf{x}, \mathbf{x}') d\mathbf{x} d\mathbf{x}' = \\ &= \iint_{r(\mathcal{X} \times \mathcal{X})_{<\beta}} p(\mathbf{x}, \mathbf{x}') d\mathbf{x} d\mathbf{x}' + \iint_{r(\mathcal{X} \times \mathcal{X})_{\geq \beta}} g(\mathbf{x}, \mathbf{x}') p(\mathbf{x}, \mathbf{x}') = \phi(g) \end{aligned}$$

Let us now compute  $\phi(g) (R(f, g, y) - R(f, g', y))$ :

$$\begin{aligned} & \phi(g) (R(f, g, y) - R(f, g', y)) = \\ &= \iint_{\mathcal{X} \times \mathcal{X}} g(\mathbf{x}, \mathbf{x}') p(\mathbf{x}, \mathbf{x}') r(\mathbf{x}, \mathbf{x}') d\mathbf{x} d\mathbf{x}' - \iint_{\mathcal{X} \times \mathcal{X}} g'(\mathbf{x}, \mathbf{x}') p(\mathbf{x}, \mathbf{x}') r(\mathbf{x}, \mathbf{x}') d\mathbf{x} d\mathbf{x}' = \\ &= \iint_{\mathcal{X} \times \mathcal{X}} g(\mathbf{x}, \mathbf{x}') p(\mathbf{x}, \mathbf{x}') r(\mathbf{x}, \mathbf{x}') d\mathbf{x} d\mathbf{x}' - \iint_{r(\mathcal{X} \times \mathcal{X})_{<\beta}} p(\mathbf{x}, \mathbf{x}') r(\mathbf{x}, \mathbf{x}') d\mathbf{x} d\mathbf{x}' - \\ & \quad \iint_{r(\mathcal{X}, \mathcal{X}')_{\geq \beta}} g(\mathbf{x}, \mathbf{x}') p(\mathbf{x}, \mathbf{x}') r(\mathbf{x}, \mathbf{x}') d\mathbf{x} d\mathbf{x}' = \\ &= \iint_{r(\mathcal{X} \times \mathcal{X})_{<\beta}} g(\mathbf{x}, \mathbf{x}') p(\mathbf{x}, \mathbf{x}') r(\mathbf{x}, \mathbf{x}') d\mathbf{x} d\mathbf{x}' + \iint_{\tilde{\mathcal{X}}} g(\mathbf{x}, \mathbf{x}') p(\mathbf{x}, \mathbf{x}') r(\mathbf{x}, \mathbf{x}') d\mathbf{x} d\mathbf{x}' - \\ & \quad \iint_{r(\mathcal{X} \times \mathcal{X})_{<\beta}} p(\mathbf{x}, \mathbf{x}') r(\mathbf{x}, \mathbf{x}') d\mathbf{x} d\mathbf{x}' = \\ &= \iint_{r(\mathcal{X} \times \mathcal{X})_{<\beta}} (g(\mathbf{x}, \mathbf{x}') - 1) p(\mathbf{x}, \mathbf{x}') r(\mathbf{x}, \mathbf{x}') d\mathbf{x} d\mathbf{x}' + \iint_{\tilde{\mathcal{X}}} g(\mathbf{x}, \mathbf{x}') p(\mathbf{x}, \mathbf{x}') r(\mathbf{x}, \mathbf{x}') \end{aligned}$$

Now, we can re-write the last equation as follows, by noticing that Eq. 7 and Eq. 8 imply that:

$$\begin{aligned} & \iint_{r(\mathcal{X} \times \mathcal{X}) < \beta} (g(\mathbf{x}, \mathbf{x}') - 1) p(\mathbf{x}, \mathbf{x}') r(\mathbf{x}, \mathbf{x}') d\mathbf{x} d\mathbf{x}' + \iint_{\mathcal{X}} g(\mathbf{x}, \mathbf{x}') p(\mathbf{x}, \mathbf{x}') r(\mathbf{x}, \mathbf{x}') \geq \\ & \iint_{r(\mathcal{X} \times \mathcal{X}) < \beta} (g(\mathbf{x}, \mathbf{x}') - 1) p(\mathbf{x}, \mathbf{x}') r(\mathbf{x}, \mathbf{x}') d\mathbf{x} d\mathbf{x}' + \beta \iint_{r(\mathcal{X} \times \mathcal{X}) < \beta} (1 - g(\mathbf{x}, \mathbf{x}')) p(\mathbf{x}, \mathbf{x}') d\mathbf{x} d\mathbf{x}' = \\ & \iint_{r(\mathcal{X} \times \mathcal{X}) < \beta} p(\mathbf{x}, \mathbf{x}') (1 - g(\mathbf{x}, \mathbf{x}')) (\beta - r(\mathbf{x}, \mathbf{x}')) d\mathbf{x} d\mathbf{x}' > 0 \end{aligned}$$

Hence, if  $p1$  is not holding,  $g(\mathbf{x}, \mathbf{x}')$  is not optimal.

**Case 2: violation p2** Let us assume that  $p1$  is satisfied, but  $p2$  is violated, i.e.,

$$\iint_{r(\mathcal{X} \times \mathcal{X}') = \beta} g(\mathbf{x}, \mathbf{x}') p(\mathbf{x}, \mathbf{x}') d\mathbf{x} d\mathbf{x}' < c \iint_{r(\mathcal{X} \times \mathcal{X}') < \beta} p(\mathbf{x}, \mathbf{x}') d\mathbf{x} d\mathbf{x}' > 0$$

In this case, we can define a  $g' : \mathcal{X} \times \mathcal{X} \rightarrow [0, 1]$  such that

$$g'(\mathbf{x}, \mathbf{x}') = \begin{cases} g(\mathbf{x}, \mathbf{x}') & \text{if } r(\mathbf{x}, \mathbf{x}') < \beta \\ 0 & \text{if } r(\mathbf{x}, \mathbf{x}') > \beta \end{cases} \quad (10)$$

and it satisfies the following condition

$$\begin{aligned} & \iint_{r(\mathcal{X} \times \mathcal{X}') = \beta} g'(\mathbf{x}, \mathbf{x}') p(\mathbf{x}, \mathbf{x}') d\mathbf{x} d\mathbf{x}' = \\ & = \iint_{r(\mathcal{X} \times \mathcal{X}') = \beta} g(\mathbf{x}, \mathbf{x}') p(\mathbf{x}, \mathbf{x}') d\mathbf{x} d\mathbf{x}' + \iint_{r(\mathcal{X} \times \mathcal{X}') > \beta} g(\mathbf{x}, \mathbf{x}') p(\mathbf{x}, \mathbf{x}') d\mathbf{x} d\mathbf{x}' \end{aligned} \quad (11)$$

Now, we can see that  $\phi(g) = \phi(g')$  as:

$$\begin{aligned} \phi(g') &= \iint_{\mathcal{X} \times \mathcal{X}} g'(\mathbf{x}, \mathbf{x}') p(\mathbf{x}, \mathbf{x}') d\mathbf{x} d\mathbf{x}' = \\ &= \iint_{r(\mathcal{X} \times \mathcal{X}') < \beta} g'(\mathbf{x}, \mathbf{x}') p(\mathbf{x}, \mathbf{x}') d\mathbf{x} d\mathbf{x}' + \iint_{r(\mathcal{X} \times \mathcal{X}') = \beta} g'(\mathbf{x}, \mathbf{x}') p(\mathbf{x}, \mathbf{x}') d\mathbf{x} d\mathbf{x}' = \\ &= \iint_{r(\mathcal{X} \times \mathcal{X}') < \beta} g(\mathbf{x}, \mathbf{x}') p(\mathbf{x}, \mathbf{x}') d\mathbf{x} d\mathbf{x}' + \iint_{r(\mathcal{X} \times \mathcal{X}') = \beta} g(\mathbf{x}, \mathbf{x}') p(\mathbf{x}, \mathbf{x}') d\mathbf{x} d\mathbf{x}' + \\ & \quad + \iint_{r(\mathcal{X} \times \mathcal{X}') > \beta} g(\mathbf{x}, \mathbf{x}') p(\mathbf{x}, \mathbf{x}') d\mathbf{x} d\mathbf{x}' = \phi(g) \end{aligned}$$

Hence, we can consider the following:

$$\begin{aligned} & \phi(g) (R(f, g, y) - R(f, g', y)) = \\ & \beta \iint_{r(\mathcal{X} \times \mathcal{X}') = \beta} g(\mathbf{x}, \mathbf{x}') p(\mathbf{x}, \mathbf{x}') d\mathbf{x} d\mathbf{x}' + \iint_{r(\mathcal{X} \times \mathcal{X}') > \beta} g(\mathbf{x}, \mathbf{x}') p(\mathbf{x}, \mathbf{x}') r(\mathbf{x}, \mathbf{x}') d\mathbf{x} d\mathbf{x}' - \\ & \quad \beta \iint_{r(\mathcal{X} \times \mathcal{X}') = \beta} g'(\mathbf{x}, \mathbf{x}') p(\mathbf{x}, \mathbf{x}') d\mathbf{x} d\mathbf{x}' = \\ & = \iint_{r(\mathcal{X} \times \mathcal{X}') > \beta} g(\mathbf{x}, \mathbf{x}') p(\mathbf{x}, \mathbf{x}') r(\mathbf{x}, \mathbf{x}') d\mathbf{x} d\mathbf{x}' - \beta \iint_{r(\mathcal{X} \times \mathcal{X}') > \beta} g(\mathbf{x}, \mathbf{x}') p(\mathbf{x}, \mathbf{x}') d\mathbf{x} d\mathbf{x}' > \\ & \quad \beta \iint_{r(\mathcal{X} \times \mathcal{X}') > \beta} g(\mathbf{x}, \mathbf{x}') p(\mathbf{x}, \mathbf{x}') d\mathbf{x} d\mathbf{x}' - \beta \iint_{r(\mathcal{X} \times \mathcal{X}') > \beta} g(\mathbf{x}, \mathbf{x}') p(\mathbf{x}, \mathbf{x}') d\mathbf{x} d\mathbf{x}' = 0 \end{aligned}$$

Hence,  $g$  is not optimal.

**Case 3. Violation of  $p2$  or  $p3$ .** Let us consider the case when  $g$  is such that  $\phi(g) > c$ , i.e., either one of the following conditions hold:

$$\iint_{r(\mathcal{X} \times \mathcal{X}') = \beta} g(\mathbf{x}, \mathbf{x}') p(\mathbf{x}, \mathbf{x}') d\mathbf{x} d\mathbf{x}' > c - \iint_{r(\mathcal{X} \times \mathcal{X}') < \beta} p(\mathbf{x}, \mathbf{x}') d\mathbf{x} d\mathbf{x}' \quad (12)$$

$$\iint_{r(\mathcal{X} \times \mathcal{X}') > \beta} g(\mathbf{x}, \mathbf{x}') p(\mathbf{x}, \mathbf{x}') d\mathbf{x} d\mathbf{x}' > 0 \quad (13)$$

We notice that for every  $\alpha \in \mathbb{R}^+$ , it holds that  $R(f, g, y) = R(f, \alpha \cdot g, y)$ . Now we consider  $g' : \mathcal{X} \times \mathcal{X}' \rightarrow [0, 1]$  such that  $g' = \frac{c}{\phi(g)} g$ . It is straightforward to notice that  $\phi(g') = c$  and the following holds:

$$\begin{aligned} & \iint_{r(\mathcal{X} \times \mathcal{X}') < \beta} g'(\mathbf{x}, \mathbf{x}') p(\mathbf{x}, \mathbf{x}') d\mathbf{x} d\mathbf{x}' = \\ & = \frac{c}{\phi(g)} \iint_{r(\mathcal{X} \times \mathcal{X}') < \beta} g(\mathbf{x}, \mathbf{x}') p(\mathbf{x}, \mathbf{x}') d\mathbf{x} d\mathbf{x}' < \iint_{r(\mathcal{X} \times \mathcal{X}') < \beta} p(\mathbf{x}, \mathbf{x}') d\mathbf{x} d\mathbf{x}' \end{aligned} \quad (14)$$

This implies that  $g'$  violates condition  $p1$  and is therefore not optimal. Consequently, since  $R(f, g', y) = R(f, g, y)$ ,  $g$  is also not optimal.  $\square$

### Proof of Theorem 3.2

*Proof.* Clearly,  $g^*$  satisfies  $p1$  and  $p3$ . If  $\iint_{r(\mathcal{X} \times \mathcal{X}') = \beta} p(\mathbf{x}, \mathbf{x}') d\mathbf{x} d\mathbf{x}' = 0$ , then condition  $p2$  is met as  $\iint_{r(\mathcal{X} \times \mathcal{X}') < \beta} p(\mathbf{x}, \mathbf{x}') d\mathbf{x} d\mathbf{x}' = c$ . Otherwise, by the definition of  $g^*$  it holds that:

$$\iint_{r(\mathcal{X} \times \mathcal{X}') = \beta} \left( c - \frac{\iint_{r(\mathcal{X} \times \mathcal{X}') < \beta} p(\mathbf{z}, \mathbf{z}') d\mathbf{z} d\mathbf{z}'}{\iint_{r(\mathcal{X} \times \mathcal{X}') = \beta} p(\mathbf{z}, \mathbf{z}') d\mathbf{z} d\mathbf{z}'} \right) p(\mathbf{x}, \mathbf{x}') d\mathbf{x} d\mathbf{x}' = c - \iint_{r(\mathcal{X} \times \mathcal{X}') < \beta} p(\mathbf{x}, \mathbf{x}') d\mathbf{x} d\mathbf{x}'$$

which means condition  $p2$  is met. Hence,  $g^*$  is optimal.  $\square$

### Proof of Proposition 3.3

*Proof.* Let us consider the 0-1 loss, hence the conditional risk is:

$$r_{0-1}(\mathbf{x}, \mathbf{x}') = p(1 | \mathbf{x}, \mathbf{x}') \mathbb{I}_{\hat{y} = -1, 0} + p(0 | \mathbf{x}, \mathbf{x}') \mathbb{I}_{\hat{y} = -1, 1} + p(-1 | \mathbf{x}, \mathbf{x}') \mathbb{I}_{\hat{y} = 0, 1},$$

where  $\hat{y} = \arg \max_{y \in \{-1, 0, 1\}} \{p(-1 | \mathbf{x}, \mathbf{x}'), p(0 | \mathbf{x}, \mathbf{x}'), p(1 | \mathbf{x}, \mathbf{x}')\}$  is the predicted label by the pairwise ranker.

Now let us consider the case where  $p(-1 | \mathbf{x}, \mathbf{x}') = \max_{y \in \{-1, 0, 1\}} \{p(-1 | \mathbf{x}, \mathbf{x}'), p(0 | \mathbf{x}, \mathbf{x}'), p(1 | \mathbf{x}, \mathbf{x}')\}$ .

Then it holds that:

$$\begin{aligned} r_{0-1}(\mathbf{x}, \mathbf{x}') &= p(0 | \mathbf{x}, \mathbf{x}') + p(1 | \mathbf{x}, \mathbf{x}') = 1 - p(-1 | \mathbf{x}, \mathbf{x}') = \\ &= 1 - \max_{y \in \{-1, 0, 1\}} \{p(-1 | \mathbf{x}, \mathbf{x}'), p(0 | \mathbf{x}, \mathbf{x}'), p(1 | \mathbf{x}, \mathbf{x}')\}, \end{aligned}$$

where the first equality comes from the fact the prediction is  $\hat{y} = -1$ . By considering the remaining two cases, we can see that the result holds also when  $p(0 | \mathbf{x}, \mathbf{x}') = \max_{y \in \{-1, 0, 1\}} \{p(-1 | \mathbf{x}, \mathbf{x}'), p(0 | \mathbf{x}, \mathbf{x}'), p(1 | \mathbf{x}, \mathbf{x}')\}$  and  $p(1 | \mathbf{x}, \mathbf{x}') = \max_{y \in \{-1, 0, 1\}} \{p(-1 | \mathbf{x}, \mathbf{x}'), p(0 | \mathbf{x}, \mathbf{x}'), p(1 | \mathbf{x}, \mathbf{x}')\}$ , concluding the proof.  $\square$

## B Additional results

**Discussion of entropy-based methods** We showcase here an example of the erratic behaviour of the entropy baseline. Figure 5 provides the plots for the estimated density functions over MQ2007 Fold 1 calibration set for both entropy and BALToR. On the one hand, we can observe that the shapes of the density functions differ when using the BT model, thus the entropy-baseline fails to correctly detect pairs to abstain on. On the other hand, when using TM model, the entropy's distribution is similar to BALToR's, thus achieving similar results. We argue this pattern occurs as the BT model tends to provide predicted probabilities that are less peaked, hence increasing the overall entropy.

**Additional Results** We provide here the additional results for (i) coverage (Figure 6) and *SelRate* (Figure 7) when using the TM model and the XGBoost ranker; (ii) for all the metrics when using the CatBoost and LightGBM implementations of ranking (Figure 9-Figure 16). Overall results are comparable, with small difference among the different implementations.

## 7.1 Bounded-Abstention Pairwise Learning to Rank

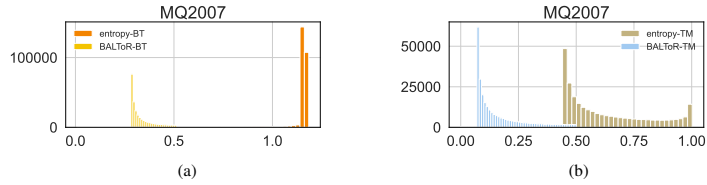


Figure 5: Estimated density functions over MQ2007 Fold 1 calibration set for BT (Figure 5a) and TM (Figure 5b) when using an XGBRanker. The shapes of the density functions differ (are similar) when using BT (TM) model.

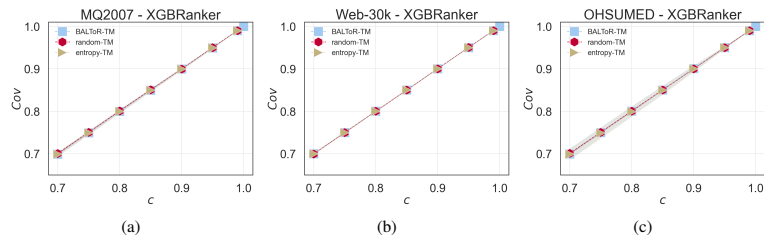


Figure 6: Actual (empirical) coverage  $Cov$  on the test set ( $mean \pm std$  over five folds) for the TM model. The actual coverage remains very close to the target coverage  $c$ .

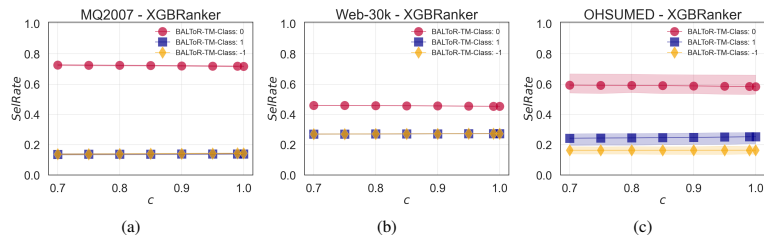


Figure 7: Distribution of classes  $SelRate$  on the selected pairs ( $mean \pm std$  over five folds) for the TM model. While the target coverage  $c$  varies, BALToR maintains stable the proportions of the classes in  $\mathcal{Y} = \{-1, 0, 1\}$ .

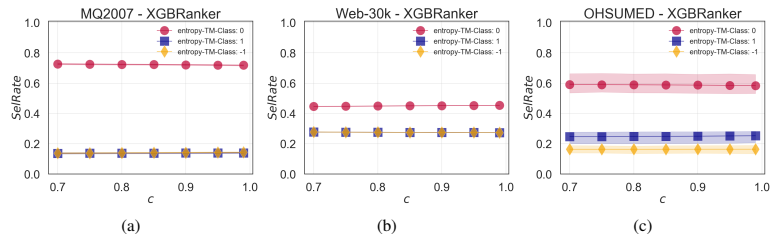


Figure 8: Distribution of classes  $SelRate$  on the selected pairs ( $mean \pm std$  over five folds) for the entropy model. While the target coverage  $c$  varies, entropy maintains stable the proportions of the classes in  $\mathcal{Y} = \{-1, 0, 1\}$ .

## 7.1 Bounded-Abstention Pairwise Learning to Rank

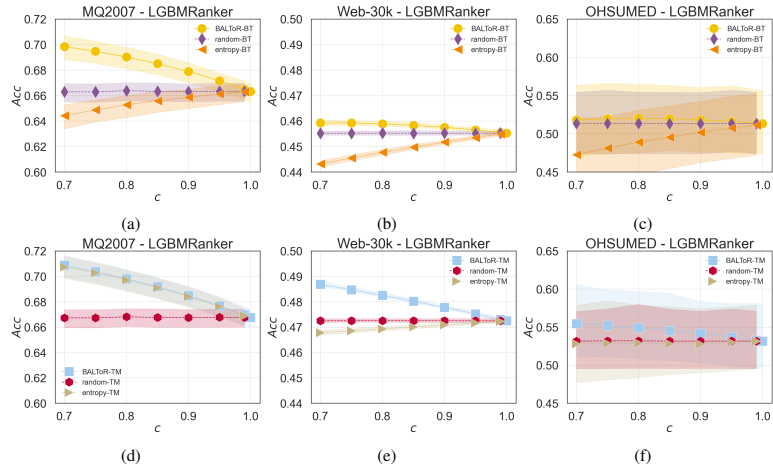


Figure 9: *Acc* results (*mean*  $\pm$  *std* over five folds) for the BT model (top line) and the TM model (bottom line) when using LightGBM.

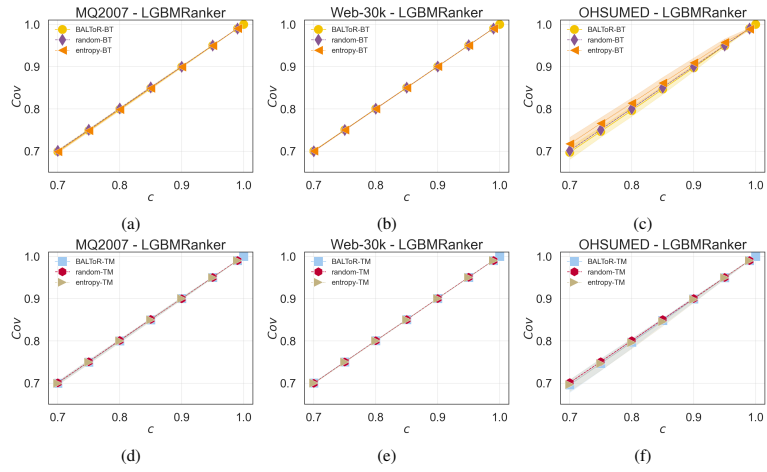


Figure 10: *Cov* results (*mean*  $\pm$  *std* over five folds) for the BT model (top line) and the TM model (bottom line) when using LightGBM.

## 7.1 Bounded-Abstention Pairwise Learning to Rank

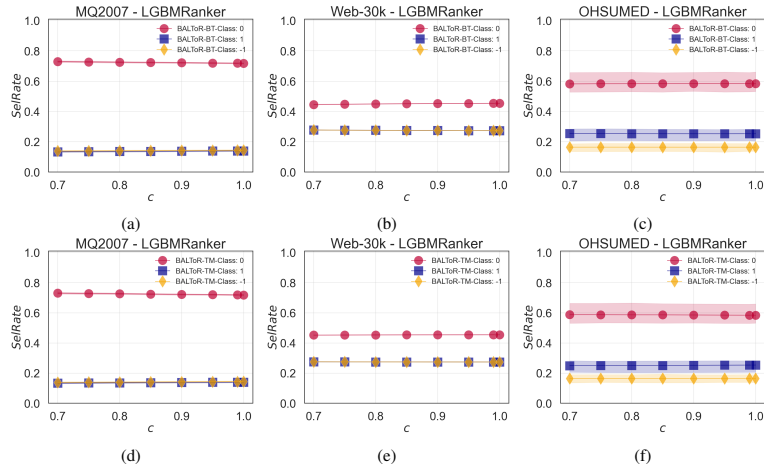


Figure 11: *SelRate* results (*mean*  $\pm$  *std* over five folds) for the BT model (top line) and the TM model (bottom line) when using LightGBM and BALToR.

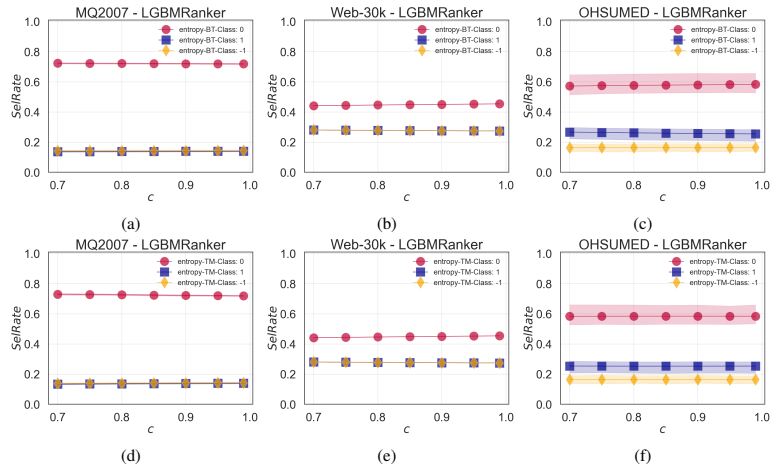


Figure 12: *SelRate* results (*mean*  $\pm$  *std* over five folds) for the BT model (top line) and the TM model (bottom line) when using LightGBM and entropy.

## 7.1 Bounded-Abstention Pairwise Learning to Rank

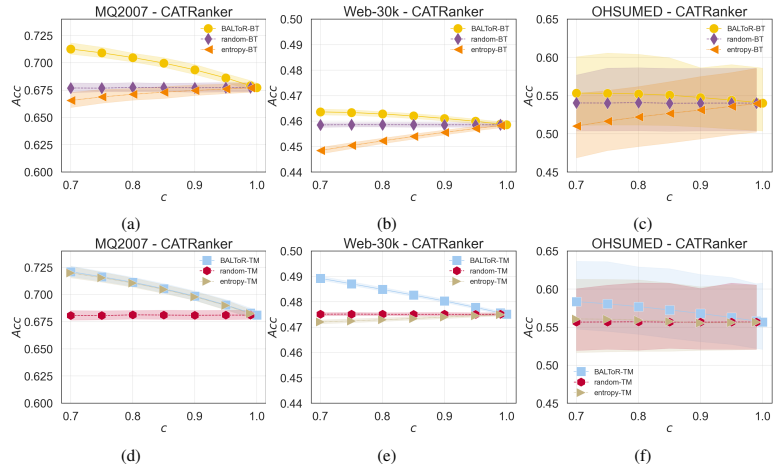


Figure 13: *Acc* results (*mean ± std* over five folds) for the BT model (top line) and the TM model (bottom line) when using CatBoost.

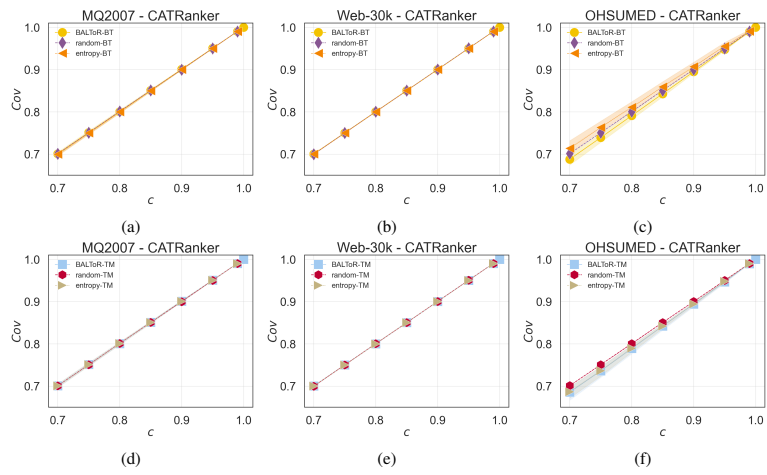


Figure 14: *Cov* results (*mean ± std* over five folds) for the BT model (top line) and the TM model (bottom line) when using CatBoost.

## 7.1 Bounded-Abstention Pairwise Learning to Rank

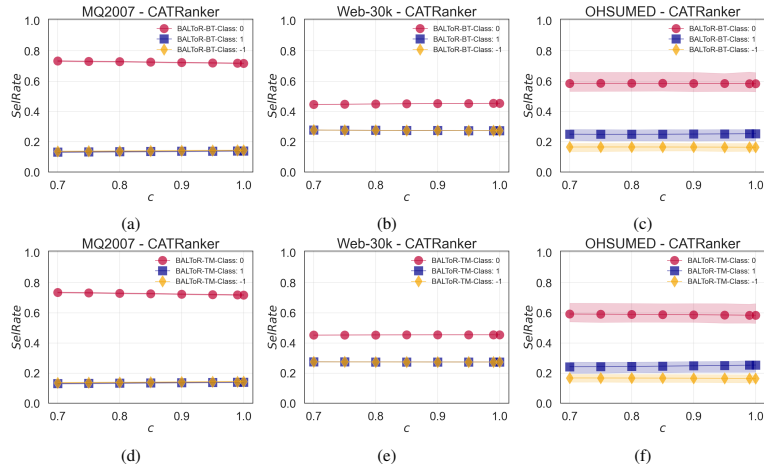


Figure 15: *SelRate* results ( $mean \pm std$  over five folds) for the BT model (top line) and the TM model (bottom line) when using CatBoost and BALToR.

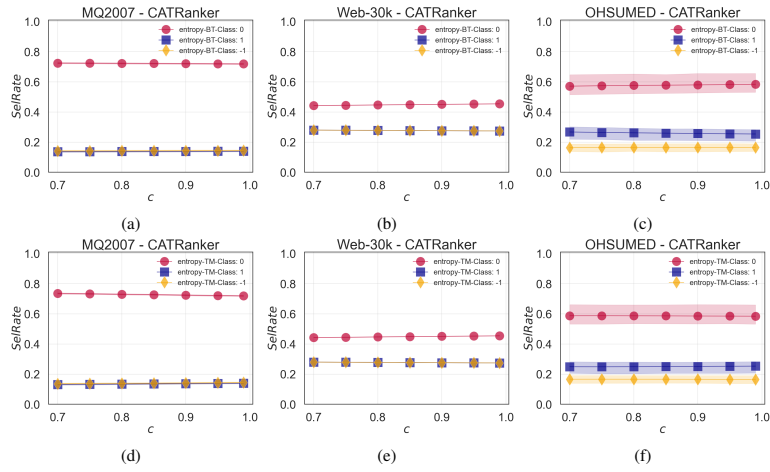


Figure 16: *SelRate* results ( $mean \pm std$  over five folds) for the BT model (top line) and the TM model (bottom line) when using CatBoost and entropy.

## 7.2 Policy Advice and Best Practices on Bias and Fairness in AI

While algorithmic interventions can improve fairness and reliability at the model level, ensuring trustworthy AI requires a broader perspective that considers the entire lifecycle of AI systems. Bias and unreliability can emerge at multiple stages, including data collection, model development, deployment, and ongoing use. Addressing these challenges therefore requires not only technical solutions but also organizational and regulatory practices.

This work synthesizes the technical contributions of the thesis into a set of policy recommendations and best practices for managing bias and ensuring reliability in AI systems. Central to this approach is a holistic bias management framework, which emphasizes that fairness cannot be achieved through isolated, post-hoc corrections but must instead be addressed systematically across all stages of the pipeline.

The framework highlights several key challenges. First, regulatory constraints, such as those imposed by data protection laws, can limit access to sensitive attributes, complicating fairness auditing and mitigation efforts. Second, AI systems are subject to temporal dynamics, including distribution shifts and feedback loops, which can degrade performance and fairness over time. Third, tools such as explainable AI, while useful, may introduce additional instability or biases if not applied carefully.

To address these issues, the work outlines practical recommendations, including the adoption of continuous monitoring, the integration of causal reasoning to better understand discriminatory mechanisms, and the explicit documentation of data generation processes and human involvement. These practices aim to ensure that AI systems remain reliable, auditable, and aligned with societal and regulatory requirements.

### Authors' Contributions

---

<b>Contribution</b>	<b>Authors</b>
<b>Conceptualization:</b>	J.M. Alvarez and all authors
<b>Writing:</b>	J.M. Alvarez and all authors A. Ferrara mainly wrote the Mitigating bias section
<b>Methodology:</b>	J.M. Alvarez and all authors

---



## Policy advice and best practices on bias and fairness in AI

Jose M. Alvarez<sup>1,2</sup> · Alejandra Bringas Colmenarejo<sup>3</sup> · Alaa Elobaid<sup>4,5</sup> · Simone Fabbri<sup>4,6,7</sup> · Miriam Fahimi<sup>8</sup> · Antonio Ferrara<sup>9,10</sup> · Siamak Ghodsi<sup>5,6</sup> · Carlos Mougán<sup>3</sup> · Ioanna Papageorgiou<sup>6</sup> · Paula Reyro<sup>11</sup> · Mayra Russo<sup>6</sup> · Kristen M. Scott<sup>12</sup> · Laura State<sup>1,2</sup> · Xuan Zhao<sup>13</sup> · Salvatore Ruggieri<sup>2</sup>

Accepted: 16 January 2024 / Published online: 29 April 2024  
© The Author(s) 2024

### Abstract

The literature addressing bias and fairness in AI models (*fair-AI*) is growing at a fast pace, making it difficult for novel researchers and practitioners to have a bird's-eye view picture of the field. In particular, many policy initiatives, standards, and best practices in fair-AI have been proposed for setting principles, procedures, and knowledge bases to guide and operationalize the management of bias and fairness. The first objective of this paper is to concisely survey the state-of-the-art of fair-AI methods and resources, and the main policies on bias in AI, with the aim of providing such a bird's-eye guidance for both researchers and practitioners. The second objective of the paper is to contribute to the policy advice and best practices state-of-the-art by leveraging from the results of the NoBIAS research project. We present and discuss a few relevant topics organized around the NoBIAS architecture, which is made up of a Legal Layer, focusing on the European Union context, and a Bias Management Layer, focusing on understanding, mitigating, and accounting for bias.

**Keywords** Artificial Intelligence · Bias · Fairness · Policy advice · Best practices

### Introduction

The last decade has witnessed a renaissance of Artificial Intelligence (AI), leading to an increasingly pervasive usage in many socially sensitive tasks. However, many concerns have been raised about the—intentional or unintentional—negative impacts on individuals and society due to biases embedded in AI models<sup>1</sup> (Future of Privacy Forum, 2017; Shelby et al., 2023). A few AI incident databases report collections of harms or near harms realized in the real world by intelligent systems (Turri & Dzombak, 2023), the most relevant one being illegal discrimination against social groups protected by non-discrimination law (Altman, 2020). In fact, there is a deep academic and social discussion around the need to evaluate the claims, decisions, actions and policies that are being made based on the AI's alleged neutrality as more examples confirm that algorithmic systems “are value-laden in that they (1) create moral consequences,

(2) reinforce or undercut ethical principles, or (3) enable or diminish stakeholder rights and dignity” (Martin, 2019).

The objective of this paper is twofold.

*First*, we aim at providing the reader with an up-to-date entry-point to the state-of-the-art of the multidisciplinary research on bias and fairness in AI. We take a bird's-eye view of the methods and resources, with links to specialized surveys, and of the issues and challenges related to policies on bias and fairness in AI. Such an overview provides guidance for both new researchers and AI practitioners that want to find their way in the blooming literature of the area.

*Second*, we contribute towards the objective of providing policy advice and best practices for dealing with bias and fairness in AI by leveraging from the results of the NoBIAS project<sup>2</sup>. We present and discuss a few topics that emerged during the execution of the project, whose focus was on legal challenges in the context of the European Union (EU) legislation, and on understanding, mitigating, and accounting for bias from a multidisciplinary perspective. The presented

<sup>1</sup> Due to the large body of literature, we prioritize the citation of survey papers, where applicable, and recent works.

<sup>2</sup> <https://nobias-project.eu/>.

Extended author information available on the last page of the article

issues are relevant but not sufficiently developed or acknowledged in the literature. As such, the paper can contribute to the advancement of the research and to increase awareness on bias and fairness in AI.

### Introducing fair-AI

In general, bias can be defined as “an attitude that always favors one way of feeling or acting over any other” (Bias, 2023). In human cognition and reasoning, this is the result of evolution (Haselton et al., 2005), for which some heuristics work well in most circumstances, or have a smaller cost than alternative strategies. In AI, biases can originate in the data (*pre-existing bias*), in the design of AI algorithms and systems (*technical bias*), and in the organizational processes using AI models (*emerging bias*). Most AI models are data-driven, hence they may inherit bias embedded in representations of reality encoded in raw data (Shahbazi et al., 2023). In fact, data are not neutral but are instead value-laden (Gitelman, 2013). Biases in AI algorithms have similar foundations as human cognitive biases, namely the reliance on heuristic algorithmic-search strategies that work well on average (Hellström et al., 2020). Quantitative loss metrics that are optimized by AI algorithms may result in an oversimplification of the complexity of reality, hence leading to a systematic difference between what AI actually models and the reality it is intended to abstract (Grimes & Schulz, 2002; Danks and London, 2017) (*internal validity*). Moreover, the usage of AI in complex socio-technical processes under untested or unplanned conditions may suffer from a lack of generalizability of the AI models (*external validity*). Several categorizations of the sources of bias and fairness in AI have been proposed in contexts such as social data (Olteanu et al., 2019), Machine Learning (ML) representations (Shahbazi et al., 2023), ML algorithms (Mehrabi et al., 2021), recommender systems (Chen et al., 2023a), algorithmic hiring (Fabris et al., 2023), large language models (Gallegos et al., 2023), and industry standards (ISO/IEC, 2021) to cite a few.

Fairness in AI (or simply, *fair-AI*) aims at designing methods for detecting, mitigating, and controlling biases in AI-supported decision making (Schwartz et al., 2022; Ntoutsis et al., 2020), especially when such biases lead to (in an ethical sense) unfair or (in a legal sense) discriminatory decisions. Fairness research in human decision-making was triggered by the US Civil Rights Act of 1964 (Hutchinson & Mitchell, 2019), while bias in procedural (i.e., hand-written by humans) algorithms has been considered since the mid 1990’s (Friedman & Nissenbaum, 1996)—with the first known case tracing back to 1986 (Lowry & Macpherson, 1986). Instead, fair-AI research is only 15 years old, starting with the pioneering

works of Pedreschi et al. (2008) and Kamiran and Calders (2009). The area originally addressed discrimination and unfairness in ML, and it has been rapidly expanding to all sub-fields of AI and to any possible harm to individuals and collectivities. The state-of-the-art has been mainly developing on the technical side, often reducing the problem to a numeric optimization of some fairness metric (Ruggieri et al., 2023; Carey & Wu, 2023; Weinberg, 2022). Such critiques to the hegemonic (i.e., dominant) theory of fair-AI are not new to the AI community. For instance, Wagstaff (2012) questioned the hyper-focus of ML on abstract metrics “in that they explicitly ignore or remove problem-specific details, usually so that numbers can be compared across domains” but the true significance and impact of the metrics are neglected. Likewise, Mittelstadt et al. (2023) pointed out how “the majority of measures and methods to mitigate bias and improve fairness in algorithmic systems have been built in isolation from policy and civil societal contexts and lack serious engagement with philosophical, political, legal, and economic theories of equality and distributive justice”, and proposed to address future discussion more towards substantive equality of opportunities and away from strict egalitarianism by default. The issue of engineering fairness is, without doubts, challenging (Scantamburlo, 2021), and likely to require domain-specific approaches (Lee & Floridi, 2021; Chen et al., 2023b) and the ability to distinguish whether and when to use AI (Lin et al., 2020), or how to enhance and extend human capabilities with AI (*human-centered AI*) (Xu, 2019; Garibay et al., 2023). A paradigmatic case is presented in Silberzahn and Uhlmann (2015), where 29 teams of researchers approached the same research question (about football players’ skin colour and red cards) on the same dataset with a wide array of analytical techniques, and obtaining highly varied results. The authors concluded that “bringing together many teams of skilled researchers can balance discussions, validate scientific findings and better inform policy-makers”.

### The NoBIAS project

The NoBIAS project (January 2020–June 2024) was a Marie Skłodowska-Curie Innovative Training Network funded by the European Union’s Horizon 2020 research and innovation program. The core objective of NoBIAS was to research and develop novel interdisciplinary methods for AI-based decision making without bias. Fig. 1 shows the NoBIAS architecture, which is designed to integrate bias management with the AI-system pipeline layer. The Bias Management Layer is made up of the various components contributed by the research projects of fifteen Early-Stage Researchers (ESRs). Together, these components aim to achieve three

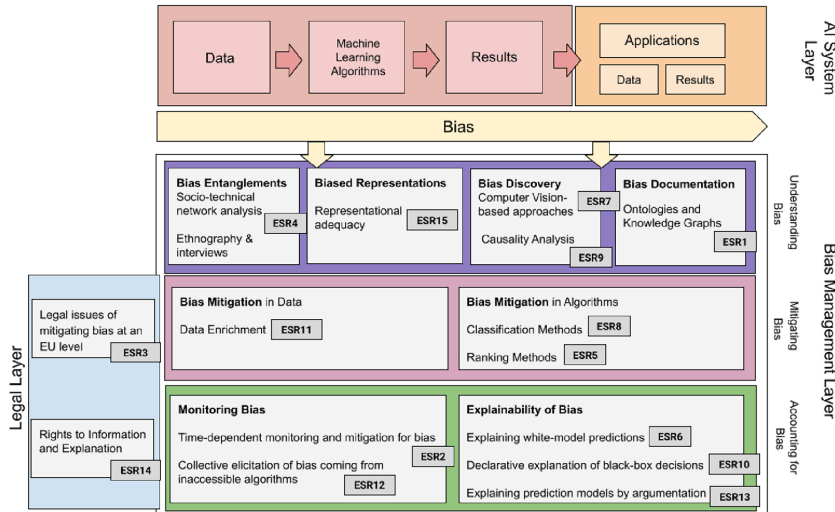


**Fig. 1** The NoBIAS architecture integrates the components necessary to understand, mitigate, and account for bias, addressing the whole AI-System decision-making pipeline

main research objectives: understanding bias, mitigating bias, and accounting for bias in data and AI-systems. An orthogonal Legal Layer provides the necessary EU legal grounds supporting the research objectives. The purpose is not to produce one single bias management framework but rather to combine technologies and techniques for generating bias-aware AI-systems in different application domains and contexts.

#### Summary of contributions

The contributions of this paper are twofold:

- we concisely survey the state-of-the-art of fair-AI methods and resources, and the main topics about policies on bias in AI (Sect. “[The landscape of policies on bias and fairness in AI](#)”), thus providing guidance for both researchers and practitioners;
- we discuss the main policy suggestions and the best practices that, in light of the execution of the NoBIAS project, are deemed relevant and under-developed (Sect. “[Lessons from the NoBIAS project](#)”). These topics are presented w.r.t. the pillars of the NoBIAS architecture (legal challenges, bias understanding, bias mitigation, and accounting for bias).

We take a multidisciplinary approach, thus facilitating cross-fertilization.

#### The landscape of policies on bias and fairness in AI

In this section, we provide a concise overview of state-of-the-art fair-AI methods and policy topics. We point to the main contributions and resources in the area to provide guidance for both researchers and practitioners.

#### Fair-AI methods and resources

Multiple measures of the degree of (un)fairness in (automated) decision making have been introduced in ML and AI (Castelnuovo et al., 2022; Mehrabi et al., 2021; Berk et al., 2021; Verma & Rubin, 2018; Zliobaite, 2017; Caton & Haas, 2024). Some of them were originally proposed and investigated in other disciplines, such as philosophy, economics, and social science (Lee et al., 2021b; Hutchinson & Mitchell, 2019; Binns, 2018a; Romei & Ruggieri, 2014). *Group fairness* metrics aim at measuring the statistical difference in distributions of decisions across social groups. *Individual fairness* metrics bind the

distance in the decision space to the distance in the feature space describing people's characteristics. *Causal fairness* metrics exploit knowledge beyond observational data to infer causal relations between membership to a protected group and decisions, and to estimate interventional consequences. As with other performance objectives, the choice of a fairness metric is crucial for optimizing AI models. See the previous surveys and Rüz (2021); Wachter et al. (2021a); Hertweck et al. (2021); Binns (2020); Tang et al. (2023); Binns et al. (2023) for a discussion of the moral/legal bases and relative merits of the various fairness notions and metrics.

Fairness metrics are the building block for numerous methods and tools of fair-AI. They aim at bias detection (a.k.a. *discrimination discovery* or *fairness testing*) (Chen et al., 2022), at data de-biasing through data processing (*pre-processing approaches*) (Shahbazi et al., 2023; Zhang et al., 2023), at fair learning of AI models and representations (*in-processing approaches*) (Wan et al., 2023), at correcting existing models (*post-processing approaches*), and at monitoring models' decisions (*monitoring*) (Kenthapadi et al., 2022; Barrainkua et al., 2022). We also refer to Pessach and Shmueli (2022); Hort et al. (2022); Mehrabi et al. (2021); Ashurst and Weller (2023) and to Fabris et al. (2022); Quy et al. (2022), respectively, for surveys of the techniques and of the experimental datasets commonly used in the field. Several off-the-shelf software libraries are available to practitioners, expanding at a fast pace. Some critical gaps to be addressed by such systems are discussed in Richardson and Gilbert (2021); Lee and Singh (2021); Balayn et al. (2023). A few papers critically discuss the inherent limitations of fair-AI (Friedler et al., 2021; Buyl & Bie, 2024; Ruggieri et al., 2023; Castelnuovo et al., 2023).

Research in fair-AI originated from the supervised ML area, but it has been rapidly expanding to all sub-fields of AI, including unsupervised (Chhabra et al., 2021; Dong et al., 2023) and reinforcement learning (Gajane et al., 2022), natural language processing (NLP) (Blodgett et al., 2020; Czarnowska et al., 2021; Gallegos et al., 2023), computer vision (Fabrizzi et al., 2022), speech processing, recommender systems (Chen et al., 2023a), and knowledge representation (Kraft & Usbeck, 2022) among others. Major AI scientific conferences regularly include papers and workshops on bias and fairness. A few global events are targeted at multidisciplinary aspects of bias, fairness and other ethical issues in AI and algorithmic decision making. These include ACM FAccT<sup>3</sup>, AAAI/ACM AIES<sup>4</sup>, ACM EAAMO<sup>5</sup>, and FoRC<sup>6</sup>.

<sup>3</sup> <https://faccconference.org/>.

<sup>4</sup> <https://www.aies-conference.com/>.

A number of initiatives have started to standardize, audit, and certify algorithmic bias and fairness (Szczekocka et al., 2022), such as the IEEE P7003<sup>TM</sup> Standard on Algorithmic Bias Considerations<sup>7</sup>, the IEEE Ethics Certification Program for Autonomous and Intelligent Systems<sup>8</sup>, the ISO/IEC TR 24027:2021—Bias in AI systems and AI aided decision making<sup>9</sup>, and the NIST AI Risk Management Framework<sup>10</sup>. Challenges of certification schemes are discussed in Anisetti et al. (2023). Moreover, very few works attempt at investigating the practical applicability of fairness in AI (Madaio et al., 2022; Makhoul et al., 2021b; Beutel et al., 2019), whilst several external audits of AI-based systems have been conducted (Koshiyama et al., 2021), sometimes with extensive media coverage (Camilleri et al., 2023). Finally, on the educational side, bias and fairness have become common topics of university courses on technology ethics (Fiesler et al., 2020), albeit they are not sufficiently included in core technical courses (Saltz et al., 2019) nor sufficiently transversal and interdisciplinary (Raji et al., 2021b; Memarian & Doleck, 2023).

#### the NoBIAS bias and fairness in AI

Bias and fairness can imply different meanings to different stakeholders depending on the application context, the people's culture and moral values, and the reference discipline (Mitchell et al., 2021; Mulligan et al., 2019). Policy initiatives, standards, and best practices in fair-AI set principles, procedures, and knowledge bases to guide and operationalize the detection, mitigation, and control of bias in AI models. Paradoxically, the uncoordinated selection and usage of fair-AI techniques may worsen off some protected groups as side-effects. Examples of such behaviors are described in the literature, including the Yule's effect (Ruggieri et al., 2023) and long-run effects of imposing fairness constraints (Liu et al., 2018).

#### Policy and guideline inventories

The AI Ethics Guidelines Global Inventory<sup>11</sup> by AlgorithmWatch lists 167 frameworks "that seek to set out principles of how systems for automated decision-making can be developed and implemented ethically". There are 8 binding

<sup>5</sup> <https://eaamo.org/>.

<sup>6</sup> <https://responsiblecomputing.org/>.

<sup>7</sup> <https://standards.ieee.org/project/7003.html>.

<sup>8</sup> <https://standards.ieee.org/industry-connections/ecpais.html>

<sup>9</sup> <https://www.iso.org/standard/77607.html>.

<sup>10</sup> <https://www.nist.gov/itl/ai-risk-management-framework>.

<sup>11</sup> <https://inventory.algorithmwatch.org/>.

agreements, 44 voluntary commitments, and 115 recommendations. The EU Agency for Fundamental Rights<sup>12</sup> has collected a list of 349 policy initiatives at the national level, and also including examples at the EU and international level. The OECD.AI Policy Observatory<sup>13</sup> provides a live repository of over 800 AI policy initiatives.

An early survey of 84 ethics guidelines (mostly from Western countries) found an apparent agreement that AI should be ethical, and it identified shared principles of transparency, justice and fairness, non-maleficence, responsibility and privacy. Authors highlight, however, a “substantive divergence in relation to how these principles are interpreted, [...] and how they should be implemented” (Jobin et al., 2019). Despite these various contributions, universal standards or blueprints of fair-AI have not yet been provided by policy-makers, regulators or scientific experts (Wachter et al., 2021b). Even if there were such standards or blueprints, computer/data scientists and practitioners still need to translate these into their academic and industrial contexts and specific situations (Hillman, 2011; Kiviat, 2019).

#### The option not to use AI

Some scholars argue that, while AI is biased, it is less biased than humans (Lin et al., 2020). For example, humans tend to resort to judgement heuristics when making decisions, leading to biased outcomes (Kahneman, 2011). Humans can also be inconsistent and sometimes opaque and unreliable decision-makers (Kahneman et al., 2021). Given that as the alternative, the option of a noise-free, consistent algorithm is understandably appealing to some. This rationale has supported the push for algorithmic-decision-making system across domains (Miller, 2018). Notwithstanding, it is essential to acknowledge the false sense of objectivity attributed to AI as well as to revise the narrative that AI’s deployment and use is inevitable. Technology alone cannot solve complex real world problems (D’Ignazio & Klein, 2020; Costanza-Chock, 2020), let alone in an equitable way (Costanza-Chock, 2020; Alkhatib, 2021). In underpinning the non-use of AI, or by-effect, prohibiting it or supporting its dismantlement, the following arguments have been documented and researched: potential or realized health and safety harms, human rights violations, opposition to deceptive predictive tools, e.g., predictive optimization (Wang et al., 2023), and organizational factors (Alkhatib, 2021). Existing community-led efforts, such as Stop LAPD Spying

Coalition<sup>14</sup>, invest their efforts in awareness campaigns on the risks and implications of the hyper surveillance of marginalized and racialized communities, thus opposing the deployment of predictive policing tools across cities. Moreover, emerging research (Pruss, 2023) has been able to demonstrate that despite the best efforts to automate high-stake decision-making, humans operating these systems can still “opt-out”, or choose to not use/interact with these tools.

An underdeveloped research line consists of rejecting the low-confidence outputs of an AI system in favor of escalating the decisions to a human agent who could possibly take into account additional (qualitative) information. This is considered in the area of classification with a *reject option* (or *selective classification*) (Hendrickx et al., 2021). There is a trade-off here between the performance of an AI system on the accepted region, which should be maximized, and the probability of rejecting, which should be minimized, as human agents’ effort is limited.

Regarding legal regimes, the EU law of General Data Protection Regulation (GDPR) (European Parliament and Council of the European Union, 2016) establishes some restrictions on the use of automated decision-making over individuals when the legal rights or legal status of an individual are impacted. Concretely, individuals should not be subject to a decision that is based solely on automated processing when it is legally binding or has similarly significant effects on them. Whether Article 22 of GDPR provides the data subjects with a right to object or establishes a general prohibition on automated decision-making is still uncertain and is the object of academics and practitioners debate (Mendoza and Bygrave, 2017; Article 29 Data Protection Working Party, 2018). The position of the regulator, then, seems to either offer people the option to opt-out or to provide them with strong safeguards to protect them from potential risks and harms. The upcoming EU AI Act (European Commission, 2021), will introduce in the EU legal framework a substantial advance in this regard by adopting a risk-based approach to assess AI systems’ legal compliance. AI systems could only be placed in the EU market if they comply with certain requirements that mainly aim to avoid the bias. The proposed risk-based approach differentiates between minimal risk, low risk, high-risk, and unacceptable risk, advocating, likewise, for a gradually stricter set of obligations and duties proportionate to each level of risk. The AI Act bans six practices due to their particularly harmful and abusive nature that contradicts the values of respect for human dignity, freedom, equality, and the rule of law. Specifically, the text recognises the threat that AI practices concerning: (1) biometric categorization systems

<sup>12</sup> <https://fra.europa.eu/en/project/2018/artificial-intelligence-big-data-and-fundamental-rights/ai-policy-initiatives>.

<sup>13</sup> <https://oecd.ai/en/dashboards/overview>.

<sup>14</sup> <https://stoplapdspying.org/wp-content/uploads/2018/05/Before-the-Bullet-Hits-the-Body-May-8-2018.pdf>.

using sensitive attributes, (2) facial recognition, (3) emotion recognition, (4) social scoring, (5) human manipulation, and (6) the exploitation of people's vulnerabilities can pose to peoples' rights and democracy values. Notwithstanding the prohibition, the use of real-time and post-remote biometric identification systems in public accessible spaces for law enforcement purposes would be permitted under specific safeguards and strict conditions.

#### Using fair-AI with a guidance

Fairness metrics are at the core of the technical approaches for fair-AI. However, theoretical results state that it is impossible to satisfy different fairness notions at the same time (Chouldechova, 2017; Kleinberg et al., 2017). Not only fairness notions are in tension among each other (Alves et al., 2023), but also with other quality requirements of AI systems, such as predictive accuracy (Menon & Williamson, 2018), calibration (Pleiss et al., 2017), impact (Jorgensen et al., 2023), and privacy (Cummings et al., 2019), for which Pareto optimality should be considered (Wei & Niethammer, 2022). Moreover, the choice of a fairness metric requires to take into account several contrasting objectives: stakeholders' utility, human value alignment (Friedler et al., 2021), people's actual perception of fairness (Saha et al., 2020; Srivastava et al., 2019), and legal and normative constraints (Xenidis, 2020; Kroll et al., 2017). Decision diagrams or rules-of-thumb for guiding practitioners in the choice of the fairness metrics are offered by (Makhlouf et al., 2021a; Buijsman, 2023; Majumder et al., 2023), highlighting the complexity of the choice. The way that the various objectives and requirements are looked for, expressed and formalized, impacts on the choice of the fairness metrics and, a fortiori, on the design of an AI system (Passi & Barocas, 2019)—an instance of the *framing effect* bias, as shown e.g., in Hsee and Li (2022). For example, in the famous case analysed by *ProPublica*<sup>15</sup>, the COMPAS algorithm for recidivism prediction fails to meet equal false positive rate among groups, but it achieves equal calibration (Corbett-Davies et al., 2017), possibly as the result of different perspectives taken by the designers of the algorithm and the *ProPublica* journalists. Even when restricting to a specific fairness notion, there is a problem on how to quantify the degree of unfairness. In fact, even the apparently innocuous choice among algebraic operators (e.g., difference or ratio of proportions), may have an impact. Pedreschi et al. (2012) show that the top-*k* protected-by-law sub-groups with the highest risk difference and the top-*k* with the highest selective risk ratio do not coincide.

<sup>15</sup> <https://www.propublica.org/article/how-we-analyzed-the-compas-recidivism-algorithm>.

Hence, cases of possible discrimination with one choice may be undetected or unprevented with another choice.

#### Beyond debiasing: addressing the origins of AI harms

The report by Balayn and Gürses (2021) studies several EU policy documents, including the AI Act. The authors find that such documents rely on technocentric approaches to address AI harms, while simultaneously not adequately specifying which harms are being referred to. They argue that there is an overemphasis and overreliance specifically on the approach of debiasing data and models. Here, debiasing is used as it is in the fair-AI literature, to refer to improving model performance on specific fairness metrics, as well as to improving representation of certain groups in datasets. This is described as a limited approach as it fails to acknowledge potential harms caused by a myriad of other system design decisions, such as what is being optimized for or what attributes are being used to represent aspects of the real world. Authors also point out that the documents provide no guidance on how to address the inevitable question of which stakeholders view of what is acceptable or unacceptable bias in a system, nor do they acknowledge that any dataset or system is biased, in the sense that it was created by people, with and for a specific view or goal. They advocate for the EU to utilize other governance strategies beyond technical debiasing solutions, so as not to transfer the responsibility, and power, to determine complex political questions to designers and technicians building AI systems. One alternative perspective about the impact of AI systems they address is the organizational view. Specifically, they identify the need to consider what impacts the adoption of extensive AI systems will have on public institutions; if they begin to rely on digitization and automation helmed by large private companies, in what ways will their resources and capacities be shifted, and what would this kind of interdependence mean for public-private relationships.

#### Bias and auditing

In algorithmic decision-making, auditing involves using experimental approaches to investigate potential discrimination by controlling factors that may influence decision outcomes (Romei & Ruggieri, 2014). Given the application scope of these systems, proposed audits span various domains, including algorithmic recruitment (Kazim et al., 2021), online housing markets (Asplund et al., 2020), resource allocation systems (Coston et al., 2021); and more general processes related to the design (Katell et al., 2019) and vision of these systems as socio-technical processes (Cobbe et al., 2021). Auditors play a crucial role in ensuring algorithmic accountability. Consequently, they involve multiple stakeholders, from product developers, government,

policy makers, and data owners to broader groups in society, such as advocacy organizations and institutional operators (Wieringa, 2020). Ultimately, audits are evaluations designed to hold stakeholders accountable. Algorithm auditing (Koshiyama et al., 2021), and specifically AI auditing (Mökander, 2023), is a concept coined to seek for the development of auditing frameworks on research and *in practice*. Moving from a case-by-case basis, audits should establish formal assurance that algorithms are legal, ethical, and safe by informing on governance and compliance with regulations and standards. Notably, the Information Commissioner's Office (ICO) of the United Kingdom has developed a such a framework for auditing AI systems in the public and private sectors<sup>16</sup>. These investigations assess how these entities process personal information and effectively deal with information rights issues. In this capacity, an audit will involve a thorough evaluation of an organisation's procedures, processes, records, and activities. We see in this example how audits are crucial in addressing issues of bias and discrimination. Specifically, by ensuring the existence of adequate policies and procedures, verifying their compliance, testing the adequacy of controls, detecting existing or potential violations, and recommending necessary changes to controls, policies and procedures.

#### Living with bias by documenting it

An emerging scholarship advocates for the development of documentation practices and accompanying artefacts that enhance AI audit pipelines (Gebru et al., 2021; Raji & Yang, 2019; Stoyanovich et al., 2022; Raji et al., 2020), thus enabling stakeholders to easily inspect all the actions performed across the many steps of the pipeline. This also contributes to increasing the trust on the development processes and the systems themselves. The AI community does not count with standardized methods to produce documentation on datasets and models, nor are there any specific regulatory frameworks that enforce this practice at the moment of writing; however, pioneering work in this area argues that “drawing on values-sensitive practices can only bring about improvements in engineering and scientific outcomes” (Bender & Friedman, 2018). Further, Gebru et al. (2021) advocate that documentation promotes the communication between “dataset consumers and producers”. Existing frameworks for the elaboration of documentation include: Datasheets for Datasets (Gebru et al., 2021), Dataset Nutrition Labels (Chmielinski et al., 2022), Data Statements (Bender & Friedman, 2018), Data Readiness Report (Afzal et al., 2021), and Model Cards for Models (Mitchell et al., 2019). Formal data models, like

ontologies and controlled vocabularies, can also support AI-related documentation needs. Examples of relevant vocabularies include: the Data Catalog Vocabulary (DCAT<sup>17</sup>), the provenance ontology (PROV-O<sup>18</sup>), and the Machine Learning Schema ontology (MLS<sup>19</sup>). Lastly, Miceli et al. (2022b) propose a shift in perspective, from documenting datasets to documenting data production processes in order to account for the intensive and precarious human labour involved in the production of datasets. More recently, the urgent call for data stewardship (Peng et al., 2021) and responsible data management practices (Stoyanovich et al., 2022) has also seen the emergence of new professional roles (Rismani & Moon, 2023).

#### Lessons from the NoBIAS project

The Bias Management Layer in the NoBIAS architecture of Fig. 1 aims at achieving three main research objectives: understanding bias, mitigating bias, and accounting for bias in AI-based systems. An orthogonal Legal Layer provides the necessary legal grounds, with regard to the EU context, supporting the research objectives. In this section, we discuss a few policy advices and best practices resulting from the execution of the NoBIAS research. The section is organized according to the NoBIAS architecture.

#### Legal challenges of bias in AI

After framing the EU legal context of AI biases, we discuss how to overcome the hegemonic theory of fair-AI beyond fairness metrics by moving towards transparency and accountability of AI systems. Finally, we consider the synergies and frictions between non-discrimination and data protection law in the specific case of EU legislation. A summary of the challenges, policy advices, and best practices in the Legal Layer is reported in Fig. 2, together with a reference to the subsection(s) where they are discussed.

#### AI biases, discrimination and unfairness

Anti-discrimination legal cases—targeted and strategically litigated—are traditionally based on causal connections between the protected group, the questioned provisions, and the discriminatory situation or unfair treatment (Foster, 2004). However, AI systems challenge that, initial, intuitive causality

<sup>16</sup> <https://ico.org.uk/media/for-organisations/documents/4022651/a-guide-to-ai-audits.pdf>.

<sup>17</sup> <https://www.w3.org/TR/vocab-dcat-2/>.

<sup>18</sup> <https://www.w3.org/TR/prov-primer/>.

<sup>19</sup> <https://github.com/ML-Schema/core>.

#### Legal Layer

- AI models often lack the auxiliary causal knowledge required to prove anti-discrimination cases as these require to show that decision is *because of* (i.e., *at cause of*) *the protected ground*. (AI biases, discrimination and unfairness)
- AI models' complexity and opaqueness make it difficult to identify individuals and groups that are treated unfairly. (AI biases, discrimination and unfairness)
- The design of AI models requires to agree on and to operationalize legal and ethical principles. (AI biases, discrimination and unfairness)
- Transparency and accountability of AI systems are a way to overcome the hegemonic theory of fairness, which reduces the fairness problem to quantitative metric optimization. (AI fairness beyond metrics: transparency and accountability of AI systems)
- There are synergies and frictions in the EU legal framework between data protection law and non-discrimination law, which demand for an integrated and interdisciplinary techno-legal framework of bias management. (EU data protection law and non-discrimination law)

**Fig. 2** Legal Layer: challenges, policy advices, and best practices. In parenthesis, references to the subsections where they are discussed

basis by performing through correlations that do not provide causal explanations for the connections between the input data and the target variable (see Bathaee (2018) and also later Sect. “Bias as a causal-thing”). AI systems operate in such a complex manner that they defy human understanding, leaving the potential victim unaware of the scope and magnitude of the extent to which they have been discriminated against and disadvantaged. Establishing a case of AI discrimination is undoubtedly difficult, as seen in the following brief analysis. Firstly, the potential claimants may not be aware of their disadvantage and the information required to prove that such algorithmic discrimination may be difficult to discover, gather, or access (Wachter et al., 2021b). Secondly, anti-discrimination law protects on the grounds of protected attributes; however, the sources of algorithmic discrimination and the individuals and groups affected by it may not be straightforwardly correlated with those attributes (Zuiderveen Borgesius, 2020). Protected groups may be treated in a biased or unfair way, but the use of proxies can cover such treatment as the features of the model would not directly reveal the use of any sensitive attribute. A second challenge arises from the limited personal scope of EU non-discrimination law, restricted by an exhaustive list of protected grounds. By utilizing proxies-i.e., “neutral” variables closely correlated with the protected ones-the use of AI systems poses a significant risk of circumventing the scope of legal protection [often referred as proxy discrimination (European Commission et al., 2021; Zuiderveen Borgesius, 2020)]. The way AI systems operate reinforce an existing challenge in EU equality protection, that of intersectional discrimination, arising when discriminatory effects occur at the intersection of two or more vectors of disadvantage. While concepts of intersectionality have been advanced by legal scholarship, the Court of Justice of the EU has so far failed to explicitly recognize intersectional discrimination as a special type of discrimination (Xenidis, 2018; Roy et al., 2023; European Court

of Justice, 2016), creating a potential gateway for algorithmic discrimination within the realm of EU non-discrimination law. Thirdly, the current legal procedure to establish a case of discrimination may also set some limitations to bring and present a case of algorithmic discrimination effectively (Wachter et al., 2021b). Furthermore, what makes an algorithm biased and its outcomes unfair is the subject of a contested debate (Rovatsos et al., 2019; Barocas & Selbst, 2016; Jacobs, 2021; Wachter et al., 2021a). Fairness is essentially a contested concept as it is context-dependent and highly conflicts with different ethical, political, and cultural understandings. Still, fairness needs to be mathematically defined to build fair-AI systems, leaving the question of which values need to be operationalized into variables unsolved. For this reason, the literature of fair-AI mainly derives its fairness constructs from a legal context where a process or decision is considered fair if it does not discriminate against people based on their membership to a protected group (Tolan, 2019; Mehrabi et al., 2021; Romei & Ruggieri, 2014). Fairness can be understood as equality or as equity, which are different concepts (Minow, 2021), so the instruments and ways to achieve and ensure the goals of each highly differ. Fairness, in essence, can be understood in different manners depending on its nature, formal or substantive; the context it applies to, legal or technical, or the actor it refers to, public or private. Selecting the appropriate principles and operationalizing the preferred construct requires understanding how people assess fairness and questioning whose perceptions should be captured or discharged (Binns, 2018b).

#### AI fairness beyond metrics: transparency and accountability of AI systems

Carey and Wu (2023); Weinberg (2022) survey the existing critiques on the hegemonic theory of fairness that draw from non-computing disciplines, including philosophy,

law, critical race and ethnic studies, and feminist studies. The hegemonic (i.e., dominant) theory of fairness in the ML community reduces the fairness problem “in terms of a domain-general procedural or statistical guideline [...] so long as the chosen fairness criteria are satisfied, the resulting procedures and outcomes of the system are necessarily fair” (Green & Hu, 2018). Beyond those critics, AI systems’ opaqueness and the potential to impact individuals’ lives are frequently described as the main motivations to demand disclosures of information and provision of explanations about their internal processes and final outcomes, understanding these requirements as necessary to ensure effective governance of the AI context (Almada, 2021) and for allowing applicants to make cases of discrimination (Xenidis and Senden, 2020). On the one hand, algorithms are considered powerful procedures that create “a growing need to evaluate the claims, decisions, actions, and policies that are being made on the bases of them. This evaluation requires gauging the reasons for an algorithmic decision, its components, and the weight assigned to them” (Vedder & Naudts, 2017), in short, requiring *AI accountability*. On the other hand, the “individual adversely affected by a predictive process has the right to understand why and frames this in familiar terms of autonomy and respect as a human being” (Edwards & Veale, 2017), in short *AI transparency*.

An extensive review of algorithmic accountability is provided by Wieringa (2020), while Percy et al. (2021) brings to life the notion of AI accountability in industry work programs, aiming to implement industry-specific technical requirements. Algorithmic impact assessments are accountability governance practices rendering visible the (possible) harms caused by algorithmic systems (Metcalf et al., 2021). Reviewability, introduced by Cobbe et al. (2021), is a way to break down the algorithmic decision-making process into technical and organisational elements which help in determining the contextually appropriate record-keeping mechanisms to facilitate meaningful review both of individual decisions and of the process as a whole. The design of interpretable AI models and the development of methods to explain black box models are comprised in the area of *eXplainable AI (XAI)* (Guidotti et al., 2019; Minh et al., 2022). Such techniques respond to a societal desire to understand the obscure systems that can greatly affect our lives when allocating services or granting and denying rights. Transparency and information obligations can publicly assess the consistent compromise and dutifulness of AI systems with legal principles such as fairness, lawfulness, or information privacy, improving the legitimacy and acceptance of their use by the individuals affected by them at last stay, and supporting the contestability of their outcomes (Henin & Métayer, 2022). However, in most situations where there are obligations to provide information and explanations about automated decision-making systems,

the context is adversarial, and the interests of the parties involved are, if not opposite, different (Bordt et al., 2022). The interest of the users and providers of AI systems and the persons affected by them are opposed to the extent that the former will want to address its transparency and information obligations in a way that ensures compliance but does not harm its private interests, whilst the person subjected to the AI systems will expect a level of compliance that is sufficiently rigorous to enable an effective exercise of her rights and protect her interests and freedoms. Consequently, the interests to be protected or respected will largely condition the method of explanation and the information and explanations expected to be received (see also later Sect. “The need for trustworthy AI, and XAI in particular”).

#### EU data protection law and non-discrimination law

The uptake of (fair-)AI has brought two distinct EU legal regimes to the forefront: data protection law and non-discrimination law. As data-driven technology, AI relies today on the processing of big volumes of data, which often relate to identified or identifiable individuals. This processing brings the development and deployment of many AI systems directly under the scope of the GDPR (European Parliament and Council of the European Union, 2016). On the other hand, due to the issue of bias, AI applications have the potential to infringe upon non-discrimination rights and interfere with existing non-discrimination regulations. Considering that both data protection and non-discrimination rights constitute fundamental rights that are as such equally protected in EU primary (art. 8 and 21 of the Charter of Fundamental Rights (European Union, 2000)) and secondary law (GDPR and EU non-discrimination directives (Council of the European Union, 2000a; European Parliament and Council of the European Union, 2006; Council of the European Union, 2000b, 2004)), mapping aspects of their intersection becomes highly relevant. We refer to Gellert et al. (2013) for a comparative analysis of the two. Here, we highlight a few relevant synergies and frictions.

Since the emergence of the AI bias discourse, EU legal scholars have approached the existing non-discrimination and data protection legal frameworks in an integrated way in order to deal with the challenges of AI in the digital age (Zuiderveen Borgesius, 2020; Hacker, 2018; European Parliament et al., 2022). Confronted with the novel challenges of algorithmic bias, commentators have mainly sought recourse to the GDPR, as a means to compensate enforcement deficiencies of the EU non-discrimination legal apparatus. Tools such as individual access rights (Article 15 (1)), data protection audits (Article 58 (1) (b)), Data Protection Impact Assessments (Article 35 et seq.) and the principle of “fairness” (art. 5 (1) (a)) along with the provision of administrative fines for violation of associated obligations (art. 83) are

among those highlighted for their potential to fight against AI bias and support the protection of non-discrimination rights. However, recourse to data protection law cannot be forever a panacea for the challenges of AI discrimination. Not only is the GDPR not *rationae materiae primarily* concerned with the right to non-discrimination but it is also *de facto* considerably ineffective in achieving this goal (Zuiderveen Borge-sius, 2020; European Parliament et al., 2022). It is important that EU and national legislature and judiciary engage with the limitations of existing non-discrimination frameworks and the nuances of AI application in order to consider tailored legislative amendments or interpretative approaches. Specific recommendations or guidelines by relevant independent bodies such as the European Data Protection Board (EDPB) that adapt the application of existing legislation to the specificities of AI technologies will particularly serve this effort. Striking the right balance between legal certainty and agile application across different domains, Member States and technological developments represent a key challenge in this undertaking. See Gerards and Zuiderveen Borge-sius (2022); European Parliament et al. (2022); Xenidis (2020) for suggestions on different legislative and interpretative approaches in the context of fair-AI.

The fair-AI ecosystem may bring about a clash between the objectives of data protection and non-discrimination legislation, as debiasing approaches may interfere with well-established data protection rights and principles (Veale & Binns, 2017). First of all, the lack of representative training datasets has been consistently described as one of the sources of AI bias (Barocas & Selbst, 2016; Buolamwini & Gebru, 2018; Ntoutsis et al., 2020) (see also Sect. “[Understanding bias](#)”). This line of reasoning has been adopted by the proposed AI Act (European Commission, 2021). Specifically, art. 10 para 3 mandates that providers of high-risk AI systems shall ensure representative training, validation and testing data sets, as part of the prescribed data governance practices. It is thus conceivable that such legislative calls might risk motivating an increasing collection of personal data particularly from data subjects that belong to hitherto underrepresented groups, who are often the most vulnerable in terms of data protection. Furthermore, fair-AI frameworks centered around bias detection, monitoring, and correction often imply the processing of data on characteristics protected by the EU non-discrimination law. This often corresponds to the collection and/or the processing of special categories of personal data (hereafter sensitive data), despite the fact that they are, as such, extensively protected by the GDPR (European Parliament and Council of the European Union, 2016). Moreover, special attention must be given to the way that bias mitigation approaches, and particularly the modification of training data through pre-processing (see Sect. “[Fair-AI methods and resources](#)”), may interfere, or

at least may introduce a layer of complexity, with GDPR principles such as the principle of “accuracy” outlined in Article 5(1) (d) of GDPR.

Since the practice of removing or ignoring sensitive attributes shows to be ineffective to tackle the issue of AI bias (Barocas et al., 2019; Zliobaite and Custers, 2016; Haeri & Zweig, 2020), data scarcity due to regulation constraints is essentially seen as a hurdle to the realisation of fair-AI. There is an effort in the European Parliament’s negotiated version of the AI Act to minimize and circumscribe the width of this obligation, by requiring “*sufficiently* representative” (*sic*) training datasets. However, this choice can also be seen critically as compromising and relativizing the obligation of AI providers to engage with representation biases. As the notion of “sufficiency” is not legally defined and until specific standards or guidelines elaborate on the matter, it is at the discretion of AI providers to weight up their datasets against the “sufficiency” scale, considering the application and the context at hand. A level of legal uncertainty arises in that regard.

The proposed AI Act comes to mediate this tension and opens up the possibility of processing sensitive personal data for the case of bias monitoring, detection and correction in high-risk AI systems [art. 10 (5)]. This possibility comes together with various requirements, intended to ensure a balance between the right to data protection and non-discrimination and prevent an excessive processing of sensitive data in the name of debiasing. However, once again these requirements entail indefinite legal concepts (e.g. “necessity”), with no existing guidance on the way they shall be operationalized in the context of fair-AI. Entrusting the lawful interpretation and implementation of fundamental requirements to the discretion of AI providers entail the risk of a purposeful and inconsistent legal application to the detriment of the right to data protection. In addition, infringements upon provisions of the GDPR or the AI Act might result in severe financial penalties (art. 83, 84 GDPR, art. 71 AI Act).

The tensions between different regulatory tools and the abundance of vague binding textual requirements generate thus a great level of legal uncertainty for all bodies concerned, which explains the urgent need for adequate guidance. Considering the novelty, the fast-evolving nature and the complexity of different debiasing approaches, the desired guidance requires targeted research efforts. Rather than focusing solely on non-discrimination desiderata and sustaining an adversarial conceptualisation of “fairness” vs “privacy”, it is important that interdisciplinary research and good practices on fair-AI transition to a more integrated model. This model should account for the deep intertwinement between data protection and non-discrimination legal regimes and seek to enhance privacy while engaging in debiasing.

### Bias Management Layer - Understanding Bias

- We should acknowledge that there are many forms of bias, with different roots and effects. (Understanding biases, not bias)
- The “ground truth” is a myth. It does not exist in a structurally unjust and unequal society. (The ground truth is biased)
- Data curation in AI should import source criticism and archival practices from historical and humanistic disciplines. (Beyond documenting bias: source criticism and archival practices)
- There is an hyper-fixation on data as the primary source of bias, but the whole AI pipeline needs to be addressed, including the data annotation process and data labourers’ exploitation. (Don’t blame the data, don’t blame the annotator)
- Different data types require specific regulatory guidelines and standards. (Consider the data type)

**Fig. 3** Bias management layer—understanding bias: challenges, policy advices, and best practices. In parenthesis, references to the subsections where they are discussed

### Understanding bias

Bias in data is not as clear-cut as it is often presented. What we mean by bias, what we consider its sources, and what we view as its materialization are all, among other, complex questions with considerable implications on policies for addressing unfair AI models. In this section, we present different angles to better understand and be critical about bias(es) in data. First, we argue on understanding biases, not bias, as a multifaceted issue. Then, we criticize the AI assumption of ground truth, quest for source criticism and archival practices, and discuss the issue of reliable data annotation. Finally, we claim for approaches specific to data types and domain types. A summary of the challenges, policy advices, and best practices in understanding bias is reported in Fig. 3.

### Understanding biases, not bias

Bias is primarily understood as a difference between what is seen as “truth” or “fact” and the respective results of an algorithmic function (a prediction or a representation). Such definitions of bias have in common that they do not relate to the harmful and discriminative impact of statistical errors nor to the underlying social conditions leading to bias. Recent research not least in Computer Science has therefore elaborated how bias is also entangled with social and historical prejudice and discrimination. For instance, the terminology “gender bias” refers not only to a statistical error but also to the algorithmic amplification of already existing discrimination against women and LGBTIQ\* persons like in the case of the Austrian public employment service algorithm (Lopez, 2019). Further studies grounded in Social Science and Science and Technology Studies have explored the “empirical grounded accounts of practices” (Jaton, 2020) of

Computer Science, folded into algorithmic bias and fairness. These contributions have in common that they approach bias not as a statistical error in the predictive performance of an algorithm, but as socio-technical, procedural and constitutive to algorithms (Jaton, 2020; Ziewitz, 2016; Draude et al., 2019; Seaver, 2017).

We think it is crucial to acknowledge that there is not just a singular bias, but rather a multitude of biases, having different (social, technical and socio-technical) roots and exerting distinct effects when employed. In the realm of policy-oriented research, a suggested approach is to “study up” (Nader, 1972) and embrace a framework that considers power dynamics, rather than solely focusing on identifying (singular) bias(es) (Miceli et al., 2022a). By doing so, *understanding biases* can even inform policy-making as it acts as a synecdoche for structural inequalities that persist in society.

### The ground truth is biased

AI models are trained on historical data to accomplish a certain task, e.g., to predict recidivism of defendants. The data used for training is assumed to encode the ground “truth” of the task, e.g., the actual outcome of recidivism for each defendant in case the defendant would have been released. In most cases, collecting the ground “truth” is difficult, expensive, or even unethical, as it would require to obtain counterfactual outcomes, such as releasing potential criminals, not treating sick patients, etc. (Tal, 2023). In the analysis of the COMPAS algorithm, for example, ground truth was approximated by the actual re-arrest outcome of defendants in the 2 years period after they were scored. First, due to unobservability of crime, re-arrest does not coincide with re-offense (Bao et al., 2021), which is the recidivism outcome intended to be predicted. Second, we do not know whether or not defendants who were not released would have recidivated in case they would have been released. Similarly, we do not

know whether an applicant with denied credit would have repaid the credit if granted, a sample selection bias problem tackled by reject inference in credit scoring (Ehrhardt et al., 2021). An idea close to reject inference has been considered in (Ji et al., 2020) for group fairness. Such sampling bias in collected ground truth has been called *negative legacy unfairness* (Kamishima et al., 2012), or the *selective label problem* (Lakkaraju et al., 2017), and it is an instance of data missingness (Goel et al., 2021). Recognizing that ground truth in collected data is biased help to solve the illusive tension between fairness and accuracy (Wick et al., 2019). In NLP, the ground truth is obtained by human annotation, typically aggregating annotators' labels through majority voting. Here, the simplifying assumption of a *single* ground truth is used. A perspectivist approach is emerging in favor of granting significance to divergent opinions, by designing methods over non-aggregated data (Cabitzta et al., 2023). Uncertainty and inconsistency in expert annotations have been pointed out also in the domain of healthcare (Lebovitz et al., 2021; Sylolypavan et al., 2023). In the absence of unbiased ground truth, however, practitioners train AI classification models by setting the target feature using historical data. Any bias in the historical data risks to be lifted to the AI model with a false claim of fairness. Looking at other disciplines, Zajko (2022) points that AI students are untrained and unprepared for the reality of an unfair society. We support the author's claim that "AI developers refer to the reality that exists outside of their models as the 'ground truth', and bias is often defined as deviations from this truth, or inaccurate representations and predictions. But when the truth is that society is deeply, structurally unjust and unequal, and that technologies are part of these structures, the question is whether our algorithms should accurately reproduce inequality or work to change it".

#### **Beyond documenting bias: source criticism and archival practices**

Data curation is central in Computer Science approaches to data bias management (Demartini et al., 2023; Balayn et al., 2021) and information resilience (Sadiq et al., 2022). Here, we highlight instead the issue of source criticism, which is central in historical disciplines and in the humanities, but still in its infancy in Computer Science and AI. Source criticism relates to the practice of understanding the provenance, authenticity, and completeness of sources used in scholarship (Koch and Kinder-Kurlanda, 2020). In the historical disciplines and in the humanities more generally, the practice is considered as required for assessing the validity and reliability of findings based on the source, usually a document. The adoption of source critical practices, applied to datasets, in fair-AI would allow us to give a better picture of the data being used and the individual instances it

contains. Questions of provenance, which is defined as "the question of who has created it with what intention, in which institutional and socio-cultural context" (Koch and Kinder-Kurlanda, 2020), have gone particularly under-examined in AI research and development work. There is now a growing body of works examining the lack of quality, offensiveness, and un-curated nature of some of the massive datasets used for common text and image AI applications (Birhane & Prabhu, 2021; Birhane et al., 2021) as well as works attempting to identify the 'genealogy' of commonly used datasets and benchmarks, with a focus on understanding the norms and values embedded in them (Raji et al., 2021a; Denton et al., 2021).

Many existing datasets used in fair-AI research have minimal information available about the reasons and decisions behind their creation (Fabris et al., 2022; Quay et al., 2022), which are needed for effective source criticism. There have been recent works proposing specific implementations for ensuring that newly created datasets are both well documented and designed as suitable for their intended purposes. In this way, AI practitioners will have a better understanding of the provenance, authenticity, and completeness of the datasets that they use, and of what the implications of results drawn from them are. Hutchinson et al. (2021) present a framework for dataset creation drawn from software development best practices. This framework is intended to support transparency and accountability regarding all steps of the dataset creation life cycle, with a particular focus on the often forgotten *maintenance* phase. Jo and Gebru (2020) propose the creation of an interdisciplinary sub-field of dataset archiving as a way to ensure capacity for the extensive and specialized work required for responsible data creation and management. The authors explain that the existing field of archiving already has established standards and practices for responsible archival processes that can be transferred to this new sub-field.

#### **Don't blame the data, don't blame the annotator**

The current paradigm of AI research and development is heavily dependent on data. Consequently, and despite the extensive resources that have been allocated to research pertaining to bias detection and mitigation in datasets and AI models, the common misconception that bias originates in the data persists, especially in circles outside fair-AI research. The hyper-fixation on data as the primary source of bias can wrongfully lead to treating the negative societal impacts of ML-systems' deployment as an oversimplified problem that can be tackled by "removing" bias from data. Instead, it is essential to reinforce the need to assess algorithmic harms through a holistic assessment that contemplates the whole of the AI pipeline throughout its entire life cycle, whilst also accounting for the societal context for its

intended use (Suresh & Guttag, 2021). With this in mind, we restate how biases can arise at any point of the pipeline as they are derived from the series of choices and practices that go into making these systems, and that eradicating all the biases is a near impossible task (Olteanu et al., 2019). Suresh and Guttag (2021) propose a framework that supports the understanding of sources of harm that can be mapped to different stages across the ML life cycle, accompanied by a non-comprehensive taxonomy of biases that can be attributed to each stage. Here, we emphasize on *non-comprehensive*, because in the same way humans are plagued by innumerable types of biases, datasets and models are also subjected to this problem (Olteanu et al., 2019).

Ultimately, decoupling the AI pipeline in stages can support the careful examination of harms, and help anticipate unforeseen negative implications that these technologies can go on to have upon deployment. Moreover, assessing algorithmic harms from a holistic point of view, also instils a degree of accountability from all those involved in the process of deploying them, instead of doing away with it by simply tackling bias during data pre-processing.

Another localized issue associated with the need for vast amounts of annotated data to train and validate AI-powered systems, in particular those resorting to supervised ML methods, is the one concerned with attributing data bias and, consequently, bad dataset quality, to human annotators, or by-effect, data labourers (Li et al., 2023). In particular, research focused on crowdsourcing dataset annotations tend to make the case for bias in human annotations as being one of the main causes of unfairness in downstream ML tasks (Demartini et al., 2023). The reason for this can be closely intertwined with the interpretative nature of tasks such as data labelling (see also Sect. “The ground truth is biased”), where data labourers are expected to fit complex and divergent world-views into rigid categories (Lin and Jackson, 2023). However, identifying “annotator bias” as the root problem of biased datasets, has become as of late a contentious issue in discussing ethical practices and AI development, as it overlooks the need to acknowledge opaque dataset production processes that require an intensive amount of human labour<sup>20</sup>. Emerging research on this spectrum calls to instead consider biases in datasets as the result of “instruction bias” (Parmar et al., 2023), where bias enters the data collection process at the hand of those designing the instructions for the requested tasks (requestors). Going further than that, Miceli et al. (2022b) propose shifting the discussion away from “annotator bias” altogether, and instead towards the critical assessment of existing work practices and conditions associated with dataset production. Specifically in this

context, they allude to their restricted ability to ask questions in instructions, raise concerns about tasks, low pay, and the elevated surveillance of the labourers. To alleviate this, Miceli et al. (2022b); Li et al. (2023) advocate for centring data labourers’ well-being, and propose frameworks that, for starters, incorporate their input and feedback into production processes, with the aim to empower them.

### Consider the data type

We have already displayed how bias is an umbrella term that comprehends many different characterisations and ranges across different disciplines (e.g., Statistics, Psychology, Social Science, Science and Technology Studies, Gender Studies, etc.), as further demonstrated by the extensiveness of the projects<sup>21,22</sup> that try to catalogue human biases. Especially for big (non-tabular) data, there is a great amount of different biases that can co-occur in the same dataset and often depend on the data type itself. In visual data, for example, framing bias is defined in Fabbri et al. (2022) as “any associations or disparities that can be used to convey different messages and/or that can be traced back to the way in which the visual content has been composed”. It is clear how this definition makes sense only if we rely on further knowledge on how visual communication works (also from the very practical point of view). Furthermore, a typical example of bias in hate speech detection is that African American English (AAE) tends to be labelled as offensive (Harris et al., 2022). Outside the specific example of this case study based on Twitter data, for which the bias was due to a different use of swearing by AAE speakers, it is evident how searching for such a bias in general is not straightforward and requires a certain understanding of how languages work and of the relationships between different dialects of the same language. It is to be considered a best practice, then, to analyse data in search for bias having clear the peculiarities of each data types. Furthermore, any policies that aim at regulating AI adequately need to be either general enough to comprehend the specificity of each data type or differentiate among different data types. For example, the “horizontal”<sup>23</sup> data governance approach of the AI Act w.r.t. bias in training, testing and validation datasets (art. 10 of AI Act) might raise considerable challenges in that respect. While different types of data imply different challenges in terms of fairness and data protection, horizontal legal requirements lean arguably towards the paradigm of tabular data. This

<sup>20</sup> <https://www.noemamag.com/the-exploited-labor-behind-artificial-intelligence/>.

<sup>21</sup> <https://catalogofbias.org/biases/>.

<sup>22</sup> [https://en.wikipedia.org/wiki/List\\_of\\_cognitive\\_biases](https://en.wikipedia.org/wiki/List_of_cognitive_biases).

<sup>23</sup> “Horizontal” is to be understood here as applying uniformly to any training, testing and validation dataset used in high-risk AI systems irrespective of the data-type.

#### Bias Management Layer - Mitigating Bias

- Multi-stakeholders participatory design and human-centered AI can be a valid alternative to technological solutionism. (Multi-stakeholder participatory design, Prioritizing Human-centric AI)
- Intersectionality requires special attention and specific methods to account for the interplay of the different (protected) attributes. (Intersectionality)
- A principled way of tackling bias is to rely on causal reasoning. (Bias as a causal-thing)
- Relying exclusively on raw data for a given task is often not sufficient. External sources can support the so-called knowledge-intensive tasks. (Knowledge-informed AI models)
- There is an urgent need for expanding the fair-AI research on the non i.i.d. case. (The non i.i.d. case: bias in unsupervised learning and graph-mining)

**Fig. 4** Bias management layer—mitigating bias: challenges, policy advices, and best practices. In parenthesis, references to the subsections where they are discussed

might impede their consistent application to a large amount of high-risk AI systems that utilize visual data. The development of corresponding regulatory guidelines and standards tailored to different data types can increase legal certainty and enhance compliance.

#### Mitigating bias

Bias mitigation is a crucial aspect in the development of fair-AI models, aimed at reducing or eliminating biases that can skew outcomes and perpetuate discrimination. As mentioned in Sect. “[Fair-AI methods and resources](#)”, bias mitigation can happen in multiple crucial stages, including data processing approaches (*pre-processing*), specialized fair-AI algorithms (*in-processing*), and model sanitization (*post-processing*). The effectiveness of mitigations at those stages presents some challenges. Pre-processing approaches may inadvertently remove relevant or informative data, with the risk of overgeneralizing and ignoring legitimate differences that may exist among subgroups. This is a problem shared with the data processing for privacy-enforcement (Shahriar et al., 2023). In-processing approaches follow the optimization of some trade-off between performance and fairness metrics. Finally, post-processing approaches may not address the root causes of biases, hence having a limited impact and potentially leading to new biases or feedback loops. In this section, we present issues that deserve specific attention by the practitioners when implementing bias mitigation strategies. A summary of the challenges, policy advices, and best practices in the mitigating bias is reported in Fig. 4.

#### Multi-stakeholder participatory design

As observed in Sect. “[Don’t blame the data, don’t blame the annotator](#)”, every technical decision, yet apparently-neutral, in any stage of the AI pipeline can impact on the biases of the final AI system. For instance, fairness is affected by imputation

of missing values (Caton et al., 2022), by encodings of categorical features (Mougan et al., 2023), by feature selection strategies (Galhotra et al., 2022), and even by hyper-parameter settings (Tizpaz-Niari et al., 2022). More importantly, the composition of data transformations and AI models that are fair in isolation may not be fair in the end (Dwork & Ilvento, 2019). Observe that this also applies to AI-based complex socio-technical systems resulting from the composition of AI, algorithms, people, and procedures (Kulynych et al., 2020). The lack of compositionality requires that the bias analysis of a socio-technical system is conducted as a whole, not by pieces. This is also because the objectives and requirements of the designers of AI, of the users of AI, and of the population subject to the AI decisions are unlikely to be the same. Fair-AI methods are currently not sufficiently robust and they can be incomplete in modelling the complexity and dynamic of the deployment scenario. Multi-stakeholders participatory design (Feffer et al., 2023) and policy actions that take into account qualitative contextual information and feedback from reality may be a valid alternative to technological solutionism. For instance, the NoBIAS project contributed in Scott et al. (2022) to a participatory approach in the design of algorithmic systems in support of public employment services.

#### Prioritizing human-centric AI

In addition to the issues discussed in Sect. “[Multi-stakeholder participatory design](#)”, involving the interested communities during the whole development process of a decision-making system is also a crucial aspect for prioritising AI systems that respond to human values—an objective known as *AI alignment* (Ji et al., 2023) or *socially responsible AI* (Cheng et al., 2021). Inclusion should go beyond the provision of “low-resource” methods (Gururangan et al., 2022), i.e., framing the under-representation of social minorities as a data scarcity problem. Instead, it should account for preventive considerations that respond to diverse human needs and preferences.

This concept is the basis for a *human-centered AI* (Mosqueira-Rey et al., 2023; Xu, 2019; Garibay et al., 2023). Active participation during the whole construction process of an AI system can be a key part of addressing the representation bias that prevails in current systems. Involving a diverse group of people has shown to be critical in stages such as selecting the preferences instructed to the model to make decisions (Organizers Of QueerInAI et al., 2023). Such practices elucidate how systems align with values from specific social groups, which frequently reflect structural and power inequalities. Adjusting to and uncovering the variations on how the data captures under-represented communities can help to represent them more fairly. For example, these practices can help to build socially aware language technologies that are adept for different dialects (Ziems et al., 2022) (see also the AAE example in Sect. “Consider the data type”). Further examples will be considered in Sect. “The need for trustworthy AI, and XAI in particular”.

#### Intersectionality

Many bias mitigation techniques assume in input the specification of one or more protected attributes to mitigate the bias against. However, different dimensions of identity cannot be understood in isolation but must be considered collectively to grasp the full complexity of individuals. A special effort must hence be employed to consider the interplay of the different (protected) attributes (Ovalle et al., 2023). It is further worth noticing that debiasing for a group can reduce even more the representation of already under-represented subgroups (Smirnov et al., 2021). The phenomenon of debiasing paradox (Smirnov et al., 2021; Hughes, 2011), refers to situations where efforts to reduce bias towards certain groups based on a characteristic can actually exacerbate the underrepresentation of already marginalized or even the most marginalized subgroups. This paradox arises when additional attributes, which may be sensitive but overlooked or disregarded, are associated with the characteristic being targeted for bias reduction. Such correlations can occur naturally in real-life scenarios. For instance, the gender pay gap, which can be partially attributed to the wage penalty for motherhood (Budig & England, 2001), serves as an example. In this case, two attributes, namely “being a woman” and “taking care of children” are correlated and both can have detrimental effects on salary. Attempting to address bias solely based on gender may unintentionally disadvantage certain minority groups, such as women without caregiving responsibilities or men who do have such responsibilities. Hence, when considering mitigation strategies, side effects on different subgroups should be carefully analyzed. Beyond its legal challenges (see Sect. “AI biases, discrimination and unfairness”), intersectionality is currently actively addressed also by technical research (Gohar & Cheng, 2023) and Science and Technology Studies (van Nuenen et al., 2022).

#### Bias as a causal-thing

As observed in Sect. “AI biases, discrimination and unfairness”, most ML models are purely observational and rely on correlation among features. Consequently, they are not able to account for spurious effects. A principled way of tackling bias is to rely on causal reasoning (Nogueira et al., 2022; Spirtes & Zhang, 2016). The preferred causal framework used within ML is that of Perlian Causality, or Structural Causal Models (SCM) (Pearl, 2009). Under SCM, causes and effects among a set of variables are denoted using a directed acyclical graph (DAG) that, in turn, represents a set of structural equations that encode directed effects (i.e.,  $X \rightarrow Y$  for attributes  $X$  and  $Y$ ) rather than non-directed effects (i.e.,  $X \rightarrow Z \rightarrow Y$  for one or more intermediate attributes  $Z$ ). Further, human thinking is often framed as causal. Causal DAGs have allowed to formalize human reasoning in a ML-readable manner (Schölkopf et al., 2021).

Causal DAGs are able to graphically represent a worldview on a given fairness context, to highlight the (structural) assumptions, and to formalize the potential bias in a dataset (Pearl & Mackenzie, 2018). Causal DAGs have motivated the rise of causal fairness metrics (Makhlouf et al., 2020; Carey & Wu, 2022), including *total fairness* (Zhang & Bareinboim, 2018), *path-specific fairness* (Zhang et al., 2017), and *counterfactual fairness* (Kusner et al., 2017). Compared with the fairness notions based on correlation, causality-based fairness notions and methods include additional knowledge of the causal structure of the problem. This knowledge often reveals the mechanism of data generation, which helps comprehend and interpret the influence of sensitive attributes on the output of a decision process. This additional auxiliary causal knowledge, e.g., is often the basis for moving from testing unfairness to testing discrimination (Álvarez & Ruggieri, 2023). A common limitation is defining a causal DAG, which requires an agreement on its existence and, in turn, structure. It is not a straightforward task, but it also forces practitioners to state otherwise implicit assumptions about the data and encourages discussions among stakeholders (Kusner et al., 2017; Álvarez & Ruggieri, 2023).

Overall, while approaches for causal discovery from data can be adopted, specifically in the context of fairness (Binkyte-Sadauskiene et al., 2022), they definitively need to be complemented with domain expert knowledge—but, with no guarantee of an unanimous agreement among experts (Rahmattalabi & Xiang, 2022). Moreover, a number of assumptions are typically made which might not be met in practice, such as sufficiency (all causes are known), and faithfulness (the graph completely characterizes the conditional independences among features) (Spirtes et al., 2000). Further, causal fairness metrics may suffer from the identifiability problem (Makhlouf et al., 2022), namely the impossibility to compute them from observational data only.

#### Bias Management Layer - Accounting for Bias

- Fair-AI should be framed and complemented with other requirements under the umbrella of trustworthy AI. (The need for trustworthy AI, and XAI in particular)
- A large potential stems from the convergence of research on fair-AI methods and XAI, although current methods of XAI have shortcomings such as stability issues, for which they should be used very carefully. (The need for trustworthy AI, and XAI in particular, XAI can be biased)
- Bias is not a static problem, but subject to distribution shift over time, or over domains. (Monitoring bias, Bias-aware transfer learning)
- The reproducibility crisis is a major practical limitation in accounting for bias in AI, for which specialized solutions should be devised in high-stakes application scenarios. (The reproducibility crisis)

**Fig. 5** Bias management layer—accounting for bias: challenges, policy advices, and best practices. In parenthesis, references to the subsections where they are discussed

Finally, the use of causal DAGs in fairness has not been free of criticism (e.g., Kasirzadeh and Smart (2021)). Arguments against the manipulability of the sensitive features, e.g., race, in counterfactual reasoning have been raised (Kohler-Hausmann, 2019; Hu & Kohler-Hausmann, 2020). These works argue that it is difficult, if not impossible, to disentangle the causal effects of the sensitive attributes on and from the other attributes in a meaningful way.

#### Knowledge-informed AI models

Relying exclusively on raw data for a given task is often not sufficient. Primarily, models trained on raw data fail to capture the nuances found in the less-represented segments of the data distribution (Mallen et al., 2023), which often correspond to underprivileged communities. While using external knowledge sources to compensate these inequalities holds promise (Lobo et al., 2023), this objective is not central to current knowledge-informed approaches. Typically, external sources support the so-called *knowledge-intensive tasks*, which are those tasks requiring a significant amount of real-world knowledge (e.g., fact verification) (Petroni et al., 2021). External knowledge sources are then used to update the model, provide higher interpretability, and enhance the reliability of its predictions (Asai et al., 2023). Other possible applications where informing predictions can be useful are based on using a combination of sources to enhance the generalizability of a model (Chiril et al., 2022). Particularly, leveraging data to improve performance outside the training distribution for a specific AI task. On issues closely related to discrimination, the integration of additional data and knowledge sources is gaining presence in the development of social-aware ML models (Wiegand et al., 2022). Such models are tailored to fill the gaps of individuals or groups with limited access to technology or who experience discriminatory representation, to frame AI systems within the specific social contexts in which they are applied.

#### The non-i.i.d. case: bias in unsupervised learning and graph-mining

The majority of traditional fair-AI metrics and methods are developed based on the independent and identically distributed (i.i.d.) data assumption: every instance in a dataset is drawn independently from a same statistical distribution. However, many real-world problems include graph-structured (network) data reflecting the connection between subjects, and such connections are not independent nor random—for instance, people connect due to similarity, local proximity, or common interests (Aiello et al., 2012). The studies centered on i.i.d. data are unable to reflect the bias exhibited by the relational information (i.e., the topology) in graph data. Fairness in graph mining can be non-trivial and it has exclusive backgrounds, taxonomies, and fulfilling techniques. Overviews papers by Dong et al. (2023); Chhabra et al. (2021); Choudhary et al. (2022), categorize a few of the current challenges and urgent needs in the field that we agree with. They include: (1) formulating (individual and group) fairness notions according to different types of biases and corresponding harms; (2) balancing model utility and algorithmic fairness; (3) explanation of bias in graph-based methods; and (4) enhancing the robustness of algorithms especially in cases of biased human annotations or malicious attacks. Harms of bias in the context of graphs, and in particular social networks, may go beyond discrimination, and include segregation (Baroni & Ruggieri, 2018; Ferrara et al., 2022), polarization (Tölle & Trier, 2023), filter bubbles (Pariser, 2011), and censorship (Aceto and Pescapè 2015). We see an urgent need for expanding the fair-AI research on the non-i.i.d. cases in the future.

#### Accounting for bias

In this section, we consider two technical aspects of accounting for bias, which complement the legal discussion of Sect. “AI fairness beyond metrics: transparency and accountability of AI systems”: monitoring and explaining

bias. We claim the need for trustworthy AI as an holistic approach beyond fairness and bias issues. We warn, however, about the limitations of the young research field of XAI. Also, we discuss bias issues in tasks related to monitoring, including transferring AI models from a domain to another, and in reproducing evaluation scenarios. A summary of the challenges, policy advices, and best practices in accounting for bias is reported in Fig. 5.

#### The need for trustworthy AI, and XAI in particular

We think that the use of fair-AI methods should be complemented with design, development, and verification practices that are commonly summarized under the umbrella of *trustworthy AI* (Kaur et al., 2023). Such practices include: human agency and oversight, accountability, explainability, robustness and safety, privacy, diversity, reproducibility, and societal and environmental well-being. The research on the interplay between bias and those other non-functional requirements has been developing at different speeds. We refer to surveys on human-centered algorithmic fairness (Wu & Liu, 2022) (see also Sections 3.3.2), differential privacy and fairness (Fioretto et al., 2022), fairness and diversity constraints in ranking (Zehlike et al., 2023), trust and fairness (Knowles et al., 2022), and fairness and robustness (Lee et al., 2021a). A large potential stems from the convergence of fairness and XAI (Balkir et al., 2022; Rawal et al., 2022). XAI methods for model inspection, such as variable importance, can be used to test the influence/independence of protected attributes on a model's output (Grabowicz et al., 2022). Adding explanations to an AI system's output can increase users' trust and fairness perception (Tal et al., 2022) and ultimately control for the exercise of power (Lazar, 2022). In particular, local explanation methods that describe why a specific output was produced (*factual explanation*) and what could have changed the output (*counterfactual explanation*) can help to identify reasons of discriminatory decisions (Manerba & Guidotti, 2021) and to support actionable recourse (Karimi et al., 2023). XAI methods that aim to answer causal questions are referred to as causal interpretable models (Moraffah et al., 2020; Ganguly et al., 2023). Results of the NoBIAS project have considered desiderata for XAI in general, based on symbolic logic reasoning (State, 2022), and for the specific domain of central banking (Mougan et al., 2021). Different user profiles require a different level of explanations as well as different ways of integration to create a human-aligned conversational explanation system (Dazeley et al., 2021). Alarmingly, human evaluation is not the norm in the XAI field: considering the case of counterfactual explanations, Keane et al. (2021) found that only 21% of the approaches are validated with human subject experiments. For a summary of recent empirical findings and user studies in XAI research, see Vainio-Pekka et al. (2023);

Rong et al. (2024). Moreover, the critical survey of Deck et al. (2023) points out a misalignment between fairness desiderata and the actual capabilities of the state-of-the-art in XAI.

#### XAI can be biased

Decision-making processes that affect individuals' rights and freedoms often require explanation (Kroll et al., 2017) (recall Sect. "AI fairness beyond metrics: transparency and accountability of AI systems"). While XAI methods offer a (non-exhaustive) way to hold AI systems accountable (Doshi-Velez et al., 2017), there are a number of limitations of current state-of-the-art that need to be acknowledged, and that should caution us from using these methods blindly. These limitations partly stem from the fact that research in XAI is relatively young (Confalonieri et al., 2021). A major problem is that when explaining black box models, multiple explanations are possible, possibly leading to disagreement about the reasons for the model's output (Krishna et al., 2022). Most prominently, post-hoc explainability methods, which typically rely on a surrogate interpretable model of a black box, are not guaranteed to be stable nor faithful to the underlying black box (Ghassemi et al., 2021). Possible gaps in faithfulness w.r.t. different sub-populations results then in potential biases also in the explanations, as shown for LIME and SHAP in Balagopalan et al. (2022). In an adversarial setting, i.e. a setting with different interests of the party explaining the ML model and the party receiving the explanation, this might allow for (intentionally) misleading explanations (Bordt et al., 2022). In line with this, other scholars argue that highly faithful explanations might not be desirable from a business perspective, and thus only carefully adopted, specifically regarding possible conflicts with Intellectual Property Rights (IPRs) and the potential to "game" the system (Barocas et al., 2020).

We highlight a few further issues of XAI. While there is a pool of explanation methods to pick from, most of them focus on classification tasks (and not, e.g., on unsupervised problems), and on tabular, image and text data (and not, e.g., on time series data). Being able to use an explainable AI method then implies that the problem might need to be adapted to the methods currently available, leading to possible losses of information and lower prediction accuracy (State et al., 2022). Also, interpreting explainability methods requires significant amounts of domain knowledge regarding the application context; a lack of such knowledge might render the explanations meaningless to (lay) end-users. Integration can be either achieved by involving the respective experts into the evaluation (see Sect. "Multi-stakeholder participatory design"), or by directly integrating it via symbolic approaches (Calegari et al., 2020), or knowledge-informed AI methods (see Sect. "Knowledge-informed AI models"). Beyond solving the technical issues of explainability methods as outlined above, there is also the need to adopt a holistic

perspective towards XAI, such as making sure that development teams are diverse, integrating all involved stakeholders into the design process (see Sect. “[Multi-stakeholder participatory design](#)”), evaluating XAI methods in context (see Sect. “[The reproducibility crisis](#)”), etc. Further, it might be worth investigating XAI methods and values embedded into these systems from other perspectives, such as that of historically marginalized groups (see Sect. “[Intersectionality](#)”). More research towards this is needed, and we point out emerging work such as State and Fahimi (2023), investigating explanations from a feminist perspective.

### Monitoring bias

Model monitoring aims to evaluate model performance metrics, also w.r.t. bias and fairness, once the model has been deployed (Kenthapadi et al., 2022; Barrainkua et al., 2022). A common assumption in traditional batch ML is that bias is a static problem. This assumption is unrealistic for the many domains that have underlying *distribution shift* over time (Quiñero-Candela et al., 2009). Subsequently, the problem of bias needs to be studied in continual (a.k.a. lifelong) learning scenarios (Lange et al., 2022), where AI models are continuously adapted to changing data. Another problem is the occurrence of *feedback loops* (Pagan et al., 2023; EU Agency for Fundamental Rights, 2022) (see also the notion of *performative predictions* (Perdomo et al., 2020)) which occur when the outputs of AI models subsequently affect the inputs to downstream systems. These vicious cycles can perpetuate unfairness even if static fair-AI models are used (Liu et al., 2018).

We distinguish two main categories of model monitoring. Supervised monitoring approaches rely on the availability of labelled data to compare the model’s predictions against a set of ground truth labels. By evaluating the model’s performance on this labelled data, we can identify performance deviations or biases that may have emerged during deployment. The NoBIAS project has contributed to this research by proposing approaches that use XAI methods for model monitoring and fairness auditing (Mougan and Nielsen, 2023; Mougan et al., 2022). However, labelled data may be available with an excessive delay (Lange et al., 2022), e.g., the data about defaults in loan repayment used to evaluate model’s predictive accuracy. In some cases, labelled data may not be available at all, e.g., sensitive personal attributes to compare model’s fairness across social groups may not be collectable due to data protection law (see Sect. “[EU data protection law and non-discrimination law](#)”). This is the case of the second category of model monitoring, namely unsupervised monitoring. Estimating the performance and fairness of AI models in the absence of labelled data is a very challenging task with impossibility theorems delimiting the work (Garg et al., 2022; Zhang et al., 2021; Fang et al., 2022).

### Bias-aware transfer learning

It is common practice to adapt an upstream “pre-trained” model to a downstream task creating a downstream “target” model. Biases tend to be propagated when fine-tuning the source models to the downstream tasks (Salman et al., 2022). This propagation of biases is known as “bias transfer” (Steed et al., 2022). While bias transfer is a well-defined concept, it has mostly been explored within the context of NLP (Ladhak et al., 2023; Feng et al., 2023; Jin et al., 2021) except for (Salman et al., 2022) in the area of computer vision. Furthermore, since upstream bias mitigation is known to reduce bias transfer to the target models (Jin et al., 2021), we raise awareness about it as an effective bias mitigation step and encourage more research on its potential. Recent work by Álvarez et al. (2023) on decision tree classifiers under transfer learning, for instance, shows that incorporating partial knowledge from the target population (i.e., that on which the pre-trained model is to be deployed upon) when training the model can increase model performance and reduce the risk of unfair classifications. To some extent, this is again an instance of the knowledge-informed AI approach of Sect. “[Knowledge-informed AI models](#)”.

### The reproducibility crisis

The evaluation of AI models should replicate the operational scenario where the model will be deployed as closely as possible. Similarly, the auditing of AI models should replicate the operational scenario where the system has been deployed. Sometimes, “stress test” scenarios are also considered to assess the impact of improper usage of the AI models—this is the case of high-risk applications in the AI Act (see Sect. “[The option not to use AI](#)”). However, the lack of good documentation on AI development and bias management processes, including definitions, software, and datasets (see Sect. “[Living with bias by documenting it](#)”), are key factors affecting evaluation and reproducibility, giving raise to the *reproducibility crisis* (Gundersen, 2020). For instance, an issue has been raised about the arbitrariness of predictions of ML models trained across different samples (Cooper et al., 2023), showing that most fairness classification benchmarks are close-to-fair when taking into account such an arbitrariness. We see reproducibility as a major practical limitation in accounting for bias in AI, for which specialized solutions should be devised based on specific application scenarios. As an example, in the high-risk domain of credit scoring, the European Banking Authority<sup>24</sup> provides detailed guidelines and discussion papers including the monitoring of bias in ML models.

<sup>24</sup> <https://www.eba.europa.eu/regulation-and-policy/credit-risk>.

## Conclusions

Many concerns about the risks and harms of bias in AI have been motivating the fast growing multidisciplinary research on fair-AI.

First, we have concisely summarized topics in policies and best practices, thus providing to researchers and practitioners pointers to inventories, guidelines and survey papers. On the one side of the spectrum of possible actions to prevent those risks and harms, there is the option not to use AI. On the other side of the spectrum, there is the option to address the origins of AI harms at societal level. In between the two options, there are methods for documenting bias, techniques for mitigating bias, and approaches for auditing AI systems.

Second, we have contributed to the ongoing fair-AI discussion with additional challenges, policy advice, and best practices that resulted from the execution of the NoBIAS project. We argue that these are, although deemed relevant, not sufficiently developed nor acknowledged in the literature. These are summarized in Figs. 2, 3, 4, 5, with in parenthesis the reference to the section of the paper where they are discussed in. While we do not claim for their completeness, we hope that those advices and best practices will contribute to the conventional wisdom in research and practice of managing bias and fairness in AI.

**Acknowledgements** This work has received funding from the European Union's Horizon 2020 research and innovation program under Marie Skłodowska-Curie Actions (Grant Agreement Number 860630) for the project "NoBIAS—Artificial Intelligence without Bias". This work reflects only the authors' views and the European Research Executive Agency (REA) is not responsible for any use that may be made of the information it contains.

**Funding** Open access funding provided by Università di Pisa within the CRUI-CARE Agreement.

## Declarations

**Conflict of interest** We have no conflict of interest to disclose.

**Open Access** This article is licensed under a Creative Commons Attribution 4.0 International License, which permits use, sharing, adaptation, distribution and reproduction in any medium or format, as long as you give appropriate credit to the original author(s) and the source, provide a link to the Creative Commons licence, and indicate if changes were made. The images or other third party material in this article are included in the article's Creative Commons licence, unless indicated otherwise in a credit line to the material. If material is not included in the article's Creative Commons licence and your intended use is not permitted by statutory regulation or exceeds the permitted use, you will need to obtain permission directly from the copyright holder. To view a copy of this licence, visit <http://creativecommons.org/licenses/by/4.0/>.

## References

- Aceto, G., & Pescapè, A. (2015). Internet censorship detection: A survey. *Computer Networks*, 83, 381–421.
- Afzal, S., C., R., Kesarwani, M., et al. (2021). Data readiness report. In *SMDs. IEEE*, pp. 42–51
- Aiello, L. M., Barrat, A., & Schifanella, R., et al. (2012). Friendship prediction and homophily in social media. *ACM Transactions on the Web*, 6(2), 1–33.
- Alkhatib, A. (2021). To live in their utopia: Why algorithmic systems create absurd outcomes. In: *CHI. ACM*, pp. 95:1–9
- Almada, M. (2021). Automated decision-making as a data protection issue. Available at SSRN 3817472
- Altman, A. (2020). Discrimination. In E. N. Zalta (Ed.), *The Stanford encyclopedia of philosophy*. Stanford University.
- Álvarez, J.M., & Ruggieri, S. (2023). Counterfactual situation testing: Uncovering discrimination under fairness given the difference. In: *EAAMO. ACM*, pp. 2:1–11
- Álvarez, J.M., Scott, K.M., & Berendt, B., et al. (2023). Domain adaptive decision trees: Implications for accuracy and fairness. In: *FAccT. ACM*, pp. 423–433
- Alves, G., Bernier, F., Couceiro, M., et al. (2023). Survey on fairness notions and related tensions. *EURO Journal on Decision Processes*, 11, 100033.
- Anisetti, M., Ardagna, C. A., Bena, N., et al. (2023). Rethinking certification for trustworthy machine-learning-based applications. *IEEE Internet Computing*, 27(6), 22–28.
- Article 29 Data Protection Working Party. (2018). Guidelines on automated individual decision-making and profiling for the purposes of regulation 2016/679 (wp251rev.01). <https://ec.europa.eu/newsroom/article29/items/612053>
- Asai, A., Min, S., & Zhong, Z., et al. (2023). Retrieval-based language models and applications. In: *ACL (tutorial)*. Association for Computational Linguistics, pp. 41–46
- Ashurst, C., & Weller, A. (2023). Fairness without demographic data: A survey of approaches. In: *EAAMO. ACM*, pp 14:1–14
- Asplund, J., Eslami, M., & Sundaram, H., et al. (2020). Auditing race and gender discrimination in online housing markets. In: *ICWSM. AAAI Press*, pp. 24–35
- Balagopalan, A., Zhang, H., & Hamidieh, K., et al. (2022). The road to explainability is paved with bias: Measuring the fairness of explanations. In: *FAccT. ACM*, pp. 1194–1206
- Balayn, A., & Gürses, S. (2021). *Beyond debiasing: Regulating AI and its inequalities*. European Digital Rights (EDRi): Tech. rep.
- Balayn, A., Lofi, C., & Houben, G. (2021). Managing bias and unfairness in data for decision support: A survey of machine learning and data engineering approaches to identify and mitigate bias and unfairness within data management and analytics systems. *The VLDB Journal*, 30(5), 739–768.
- Balayn, A., Yurrita, M., & Yang, J., et al. (2023). Fairness toolkits, a checkbox culture? On the factors that fragment developer practices in handling algorithmic harms. In: *AIES. ACM*, pp. 482–495
- Balkir, E., Kiritchenko, S., Nejadgholi, I., et al. (2022). Challenges in applying explainability methods to improve the fairness of NLP models. *CoRR abs/2206.03945*
- Bao, M., Zhou, A., Zottola, S., et al. (2021). It's compaslicated: The messy relationship between RAI datasets and algorithmic fairness benchmarks. In: *NeurIPS Datasets and Benchmarks*
- Barocas, S., & Selbst, A. D. (2016). Big data's disparate impact. *California Law Review*, 104, 671–732.
- Barocas, S., Hardt, M., & Narayanan, A. (2019). Fairness and machine learning. [fairmlbook.org](http://www.fairmlbook.org), <http://www.fairmlbook.org>
- Barocas, S., Selbst, A.D., & Raghavan, M. (2020). The hidden assumptions behind counterfactual explanations and principal reasons. In: *FAT\*. ACM*, pp. 80–89

- Baroni, A., & Ruggieri, S. (2018). Segregation discovery in a social network of companies. *Journal of Intelligent Information Systems*, 51(1), 71–96.
- Barrainkua, A., Gordaliza, P., & Lozano, J.A., et al. (2022). A survey on preserving fairness guarantees in changing environments. CoRR abs/2211.07530
- Bathae, Y. (2018). The Artificial Intelligence black box and the failure of intent and causation. *Harvard Journal of Law & Technology*, 31(2), 889–938.
- Bender, E. M., & Friedman, B. (2018). Data statements for natural language processing: Toward mitigating system bias and enabling better science. *Transactions of the Association for Computational Linguistics*, 6, 587–604.
- Berk, R., Heidari, H., Jabbari, S., et al. (2021). Fairness in criminal justice risk assessments: The state of the art. *Sociological Methods & Research*, 50(1), 3–44.
- Beutel, A., Chen, J., & Doshi, T., et al. (2019). Putting fairness principles into practice: Challenges, metrics, and improvements. In: AIES. ACM, pp. 453–459
- Bias (2023) Merriam-Webster.com Dictionary. Merriam-Webster, Inc.
- Binkyte-Sadauskienė, R., Makhlof, K., & Pinzón, C., et al. (2022). Causal discovery for fairness. CoRR abs/2206.06685
- Binns, R. (2018). Fairness in machine learning: Lessons from political philosophy. *Proceedings of Machine Learning Research*, 81, 149–159.
- Binns, R. (2018). What can political philosophy teach us about algorithmic fairness? *IEEE Security & Privacy*, 16(3), 73–80.
- Binns, R. (2020). On the apparent conflict between individual and group fairness. In: FAT\*. ACM, pp. 514–524
- Binns, R., Adams-Prassl, J., & Kelly-Lyth, A. (2023). Legal taxonomies of machine bias: Revisiting direct discrimination. In: FAccT. ACM, pp. 1850–1858
- Birhane, A., & Prabhu, V.U. (2021). Large image datasets: A pyrrhic win for computer vision? In: WACV. IEEE, pp. 1536–1546
- Birhane, A., Prabhu, V.U., Kahembwe, E. (2021). Multimodal datasets: Misogyny, pornography, and malignant stereotypes. CoRR abs/2110.01963
- Blodgett, S.L., Barocas, S., & III, H.D., et al. (2020). Language (technology) is power: A critical survey of bias in NLP. In: ACL. Association for Computational Linguistics, pp. 5454–5476
- Bordt, S., Finck, M., & Raidl, E., et al. (2022). Post-hoc explanations fail to achieve their purpose in adversarial contexts. In: FAccT. ACM, pp. 891–905
- Budig, M. J., & England, P. (2001). The wage penalty for motherhood. *American Sociological Review*, 66(2), 204–225.
- Buijsman, S. (2023). Navigating fairness measures and trade-offs. AI and Ethics
- Buolamwini, J., & Gebru, T. (2018). Gender shades: Intersectional accuracy disparities in commercial gender classification. *Proceedings of Machine Learning Research*, 81, 77–91.
- Buyl, M., Bie, T.D. (2024). Inherent limitations of AI fairness. Commun ACM p to appear
- Cabitza, F., Campagner, A., & Basile, V. (2023). Toward a perspectivist turn in ground truthing for predictive computing. In: AAAI. AAAI Press, pp. 6860–6868
- Calegari, R., Ciatto, G., & Omicini, A. (2020). On the integration of symbolic and sub-symbolic techniques for XAI: A survey. *Intelligenza Artificiale*, 14(1), 7–32.
- Camilleri, H., Ashurst, C., & Jaisankar, N., et al. (2023). Media coverage of predictive policing: Bias, police engagement, and the future of transparency. In: EAAMO. ACM, pp. 28:1–28:19
- Carey, A. N., & Wu, X. (2022). The causal fairness field guide: Perspectives from social and formal sciences. *Frontiers Big Data*, 5, 892837.
- Carey, A. N., & Wu, X. (2023). The statistical fairness field guide: Perspectives from social and formal sciences. *AI Ethics*, 3(1), 1–23.
- Castelnuovo, A., Crupi, R., Greco, G., et al. (2022). A clarification of the nuances in the fairness metrics landscape. *Scientific Reports*, 12(1), 4209.
- Castelnuovo, A., Inverardi, N., & Nanino, G., et al. (2023). Fair enough? A map of the current limitations of the requirements to have fair algorithms. CoRR abs/2311.12435
- Caton, S., & Haas, C. (2024). Fairness in machine learning: A survey. ACM Comput Surv p to appear
- Caton, S., Malisetty, S., & Haas, C. (2022). Impact of imputation strategies on fairness in machine learning. *Journal of Artificial Intelligence Research*, 74, 1011–1035.
- Chen, J., Dong, H., Wang, X., et al. (2023). Bias and debias in recommender system: A survey and future directions. *ACM Transactions on Information Systems*, 41(3), 1–39.
- Chen, R. J., Wang, J. J., Williamson, D. F. K., et al. (2023). Algorithmic fairness in Artificial Intelligence for medicine and healthcare. *Nature Biomedical Engineering*, 7(6), 719–742.
- Chen, Z., Zhang, J.M., & Hort, M., et al. (2022). Fairness testing: A comprehensive survey and analysis of trends. CoRR abs/2207.10223
- Cheng, L., Varshney, K. R., & Liu, H. (2021). Socially responsible AI algorithms: Issues, purposes, and challenges. *Journal of Artificial Intelligence Research*, 71, 1137–1181.
- Chhabra, A., Masalkovaite, K., & Mohapatra, P. (2021). An overview of fairness in clustering. *IEEE Access*, 9, 130698–130720.
- Chiril, P., Pamungkas, E. W., Benamara, F., et al. (2022). Emotionally informed hate speech detection: A multi-target perspective. *Cognitive Computation*, 14(1), 322–352.
- Chmielinski, K.S., Newman, S., Taylor, M., et al. (2022). The dataset nutrition label (2nd gen): Leveraging context to mitigate harms in Artificial Intelligence. CoRR abs/2201.03954
- Choudhary, M., Laclau, C., Langeron, C. (2022). A survey on fairness for machine learning on graphs. CoRR abs/2205.05396
- Chouldechova, A. (2017). Fair prediction with disparate impact: A study of bias in recidivism prediction instruments. *Big Data*, 5(2), 153–163.
- Cobbe, J., Lee, M.S.A., & Singh, J. (2021). Reviewable automated decision-making: A framework for accountable algorithmic systems. In: FAccT. ACM, pp. 598–609
- Confalonieri, R., Coba, L., Wagner, B., et al. (2021). A historical perspective of explainable Artificial Intelligence. *Wiley Interdisciplinary Reviews: Data Mining and Knowledge Discovery*, 11(1), e1391.
- Cooper, A.F., Lee, K., Barocas, S., et al. (2023). Is my prediction arbitrary? Measuring self-consistency in fair classification. CoRR abs/2301.11562
- Corbett-Davies, S., Pierson, E., Feller, A., et al. (2017). Algorithmic decision making and the cost of fairness. In: KDD. ACM, pp. 797–806
- Costanza-Chock, S. (2020). *Design justice: Community-led practices to build the worlds we need*. The MIT Press.
- Coston, A., Guha, N., & Ouyang, D., et al. (2021). Leveraging administrative data for bias audits: Assessing disparate coverage with mobility data for COVID-19 policy. In: FAccT. ACM, pp. 173–184
- Council of the European Union (2000a) Council Directive 2000/43/EC of 29 June 2000 implementing the principle of equal treatment between persons irrespective of racial or ethnic origin. Official Journal of the European Communities L 180. <http://data.europa.eu/eli/dir/2000/43/oj>
- Council of the European Union (2000b) Council Directive 2000/78/EC of 27 November 2000 establishing a general framework for equal treatment in employment and occupation. Official Journal of the European Communities L 303. <http://data.europa.eu/eli/dir/2000/78/oj>
- Council of the European Union (2004) Council Directive 2004/113/EC of 13 December 2004 implementing the principle of equal treatment between men and women in the access to and supply

- of goods and services. Official Journal of the European Union L 373. <http://data.europa.eu/eli/dir/2004/113/oj>
- Cummings, R., Gupta, V., & Kimpara, D., et al. (2019). On the compatibility of privacy and fairness. In: UMAP (Adjunct Publication). ACM, pp. 309–315
- Czarnowska, P., Vyas, Y., & Shah, K. (2021). Quantifying social biases in NLP: A generalization and empirical comparison of extrinsic fairness metrics. *Transactions of the Association for Computational Linguistics*, 9, 1249–1267.
- Danks, D., & London, A.J. (2017). Algorithmic bias in autonomous systems. In: IJCAI. [ijcai.org](http://ijcai.org), pp. 4691–4697
- Dazeley, R., Vamplew, P., Foale, C., et al. (2021). Levels of explainable Artificial Intelligence for human-aligned conversational explanations. *Artificial Intelligence*, 299, 103525.
- Deck, L., Schoeffler, J., & De-Arteaga, M., et al. (2023). A critical survey on fairness benefits of XAI. CoRR abs/2310.13007
- Demartini, G., Roitero, K., & Mizzaro, S. (2023). Data bias management. *Communication ACM*, 67(1), 28–32.
- Denton, E., Hanna, A., & Amironesei, R., et al. (2021). On the genealogy of machine learning datasets: A critical history of ImageNet. *Big Data Society*. <https://doi.org/10.1177/20539517211035955>
- D’Ignazio, C., & Klein, L. F. (2020). *Data feminism*. MIT press.
- Dong, Y., Ma, J., Chen, C., et al. (2023). Fairness in graph mining: A survey. *IEEE Transactions on Knowledge and Data Engineering*, pp. 1–22
- Doshi-Velez, F., Kortz, M., & Budish, R., et al. (2017). Accountability of AI under the law: The role of explanation. CoRR abs/1711.01134
- Draude, C., Klumbyte, G., Lücking, P., et al. (2019). Situated algorithms a sociotechnical systemic approach to bias. *Online Information Review*, 44(2), 325–342.
- Dwork, C., Ilvento, C. (2019). Fairness under composition. In: ITCS, LIPICs, vol 124. Schloss Dagstuhl - Leibniz-Zentrum für Informatik, pp. 1–33
- Edwards, L., & Veale, M. (2017). Slave to the algorithm? Why a right to an explanation is probably not the remedy you are looking for. *Tech Rev*, 16, 18.
- Ehrhardt, A., Biernacki, C., Vandewalle, V., et al. (2021). Reject inference methods in credit scoring. *Journal of Applied Statistics*, 48, 2734–2754.
- EU Agency for Fundamental Rights (2022) Bias in algorithms: Artificial intelligence and discrimination. Publications Office of the European Union, <https://data.europa.eu/doi/10.2811/25847>
- European Commission (2021) Proposal for a Regulation of the European Parliament and of the Council Laying down harmonised rules on Artificial Intelligence (AI Act) and amending certain Union legislative acts. <https://eur-lex.europa.eu/legal-content/EN/TXT/?uri=CELEX:52021PC0206>
- European Commission, Directorate-General for Justice and Consumers, & Gerards J, et al. (2021). Algorithmic discrimination in Europe: Challenges and opportunities for gender equality and non-discrimination law. Publications Office, <https://data.europa.eu/doi/10.2838/544956>
- European Court of Justice. (2016). *Parris v trinity college Dublin and others*. (Case C-443/15)
- European Parliament, Council of the European Union. (2006). Directive 2006/54/EC of the European Parliament and of the Council of 5 July 2006 on the implementation of the principle of equal opportunities and equal treatment of men and women in matters of employment and occupation (recast). Official Journal of the European Union L 204. <http://data.europa.eu/eli/dir/2006/54/oj>
- European Parliament, Council of the European Union. (2016). Regulation (EU) 2016/679 of the European Parliament and of the Council of 27 April 2016 on the protection of natural persons with regard to the processing of personal data and on the free movement of such data, and repealing Directive 95/46/EC (General Data Protection Regulation). Official Journal of the European Union L 119. <http://data.europa.eu/eli/reg/2016/679/oj>
- European Parliament, Directorate-General for Parliamentary Research Services, & Beriain M., et al. (2022). Auditing the quality of datasets used in algorithmic decision-making systems. <https://data.europa.eu/doi/10.2861/98930>
- European Union. (2000). Charter of Fundamental Rights of the European Union. Official Journal of the European Union C 364. [http://data.europa.eu/eli/treaty/char\\_2012/oj](http://data.europa.eu/eli/treaty/char_2012/oj)
- Fabbrizzi, S., Papadopoulos, S., Ntoutsis, E., et al. (2022). A survey on bias in visual datasets. *Computer Vision and Image Understanding*, 223, 103552.
- Fabris, A., Messina, S., & Silvello, G., et al. (2022). Algorithmic fairness datasets: The story so far. *Data Mining and Knowledge Discovery*, 36, 2074–2152
- Fabris, A., Baranowska, N., & Dennis, M.J., et al. (2023). Fairness and bias in algorithmic hiring. CoRR abs/2309.13933
- Fang, Z., Li, Y., & Lu, J., et al. (2022). Is out-of-distribution detection learnable? In: NeurIPS
- Feffer, M., Skirpan, M., & Lipton, Z., et al. (2023). From preference elicitation to participatory ML: A critical survey & guidelines for future research. In: AIES. ACM, pp. 38–48
- Feng, S., Park, C.Y., & Liu, Y., et al. (2023). From pretraining data to language models to downstream tasks: Tracking the trails of political biases leading to unfair NLP models. In: ACL (1). Association for Computational Linguistics, pp. 11737–11762
- Ferrara, A., Noboa, L.E., & Karimi, F., et al. (2022). Link recommendations: Their impact on network structure and minorities. In: WebSci. ACM, pp. 228–238
- Fiesler, C., Garrett, N., Beard, N. (2020). What do we teach when we teach tech ethics?: A syllabi analysis. In: SIGCSE. ACM, pp. 289–295
- Fioretto, F., Tran, C., & Hentenryck, P.V., et al. (2022). Differential privacy and fairness in decisions and learning tasks: A survey. In: IJCAI. [ijcai.org](http://ijcai.org), pp. 5470–5477
- Foster, S. R. (2004). Causation in antidiscrimination law: Beyond intent versus impact. *Houston Law Review*, 41(5), 1469–1548
- Friedler, S. A., Scheidegger, C., & Venkatasubramanian, S. (2021). The (im)possibility of fairness: Different value systems require different mechanisms for fair decision making. *Communications of the ACM*, 64(4), 136–143.
- Friedman, B., & Nissenbaum, H. (1996). Bias in computer systems. *ACM Transactions on Information Systems*, 14(3), 330–347.
- Future of Privacy Forum. (2017). Unfairness by algorithm: Distilling the harms of automated decision-making. <https://fpf.org/blog/unfairness-by-algorithm-distilling-the-harms-of-automated-decision-making/>
- Gajane, P., Saxena, A., Tavakol, M., et al. (2022). Survey on fair reinforcement learning: Theory and practice. CoRR abs/2205.10032
- Galhotra, S., Shanmugam, K., & Sattigeri, P., et al. (2022). Causal feature selection for algorithmic fairness. In: SIGMOD Conference. ACM, pp. 276–285
- Gallegos, I.O., Rossi, R.A., Barrow, J., et al. (2023). Bias and fairness in large language models: A survey. CoRR abs/2309.00770
- Ganguly, N., Fazliza, D., & Badar, M., et al. (2023). A review of the role of causality in developing trustworthy AI systems. CoRR abs/2302.06975
- Garg, S., Balakrishnan, S., Lipton, Z.C., et al. (2022). Leveraging unlabeled data to predict out-of-distribution performance. In: ICLR. OpenReview.net
- Garibay, Ó. Ó., et al. (2023). Six human-centered Artificial Intelligence grand challenges. *International Journal of Human-Computer Interaction*, 39(3), 391–437.
- Gebru, T., Morgenstern, J., Vecchione, B., et al. (2021). Datasheets for datasets. *Communications of the ACM*, 64(12), 86–92.
- Gellert, R., Vries, K.D., de Hert, P., et al. (2013). A comparative analysis of anti-discrimination and data protection legislations. In: *Discrimination and Privacy in the Information Society, Studies in Applied Philosophy, Epistemology and Rational Ethics*, vol 3. Springer, pp. 61–89

- Gerards, J., & Zuiderveen Borgesius, F. J. (2022). Protected grounds and the system of non-discrimination law in the context of algorithmic decision-making and Artificial Intelligence. *Colorado Technology Law Journal*, 20, 1.
- Ghassemi, M., Oakden-Rayner, L., & Beam, A. L. (2021). The false hope of current approaches to explainable Artificial Intelligence in health care. *Lancet Digit Health*, 3(11), e745–e750.
- Gitelman, L. (2013). *Raw data is an oxymoron*. MIT Press.
- Goel, N., Amayuelas, A., Deshpande, A., et al. (2021). The importance of modeling data missingness in algorithmic fairness: A causal perspective. In: AAAI. AAAI Press, pp. 7564–7573
- Gohar, U., Cheng, L. (2023). A survey on intersectional fairness in machine learning: Notions, mitigation, and challenges. In: IJCAI. ijcai.org, pp. 6619–6627.
- Grabowicz, P.A., Perello, N., & Mishra, A. (2022). Marrying fairness and explainability in supervised learning. In: FAccT. ACM, pp. 1905–1916.
- Green, B., & Hu, L. (2018). The myth in the methodology: Towards a recontextualization of fairness in machine learning. In: Debates@ICML. [https://econcs.seas.harvard.edu/files/econcs/files/green\\_icml18.pdf](https://econcs.seas.harvard.edu/files/econcs/files/green_icml18.pdf)
- Grimes, D. A., & Schulz, K. F. (2002). Bias and causal associations in observational research. *Lancet*, 359, 248–252.
- Guidotti, R., Monreale, A., Ruggieri, S., et al. (2019). A survey of methods for explaining black box models. *ACM Computing Surveys*, 51(5), 1–42.
- Gundersen, O. E. (2020). The reproducibility crisis is real. *AI Magazine*, 41(3), 103–106.
- Gururangan, S., Card, D., Dreier, S.K., et al. (2022). Whose language counts as high quality? Measuring language ideologies in text data selection. In: EMNLP. Association for Computational Linguistics, pp. 2562–2580
- Hacker, P. (2018). Teaching fairness to Artificial Intelligence: Existing and novel strategies against algorithmic discrimination under EU law. *Common Market Law Review*, 55(4), 1.
- Haeri, M.A., Zweig, K.A. (2020). The crucial role of sensitive attributes in fair classification. In: SSCI. IEEE, pp. 2993–3002
- Harris, C., Halevy, M., Howard, A.M., et al. (2022). Exploring the role of grammar and word choice in bias toward African American English (AAE) in hate speech classification. In: FAccT. ACM, pp. 789–798
- Haselton, M.G., Nettle, D., Andrews, P.W. (2005). The evolution of cognitive bias. In: Zalta EN (Eds.) *Handbook of Evolutionary Psychology*. John Wiley & Sons Inc., pp. 724–746
- Hellström, T., Dignum, V., Bensch, S. (2020). Bias in machine learning - what is it good for? In: NeHuAI@ECAI, CEUR Workshop Proceedings, vol 2659. CEUR-WS.org, pp. 3–10
- Hendrickx, K., Perini, L., der Plas, D.V., et al. (2021). Machine learning with a reject option: A survey. CoRR <http://arxiv.org/abs/2107.11277>
- Henin, C., & Métayer, D. L. (2022). Beyond explainability: Justifiability and contestability of algorithmic decision systems. *AI Society*, 37(4), 1397–1410.
- Hertweck, C., Heitz, C., & Loi, M. (2021). On the moral justification of statistical parity. In: FAccT. ACM, pp. 747–757
- Hillman, T. (2011). The inscription, translation and re-inscription of technology for mathematical learning. *Technology, Knowledge and Learning*, 16(2), 103.
- Hort, M., Chen, Z., Zhang, J.M., et al. (2022). Bias mitigation for machine learning classifiers: A comprehensive survey. CoRR <http://arxiv.org/abs/2207.07068>
- Hsee, C. K., & Li, X. (2022). A framing effect in the judgment of discrimination. *Proceedings of the National Academy of Sciences*, 119(47), e2205988119.
- Hu, L., & Kohler-Hausmann, I. (2020). What's sex got to do with machine learning? In: FAT\*. ACM, p. 513
- Hughes, M. M. (2011). Intersectionality, quotas, and minority women's political representation worldwide. *American Political Science Review*, 105(3), 604–620.
- Hutchinson, B., Mitchell, M. (2019). 50 years of test (un)fairness: Lessons for machine learning. In: FAT. ACM, pp. 49–58
- Hutchinson, B., Smart, A., Hanna, A., et al. (2021). Towards accountability for machine learning datasets: Practices from software engineering and infrastructure. In: FAccT. ACM, pp. 560–575
- ISO/IEC. (2021). ISO/IEC TR 24027:2021 - Information Technology - Artificial Intelligence (AI) - Bias in AI systems and AI-aided decision making. <https://www.iso.org/standard/77607.html>
- Jacobs, A.Z. (2021). Measurement and fairness. In: FAccT. ACM, pp. 375–385
- Jaton, F. (2020). *The Constitution of Algorithms*. Ground-Truthing, Programming, Formulating: Inside technology, The MIT Press
- Ji, D., Smyth, P., Steyvers, M. (2020). Can I trust my fairness metric? assessing fairness with unlabeled data and bayesian inference. In: NeurIPS
- Ji, J., Qiu, T., Chen, B., et al. (2023). AI alignment: A comprehensive survey. CoRR <http://arxiv.org/abs/2310.19852>
- Jin, X., Barbieri, F., Kennedy, B., et al. (2021). On transferability of bias mitigation effects in language model fine-tuning. In: NAACL-HLT. Association for Computational Linguistics, pp. 3770–3783
- Jo, E.S., Geburu, T. (2020). Lessons from archives: Strategies for collecting sociocultural data in machine learning. In: FAT\*. ACM, pp. 306–316
- Jobin, A., Ienca, M., & Vayena, E. (2019). The global landscape of AI ethics guidelines. *Nature Machine Intelligence*, 1(9), 389–399.
- Jorgensen, M., Richert, H., Black, E., et al. (2023). Not so fair: The impact of presumably fair machine learning models. In: AIES. ACM, pp. 297–311
- Kahneman, D. (2011). *Thinking*. Farrar, Straus and Giroux: Fast and Slow
- Kahneman, D., Sibony, O., Sunstein, C. (2021). *Noise: A Flaw in Human Judgment*. William Collins
- Kamiran, F., Calders, T. (2009). Classifying without discriminating. In: International conference on computer, control and communication. IEEE, pp. 1–6
- Kamishima, T., Akaho, S., Asoh, H., et al. (2012). Fairness-aware classifier with prejudice remover regularizer. In: ECML/PKDD (2), LNCS, vol 7524. Springer, pp. 35–50
- Karimi, A., Barthe, G., Schölkopf, B., et al. (2023). A survey of algorithmic recourse: Contrastive explanations and consequential recommendations. *ACM Computing Surveys*, 55(5), 1–29.
- Kasirzadeh, A., & Smart, A. (2021). The use and misuse of counterfactuals in ethical machine learning. In: FAccT. ACM, pp. 228–236
- Katell, M.A., Young, M., Herman, B., et al. (2019). An algorithmic equity toolkit for technology audits by community advocates and activists. CoRR <http://arxiv.org/abs/1912.02943>
- Kaur, D., Uslu, S., Rittichier, K. J., et al. (2023). Trustworthy artificial intelligence: A review. *ACM Computing Surveys*, 55(2), 1–38.
- Kazim, E., Koshiyama, A. S., Hilliard, A., et al. (2021). Systematizing audit in algorithmic recruitment. *Journal of Intelligence*, 9(3), 46.
- Keane, M.T., Kenny, E.M., Delaney, E., et al. (2021). If only we had better counterfactual explanations: Five key deficits to rectify in the evaluation of counterfactual XAI techniques. In: IJCAI. ijcai.org, pp. 4466–4474
- Kenthapadi, K., Lakkaraju, H., Natarajan, P., et al. (2022). Model monitoring in practice: Lessons learned and open challenges. In: KDD. ACM, pp. 4800–4801
- Kiviat, B. (2019). The art of deciding with data: evidence from how employers translate credit reports into hiring decisions. *Socio-Economic Review*, 17(2), 283–309.
- Kleinberg, J.M., Mullainathan, S., Raghavan, M. (2017). Inherent trade-offs in the fair determination of risk scores. In: ITCS,

- LIPics, vol 67. Schloss Dagstuhl - Leibniz-Zentrum für Informatik, pp. 43:1–23
- Knowles, B., Richards, J.T., Kroeger, F. (2022). The many facets of trust in AI: Formalizing the relation between trust and fairness, accountability, and transparency. CoRR <http://arxiv.org/abs/2208.00681>
- Koch, G., & Kinder-Kurlanda, K. (2020). Source criticism of data platform logics on the internet. *Historical Social Research*, 45(3), 270–287.
- Kohler-Hausmann, I. (2019). Eddie murphy and the dangers of counterfactual causal thinking about detecting racial discrimination. *Northwestern University Law Review*, 113(5), 1163–1227.
- Koshiyama, A., Kazim, E., Treleaven, P., et al. (2021). Towards algorithm auditing: A survey on managing legal, ethical and technological risks of AI, ML and associated algorithms. Available at SSRN: <https://doi.org/10.2139/ssrn.3778998>
- Kraft, A., & Usbeck, R. (2022). The lifecycle of "facts": A survey of social bias in knowledge graphs. In: *AACL/IJCNLP (1)*. Association for Computational Linguistics, pp. 639–652
- Krishna, S., Han, T., Gu, A., et al. (2022). The disagreement problem in explainable machine learning: A practitioner's perspective. CoRR <http://arxiv.org/abs/2202.01602>
- Kroll, J. A., Huey, J., Barocas, S., et al. (2017). Accountable algorithms. *U of Penn Law Review*, 165, 633–705.
- Kulynych, B., Overdorf, R., Troncoso, C., et al. (2020). Pots: protective optimization technologies. In: *FAT\**. ACM, pp. 177–188
- Kusner, M.J., Loftus, J.R., Russell, C., et al. (2017). Counterfactual fairness. In: *NIPS*, pp. 4066–4076
- Ladhak, F., Durmus, E., Suzgun, M., et al. (2023). When do pre-training biases propagate to downstream tasks? A case study in text summarization. In: *EACL*. Association for Computational Linguistics, pp. 3198–3211
- Lakkaraju, H., Kleinberg, J.M., Leskovec, J., et al. (2017). The selective labels problem: Evaluating algorithmic predictions in the presence of unobservables. In: *KDD*. ACM, pp. 275–284
- Lange, M. D., Aljundi, R., Masana, M., et al. (2022). A continual learning survey: Defying forgetting in classification tasks. *IEEE transactions on Pattern Analysis and Machine Intelligence*, 44(7), 3366–3385.
- Lazar, S. (2022). Legitimacy, authority, and the political value of explanations. CoRR [abs/2208.08628](https://arxiv.org/abs/2208.08628)
- Lebovitz, S., Levina, N., & Lifshitz-Assaf, H. (2021). Is AI ground truth really true? The dangers of training and evaluating AI tools based on experts' know-what. *MIS Q* 45(3)
- Lee, J., Roh, Y., Song, H., et al. (2021a). Machine learning robustness, fairness, and their convergence. In: *KDD*. ACM, pp. 4046–4047
- Lee, M. S. A., & Floridi, L. (2021). Algorithmic fairness in mortgage lending: from absolute conditions to relational trade-offs. *Minds and Machines*, 31(1), 165–191.
- Lee, M.S.A., Singh, J. (2021). The landscape and gaps in open source fairness toolkits. In: *CHI*. ACM, pp. 1–13
- Lee, M. S. A., Floridi, L., & Singh, J. (2021). Formalising trade-offs beyond algorithmic fairness: Lessons from ethical philosophy and welfare economics. *AI Ethics*, 1(4), 529–544.
- Li, H., Vincent, N., Chancellor, S., et al. (2023). The dimensions of data labor: A road map for researchers, activists, and policymakers to empower data producers. In: *FACCT*. ACM, pp. 1151–1161
- Lin, C. K., & Jackson, S. J. (2023). From bias to repair: Error as a site of collaboration and negotiation in applied data science work. *Proceedings of the ACM on Human-Computer Interaction*, 7(CSCW1), 1–32.
- Lin, Z. J., Jung, J., Goel, S., et al. (2020). The limits of human predictions of recidivism. *Science Advances*, 6(7), 0652.
- Liu, L. T., Dean, S., Rolf, E., et al. (2018). Delayed impact of fair machine learning. *International Conference on Machine Learning*, 80, 3156–3164.
- Lobo, P. R., Daga, E., Alani, H., et al. (2023). Semantic web technologies and bias in Artificial Intelligence: A systematic literature review. *Semantic Web*, 14(4), 745–770.
- Lopez, P. (2019). Reinforcing intersectional inequality via the AMS algorithm in Austria. In: *Proc. of the STS Conference*. Verlag der Technischen Universität Graz, pp. 289–309
- Lowry, S., & Macpherson, G. (1986). A blot on the profession. *British Medical Journal*, 296(6623), 657–658.
- Madaio, M., Egede, L., Subramonyam, H., et al. (2022). Assessing the fairness of AI systems: AI practitioners processes, challenges, and needs for support. *Proceedings of the ACM on Human-Computer Interaction*, 6, 1–26.
- Majumder, S., Chakraborty, J., Bai, G. R., et al. (2023). Fair enough: Searching for sufficient measures of fairness. *ACM Transactions on Software Engineering and Methodology*, 32(6), 1–22.
- Makhlouf, K., Zhioua, S., & Palamidessi, C. (2020). Survey on causal-based machine learning fairness notions. CoRR [abs/2010.09553](https://arxiv.org/abs/2010.09553)
- Makhlouf, K., Zhioua, S., & Palamidessi, C. (2021). Machine learning fairness notions: Bridging the gap with real-world applications. *Information Processing & Management*, 58(5), 102642.
- Makhlouf, K., Zhioua, S., & Palamidessi, C. (2021). On the applicability of machine learning fairness notions. *SIGKDD Explorations Newsletter*, 23(1), 14–23.
- Makhlouf, K., Zhioua, S., & Palamidessi, C. (2022). Identifiability of causal-based fairness notions: A state of the art. CoRR [abs/2203.05900](https://arxiv.org/abs/2203.05900)
- Mallen, A., Asai, A., Zhong, V., et al. (2023). When not to trust language models: Investigating effectiveness of parametric and non-parametric memories. In: *ACL (1)*. Association for Computational Linguistics, pp. 9802–9822
- Manerba, M.M., & Guidotti, R. (2021). Fairshades: Fairness auditing via explainability in abusive language detection systems. In: *CogMI*. IEEE, pp. 34–43
- Martin, K. (2019). Ethical implications and accountability of algorithms. *Journal of Business Ethics*, 160(4), 835–850.
- Mehrabi, N., Morstatter, F., Saxena, N., et al. (2021). A survey on bias and fairness in machine learning. *ACM Computing Surveys*, 54(6), 1–35.
- Memarian, B., & Doleck, T. (2023). Fairness, accountability, transparency, and ethics (FATE) in Artificial Intelligence (AI) and higher education: A systematic review. *Computers and Education: Artificial Intelligence*, 5, 100152.
- Mendoza, I., & Bygrave, L. A. (2017). *The right not to be subject to automated decisions based on profiling* (pp. 77–98). EU Internet Law: Regulation and Enforcement
- Menon, A. K., & Williamson, R. C. (2018). The cost of fairness in binary classification. *Proceedings of Machine Learning Research*, 81, 107–118.
- Metcalfe, J., Moss, E., Watkins, E.A., et al. (2021). Algorithmic impact assessments and accountability: The co-construction of impacts. In: *FACCT*. ACM, pp. 735–746
- Miceli, M., Posada, J., & Yang, T. (2022). Studying up machine learning data: Why talk about bias when we mean power? *Proceedings of the ACM on Human-Computer Interaction*, 6, 1–14.
- Miceli, M., Yang, T., Garcia, A. A., et al. (2022). Documenting data production processes: A participatory approach for data work. *Proceedings of the ACM on Human-Computer Interaction*, 6(CSCW2), 1–34.
- Miller, A.P. (2018). Want less-biased decisions? Use algorithms. *Harvard Business Review*
- Minh, D., Wang, H. X., Li, Y. F., et al. (2022). Explainable Artificial Intelligence: A comprehensive review. *Artificial Intelligence Review*, 55(5), 3503–3568.
- Minow, M. (2021). Equality vs. Equity. *American Journal of Law and Equality*, 1, 167–193.
- Mitchell, M., Wu, S., Zaldivar, A., et al. (2019). Model cards for model reporting. In: *FAT*. ACM, pp. 220–229

- Mitchell, S., Potash, E., Barocas, S., et al. (2021). Algorithmic fairness: Choices, assumptions, and definitions. *Annual Review of Statistics and Its Application*, 8, 141–163.
- Mittelstadt, B.D., Wachter, S., & Russell, C. (2023). The unfairness of fair machine learning: Levelling down and strict egalitarianism by default. *CoRR abs/2302.02404*
- Mökander, J. (2023). Auditing of AI: legal, ethical and technical approaches. *Digital Society*, 2(3), 49.
- Moraffah, R., Karami, M., Guo, R., et al. (2020). Causal interpretability for machine learning - problems, methods and evaluation. *SIGKDD Explorations Newsletter*, 22(1), 18–33.
- Mosqueira-Rey, E., Hernández-Pereira, E., Alonso-Ríos, D., et al. (2023). Human-in-the-loop machine learning: A state of the art. *Artificial Intelligence Review*, 56(4), 3005–3054.
- Mougan, C., & Nielsen, D.S. (2023). Monitoring model deterioration with explainable uncertainty estimation via non-parametric bootstrap. In: *AAAI*. AAAI Press, pp. 15037–15045
- Mougan, C., Kanellos, G., & Gottron, T. (2021). Desiderata for explainable AI in statistical production systems of the european central bank. In: *PKDD/ECML Workshops (1)*, Communications in Computer and Information Science, vol 1524. Springer, pp. 575–590
- Mougan, C., Broelemann, K., Kasneci, G., et al. (2022). Explanation shift: Detecting distribution shifts on tabular data via the explanation space. In: *NeurIPS 2022 Workshop on Distribution Shifts: Connecting Methods and Applications*
- Mougan, C., Álvarez, J.M., Ruggieri, S., et al. (2023). Fairness implications of encoding protected categorical attributes. In: *AIES*. ACM, pp. 454–465
- Mulligan, D. K., Kroll, J. A., Kohli, N., et al. (2019). This thing called fairness: Disciplinary confusion realizing a value in technology. *Proceedings of the ACM on Human-Computer Interaction*, 3, 1–36.
- Nader, L. (1972). Up the anthropologist: Perspectives gained from studying up. *Tech. Rep.* ED065375, ERIC, <https://eric.ed.gov/?id=ED065375>
- Nogueira, A. R., Pugnana, A., Ruggieri, S., et al. (2022). Methods and tools for causal discovery and causal inference. *Wiley Interdisciplinary Reviews: Data Mining and Knowledge Discovery*, 12(2), e1449.
- Ntoutsis, E., Fafalios, P., Gadiraju, U., et al. (2020). Bias in data-driven Artificial Intelligence systems - An introductory survey. *Wiley Interdisciplinary Reviews: Data Mining and Knowledge Discovery*, 10(3), e1356.
- van Nuenen, T., Such, J. M., & Coté, M. (2022). Intersectional experiences of unfair treatment caused by automated computational systems. *Proceedings of the ACM on Human-Computer Interaction*, 6(CSCW2), 1–30.
- Olteanu, A., Castillo, C., Diaz, F., et al. (2019). Social data: Biases, methodological pitfalls, and ethical boundaries. *Frontiers Big Data*, 2, 13.
- Organizers Of QueerInAI, et al. (2023). Queer in AI: A case study in community-led participatory AI. In: *FAccT*. ACM, pp. 1882–1895
- Ovalle, A., Subramonian, A., Gautam, V., et al. (2023). Factoring the matrix of domination: A critical review and reimagining of intersectionality in AI fairness. In: *AIES*. ACM, pp. 496–511
- Pagan, N., Baumann, J., Elokda, E., et al. (2023). A classification of feedback loops and their relation to biases in automated decision-making systems. *CoRR abs/2305.06055*
- Pariser, E. (2011). *The filter bubble: What the Internet is hiding from you*. Penguin Press.
- Parmar, M., Mishra, S., Geva, M., et al. (2023). Don't blame the annotator: Bias already starts in the annotation instructions. In: *EACL*. Association for Computational Linguistics, pp. 1771–1781
- Passi, S., Barocas, S. (2019). Problem formulation and fairness. In: *FAT*. ACM, pp. 39–48
- Pearl, J. (2009). *Causality: models, reasoning and inference*, Second Edition. Cambridge University Press
- Pearl, J., Mackenzie, D. (2018). *The book of why: The new science of cause and effect*. Basic Books
- Pedreschi, D., Ruggieri, S., Turini, F. (2008). Discrimination-aware data mining. In: *KDD*. ACM, pp. 560–568
- Pedreschi, D., Ruggieri, S., Turini, F. (2012). A study of top-k measures for discrimination discovery. In: *SAC*. ACM, pp. 126–131
- Peng, K., Mathur, A., Narayanan, A. (2021). Mitigating dataset harms requires stewardship: Lessons from 1000 papers. In: *NeurIPS Datasets and Benchmarks*
- Percy, C., Dragicevic, S., Sarkar, S., et al. (2021). Accountability in AI: from principles to industry-specific accreditation. *AI Communications*, 34(3), 181–196.
- Perdomo, J. C., Zrnic, T., Mendler-Dünner, C., et al. (2020). Performative prediction. *Proceedings of Machine Learning Research*, 119, 7599–7609.
- Pessach, D., & Shmueli, E. (2022). A review on fairness in machine learning. *ACM Computing Surveys*, 55(3), 1–44.
- Petroni, F., Piktus, A., Fan, A., et al. (2021). KILT: a benchmark for knowledge intensive language tasks. In: *NAACL-HLT*. Association for Computational Linguistics, pp. 2523–2544
- Pleiss, G., Raghavan, M., Wu, F., et al. (2017). On fairness and calibration. In: *NIPS*, pp. 5680–5689
- Pruss, D. (2023). Ghosting the machine: Judicial resistance to a recidivism risk assessment instrument. In: *FAccT*. ACM, pp. 312–323
- Quiñero-Candela, J., Sugiyama, M., Lawrence, N. D., et al. (2009). *Dataset shift in machine learning*. MIT Press.
- Quy, T. L., Roy, A., Iosifidis, V., et al. (2022). A survey on datasets for fairness-aware machine learning. *Wiley Interdisciplinary Reviews: Data Mining and Knowledge Discovery*, 12(3), e1452.
- Rahmatalabi, A., Xiang, A. (2022). Promises and challenges of causality for ethical machine learning. *CoRR abs/2201.10683*
- Raji, I. D., Yang, J. (2019). ABOUT ML: annotation and benchmarking on understanding and transparency of machine learning lifecycles. *CoRR abs/1912.06166*
- Raji, I. D., Smart, A., White, R. N., et al. (2020). Closing the AI accountability gap: defining an end-to-end framework for internal algorithmic auditing. In: *FAT\**. ACM, pp. 33–44
- Raji, I. D., Bender, E. M. et al. (2021a). AI and the everything in the whole wide world benchmark. In: *NeurIPS Datasets and Benchmarks*
- Raji, I. D., Scheuerman, M. K., Amironesei, R. (2021b). You can't sit with us: Exclusionary pedagogy in AI ethics education. In: *FAccT*. ACM, pp. 515–525
- Rawal, A., McCoy, J., Rawat, D. B., et al. (2022). Recent advances in trustworthy explainable Artificial Intelligence: Status, challenges, and perspectives. *IEEE Transactions on Artificial Intelligence*, 3(6), 852–866.
- Rüz T (2021) Group fairness: Independence revisited. In: *FAccT*. ACM, pp. 129–137
- Richardson, B., Gilbert, J. E. (2021). A framework for fairness: A systematic review of existing fair AI solutions. *CoRR abs/2112.05700*
- Rismani, S., Moon, A. (2023). What does it mean to be a responsible AI practitioner: An ontology of roles and skills. In: *AIES*. ACM, pp. 584–595
- Romei, A., & Ruggieri, S. (2014). A multidisciplinary survey on discrimination analysis. *The Knowledge Engineering Review*, 29(5), 582–638.
- Rong, Y., Leemann, T., Nguyen, T., et al. (2024). Towards human-centered explainable AI: A survey of user studies for model explanations. *IEEE Trans Pattern Anal Mach Intell* p to appear
- Rovatsos, M., Mittelstadt, B., Koene, A. (2019). *Landscape Summary: Bias In Algorithmic Decision-Making: What is bias in algorithmic decision-making, how can we identify it, and how can we mitigate it?* UK Government

- Roy, A., Horstmann, J., Ntoutsis, E. (2023). Multi-dimensional discrimination in law and machine learning - A comparative overview. In: *FAccT*. ACM, pp. 89–100
- Ruggieri, S., Álvarez, J. M., Pugnana, A., et al. (2023). Can we trust fair-AI? In: AAAI. AAAI Press, pp. 15421–15430
- Sadiq, S. W., Aryani, A., Demartini, G., et al. (2022). Information resilience: the nexus of responsible and agile approaches to information use. *The VLDB Journal*, 31(5), 1059–1084.
- Saha, D., Schumann, C., McElfresh, D. C., et al. (2020). Measuring non-expert comprehension of machine learning fairness metrics. *Proceedings of Machine Learning Research*, 119, 8377–8387.
- Salman, H., Jain, S., Ilyas, A., et al. (2022). When does bias transfer in transfer learning? CoRR abs/2207.02842
- Saltz, J. S., Skirpan, M., Fiesler, C., et al. (2019). Integrating ethics within machine learning courses. *ACM Transactions on Computing Education*, 19(4), 1–26.
- Scantamburlo, T. (2021). Non-empirical problems in fair machine learning. *Ethics and Information Technology*, 23(4), 703–712.
- Schölkopf, B., Locatello, F., Bauer, S., et al. (2021). Toward causal representation learning. *Proc IEEE* 109(5), 612–634.
- Schwartz, R., Vassilev, A., Greene, K., et al. (2022). Towards a standard for identifying and managing bias in Artificial Intelligence. Tech. Rep. 1270, NIST Special Publication
- Scott, K. M., Wang, S. M., Miceli, M., et al. (2022). Algorithmic tools in public employment services: Towards a jobseeker-centric perspective. In: *FAccT*. ACM, pp. 2138–2148
- Seaver, N. (2017). Algorithms as culture. Some tactics for the ethnography of algorithmic systems. *Big Data & Society*, 4(2), 2053951717738104.
- Shahbazi, N., Lin, Y., Asudeh, A., et al. (2023). Representation bias in data: A survey on identification and resolution techniques. *ACM Computing Surveys*. <https://doi.org/10.1145/3588433>
- Shahriar, S., Allana, S., Hazratifard, S. M., et al. (2023). A survey of privacy risks and mitigation strategies in the Artificial Intelligence life cycle. *IEEE Access*, 11, 61829–61854.
- Shelby, R., Rismani, S., Henne, K., et al. (2023). Sociotechnical harms of algorithmic systems: Scoping a taxonomy for harm reduction. In: AIES. ACM, pp. 723–741
- Silberzahn, R., & Uhlmann, E. L. (2015). Crowdsourced research: Many hands make tight work. *Nature*, 526, 189–191.
- Smirnov, I., Lemmerich, F., & Strohmaier, M. (2021). Quota-based debiasing can decrease representation of the most under-represented groups. *Royal Society Open Science*, 8(9), 210821.
- Spirtes, P., & Zhang, K. (2016). Causal discovery and inference: concepts and recent methodological advances. *Applied Informatics*, 3(3), 1–38.
- Spirtes, P., Glymour, C., & Scheines, R. (2000). *Causation, Prediction, and Search* (2nd ed.). Adaptive computation and machine learning: MIT Press.
- Srivastava, M., Heidari, H., Krause, A. (2019). Mathematical notions vs. human perception of fairness: A descriptive approach to fairness for machine learning. In: KDD. ACM, pp. 2459–2468
- State, L. (2022). Constructing meaningful explanations: Logic-based approaches. In: AIES. ACM, p. 916
- State, L., Fahimi, M. (2023). Careful explanations: A feminist perspective on XAI. In: EWAF, CEUR Workshop Proceedings, vol 3442. CEUR-WS.org
- State, L., Salat, H., Rubrichi, S., et al. (2022). Explainability in practice: Estimating electrification rates from mobile phone data in senegal. CoRR abs/2211.06277
- Steed, R., Panda, S., Kobren, A., et al. (2022). Upstream mitigation is not all you need: Testing the bias transfer hypothesis in pre-trained language models. In: ACL (1). Association for Computational Linguistics, pp. 3524–3542
- Stoyanovich, J., Abiteboul, S., Howe, B., et al. (2022). Responsible data management. *Communications of the ACM*, 65(6), 64–74.
- Suresh, H., Gutttag, J. V. (2021). A framework for understanding sources of harm throughout the machine learning life cycle. In: EAAMO. ACM, pp. 17:1–17:9
- Sylolypavan, A., Sleeman, D. H., Wu, H., et al. (2023). The impact of inconsistent human annotations on AI driven clinical decision making. *NPI Digit Medicine*, 6, 26.
- Szczekocka, E., Tarnec, C., Pieczrak, J. (2022). Standardization on bias in Artificial Intelligence as industry support. In: Big Data. IEEE, pp. 5090–5099
- Tal, A. S., Kuflik, T., & Kliger, D. (2022). Fairness, explainability and in-between: Understanding the impact of different explanation methods on non-expert users' perceptions of fairness toward an algorithmic system. *Ethics and Information Technology*, 24(1), 2.
- Tal, E. (2023). Target specification bias, counterfactual prediction, and algorithmic fairness in healthcare. In: AIES. ACM, pp. 312–321
- Tang, Z., Zhang, J., & Zhang, K. (2023). What-is and how-to for fairness in machine learning: A survey, reflection, and perspective. *ACM Computing Surveys*, 55, 1–37.
- Tizpaz-Niari, S., Kumar, A., Tan, G., et al. (2022). Fairness-aware configuration of machine learning libraries. In: ICSE. ACM, pp. 909–920
- Tolan, S. (2019). Fair and unbiased algorithmic decision making: Current state and future challenges. arXiv preprint [arXiv:1901.04730](https://arxiv.org/abs/1901.04730)
- Tölle, L., Trier, M. (2023). Polarization in online social networks: A review of mechanisms and dimensions. In: ECIS
- Turri, V., Dzombak, R. (2023). Why we need to know more: Exploring the state of AI incident documentation practices. In: AIES. ACM, pp. 576–583
- Vainio-Pekka, H., otse Agbese MO, Jantunen M, et al. (2023). The role of explainable AI in the research field of AI ethics. *ACM Transactions on Interactive Intelligent Systems*, 13(4), 1.
- Veale, M., & Binns, R. (2017). Fairer machine learning in the real world: Mitigating discrimination without collecting sensitive data. *Big Data & Society*, 4(2), 2053951717743530.
- Vedder, A., & Naudts, L. (2017). Accountability for the use of algorithms in a big data environment. *International Review of Law, Computers & Technology*, 31(2), 206–224.
- Verma, S., Rubin, J. (2018). Fairness definitions explained. In: FairWare@ICSE. ACM, pp. 1–7
- Wachter, S., Mittelstadt, B., & Russell, C. (2021). Bias preservation in machine learning: The legality of fairness metrics under EU non-discrimination law. *W Va L Rev*, 123(3), 735–790.
- Wachter, S., Mittelstadt, B., & Russell, C. (2021). Why fairness cannot be automated: Bridging the gap between EU non-discrimination law and AI. *Computer Law & Security Review*, 41, 105567.
- Wagstaff, K. (2012). Machine learning that matters. In: ICML. icml.cc/Omnipress
- Wan, M., Zha, D., Liu, N., et al. (2023). In-processing modeling techniques for machine learning fairness: A survey. *ACM Transactions on Knowledge Discovery from Data*, 17(3), 1–27.
- Wang, A., Kapoor, S., Barocas, S., et al. (2023). Against predictive optimization: On the legitimacy of decision-making algorithms that optimize predictive accuracy. In: *FAccT*. ACM, p. 626
- Wei, S., & Niethammer, M. (2022). The fairness-accuracy Pareto front. *Statistical Analysis and Data Mining*, 15(3), 287–302.
- Weinberg, L. (2022). Rethinking fairness: An interdisciplinary survey of critiques of hegemonic ML fairness approaches. *Journal of Artificial Intelligence Research*, 74, 75–109.
- Wick, M. L., Panda, S., Tristan, J. (2019). Unlocking fairness: A trade-off revisited. In: *NeurIPS*, pp. 8780–8789
- Wiegand, M., Eder, E., Ruppenhofer, J. (2022). Identifying implicitly abusive remarks about identity groups using a linguistically informed approach. In: NAACL-HLT. ACL, pp. 5600–5612
- Wieringa, M. (2020). What to account for when accounting for algorithms: A systematic literature review on algorithmic accountability. In: *FAT\**. ACM, pp. 1–18

- Wu, D., Liu, J. (2022). Involve humans in algorithmic fairness issue: A systematic review. In: *iConference* (1), LNCS, vol 13192. Springer, pp. 161–176
- Xenidis, R. (2018). Multiple discrimination in EU anti-discrimination law: Towards redressing complex inequality? In: Belavusau, U., Henrard, K. (Eds.) *EU anti-discrimination law beyond gender*. Hart Publishing, pp. 41–74
- Xenidis, R. (2020). Tuning EU equality law to algorithmic discrimination: Three pathways to resilience. *Maastricht Journal of European and Comparative Law*, 27(6), 736–758.
- Xenidis, R., & Senden, L., et al. (2020). EU non-discrimination law in the era of Artificial Intelligence: Mapping the challenges of algorithmic discrimination. In U. Bernitz (Ed.), *General principles of EU law and the EU digital order* (pp. 151–182). Kluwer Law International.
- Xu, W. (2019). Toward human-centered AI: A perspective from human-computer interaction. *Interactions*, 26(4), 42–46.
- Zajko, M. (2022). Artificial Intelligence, algorithms, and social inequality: Sociological contributions to contemporary debates. *Sociology Compass*, 16(3), e12962.
- Zehlke, M., Yang, K., & Stoyanovich, J. (2023). Fairness in ranking, part I: Score-based ranking. *ACM Computing Surveys*, 55, 1–36.
- Zhang, J., Bareinboim, E. (2018). Fairness in decision-making - the causal explanation formula. In: AAAI. AAAI Press, pp. 2037–2045
- Zhang, L., Wu, Y., Wu, X. (2017). A causal framework for discovering and removing direct and indirect discrimination. In: IJCAI. ijcai.org, pp. 3929–3935
- Zhang, L. H., Goldstein, M., & Ranganath, R. (2021). Understanding failures in out-of-distribution detection with deep generative models. *Proceedings of Machine Learning Research*, 139, 12427–12436.
- Zhang, Z., Wang, S., & Meng, G. (2023). A review on pre-processing methods for fairness in machine learning. *Advances in natural computation, Fuzzy Systems and Knowledge Discovery* (pp. 1185–1191). Springer.
- Ziems, C., Chen, J., Harris, C., et al. (2022). VALUE: understanding dialect disparity in NLU. In: ACL (1). Association for Computational Linguistics, pp. 3701–3720
- Ziewitz, M. (2016). Governing algorithms. Myth, mess, and methods. *Science Technology Human Values*, 41(1), 3–16.
- Zliobaite, I. (2017). Measuring discrimination in algorithmic decision making. *Data Mining and Knowledge Discovery*, 31(4), 1060–1089.
- Zliobaite, I., & Custers, B. (2016). Using sensitive personal data may be necessary for avoiding discrimination in data-driven decision models. *Artificial Intelligence and Law*, 24(2), 183–201.
- Zuiderveen Borgesius, F. J. (2020). Strengthening legal protection against discrimination by algorithms and Artificial Intelligence. *The International Journal of Human Rights*, 24(10), 1572–1593.

**Publisher's Note** Springer Nature remains neutral with regard to jurisdictional claims in published maps and institutional affiliations.

## Authors and Affiliations

Jose M. Alvarez<sup>1,2</sup> · Alejandra Bringas Colmenarejo<sup>3</sup> · Alaa Elobaid<sup>4,5</sup> · Simone Fabbrizzi<sup>4,6,7</sup> · Miriam Fahimi<sup>8</sup> · Antonio Ferrara<sup>9,10</sup> · Siamak Ghodsi<sup>5,6</sup> · Carlos Mougán<sup>3</sup> · Ioanna Papageorgiou<sup>6</sup> · Paula Reyero<sup>11</sup> · Mayra Russo<sup>6</sup> · Kristen M. Scott<sup>12</sup> · Laura State<sup>1,2</sup> · Xuan Zhao<sup>13</sup> · Salvatore Ruggieri<sup>2</sup>

✉ Jose M. Alvarez  
jose.alvarez@sns.it

✉ Salvatore Ruggieri  
salvatore.ruggieri@unipi.it

Alejandra Bringas Colmenarejo  
Alejandra.Bringas-Colmenarejo@soton.ac.uk

Alaa Elobaid  
elobaida@iti.gr

Simone Fabbrizzi  
simone.fabbrizzi@unibz.it

Miriam Fahimi  
miriam.fahimi@aau.at

Antonio Ferrara  
antonio.ferrara@centai.eu

Siamak Ghodsi  
ghodsi@l3s.de

Carlos Mougán  
c.mougan@soton.ac.uk

Ioanna Papageorgiou  
ioanna.papageorgiou@iri.uni-hannover.de

Paula Reyero  
paula.reyero-lobo@open.ac.uk

Mayra Russo  
mrusso@l3s.de

Kristen M. Scott  
kristen.scott@kuleuven.be

Laura State  
laura.state@di.unipi.it

Xuan Zhao  
xuan.zhao@schufa.de

<sup>1</sup> Scuola Normale Superiore, Pisa, Italy

<sup>2</sup> University of Pisa, Pisa, Italy

<sup>3</sup> University of Southampton, Southampton, UK

<sup>4</sup> CERTH, Thessaloniki, Greece

<sup>5</sup> Free University of Berlin, Berlin, Germany

<sup>6</sup> Leibniz University Hannover, Hannover, Germany

<sup>7</sup> Free University of Bozen-Bolzano, Bolzano, Italy

<sup>8</sup> University of Klagenfurt, Klagenfurt, Austria

<sup>9</sup> GESIS - Leibniz Institute, Mannheim, Germany

<sup>10</sup> RWTH Aachen University, Aachen, Germany

<sup>11</sup> The Open University, Milton Keynes, UK

<sup>12</sup> KU Leuven, Leuven, Belgium

<sup>13</sup> SCHUFA Holding AG, Wiesbaden, Germany

## 8 Conclusions, Limitations and Future Work

*“All that you touch  
You Change.  
All that you Change  
Changes you.  
The only lasting truth  
is Change.”*

– Octavia E. Butler [77]

### Conclusions

This thesis argued that algorithmic fairness must evolve along two fundamental dimensions: it must become statistically robust and structurally aware. As algorithmic systems increasingly function as institutional gatekeepers, fairness can neither be assessed through deterministic point estimates nor ensured by adjusting outputs alone. It must be grounded in reliable inference and embedded into the relational mechanisms that govern how opportunities are distributed. On the diagnostic side, this work reframed fairness auditing as a problem of statistical and causal inference. Instead of relying on brittle point estimates, it introduced size-adaptive testing procedures that account for sampling variability in intersectional groups, conditional independence tests that isolate residual bias in opaque ranking systems, and explanation-based analyses that detect disparate treatment even when outcome distributions appear equal. Together, these contributions move fairness evaluation from threshold comparison to evidence-based decision-making, addressing statistical reliability, causal validity, and procedural neutrality in a unified framework. On the structural side, the thesis demonstrated that unfairness often emerges from topology and interaction rather than isolated predictions. In routing systems, strict efficiency objectives can structurally concentrate exposure; in link recommendation, feedback loops amplify homophily and popularity bias; in urban inference, coarse measurements obscure localized inequalities; and in ranking pipelines, evaluator bias, skewed sampling, and aggregation dynamics can crystallize prejudice into hierarchical disadvantage. Across these domains, one of the central insights is that fairness must intervene in the inputs, mechanisms, and connectivity patterns that shape visibility and comparison, not only in final outcomes. Finally, the thesis connected fairness to reliability and governance. By introducing abstention mechanisms

for ranking systems and articulating a holistic bias-management architecture, it emphasized that trustworthy AI requires continuous monitoring, explicit modeling of uncertainty, and lifecycle-wide oversight. In sum, this work advances a comprehensive view of algorithmic fairness as a systemic property: statistically grounded, structurally informed, and operationally embedded. Ensuring fairness in modern AI systems is not a matter of satisfying isolated metrics, but of designing and auditing the institutional processes through which algorithms shape opportunity.

## Limitations

In this thesis, we acknowledge that theoretical definitions of algorithmic fairness rely on mathematical abstractions that cannot fully capture the highly complex nature of political philosophy and distributive justice. Consequently, deploying a mathematically fair algorithmic technique does not automatically guarantee fairness within the broader, complex socio-technical system it inhabits. This disconnect between mathematical abstraction and social reality is perhaps most evident in the pervasive necessity of treating human identity as discrete, fixed categories. Whether defining groups for fairness testing or mitigation, these models rely on reducing complex, fluid, and continuous human identities into rigid bins, such as binary gender or predefined racial categories. This epistemological reduction inherently fails to capture the true sociological nuances of identity and marginalization.

Beyond the categorization of identity, this reductionist approach also extends to the evaluation of individuals, leading to a “ground truth” illusion regarding merit. Several structural interventions in this thesis, particularly in recovering fair rankings from pairwise comparisons or aggregating crowd-sourced judgments, rely on modeling and isolating human bias to uncover a candidate’s latent quality. However, in complex socio-technical systems, ground truth or merit is often inherently subjective, socially constructed, or historically distorted. While mathematical models can elegantly correct for observed statistical deviations, they cannot entirely resolve the philosophical ambiguity of what constitutes an objectively correct ranking.

Even if individual identities and subjective merit could be perfectly quantified, the mathematical models used to process them face their own systemic boundaries. The structural interventions proposed in this thesis, whether redistributing exposure in physical routing networks, mitigating homophily in link recommendations, or aggregating hierarchical rankings, implicitly model these platforms

as closed, self-contained environments. In reality, users and opportunities exist within interconnected, open-world ecosystems. A limitation of these structural approaches is that mitigating bias on isolated graphs or ranking systems does not account for how advantages and disadvantages cascade across other platforms, or how users simultaneously use different, potentially biased systems.

Finally, compounding these theoretical and structural limitations are the practical barriers encountered during real-world deployment. The practical implementation of demographic auditing and debiasing frameworks is often severely complicated by real-world privacy restrictions. Data protection regimes, such as the GDPR, strictly limit access to the exact sensitive attributes needed to effectively run these statistical tests and monitor compliance. This creates an ongoing regulatory friction between privacy mandates and non-discrimination goals, presenting a formidable final hurdle to comprehensive AI auditing.

## Future Work

Just as foundational methods in statistics, optimization, and linear algebra were developed long before deep learning could build upon them, this thesis aims to establish rigorous statistical and structural foundations for algorithmic fairness. Several frameworks introduced in the thesis, including hypothesis testing for fairness auditing, causal diagnostics for opaque systems, and bias-aware preference modeling, are deliberately general: they do not depend on a specific model architecture or application domain. This generality positions them to be extended to the next generation of AI systems, where the challenges of fairness are amplified rather than resolved. In what follows, we outline several broad directions along which this work could be developed further.

On the diagnostic side, the hypothesis-testing frameworks presented here operate mostly in a static setting. Deployed systems, however, require continuous monitoring as new data arrives and distributions shift. Extending size-adaptive fairness testing to a sequential setting, where statistical guarantees must be maintained over time while adapting to distributional drift, would provide the formal underpinning for the continuous monitoring advocated in the policy chapter of this thesis. Furthermore, the resolution limit introduced in this thesis raises deeper information-theoretic questions about the minimum amount of data required to certify a system as fair, and how such minima should inform regulatory standards for deployment.

On the structural side, this thesis studies fairness in routing, link recommendation, and socioeconomic inference as separate problems on distinct networks.

In reality, these processes coexist on overlapping topologies: the same urban graph supports both traffic flow and economic activity, the same social network mediates both information propagation and access to opportunity. Understanding how a fairness intervention in one process affects the others requires a unified multi-process perspective that this thesis does not yet provide.

Regarding the bias-aware preference modeling developed in this thesis, a direct frontier is its extension to the alignment of large language models. Modern alignment pipelines such as Reinforcement Learning from Human Feedback [78] train reward models from human pairwise preferences, a setting that directly instantiates the problem addressed by BARP. Current approaches assume that annotators are unbiased sensors of helpfulness, yet evaluators carry cultural biases and favoritism, precisely the distortions that BARP models through its evaluator-specific bias parameters. Integrating bias-aware preference modeling into reward model training could prevent demographic prejudice from contaminating the alignment signal. This also raises a deeper open question: correcting annotator bias may conflict with other alignment objectives, creating a fairness-alignment trade-off whose characterization remains an open problem.

Finally, these frameworks extend naturally to agentic AI systems [79]. Modern architectures increasingly rely on multi-agent pipelines where multiple components generate, evaluate, and aggregate information, a compositional structure that mirrors the ranking pipeline studied in this thesis. In such systems, bias may enter at each stage and compound across agents with heterogeneous distortions. When AI agents serve as evaluators, the bias parameters no longer represent human prejudice but the systematic distortions of AI systems, which may be subtler and more correlated than those of human annotators. Similarly, the abstention mechanisms introduced for ranking naturally generalize to agent delegation: determining when an agent should act versus defer to a human based on estimated risk. Developing fairness frameworks for these multi-agent dynamics, where unfairness emerges from the interaction of components rather than from any single one, represents a critical open challenge.

## Bibliography

- [1] M. Kranzberg, “Technology and history: Kranzberg’s laws,” *Technology and culture*, vol. 27, no. 3, pp. 544–560, 1986.
- [2] C. Dwork, M. Hardt, T. Pitassi, O. Reingold, and R. Zemel, “Fairness through awareness,” in *Proceedings of the 3rd innovations in theoretical computer science conference*, 2012, pp. 214–226.
- [3] M. Hardt, E. Price, and N. Srebro, “Equality of opportunity in supervised learning,” *Advances in neural information processing systems*, vol. 29, 2016.
- [4] I. Greenberg, “An analysis of the eoccc “four-fifths” rule,” *Management Science*, vol. 25, no. 8, pp. 762–769, 1979.
- [5] B. Schölkopf and A. J. Smola, *Learning with Kernels: Support Vector Machines, Regularization, Optimization, and Beyond*. MIT Press, 2002.
- [6] M. McPherson, L. Smith-Lovin, and J. M. Cook, “Birds of a feather: Homophily in social networks,” *Annual review of sociology*, vol. 27, no. 1, pp. 415–444, 2001.
- [7] A.-L. Barabási and R. Albert, “Emergence of scaling in random networks,” *science*, vol. 286, no. 5439, pp. 509–512, 1999.
- [8] A. Ferrara, F. Cozzi, A. Perotti, A. Panisson, and F. Bonchi, “Size-adaptive hypothesis testing for fairness,” *Advances in neural information processing systems*, vol. 38, 2025.
- [9] A. Ferrara, C. Abrate, F. Vitale, and F. Bonchi, “Auditing for demographic bias in opaque rankings,” *Proceedings of the VLDB Endowment*, vol. 19, 2026.
- [10] A. Ferrara, D. García-Soriano, and F. Bonchi, “Beyond shortest paths: Node fairness in route recommendation,” *Proceedings of the VLDB Endowment*, vol. 18, no. 9, pp. 3230–3242, 2025.
- [11] A. Ferrara, F. Bonchi, F. Fabbri, F. Karimi, and C. Wagner, “Bias-aware ranking from pairwise comparisons,” *Data Mining and Knowledge Discovery*, vol. 38, no. 4, pp. 2062–2086, 2024.
- [12] A. Ferrara, L. Espín-Noboa, F. Karimi, and C. Wagner, “Link recommendations: Their impact on network structure and minorities,” in *Proceedings of the 14th ACM Web Science Conference 2022*, 2022, pp. 228–238.

- [13] A. Ferrara\*, A. Pugnana\*, F. Bonchi, and S. Ruggieri, “Bounded-abstention pairwise learning to rank,” in *Proceedings of the 32nd ACM SIGKDD Conference on Knowledge Discovery and Data Mining*, 2026.
- [14] J. M. Alvarez, A. B. Colmenarejo, A. Elobaid, S. Fabbriizzi, M. Fahimi, A. Ferrara, S. Ghodsi, C. Mougán, I. Papageorgiou, P. Reyeró, et al., “Policy advice and best practices on bias and fairness in ai,” *Ethics and Information Technology*, vol. 26, no. 2, p. 31, 2024.
- [15] G. Ahnert, A. Ferrara, and C. Wagner, “Fairness-aware ranking recovery from pairwise comparisons,” in *Proceedings of the 18th ACM Web Science Conference 2026*, 2026, pp. 289–298. DOI: 10.1145/3795766.3799744
- [16] C. Balestra, A. Ferrara, and E. Müller, “Fairmc fair–markov chain rank aggregation methods,” in *International Conference on Big Data Analytics and Knowledge Discovery*, Springer, 2024, pp. 315–321.
- [17] F. P. Nerini, C. Borile, A. Ferrara, and A. Panisson, “Super-resolution of urban socioeconomic indicators via graph-based recommender systems,” *Web and the City, workshop at the WebConference*, 2026.
- [18] C. Mougán, L. State, A. Ferrara, S. Ruggieri, and S. Staab, “Beyond demographic parity: Redefining equal treatment,” *arXiv preprint arXiv:2303.08040*, 2023.
- [19] P. Reyeró Lobo, J. Kwarteng, M. Russo, M. Fahimi, K. Scott, A. Ferrara, I. Sen, and M. Fernandez, “A multidisciplinary lens of bias in hate speech,” in *Proceedings of the International Conference on Advances in Social Networks Analysis and Mining*, 2023, pp. 121–125.
- [20] S. Kierkegaard, *Soren Kierkegaard’s Journals and Papers, 1845-1855*. Indiana University Press, 1967, vol. 6.
- [21] C. J. Rowe, S. Broadie, et al., *Nicomachean ethics*. Oxford University Press, 2002.
- [22] D. García-Soriano and F. Bonchi, “Maxmin-fair ranking: Individual fairness under group-fairness constraints,” in *Proceedings of the 27th ACM SIGKDD Conference on Knowledge Discovery & Data Mining*, 2021, pp. 436–446.
- [23] D. García-Soriano and F. Bonchi, “Fair-by-design matching,” *Data Mining and Knowledge Discovery*, vol. 34, no. 5, pp. 1291–1335, 2020.
- [24] J. Rawls, “A theory of justice,” in *Applied ethics*, Routledge, 2017, pp. 21–29.
- [25] S. Verma and J. Rubin, “Fairness definitions explained,” in *Proceedings of the international workshop on software fairness*, 2018, pp. 1–7.

- [26] J. Kleinberg, S. Mullainathan, and M. Raghavan, “Inherent trade-offs in the fair determination of risk scores,” *arXiv preprint arXiv:1609.05807*, 2016.
- [27] A. Chouldechova, “Fair prediction with disparate impact: A study of bias in recidivism prediction instruments,” *Big data*, vol. 5, no. 2, pp. 153–163, 2017.
- [28] M. J. Kusner, J. Loftus, C. Russell, and R. Silva, “Counterfactual fairness,” *Advances in neural information processing systems*, vol. 30, 2017.
- [29] J. Pearl, “Causal inference in statistics: An overview,” *Statistics Surveys*, vol. 3, pp. 96–146, 2009. DOI: 10.1214/09-SS057 [Online]. Available: <https://projecteuclid.org/journals/statistics-surveys/volume-3/issue-none/Causal-inference-in-statistics-An-overview/10.1214/09-SS057.full>
- [30] D. Ji, P. Smyth, and M. Steyvers, “Can i trust my fairness metric? assessing fairness with unlabeled data and bayesian inference,” *Advances in Neural Information Processing Systems*, vol. 33, pp. 18 600–18 612, 2020.
- [31] J. J. Cherian and E. J. Candès, “Statistical inference for fairness auditing,” *Journal of machine learning research*, vol. 25, no. 149, pp. 1–49, 2024.
- [32] P. Besse, E. del Barrio, P. Gordaliza, J.-M. Loubes, and L. Risser, “A survey of bias in machine learning through the prism of statistical parity,” *The American Statistician*, vol. 76, no. 2, pp. 188–198, 2022.
- [33] H. Weerts, M. Dudík, R. Edgar, A. Jalali, R. Lutz, and M. Madaio, “Fair-learn: Assessing and improving fairness of ai systems,” *Journal of Machine Learning Research*, vol. 24, no. 257, pp. 1–8, 2023.
- [34] E. Del Barrio, P. Gordaliza, and J.-M. Loubes, “A central limit theorem for lp transportation cost on the real line with application to fairness assessment in machine learning,” *Information and Inference: A Journal of the IMA*, vol. 8, no. 4, pp. 817–849, 2019.
- [35] V. S. Lo, S. Datta, and Y. Salami, “Bringing practical statistical science to ai and predictive model fairness testing,” *AI and Ethics*, vol. 5, no. 3, pp. 2149–2164, 2025.
- [36] C. Marx, R. Phillips, S. Friedler, C. Scheidegger, and S. Venkatasubramanian, “Disentangling influence: Using disentangled representations to audit model predictions,” *Advances in Neural Information Processing Systems*, vol. 32, 2019.

- [37] P. Adler, C. Falk, S. A. Friedler, T. Nix, G. Rybeck, C. Scheidegger, B. Smith, and S. Venkatasubramanian, “Auditing black-box models for indirect influence,” *Knowledge and Information Systems*, vol. 54, no. 1, pp. 95–122, 2018.
- [38] K. Zhang, J. Peters, D. Janzing, and B. Schölkopf, “Kernel-based conditional independence test and application in causal discovery,” in *Proceedings of the 27th Conference on Uncertainty in Artificial Intelligence (UAI)*, Barcelona, Spain: AUAI Press, 2011, pp. 804–813.
- [39] G. J. Szekely and M. L. Rizzo, “Partial distance correlation with methods for dissimilarities,” *Annals of Statistics*, vol. 42, no. 6, pp. 2382–2412, 2014. DOI: 10.1214/14-AOS1255
- [40] B. Salimi, L. Rodriguez, B. Howe, and D. Suciu, “Interventional fairness: Causal database repair for algorithmic fairness,” in *Proceedings of the 2019 international conference on management of data*, 2019, pp. 793–810.
- [41] F. Kamiran and T. Calders, “Data preprocessing techniques for classification without discrimination,” *Knowledge and information systems*, vol. 33, no. 1, pp. 1–33, 2012.
- [42] M. Feldman, S. A. Friedler, J. Moeller, C. Scheidegger, and S. Venkatasubramanian, “Certifying and removing disparate impact,” in *proceedings of the 21th ACM SIGKDD international conference on knowledge discovery and data mining*, 2015, pp. 259–268.
- [43] L. C. Freeman, “Centrality in social networks conceptual clarification,” *Social networks*, vol. 1, no. 3, pp. 215–239, 1978.
- [44] L. Page, S. Brin, R. Motwani, and T. Winograd, “The pagerank citation ranking: Bringing order to the web.,” Stanford infolab, Tech. Rep., 1999.
- [45] J. Bachmann, S. Martin-Gutierrez, L. Espín-Noboa, N. Cinardi, and F. Karimi, “Network inequality through preferential attachment, triadic closure, and homophily,” *Scientific Reports*, 2026.
- [46] A. Saxena, G. Fletcher, and M. Pechenizkiy, “Fairsna: Algorithmic fairness in social network analysis,” *ACM Computing Surveys*, vol. 56, no. 8, pp. 1–45, 2024.
- [47] Y. Dong, J. Ma, S. Wang, C. Chen, and J. Li, “Fairness in graph mining: A survey,” *IEEE Transactions on Knowledge and Data Engineering*, vol. 35, no. 10, pp. 10 583–10 602, 2023.
- [48] F. Karimi, M. Oliveira, and M. Strohmaier, “Minorities in networks and algorithms,” in *Handbook of Computational Social Science*, Edward Elgar Publishing Limited, 2025, pp. 438–451.

- [49] A. Bose and W. Hamilton, “Compositional fairness constraints for graph embeddings,” in *International conference on machine learning*, PMLR, 2019, pp. 715–724.
- [50] T. Rahman, B. Surma, M. Backes, and Y. Zhang, “Fairwalk: Towards fair graph embedding,” 2019.
- [51] A. Khajehnejad, M. Khajehnejad, M. Babaei, K. P. Gummadi, A. Weller, and B. Mirzasoleiman, “Crosswalk: Fairness-enhanced node representation learning,” in *Proceedings of the AAAI Conference on Artificial Intelligence*, vol. 36, 2022, pp. 11 963–11 970.
- [52] E. Dai and S. Wang, “Learning fair graph neural networks with limited and private sensitive attribute information,” *IEEE Transactions on Knowledge and Data Engineering*, vol. 35, no. 7, pp. 7103–7117, 2022.
- [53] J. Ma, J. Deng, and Q. Mei, “Subgroup generalization and fairness of graph neural networks,” *Advances in Neural Information Processing Systems*, vol. 34, pp. 1048–1061, 2021.
- [54] S. Tsioutsoulis, E. Pitoura, P. Tsaparas, I. Kleftakis, and N. Mamoulis, “Fairness-aware pagerank,” in *Proceedings of the Web Conference 2021*, 2021, pp. 3815–3826.
- [55] E. Krasanakis, S. Papadopoulos, and I. Kompatsiaris, “Applying fairness constraints on graph node ranks under personalization bias,” in *International Conference on Complex Networks and Their Applications*, Springer, 2020, pp. 610–622.
- [56] A.-A. Stoica, C. Riederer, and A. Chaintreau, “Algorithmic glass ceiling in social networks: The effects of social recommendations on network diversity,” in *Proceedings of the 2018 World Wide Web Conference*, 2018, pp. 923–932.
- [57] A. G. Greenwald and M. R. Banaji, “Implicit social cognition: Attitudes, self-esteem, and stereotypes,” *Psychological review*, vol. 102, no. 1, p. 4, 1995.
- [58] M. Bertrand and S. Mullainathan, “Are emily and greg more employable than lakisha and jamal? a field experiment on labor market discrimination,” *American economic review*, vol. 94, no. 4, pp. 991–1013, 2004.
- [59] R. A. Bradley and M. E. Terry, “Rank analysis of incomplete block designs: I. the method of paired comparisons,” *Biometrika*, vol. 39, no. 3/4, pp. 324–345, 1952.
- [60] R. D. Luce, *Individual choice behavior: A theoretical analysis*. New York: John Wiley and Sons, 1959.

- [61] A. Khetan and S. Oh, “Achieving budget-optimality with adaptive schemes in crowdsourcing,” in *Advances in Neural Information Processing Systems*, vol. 29, 2016.
- [62] N. B. Shah, S. Balakrishnan, and M. J. Wainwright, “A permutation-based model for crowd labeling: Optimal estimation and robustness,” *arXiv preprint arXiv:1606.09632*, 2016.
- [63] N. B. Shah, S. Balakrishnan, J. Bradley, A. Parekh, K. Ramchandran, and M. J. Wainwright, “Estimation from pairwise comparisons: Sharp minimax bounds with topology dependence,” *Journal of Machine Learning Research*, vol. 17, no. 58, pp. 1–47, 2016.
- [64] M. Zehlike, F. Bonchi, C. Castillo, S. Hajian, M. Megahed, and R. Baeza-Yates, “FA\*IR: A fair top-k ranking algorithm,” in *Proceedings of the 26th ACM on International Conference on Information and Knowledge Management*, 2017, pp. 1569–1578.
- [65] A. Singh and T. Joachims, “Fairness of exposure in rankings,” in *Proceedings of the 24th ACM SIGKDD International Conference on Knowledge Discovery & Data Mining*, 2018, pp. 2219–2228.
- [66] A. J. Biega, K. P. Gummadi, and G. Weikum, “Equity of attention: Amortizing individual fairness in rankings,” in *The 41st International ACM SIGIR Conference on Research & Development in Information Retrieval*, 2018, pp. 405–414.
- [67] J.-C. de Borda, “Mémoire sur les élections au scrutin,” *Histoire de l’Académie Royale des Sciences*, vol. 1, pp. 657–665, 1781.
- [68] C. Dwork, R. Kumar, M. Naor, and D. Sivakumar, “Rank aggregation methods for the web,” in *Proceedings of the 10th International Conference on World Wide Web*, ACM, 2001, pp. 613–622.
- [69] A. Schopenhauer, *Parerga and paralipomena: Short philosophical essays*. Oxford University Press, 2000, vol. 1.
- [70] G. Jeh and J. Widom, “Scaling personalized web search,” in *Proceedings of the 12th international conference on World Wide Web*, 2003, pp. 271–279.
- [71] P. Gupta, A. Goel, J. Lin, A. Sharma, D. Wang, and R. Zadeh, “Wtf: The who to follow service at twitter,” in *Proceedings of the 22nd international conference on World Wide Web*, ACM, 2013, pp. 505–514.
- [72] A. Grover and J. Leskovec, “Node2vec: Scalable feature learning for networks,” in *Proceedings of the 22nd ACM SIGKDD international conference on Knowledge discovery and data mining*, 2016, pp. 855–864.

- [73] Voltaire, *Voltaire in His Letters: Being a Selection from His Correspondence*. GP Putnam's Sons, 1919.
- [74] J. Muir, "My first summer in the sierra," in *British Politics and the Environment in the Long Nineteenth Century*, Routledge, 2023, pp. 291–296.
- [75] C. G. Jung and R. F. C. Hull, "The archetypes of the collective unconscious," in *Collected works of CG Jung*, Routledge, 2023, v7\_90–v7\_113.
- [76] A. de Saint-Exupéry, *The Little Prince*. Reynal & Hitchcock, 1943.
- [77] O. E. Butler, *Parable of the Sower*. Four Walls Eight Windows, 1993.
- [78] P. F. Christiano, J. Leike, T. Brown, M. Martic, S. Legg, and D. Amodei, "Deep reinforcement learning from human preferences," *Advances in neural information processing systems*, vol. 30, 2017.
- [79] Z. Xi, W. Chen, X. Guo, W. He, Y. Ding, B. Hong, M. Zhang, J. Wang, S. Jin, E. Zhou, et al., "The rise and potential of large language model based agents: A survey," *Science China Information Sciences*, vol. 68, no. 2, p. 121 101, 2025.